Computer Simulation and Analysis Methods in the Development of the Hydraulic Ram Pump

Eur Ing Peter B.M. Glover BSc MSc C.Eng MIMechE

Thesis submitted for PhD by Research

University of Warwick Department of Engineering

January 1994

TEXT BOUND CLOSE TO THE SPINE IN THE ORIGINAL THESIS

TEXT CUT OFF IN THE ORIGINAL

PAGE NUMBERING AS ORIGINAL

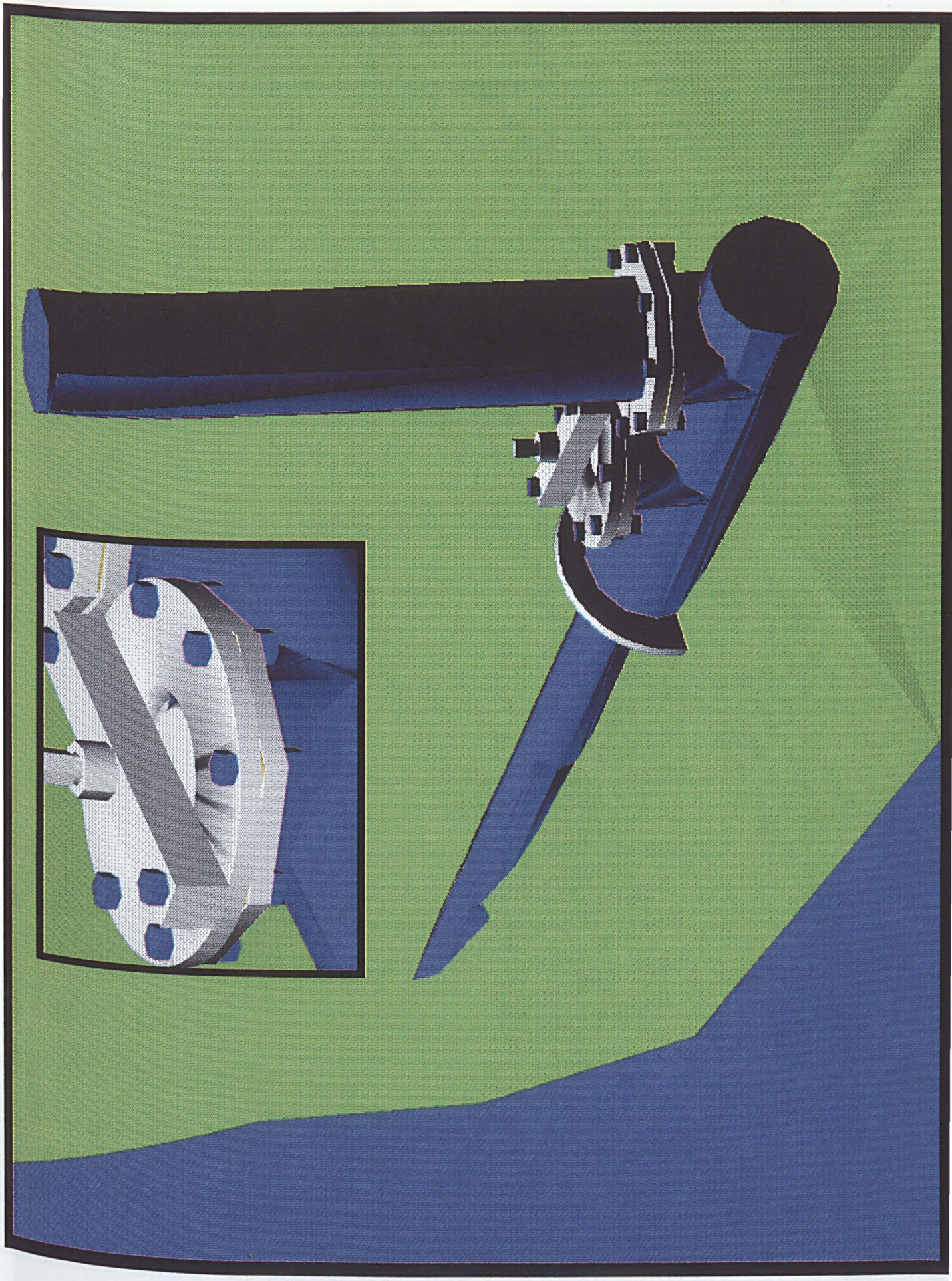

Dedication

To Stephanie

Declaration

The research described in this thesis has been undertaken as part of an ongoing research, development and dissemination programme undertaken at the University of Warwick by its Development Technology Unit. The work described in this thesis represents original work carried out in collaboration with the Development Technology Unit. Except where otherwise stated, the described work has been undertaken by the author.

Acknowledgments

The author would like to particularly acknowledge Dr Adrian Boldy for his inspiration and motivation throughout the research programme.

Further acknowledgment is offered to Mott MacDonald for providing the author with the financial support required to undertake this research; and to the University of Warwick's Civil Engineering Research Fund for providing research funds.

The author would also like to acknowledge the Development Technology Unit (D.T.U.) under Dr Terry Thomas for undertaking such important research and development work, and providing staff and equipment resources. Further acknowledgment is offered to Paul Fountain of Tear Fund for his pioneering work deploying hydraulic ram pumps for water supply in developing countries, and his role in the instigation of the hydraulic ram pump research and development programme.

Table of Contents

List of Figures

Nomenclature

a = *Wave propagation velocity (m/s)*

α = *Acceleration* (ms^{-2})

A = *Area* (m^2)

C_d = *Drag coefficient*

C_L = *Head loss coefficient for fittings*

D = *Diameter (m,mm)*

E = *Youngs Modulus* (Nm^{-2})

F = *Force (N)*

g = *Acceleration due to gravity* (9.80665 ms^{-2})

γ = *Ratio of isobaric and isochoric specific heat capacity for air and dynamic viscosity*

h = *Delivery head (m)*

H = *Drive head (m)*

K_h, K_f = *Coefficients of head loss and force*

L = *Drive pipe length (m)*

M = *Mass (kg)*

μ = *Poissons Ratio*

N = *Integer number of velocity steps in cut-off velocity*

q = *Delivery flow* (*l/s*, m^3/s)

Q = *Flow, total drive pipe flow* (*l/s*, m^3/s)

t = *Pipe wall thickness (mm)*

T,t = *Time (s)*

V = *Velocity (m/s)*

x = *Valve Displacement (mm)*

Chapter 1: Introduction

The work described in this thesis was undertaken on behalf of the University of Warwick's Development Technology Unit, under the auspices of the HYDROtransient SIMulation unit.

The HYDROtransient SIMulation Unit in the Department of Engineering represents a centre of excellence in the modeling of hydraulic transients in pressure systems. The unit has its foundations in the expertise of Dr Adrian Boldy whose research and consultancy has ordained his position among the world leaders in the field. Much of the work undertaken by the unit uses the simulation package PTRAN developed by Dr Boldy for the simulation of transients in complex networks.

The Development Technology Unit (D.T.U.) is run by a group of professionals and volunteers committed to promoting third world development. The unit is the brain child of Dr Terry Thomas, and operates on many different levels. The majority of work undertaken is in the form of research and development of technologies appropriate to the needs, skills and resources of developing countries. In recent years, this has involved the development of technologies for solar refrigeration, water pumping, micro hydro, and biomass..

The D.T.U. has also been involved in the dissemination of these and similar technologies working with local organisations throughout the world including: Sri Lanka, Zaire, South Africa, Nigeria, Zambia, Zimbabwe, and Rwanda. Much of this dissemination has involved the setting up of teaching programmes and providing consultancy on hydraulic ram pump projects.

The D.T.U. first became involved with the development of hydraulic ram pumps in the early 1980s when it undertook the assessment of the I.T.D.G. hydraulic ram pump (Intermediate Technology Development Group-S.B.Watt[1]). This design was cheap to manufacture, and could be manufactured in a small, poorly equipped workshop and in this respect was highly attractive. The design was found to give poor performance, poor reliability, and was found to lack performance prediction data.

The D.T.U then started a series of parallel research and development programmes investigating plastic pumps, rubberised rocking valves, the use of hydraulic ram pumps in irrigation channels.

The above work culminated in the initiation of the main D.T.U. hydraulic ram pump (hydram) development programme. This was initially co-funded by the Overseas Development Administration and Tear Fund, and comprised a research and development component together with a dissemination component.

The objective of the research and development programme was to improve current hydraulic ram pump designs to make them more suitable for manufacture and maintenance in a third world environment and to identify design parameters and means of performance prediction. The dissemination programme initially involved direct support for a hydraulic ram pump orientated water programme in Zaire, but then included further training in Zimbabwe, and consultancy on projects in other countries.

This thesis outlines the ways in which computer methods in simulation and analysis have been deployed by the author to contribute to the objectives of the above programmes. The author has undertaken the described work in conjunction with the above development programmes, and within the research programme has visited hydraulic ram pump projects in Columbia, Zaire, and South Africa, and has further provided consultancy for projects in other countries.

A century of scientific analyses and experimental work had failed to provide a full understanding of the behaviour of the

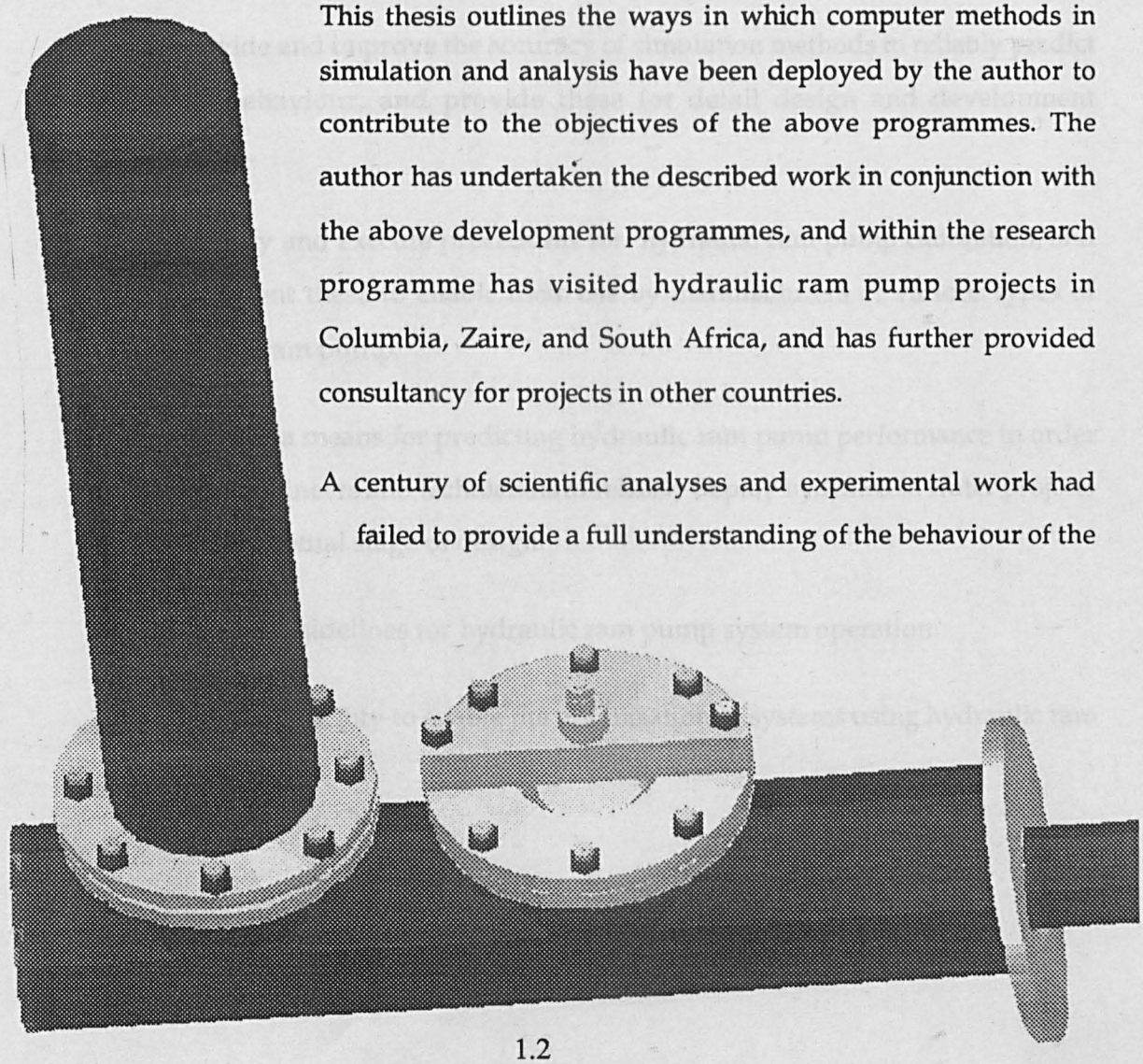

hydraulic ram pump, and provide reliable means for performance prediction. This thesis describes how the author has used modern computing methods to gain a full understanding of pump operation, identify methods of pump calibration, and performance prediction.

1.1 Research Objectives.

The research described in this thesis has been undertaken in conjunction with a research and development programme at the University of Warwick to develop the Hydraulic Ram Pump to allow its wider deployment and manufacture in developing countries. Many of the research objectives have thus been set by the needs of the programme, although significant aspects have been undertaken with regard to wider deployment of hydraulic ram pumps generally.

A summary of some of the research objectives is given below. These are:

- To provide an improved understanding of the hydraulic ram pump so as to provide an educated environment for development of the device.
- To provide and improve the accuracy of simulation methods to reliably predict pump behaviour, and provide these for detail design and development purposes.
- To identify and execute procedures for hydraulic ram pump calibration, and to document these to enable their use by manufacturers of various types of hydraulic ram pump.
- To provide a means for predicting hydraulic ram pump performance in order to allow engineers and technicians to reliably deploy hydrams in water projects at the conceptual stage of design.
- To identify guidelines for hydraulic ram pump system operation.
- To provide a facility to enable the optimisation of systems using hydraulic ram pumps.

1.2 The Need.

The main motivation behind this research programme was the opportunity to enhance the accessibility of a technology that is ideally suited to small scale third world water supply programmes. The hydraulic ram pump is basically a very simple and reliable device capable of operating continuously over long periods of time with the minimum of maintenance.

In many developing countries there is a massive need for reliable water pumping. In addition to this, sophisticated technologies are not generally suitable because of inadequately trained technicians, and poor maintenance capability. Also in many rural areas the availability of electrical supplies is poor and where supplies are available, connection to the supply is usually prohibitively expensive. Alternative prime mover technologies such as diesel or petrol engines are also expensive, require maintenance, and have a requirement for regular supplies and storage of expensive fuels.

The hydraulic ram pump is a water pump that uses the energy present in water falling naturally, to pump some of the falling water to a higher elevation than it originated. As such, the hydraulic ram represents a renewable energy device. It operates around two simple valves and therefore, is theoretically adaptable for manufacture in developing countries, and maintenance at village level.

There is significant potential for wider deployment of hydraulic ram pumps within the developed world, but the main motivation behind this research programme is to allow their wider deployment in developing countries.

The following quotations come from papers published at a 1985 conference on the hydraulic ram pump in Tanzania:

> "Information on practical hydram sizes and installation limitations is often not available. Such information is necessary to prevent expensive failures in the field and arbitrary hydram designs and installation." - P.O. Kahangire[(2)]1986

"From the point of view of water supply design, the engineers are only awaiting a hydraulic ram with established performance data so as to confidently incorporate it in their schemes." - T.S.A. Mbwette and E.Th.Protzen[3]1986

1.3 History of hydraulic ram pump analysis

Chapter 3 summarises the previous research work undertaken on the hydraulic ram pump. The difficulty of this is due to the large number of investigations undertaken over the last century, and the great degree of replication within these. Very few of the analyses have used the more modern computational techniques, but the results of those which did are also discussed.

1.4 The simulation

Chapter 4 describes the computer simulation that was developed as part of the author's MSc research, and then significantly enhanced during this research. The chapter describes the detail of the simulation, and the applications for which the simulation has given the most insight. Much of the understanding described in chapter 2 was only achieved as a result of being able to visualise pump operation through simulation, in the knowledge that the simulation provided a reliable representation of reality. Experimental data demonstrating the accuracy of the simulation is given.

1.5 The Predictive Model

A major development described in this thesis is the development of the predictive model. This is described in detail in chapter 5. The described model is able to provide the quantity of data required to produce design charts. It became apparent that the computational overhead associated with the simulation of a single pumping condition made the simulation package unsuitable for generating the required volume of data. For this reason, the predictive model was developed using the insight provided by the computer simulation.

The main purpose for developing the predictive model was the creation of design charts as illustrated in chapter 6. These are already being used in the field. The predictive model can also be deployed as a stand alone package.

1.6 Other Hydraulic Ram Pump Designs

The majority of the analyses described in the following chapters relate to the D.T.U. Pumps, the designs of which are given in Appendix H. It is anticipated that the described methods will be adaptable to all currently available designs of hydraulic ram pumps, and that manufacturers adopting the methods will benefit greatly by improving the accessibility of their products. Chapter 7 attempts to identify possible approaches to adopt the described methods to some of the more difficult designs.

1.7 Further Research

The research has identified areas of further research, and these are summarised in Chapter 8. It is hoped that the results of this research will provide the tools by which hydraulic ram pumps can become more accessible and understandable to the water engineer and the manufacturer. Furthermore, it is hoped that this will enhance the wider deployment of this fascinating and environmentally friendly technology in the developing world.

Chapter 2: How The Hydraulic Ram Pump Operates

Although the operation of the hydraulic ram pump is in principle very simple, the interaction of all its elements make a full understanding of its operation somewhat more complex. For this reason, a simple description of the pump's operation is given first, followed by a more complex analysis of the detail of its operation. It is necessary to fully understand this chapter in order to follow the steps that have been taken to provide performance prediction, and system design tools.

2.1 Simple description of the operation of the hydraulic ram pump

The hydraulic ram pump is a simple water powered pumping device that uses the phenomenon of waterhammer to transfer the potential energy of a large body of fluid to a small quantity of the same fluid. Essentially, it removes the energy from a large flow of water falling through a small distance, and transfers it to a small body of the same fluid, pumping it to a great height.

A typical installation is presented in figure 2.1. It illustrates a drop between the water source and the waste level, which supplies the energy to pump some of the water to the delivery reservoir. This is achieved by cyclically inducing a pressure transient in the drive pipe by successive rapid halting of its natural flow.

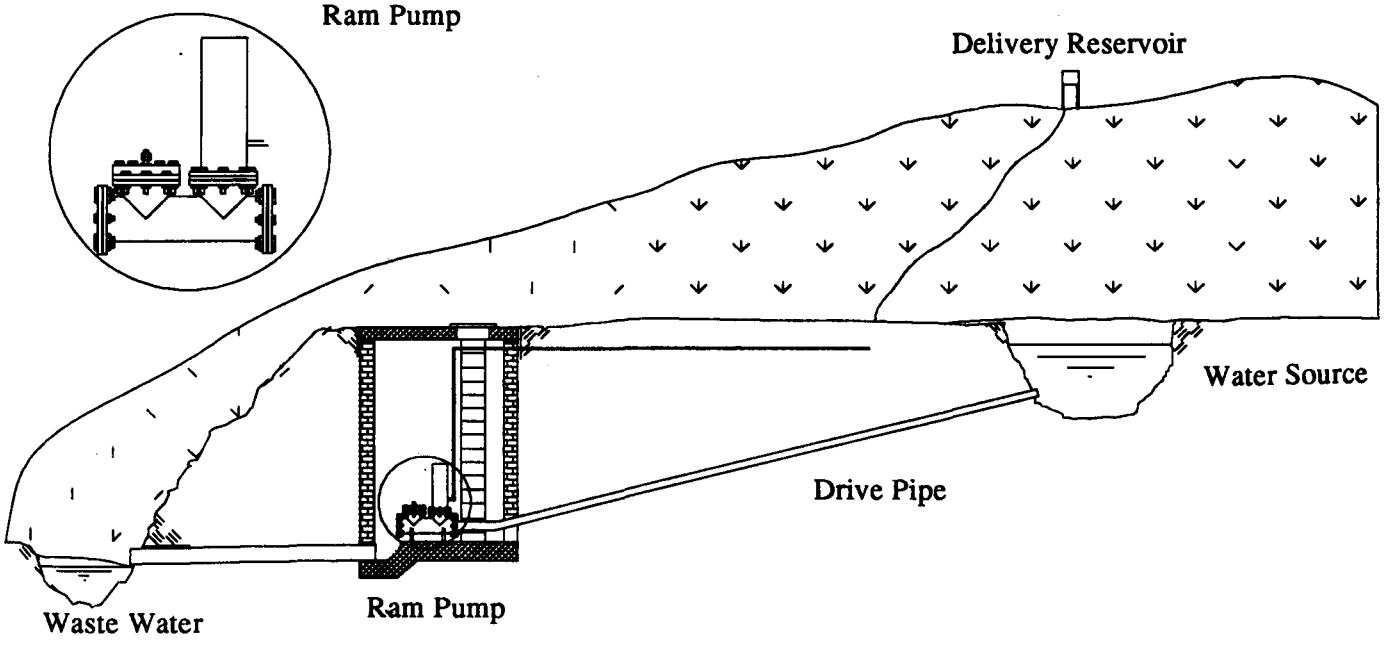

It is helpful to understand the operation of the hydraulic ram pump as a series of consecutive periods. This has been the approach of many authors on the hydraulic ram pump, which have differed greatly in their detail, accuracy, and number of cycles discussed. For simplicity, it is helpful to consider the hydraulic ram pump to function in three consecutive cycles, and to account for other factors within these. The cycles are: the acceleration period in which water accelerates in the drive pipe; the delivery period in which water is delivered to the pressure system; and the recoil period which is experienced before the whole cycle recommences.

Acceleration Period.

Water accelerates under gravity in the drive pipe from the drive tank, and discharges through the impulse valve to atmosphere. This process of acceleration continues until such time as the drag forces on the impulse valve exceed its own weight at which time the impulse valve starts to close.

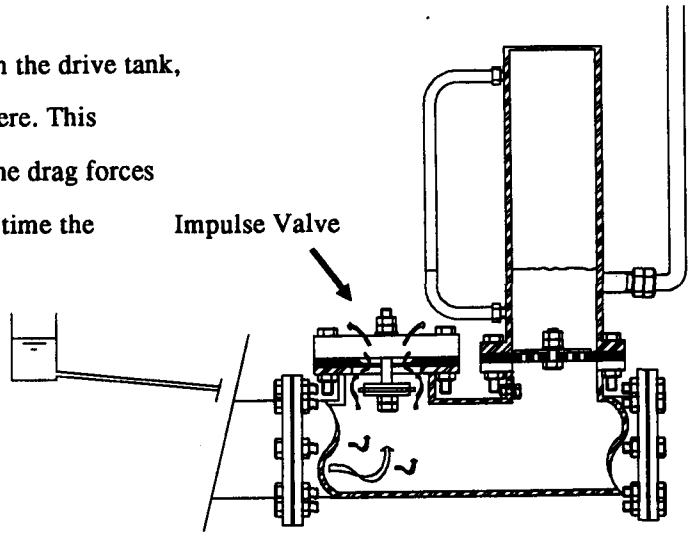

Figure 2.2 The Acceleration Period

Delivery Period

The sudden closure causes the fluid in the drive pipe to be brought to rest very rapidly. This results in a rise in pressure which is maintained as the velocity change propagates up the drive pipe. While this higher pressure is maintained, a discharge occurs through a one way valve (delivery valve) into a cushioning air vessel which is connected to the delivery system

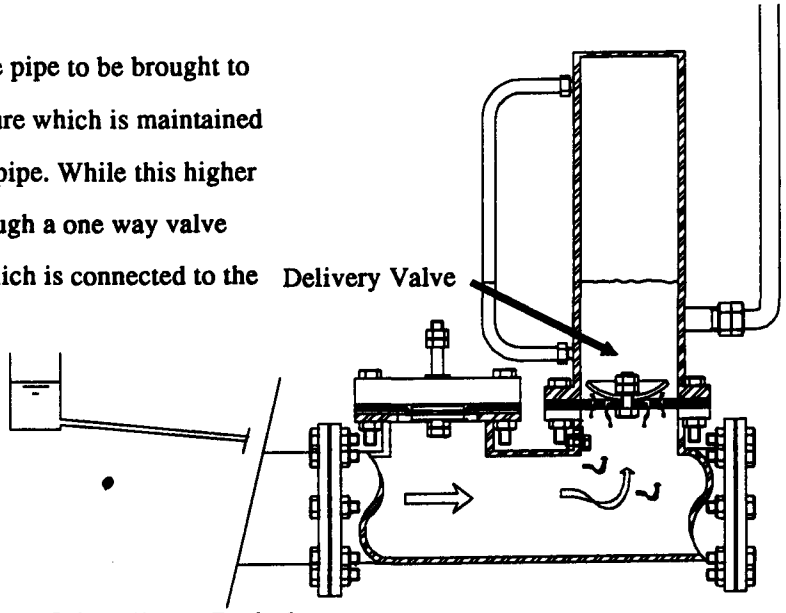

Figure 2.3 Delivery Period

Recoil Period

Once the pressure in the drive pipe begins to subside, the delivery valve closes, and a recoil is experienced. This causes a reverse of flow in the drive pipe, and reopens the impulse valve ready for the next operating cycle. It also allows a small quantity of air to be induced through the snifter valve. This air is then delivered into the air vessel on the next delivery period, and acts to replenish air in the air vessel that is lost into solution.

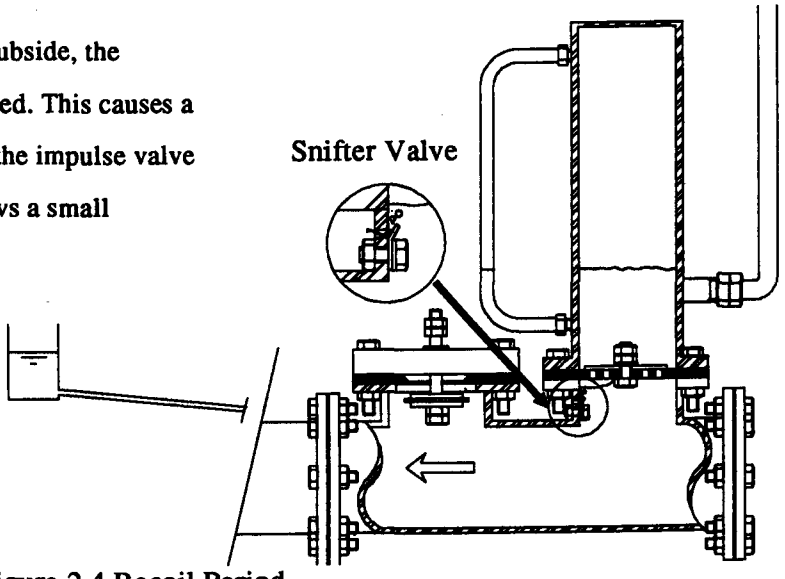

Figure 2.4 Recoil Period

2.2 The Acceleration Period

During this cycle, water accelerates from a source or collection tank, through a length of pipe known as the drive pipe (see Figure 2.1). This pipe allows the water to fall through a small distance, accelerating under the force of gravity, and is allowed to discharge at a lower level through a valve known as the impulse valve.

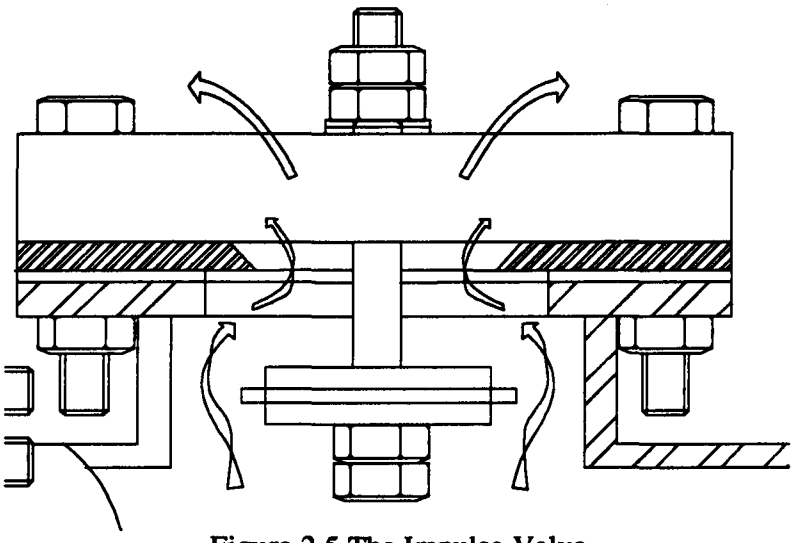

Figure 2.5 The Impulse Valve

The impulse valve is a simple valve (see Figure 2.5) that is closed by the drag force induced by a high through flow. The geometry of the valve is such that these drag forces increase rapidly as the valve moves towards its closed position, so inducing a rapid "snap" closure. See Figure 2.2.

2.3 Delivery Period

The sudden closure of the impulse valve induces a pressure rise in the drive pipe that is proportional to the velocity of the fluid in the pipe immediately before the valve closure. This pressure is maintained while pressure waves propagate along the drive pipe.

During this period in which the drive pipe sustains a high pressure, a small discharge occurs through a non-return valve (delivery valve) into a vessel containing air at a pressure approximating to the delivery pressure of the pump. This discharge continues until such time as the pressure in the drive pipe subsides, at which stage, the non-return valve closes, and the discharge ceases. See Figure 2.3.

2.4 Recoil Period

A small remaining velocity in the drive pipe fluid induces a recoil, which in turn induces a pressure drop at the impulse valve, so allowing it to reopen, and the cyclic operation to recur.

A small air inlet valve (snifter valve) allows a small quantity of air into the drive pipe during low pressure periods. This is forced through the delivery valve and into the air vessel on the delivery cycle. This air replaces air that is lost into solution in the air vessel.

The device operates with a cyclic operation of typically 1Hz. The three described phases are summarised in illustration by figures 2.2, 2.3 and 2.4.

2.5 Detail Function of the Hydraulic Ram Pump

The detailed operation of a hydraulic ram pump as described in the following sections has been determined as a result of a long term study of hydraulic ram pumps involving extensive experimental measurement, computer modelling and simulation.

2.6 Acceleration Period in Detail

The acceleration cycle commences with the opening of the impulse valve. This will usually open under the force of gravity, but is often assisted by the recoil of the previous pumping cycle. The fluid is either stationary, or travelling up the drive pipe towards the feed tank following a velocity recoil in the drive pipe at the end of the previous cycle (this recoil is covered in the following sections).

The fluid in the drive pipe then accelerates under gravity towards the impulse valve. If it is initially in recoil, it decelerates under the differential pressure along the length of the drive pipe imposed by the water level in the drive tank, and this deceleration is increased by friction effects. The equation given in Figure 2.6 gives the deceleration force on the column of fluid in the drive pipe at any instant in time. It should be noted, that this equation assumes the fluid to be a rigid column, and as the wave propagation time is very short compared with the deceleration period, this gives an acceptable approximation for most purposes.

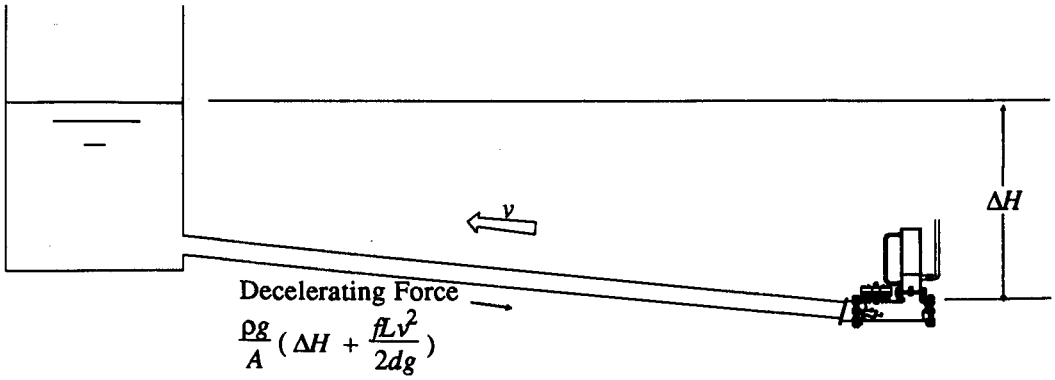

Figure 2.6 The Beginning of the Cycle

Once the fluid is flowing towards the impulse valve, and discharging from it, it accelerates under the action of gravity. This acceleration is reduced by frictional effects.

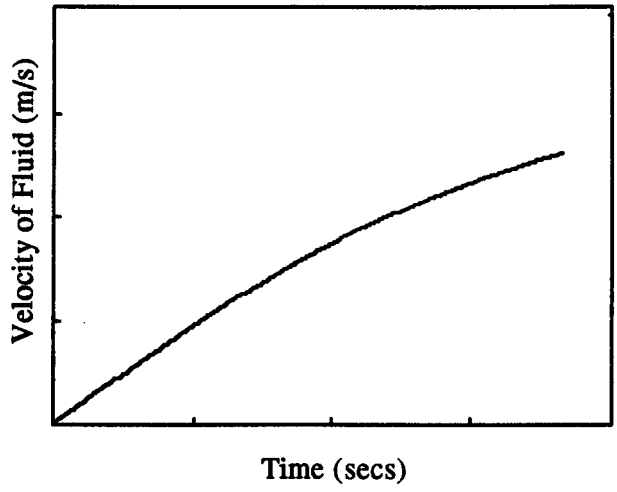

Figure 2.8 Velocity History for Acceleration Period

The described acceleration may not be linear because of residual transients propagating in the drive pipe from the previous pumping cycle as well as changing friction effects. Figure 2.8 illustrates the shape of the velocity history that results from a typical acceleration phase.

2.7 Valve Closure Period in Detail

The impulse valve disc experiences a drag force as a result of the fluid flowing past it. This drag force is approximately proportional to the square of the velocity of the fluid flow, and

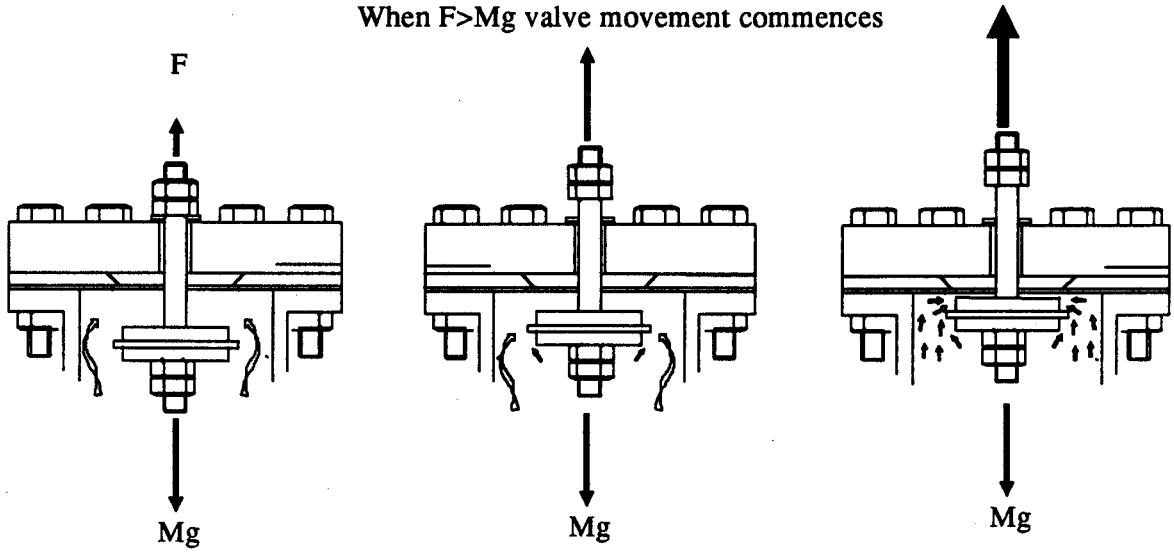

Figure 2.7 Impulse Valve Closure

proportional to a coefficient of drag for the valve. Once the flow in the drive pipe reaches a level at which the drag force on the valve exceeds the force keeping it open (typically its weight), the impulse valve accelerates towards its closed position.

As the impulse valve disc starts to move, the coefficient of drag increases as the distance between the valve disc and its seat reduces. Similarly the head loss coefficient across the valve will also increase. This increase in head loss coefficient will act to reduce the acceleration of the flow. The increase in the coefficient of drag will act to increase the acceleration of the impulse valve towards its position of closure.

The valves coefficient of drag increases exponentially as the valve face moves towards the valve seat (this is a characteristic of the type of valve, but is common to the majority of hydraulic ram pumps). This causes an exponentially increasing acceleration on the valve, which in turn leads to a very rapid closure. This valve acceleration is reduced by drag forces restraining the movement of the valve through the fluid in the final stages of closure when the valve velocity exceeds that of the fluid.

The increasing head loss coefficient is significant with respect to the length of the drive pipe, and the acceleration of the fluid. If the drive pipe is relatively short, or the fluid acceleration relatively low, it is possible that the increasing head loss will reduce the velocity of the fluid to such an extent that the drag force on the valve is no longer sufficient to maintain the closure. In this situation, the impulse valve will "bob" up and down, but not reach its seat.

Once the impulse valve reaches its seat, the fluid immediately upstream is brought to a halt. This induces a pressure rise immediately upstream of the valve which helps to make a seal with the valve disc.

2.8 Delivery Period in Detail

The velocity drop and pressure rise propagate upstream in the opposite direction to the direction of flow. A high pressure wave is also communicated from the three way junction towards the air vessel. The high pressure wave front will generally reach the delivery valve well before it reaches the feed tank. The pressure rise experienced is related to the initial velocity by the equation:

$$\Delta H = \frac{aV_0}{g} \qquad \text{- (2.1)}$$

where: ΔH = the rise in pressure head (m); a = the velocity of sound in the drive pipe (m/s); g = the acceleration due to gravity (m/s^{-2}); V_0 = the velocity of the fluid before closure(m/s).

This is generally referred to as the Joukowsky[4] (1904) pressure head. When this pressure rise reaches the delivery valve, the valve is forced open and fluid is free to flow into the air vessel. The pressure in the air vessel at this stage is at the delivery head. This flow causes an instantaneous drop in pressure in the main body of the pump. A high frequency pressure oscillation is induced between the impulse valve and the air vessel water surface on account of the compressibility of the fluid in the body of the ram.

The opening of the delivery valve causes a new pressure to be sustained. This new pressure is slightly higher than the pressure in the air vessel on account of the head losses occuring through the delivery valve. The first pressure wave to propagate up the length of the drive pipe causes a large pressure rise, and brings the velocity in the drive pipe to a halt. The opening of the delivery valve causes a second pressure wave to travel up the drive pipe. This wave front will induce a velocity increase in the drive pipe to allow the delivery flow to continue, and an associated drop in pressure that is proportional to the increase in velocity.

When the wave front meets the feed tank, the pressure rise is no longer maintained, as there is no inertial change experienced at the reservoir. This effectively transfers a constant head to the drive pipe. The effect is a wave reflection. The high pressure in the drive pipe is relieved by this pressure wave reflection, and as this wave form propagates back down the drive pipe, it induces a "bounce back" velocity drop. As this pressure wave travels towards the delivery

The impulse valve closes, and the resulting high pressure propagates upstream, and towards the delivery valve. The fluid in the drive pipe is brought instantaneously to rest.

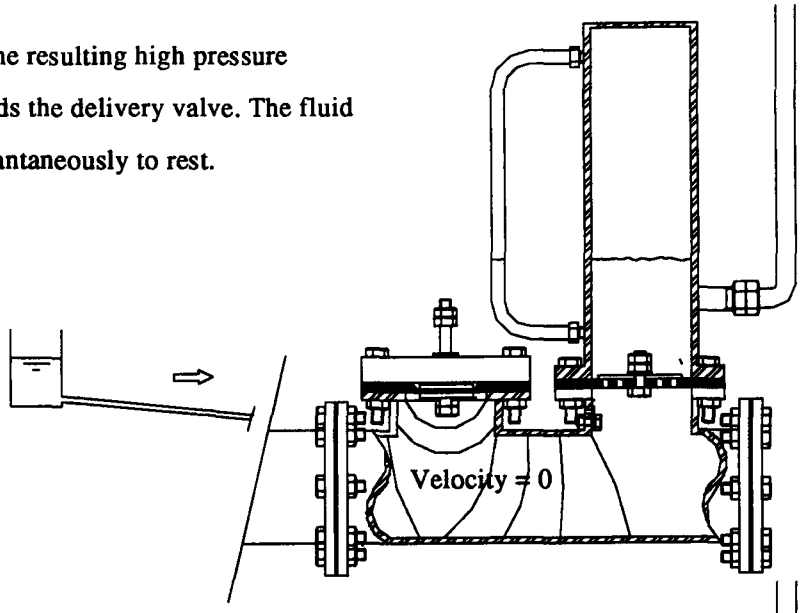

The high pressure in the drive pipe forces the delivery valve to open. This causes a flow in the drive pipe, which propagates along the drive pipe with an associated pressure drop.

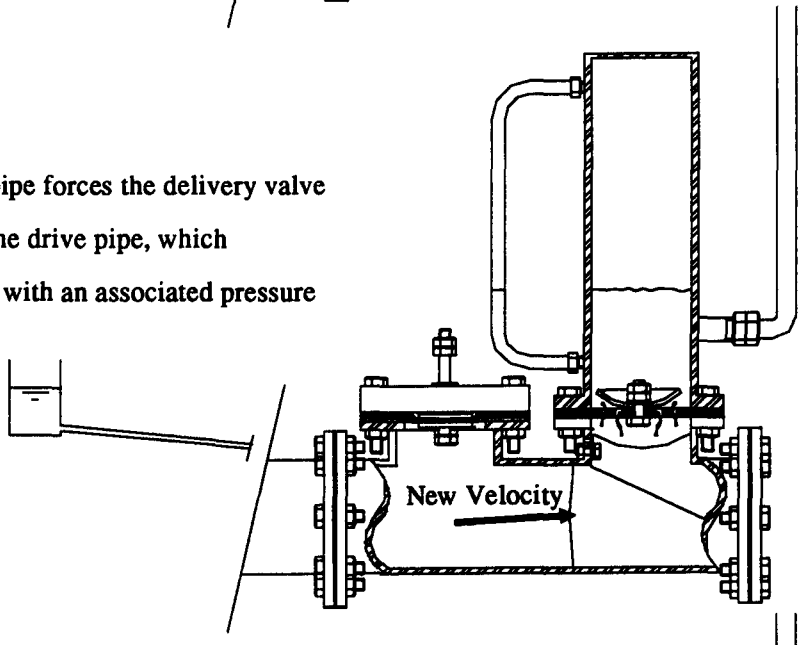

Once all the flow in the drive pipe reaches this new value, a small recoil in velocity proportional to the effective step down in velocity commences at the drive tank. On reaching the impulse valve the associated pressure drop causes the delivery valve to close. Remaining velocity will instigate a second delivery stage.

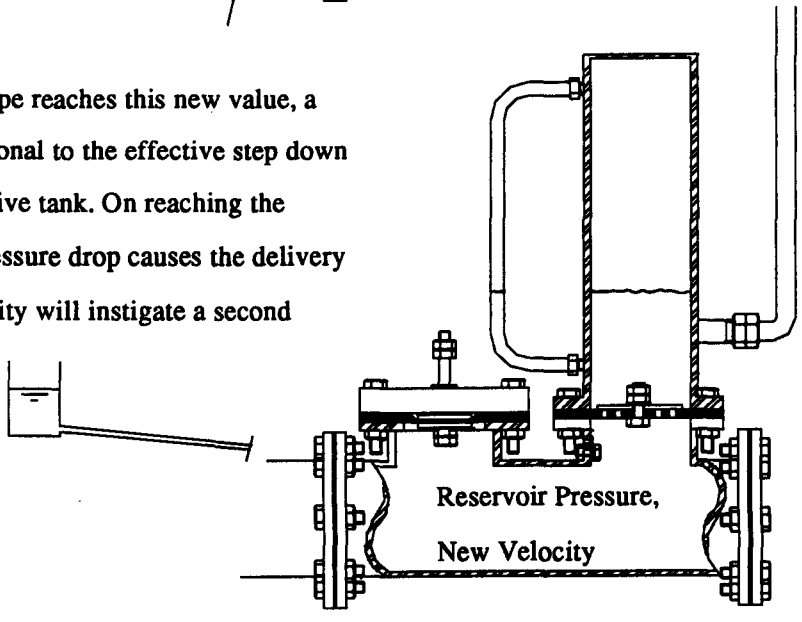

Figure 2.9 Delivery Cycle

valve, the magnitude of the relieving pressure becomes smaller because of the friction that exists in the drive pipe. The pressure that finally arrives at the delivery valve is equal to the static head supplied by the feed tank, less the friction losses at the new reduced velocity. (See Figure 2.9).

This new pressure is not sufficient to maintain the delivery pressure, and so the delivery valve moves towards its closed position. The nature of the delivery valve is such that there will be a degree of back flow, and this will vary with operating conditions, but will typically be equal to the swept volume of the valve. At this stage, the delivery period has undergone its first delivery cycle. There remains a new reduced steady state velocity in the drive pipe. This velocity effectively meets a closed valve as the delivery valve closes under the normalised pressures. A pressure rise is induced at the delivery valve that is proportional to the new velocity in the drive pipe. A new pressure wave then propagates down the drive pipe, incorporating a Joukowsky pressure rise, and an associated halting of the velocity in the pipe. This wave propagates up the drive pipe towards the feed tank, but is followed by another wave front of reduced pressure, and increased velocity associated with the

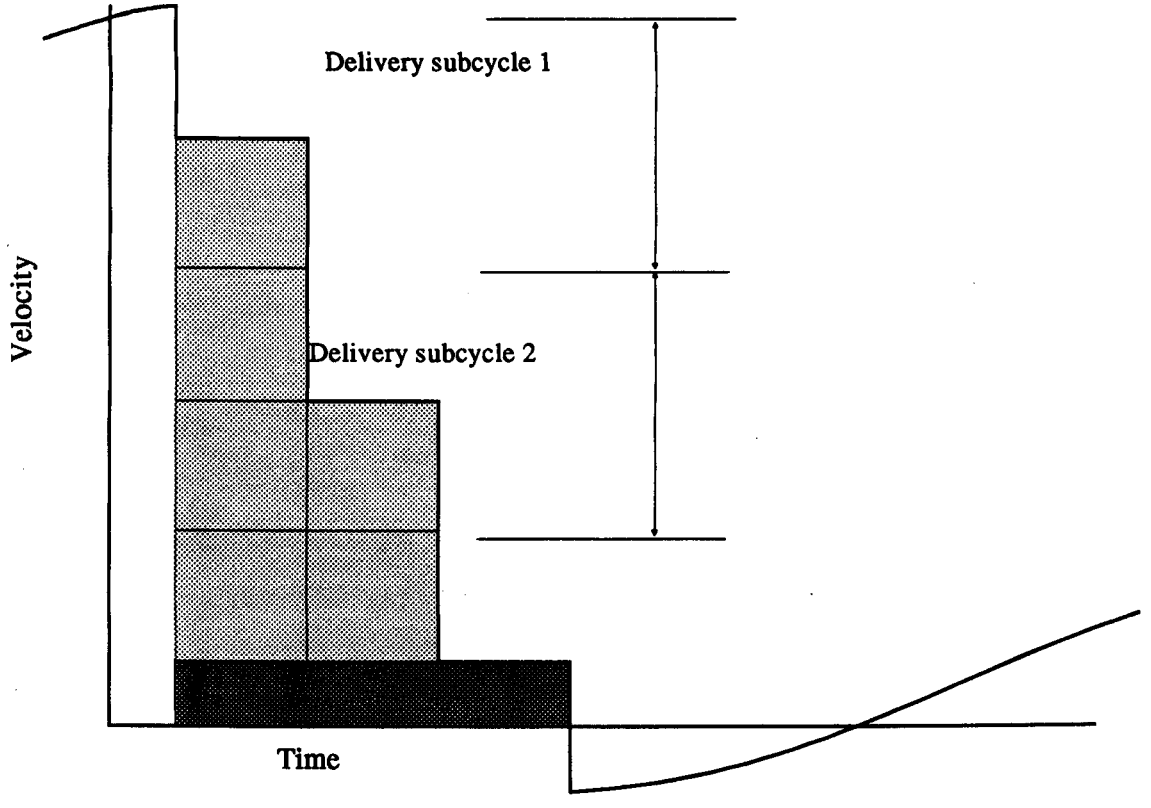

Figure 2.10 Drive Pipe Velocity History

reopening of the delivery valve.

A typical drive pipe velocity history for the delivery period is given in Figure 2.10. This illustrates the multiple delivery subcycles. The shaded area represents the volume of water delivered when multiplied by the drive pipe area.

2.9 Recoil Period in Detail

As before, these waves are reflected at the reservoir, in a normalising pressure wave which also induces a drop in velocity. When this arrives at the delivery valve, the delivery valve once again closes (or starts to), and the above cycle recurs. This process of velocity steps continues until such time as the velocity remaining in the drive pipe is such that the induced pressure is smaller than the delivery pressure. If this occurs, the whole of the drive pipe becomes pressurised at the new lower pressure and the pressure wave propagates up the drive pipe. On reaching the reservoir, there is again a reflection involving a reduction in velocity, and a normalisation of pressure. As the velocity reduction associated with the previous pressure wave travelling up the drive pipe reduced the fluid velocity to zero, this

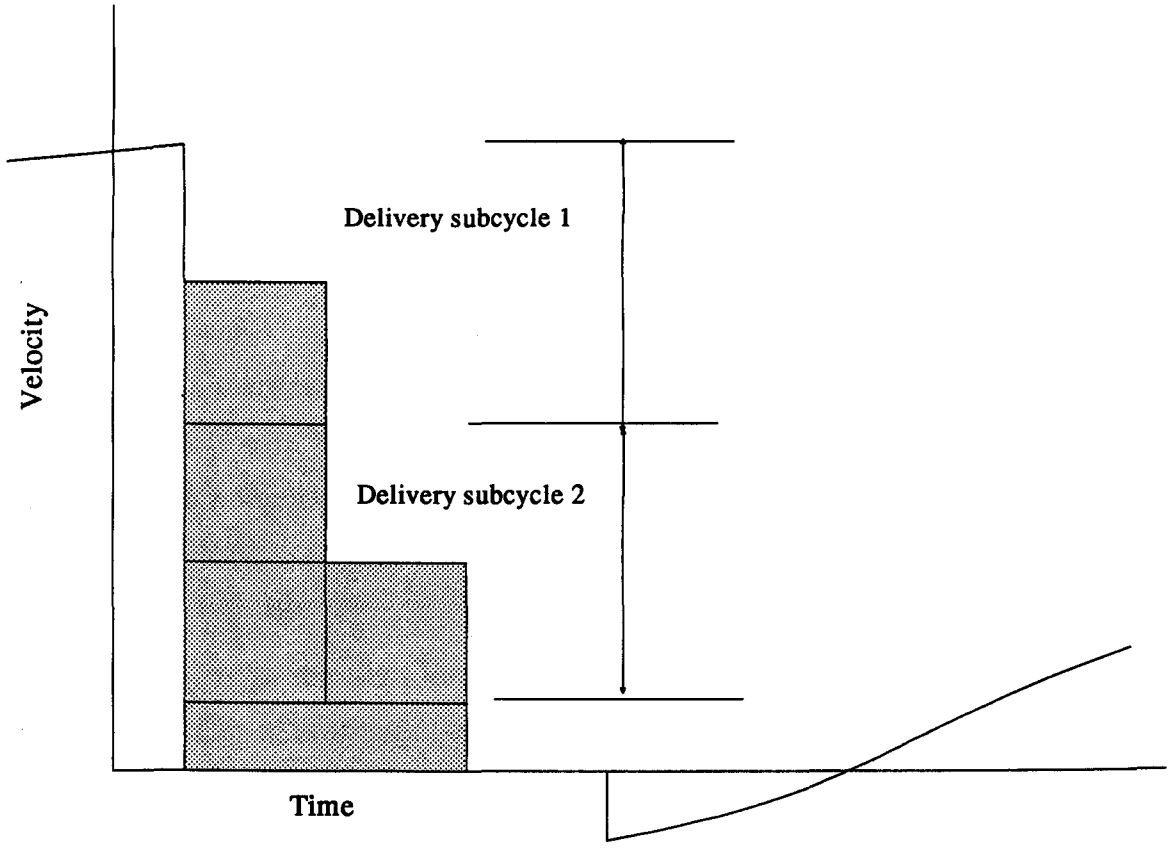

Figure 2.11 Drive Pipe Velocity History

pressure reduction induces a negative velocity known as the recoil. This propagates down the drive pipe towards the delivery valve. This represents an entire wave reflection in which no delivery occures.

When this negative velocity and pressure normalisation arrives at the delivery valve, the delivery valve closes. A negative pressure is then created at the delivery valve, the downward pressure transient being proportional to the magnitude of the recoil velocity. This low pressure allows a quantity of air to be induced through a snifter valve located at the delivery valve. This in turn acts to reduce the magnitude of the drop in pressure, and allows some of the recoil velocity to be sustained.

When this negative pressure is communicated to the delivery valve, the impulse valve will typically open under its own weight. If this negative pressure wave is of insufficient magnitude, the valve will fail to reopen. This represents a common reason for pump failure.

This negative velocity pressure wave then proceeds up the full length of the drive pipe. On reaching the feed reservoir, a reflected wave propagates down the drive pipe normalising the pressures to reservoir pressure. Small damped pressure oscillations then occur on account of friction effects. This marks the beginning of the next acceleration cycle.

The velocity history given in Figure 2.11 illustrates the recoil period as described above. This recoil can be seen to differ from that illustrated in Figure 2.10. In Figure 2.10, the velocity drop associated with a reflected pressure wave from the reservoir brings the drive pipe velocity negative which allows the delivery valve to close and the impulse valve to reopen as above. In this case, there is no residual forward velocity and no additional pressure rise, and the next cycle can begin immediately. This will marginally increase the frequency, and therefore the power ouput of the device.

2.10 The Snifter Valve

As mentioned in the above section, the snifter valve operates during the recoil period to allow a small quantity of air to be induced into the body of the hydraulic ram pump. This will rest as an air pocket just below the delivery valve. This air will then be transfered to the air vessel as soon as the delivery valve next opens. The effect of this is to sustain the volume of air in the air vessel, as air is continuously lost into solution under pressure.

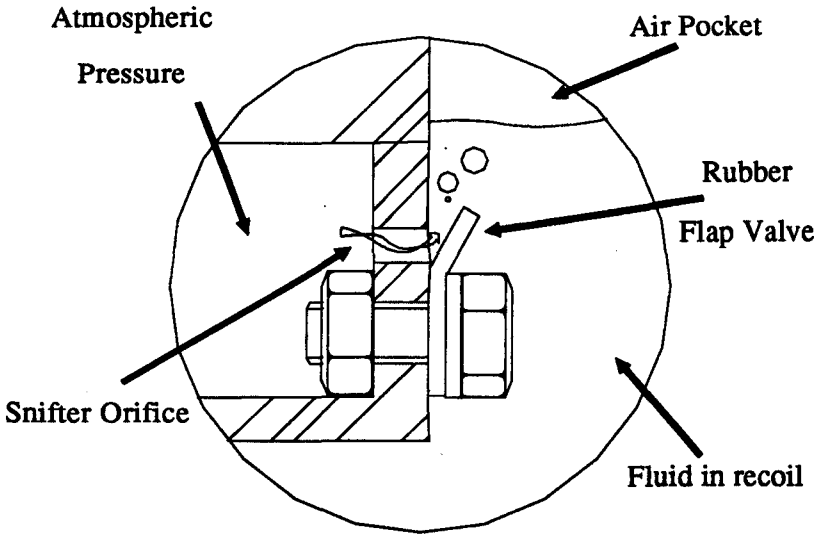

Figure 2.12 The Snifter Valve

There are a number of snifter valve designs used, and the most typical of these is illustrated in Figure 2.12 . It incorporates a simple flap seal over an air inlet orifice. The sizing of this orifice directly influences the volume of air induced on each cycle. It also effects the severity of the negative pressure associated with the recoil, and the magnitude of recoil velocity attained.

The orifice is sized empirically to ensure that the quantity of air induced is in excess of that lost into solution. This results in a continuous air discharge into the delivery pipe. This can cause problems downstream, so an air release valve is required immediately downstream of the air vessel.

2.11 The Significance of this Understanding on Pump Design.

2.11.1 Two modes of recoil effect pump performance.

The observation that there are two ways in which the hydraulic ram pump cycle finishes is helpful in interpreting sudden frequency shifts in operating pumps and unreliable behaviour at some delivery heads, and also provides important insight necessary to reliably predict ram pump performance.

2.11.2 Acceleration efficiency

The concept of acceleration efficiency in this thesis represents the amount of potential energy expended in attaining the kinetic energy present before closure of the impulse valve.

The acceleration efficiency in a hydraulic ram pump is closely dependent on the friction experienced in the drive pipe. Similarly, it is also dependent on the acceleration of the fluid in the drive pipe. This is because with a low acceleration that diminishes significantly with speed the acceleration period is greatly extended, while the resulting kinetic energy of the fluid in the pipe is the same for a given final velocity. The result is a significant quantity of wasted water, and therefore a reduction in pump efficiency and power.

2.11.3 Delivery Efficiency

The concept of delivery efficiency was also invented by the author, and represents the potential energy attained through the discharge of water to the delivery head as a proportion of the kinetic energy in the drive pipe at the beginning of the delivery cycle (closure of the impulse valve).

The efficiency of the delivery cycle has been found to be of some significance. A direct influence on this is the friction coefficient of the delivery valve. However, other very significant factors include the swept volume of the delivery valve, and the mode of delivery.

If a hydraulic ram pump incorporates a delivery valve which has a returning force applied to it, the head loss associated with delivery may be much increased, however, the loss of water as a result of back flow is also greatly reduced. This may compensate for the extra losses associated with delivery. The significance of this effect increases with higher delivery heads.

2.11.4 High Frequency Oscillations.

The high frequency oscillations visible in the pressure history given in Figure 2.13, can be seen to be oscillations between the impulse valve and the air vessel. If, for reasons of durability, it is necessary to alter the frequency or magnitude of the oscillations, this can be achieved by dimensional changes within the pump itself. A study of this is illustrated in chapter 4. A lower frequency oscillation is obtained by increasing the distance between the impulse valve and the air vessel. The magnitude of the oscillations are reduced by increasing the diameter of the pipework connecting the two. This study was the cause of major changes in the characteristic of the hydraulic ram pump designs adopted by the D.T.U.

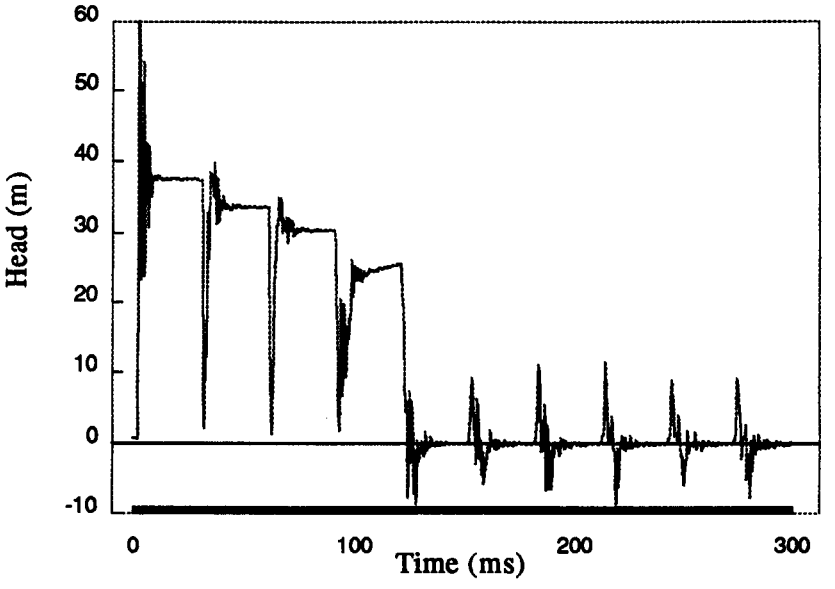

Figure 2.13 Simulated Pressure Transient in Ram Pump

2.11.5 Snifter Valve Sizing

The quantity of air induced into the drive pipe through the snifter valve is quite critical. Too large a quantity will result in failure of operation of the pump as air will travel up the drive pipe, and affect the behaviour of the propagating transients. A snifter valve orifice which is too small will result in insufficient air being induced into the air vessel to replenish that lost into the delivered water. The result of this will be an empty air vessel, which can potentially cause significant damage to the pump and delivery pipe work, and will certainly have a negative effect on performance.

It is evident from the explanation that the quantity of air induced into the drive pipe is also dependent on the magnitude of the recoil velocity that occurs in the drive pipe. The snifter valve should therefore be sized or adjusted accordingly.

2.11.6 Time for Valve Closure

From the description of the valve closure period, it is possible to perceive that the major factor effecting this is the acceleration of the fluid in the drive pipe. As this has a direct effect on the performance of the pump, it is important that the acceleration of the fluid column is of a suitably high magnitude when the impulse valve begins to close, to ensure rapid closure of the valve.

2.11.7 Impulse Valve Failure To Close

From the description of the delivery valve closure it is possible to understand the interaction between the impulse valve and the drive pipe during the closure. As the impulse valve begins to close, the head loss across the valve increases, and this will slow down the fluid in the drive pipe after a wave reflection time of 2L/a. A lower velocity will reduce the drag force on the valve causing it to close, however, the movement of the valve will have increased the force coefficient for the valve. The net effect is a trade off between an increasing drag coefficient and a decreasing flow. If the net effect is a force that is less than the weight of the valve, the valve will decelerate. Depending on the severity of the deceleration, and the velocity of the valve, the valve may never reach its seat, but only "bob" up and down.

The above illustrates a problem that is highly dependent on a particular valve's characteristics. The problem is exacerbated on installations in which the fluid acceleration is small. Minimum drive pipe lengths and fluid accelerations during the closure cycle should be quantifiable for a given impulse valve geometry and settings.

2.11.8 Drive Pipe Length

The drive pipe length greatly effects the nature of operation of a hydraulic ram pump. However, many of the factors that are greatly affected by drive pipe length are cancelling. For example, a long drive pipe will have a relatively long and inefficient acceleration period, but will require fewer ram cycles for a given delivery volume. So increased losses associated with inefficient acceleration are cancelled by reduced losses associated with each valve closure. For this reason, within a design operating range, the overall performance is largely unaffected by drive pipe length.

An enhanced understanding of the operation of the hydraulic ram pump enables this operating range to be more usefully specified.

The acceleration cycle is greatly affected by the length of the drive pipe. The longer the drive pipe, the more mass that exists to be accelerated by the drive head, and so the slower the acceleration. Similarly the longer the drive pipe, the more friction that exists on the column of accelerating water, and therefore the more energy that is lost during the acceleration cycle.

The valve closure period is affected by the length of the drive pipe. This affects pump performance as a short valve closure period will generally be more efficient. The interaction between the two is discussed in the above explanation, and more detail is given in Chapter 4 which refers to a study undertaken by the author on this effect using the method of characteristics simulation.

The delivery cycle is also significantly affected by the length of the drive pipe. The longer the drive pipe, the longer each of the delivery phases, as each delivery phase lasts a full wave reflection period. A longer delivery phase will deliver proportionately more water.

The recoil period is also directly affected by the length of drive pipe. A recoil on a long drive pipe will involve more kinetic energy, and will therefore take longer to slow down. This will reduce the pump beat frequency, and so reduce the output power of the device.

2.12 Summary

This chapter has given a detailed description of the operation of the hydraulic ram pump, and the interaction of the parameters affecting its performance. Chapter 3 gives a summary of other analyses undertaken on the hydraulic ram pump, while Chapters 4 and 5 illustrate the methods employed to obtain and use the described understanding of hydraulic ram pump operation.

Chapter 3: History of the Hydraulic Ram Pump and Analyses.

The hydraulic ram in its earliest form was invented by John Whithurst of Derby [5] 1772. The device he created bears little resemblance to the devices of today, and was discovered by chance. He found that a length of pipe that discharged from a reservoir to a low level valve was prone to failure adjacent to the valve. To solve the problem, a small air vessel was connected to the system. This was connected through a one way valve, and a delivery pipework was connected to it. To the surprise of many, water was delivered in this pipe to a level higher than the original source. Unfortunately a continuous delivery was only possible if an individual was deployed to continuously open and close the discharge valve.

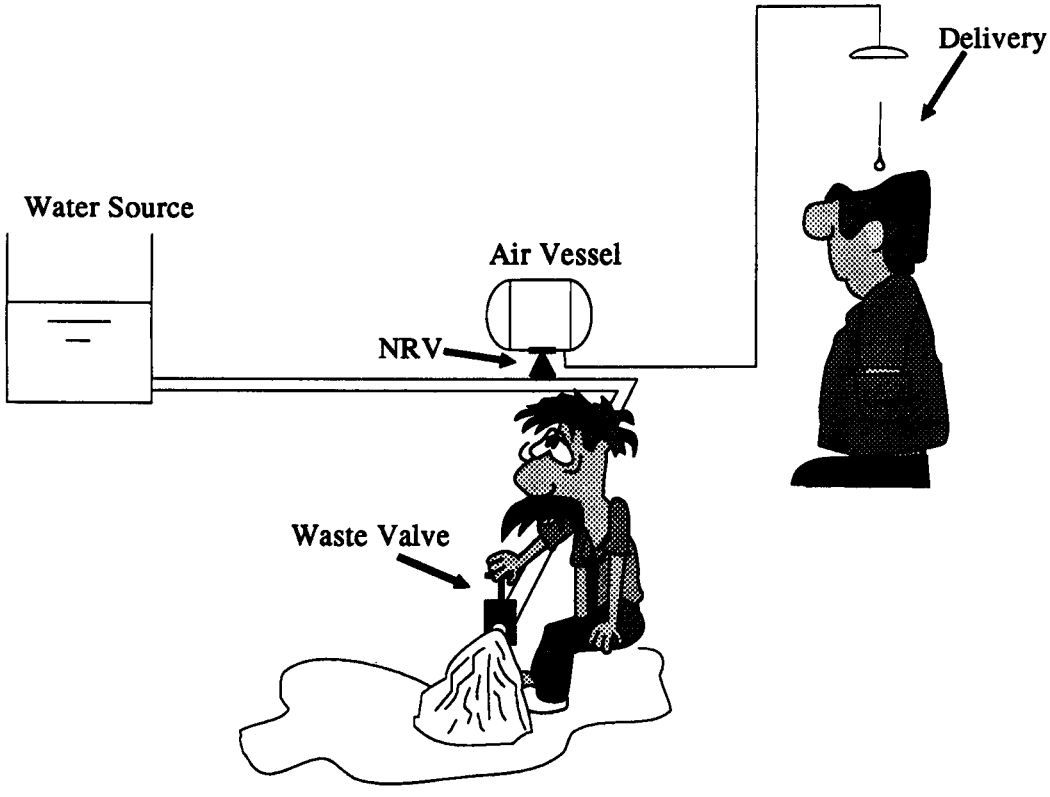

Figure 3.1 The Hydraulic Ram Pump after John Whithurst

The inventor of the automatic hydraulic ram was the French engineer Montgolfier [6]1775. Although more highly famed for his invention of the hot air balloon, Montgolfier's design of the hydraulic ram pump fundamentally transformed the device by allowing it to be operated automatically. Montgolfier produced an impulse valve that closed rapidly under the effect of drag forces, and reopened as a result of recoil.

A wide variety of hydraulic ram pump devices followed, and hydraulic rams were very widely deployed, and a large quantity of literature produced before the turn of the century. Manufacturers also produced dual flow ram pumps capable of pumping clean potable water using the energy available in falling waste water. Even air compressors were produced that compressed air by the same operation as a conventional hydraulic ram pump.

3.1 Experimental Research

In the early days of hydraulic ram pumps, extensive experimental work was undertaken on the device. Documented works include: Eytelwein[7]1805, d'Aubuisson[8]1840, Morin[9]1863, Tresca[10]1864, Carpenter[11]1894, Richards[12]1898, Church[13]1899, Clark[14]1900, Anderson[15]1922 and Clavert[16]1957.

These analyses were invariably based on a single experimental facility and often resulted in the drawing of sweeping conclusions on hydraulic ram pump design and operation. A helpful summary of these is offered by Rennie and Bunt [17]1981. Some of these conclusions were of significant value in design, but with the lack of theoretical analyses, the conclusions were often adopted completely regardless of their validity.

3.2 Theoretical Analyses

A number of theoretical analyses of the hydraulic ram pump developed alongside the above research. Significant works were provided by Montgolfier[6], Venturoli[18]1818, Navier[19]1839, Weissbach[20]1897, Rankine[21]1872, Mirapeix[22]1907, Lorenz[23]1910, and Bergeron[24]1932. None of the above were based on empirical data, and all involved some erroneous assumptions. A summary of these is also available in the work by Rennie and Bunt[17].

The above analyses differed in the sophistication with the pumping cycle being subdivided to varying degrees, from two divisions in the theory proposed by Navier to typically four divisions adopted by the majority to represent a range of different theoretical periods. Although the above theories offered a wider perspective than the purely empirical studies, errors in assumptions and the crudeness of the analyses severely hampered their usefulness.

An attempt to combine experimental data with theoretical analyses was first undertaken by Harza[25]1908. His work was also hampered by the inadequacy of his experimental facility

but he was able to confirm a correlation between experimental and theoretical behaviour during the acceleration period.

As measurement technologies became more sophisticated, the understanding of the transient behaviour in the hydraulic ram pump developed. In the 1930's O'Brien and Gosline[26] using the research undertaken by Harza[25], provided a theoretical and experimental investigation into hydraulic ram pumps which in retrospect was inspired. They provided a theoretical analysis of the transient behaviour in the drive pipe during the delivery cycle. The simulation work undertaken in this study largely verifies the analysis proposed. Unfortunately many subsequent analysis did not acknowledge or adopt the development attained, and later work by Krol[27]1947 provided a detailed analysis that was widely adopted, but failed to incorporate the work of O'Brien and Gosline.

A brief summary of the analytical results obtained by O'Brien and Gosline is given in the following section. Beyond this analysis, there were attempts to utilise the graphical method of transient analysis for which Schyder[28]1932 and Bergeron[24] are famed. The work of Krol has been adopted by a number of more recent studies.

3.3 Summary of more recent Analyses of the Hydraulic Ram Pump

3.3.1 O'Brien and Gosline[26]1933

A diagrammatic summary of O'Brien and Gosline's theoretical analysis of the hydraulic ram pump given in Figure 3.2 shows that the researchers were able to predict the characteristic behaviour identified by the simulation developed within this research. In this respect, their research is unique, and unfortunately largely unrecognised except within the work of Rennie and Bunt. The analysis offered for much of the hydraulic ram cycle was typical of such analyses, but their analysis of the delivery cycle was unique, and they were able to predict the intricacies of the delivery cycle that are modelled in detail in chapter 5 of this thesis.

O'Brien and Gosline avoid providing a prediction of overall efficiency on the grounds that such a calculation would be excessively complex. However, they do offer an expression for acceleration efficiency. This is a valuable concept, and is covered in the proposed design charts in Chapter 6. The reason given for this is that acceleration efficiency dominates in hydraulic ram pump overall performance. This assumption is valid under many operating

but is, however, fundamentally flawed, as other inefficiencies such as poor valve closure times can rapidly dominate.

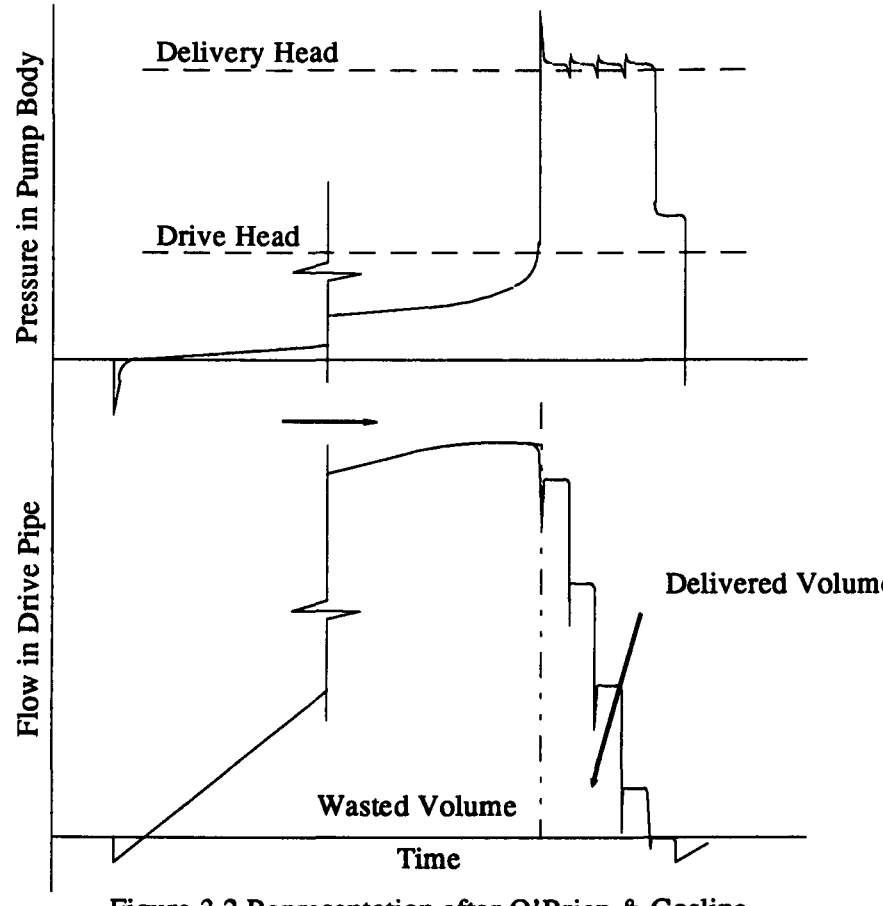

Figure 3.2 Representation after O'Brien & Gosline

3.3.2 Krol[27] 1947

A very detailed analysis was provided by Krol using calibrated data from a hydraulic ram pump. It is interesting to note Krol's use of friction and head loss coefficients to determine closure times and flows. It is also interesting to note the degree of success he attained with these. The major failings of his analysis were as a result of his denial of the transient wave propagation during the delivery cycle. His modelling of the impulse valve was valuable, but limited in that it assumed constant drag coefficients. It is possible to see from the calibrations undertaken in chapter 4 that this is clearly an unacceptable assumption.

3.3.3 Rennie and Bunt[17] 1981

Rennie and Bunt offered a further development by attempting to unite the successes of the work by Krol with that of O'Brien and Gosline. Their work involved the collation of extensive empirical data, and the production of a theoretical analysis. To further develop the work of

Krol, they adopted the graphical method[24] to solve the behaviour of the impulse valve during closure and the transient regime that followed. In spite of the difficulty involved with representing complex transients using the graphical method, useful results were obtained.

3.3.4 Yau-Chung Chiang[29] 1984 University of Wisconsin-Madison

This was an interesting study into simulation and optimisation of transient oscillation flow and sound in complex piping systems. The study utilised the hydraulic ram pump as a case study, and created a crude "method of characteristics" simulation of the device, and then proceeded to apply the optimisation routines to the device. The study suffered considerably as a result of the crudeness of the hydraulic ram model adopted. Further problems found were similar to those described in chapter 4, where the quantity of data and variables existing in a single simulation are so great that attempts at optimisation are severely hampered. Chiang attempted to overcome this by considering aspects of design in isolation. This was a valuable approach, but the results obtained suggested improvements in efficiencies to levels far below those currently attained.

An aspect of the work of particular interest was an attempt to find the optimal shape of a drive pipe of variable diameter. This is conceptually very exciting as the optimisation of the transient wave shape in a hydram may have major consequences with respect to performance. However, the optimisation algorithms used appear to have been unsurprisingly inadequate for a task of this complexity providing slightly obscure optimal shapes, and insignificant predicted efficiencies. This concept remains exciting, and may be adaptable to be incorporated within the simulation described in chapter 4 in the hope that using the sophisticated optimisation algorithms on a detailed and calibrated simulation may provide more useful results. The studies described in the following chapters illustrate the significance of the interaction between the shape of the transient wave front and the elements of the pump it interacts with. Unfortunately the work of Chiang was unable to determine this because of the crudeness of his boundary conditions. His interesting work does seem to be the first instance in which the "method of characteristics" was used to provide a simulation of the hydraulic ram pump for the purpose of analysis.

3.4 Summary

It is clear that there has been significant research into the hydraulic ram pump, and much of it highly replicatory. The reason for this is largely due to the massive complexity of interacting variables that are involved in an apparently very simple phenomenon. Poor results in much of the early work were a result of poor measurement technologies.

It is interesting to note that as the measurement technologies improved so did the theoretical analyses. The theoretical success of O'Brien and Gosline seemed to be closely related to their ability to measure transient pressures. The work of Krol some years later however, failed to achieve the insight offered by O'Brien and Gosline.

Rennie and Bunt where able to progress Krol's understanding with an improved understanding of hydraulic transients, although the methods used to analyse these are somewhat antiquated, and not without their inadequacies.

The present day availability of good computing facilities and measurement equipment makes it more possible to progress the understanding and theory of hydraulic ram pump operation. The work done by Chiang appears to have valuable vision in this respect, but fails in its total isolation from empirical analysis.

Chapter 4: Computer Simulation of the Hydraulic Ram Pump

4.1 Summary of simulation

An important tool in the analysis of the hydraulic ram pump was a computer simulation of the device. The development of the simulation was initiated during the author's MSc research. This simulation utilised the extensively documented "method of characteristics" to solve the partial differential equations of motion and continuity together with standard algorithms for the modelling of boundary conditions for the reservoir and air vessel present in a hydraulic ram. Some innovation was required with respect to modelling some of the more dynamic boundary elements.

4.2 The modelling of pressure transients in a pipe

A method of characteristics simulation enables an accurate modelling of pressure transients in a pipe. Although developed during the 1950's the method was popularised by Victor Streeter and Ben Wylie[30]1993 of the University of Michigan. The majority of modern transient simulation work currently undertaken utilises this explicit finite difference method known as the "method of characteristics". The equations used to determine transient flows and pressures in a pipe using a fixed time step are given in Appendix B.

Recent attempts have been made to employ finite element techniques for transient analysis, but these have involved severe limitations (Watt and Boldy[31]) . The decision to use a method of characteristics simulation was made for the following reasons:

- The finite element methods available are not readily suited to sharp wave front transients of the type induced in a hydraulic ram pump.
- The use of finite element techniques for complex pipe systems involves the production of some highly sophisticated shape functions which although quick to solve, do not allow minor modifications at a later stage.
- It was anticipated that drastic modification to both program structure and boundary conditions would be carried out in an evolutionary manner. Such modifications are well suited to a "method of characteristics" simulation as it allows modification to a section or boundary condition to take place, without

effecting the integrity of the rest of the simulation.

- The "method of characteristics" is used widely in the simulation of hydraulic transients in water pumping systems, and much research has been published on the most accurate means to represent various commonly occurring boundary conditions. Streeter and Wylie[30],Chaudry[32],Fox[33],Swaffield and Boldy[34],Thorley[35].

The "method of characteristics" requires a good estimate for the transient wave propagation velocity for each pipe section. To determine this, Joukowsky[4](1898) and Gibson[36](1908) developed a concept of a "Virtual Bulk Modulus of Elasticity" which also accounts for the pipe materials and dimensions. Joukowsky's calculation assumed a linear constraint on the pipe, and so has become the more widely adopted solution. This led to the following equation for pressure wave propagation velocity of:

$$a = \frac{1}{\sqrt{\rho \left[\frac{1}{K} + \frac{Dc_1}{tE}\right]}} \qquad (4.1)$$

where:

a = *propagation velocity (m/s)*

ρ = *the density of the fluid* (kg/m^3)

K = *the fluid's bulk modulus* (2.1×10^9 N/m^2 *for water at 20deg)*

D = *the pipe diameter(mm)*

t = *the pipe wall thickness(mm)*

E = *the Young's modulus for the pipe material* (N/m^2)

in which c_1 *may take one of the following values dependent on the means by which the pipe is restrained:*

For pipes restrained at one end only : $c_1 = 1 - \frac{\mu}{2}$

For pipes anchored throughout their length: $c_1 = 1 - \mu^2$

For pipes with expansion joints along their entire length: $c_1 = 1$

where μ =*Poissons Ratio for the given pipe material.*

Equation *(4.1)* has been used extensively in this study to predict the speed of pressure wave propagation. The wave speed propagation time was also monitored using sequentially placed pressure transducers which were sampled using a 500kHz analogue to digital converter. This system was used to verify the calculated pressure wave propagation speeds as well as experimentally monitor pressure transients in pipelines.

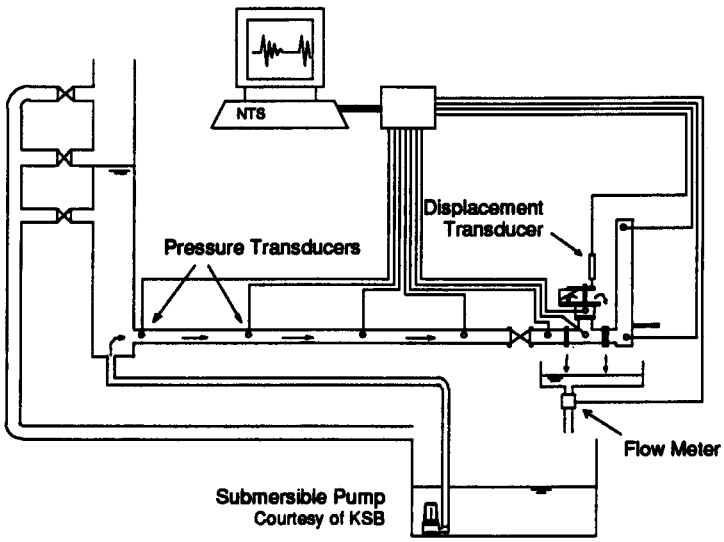

Figure 4.1 Experimental Rig

4.3 The Reservoir Boundary

The reservoir boundary condition used is a standard boundary condition used for transient simulation. The equation that describes the boundary condition for outflowing water is simply

$$H_x = Reservoir\ Level - \frac{V^2}{2g} \qquad (4.2)$$

where Hx is the pressure at the exit from the reservoir; V is the exit velocity, and g is the acceleration due to gravity.

The boundary condition is then solved simultaneously with the negative characteristic compatibility equation. The accuracy of this boundary condition was further improved by accounting for fitting losses at the discharge from the reservoir.

4.4 The three way junction

The schematic diagram of a hydraulic ram pump given in figure 4.2 has a central three way junction that links the various elements that make up the computer model of a hydraulic ram pump. To provide a simple model of the device, it was assumed that there were no headlosses experienced across the junction to allow a common pressure to be assumed for each of the branches. The solution used for the branch was obtained directly from the work of Streeter and Wylie (30).

$$H_p = \frac{\left(\frac{C_{p1}A_1}{a_1} + \frac{C_{m2}A_2}{a_2} + \frac{C_{m3}A_3}{a_3}\right)}{\sum\left(\frac{A}{a}\right)}, \qquad (4.3)$$

where:

H_p = *the calculated pressure at the junction boundary after a period* Δt

C_p, C_m = *determinable constants for each pipe at a given time (see definition in Appendix B).*

a = *the wave speed for each of the pipes connected by the junction*

A = *the area of each of the three pipes*

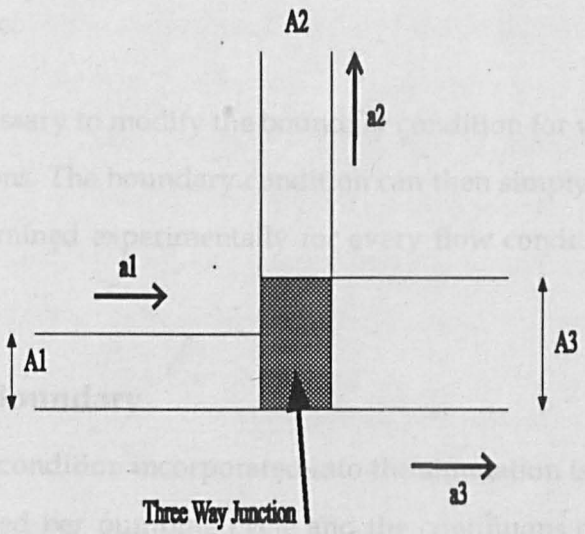

Figure 4.2 Three Way Junction

4.5 The Delivery Valve Boundary

The delivery valve boundary condition initially adopted was one of a simple two way junction with a facility for a diameter variation across the valve, and a mechanism to ensure that any backward flows calculated are forced to zero. This represents a highly crude modelling as it does not account for friction across the valve, or the swept volume of the delivery valve. No attempt was made to account for the swept volume of the valve until the model described in chapter 5 included a facility to account for its operation.

The losses experienced at the valve during discharge were, however, incorporated by experimentally determining a head loss coefficient. It was anticipated that the coefficient would be easily incorporated in the form $H_f = Cl\frac{v^2}{2g}$. However, it was found that the experimental results for some of the valves tested produced a rather more linear loss characteristic. The reason for this was believed to be on account of two parallel mechanisms of friction in the valve. In the first instance, there is a simple orifice mechanism associated with the fluid passing through the valve orifice(s). Beyond this there is a friction mechanism associated with the type of valve. The most common type of valve incorporates a rubber disc, which distorts to allow flow through in the delivery direction, and recovers its shape to seal the valve's orifices. The valve, therefore will distort to a greater degree for higher flows, so significantly reducing the friction coefficient. It is this part of the mechanism that explains the more linear characteristic.

For this reason, it is necessary to modify the boundary condition for various typesof delivery valve boundary conditions. The boundary condition can then simply adopt the steady state friction coefficient determined experimentally for every flow condition experienced under simulation.

4.6 The Air Vessel Boundary

The air vessel boundary condition incorporated into the simulation is used to determine the quantity of fluid delivered per pumping cycle and the continuous delivery flow rate. The quantity delivered per pumping cycle is dependent on the pressure in the air vessel which is

determined using the gas law given below:

$$H.V^{\gamma} = Constant \qquad (4.4)$$

where:

H = *Absolute pressure head (m)*

V = *Air volume present (m^3)*

γ = *Ratio of isobaric and isochoric specific heat capacities for air*

The continuous delivery flow rate is determined using a throttled valve head loss characteristic of the form:

$$Hf = K.Q^2 \qquad (4.5)$$

where:

Hf = *Head loss due to friction (m)*

Q = *The discharge flow(l/s)*

K = *Constant coefficient of friction*

A simple algorithm was set up to determine the flow into the air vessel for a given time step. This integrated flow represents a net incoming volume. If this is subtracted from the net out going volume calculated using the $K.Q^2$ relationship, the net change in volume in the air vessel can be determined.

This method was used in conjunction with the perfect gas law to determine what the resulting pressure change would be. It should be noted that if the process of air compression is reversible and adiabatic, the effective variations in pressure for a given fluid volume will be greater than if significant heat exchange occurs. This is accounted for in the gas law equation with $\gamma = 1.4$ for adiabatic, reversible compression and $\gamma = 1$ for isothermal compression. The general opinion within water supply is to assume an average of $\gamma = 1.2$ unless the operating conditions of the air vessel should suggest otherwise.

The air vessels associated with hydraulic ram pumps are generally small and of a simple geometry suggesting a low surface area to volume ratio. Intuitively this would suggest an adiabatic reversible tendency to be most likely if all losses are convectional. However, in view of the quantity of wet surfaces, and the likelihood of a cooling spray during delivery periods,

it seems reasonable to assume $\gamma = 1.2$ unless extensive experimental testing should prove otherwise.

4.7 The Impulse Valve Boundary

One of the most original aspects of the computer simulation was the way it included an experimentally calibrated boundary condition for the Impulse Valve.

In the early stages of simulation development, it was believed that a linearly varying dimensionless valve opening would provide an adequate approximation of the impulse valve's behaviour for the purposes of the simulation. This was incorporated into an early version using an estimated valve closure time. The form of the dimensionless valve opening used, given in equation (4.6) was obtained from the work of Streeter and Wylie(30). The value of the dimensionless parameter(τ) was reduced linearly from unity to zero in the valve closure time specified.

$$\tau = \frac{C_d A_g}{(C_d A_g)_0} \qquad (4.6)$$

where:

C_d = *The coefficient of drag on the valve.*

A_g = *The area of the open valve orifice(m^2)*

o = *Subscript to represent initial values.*

It became apparent from both qualitative assessment and empirical data that the above method did not adequately describe the behaviour of the valve. The short lengths of pipe existing in a hydraulic ram pump provide very short transient pressure wave travel times requiring the source of the transient to be accurately specified. The linear closure proposed provides only a marginal improvement on a simulation based on an instantaneous closure.

An example trace from a linearly variable differential transformer used as a displacement transducer for the valve is given in Figure 4.3. It can be seen that the valve travels with an increasing velocity, and acceleration. As the relationship between valve area (resistance) and valve position was not believed to be linear either, the linearly varying dimensionless valve opening boundary condition was abandoned. This was replaced by a two step linearly varying dimensionless valve opening, which seemed qualitatively to be an improvement but

still very limited.

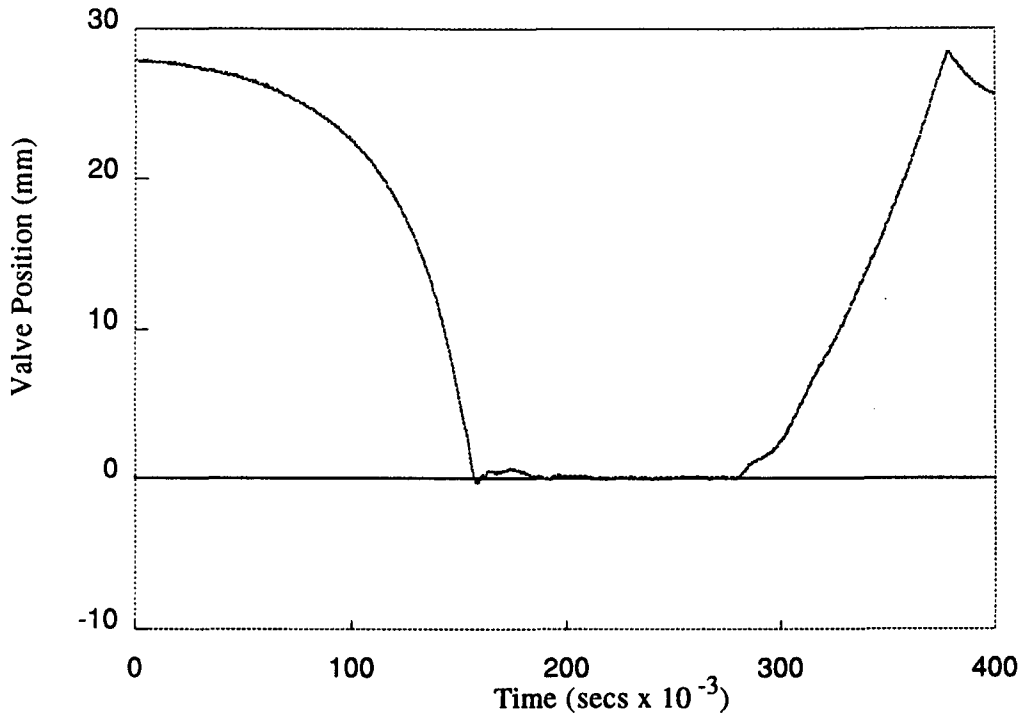

Figure 4.3 Position/Time History for Impulse Valve

This boundary condition provided a usable representation of the impulse valve for one pumping cycle, and accuracy could be improved using empirical data by increasing the number of linear steps in the simulated valve closure.

A major limitation of the boundary representation was that it only covered a single cycle. This meant that the calculated transient was based on initial conditions produced using steady state calculations carried out in the initial set up procedure. This situation was not ideal, as many hydraulic ram pump installations exist in which steady state conditions are not reached before the new pumping cycle occurs. In an attempt to simulate the cyclic action of the valve, and so allow for this difficulty, the dimensionless valve opening was returned to unity as soon as negative pressures were calculated immediately upstream of the valve. It was hoped that the third or fourth simulated pumping cycle could then be taken as typical for a given pump configuration, accounting for the superposition of transients initiated by the previous valve closure. This modification represented a major step forward in the production of a simulation, and output graphs began to take on the appearance of pressure transducer traces obtained from various hydraulic ram pumps. However, there remained some

significant restrictions which severely limited the value of the simulation as a design tool. For a simulation to be readily beneficial as a design tool, input parameters should be easily measurable, and should be related as closely as possible to the parameters that are altered in the setting up and tuning of a pump. The described boundary condition failed in this respect as input parameters such as valve closure time and flow at which closure commences, were required. The simulation provided a useful general solution for the impulse valve boundary condition, but to overcome its limitations, a completely new approach was necessary. It was decided that if useful accuracy was to be expected from the simulation, the valve boundary condition would have to represent a calibrated valve. This would appear to limit the usefulness of the simulation to identifying optimum hydraulic ram pump configurations for a given valve.

4.7.1 Experimental Procedure

The equipment and services of the D.T.U. were employed under the direction of the author, for the acquisition of valve calibration data since such experimental work was deemed to be mutually beneficial. The author was actively involved in supervising the D.T.U. work and recording results.

The D.T.U. have been developing a series of simple valves for use on hydraulic ram pumps. It was decided that the first valve to be calibrated should be a simple linearly moving valve. If the technique of calibration was found to be successful, the method of calibration could then be adapted for more complex valve systems.

A hydraulic ram pump was set up to receive flow directly from a centrifugal pump. Pressure tappings were installed directly below the valve, and flow was monitored using a Rotameter flow meter. The force on the valve was measured by employing a system of calibrated masses and a spring balance.

The impulse valve was fixed in a partially open state. One set of readings were taken for each position in which the impulse valve was restrained, and these positions were linearly incremented between full stroke and closed positions. Each record contained the measured

Impulse Valve Headloss Calibration Data.

Each graph gives the recorded data and a curve fit for a given valve displacement.

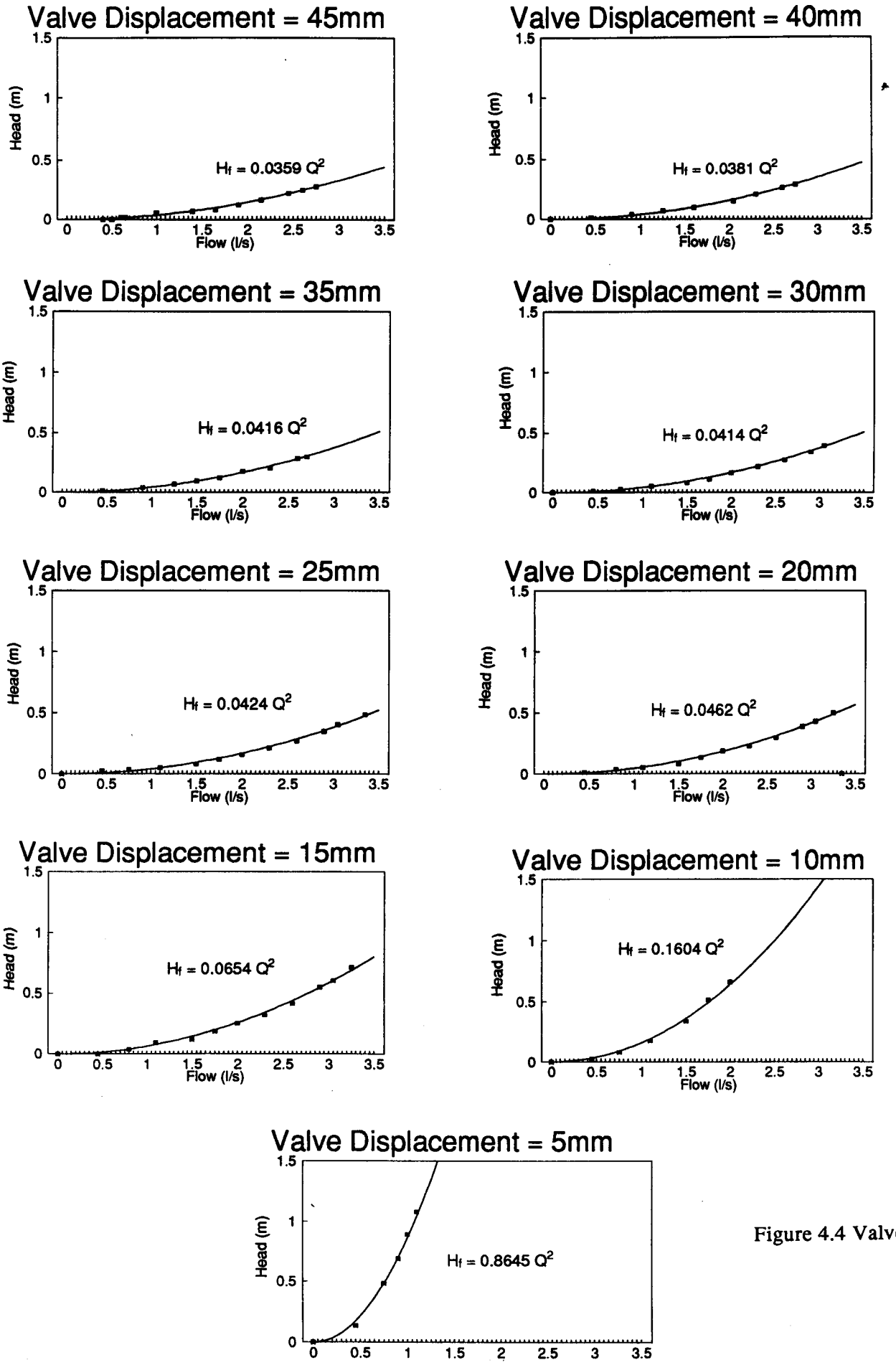

Figure 4.4 Valve Calibration

head loss across the valve and the force on the valve for a wide range of steady state flows. The graphs in Figure 4.4 give the measured results in graphical form alongside curve fits that were obtained using Nelder-Mead simplex algorithm[38] for minimising a non-linear function of several variables. The ordinate for each graph is "Head loss across valve (m)". Similar graphs were produced illustrating the variation of force on the valve with flow, for the various valve positions.

4.7.2 Curve fitting

The Nelder-Mead simplex algorithm was employed to minimise an error function. The error function described algebraically the sum of the errors that existed between an anticipated curve fit that was described algebraically, and the data points obtained from experimental work. The values of the function's parameters that forced it to a minimum were then incorporated into the initial anticipated function to obtain the curve fit. For the head loss characteristic it was assumed that the curve would be of the form:

$$H_f = K_h Q^2 \qquad (4.7)$$

where:

H_f = the head loss across the valve (m)

K_h = the valve's head loss coefficient

Q = the flow through the valve (l/s)

However, as a precautionary measure an attempt was also made to fit the data to a function of the form $H_f = K_h Q^n$, in case the valve's characteristic varied significantly from a simple parabola. The error function to be minimised for the parabolic and alternative function are given respectively as:

$$F = S(h - K_h Q^2)^2 \qquad (4.8)$$

$$F = S(h - K_h Q^n)^2 \qquad (4.9)$$

where S is a function and:

K_h = is the frictional coefficient to be determined.

h = is the measured head loss (m) for a given measured flow rate Q(l/s)

n and Kh are the output variables to be determined.

The algorithm was run for all the recorded data with both error functions, and it was found that the deviation from a parabolic fit was generally insignificant with respect to experimental error. However with the data obtained at a valve displacement of 10mm an acceptable fit was obtained with a cubic function, which failed to tally with any of the other data. It was suspected that the last reading taken may have been spurious; and with this removed from the input data, an adequate parabolic fit was obtained. The same procedure was carried out for the calibration of the valve with respect to the force experienced under steady state flow conditions with the assumed fit again being of the form:

$$F = K_f Q^2 \qquad (4.9)$$

where:

K_f= *Valve force coefficient to be determined*

F= *Force on the valve (kgf)*

Table 4.1 gives the values of the head loss coefficient (Kh) and force coefficient (Kf) obtained with the Nelder-Mead algorithm for each of the recorded valve positions. Figure 4.7 shows some of the curve fits for the headloss data given in Figure 4.6, demonstrating the variation with valve position.

Valve Position (mm)	Kh	Kf
40	0.0381	-
35	0.0416	-
30	0.0414	-
25	0.0424	0.424
20	0.0462	0.43
15	0.0654	0.736
10	0.1604	2.612
5	0.8845	20.13

Table 4.1 Determined head loss and force coefficients

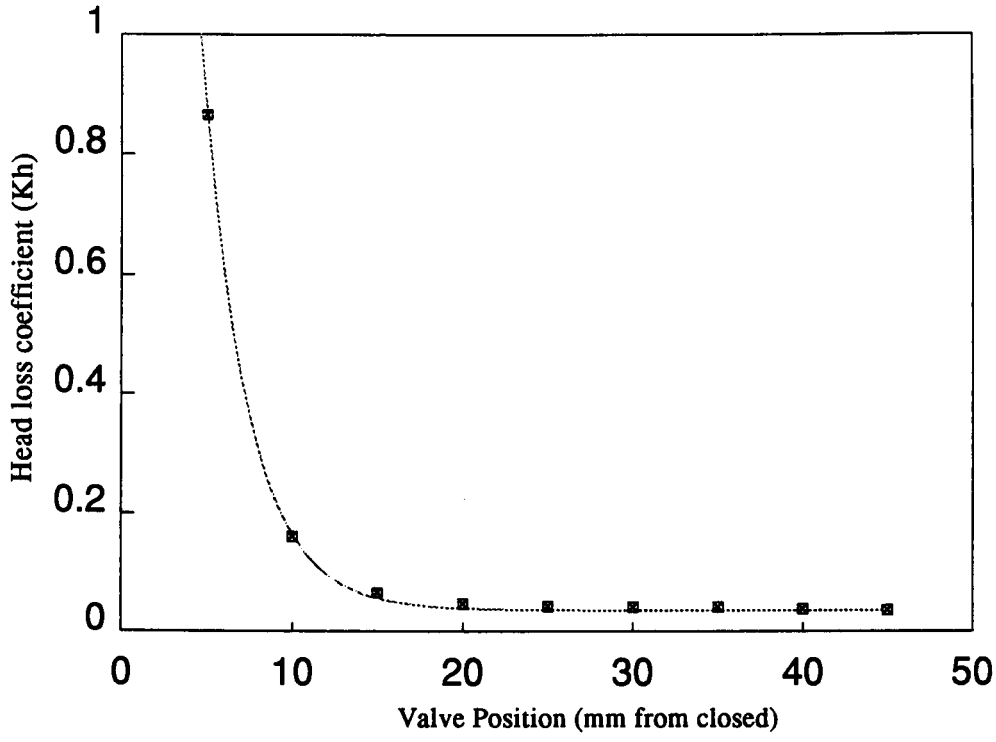

Figure 4.5 Variation of head loss coefficient

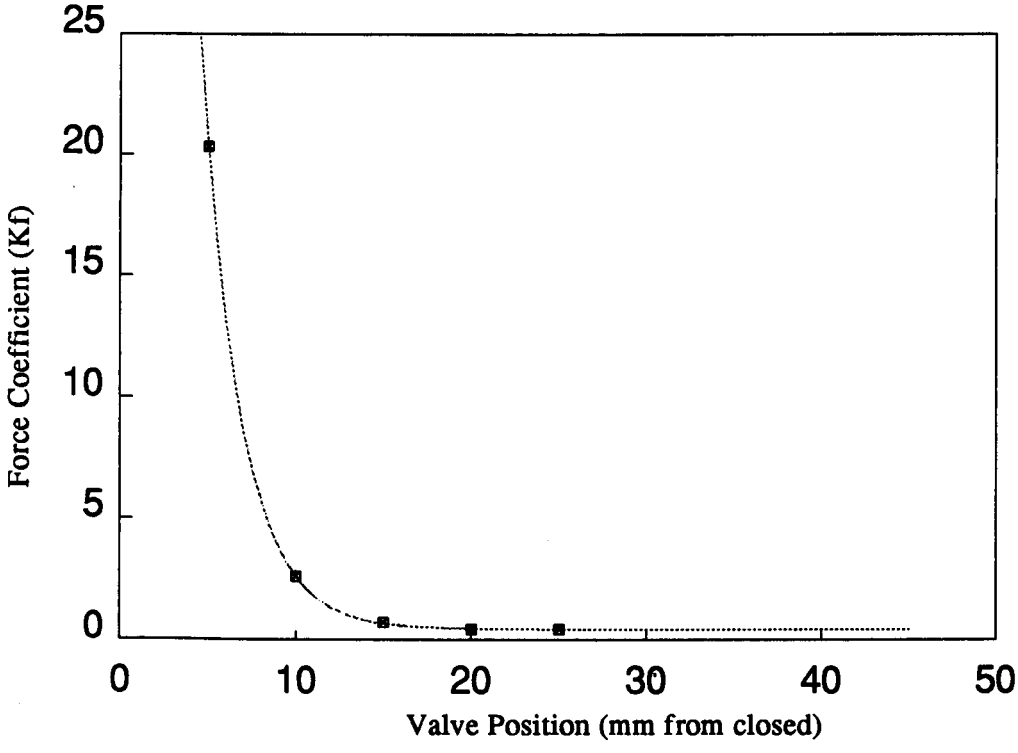

Figure4.6 Variation of force coefficient with position

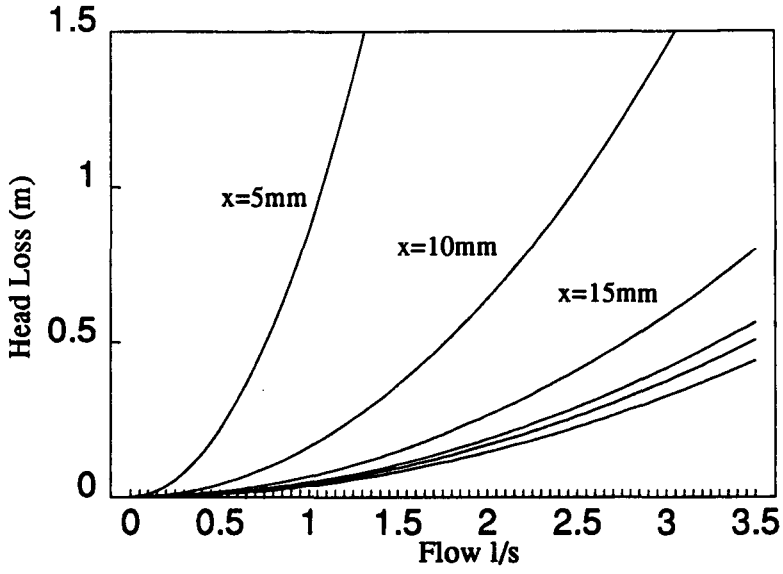

Figure 4.7 Head loss characteristic curve fits

The coefficients in Table 4.1 appear to vary exponentially (Figures 4.5 and 4.6) with respect to the valve position, and for this reason an exponential form was chosen for use with the Nelder-Mead simplex curve fitting technique.

An equation was chosen of the form:

$$K(f\,or\,h) = Ae^{-Bx} + C \qquad (4.10)$$

where A,B and C represent constants relating to the curve fit and x is the valve displacement. Figures 4.5 and 4.6 graph the variation of the head loss and force coefficients with displacement. The graphs show the values and the curves fitted to the form given above.

4.7.3 The Production of a Valve Boundary Algorithm

The basic results of the calibration work above are in the form of two equations which can be used to fully describe the behaviour of the valve for all positive flow situations. These equations are:

$$K_f = 180e^{-0.4407x} + 0.43 \qquad (4.11)$$

$$K_h = 5.338e^{-3.726x} + 0.0355 \qquad (4.12)$$

where K_h and K_f are the Head loss and Force coefficients respectively and x is the valve displacement.

The behaviour of the valve under negative flow situations was assumed to be dominated by gravitational acceleration once the valve was open, and reopening was determined by monitoring the instantaneous pressure simulated for the valve face. No allowance was made for fluid churning, or the drag caused by induced air. If this proves inaccurate more sophisticated test facilities and experimental procedures will be necessary to create an algorithm to account for these. This work is not included in the scope of this thesis and the need for it will be determined during the extensive application of the simulation to design problems. Using the equations above along with basic physical laws the author created a basic set of algorithms to describe the characteristics of the valve. The boundary condition operates by initially calculating the valve displacement and velocity based on values of valve displacement velocity and acceleration calculated for the previous time step or in the initial setup. This is done using the fundamental equations of motion given below:

$$X = X_0 + V_0 \Delta T + \frac{\alpha \Delta T^2}{2} \qquad (4.13)$$

$$V = V_0 + \alpha \Delta T \qquad (4.14)$$

Where

X & X_o = *the present and previous valve displacements,*

V & V_o = *the present and previous valve velocities,*

α = *the valve acceleration*

ΔT = *the time increment used.*

Once these values have been determined, the force on the valve and the head loss across the valve can be calculated using the equations (4.13) and (4.14). Once the force on the valve is known the acceleration can be determined for the next time step calculation. The new head loss characteristics can be used to describe the instantaneous hydraulic character of the valve, which is used in conjunction with the C^+ characteristic to solve the boundary condition for the given time period. Using the equations above along with basic physical laws the author created a basic set of algorithms to describe the characteristics of the valve. The boundary condition operates by initially calculating the valve displacement and velocity based on values of valve displacement velocity and acceleration calculated for the previous time step or in the initial setup.

4.8 Summary

The above sections illustrate the detail of modelling that is involved in the developed computer simulation. As is shown, the most significant aspect for modelling was seen as the impulse valve boundary condition. The accurate modelling of this involved significant innovation.

Appendix D gives a listing of the main body of code that was used to produce the simulation. Extensive developments have since occurred to the simulation, and these are described in the following sections. The resulting code for these is given in Appendix E.

4.9 Further Development of the Simulation

One of the main factors that has severely hampered the direct use of simulation in design has been its speed of execution. For this reason, extensive attempts were made to improve its speed of operation. Initially, this was by the use of programming methods which enable the time consuming calculations to be monitored. Once identified, the efficiency of these time expensive loops could be improved. Significant improvements were obtained by reducing the number of variables used, and more importantly, reducing the number of calculations required.

There remained a need to further reduce the time of execution. The simulation was originally running on a 16 bit PC compatible machine. This was transferred to a 32bit Intel 486 workstation. In order to exploit the full power of a 32bit processor, it was necessary to use a full 32 bit compiler. To reasonably achieve this, it was necessary to manually translate the simulation from the original Pascal language to C which is a very widely adopted programming language that is known particularly for its efficiency, and ability to produce very high speed code. The compiler used to build this translated simulation was specifically optimised for the Intel 486 processor, and efficiently exploited the Weitek 4167 floating point coprocessor.

A significant performance gain was experienced. Simulation runs that previously took 48hrs to run would complete in under 6 hrs. In addition to this, these simulations offered greater accuracy as all floating point operations were undertaken at 32bit resolution namely 38

significant figures.

The translation of the code to the C language also enabled minor adaptions to be made to allow the exploitation of alternative computer architectural platforms. The simulation was made to run on a sun4 system approximately 4 times faster. This was not adopted as a full time solution as the execution time was found to be very highly dependent on other users. In addition to this, great difficulty was experienced in trying to remove calculation errors caused by variations in compiler type.

The version of the simulation that resulted was significantly more useful as an analytical tool than the version that was originally produced as part of the MSc research programme.

4.10 Valve Recalibration

The methods used to calibrate the impulse valve as described above were certainly revolutionary. However, the use of calibrated masses and spring balances under such turbulent conditions provided limited accuracy. To address this, a load cell was acquired. Figure 4.8 illustrates the experimental apparatus adopted to provide an enhanced calibration of the impulse valve. The illustrated calibration equipment provided a significantly more robust means of valve calibration, allowing small increments of stroke to be calibrated. Furthermore, at the extremes of operation where the use of calibrated masses and spring balances proved impractical, the use of a load cell provided no difficulty in measurement.

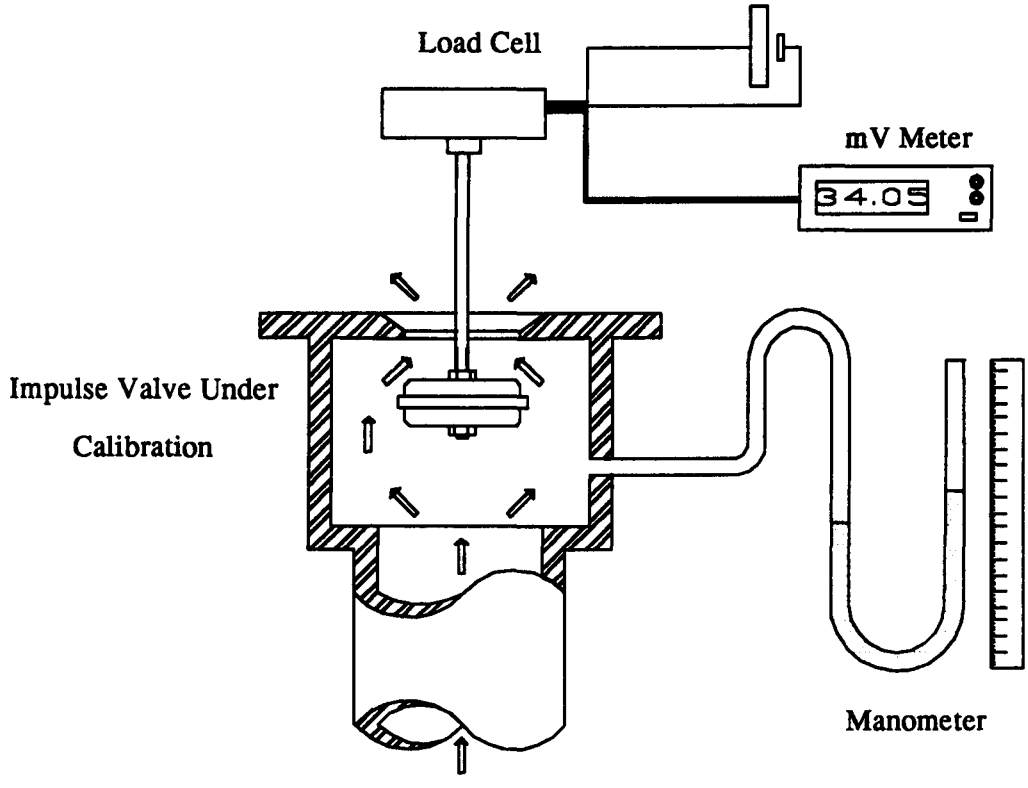

Figure 4.8 Enhanced Experimental Equipment

Figures 4.9 and 4.10 illustrate the results obtained for one of the valves calibrated with the new apparatus. The experimental data in these charts is given in Appendix G. Further calibration was undertaken by the University's D.T.U. under the author's supervision for a range of valve geometries. The results of these experiments are also given in Appendix G.

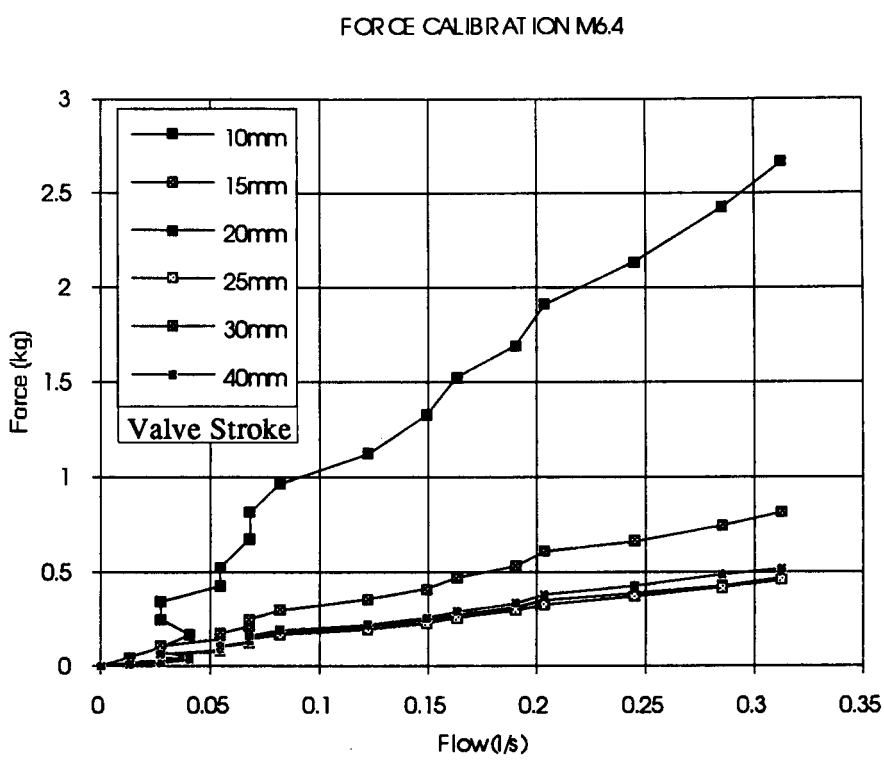

Figure 4.9 Force Calibration Results

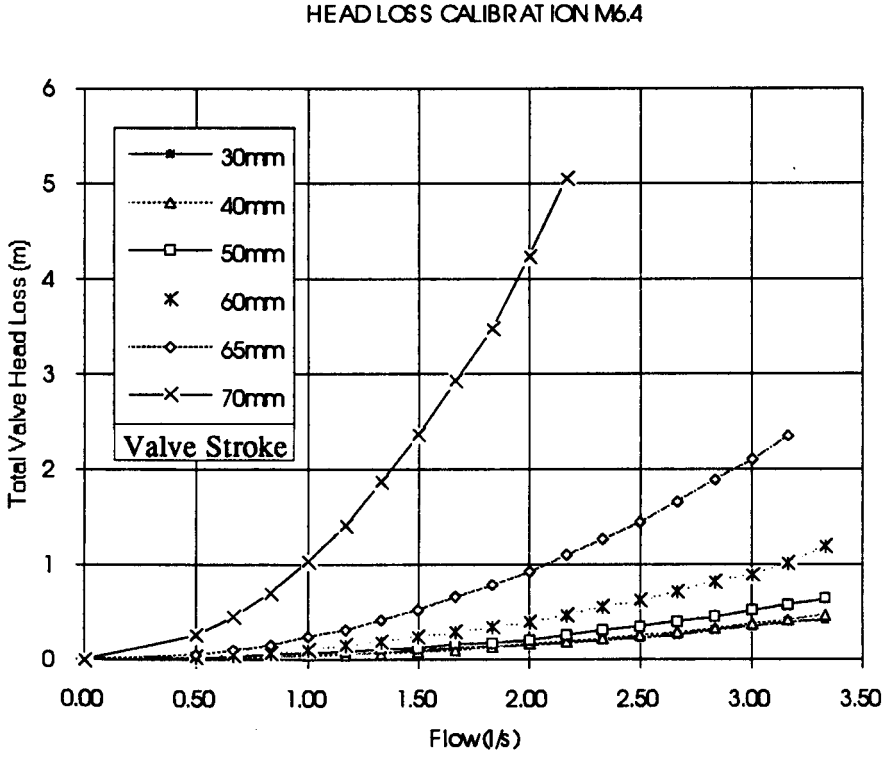

Figure 4.10 Head loss calibration results

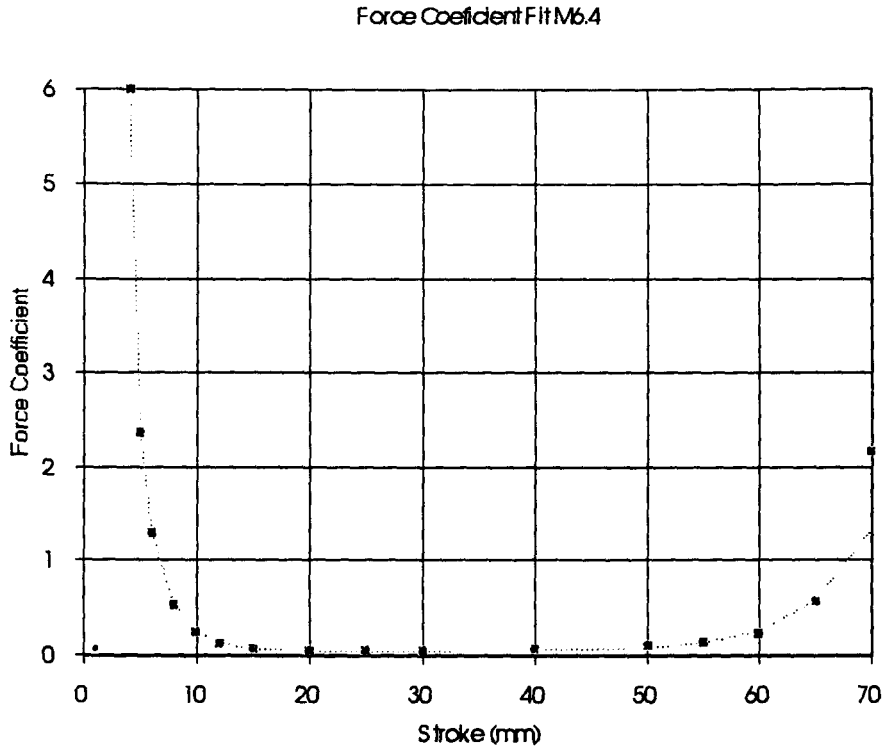

Figure 4.11 Curve Fit to Force Coefficients

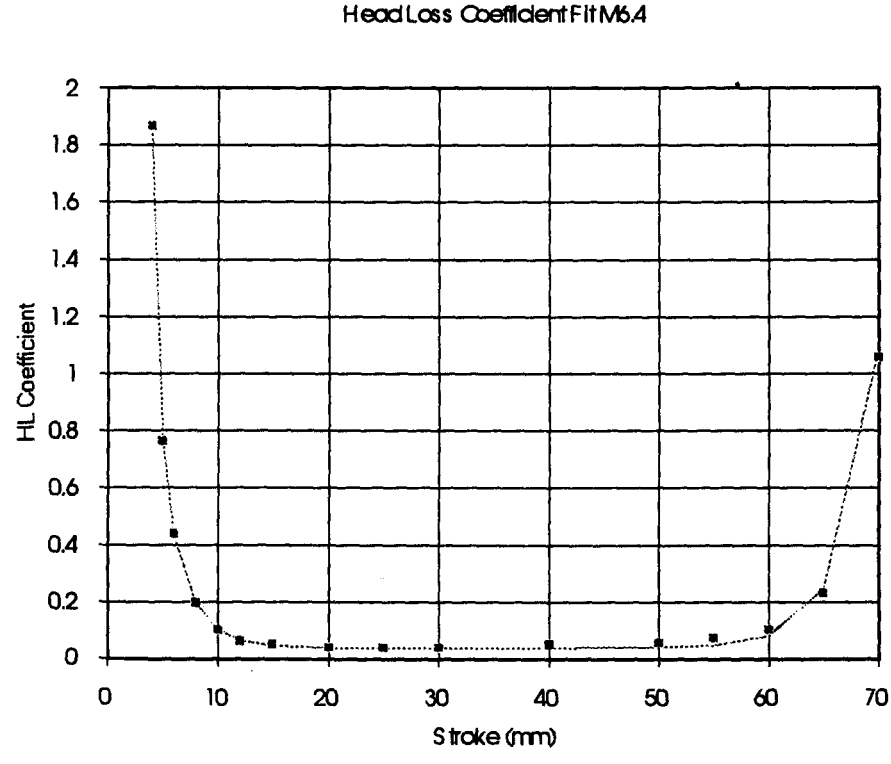

Figure 4.12 Curve fit to head loss coefficients

The given data was the fitted to Q^2 curves as described in section 4.7.2 , and detailed fitting of the resulting coefficients was also carried out. The use of the load cell allowed the valve to be calibrated over its full range of movement. The fitted curves given in figures 4.11 and 4.12 illustrate more detailed curve fits than previously developed to describe the variation of the head loss and force coefficients over the whole range. Again these used the NelderMead simplex algorithm, but this time to fit the data to compound exponential equations.

The curves given in figures 4.11 and 4.12 are represented by the equations:

$$K_f = 5.2827\times10^{3}\, e^{-1.862x} + 17.1304e^{0.4459x} + 4.7\times10^{-6}e^{0.1788x} + 0.0414 \qquad (4.15)$$

$$K_h = 1.6569\times10^{3}e^{-1.8748x} + 5.1944e^{-0.436x} + 2.2887\times10^{-10}e^{0.3177x} + 0.038 \qquad (4.16)$$

where:

K_f = *the force coefficient*

K_h = *the head loss coefficient*

x = *the valve stroke*

It can be seen in Figures 4.11 and 4.12 that the curve fits provide an excellent representation of the impulse valve characteristic for strokes between 0 and 40mm. This is the normal operating range for the D.T.U. Mk 6.4 impulse valve (for valve dimensions see Appendix H). Beyond this range, there can be seen to be errors in the curve fits. It would be possible to add a fourth exponential component to equations (4.15) and (4.16) to improve the correlation over this range. As the error region is not required for the majority of modelling and ram pump operation, this has not been undertaken. In addition, the third exponential component is not required within the range 0 - 40mm, and the above equations can therefore be simplified without losing fit accuracy to:

$$K_f = 5.2827\times10^{3}\, e^{-1.862x} + 17.1304e^{0.4459x} + 0.0414 \qquad (4.17)$$

$$K_h = 1.6569\times10^{3}e^{-1.8748x} + 5.1944e^{-0.436x} + 0.038 \qquad (4.18)$$

These equation represent a significantly more sophisticated calibration of the impulse valve than was previously adopted.

4.11 Dynamic modelling of the Impulse Valve

A further improvement to the modelling of the impulse valve was an enhancement to the dynamic characteristic of the simulated valve. The modelling of the impulse valve described above assumes that the force on, and head loss across, a valve measured under steady flow and static valve condition can be mapped directly onto a dynamic valve closure. Intuitively, this would seem to be an approximate solution, and a dynamic component influencing the head loss and force coefficient would be anticipated.

The possibility of accounting for a dynamic component of force and head loss in terms of the relative velocity between the impulse valve plunger and the passing flow was investigated. An insight into a means to account for such a component was realised during the calibration process described in the preceding section.

In Figures 4.11 and 4.12 it is possible to see that the head loss and force coefficients measured remain constant in the approximate range of valve positions 20 to 40mm. It is suggested that the coefficients measured in this range of strokes are not influenced by turbulent effects at the discharge orifice and, therefore, an increment in stroke has no effect on the coefficients. To follow on from this, it is suggested that these coefficients will be of the same order if the valve plunger were moving, and the fluid were stationary (see Figure 4.13)

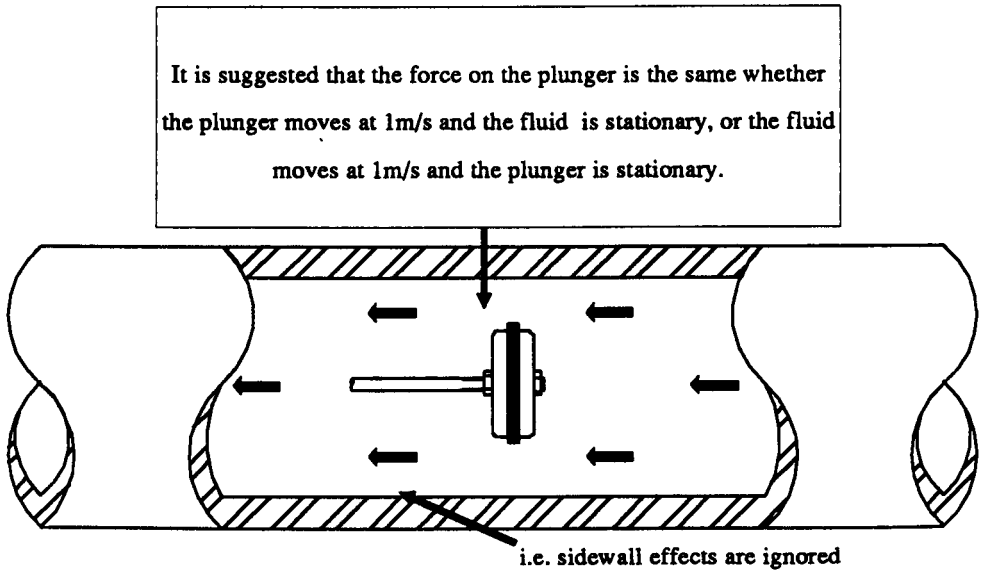

Figure 4.13 Valve plunger in free pipe

This suggestion should be valid providing the ratio between the pipe internal diameter and the valve plunger external diameter is significant. The coefficient of head loss and force for the range of strokes 20mm to 40mm can thus be assumed to equal the dynamic components of the coefficient; namely the component that is directly due to the valve plunger moving relative to the fluid flow.

Thus the new dynamic valve force calibration equations would be:

$$K_{fs} = 5.2827 \times 10^3 \, e^{-1.862x} + 17.1304 e^{0.4459x} \qquad (4.19)$$

$$K_{fd} = 0.0414 \qquad (4.20)$$

where:

K_{fs} = *static component of the force varying with displacement x*

K_{fd} = *dynamic component of force coefficient*

The dynamic boundary condition is then solved as before, except that for every calculation of force on the valve, a dynamic component is summed with the statically calibrated component. To calculate the force on the valve at any time step knowing the flow through the valve, the following formula is used:

$$Force = K_{fs} \cdot Q^2 + K_{fd} \cdot A^2 \cdot V_r \cdot |V_r| \qquad (4.21)$$

where:

Q = *Flow through the impulse valve*

A = *Area of the Valve body*

V_r = *Relative velocity between the valve disc and the fluid.*

4.12 Analysis of the Hydraulic Ram Pump Geometry

It was suggested that the geometry of the Hydraulic Ram Pump may affect its performance, and to investigate this, a series of simulations were undertaken to assess the effect of geometry changes. Figure 4.14 is an assembly drawing of the D.T.U. Mk 6.4 hydraulic ram that was drawn by the D.T.U. It is this version of the hydraulic ram pump that was used to develop the simulation described in the preceding sections, and to monitor its accuracy. Note that the body of the pump is made of 50mm fittings.

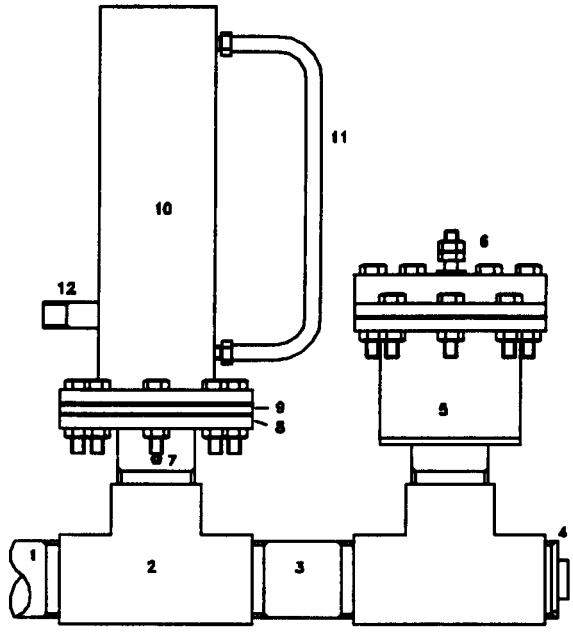

Parts List
1 Drive Pipe
2 2" Galv. Tee
3 2" Galv. Nipple
4 2" Galv. Plug
5 Impulse Valve Body
6 Impulse Valve Assembly
7 Snifter Valve
8 Snifter Housing
9 Delivery Valve
10 Air Vessel
11 Air Sight Tube
12 Delivery Pipe

Figure 4.14 D.T.U. Mk6.4 Hydraulic Ram Pump

Extensive simulation runs were undertaken to assess the significance of changing the length and diameter of the pipe sections linking the air vessel to the impulse valve. The size of the body diameter was found to have a significant effect on the magnitude of the high frequency pressure oscillations experienced during the delivery cycle, while the length of this interconnection was found to have influence on the frequency of the oscillations.

Figure 4.15 illustrates a typical simulated pressure trace for a Mk 6.4 pump using a standard Mk6.4 Impulse Valve as calibrated. It shows the typical pressure oscillations that are experienced in the body of the ram pump during a delivery cycle. The second trace shows the oscillations in the air vessel. In contrast, Figure 4.16 illustrates the simulated pressure transients experienced for an identical operating condition, but assuming the body of the

pump to be 100mm instead of 50mm.

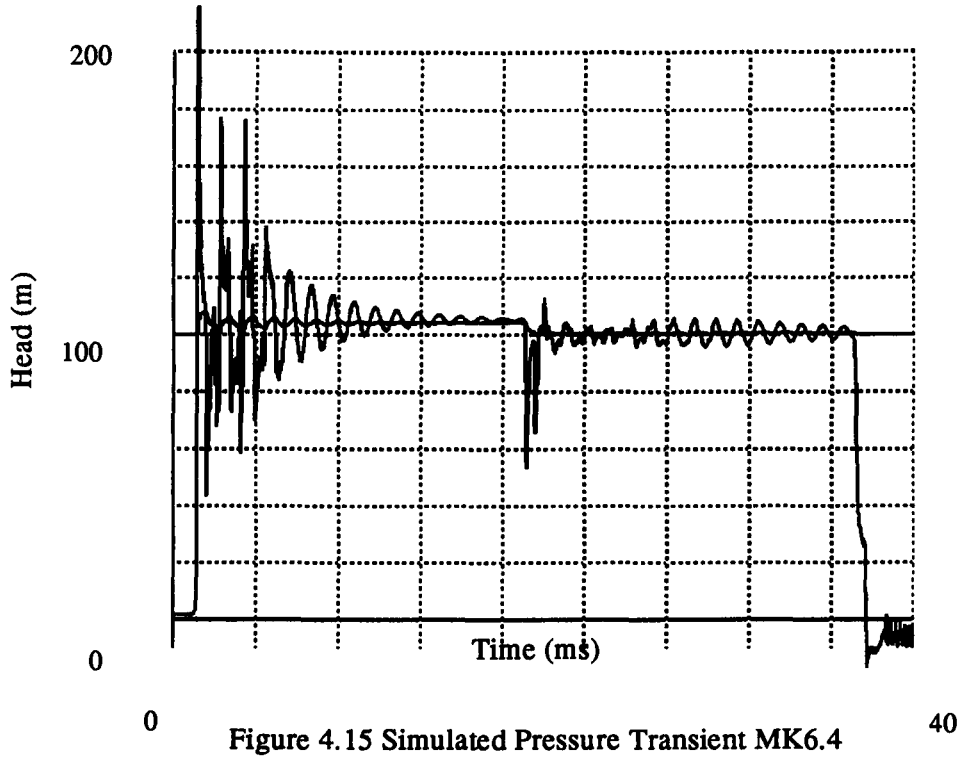

Figure 4.15 Simulated Pressure Transient MK6.4

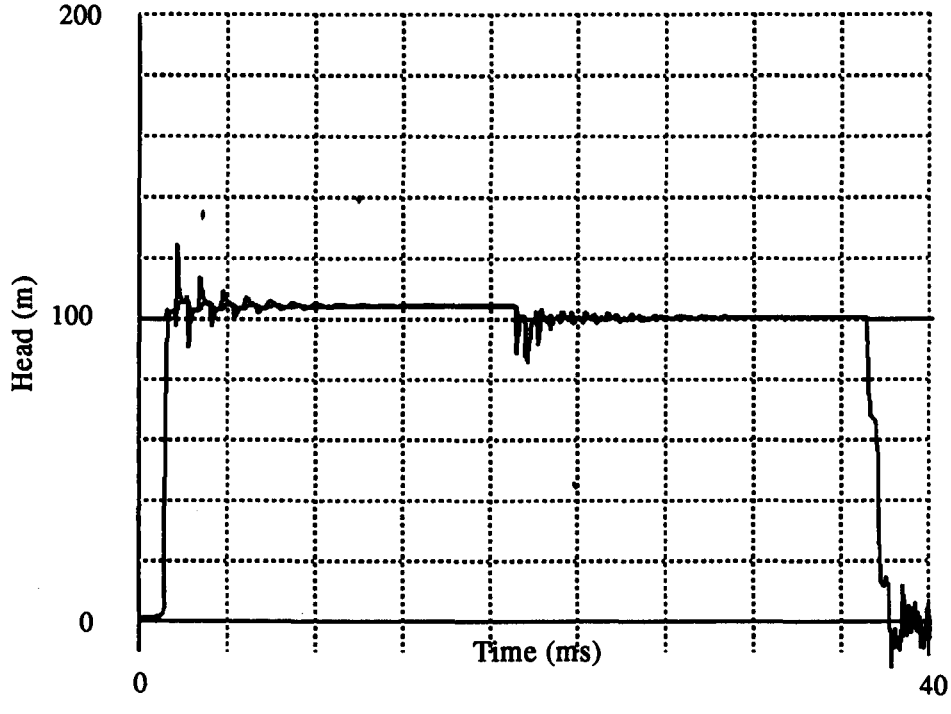

Figure 4.16 Simulated Pressure Transient Mk8

It is evident that the magnitude of the high frequency oscillations is massively reduced when the larger diameter pump body is deployed. This would be expected to reduce fatigue of the various pump elements, and enhance the pump's reliability. The described analysis led to the production of the D.T.U. Mk 8 pump. A D.T.U. assembly drawing of the Mk 8 is given in Figure 4.17. Note that the body of the pump is now 100mm diameter.

This design has been found to offer improved throughput, as well as inducing lower magnitude high frequency oscillations.

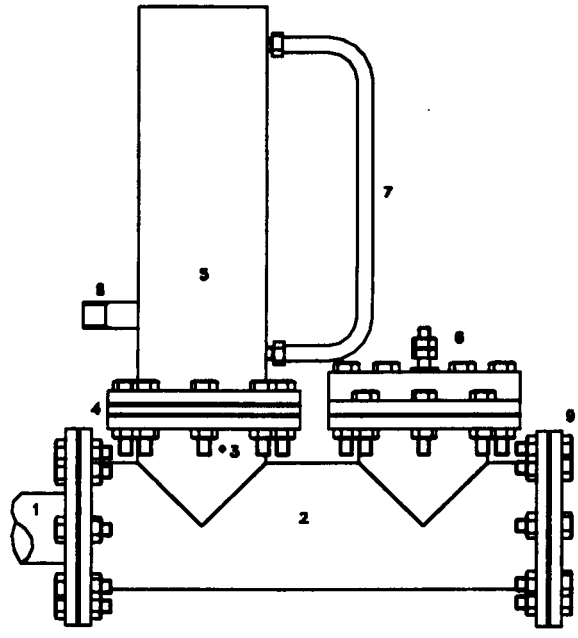

Figure 4.17 D.T.U. Mk 8 Hydraulic Ram Pump

4.13 Pump Performance Prediction

One of the most significant objectives of this study was to provide a reliable means of pump performance prediction to provide the water engineer a means by which he can reliably incorporate hydraulic ram pumps into systems. The limitations of the simulation have already been discussed in section 4.9. In spite of these limitations, attempts were made to use the simulation for pump performance prediction. The chart given in Figure 4.18 is the result of many consecutive simulations. The graph shows the variation of power and efficiency with respect to a Joukowsky ratio. This is defined as the delivery pressure over the maximum attainable head at a given drive pipe cut off velocity. This is determined using the Joukowsky formula.

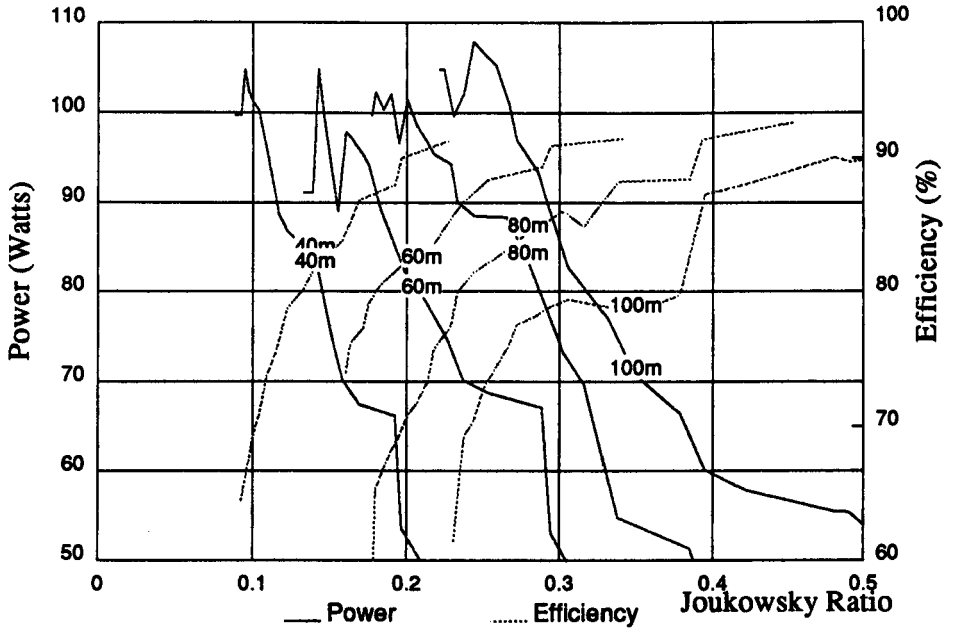

Figure 4.18 Pump Performance & Joukowsky Ratio

The quantity of data stored in the above chart is immense, but its usefulness is restricted by the lack of uniformity in the curves given, and the discovery of a flaw in an assumption used in its creation. It was discovered with extensive simulation work, that a given valve setting could allow significant variation in final fluid velocity. It was found that the velocity of the fluid at valve closure was significantly dependent on the acceleration of the fluid under gravity. In view of this, the direct mapping of the data given on the above chart was open to significant error.

4.14 Use of simulation in the creation of a predictive model.

In view of the described limitations of the simulation developed, it was decided that for the creation of design charts, it was necessary to produce a computational model based on the data obtained from the simulation. Chapter 5 describes the development of the model, and its use. Some of the work undertaken in order to attempt to provide a simplified model for the operation of the impulse valve is described here.

It became apparent from the results of the simulation that the period in which the impulse valve closed was highly variable, and also represented a major loss of pumping energy. In order to develop a useful means by which the period of impulse valve closure could be

assessed, the simulation was used. It was assumed that the factors affecting the closure time of the impulse valve were: the acceleration of the fluid in the drive pipe at the time valve closure commences, the length of the drive pipe, the stroke and mass of the impulse valve, and the velocity of the fluid at the commence of valve closure.

To simplify modelling, it was necessary to reduce the number of variables that were being analysed. It was therefore suggested that for a given impulse valve stroke and mass, the fluid velocity at which the impulse valve would start closing would be fixed. It should therefore be possible to provide different solutions for a range of standard valve masses and settings. An accurate prediction of valve closure time was required, and this is predicted to depend on drive pipe length, and acceleration of the fluid at the start of valve closure, if the valve setting is assumed to be fixed. In view of the above, it should be possible to obtain a reference value for valve closure time, and providing increments of the variables are small, obtain a function to describe the variation:

$$\Delta t = \Delta L \cdot \frac{\partial t}{\partial L} + \Delta A \cdot \frac{\partial t}{\partial A} \qquad (4.21)$$

where :

Δt = *the increment in valve closure time*

ΔL = *an increment in Length of the drive pipe*

ΔA = *an associated increment in the Acceleration at the commence of closure.*

If it is possible to obtain values or equations to describe the partial derivatives shown in equation (4.21), the above equation could then be utilised within a model to predict the time of closure relative to some reference time. To determine these values, a series of consecutive simulations were undertaken.

An algorithm was required to determine the time of the commencement of the valve closure. This was provided as a simple internal counter in the simulation. This counter required enough sophistication to ensure a reset if a slight bounce happened on the valve. This condition often occurs in hydraulic ram pumps as there are often stray pressure transients in

the system from previous cycles. Similarly, a computational switch was required to determine the exact time of closure of the valve.

A further modification was required to the simulation on account of the initial steady state that is given for the simulation to run. The current version of the simulation calculates the initial steady state operating condition of the hydraulic ram pump as if the impulse valve were initially held at full bore. This method , although reliable, induces a much higher initial velocity in the hydraulic ram body, than would be experienced under normal operating conditions. The resulting pressure transients are therefore much greater, and the results not indicative of typical hydraulic ram pump operation. For this reason, it was necessary for the simulation to undertake a series of simulation cycles to enable a stable operating condition to be set up. As with a normal hydraulic ram pump, the simulated delivery cycles were found to vary naturally. For this reason, it was necessary to introduce some level of statistical analysis in order to account for these variations.

The statistical method adopted for the study dictated that each operating condition should be run through a number of cycles to allow stabilisation before any of the data was recorded, and following this, a series of consecutive delivery cycles were recorded, and the relevant data analysed to obtain an accurate mean and standard deviation for valve closure at every operating condition. The above involved a major computing load, as each simulation required a minimum of ten pump cycles for a given pump setting.

4.14.1 Partial differential coefficient of Pipe Length with respect to time

The pump settings chosen for the simulations to determine $\frac{\partial t}{\partial L}$ were chosen using the model described in Chapter 5. The settings were chosen to ensure that as the length of each varied, the fluid acceleration at the commencement of each pump closure remained constant. Figure 4.19 gives the results calculated for a fixed acceleration of $3.03ms^{-2}$.

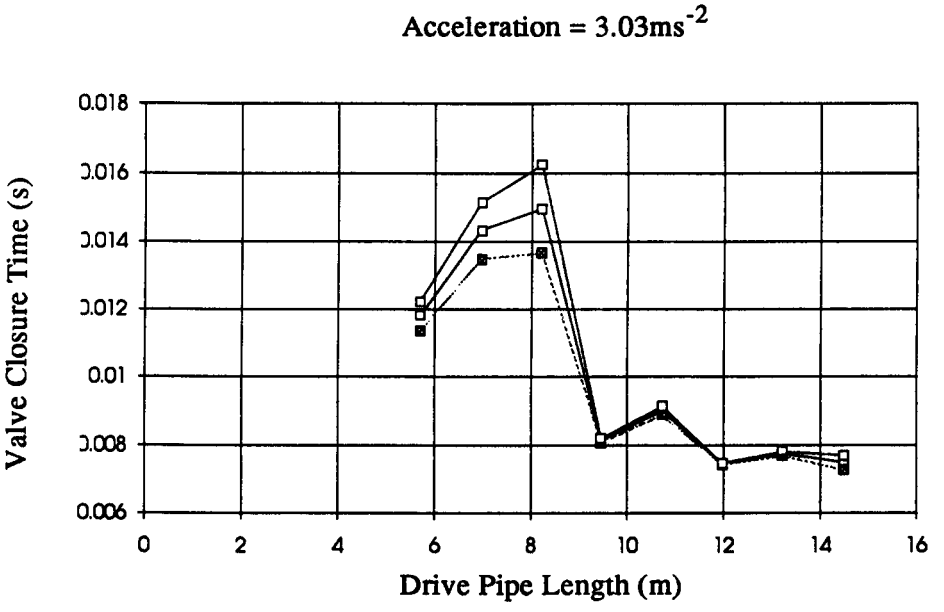

Figure 4.19 Valve Closure Time with fixed acceleration

The result illustrated in Figure 4.19 is disappointing as far as obtaining a simple value or formula to describe $\frac{\partial t}{\partial L}$. The three lines given on the chart illustrate the mean value of valve closure time calculated (center) and lines representing the standard deviation above and below this mean for the data obtained.

The results given would suggest that valve closure time is very dependent on length for drive pipe lengths between 5 and 8m. It is interesting to note that the standard deviation from the mean increases up to a length of 8 m and then drops to a minimum for the longer drive pipe lengths. This suggests that there is an erratic behaviour of the valve that develops with a drive pipe length of approximately 8m. It would seem that there is somehow a wave

reflection interfering with the closure of the valve. To gain a greater understanding, more data may be valuable. Figure 4.20 represents the data from 4.19 alongside data for accelerations of 1.04 and 2.04ms^{-2}

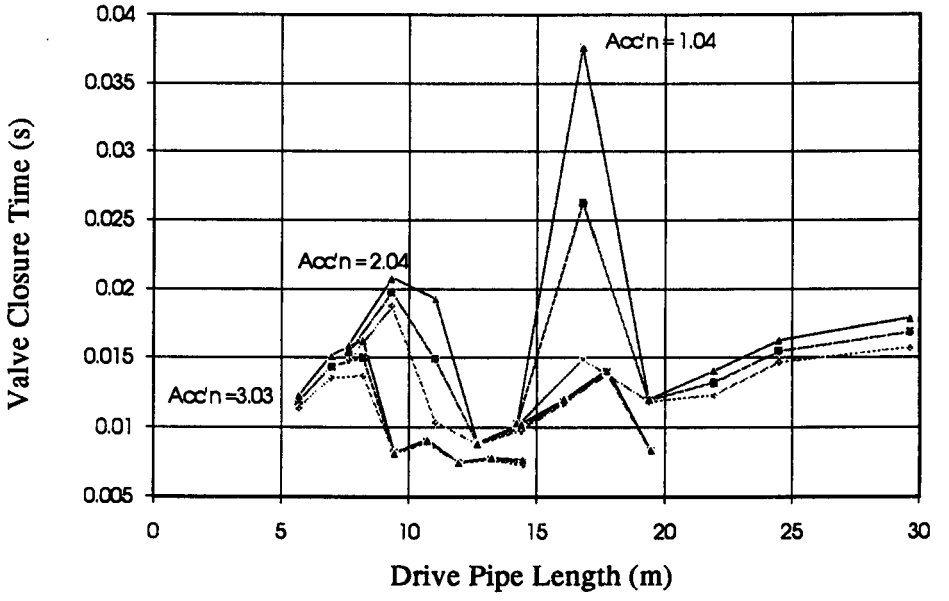

Figure 4.20 Impulse Valve Closure Times.

The data for the other acceleration values can be seen to follow a similar characteristic. There is a definite step at which the time for valve closure reduces by about 50%. For all of the sets of data, this step is marked by a significant divergence of the standard deviation lines from the mean valve closure time values. Following this step there would appear to be again a linear increase in closure time with drive pipe length, but at a reduced gradient than previously.

The key factor relating pipe length to valve closure time would evidently be fluid acceleration, but the above data is collated for instances of identical fluid acceleration. Another factor of influence could be the time taken for a wave reflection from the free surface.

Figure 4.21 illustrates the above data lines alongside lines representing the time taken for a pressure wave to travel one length of the drive pipe (L/a), the time taken for a pressure wave to travel 3 lengths of the drive pipe (3L/a).

The lines representing wave reflection times clearly have a bearing on the valve closure time calculated by the simulation. However, the relationship illustrated is by no means simple, and, therefore, does not easily lend itself to the impulse valve solution suggested in equation 4.21. The above does, however, illustrate that simple modelling of the impulse valve closure without accounting for wave reflection times will be inadequate under some operating conditions.

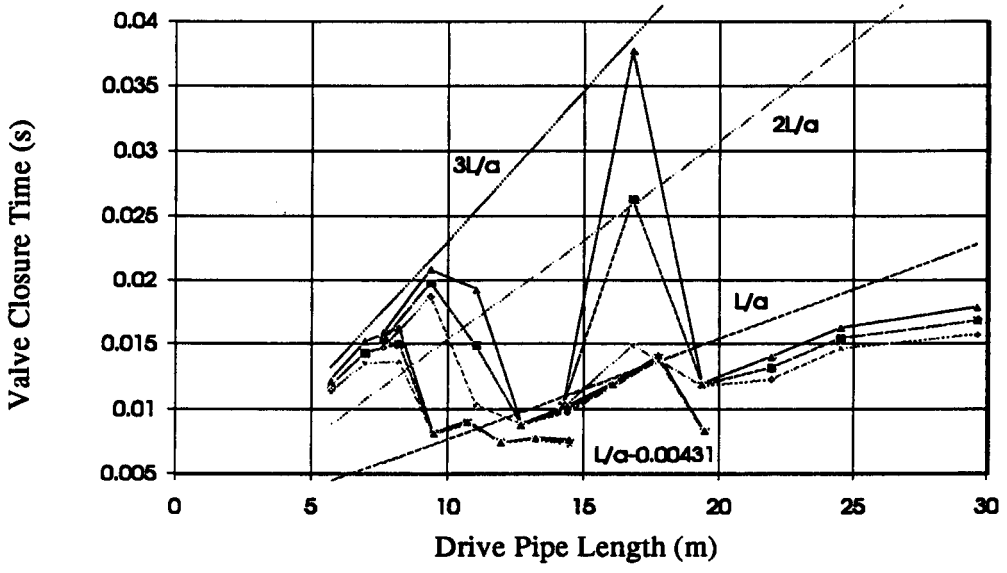

Figure 4.21 Valve Closure and Wave Reflection Times

It is possible to provide an explanation for the above behaviour in terms of the closing impulse valve. If the impulse valve moves from fully open to fully closed state in a time less than 2L/a, the reflection of the wave will have no effect on the closure time. If however, the valve reaches its seat in a time greater than 2L/a, the reflected velocity wave will effectively reduce the closure force on the valve, and delay its ultimate closure.

This is illustrated quite clearly if the data given is considered with reference to the line representing the wave reflection 2L/a in Figure 4.21. It can be seen clearly that if the closure time approaches the wave reflection time, the valve closure time is erratic. This is illustrated by the deviation between the mean data line, and the line representing the standard deviation. It is then possible to see that for valve closure times greater than this, there is a marked stepped increase in the time for closure. This is is well illustrated by the lines representing closure times with fluid acceleration of $1.04ms^{-2}$. At the position where the mean

closure time is almost exactly equal to the time for a full wave reflection, the standard deviation from the mean is at its largest, and illustrates the step in closure time experienced. The above information does not provide a solution for the impulse valve that was required for predictive modelling. An alternative solution to this was implemented, and is described in detail in chapter 5. The above analysis does however allow a series of interesting conclusions to be drawn.

- The impulse valve closure time is not always small compared with the wave reflection time as some analyses would assume.

- To maximise the efficiency of a hydraulic ram pump, it is necessary to minimise the valve closure time. To do this, it is preferable to have a valve closure time shorter than the wave reflection time.

- For good operating efficiency there is a critical minimum drive pipe length that should not be reduced.

- From the data shown, it can be seen that this minimum length can be reduced if greater fluid accelerations are experienced during the valve closure. This is a characteristic of the D.T.U. impulse valve which like the majority of designs closes under drag forces provided by the discharging fluid. The higher the acceleration, the more rapid the closure, the shorter the minimum pipe length for a given valve setting. For the D.T.U. valve, a minimum drive length of 20m should be used with an acceleration of $1ms^{-2}$; 13m with an acceleration of $2ms^{-2}$; and 10m for an acceleration $3ms^{-2}$, in order to avoid impulse valve inefficiency.

In the interest of completeness, Figure 4.22 illustrates the variation of impulse valve closure time varying with fluid acceleration assuming drive pipe length to be constant. The figure 4.22 again has a central line representing the mean simulated valve closure time for the given fluid acceleration, while the lines above and below represent the standard deviation of the simulated results from this mean value. It is suprising to note that for the given drive pipe length, there is not a significant variation in closure time with fluid acceleration during closure. However, the reaching of a critical fluid acceleration is clearly evident, and marked by a major deviation of the standard deviation line from the mean.

The importance of ensuring the drive pipe for a hydraulic ram pump is long enough to

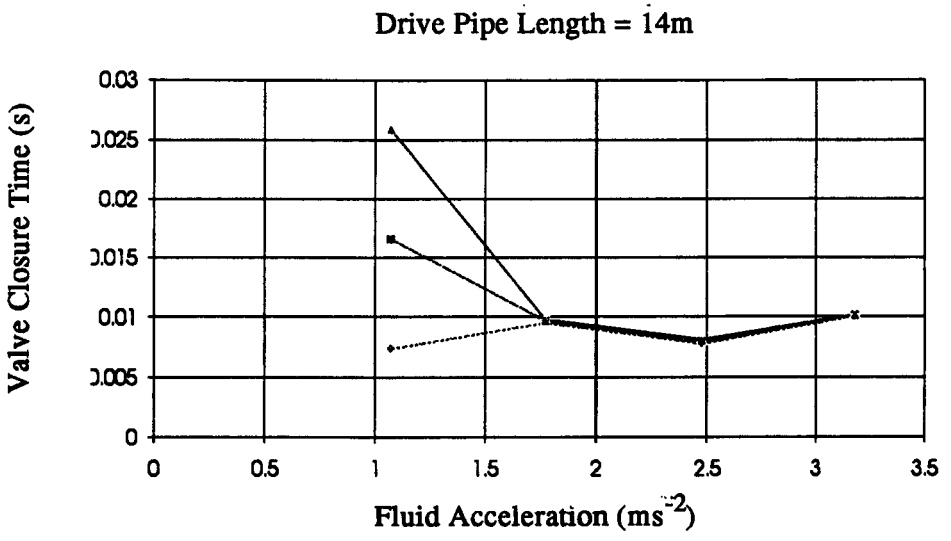

Figure 4.22 Valve Close Time varying with acceleration

ensure minimum energy losses during impulse valve closure should be balanced against the significant energy losses that are associated with the acceleration of fluid in the drive pipe. To provide an optimal hydraulic ram pump design, it is therefore necessary to discover an impulse valve capable of an extremely rapid closure. This will allow a reduction in drive pipe length, and associated cost savings, as well as a greatly enhanced performance in terms of pump efficiency (the water power delivered over the water power used) and throughput power (the water power delivered).

4.15 Conclusions.

The described computer simulation has been of direct use in the provision of understanding of the hydraulic ram pump. Relatively unsuccessful attempts have been made to use it as a tool for pump performance prediction, but these have been largely hampered by computational restrictions. The simulation has proved an invaluable tool in answering questions regarding pump geometry, and been the driving force behind some major changes in design.

The major use of the simulation has been in providing the greater understanding of the hydraulic ram pump as described in chapter 2, and also providing a quantitative insight into

elements of pump operation that have enabled the development of a pump performance prediction model as described in chapter 5.

Further to this, a valuable insight into the interaction between the impulse valve and the drive pipe has been made possible by the use of extensive simulation and statistical analysis. The Figures 4.23 and 4.24 show a comparison of simulated and measured transients in a D.T.U. Mk 6.4 hydraulic ram pump.

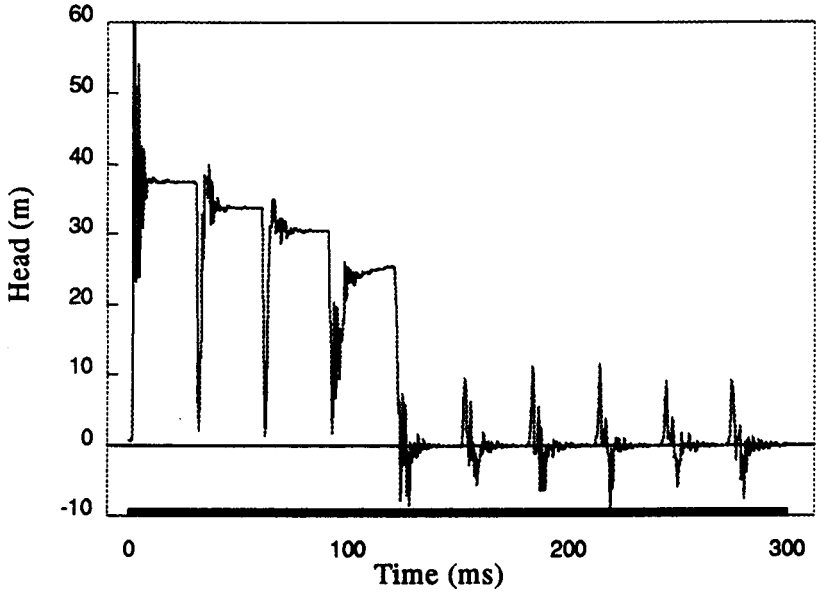

Figure 4.23 Simulated Pressure Trace

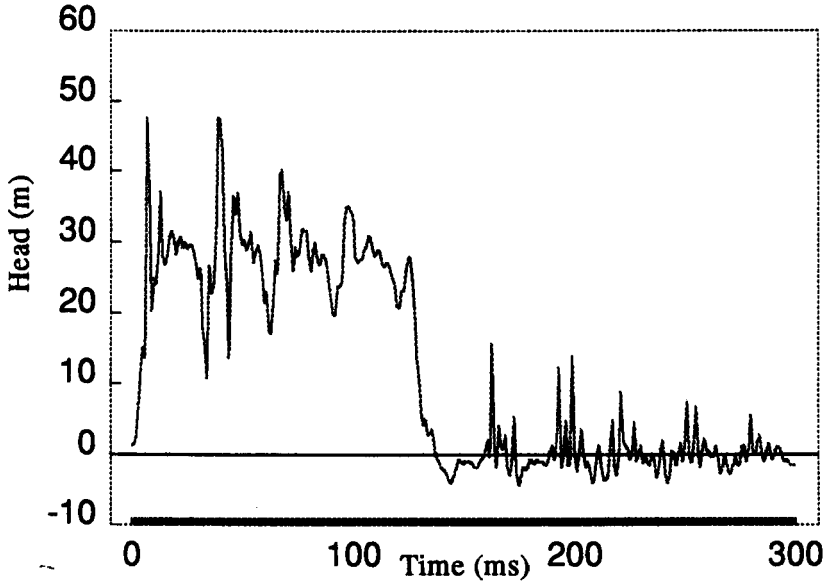

Figure 4.24 Measured Pressure Trace

Chapter 5: Development of Pump Performance Model

5.1 The need for a model

In view of the great number of variables associated with the design of hydraulic ram pumping systems, good design practices are potentially highly complex. Hitherto, the process of design has too often been based on "rules of thumb" and inaccurate formulae. It is apparent that because of this, the extent of hydraulic ram pump usage has been greatly limited. Furthermore, systems which have been deployed are often far from the optimum. A predictive model would provide a means by which the above situation could be avoided.

Other technologies exist which achieve similar results to the hydraulic ram pump. The main competing technology involves pump-turbine systems which incorporate a direct or geared linkage of a pump unit to a turbine. The cheapest of these systems utilise a reversed pump unit as the turbine. The water engineer requires a means by which such competing technologies may be compared with hydraulic ram pumps. A predictive model would allow a realistic comparison with competing technologies, and so allow reasonable deployment of optimum solutions. The present lack of the method to undertake a reasonable feasibility study means that hydraulic ram pump users have generally to be committed to the technology well before the detailed design stage.

It is apparent that a predictive model could provide the means by which hydraulic ram pump systems could be reliably designed, and so remove the main restriction on their wider deployment.

5.2 Solutions to the design vacuum

In view of the sophistication and accuracy of the computer simulation described in chapter 4, it could be proposed that system design should be undertaken using a simulation of this type. However, a standard configuration simulation of this type can take up to 3 days to run only 30 seconds of simulated time. It is therefore clearly inappropriate for regular system design analyses. This is illustrated further if one observes that each simulation represents only one set of data, and many sets would be required to produce any useful design data.

There would appear to be two possible solutions to this problem. One route would be to use the simulation in the creation of design charts of such detail and incorporating such an

extensive amount of data that they would negate the need for any computation at the detailed design stage. The alternative is to produce a set of computer algorithms based on understanding gained from the use of the simulation which predict pump behaviour over a range of operating conditions. As will be demonstrated, both of these routes have been pursued within this research. This chapter concentrates on the development of the later, computer model approach. The usefulness of a model of this type to the creation of design charts is also discussed.

5.3 The Development of Pump Prediction Algorithms

The development of these algorithms extensively uses a computer spreadsheet environment. If the reader is not already practised in the use of computer spreadsheets, it would be advantageous to refer to Appendix C before continuing in this chapter.

The chapter describes the development of a model for the Acceleration Phase as described in chapter 2, and then described the methods adopted for modelling the Delivery Phase. These two components make up the main body of the model. Further sections then describe the modelling of the Recoil Cycle, and the Impulse Valve Closure. Coverage is given to the use of the model, although its use will become more apparant in later chapters.

5.4 The Acceleration Cycle

The first attempt at modelling concentrated on the hydraulic ram pump's acceleration cycle. It was believed that this cycle represented the majority of the losses for operating hydraulic ram pump systems and therefore required immediate attention. The initial approach was to compare the efficiency of this cycle for a range of pump settings. (Each pump setting represents a different water velocity at which the impulse valve closes). As defined previously, the efficiency of the acceleration cycle is defined as the percentage of potential energy dissipated in the acceleration of the fluid in the drive pipe that is transfered to kinetic energy of the drive pipe fluid at the end of the cycle.

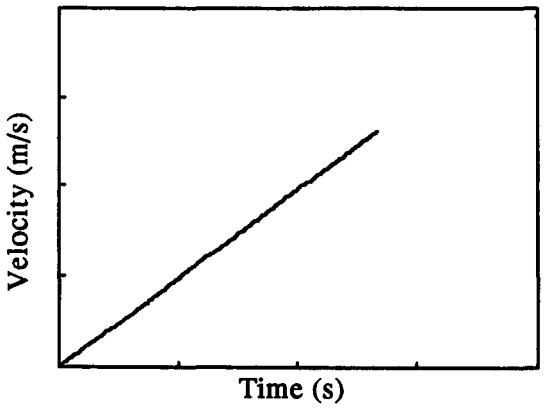

Fig.5.1 Velocity History (zero friction)

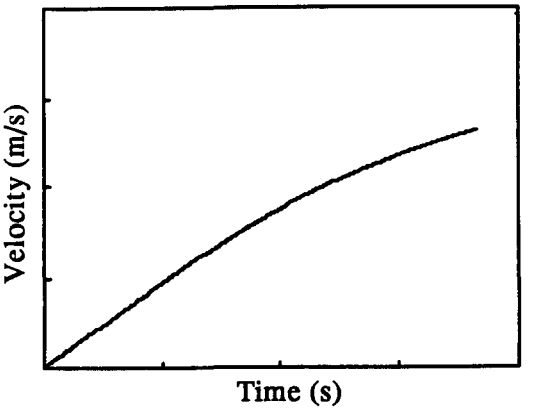

Fig.5.2 Velocity History (normal friction)

A spreadsheet environment was chosen to investigate the acceleration efficiency variations. The development of two velocity histories was considered. Firstly the velocity history for a hydraulic ram pump offering zero friction was considered. Although this zero friction is not practically possible, it provides a useful means for assessing the efficiency of the process, as no friction means no energy loss. Figure 5.1 represents a velocity history for this instance.A history assuming acceleration with normal friction effects is given in Figure 5.2 (Colebrook-White steady state formulae assumed).

In both of the graphs the velocity rises to the same "cut off" velocity. However, the time taken to reach this velocity is significantly greater in the instance involving friction, as is the volume of water that passes. The volume of water passing is determined by an integration of the flow velocity with respect to time or as the area under the velocity lines shown multiplied by the pipe area.

The curves shown can be calculated within a spreadsheet environment. An example

	A	B	C	D	E	F	G	H	I
1	Drive Head	3	Diameter	50	K (mm)		$K_{impulseV}$		
2	DeliveryHd	60	Length	12					
3									
4	Velocity	Accn1	Accn2	Time1	Time2	Q1	Q2	f	
5	0	2.4525		0	0	0	0	0	
6	0.01	2.4525							
7	0.02	2.4525							
8	0.03	2.4525							
9	0.04	2.4525							
10	0.05	2.4525							

Figure 5.3 Calculating Acceleration from Velocity

computer spreadsheet demonstrating the calculation of the flows and time taken to reach cut off velocity is given in Figure 5.3.

Column A in Figure 5.3 is a range of cells with a small increment in velocity in each (the smaller the increment the greater the accuracy of the integrations). The model at a later stage involves a series of trapezoidal integrations, and for this purpose the velocity of the water in the drive pipe was chosen as the base variable for all the calculations.

Column B represents the acceleration experienced by the column of fluid in the drive pipe assuming that there is no friction. This is a constant for a given "frictionless" system and is calculated using

$$\alpha = \frac{\rho.g.h.A}{\rho.A.L} \quad giving \quad \frac{g.h}{L} \qquad (5.1)$$

where:

α = *acceleration of water in the drive pipe*

A = *area of drive pipe, L = length of drive pipe*

ρ = *density of fluid*

g = *acceleration due to gravity*

h = *driving head*

Column C in Figure 5.4 represents the fluids acceleration in a real system. It allows for friction by accounting for a reducing driving head. A similar form of the previous equation is used but an alternative driving head H is used to account for the head loss due to friction, and is defined as:

	A	B	C	D	E	F	G	H	I
1	Drive Head	3	Diameter	50	K (mm)		$K_{impulseV}$		
2	DeliveryHd	60	Length	12					
3									
4	Velocity	Accn1	Accn2	Time1	Time2	Q1	Q2	f	
5	0	2.4525	2.4525	0	0	0	0		
6	0.01	2.4525	2.4525					0.1677	
7	0.02	2.4525	2.4522					0.0838	
8	0.03	2.4525	2.4518					0.0559	
9	0.04	2.4525	2.4513					0.0419	

Figure 5.4 Accounting for Friction

$$H = h - \frac{fLV^2}{2.d.g} - K_{ho}A^2.V^2 - \frac{C_L.V^2}{g} \qquad (5.2)$$

where:

f = *Colebrook-White friction factor using Barr approximation (see section 5.5)*

K_{ho} = *the impulse valve friction coefficient*

C_L = *Sum of loss coefficients for drive pipe fittings (inlet,outlet elbow)*

The spreadsheet formula used for cell C5 in Figure 5.4. using standard spreadsheet syntax is therefore:

*(9.81/$D$2)*($B$1((0.09+$D$1*$N$10^2+H5*$D$2/(2*0.001*$D$1*9.81)*A5*A5)* (5.3)

Cell addresses preceded by $ are absolute, while others are addresses relative to cell position. So if this cell contents is copied to the whole column, the formula in cell C6 will read:

*(9.81/$D$2)*($B$1((0.09+$D$1*$N$10^2+H6*$D$2/(2*0.001*$D$1*9.81)*A6*A6)* (5.4)

with the relative addresses changing for the new row, and the absolute addresses staying constant. In this way column C represents the acceleration which would be experienced by the fluid in the drive pipe if the velocity of the fluid is that given in the corresponding row of column A.

5.5 Friction

The implicit form of the Colebrook-White equation for the friction factor f make it difficult to use in many circumstances. There are several simplified forms which give results that approximate closely with the Colebrook-White equations. For the spreadsheet model the equation by Barr[39] was adopted:

$$1/\sqrt{f} = 2\log_{10}\left[\frac{k}{3.7D} + \frac{5.1286}{Re^{0.89}}\right] \text{ for } Re>2000 \quad (5.5)$$

k = *relative roughness coefficient (mm)*

D = *diameter (mm)*

Re = *Reynolds number* $(\frac{V.D}{\gamma})$

f = $\frac{64}{Re}$ *for Re<2000 for lamina flow*

Adopting this formula in column H of the spreadsheet yields a friction factor that is calculated for each of the velocities given in column A.

5.6 Acceleration Time

The columns A and C represent instantaneous drive pipe velocity and acceleration respectively. Using simple equations of motion, and trapezoidal integration, it is possible to use these calculated values to determine the time taken to reach these velocity and acceleration values.

From the spreadsheet illustrated in Figure 5.4, values can be obtained for velocity and acceleration corresponding to times T_0 and T_1 in figure 5.5 . If a small value for δV is adopted, δT can be calculated using simple equations of motion: $\delta T = \delta V \cdot dt/dv$. Thus the equations for the Time columns D and E are easily solved. To improve accuracy slightly, the value of dt/dv is taken as the average of the value at T_0 and T_1.

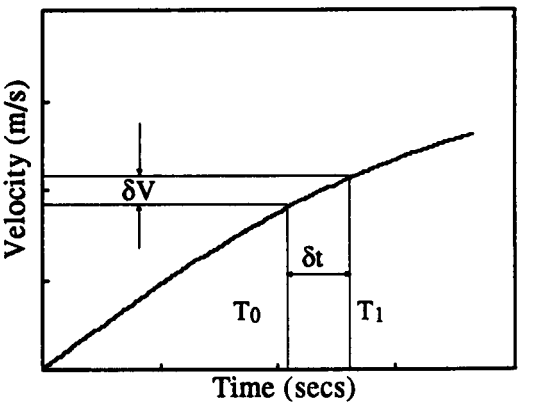

Fig.5.5 Velocity History (normal friction)

5.5 Friction

The implicit form of the Colebrook-White equation for the friction factor f make it difficult to use in many circumstances. There are several simplified forms which give results that approximate closely with the Colebrook-White equations. For the spreadsheet model the equation by Barr[39] was adopted:

$$1/\sqrt{f} = 2\log 10\left[\frac{k}{3.7D} + \frac{5.1286}{Re^{0.89}}\right] \text{ for } Re>2000 \quad (5.5)$$

k = *relative roughness coefficient (mm)*

D = *diameter (mm)*

Re = *Reynolds number* $(\frac{V.D}{\gamma})$

f = $\frac{64}{Re}$ *for* $Re<2000$

Adopting this formula in column H of the spreadsheet yields a friction factor that is calculated for each of the velocities given in column A.

5.6 Acceleration Time

The columns A and C represent instantaneous drive pipe velocity and acceleration respectively. Using simple equations of motion, and trapezoidal integration, it is possible to use these calculated values to determine the time taken to reach these velocity and acceleration values.

From the spreadsheet illustrated in Figure 5.4, values can be obtained for velocity and acceleration corresponding to times T_0 and T_1 in figure 5.5 . If a small value for δV is adopted, δT can be calculated using simple equations of motion: $\delta T = \delta V \cdot dt/dv$. Thus the equations for the Time columns D and E are easily solved. To improve accuracy slightly, the value of dt/dv is taken as the average of the value at T_0 and T_1.

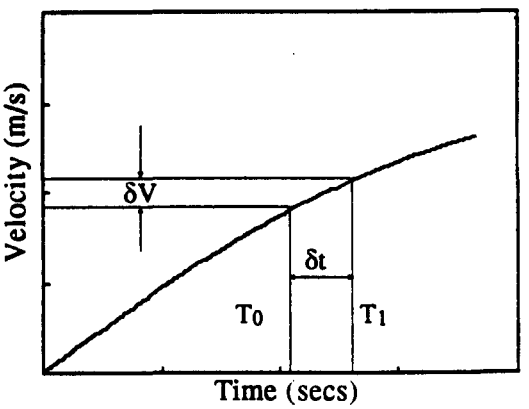

Fig.5.5 Velocity History (normal friction)

To illustrate, the equations for the time columns given in Figure 5.6 equation for cell E6 is given as (A6A5)/((C6+C5)/2) + E5. This equation when copied to all the cells in the column gives the time taken to reach a drive pipe velocity as specified in column A.

If these calculated times are plotted against velocity (switching axes) an accurate representation of the velocity history during the acceleration history is obtained, providing the velocity increments used are small. Suitable sizes for velocity increments were chosen following a simple sensitivity analysis. Figure 5.7 is a direct plot from the spreadsheet in Figure 5.6 .

	A	B	C	D	E	F	G	H	I
1	Drive Head	3	Diameter	50	K (mm)		$K_{impulseV}$		
2	DeliveryHd	60	Length	12					
3									
4	Velocity	Accn1	Accn2	Time1	Time2	Q1	Q2	f	
5	0	2.4525	2.4525	0	0	0	0		
6	0.01	2.4525	2.4525	0.00815	0.00815			0.1677	
7	0.02	2.4525	2.4522	0.01631	0.01631			0.0838	
8	0.03	2.4525	2.4518	0.02446	0.02447			0.0559	
9	0.04	2.4525	2.4513	0.03262	0.03263			0.0419	

Figure 5.6 Calculation of elapsed time

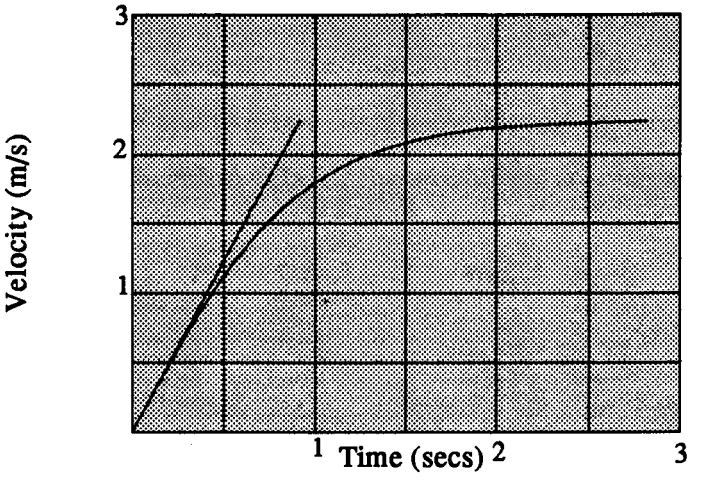

Fig.5.7 A Typical Velocity History

5.7 Using the Acceleration Algorithms

The graph in Figure 5.7 shows two calculated velocity histories which can be used to assess the performance of a given hydraulic ram system from the point of view of the acceleration cycle.

5.7.1 Acceleration Efficiency

A saw tooth velocity profile of the type illustrated in Figure 5.1 represents a competely frictionless acceleration cycle. It represents a perfect cycle with hydraulic energy being converted completely to kinetic energy in the drive pipe. The resulting kinetic energy in the drive pipe is exactly the same as would result in a normal friction environment. This is based on the assumption that the cut off velocity in the hydraulic ram is fixed by the impulse valve setting. By calculating the volume of water flowing under the two velocity histories, the efficiency of the acceleration cycle can be determined, as energy used in acceleration is proportional to the volume of water flowing through the drive pipe. In the saw tooth velocity history this energy used is turned into kinetic energy in the fluid. In the friction case (curved velocity history), the same ultimate kinetic energy is attained, but significantly more energy is expended during the acceleration cycle. An acceleration efficiency can be determined by dividing the volume used in the acceleration cycle with friction by that used in the acceleration cycle without.

Initially it is necessary to calculate the volume of water passed for each row of the spreadsheet. To do this, a simple trapezoidal integration of flow is used (see Appendix C). Two volume columns are created, one for the frictionless acceleration, and one for normal acceleration. The spreadsheet formula for these columns is given as:

$$F5 : 0.5*D5*A5*PipeArea \qquad (5.6)$$

	A	B	C	D	E	F	G	H	I
1	Drive Head	3	Diameter	50	K (mm)		$K_{impulseV}$		
2	DeliveryHd	60	Length	12					
3									
4	Velocity	Accn1	Accn2	Time1	Time2	Q1	Q2	f	
5	0	2.4525	2.4525	0	0	0	0		
6	0.01	2.4525	2.4525	0.00815	0.00815	0.00016	0.00016	0.1677	
7	0.02	2.4525	2.4522	0.01631	0.01631	0.000641	0.000641	0.0838	
8	0.03	2.4525	2.4518	0.02446	0.02447	0.001441	0.001442	0.0559	
9	0.04	2.4525	2.4513	0.03262	0.03263	0.002562	0.002563	0.0419	

Figure 5.8 Calculation of volume of water

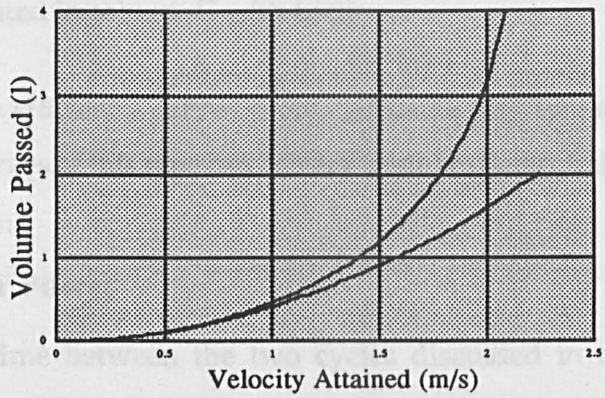

Figure 5.9 Waste Volume during Acceleration

G5: Pipe Area(A5*(D5D4)+0.5*C5*(D5D4)^2))+G4* *(5.7)*

The formula given for F5 is simply the area of a right angled triangle, and is therefore quite simple to determine. The formula for G5 represents a trapezoidal integration, treating the spreadsheet row as one incremental step in the integration. The formula gives the area covered within the period of one velocity increment, multiplied by the pipe area to give the volume within that period. This is then summed with the previous total to give the total volume passed on reaching the row's terminal velocity. Figure 5.9 shows the two flow volumes calculated in these columns.

These provide the means by which the acceleration efficiency of the hydraulic ram can be determined. For any row the volumetric efficiency of the acceleration cycle is simply the

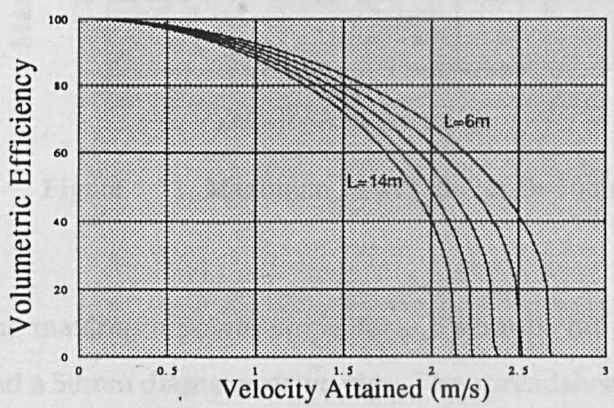

Figure 5.10 Volumetric Efficiency of Acceleration

volume passing as calculated in column F without friction (effectively the energy out) divided by that calculated in column G with friction.

Figure 5.10 shows the efficiency curves produced using this spreadsheet for a number of drive pipe lengths. Curves of this type can be very useful in determining the reasonable limits for drive system design.

5.7.2 Acceleration Power

If the difference in time between the two cycles discussed in the previous section is calculated, a mean power for the drive system during the acceleration cycle can be determined:

$$Power = (\rho \times Volume \times g \times H)/Time \qquad (5.8)$$

If the value of time we use includes a minimum delivery period 2L/a, the result is a theoretical maximum pumping power for a given hydraulic ram system. The zero friction curve will yield the maximum power possible, while the other curve will yield the maximum power for given friction characteristics. Dividing one value by the other will yield the fraction of maximum power obtainable by the given drive system.

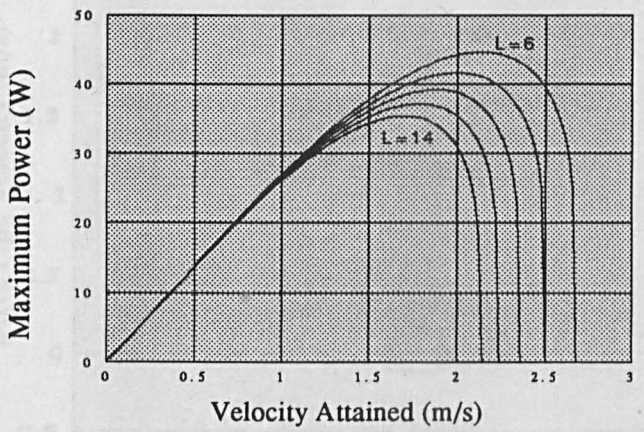

Figure 5.11 Maximum Power h=3m D=50mm

Figure 5.11 shows the maximum power curve for a hydraulic ram pump using a standard DTU Mk 8.4 or 6.4 and a 50mm diameter drive pipe. The spreadsheet allows similar curves to be produced for different valves, pipe diameters, and drive heads.

5.8 The Delivery Cycle

Although the acceleration algorithms offer significant insight, some understanding of the delivery cycle is required to allow accurate pump performance prediction.

During the delivery cycle there are a series of rapidly propagating hydraulic transients. Experimental equipment to measure instantaneous velocities is extremely expensive, and often inaccurate. So in order to get an understanding of the real time variations it is helpful to look at the computer simulation data. Chapter 2 offers a detailed explanation of the cycle. Figure 5.12 is a velocity trace for the water in the drive pipe during the delivery cycle, and was obtained directly from computer simulation.

This characteristic step nature of the velocity trace was predicted and documented by O'Brien and Gosline [26] in the 30's and subsequently ignored by many later works. The shape of the trace is a consequence of the delay in velocity and pressure changes caused by the propagation of pressure waves along the drive pipe.

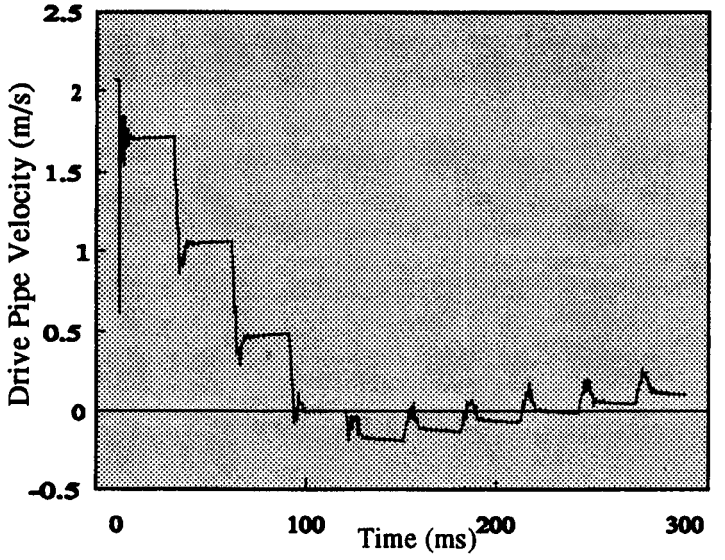

Figure 5.12 Simulated Drive Pipe Velocity

The stepped trace can be measured to have a step period approximating to the period of wave propagation 2L/a. The first step is of a magnitude approximating to gh/a. From

Joukowski[4] this represents the velocity change required to achieve a pressure of h. The remaining steps then have a magnitude of 2gh/a, unless cut short by the abscissa.

These observations provide the basis for calculating the period and volume of water passing during the delivery period. The volume delivered being defined by the area under the curve multiplied by pipe area, and the period being an integer number of wave propagation periods.

It can be seen from these observations that there are a number of possible delivery characteristics. The nature of the delivery is primarily dependent on the cutoff velocity in the drive pipe, and the delivery head. Other factors include the length of the drive pipe, the speed of sound in the drive pipe, and the headloss coefficient across the delivery valve.

In order to provide accurate predictions of ram performance it is necessary to know the period of the delivery cycle, the volume delivered, and the resulting recoil velocity.

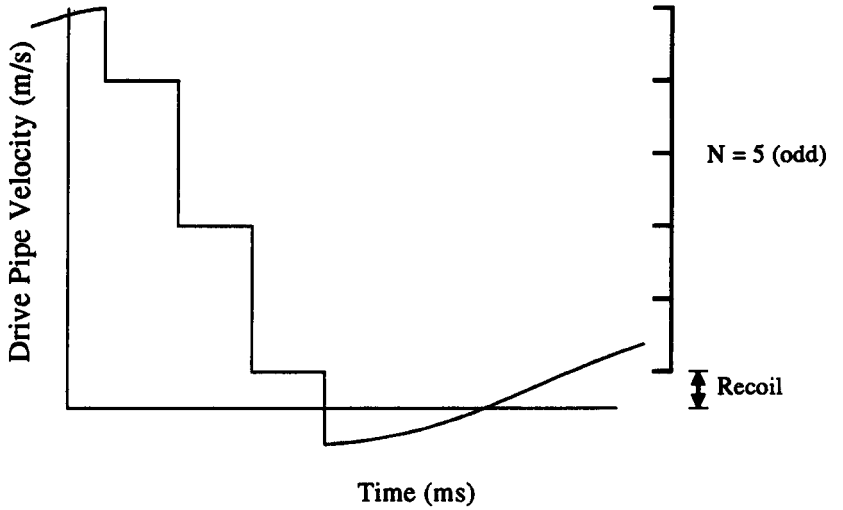

Figure 5.13 Mode 1

5.8.1 Recoil

From observations, the degree of recoil is dependent on the velocity drop associated with the final pressure spike. If this final drop is smaller or equal in magnitude to gh/a, the recoil is equal and opposite to this velocity, and occurs immediately. If the final velocity drop exceeds this by some value R, the recoil is observed to be of the same order as R. In this situation,

delivery is observed to stop immediately, and recoil only occurs after a period 2L/a.

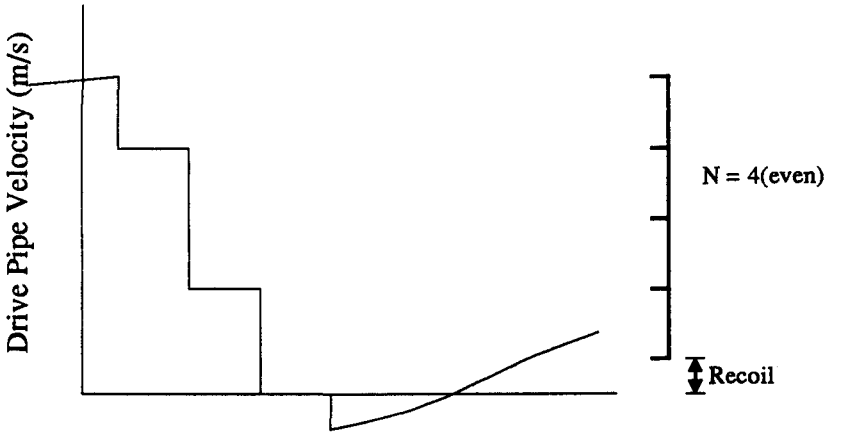

Figure 5.14 Mode 2

5.8.2 Modelling of the Delivery Cycle

In view of the recoil observations described above, it is helpful for modelling purposes to differentiate between the two modes of delivery. The mode of delivery shown in Figure 5.13 occurs when the terminal velocity divided by the Joukowsky velocity required to attain

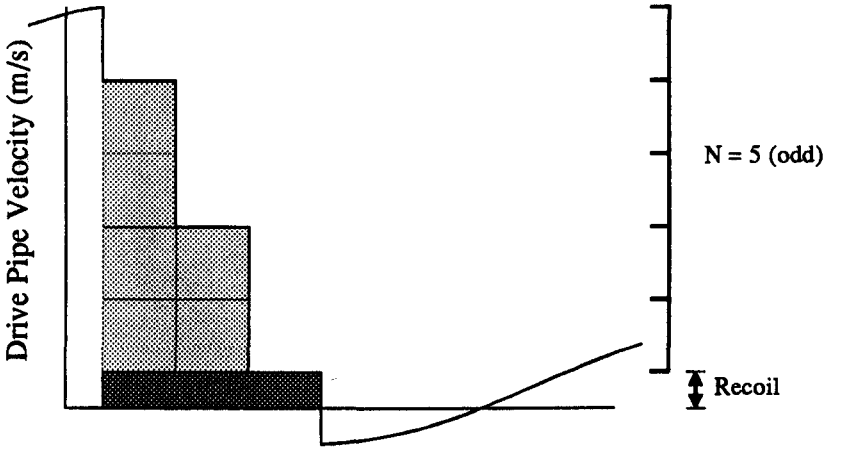

Figure 5.15 Mode 1

delivery gives an odd integer and a remainder. Similarly Figure 5.14 illustrates the delivery if this yields an even number. With this information, the period of the delivery cycle, the volume of the delivery cycle, and the size of the recoil , may be calculated.

The volume delivered is determined by calculating the number of shaded boxes as illustrated below in figures 5,15 and 5.16 , and multiplying this by the pipe area. In addition the volume associated with the remainder (dark shading) is also calculated as the product of the full period delivery, the velocity remainder and the pipe area.

Each block shown in Figure 5.15 has an area equal to the product of gh/a (velocity to achieve Joukowsky delivery head) and the wave propogation period 2l/a. To determine the volume of water, it is necessary to calculate the number of blocks.

If N is odd, observation provides the following number of blocks, and delivery period.

N	blocks	periods
1	0	1
3	2	2
5	6	3

This table can be used to determine a formula for delivery volume, where the number of blocks = $\frac{(N^2 1)}{4}$ and the number of delivery cycles = $\frac{(N+1)}{2}$, giving a formula for delivery

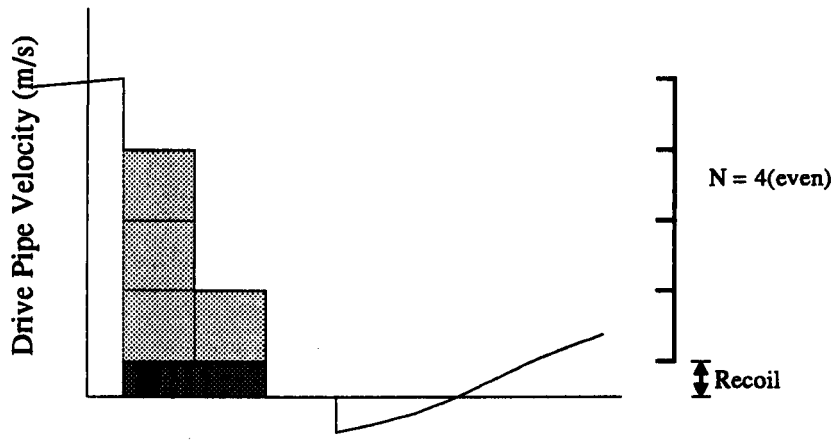

Figure 5.16 Mode 2

volume of :

$$Delivered\ Volume = \frac{(N^2 1)}{4}.\frac{gh}{a} + \frac{(N+1)}{2}.R \qquad (5.9)$$

Similarly for a "mode 2" delivery when N is even, the table for blocks and periods is:

N	blocks	periods
2	1	2
4	4	3
6	9	4

This yields a formula for delivered volume of:

$$Delivered\ Volume = \left(\frac{N^2}{4} \cdot \frac{gh}{a} + \frac{NR}{2}\right).\frac{2L}{a}.A \qquad (5.10)$$

where h = delivery head, R = remainder (diag) L = drive pipe length, A= pipe area, a=wavespeed.

These formulae are easily programmed into a spreadsheet environment, although there is need for logical statements to determine if the value of N is odd or even.

The accuracy of this delivery model is quite attractive, and allows quite simple calculation of recoil velocity, delivery period, as well as delivered volume. These values make up important

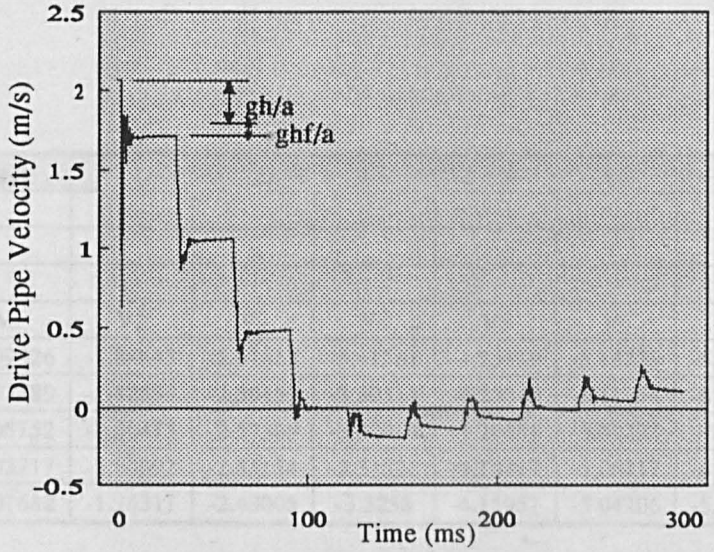

Figure 5.17 Simulated Velocity

components of the model to calculate total power of a hydraulic ram, and its beat frequency.

However, there remains a flaw in the described calculations that only becomes apparent with a high terminal velocity or high delivery valve restriction. Looking more closely at the simulated velocity trace for the delivery cycle in Figure 5.17 it is possible to see that the velocity drop associated with each step varies, decreasing with each step. According to the described theory, the first drop should be equal to gh/a, and thereafter to 2gh/a until the steps reach zero velocity. However, each step exceeds this value by a decreasing amount, and this has been found to be proportional to the square of the velocity and the delivery valve headloss coefficient.

This leaves a major problem for the creation of the model. An analytical solution of this would be highly complex, whilst ignoring it would only provide useful results under certain operating conditions. A solution was found to the problem by the use of a spreadsheet interactive environment.

5.8.3 Modelling of delivery Valve Losses

The spreadsheet environment allows the analyses of this complex behaviour to be undertaken in small steps. If a spreadsheet column is set up to represent the velocity after the first step down, at the beginning of the delivery cycle, a reasonable approximation of this velocity can be obtained using the formula:

	AA	AB	AC	AD	AE	AF	AG	AH	AI
1									
2									
3									
4	V0	V1	V2	V3	V4	V5	V6	V7	No Del.s
5	-0.36407	-1.09826	-1.84645	-2.61615	-3.41561	-4.25419	-5.14279	-6.09442	0
6	-0.34398	-1.07789	-1.82559	-2.59459	-3.39311	-4.23048	-5.11754	-6.06723	0
7	-0.32389	-1.05752	-1.80475	-2.57305	-3.37064	-4.20681	-5.09233	-6.0401	0
8	--0.30381	-1.03717	-1.78392	-2.55154	-3.34821	-4.18317	-5.06717	-6.01304	0
9	-0.28373	-1.01682	-1.76311	-2.43005	-3.3258	-4.15957	-5.04206	-5.98603	0

Figure 5.18 Velocity after each delivery step

$$Vo = V_T - \frac{gh}{a} - \frac{g\,(K_d(V_T - \frac{gh}{a})^2 A^2)}{a} \qquad (5.11)$$

where V_T = *the cutoff velocity in the drive pipe,* V_o = *the velocity after the first step down, and* K_d = *the head loss coeficient for the delivery valve (* $Hf = K_d Q^2$*).*

The formula determines the new velocity by calculating the velocity that would occur following a normal drop with no delivery valve friction, and then calculating the value of the delivery valve losses at this velocity. The further velocity drop associated with this extra frictional head is then calculated using Joukowsky again. For greater accuracy, it would be useful to undertake a series of iterations to determine the head velocity relationship for this frictional drop. However, for the sake of simplicity, a good approximation is obtained by assuming the above relationship in which the calculated head loss is determined using the cutt-off velocity less the standard velocity step gh/a.

As above, a column is set up to represent the velocity after the second velocity down step, and the formula for this is given as:

$$V_1 = V_0 - \frac{2gh}{a} - \frac{g\,(K_d(V_0 - \frac{2gh}{a})^2 A^2)}{a} \qquad (5.12)$$

The form of the equation (5.12) is the same as that of equation (5.11), but accounts for the double step down in velocity that occurs on all following steps (see velocity history). So similar columns are created for velocity step 3, 4 etc. If the velocity following the previous step down is smaller than 2 gh/a, the value of velocity calculated in the column will be below zero.

With these columns calculated, it is possible to determine the number of delivery cycles (row AI) that would occur if the cutoff velocity experienced was that represented by the given row.

This is determined by defining the column with nested "if" statements. Using the appropriate syntax, this checks columns V0, and if its value is below zero, the number of delivery cycles is given as 0. If however, the value is greater than zero, then column V1 is checked. If this value is smaller than zero, the number of deliveries is given as 1. If not, column V2 is checked;

and so on. The resulting column gives the number of velocity steps there would be in the delivery cycle if the valve shut at the velocity in the first column of the given row.

A similar set of nested "if" statements are then used to identify a column of delivered volume. Each "if" statement checks the value in the delivery cycle column, and gives a corresponding function to determine the volume of water such a cycle would deliver. These calculations are based on the calculated velocities after each velocity step down obtained from the velocity columns in Figure 5.18.

The two spreadsheet columns described provide the means by which the performance of a hydraulic ram can be predicted. The column describing the number of velocity steps can be used to predict the period of the delivery cycle, while the quantity delivered is the predicted output per cycle of the pump. Using the information in the previous sections it is possible to produce a performance characteristic for a given pump operating condition. To do this, it is necessary to know how quickly the impulse valve closes, as this is a period in which there is likely to be little acceleration, and the time delay involved will directly reduce the output power of the ram pump. Extensive analysis of the time for valve closure has been undertaken, but for an initial approximation, the valve closure time was assumed to be fixed.

5.9 Performance Characteristic.

Figure 5.19 is a performance characteristic for a hydraulic ram pump with a 50mm drive pipe, a 10m drive head, an 80m delivery head, and a 25 m drive pipe. Figure 5.19 is a graph produced directly from the described spreadsheet model. The left hand absisca refers to the power and throughflow curves, while the right hand abscissa refers to the efficiency and frequency curves. The valve characteristics used to determine the valve friction, and a typical valve closure time are taken from the D.T.U. Mk 6.4 valve.

The power curve is obtained by creating a column which divides the delivered volume by the cycle time, and to quantify power this is multiplied by the delivery head, the acceleration due to gravity, and the fluid density. The cycle time used in this situation is the summation of the acceleration time, the delivery time, the recoil time and the valve closure time.

This cycle time is also used to predict the frequency of the valve cycle given in the diagram.

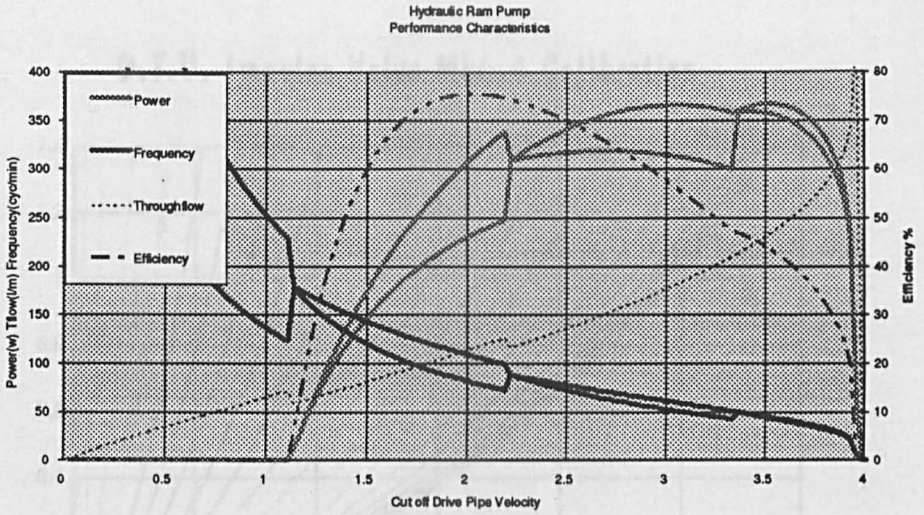

Figure 5.19 Pump Performance against Cut off Velocity

The graph gives the frequency of the hydraulic ram and its power as an area of operation. This accounts for the variation in recoil received. As explained earlier in this chapter, the recoil is calculated for each possible terminal velocity. However, due to the pressure drop caused by air travelling through the snifter and impulse valves, varying degrees of this recoil will be realised. The envelope creating the areas described is calculated assuming that this recoil is fully realised, and also that this recoil is not realised, so giving a range of possible performances.

To use the graph given, it is helpful to refer to a valve calibration chart such as that illustrated in Figure 5.20. This will give the velocity of the water in the drive pipe at the time of valve closure. This can then be used to define a position on the graph's ordinate of cut off velocity. It should be noted that it is at this abscissa value that the graph is most accurate. This is because the valve friction used to determine the pump characteristic is only correct for the given valve stroke, and this will give one cut off velocity.

The rest of the graph is therefore only a guideline to the operating range of the hydraulic ram pump, but it is the first time a global characteristic of this type that has been produced for the hydraulic ram. In terms of design, it can be used to identify the likely maximum power of a

pump, and the valve setting required to achieve it, as well as the the likely optimum efficiency.

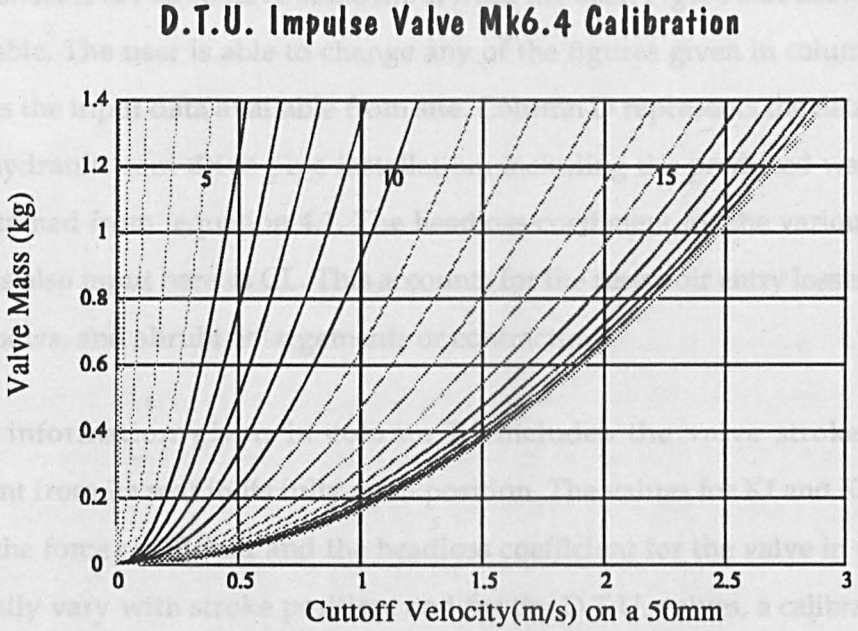

Figure 5.20

These are invaluable to any design process. However, the graph does need to be used in conjunction with the valve calibration chart. The calibration chart will enable a sensible range of strokes and valve masses to be deduced, and the likely cut off velocities these will produce. With this information, it is possible to input a valve setting for the model to use as a base value, and then to use the value of cut-off velocity to read the output graph shown in the graph in Figure 5.19

Using this procedure provides a means to predict the performance of hydraulic ram sites before installation. Although, a number of site variables are not accounted for, it will give a useful guideline for the designer.

5.10 Using the model

The spreadsheet is set up to have some input from the user. Figure 5.21 shows the layout for the input table. The user is able to change any of the figures given in columns B, D, and E. Column B is the input data available from site. Column D represents the data relating to the proposed hydraulic ram drive pipe installation, including the predicted wave propagation velocity obtained from equation 4.1. The headloss coefficient for the various fittings in the drive pipe is also input here as CL. This accounts for the reservoir entry losses, as well as any losses in elbows, and abrubt enlargements or contractions.

The valve information given in column F includes the valve stroke, which is the displacement from its seat in its fully open position. The values for Kf and Kh, are the input values for the force coefficient and the headloss coefficient for the valve in question. These values usually vary with stroke position, and for the D.T.U. valves, a calibrated function of stroke is put into these input cells. The headloss coefficient for the delivery valve is also input here, and this is assumed to be constant.

Finally, the mass of the impulse valve is input. Although this is not directly used in the spreadsheet calculations, it is needed to use the valve calibration chart, and also is used in a development of the spreadsheet in the following section.

	A	B	C	D	E	F
1	**Hydraulic Ram Pump Performance Model Input Data**					
2	SITE		DRIVE PIPE		VALVE	
3	Drive Head(m)	3	Diameter(mm)	50	Stroke(mm)	20
4	Delivery Head(m)	45	Pipe Length(m)	10	Kf	0.04
5			Rel' Rough(mm)	0.15	Kh	0.039
6			Wavespeed(m/s)	1350	Kdv	0.9
7			CL Fittings	2.06	Valve Mass (kg)	0.507

Fig. 5.21 Input Table for Model

Once the above data has been input, the spreadsheet is recalculated, and an output graph such as that in Figure 5.19 is produced. The designer is therefore able to predict the performance of a hydraulic ram site, and decide the number of pumps required, and therefore the cost and viability of a potential site. The lack of such a facility previously has severely hampered the wider adoption of the technology.

5.11 Valve Closure Modelling

The described spreadsheet model assumes that the time the impulse valve takes to close is fixed for a given valve geometry. However, studies on the impulse valve using the method of characteristics prove that this is not true, as there are significant variations in valve closure behaviour under different operating conditions. A fixed valve closure period assumes a fixed loss per cycle, and has a fixed reduction in power by reducing the cycle time by a fixed amount. If this fixed closure is inaccurate, variations in valve closure rates could have a significant effect on the accuracy of the model.

The spreadsheet model described is remarkable in its ability to determine a huge range of operating conditions with one range of calculations. Even in these calculations there is some inaccuracy associated with considering a single valve headloss coefficient for the whole range of possible closure velocities.

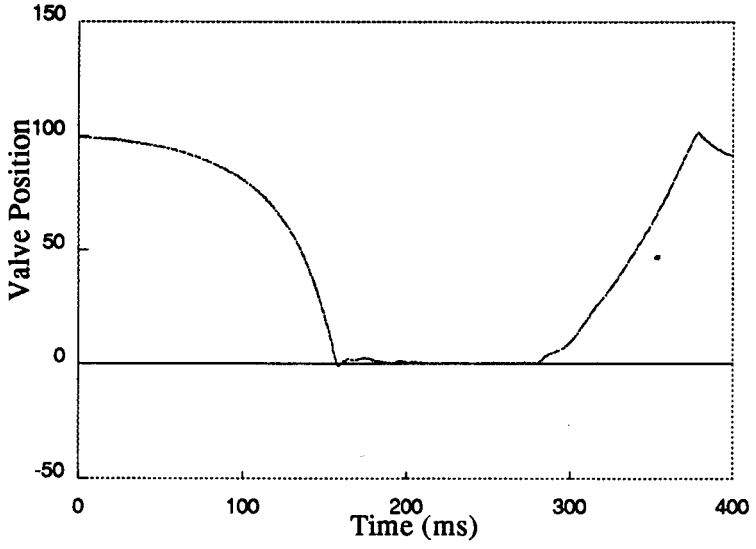

Figure 5.22 Valve Closure LVDT trace

A solution to the described inaccuracies has been obtained, but only by losing the

spreadsheet's remarkable ability to determine a range of operating conditions with only one set of calculations. The new model is able to determine only one operating condition, but with a significant improvement in accuracy.

Figure 5.22 shows a measured impulse valve closure for a hydram. The measurement was obtained using a displacement device based on a linear variable displacement transformer, and a high speed analogue to digital converter downloading to a personal computer. It is possible to see from this curve that 80% of the closure time is taken up by the first 75% of the closure sweep. For many valves including the impulse valve, positions between open and 75% closed do not create significant variations in head, so it should be possible to determine valve movement without having to resort to compressibility effects within this range of operation. This observation provides the basis for the production of the valve closure algorithm for the spreadsheet model.

The first part of the closure was modelled by using quasi-steady-state calculations. The spreadsheet model described in the previous sections, utilised a series of integrations with respect to fluid velocity. In order to incorporate a valve closure model, it is necessary to introduce a set of calculations and integrations with respect to time. This is done by creating a time series in a column of cells with very small time increments. The model uses the valve calibration equation (5.13) along with the input valve parameters to determine the drive pipe fluid velocity at which the valve closure would commence (equation 5.14). The main spreadsheet model is then used to determine the fluid acceleration and the friction factor in the drive pipe at this drive pipe velocity.

$$K_f = 5282.7\, e^{(1.862*X)} + 17.1304\, e^{(0.4459*F4)} + 4.7x10^{05}\, e^{(0.4459*F4)} + 0.0414 \quad (5.13)$$

$$V = \frac{\sqrt{M/K_f}}{A} \quad (5.14)$$

BJ	BK	BL	BM	BN	BO
Valve Closure Time Model					
Time	Fluid Velocity	Fluid Acceleration	Waste Volume	kh	kf
0.001	1.741	1.371	0.003418	0.0388	
0.002	1.742	1.371	0.006839	0.0388	

Figure 5.23

Knowing the acceleration of the fluid, and its velocity at the commencement of valve closure, it is simple to determine an approximate solution for the fluid velocity and acceleration after a small time period. To simplify the calculation, the friction factor calculated is assumed to stay constant during the closure period. However, the valve head loss characteristic varies significantly with stroke, and has a calibration equation similar in form to equation (5.13). This formula is used to calculate the reducing acceleration of the fluid column during the valve closure period. There is a delay in the increasing head loss coefficient of the valve taking effect due to the time taken for a pressure wave to travel in the pipe, this delay can be incorporated simply into the spreadsheet.

Using equation (5.13), it is possible to use the fluid velocity calculated at time zero to determine the force on the impulse valve, and the resulting acceleration. The velocity of the valve can then be determined after a small time period, and using simple equations of motion it is possible to determine the valve displacement at each time interval. The method used is identical to that adopted for the valve closure boundary condition in the method of characteristics simulation of the hydraulic ram pump described in chapter 4.

BP	BQ	BR	BS	BT	BU
VAccn	VVek	VDisp.			
0.0388	3.88E-5	19.9999			
0.0467	8.55E-5	19.9998			

Figure 5.24 Calculated Valve Parameters

The remainder of the columns making up the model incorporate these values of valve acceleration, valve displacement, and valve velocity, as shown in figure 5.24.

It should be stressed that the method adopted to simulate the delay caused by the propagating pressure waves is a very crude approximation, which avoids the need to simulate the pressure transients. For this reason, the model is only valid in the early stages of the closure where wave propagation time are insignificant as pressure changes are small.

This change to the model has been found to have a great effect on the accuracy of pump performance prediction. Section 5.13 shows correlation between experimental data and

5.12 Head reduction modelling

The described model has been used in connection with a number of water supply installations. One of the problems associated with a set of schemes using particularly high supply heads was that of the impulse valve often failed to reopen. This is a problem particularly experienced in the D.T.U.'s Rwanda schemes.

The problem arises because the recoil velocity at the end of the hydram cycle does not create enough of a downward pressure transient to overcome the static head provided from the supply reservoir, and so the valve is unable to reopen. It would be helpful to use the model to predict under what conditions this failure would occur, but in order to do this, a very accurate calculation of the recoil velocity is required.

The delivery model described in section 5.8.2 calculates every incremental velocity change occuring in the drive pipe in terms of the delivery pressure. To attain the delivery pressure, a velocity drop of a magnitude proportional to the pressure rise is required. In the previously described model this pressure rise was taken to be the summation of the delivery head and the head loss through the impulse valve. The actual pressure rise required will in fact be less than this, because the pressure in the drive pipe before the closure will not be atmospheric.

The assumption that it would be atmospheric would not usually cause unacceptable results except when the supply heads are high. However, the accuracy of calculating velocity drops is very important for determining exactly the recoil velocity induced after the delivery valve closure. If the initial recoil velocity is known, the ensuing pressure drop, assuming it is realised, could be predicted. If this pressure drop does not exceed the supply head in magnitude, the impulse valve may not reopen.

In this way, the model can predict valve settings at which the pump would fail to operate, and so avoid a potentially costly installation.

5.12.1 The method used for head reduction modelling

In chapter 2 there is a detailed account of the hydraulic ram pump's delivery cycle. To undertake the more accurate prediction described above, it is necessary to work through this account.

1) At valve closure, the velocity in the drive pipe drops by a quantity sufficient to attain a pressure equal to the delivery pressure. And this pressure-velocity transient travels up the drive pipe to the reservoir at which there is reflection. This reflection induces a further drop in velocity, and a return to atmospheric pressure. This velocity-pressure wave then propagates down the drive pipe.

Prior to valve closure, the pressure of the fluid in the drive pipe is approximately atmospheric. It in fact exceeds atmospheric pressure by the head loss through the impulse valve. This assumes that the impulse and delivery valves are at the same physical level. The initial velocity drop is calculated as being the velocity drop associated with a pressure rise equal to the delivery head minus the residual pressure in the drive pipe. This differs from the previous model in that the previous velocity drop was taken as that associated with a pressure rise equal to the delivery pressure. This refinement means the remaining velocity is greater than previously calculated.

2) When the reflected wave reaches the delivery valve, it brings with it both a pressure drop, and a velocity drop equivalent to the previous drop. This causes the delivery valve to close. This in turn induces a pressure rise to reopen the valve. The velocity drop associated with this pressure rise is equal to that required to raise the drive pipe pressure to the delivery pressure. This is calculated with the modified model as the delivery head less the supply head, accounting for friction losses in the drive pipe.

3) This new condition is maintained while the pressure transient travels upstream in the drive pipe. On reaching the reservoir, there is again a reflection as before. This gives an additional velocity drop, and normalizes the drive pipe pressure with respect to the drive tank.

The described chain of velocity drops is illustrated in figure 5.25. It can be seen in this diagram that there is an equivalent velocity drop associated with each velocity drop, but delayed by a single wave reflection period.

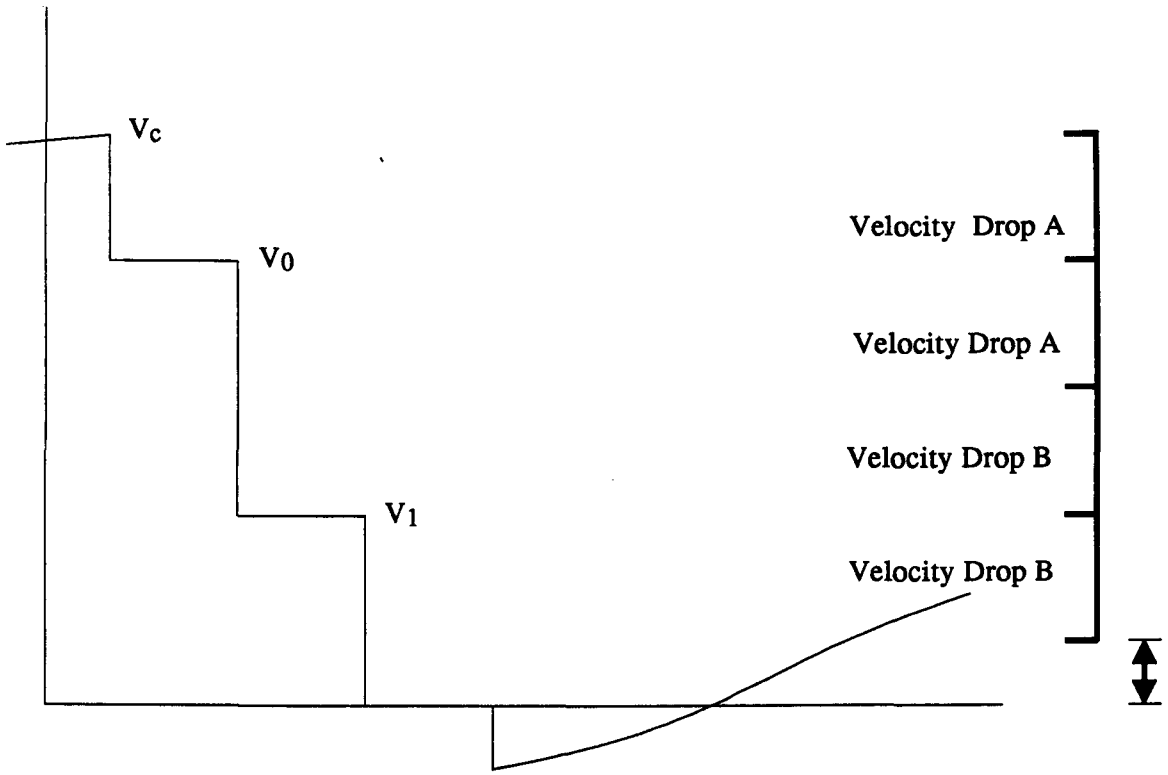

Figure 5.25 Head Reduction Delivery Modelling

Observing the notation on the Figure 5.25 It can be seen that:

$$Velocity\ drop\ A = Vc - V0 \qquad (5.15)$$

and therefore:

$$Velocity\ drop\ B = V0 - V1 - (Vc - V0) \qquad (5.16)$$

which simplifies to

$$Velocity\ drop\ B = Vc + 2V0 - V1 \qquad (5.17)$$

and similarly the following velocity drops are:

$$Velocity\ drop\ C = +Vc - 2V0 + 2V1 - V2 \qquad (5.18)$$

$$Velocity\ drop\ D = -Vc + 2V0 - 2V1 + 2V2 - V3 \qquad (5.19)$$

$$Velocity\ drop\ E = +Vc - 2V0 + 2V1 - 2V2 + 2V3 - V4 \qquad (5.20)$$

$$Velocity\ drop\ F = Vc + 2V0 - 2V1 + 2V2 - 2V3 + 2V4\ V5 \qquad (5.21)$$

This series is useful in the calculation of the velocity after each step of the delivery cycle. These are calculated using the following formulae.

$$V_2 = V_c - 2V_0 + 2V_1 - \frac{g(h - H - \frac{flV_1^2}{2dg})}{a} - \frac{g(K_dA^2(V_1 - \frac{2gh}{a})^2)}{a} \qquad (5.22)$$

When n is even:

$$V_n = V_c - 2V_0 + 2V_1 - 2V_2 \ldots\ldots - 2V_n - \frac{g(h - H - \frac{flV_{(n-1)}^2}{2dg})}{a} - \frac{g(K_dA^2(V_{(n-1)} - \frac{2gh}{a})^2)}{a} \qquad (5.23)$$

When n is odd:

$$V_n = -V_c + 2V_0 - 2V_1 + 2V_2 \ldots\ldots + 2V_n - \frac{g(h - H - \frac{flV_{(n-1)}^2}{2dg})}{a} - \frac{g(K_dA^2(V_{(n-1)} - \frac{2gh}{a})^2)}{a} \qquad (5.24)$$

This set of equations provides a much more accurate means for detecting the level of each of the velocity steps, and so allows a much greater accuracy in the prediction of recoil. This is of great value to any studies involving the prediction of valve reopening failure.

5.13 Accuracy of the model

The model can be seen to be complex, and unfortunately the facility to measure each stage of modelling is highly limited. This is primarily because of the short times involved. Some validation of aspects of the model have been undertaken using high speed data sampling methods, but this is mainly restricted to valve movement and pressure changes; both of which allow "instantaneous" measurement, and high speed sampling.

The model does much of its calculation using fluid velocities. In order to ascertain the behaviour of instantaneous velocities, it has been necessary to resort to the method of characteristics simulation.

It is possible to correlate output from the model with experimental data. The graphs in Figures 5.26 to 5.31 show modelled data alongside experimental data for the D.T.U. Mk 6.4 pump. The graphs show a good correlation between the results, although they give a consistently higher reading for pump output than experimental results. It can be seen that there is a good correlation on all of the graphs. The graphs test the hydram model over a comprehensive range of typical settings. The graphs show the delivery flow obtained from the hydraulic ram pump with a fixed drive head across an array of valve settings. These are fundamentally two weights; a standard unweighted valve, and a valve incorporating a single weight. The data shown is given for three valve settings 10mm, 15mm and 20mm. The Figures 5.26 to 5.31 show a curve to represent the data predicted by the model, and the crosses represent experimentally obtained data. The curve shows the output from the model that assumes a full recoil is realised, and accounts for the full delivery cycle prediction described in section 5.12.

The Figures demonstrate that there is an excellent correlation across the whole range of pump operation, and suggest the model could therefore be used with acceptable reliability to predict pump performance beyond the described range. However, it is apparent that the predicted flow is usually higher than that obtained in experimental measurement. A likely cause of this is an additional loss associated with the delivery valve.

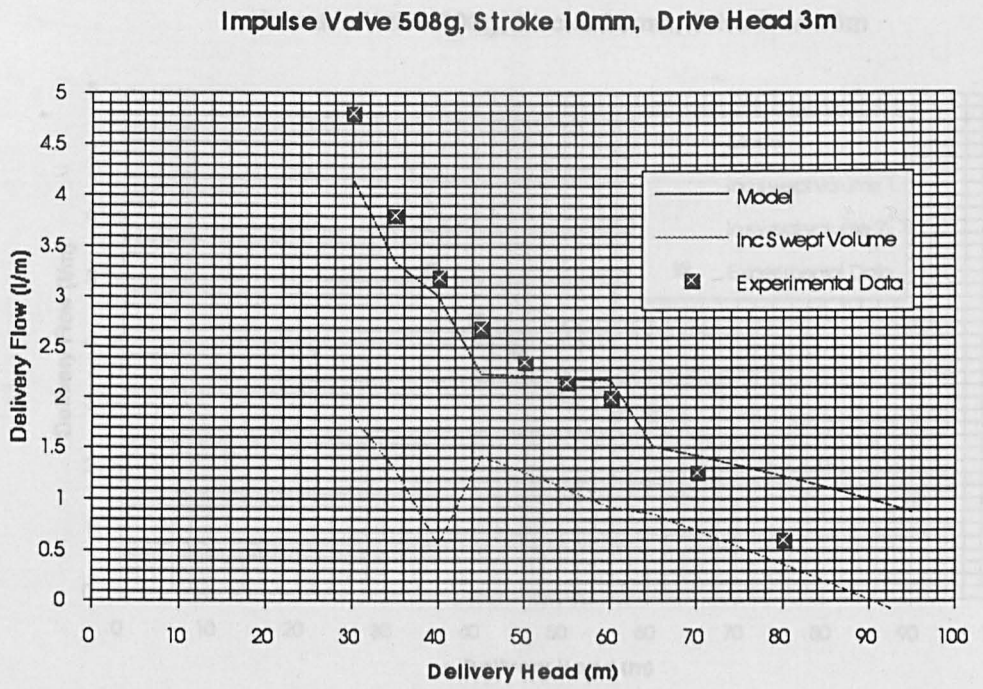

Figure 5.26

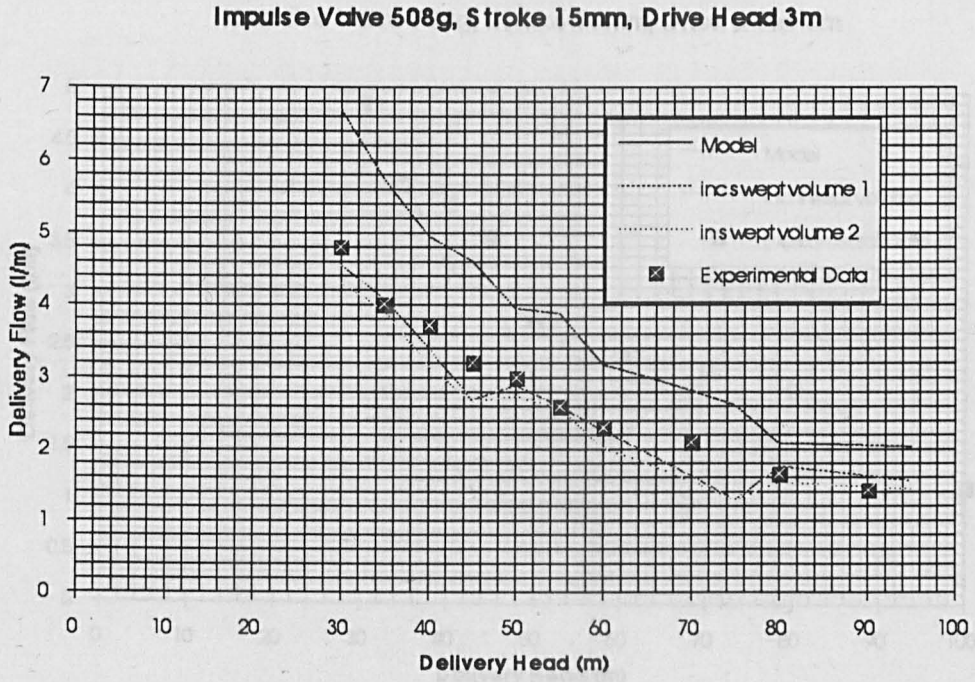

Figure 5.27

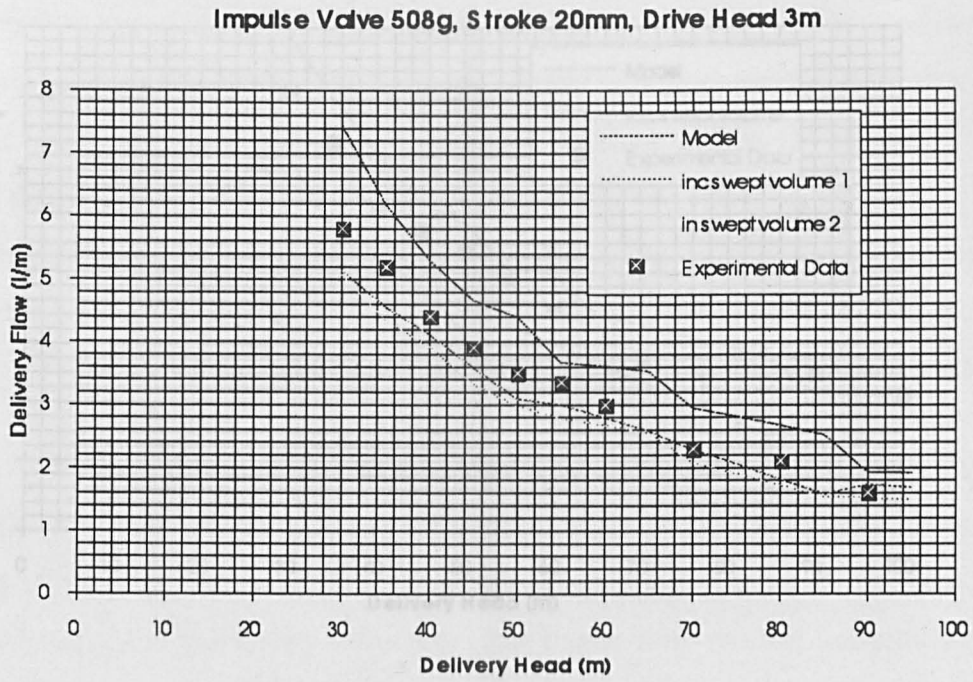

Figure 5.28

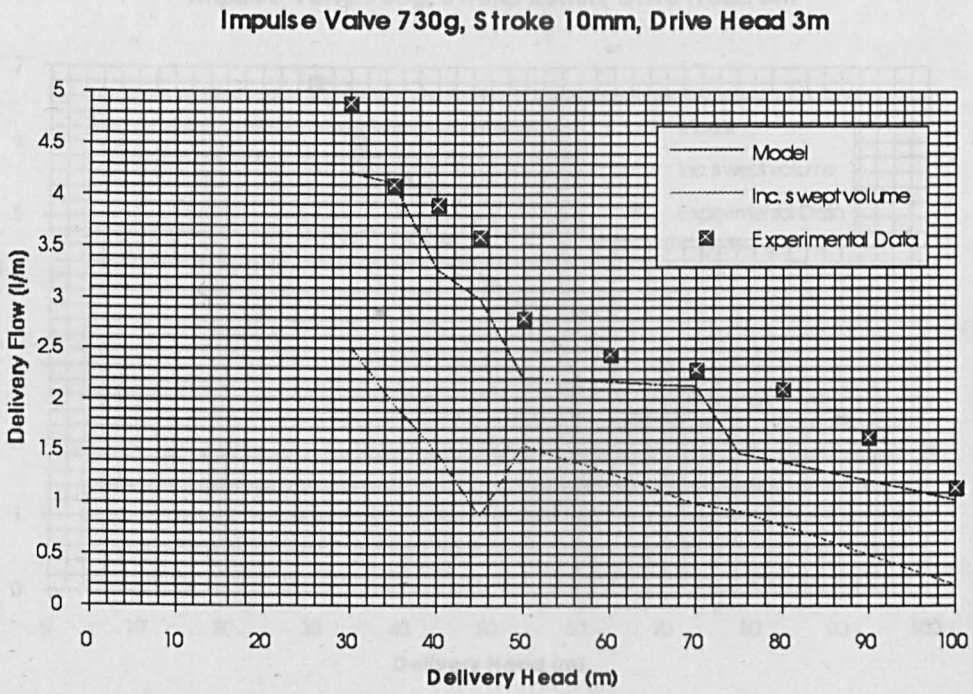

Figure 5.29

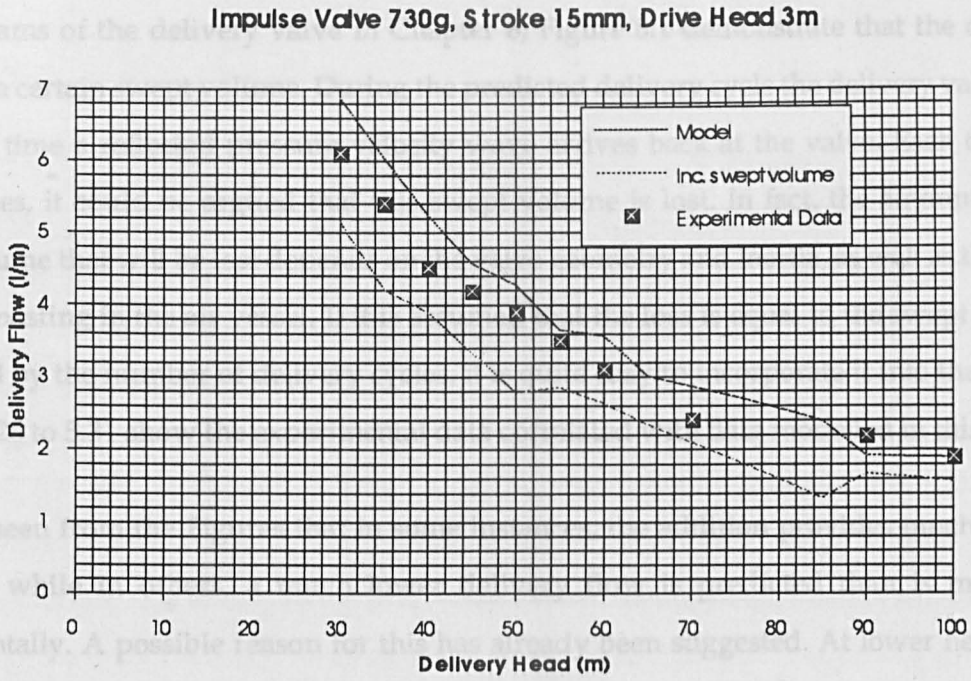

Figure 5.30

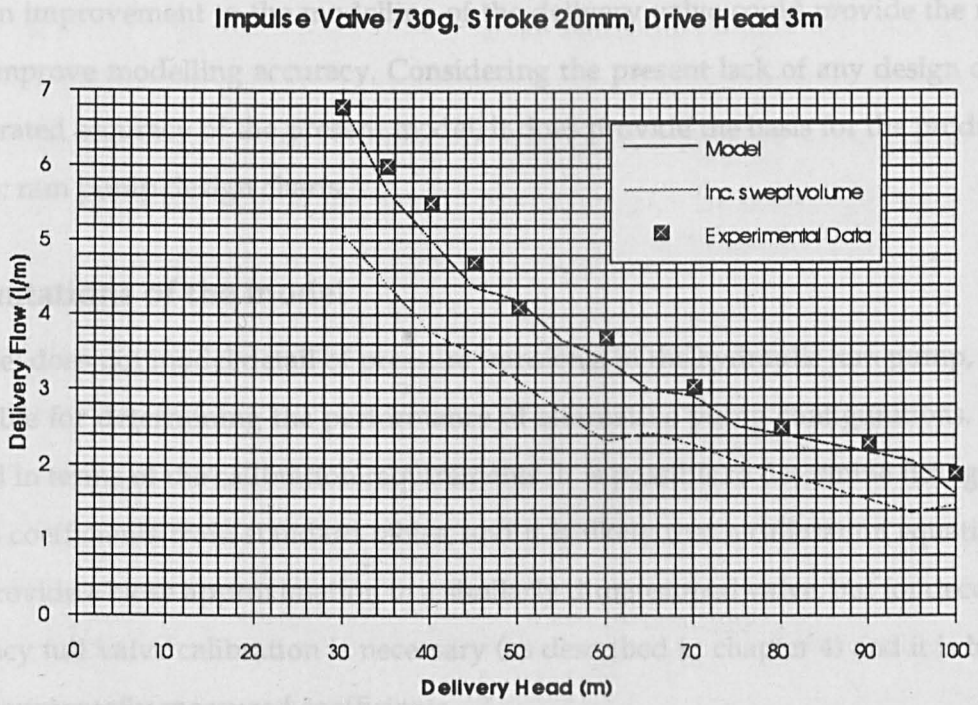

Figure 5.31

The diagrams of the delivery valve in Chapter 8, Figure 8.1 demonstrate that the delivery valve has a certain swept volume. During the predicted delivery cycle the delivery valve may shut each time a reflected pressure velocity wave arrives back at the valve. Each time the valve closes, it could be argued that this swept volume is lost. In fact, the amount of this swept volume that will be lost depends on the valve geometry and inertia, as well as the static pressure existing in the air vessel. If it is assumed that the loss is equal to the swept volume multiplied by the number of delivery cycles, it is quite easy to incorporate it into the model. Figures 5.26 to 5.31 show the experimental data correlated with data modelled in this way.

It can be seen from the Figures that in some instances, the addition provides much greater accuracy, while in others, a much lower delivery flow is predicted than is measured experimentally. A possible reason for this has already been suggested. At lower heads, the return characteristic of the valve may allow it to close before flow reversal, so reducing the quantity lost. In addition to this, at lower drive pipe velocities, the initial delivery velocity will be much reduced, and so the sweep of the valve will also be reduced.

These observations, along with the evidence in figures 5.26 to 5.31 suggest that although the simple model of the delivery valve is not suitable to improve the accuracy of the whole model, an improvement to the modelling of the delivery valve could provide the means to further improve modelling accuracy. Considering the present lack of any design data, and the illustrated accuracy of the present model, it does provide the basis for the production of hydraulic ram pump design charts.

5.14 Limitations of the model

The model does not model detail of pressure transients in the hydraulic ram pump, and so is not suitable for determining the performance of alternative pump configurations. It is also restricted in terms of the calibration requirements. It is possible to determine fitting loss and pipe loss coefficients from standard tables, and it is likely that a calibration equation given would provide a close approximation to a similarly dimensioned valve, but for decent levels of accuracy full valve calibration is necessary (as described in chapter 4) and it is helpful to have experimentally measured coefficients.

5.14.1 Delivery Valve Modelling

It has been observed that the behaviour of the delivery valve can severely affect the performance of a hydraulic ram pump. An attempt has been made in the prediction model to account for its behaviour. In figure 5.26, it can be seen that the correlation between the measured hydraulic ram pump data, and that predicted by the model diverge at higher heads and at certain stroke settings.

The reason for this divergence is believed to be directly related to the operation of the delivery valve. The behaviour of the delivery valve will vary depending on its inertia, and its mode of operation. It is anticipated that a volume approximately equal to this stroke volume is lost every time the delivery valve closes. It is this loss, that accounts for the divergence between modelled data.

It has been observed using simulation that the delivery valve closes at the end of each velocity step associated with the delivery period, see chapter 2. During experimental work, a flapping of the delivery valve during the delivery period has been observed using a transparent air vessel surface. The degree of this flapping will depend on the ease with which the valve surface moves, and the force causing it to close and reopen. The force causing it to close is provided by the delivery pressure, and so the speed and degree of closure will be directly proportional to this delivery pressure. The force causing the valve to open, and the degree of opening is directly proportional to the velocity in the drive pipe that induces the pressure rise that enables the pump to deliver.

To illustrate the above, it is valuable to consider the stages of the delivery experience by the delivery valve. The impulse valve induces a large upward pressure transient, which in turn causes the delivery valve to open. The degree of opening is dependent to a degree on the velocity of the flow through the valve, as this will create drag forces that may or may not take the valve through its full travel. Once the velocity and pressure normalises in the drive pipe, the delivery valve will start to close. The speed and degree to which the closure occurs will be proportional to the delivery pressure. The remaining velocity in the drive pipe is then translated to a second pressure rise which causes the delivery valve to reopen again, but again to a degree proportional to the lower flow in the second cycle. This process continues,

throughout the delivery cycle. It is possible that the degree of wastage could decrease on each cycle.

An additional effect may become important at low delivery heads. If the delivery valve has some return mechanism over and above that of reverse flow, such as gravity or elastic behaviour, it is conceivable that some of the stroke volume would be forced out of the way on the return stroke, and so would not be wasted by returning to the drive pipe.

Chapter 6: Hydraulic Ram Pump Design Charts

The need for design charts for Hydraulic Ram Pumps has been identified by a number of authors (see quotes on page 1.4 and 1.5). A major product of this research was the provision of design charts for the D.T.U. hydraulic ram pump, but more importantly to identify suitable means to calibrate hydraulic ram pumps, and guidlines on the provision of design charts hydraulic ram pumps generally.

This chapter will introduce the main forms of hydraulic ram design charts produced for the D.T.U. hydraulic rams, and describe the use of these charts. It is hoped that these will be adopted by other manufacturers as standard forms so that the task of the water engineer may be simplified.

6.1 Acceleration Efficiency Chart.

In many hydraulic ram installations, the energy loss in the drive pipe represents the most significant aspect of the overall losses in the pump, and therefore, good design of the drive pipe characteristic is important. Head losses in the drive pipe are proportional to the square of the velocity, and so energy losses will be proportional to the cube of the velocity. In contrast, the Joukowsky pressure rise is directly proportional to the velocity in the drive pipe. Head losses are also directly proportional to the drive pipe length For a given hydraulic ram installation it would be valuable to have an indication of the limits on drive pipe length and internal velocity for the purpose of system selection.

Chapter 5 described the use of the predictive model for the creation of an acceleration chart. An example of one of these charts is given in Figure 6.1. It can be seen from this chart that if a terminal velocity of 1.5 m/s is required a 14 m drive pipe will offer an acceleration efficiency of 71.5%, whilst a 6m drive pipe will give an acceleration efficiency of 85%. This chart is clearly of value in optimising hydraulic ram systems, but is unusable in isolation. The chart represents the acceleration efficiency for a drive pipe of 50mm diameter, utilising a 3m drive head, and assuming the D.T.U. Mk 6.4 valve with a stroke setting of 20mm for valve head losses. Many more charts will be required for different supply heads, and possibly for different diameters.

In addition to this it would be helpful to be able to interpret the final fluid velocity in terms of an impulse valve setting.

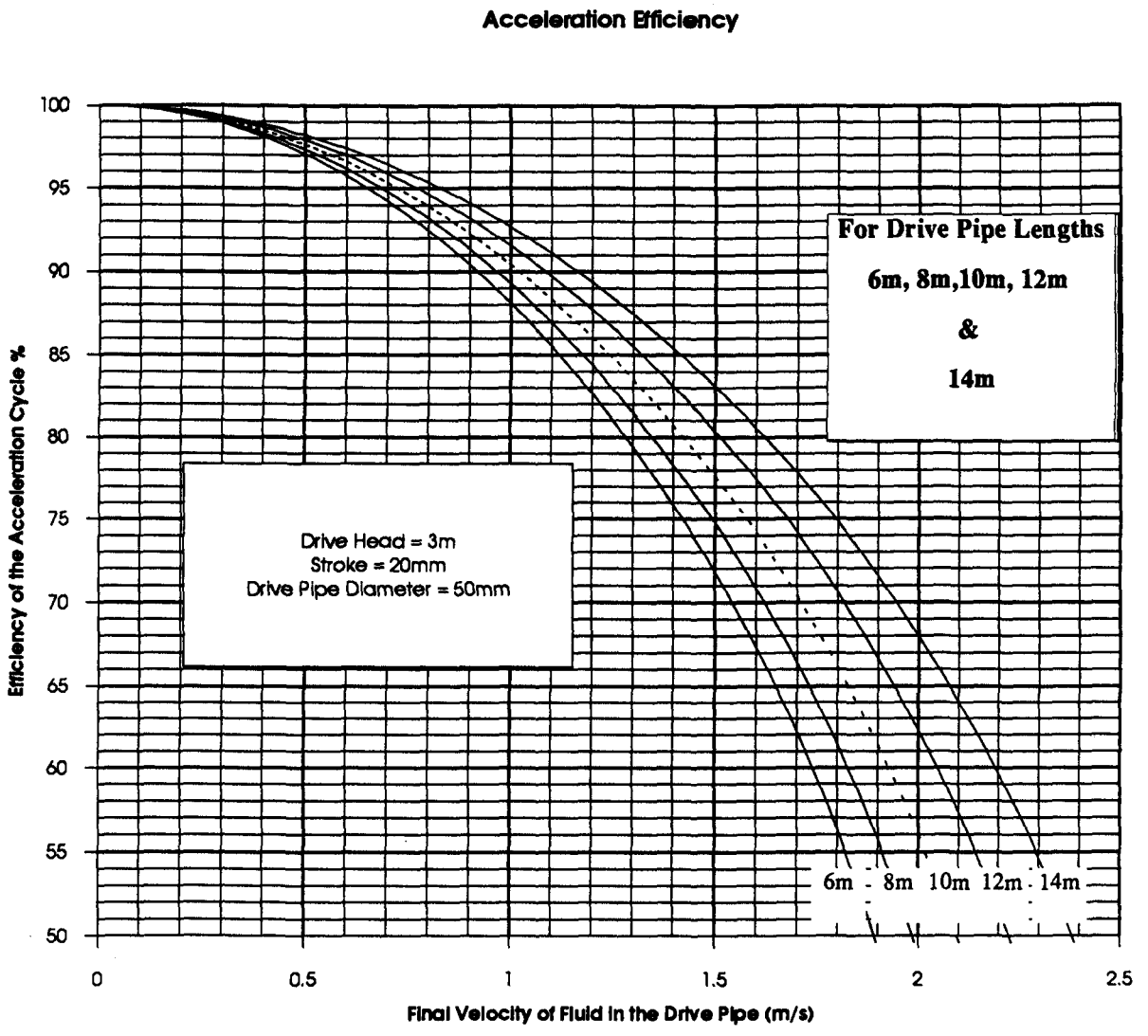

Figure 6.1 Acceleration Efficiency

6.2 The Impulse Valve Calibration Chart

An example of the author's impulse valve calibration chart is given in Figure 6.2. This chart does not give the fluid velocity at the final closure of the valve, but does provide an indicator of this. It represents the force experienced on the valve at a given fluid velocity in different drive pipe diameters. For a given valve mass, therefore, it gives the fluid velocity at which valve closure commences. This is a valuable indicator of valve behaviour, and can be used alongside the acceleration efficiency to design hydraulic ram systems.

For example, if we have a D.T.U. Impulse Valve with a mass of 0.4 kg and stroke of 20mm, it is possible to determine from this chart that the valve will commence closure at 1.5m/s fluid velocity in a 50mm drive pipe, it is then possible to determine the significance of the acceleration cycle on the efficiency of such a pump, using the acceleration chart.

It is likely that every valve manufacturer will have a minimum drive pipe length for a given impulse valve design. This should be considered in conjunction with the two charts (Accleration Figure 6.1, and Valve Calibration Figure 6.2), in the choice of an acceptable system.

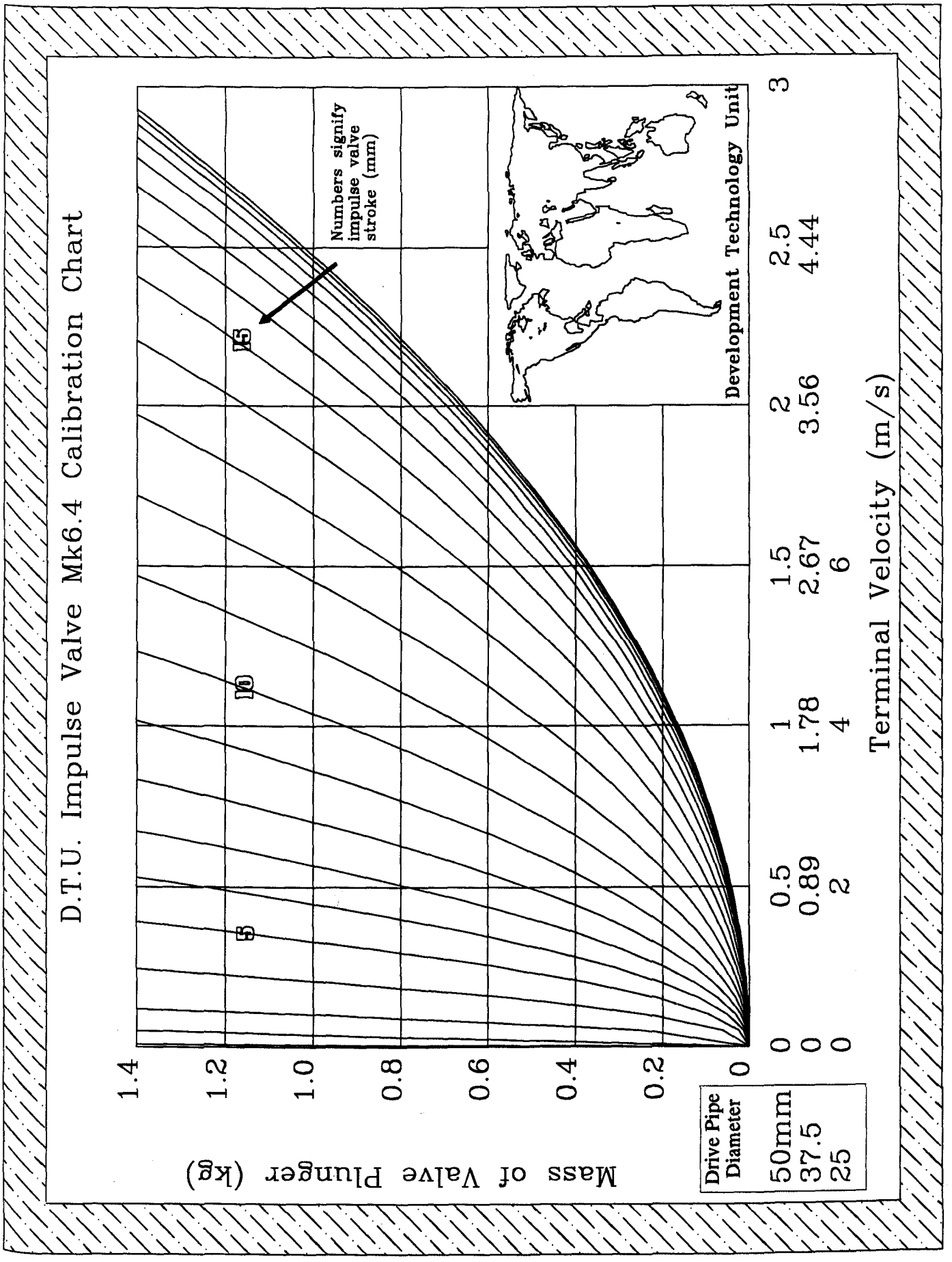

Figure 6.2 D.T.U. Mk 6.4 Valve Calibration Chart

6.3 Overall Pump Operation Chart

If from the data given in the previous charts, a hydram system with a 3m drive head, and a 10m drive pipe of 50mm diameter were chosen, it would be helpful to have a guideline as to the range of operation of the given hydram. This is obtainable directly from the predictive model described in chapter 5. The model will give the predicted performance of the ram pump for a range of different operating strokes. From the chart given in FIgure 6.3, obtained directly from the model, it is possible to choose the stroke setting for a given mass of valve in order to optimise the efficiency or power of the given hydraulic ram pump, operating on a given drive head.

The shaded marker on the abscissa indicates strokes at which the impulse valve is unlikely to reopen on account of insufficient recoil velocities.. From the chart below it can be seen that for maximum efficiency a stroke of the order of 9mm would provide the maximum pump

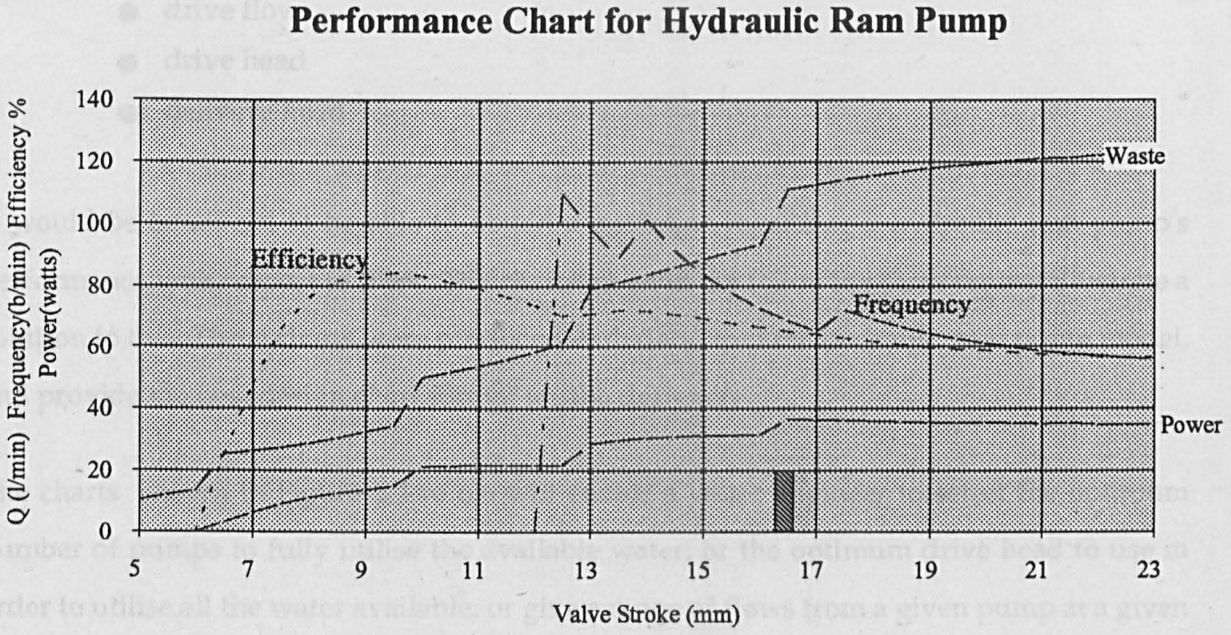

Figure 6.3 Pump Tuning Chart

efficiency while a stroke of 17mm would provide the maximum delivery power. To achieve maximum power it would probably be prudent to adopt a stroke of 19mm to ensure valve reopening occurs..

There are a large number of charts of this type reproduced in Appendix I. Each chart represents a given hydraulic ram setup, and associated with each, the model provides a chart describing the ratio of waste and delivered flows. These charts are most useful if they represent an actual installation as interpolation between charts is difficult, and unreliable. The production of a large number of such charts is obviously less than ideal, and the direct use of the model would be more useful.

Although the detail of the illustrated chart is attractive, a more widely applicable design chart would be beneficial.

6.4 Hydraulic Ram Pump Flow Charts.

A water engineer proposing a hydraulic ram pump sytem will generally have a number of fixed parameters. Typically these will include some of the following:

- delivery flow
- drive flow
- drive head
- delivery head

It would be beneficial to be able to obtain a guideline regarding a hydraulic ram pump's performance with respect to these. The charts given in the following three figures illustrate a solution to this. These charts were produced with data from the hydraulic ram pump model, and provide the best design chart format for the designer.

The charts shown in Figure 6.4 to 6.6 will enable a water engineer to select the optimum number of pumps to fully utilise the available water; or the optimum drive head to use in order to utilise all the water available; or give a range of flows from a given pump at a given head. The data in these charts is clearly in an ideal form for a design engineer. This is particularly so on account of the symmetry within the charts which allow for easy and reliable interpolation.

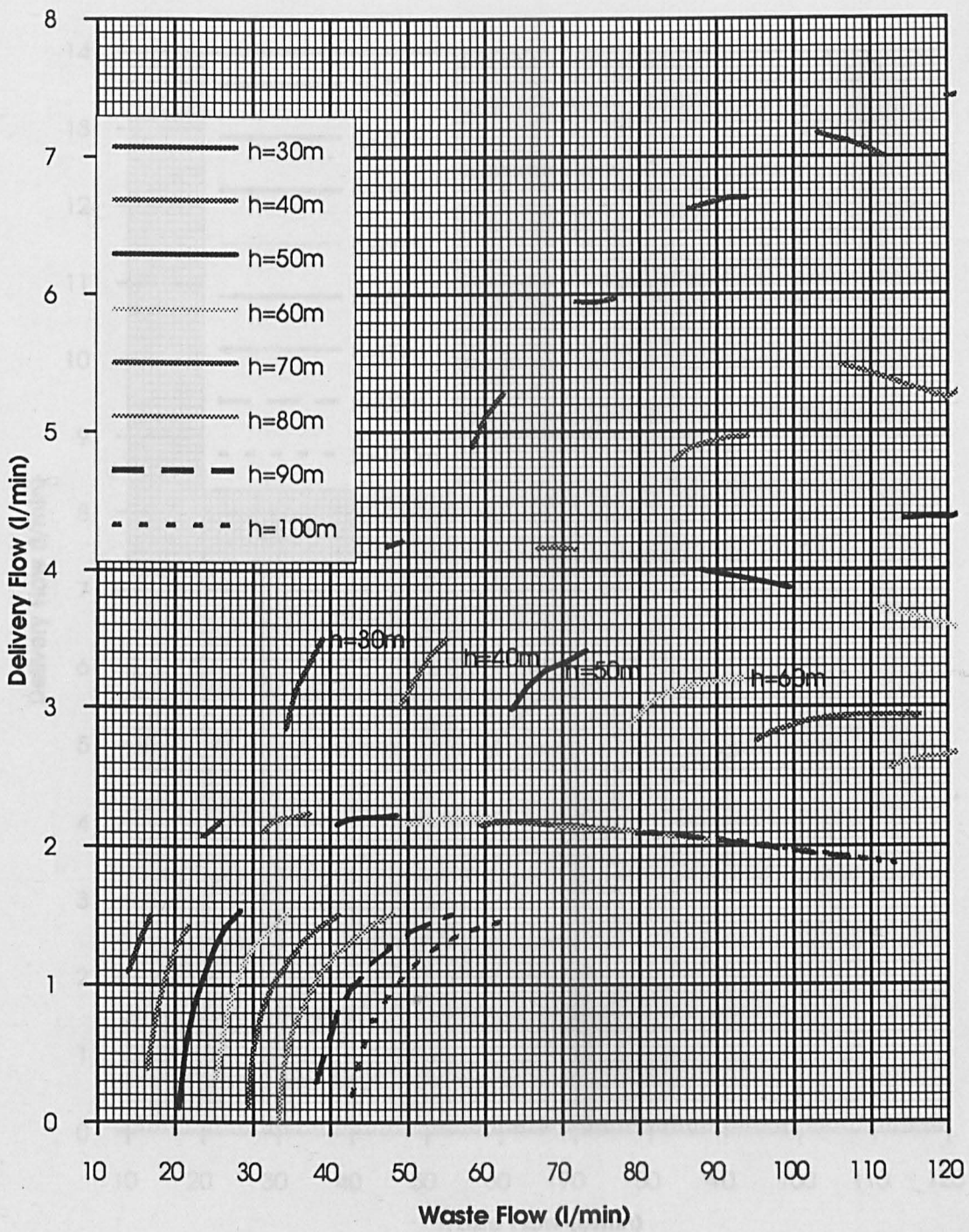

Figure 6.4 Flow Chart for 3m Drive Head

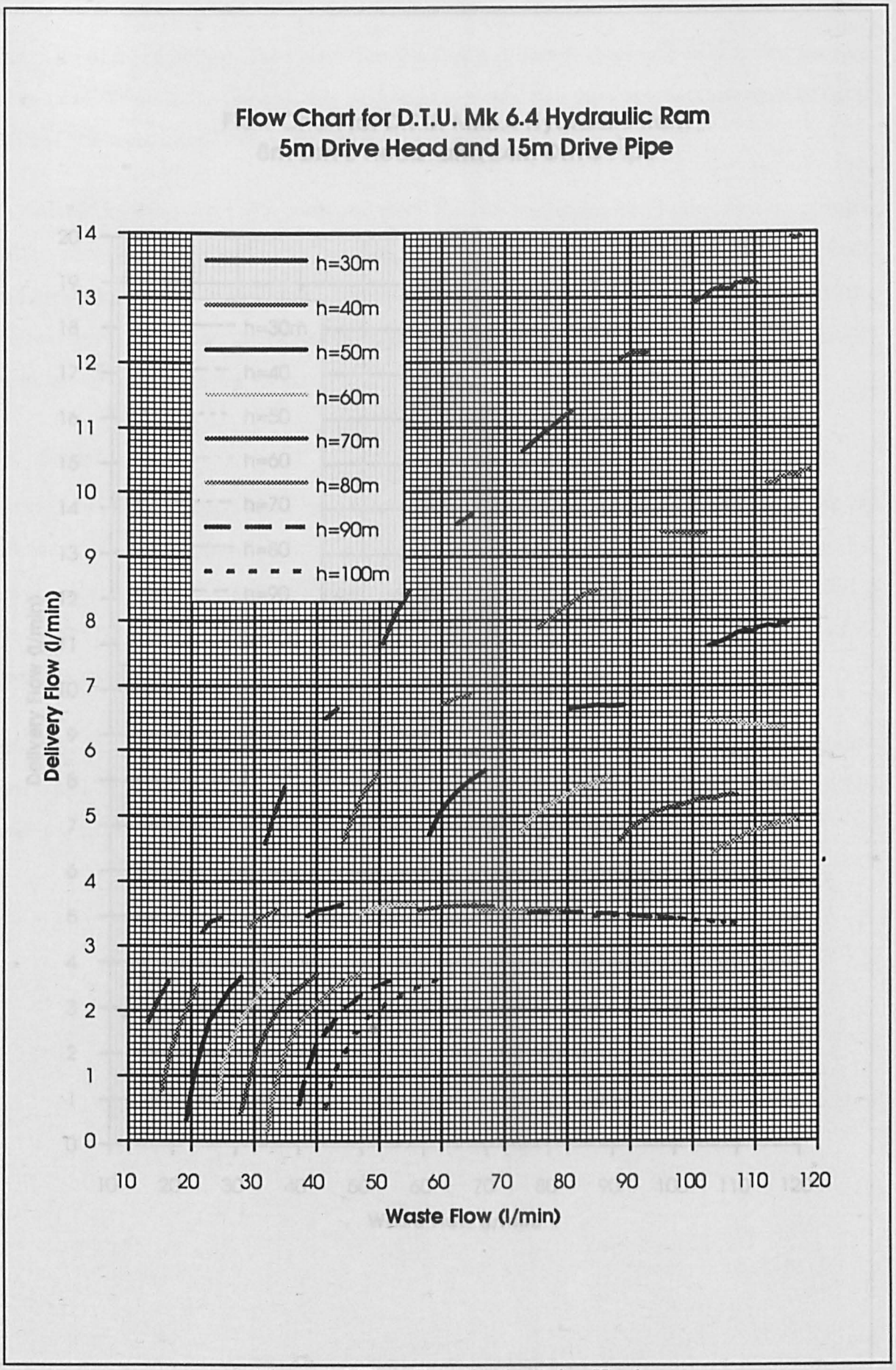

Figure 6.5 Flow Chart for 5m Drive Head

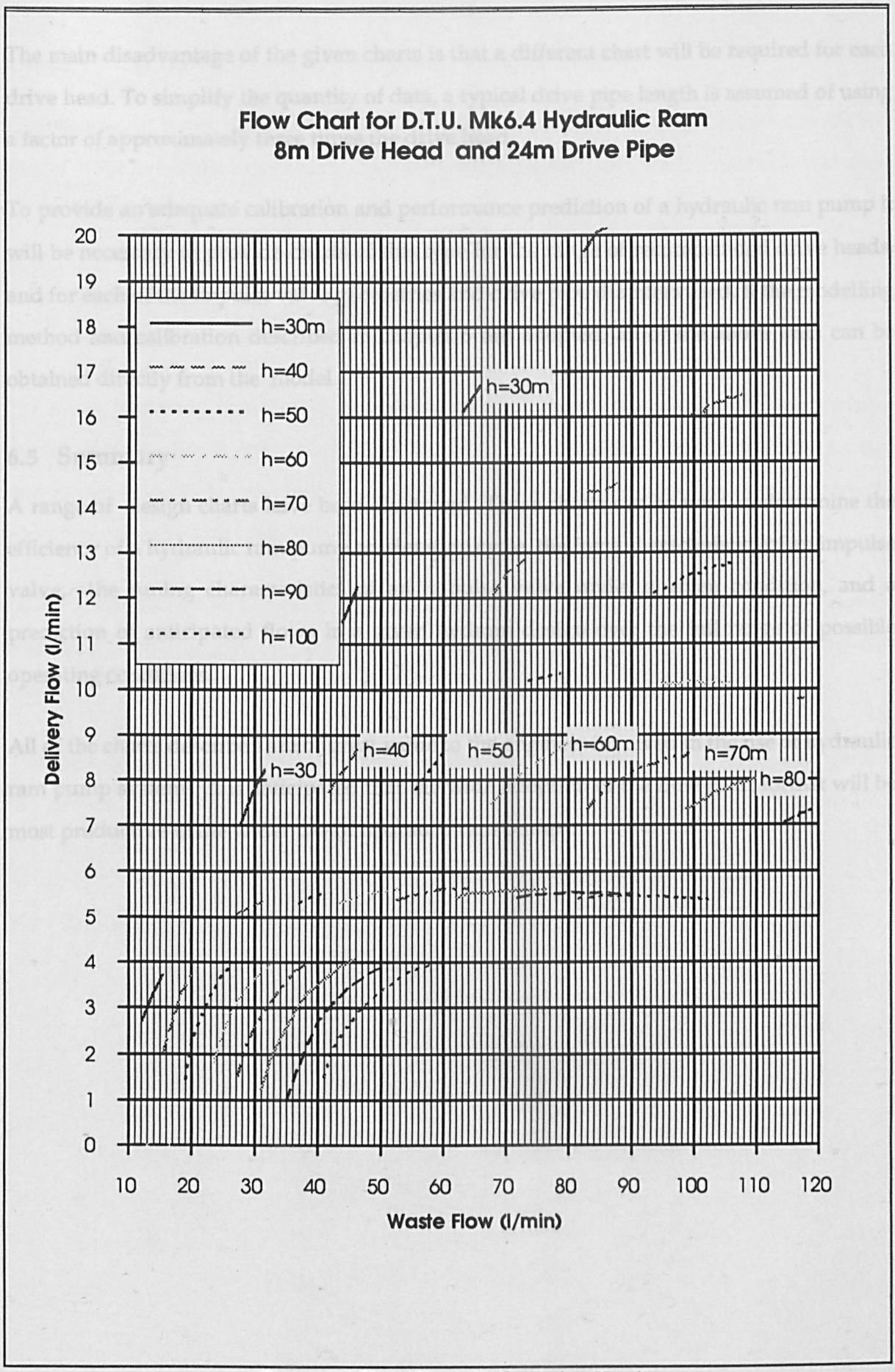

Figure 6.6 Flow Chart for 8m Drive Head

The main disadvantage of the given charts is that a different chart will be required for each drive head. To simplify the quantity of data, a typical drive pipe length is assumed of using a factor of approximately three times the drive head.

To provide an adequate calibration and performance prediction of a hydraulic ram pump it will be necessary to provide charts of this type for the range of recommended drive heads, and for each of the impulse valve geometries and drive pipe diamters used. If the modelling method and calibration described in chapter 5 are adopted, all of the above data can be obtained directly from the model.

6.5 Summary

A range of design charts have been illustrated. These charts can be used to determine the efficiency of a hydraulic ram pump acceleration cycle, the force characteristics of an impulse valve, the tuning characteristics of an impulse valve under a given condition, and a prediction of anticipated flows in a given hydram design over the full range of possible operating conditions.

All of the charts described are of great value to the engineer involved in the use of hydraulic ram pump systems. It is anticipated that the wide adoption of the flow chart format will be most productive in the wider use of hydraulic ram pumps.

Chapter 7: Other Hydraulic Ram Pump Designs.

Chapters 4 and 5 describe in detail the steps taken to provide a simulation and a predictive model of the hydraulic ram pump. Chapter 6 then proceeds to discuss the production and use of design charts. It is anticipated that the procedures discussed are directly applicable to the majority of hydraulic ram pumps currently manufactured. It is also hoped that other manufacturers of Hydraulic ram pump designs will be able to adopt the methods, and offer a relatively standard means for specifying hydraulic ram performance.

For many hydraulic ram designs, it is possible to reproduce the calibration procedures described in chapter 4. For some designs however, this will present problems. There are two designs particularly which are very widely deployed but have impulse valve operations the differ significantly from the D.T.U.Mk 6.4.

The rubber disc valve has been very widely used by Blake of the U.K. This pump uses a distorting rubber disc to cyclically shut off the flow in the drive pipe of the hydram (see Figure 7.1).

The rotating valve has been adopted by a number of manufacturers world wide, and operates in a similar way to the D.T.U. valve but differs in that it is restrained on one pivoting position. This makes the valve close in an arc shape (see Figure 7.3).

7.1 The rubber disc (BLAKE) impulse valve

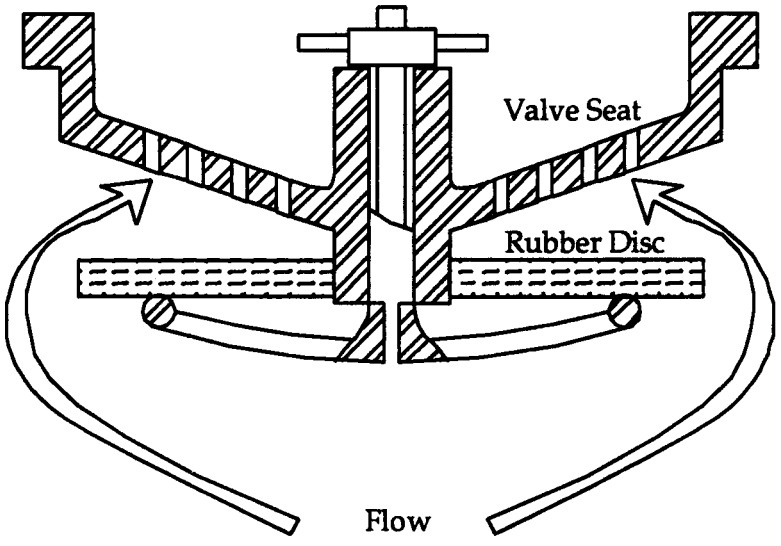

Figure 7.1 Rubber Disc Impulse Valve

Figure 7.1 illustrates the rubber disc valve manufactured by Blake. A rubber disc is supported at an adjustable distance from an impulse valve seat. As flow passes through the valve, the rubber disc experiences drag forces which act to distort the rubber disc. At a certain flow, the rubber disc is distorted to a degree which causes the drag forces to increase significantly. This will result in more rapid distortion of the valve, and ultimate valve closure.

This type of impulse valve has many attractive attributes, and is very widely used by Blake Pumps. In order to calibrate a valve like this, it is necessary to know the distorting force imposed by the water flowing past the disc, and also the bending characteristic of the disc. To determine the bending behaviour of the disc it will be necessary to use some geometric integration. This may have to be simplified to allow a single parameter to be used to represent the degree of valve opening. This impulse valve does represent the most complex type for calibration, as the closure motion is partially angular, and partially linear. The simplification will probably absorb the linear movement into an angular equation.

To determine the force on the valve under any operating conditions presents severe problems . During the closure of an impulse valve, its head loss and drag characteristics vary greatly. It is necessary therefore to determine what these characteristics are under steady state operating conditions. The characteristic of the valve is such that a full representation of dynamic components as described in chapter 4 will not be readily achieved, but a good representation of the valve's behaviour should be achievable by direct mapping of the steady state characteristics of the valve onto a dynamic model.

In the valve open position, it is possible to determine the force experienced by the valve rubber by the use of strain gauges. In order for these to make any sense, it will be necessary to stiffen the rubber disc in some way (i.e. replace it with a steel disc with a rubberised coating). If strain gauges are then placed radially and laterally on the steel disc, it will be possible to determine the loading on the valve at a range of flow rates. It is anticipated that the loadings on the valve disc under a variety of flows (Q) will approximate to a kQ^2 relationship, as the flows around the disc are highly turbulent. If this is the case, it should be easy to determine coefficients to describe the force on the valve with different flows. Head loss readings should be taken at the same time to allow head loss coefficients to be

this will also be necessary for valve calibration.

As a result of the described experimental work a coefficient (or two) should be calculable to describe the force(s) on the disc causing it to close at a range of different flows. This procedure will then need to be repeated for a series of positions approaching its closure. In order to do this, the approximate shape of the disc during closure needs to be determined in incremental stages. For each of these shapes, a stiff disc will need to be produced with strain gauges attached. This will be a time consuming task, but is the only way to produce a reliable prediction of the valve's behaviour under different operating conditions. The procedure of calibration is then progressed as before, with force and head loss coefficients being determined for each of the incremental valve positions.

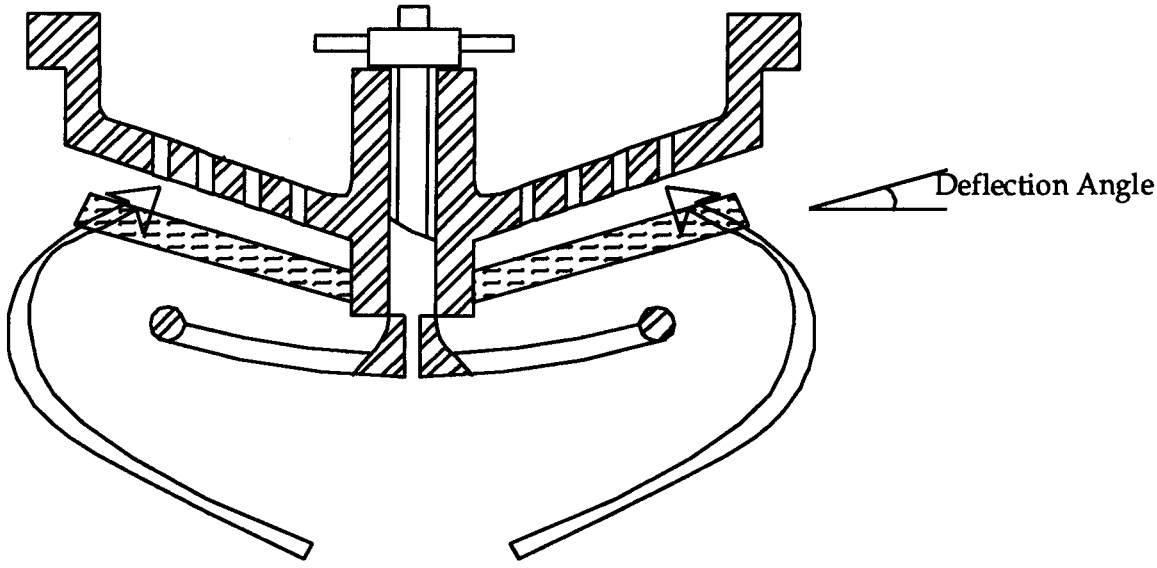

Figure 7.2. Rubber Disc Deflected During Closure

Once calibrated, modelling of the valve will be possible by a similar means to the simpler D.T.U. impulse valve. The position of the valve could be measured in degrees of deflection, and the force opposing valve closure will rise with valve deflection, and be determined analytically, and be dependent on the modulus of elasticity of the rubber. This type of valve can be used with a series of different rubber discs. This calibration procedure would have to be repeated for each new disc geometry, but repetition would not be required if the disc was identical in geometry with an alternative stiffness as this could be accounted for analytically.

The method of calibration would provide results suitable for valve modelling, but no attempts have been made to calibrate a valve of this type. It maybe necessary to modify the approach taken, depending on the quality of the results obtained.

7.2 Pivoting Valve

This type of valve represents a commonly used valve and can be calibrated using methods very similar to those used in the calibration of the D.T.U. valve There are a number of changes in approach that will need to be deployed.

The impulse valve is no longer closed by a linear force, but by a moment. It will therefore be necessary to calibrate the valve by the use of a torque meter. The type of meter used will have to account for the particular nature of the valve under calibration, and the facility for connection of a meter.

As described in chapter 4, the impulse valve can then be calibrated by using the torque meter to measure the force on the valve, and a manometer to measure the head loss across the valve.

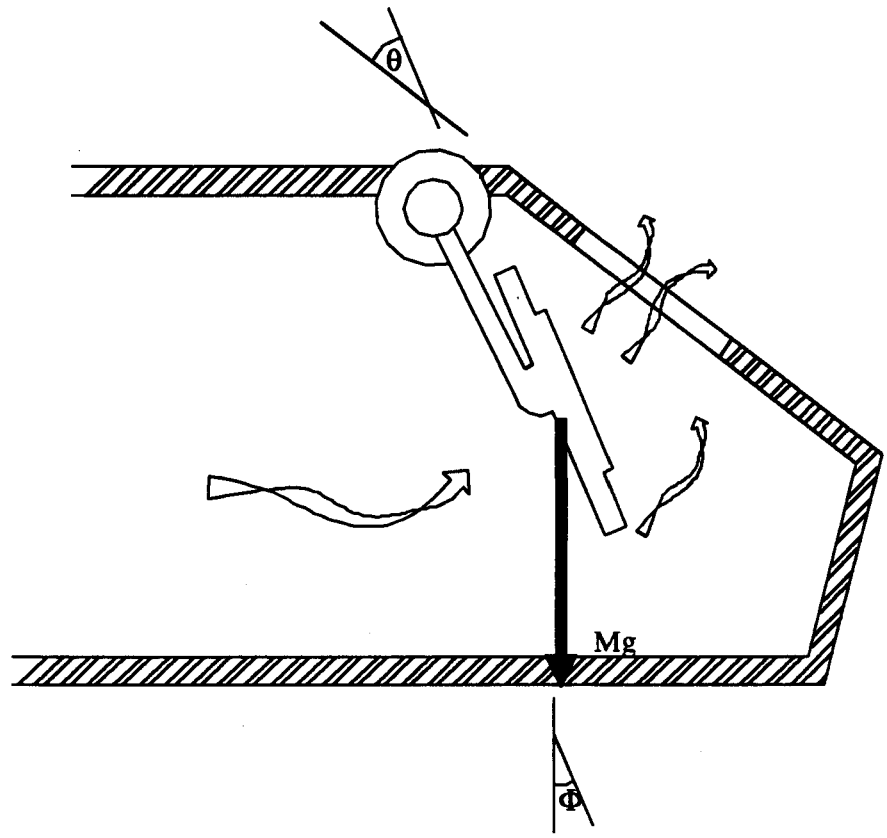

Figure 7.3 Illustration of a typical pivoting valve

These measurements should be taken for a range of flows through the valve, with the impulse valve held at various angles from its seat position.

As before, coefficients of head loss and torque can then be obtained by using curve fitting techniques on the acquired data. Some account will need to be made for the component of torque provided by the mass of the valve under gravity. This component opposes closure, and will be of the form:

$$T = Mg\sin(\Phi)\times K \qquad (6.1)$$

where:

T = *the torque on the valve*

M = *the mass of the moving part of the valve*

g = *the acceleration due to gravity*

Φ = *the angle of the valve line from the vertical*

K = *the radius of gyration of the valve about the pivot point*

Modelling of the valve can then be achieved in both simulation and model by substituting the position of the valve with θ, and the mass of the valve with its moment of inertia about the pivot point, and the velocity and acceleration of the valve with angular variables.

7.3 Summary

The methods of calibration and prediction described in chapters 4 and 5 can be adopted by the majority of hydraulic ram pump designs currently in production. The valve types for which this procedure is somewhat more complex include the rubber disc valve, and the pivoting valve. Suitable experimental and analytical approaches for these valves have been identified. No attempts have been made to calibrate these experimentally, so the approaches identified may require modification, depending on the results obtained.

It is strongly recommended that manufacturers adopting the detailed calibration methods also adopt the graphical design charts as demonstrated in Chapter 6, since a standard design chart format will simplify the task of the water engineer, and so increase the deployment of the device.

Chapter 8: Areas for Further research

There are a diverse number of areas for further research that have been identified as a result of this research. Some of these require theoretical investigation, while others require experimental research. Possible alternative hydraulic ram designs have been identified along with possible modifications to current designs.

Chapter 7 illustrated possible approaches to the calibration of differing impulse valves used by other manufacturers. The provision of performance charts and possibly simulations for hydraulic rams utilising these valves represent an area of valuable further research.

In addition to the above there are aspects of the described work than can be extended, and this may be of some benefit.

8.1 Development of the Computer Model of the Hydraulic Ram Pump.

The predictive model described in chapter 5 has been demonstrated as being highly reliable in performance prediction. As was mentioned in the chapter, there is potential to improve the model, and allow it to be adapted to differing hydraulic ram pumps. The adaptation of the impulse valve modelling is covered in Chapter 7.

The model's approach to the operation of the delivery valve was identified to be the major flaw limiting its overall accuracy. Some attempt was made to account for the swept volume of the delivery valve, and the losses associated with this volume. These amendments were found to enhance the accuracy of the model under some operating conditions. The main limitation of the model was its failure to model the inertial characteristics of the valve. An enhanced modelling of the delivery valve could provide greater accuracy in both the predictive model described in chapter 5 and the method of characteristics simulation described in chapter 4.

In terms of improving the predictive model, there is significant experimental work to quantify the degree of backflow, and the effect of the return characteristics of the valve on this. Some experimental work has been undertaken into the significance of valve

characteristics on pump performance, but this type of work would be needed to be undertaken in greater detail in order to provide a reliable predictive model of the behaviour.

8.2 Further Developments of Simulation

The method of characteristics simulation described in Chapter 4 models the delivery valve boundary condition as a simple orifice in which the head loss coefficient is calibrated experimentally. In addition to this, the simulation incorporates an algorithm to detect reverse flow. If reverse flow is detected it is reset to zero flow. In terms of simulation it is clearly possible to obtain empirically the dynamic coefficients that describe the behaviour of the delivery valve. This would be approached in a similar manner to that described for the impulse valve in chapter 4.

The type of calibration used will depend on the type of delivery valve that is used. The main types fit into two distinct groups; namely the rubber valves, and the plunger type valves.

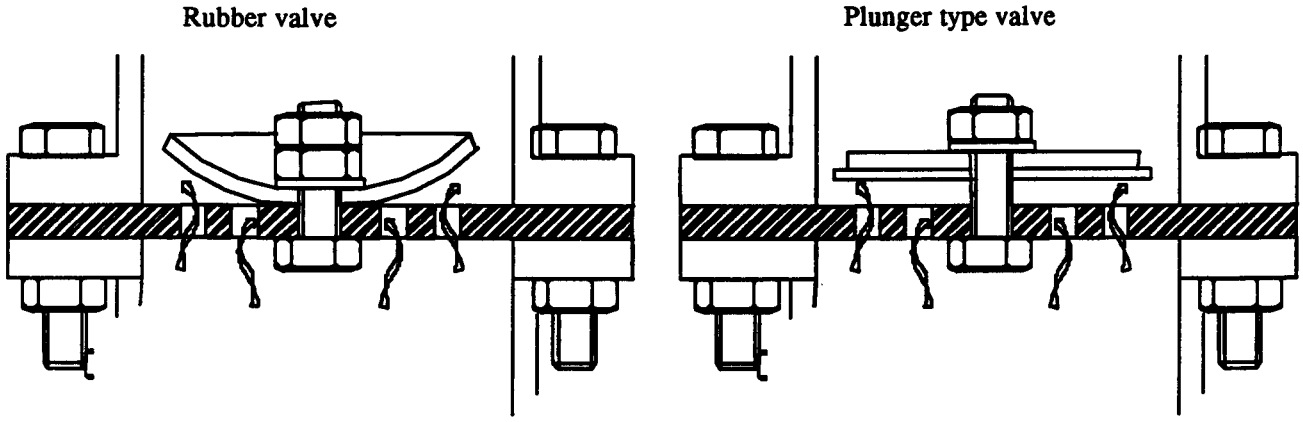

Figure 8.1 Delivery Valve Types

There are differing advantages associated with each type of valve, and as with the impulse valve the plunger type represents a simpler problem with respect to experimental calibration and modelling.

Further Development of the simulation that would be of value would be to incorporate work such as that of Dr Chiang[29] as described in chapter 3. This would bring optimisation methods to a technically accurate simulation, and so should produce more beneficial results than were obtained within the study.

8.3 Hydraulic Ram Development

Within the research programme there have been a number of possible development avenues that have been identified. Two of these are recommended for further experimental and theoretical investigation.

8.3.1 The flexible hydraulic ram (flexiram).

A large number of hydraulic ram pump installations have been visited and initiated during this research programme. It is evident at many installations that the severity of the shock loading experienced can have a detrimental effect on the life of a hydraulic ram pump. This shock loading can also become more severe if for any reason the air vessel fails to be charged. In considering the above, some possibilities for some drastic variations on hydraulic ram pump designs was identified for experimental and theoretical analysis.

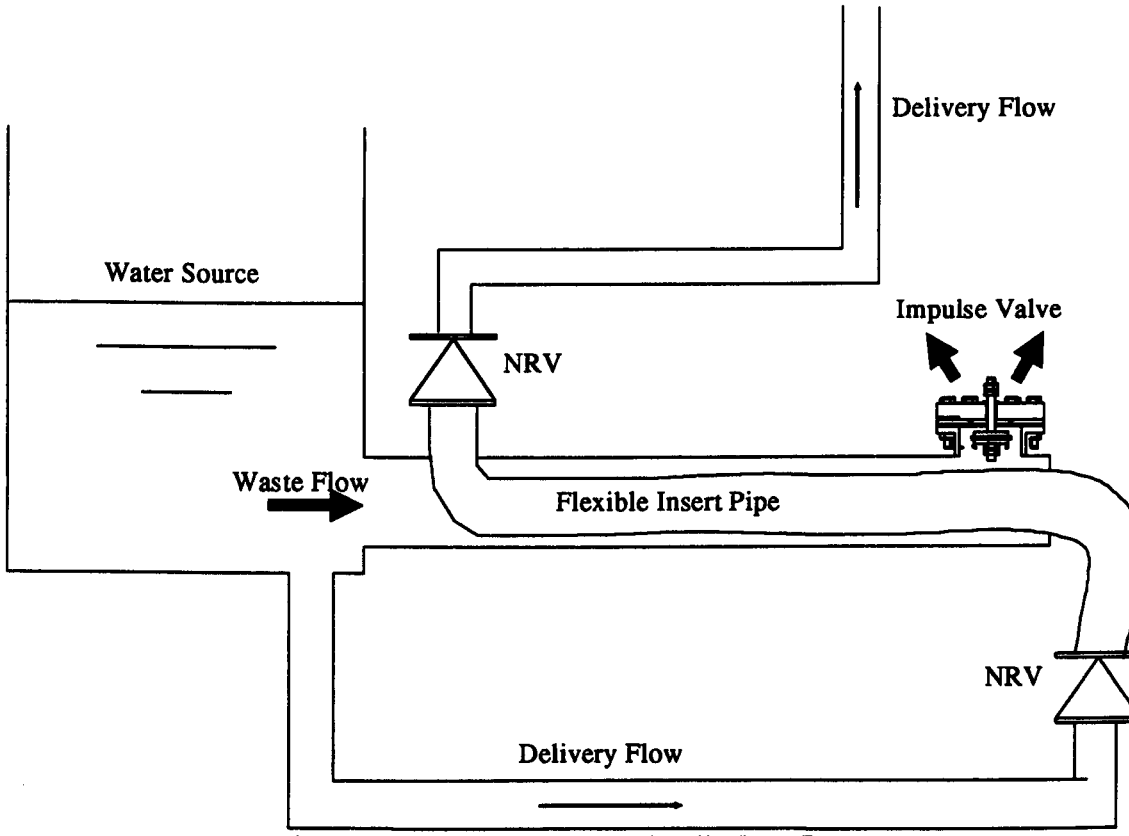

Figure 8.2 Flexible Insert Hydraulic Ram Pump

Figure 8.2 illustrates a drastic variation on the hydraulic ram pump. It is similar to a conventional hydraulic ram pump only in its use of an impulse valve and a drive pipe. The actual pumping action of a device of this type would be affected by the interaction between the fluid flowing in the drive pipe, and the fluid flowing within a flexible pipe within this drive pipe. If the impulse valve shown were able to operate as normal, and generate

transients in the drive pipe, periods of high pressure in the drive pipe would compress the flexible pipe, and transmit the high pressure to the fluid inside. The effect of this will be to force the fluid from the flexible pipe. Two non-return valves will then ensure that the fluid is forced in the right direction. Similarly during a recoil, when pressures drop , the flexible hose will return to its natural size, and water from the source will be allowed into the flexible pipe.

It is interesting to observe that the velocity of wave propagation will vary with the pressure in the delivery pipe, so therefore, the higher the delivery pressure, the higher the wave speed, and the higher the generated pressure for a given velocity. If successful, the device will have a characteristic closer to a conventional positive discplacement pump, and will have some degree of self tuning.

The factors that will influence the success of a device of this type include:

- the flexible nature of the pipe material,
- the characteristics required of an impulse valve to continue to operate with a transient regime of such varying propagation velocity,
- the response characteristics of the non-return valves,
- the relative diameters and heads,
- the length of the flexible piping with respect to the overall drive pipe length.

It is clear that the proposed device offers significant potential as a pumping device, with a particular attraction being its self adjustment with respect to shock pressures, but also the increased simplicity allowed by omitting an air vessel. This removes the requirement for a snifter valve, and could therefore improve the reliability of the device. It also resolves the problem of air being delivered into the delivery pipe work of a distribution system.

Further modification to the above "flexiram" would be possible by reversing the roles of the solid and flexible pipes. It should be possible to connect the internal flexible pipe directly to the impulse valve, and use the stiff external pipe to contain the delivery flow.

The use of simulation to assess the above would provide an extremely difficult challenge, and an experimental approach will probably provide more immediate results.

8.3.2 Hydraulic Ram Pump Performance Enhancement

During the research, and during exploratory visits to water programmes utilising hydraulic rams it became apparent that a major expense in a hydraulic ram pump installation is incurred in terms of the drive pipe cost, and the civil works on a project. Often the pumping power obtained for the expenditure incurred seems small. It would be of interest to increase the output power of a hydraulic ram pump, and so reduce the size of the drive pipe required for a given output of water, and so reduce the effective cost per litre per second pumping.

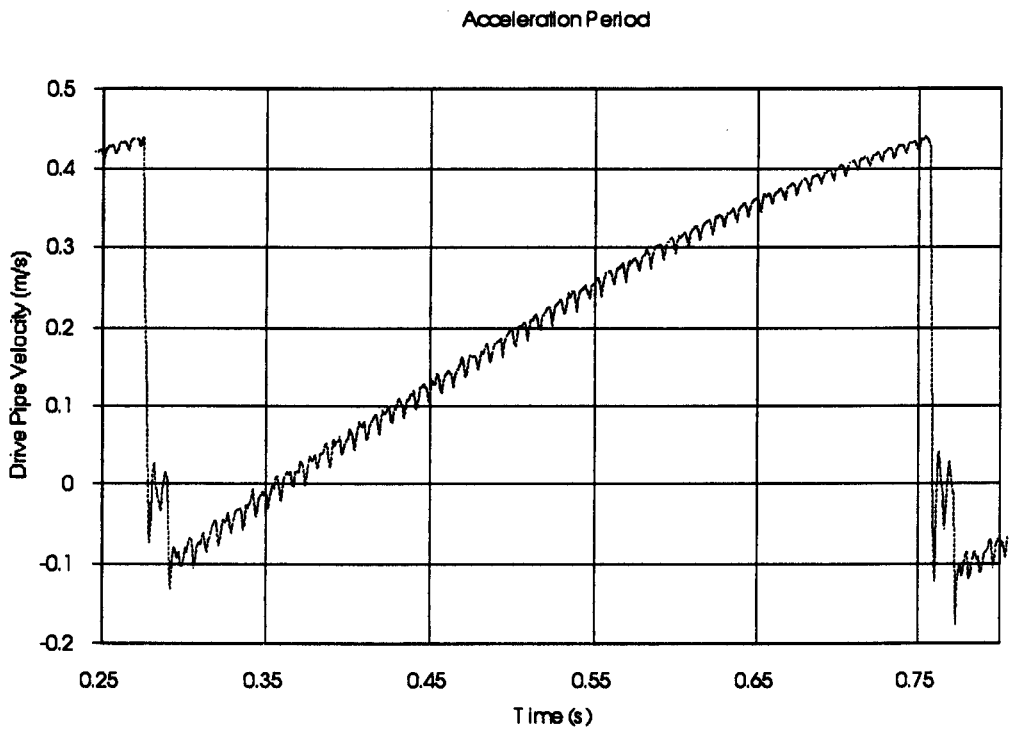

Figure 8.3 Hydraulic Ram Pumping Cycle

A possible means to achieve this is evident as a result of the detailed explanation of pump operation offered in chapter 2, and further explained in chapters 4 and 5. Figure 8.3 illustrates a full hydraulic ram pump cycle in terms of the velocity experienced in the drive pipe (obtained from simulation). Assuming that the energy flux through the pump at any time is proportional to the square of the velocity, it would seem reasonable to consider that to maximise the energy flux, it is better to keep the velocity levels high. This contrasts

significantly with the conventional operation of a hydraulic ram pump which reduces the velocity to a negative level every pumping cycle.

Considering the delivery cycle as analysed in chapter 5, it is in fact made up of a series of consecutive deliveries, each one less productive than the previous, and each one reducing the residual velocity in the drive pipe by a step amount which is proportional the the delivery head. If it is possible to stop the delivery process after only one of these cycles, a significant quantity of water will be pumped. Furthermore, there will remain a high velocity in the pipe. This will allow a given acceleration period to convert more of the potential energy held in the drive tank to kinetic energy in the drive pipe (providing friction effects do not become significant).

The delivery cycle is initiated by the closure of the impulse valve. This brings the water in the drive pipe to a halt, and in turn induces a pressure rise. This pressure rise allows the delivery valve to open, and the velocity in the drive pipe increases. At this stage there is an associated pressure drop to the delivery pressure. This propagates along the drive pipe to the reservoir. Once arriving at the reservoir, a "reflected" wave return involving a further drop in velocity, and a normalisation of pressure. Conventionally when this arrives at the delivery valve, the valve closes, the remaining velocity in the drive pipe induces a pressure rise, and the delivery process recurs. If however at this stage of the reflected wave arriving at the ram pump it were possible for the impulse valve to be reopened, the acceleration cycle would continue instead. The exact timing of the reopening should not be critical as long as it is before the arrival of the reflected wave. Poor timing may however result in poor efficiency. If a hydraulic ram pump could operate on this principle, it would not necessarily suffer a decline in efficiency, as long as friction in the drive pipe and impulse valve are kept to a minimum.

The mechanism by which such impulse valve control could be attained is rather more complex. It may be possible to incorporate a flywheel arrangement to provide rapid reopening. If this method were adopted, significant design would be required to ensure compatibility between the drive pipe frequency and the impulse valve.

In 1909 Abraham invented a device known as the hydropulsator. This device involved a cylindrical impeller that provided two flow paths. One of these was to the delivery chamber, and another discharging to atmosphere. As the impeller rotated, the connection between the

drive pipe and the two destinations was made sequentially. The device was designed for pumping large quantities of fluid to a low head.

If a device such as Abraham's Hydropulsator were calibrated to ensure that the delivery period were restricted to one wave reflection time, this may provide the solution suggested above, without being restricted to only low heads.

It is also possible that the above concept could be combined with the "flexiram" concept. If this were attempted, the impulse valve would become a higher frequency vibrating device, and may be rotated externally.

If a steel hydram operating with a cutoff velocity of 1m/s utilises a single delivery cycle, and delivering to approximately 30m, this would give a minimum velocity of approximately 0.5m/s, and a 50% increase in energy flux, with hopefully only a small decline in efficiency. It is conceivable an efficiency improvement could be experienced as the closure characteristics of the impulse valve would also be enhanced to allow such operation.

8.3.3 Internal Hydraulic Ram Pump

A hydraulic ram pump is conventionally used as a stand alone device, and is not generally used except as the sole water supply on a water scheme. There does seem to be potential for the hydraulic ram pump principle to be incorporated more widely into water projects. One of the reasons for its minimal use currently is the requirement for waste water which is usually expensive in itself, and requires to be dealt with. If water is treated, it is preferable not to waste it, and if not, why pump it?

A pressure reducing valve is an increasingly common device in water distribution. It is suggested that a device of this type could incorporate the hydraulic ram principle to enhance its function. It should be possible to deploy a hydraulic ram pump in a totally enclosed form. The waste water would then not be waste water, but pressure reduced water, and the frequency of the hydram function would adjust itself according to the pressure difference across the valve. The enhanced function of the valve would be the facility to take a small percentage of the discharge to a higher pressure than the source. This may allow delivery to high properties, without the need to pressurise the whole system.

Clearly, the presence of an entire hydraulic ram pump in a pipe system is likely to produce pressure transients in the pipe system. To overcome this, it will be necessary to incorporate an air vessel or accumulator at both ends of the drive pipe. This will minimise pressure fluctuations both upstream and downstream of the device.

In terms of experimental work, it may be possible to investigate the above to include an investigation into the previous design proposals. A flexiram with a high frequency automatic valve may be more readily incorporated into a internal hydraulic ram.

8.3.4 Tailrace

This concept represents the most straightforward of the further research suggestions. It should be feasible to connect a pipe system onto the waste valve. This will provide a partial internal hydraulic ram, with the facility to increase the overall drive head by allowing a negative pressure to exist within the tailrace.

This solution is clearly possible, but only useful if there is a surface of the waste water below the impulse valve. Research into the value of such a device could deploy simulation methods to define the relationship between the transients in the tailrace, and the reliable operation of the impulse valve. It may be necessary to have a significantly larger diameter in the tailrace than exists in the drive pipe.

8.4 Summary

There exists significant potential for further research into the use of hydraulic ram pumps. The computational methods developed within this research programme provide a valuable analytical base for this. Possibilities for improving these tools have been identified.

The potential for the wider deployment of the hydraulic ram principle has been well illustrated by the range of possible variations discussed here. In order that hydraulic ram pumps be used more widely, it is suggested that investigation into the high frequency impulse valve to provide a performance enhancement should be given priority.

Chapter 9: Conclusions

This thesis has provided results in a number of different areas. These relate to the enhancement of the computer simulation of the hydraulic ram pump, the furthering of understanding of hydraulic ram operation; the creation of a model of pump operation; and the production of design tools for users and designers of hydraulic ram pumps.

The research programme followed on from the author's MSc research, in which a method of characteristics simulation of the hydraulic ram was developed. Within this PhD research programme, this simulation was recoded with faster, more efficient code, and using a different programming language. It was then enhanced to incorporate monitoring algorithms for the relevant parameters, and enhanced by incorporating a dynamic component into the operation of the delivery valve boundary condition.

The simulation has been used widely within this research programme, and it has been valuable in providing a detailed understanding of the operation of a hydraulic ram pump, as well as identifying necessary modifications to the geometry of the D.T.U. hydraulic ram. The simulation was used extensively in studying the interaction between the impulse valve closure and pressure transients in the drive pipe of the hydraulic ram pump. This identified some performance limitations of the D.T.U. impulse valve.

A detailed understanding of the operation of the hydraulic ram pump was a necessary resource in the creation of a model of hydraulic ram pump operation. A detailed performance model of the hydraulic ram has been created to incorporate the acceleration and delivery cycles of the pump. The model also accounts for a reducing delivery head associated with reducing drive pipe velocities, and so provides an accurate prediction of recoil velocity. Adjustments to the model also account for head losses across the delivery valve, and back flow through the valve during the delivery cycle. The model accurately determines the impulse valve closure time, and the energy loss associated with it.

The model is clearly unique in the accuracy of modelling it incorporates. Extensive comparison of the output with experimental data has been undertaken, and a good correlation identified. The model is directly usable by engineers as designers or end users, providing reliable results with respect to performance, efficiency, and reliability.

The model has been deployed to produce tables of acceleration efficiency for drive pipe selection, as well as detailed performance charts for a given installation, and more general selection charts giving pump performance for a range of operating conditions.

The production of design charts is seen as a major result of this research programme, which has produced the first impulse valve calibration charts, the first known detailed performance charts, and the first pump selection charts to cover a range of operating conditions.

The research has identified a number of areas for further research. These include the adaptation of the model and simulation to different types of hydraulic ram pump; the improvement of the delivery valve modelling of the pump, and the investigation of alternative devices operating on the same principle.

The research described in this thesis has demonstrably achieved the initial objectives, and provided the data called for by authors such as Mbwette(3), Protzen, and Kahangire(2).

References

1, Watt S.B. 1977, A manual on the hydraulic ram for pumping water, Intermediate Technology Publications Ltd

2, Kahangire P.O. 1986,*The theory and design of the hydraulic ram pump*,Proceeding of a workshop on hydraulic ram pump technology,I.D.R.C

3, Mbwette T.S.A., Protzen E.Th, 1986, *Hydraulic rams as potential pumping units for rural water supply schemes in Tanzania*, Proceeding of a workshop on hydraulic ram pump technology., I.D.R.C

4, Joukowsky J.N.1904, *Water hammer, Proceedings of American Waterworks Association*, Vol 24 pp 341-424 Translated by Olga Simin

5, Whithurst J. 1775, *Account of a machine for raising water*, Philosophical Trans Royal Society, London

6, Montgolfier J.M., Montgolfier E.J., 1798, *Le belier hydraulique*, French Patent Specification

7, Eytelwein J.A.1805, *Bemerkungen über die Wirkung und Vortheilhafte Anwendung des Stosshebers*, Berlin

8, D'Aubuisson J.E.1840, *Traité d'hydraulique à l'usage des ingenieurs*, Paris

9, Morin A.1863, *Des machines et appereils destinés a l'élevation des eaux*, Paris

10, Dingler E.M.1865, *Der Stossheber von Bollée*, Polytechnisches Journal Vol 176, Augsburg

11, Kent W.1910, *Mechanical Engineers Handbook*, N.Y. and London

12, Richards J. 1898, *Hydraulic rams*, Journal Ass Engineering Societies, Boston

13, Church J.P. 1905, *Hydraulic motors*, N.Y. and London,

14, Clark J. 1900, *Hydraulic rams their principles and construction*, Batsford, London

15, Anderson E.W. 1923, *Hydraulic rams*, Proc. Inst. of Mech. Eng. Vol112 p337

16, Clavert N.G. 1957, *The hydraulic ram*, The Engineer. Vol 203 p 597

17, Rennie & Bunt 1981, *The automatic hydraulic ram*, The South African Mechanical Engineer Vol 31 p258,

18, Venturoli G.1818, *Elementi di meccanica e d'idraulica*, Milano

19, Navier M.1839, *Resumé des leçon de mecanique appliqué*, Bruxelles

20, Weissbach J. & Herman G. 1897, *The mechanics of pumping machinery*, London

21, Rankine W.J. 1874, *On the mathematical theory of the hydraulic ram*, The Engineer Vol 33

22, Mirapeix F. 1907, *Contribucion al estudio de la teoria de los arites hidraulicos*, Revista Technologico - Industrial, Barcelona

23, Lorenz H.1910, *Theorie des hydraulischen Widders*, Zeitschrift des V.D.I., Berlin

24, Bergeron L.1935, *Étude des variations de regime dans les conduites d'eau; solution graphic generale*, Revue Generale de l'Hydraulique Vol1 pp12, 69,

25, Harza L.F. 1908, *An investigation of the hydraulc ram*, Bulletin No 205 of the Univeristy of Wisconsin

26, O'Brien M.P. & Gosline J.E. 1933, *The hydraulic ram*, University of California Publications in Engineering Vol 3 No 1.

27, Krol J. 1951, *The automatic hydraulic ram*, Proc. Inst. Mech. Eng. Vol 165 p53

28, Schnyder O. 1932, *Über Druckstossen Rohrleitungen*, Wasserkraft und Wasserwirtshaft

29, Chiang Y.C. 1984, *Simulation and optimization of transient oscillations, flow, and sound in complex piping systems*, PhD at University of Wisconsin

30, Streeter V.L. & Wylie E.B. 1993, *Fluid Transients in Systems*, Prentice Hall

31, Watt C.S. & Boldy A.P. 1980, *Combination of finite difference and finite element techniques in hydraulic transient problems*, Third International Conference on Pressure Surges pp43-62, B.H.R.A.

32, Chaudhry M.H.1987, *Applied hydraulic transients, Second Edition*, Van Nostrand Reinhold Co. N.Y.

33, Fox J.A.1989, *Transient flow in pipes, open channels and sewers*, Ellis Horwood Ltd

34, Swaffield J.A. & Boldy A.P. 1993, *Pressure surges in pipe and duct systems*, Avebury Technical

35, Thorley A.R.D.1991, *Fluid transients in pipeline systems*, D&L George Ltd

36, Gibson A.H. 1908, *Water hammer in hydraulic pipelines*, Constable London

37, Jeffery T.D. Thomas T.H. Smith A.V. Glover P.B.M. Fountain P.D. 1992, *Hydraulic ram pumps a guide to ram pump water supply systems*, Intermediate Technology Publications Ltd

38, *Matlab*
Matworks Inc. U.S.A. 1987

39, Barr (1975)
Kempes Engineers Year-Book 1987

Appendix A. Publications

The following publications of the author have been included in this appendix on account of their relevance to the PhD subject matter.

1) The use of Computer Simulation and Analysis Tools in the Development of the Hydraulic Ram Pump. P.B.M. Glover, P.D.Fountain T.D.Jeffery and A.P. Boldy
Proceedings of the International Conference of Computer Methods and Water Resources CMWR91, Rabat 1991 ISBN 1853121290 (A2)

2) The application of hydraulic transient analysis tools to design optimisation on the hydraulic ram pump. P.B.M.Glover, T.D.Jeffery and Dr A.P. Boldy.
Proceedings of the International Association of Hydraulic Research Symposium. Belgrade 1990 (A13)

3) Computer Simulation of the Hydraulic Ram Pump. P.B.M.Glover and A.P.Boldy
Proceedings of the 6th International Pressure Surge Conference, B.H.R.A. 1989. ISBN0947711791 (A23) organised by B.H.R.A.

The Use of Computer Simulation and Analysis Tools in the Development of the Hydraulic Ram Pump.

P.B.M.Glover, T.D.Jeffery, P.D.Fountain, and A.P.Boldy
Department of Engineering, University of Warwick, Coventry ,U.K.

ABSTRACT

A detailed description is given of the application of computer simulation techniques in the development of the hydraulic ram pump. Details of an original and effective method of accurately modelling the dynamics of the operating valve are presented, along with details of practical application of the model. A descriptive summary is given of further computational methods used.

INTRODUCTION

The hydraulic ram arguably represents the most appropriate low power water pumping technology presently available for isolated rural regions of suitable topography. As such, it is the subject of increasing interest with reference to small scale water supply and irrigation requirements of developing countries.

The attraction of the device for rural water projects lies in its inherent simplicity, its insignificant running costs, and its potential as a VLOM device (Village Level Operation and Maintenance). The factors most drastically effecting its wider deployment include the antiquated nature and expense of models presently available, as well as the highly limited design literature provided by most manufacturers. To quote two papers from a recent workshop on the hydraulic ram pump held in Tanzania:

"Information on practical hydram sizes and installation limitations is often not available. Such information is necessary to prevent expensive failures in the field, and arbitrary hydram designs and installations." - P.O.Kahangire[1]

"From the point of view of water supply design, the engineers are only awaiting a hydraulic ram with established performance data so as to confidently incorporate it in their schemes."-T.S.A.Mbwette and E.Th.Protzen[2].

The work being undertaken at the University of Warwick in conjunction with a Zaire based field project is attempting to solve these problems, as well as produce hydraulic ram pump designs suitable for manufacture in developing countries and village level operation and maintenance(VLOM). In view of the limited success

of the various numerical models developed [13], the project has deployed a variety of sophisticated computational methods in its attempt to both calibrate and improve available designs.

The main computational element of the research programme has been the production and use of a dedicated hydraulic ram pump computer simulation. The simulation has been produced and calibrated at the University, and is being used alongside experimental work to quantify important parameters associated with the development of the pump, and provide performance data for operating conditions beyond those readily reproducible in the laboratory. Computers have also provided an important part of the development programme through less revolutionary areas such as electronic data acquisition, computer aided design, data analysis and curve fitting.

This paper will for the most part describe the application of the computer simulation, although other computational aspects will be mentioned for areas of particular significance to hydraulic ram pump development.

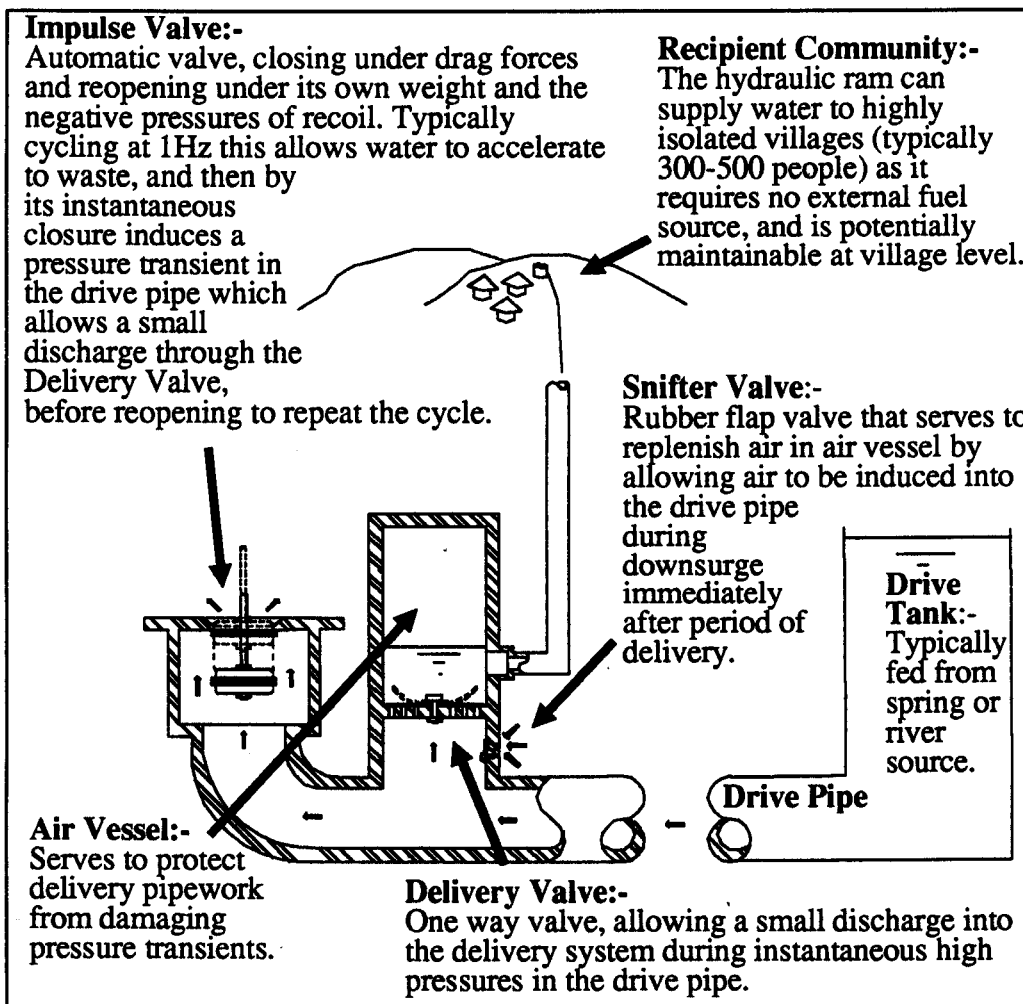

Figure 1. The Hydraulic Ram Pump

SUMMARY OF OPERATION.

The hydraulic ram pump is a fundamentally simple pumping device which operates using water power. The pump operates in sites with surface drainage, and uses the energy present in a large body of water from a spring or river as it falls through a small distance, transferring this energy to a small body of the same fluid delivering it to some height. This is achieved by inducing large pressure transients in a small length of pipe (the drive pipe: typically 5-40m). Water is accelerated under gravity through this section of pipe and discharges to waste. This process continues until such a time as the drag force on the valve situated at the position of discharge (known as the impulse valve) exceeds the force holding it open (typically gravity). At this point the impulse valve begins to move, upon which the drag forces increase, resulting in a "snap shut closure".

This rapid closure induces a temporary high pressure in the drive pipe, which in turn allows a small discharge through a delivery valve (one way valve) into an air chamber which is held at the system delivery pressure.

Once the pressure subsides, a recoil is experienced. The associated low pressure causes the delivery valve to shut, and allows the impulse valve to reopen, so allowing the cycle to recommence.

During this period of low pressure, a small quantity of air is induced into the body of the hydraulic ram through a snifter valve. On the next delivery cycle, this air will be forced into the air vessel, allowing any air lost from the air vessel through absorbtion to be replenished.

The annotated diagram in Fig 1. illustrates the basic elements of the hydraulic ram pump under operating conditions. The simplicity of the device is awe-inspiring, and the theoretical potential of the device extends well beyond its present deployment. The main limiting factors being poor design data, incomplete theoretical analyses, poor documentation, and antiquated designs.

OBJECTIVES.

The fundamental goal of the research and development work that is being undertaken by the Development Technology Unit at the University of Warwick is to improve the quality of life in some of the worlds poorer regions. To this end, the D.T.U.'s hydraulic ram pump development project aims to significantly improve the availability of the hydraulic ram pumping technology at the village level.

The project hopes to facilitate the wider dissemination of this highly appropriate technology, by producing high quality pump designs that are readily manufacturable in developing countries, and maintainable at the village level. It is also anticipated that the sophistication of the analytical work being undertaken by the Unit will enable a significant improvement in the accuracy and usefulness of pump and system design literature. This should serve to greatly reduce the problems of pump and system design experienced by today's engineers and field workers.

In addition to this, it is hoped that the calibration and performance prediction techniques being developed will be adopted by the majority of hydraulic ram pump manufacturers, and this will further improve their dissemination of the technology.

COMPUTER SIMULATION OF THE HYDRAULIC RAM PUMP

In view of the limited success of the multitude of analyses that have been undertaken on the hydraulic ram pump, and following a number of investigations by the D.T.U., it was decided that a computer simulation of the pumping device would be the only way to answer some of the more specific questions relating to hydraulic ram pump performance.

The D.T.U.'s simulation is a fixed wave speed method of characteristics simulation which reduces the pump into a four pipe network, using standard techniques [4] to model the majority of the boundary conditions.

The modelling of the Impulse Valve boundary condition has proved to be not only the most complex of the modelling problems, but also the most significant to the simulation's usefulness as a tool for design. Early attempts to model the valve were again based on standard valve modelling techniques using a timed closure. The inadequacy of this approach in modelling the dynamic behaviour of the valve was obvious and so a calibrated boundary condition was adopted in an attempt to provide sufficient accuracy to at least provide a comparative tool.

A CALIBRATED VALVE BOUNDARY CONDITION

To provide accurate reproduction of the valve's behaviour it was necessary to obtain detail of the valve's head loss and force characteristics for a number of operating conditions. This was achieved by using the apparatus shown in Fig 2.

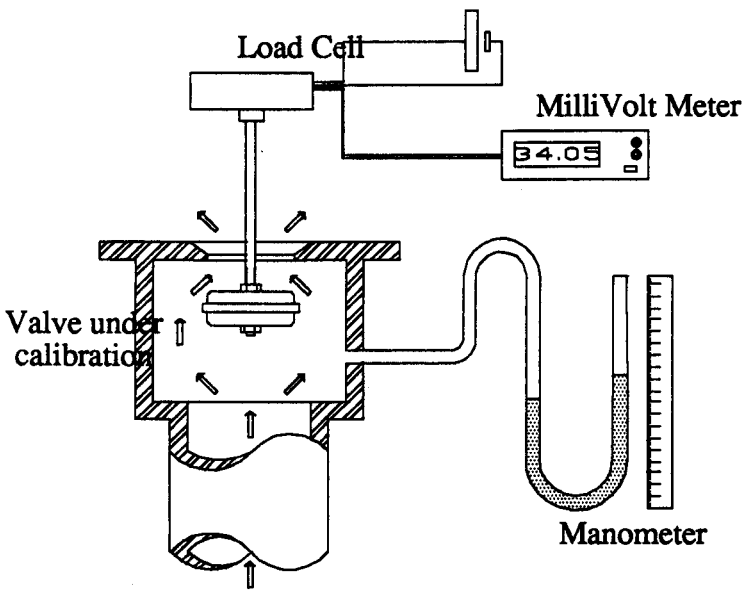

Fig.2 Valve Calibration Test Rig

A given impulse valve was set in a test rig with the valve plunger held at a measured distance from its seat. The force on the valve and the head loss across the valve were then accurately measured for a range of flows. This was repeated throughout the valve's travel, yielding a series of characteristic curves of head loss and force.

Some simple curve fitting algorithms were applied to these, and they were found to follow a Q^2 relationship (Q = Flow) as one would expect for a turbulent discharge. The curve fitting routines yielded a series of head loss and force

coefficients for the various measured valve positions. More sophisticated curve fitting algorithms were applied to these which yielded equations that described the variation of head loss and force coefficients with valve position.
Equations 1 and 2 represent the head loss and force coefficients for a D.T.U. valve model Mk 6.4 as defined in Fig 3.

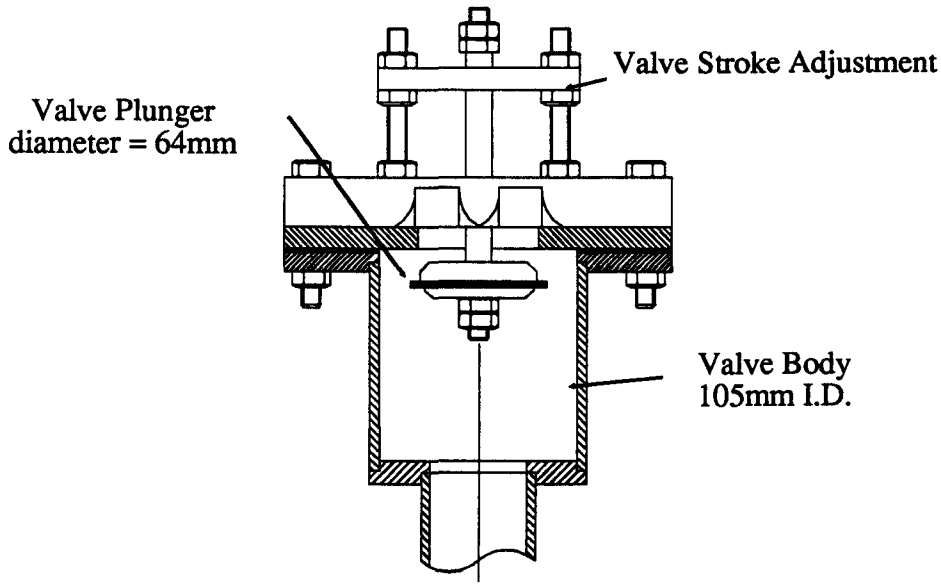

Fig. 3 D.T.U. Impulse Valve Mk 6.4.

VALVE Mk 6.4 CALIBRATION EQUATIONS

$$K_f = 5.2827 \cdot 10^3 \cdot e^{-1.862x} + 17.13 \cdot e^{-0.4459} + 0.0414 \quad (1)$$

$$K_h = 1.6569 \cdot 10^3 \cdot e^{-1.8748x} + 5.1944 \cdot e^{-0.436x} + 0.038 \quad (2)$$

Where:-

K_f = The Impulse Valve Force Coefficient
K_h = The Impulse Valve Head Loss Coefficient
and x = The position of the valve plunger relative to its seat (mm)

These equations can provide the basis for a valve boundary condition as follows. The simulation can be initialised assuming the valve is fully open. Equations 1 and 2 can be used to determine the force and head loss on the valve at this position. Following a single simulated time increment, the new position of the valve can be determined by using Newtonian laws of motion, and the value of force on the valve calculated previously. Once the new valve position is determined, equation 2. can be used to determine the instantaneous head loss characteristic of the valve, and so allow the boundary condition to be solved. This process can then continue, with the valve acceleration, velocity and position being recalculated at each time step. To solve the valves end conditions (fully open and fully closed) additional algorithms are included.
The described boundary condition represents a pseudo dynamic model of the impulse valve, based on static measurement. Its inadequacy lies in its failure to

model the significance of the relative velocity between the fluid and the valve plunger. However, it has been valuable in providing some useful insight into the pumps operation. Figs 4. and 5. illustrate some of the accuracy obtained using the described model. Fig 4. represents a measured pressure transient in a hydraulic ram pump, and Fig 5. represents the simulated transient for the same operating conditions.

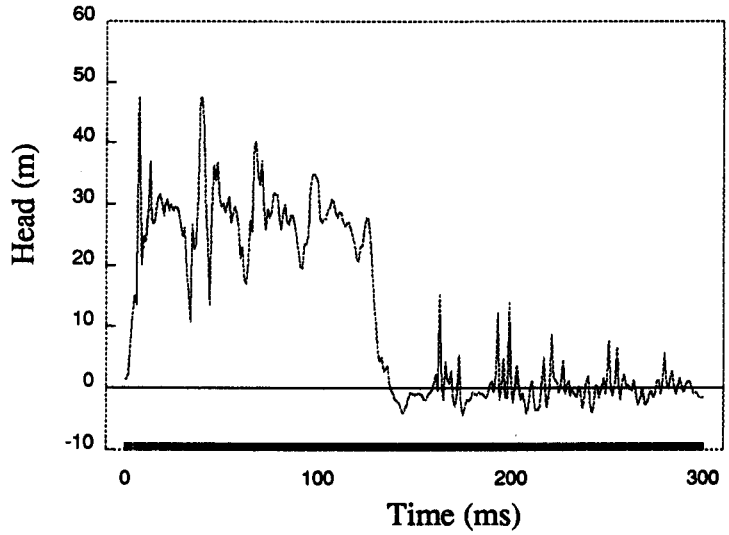

Fig 4. Measured Pressure Transient.

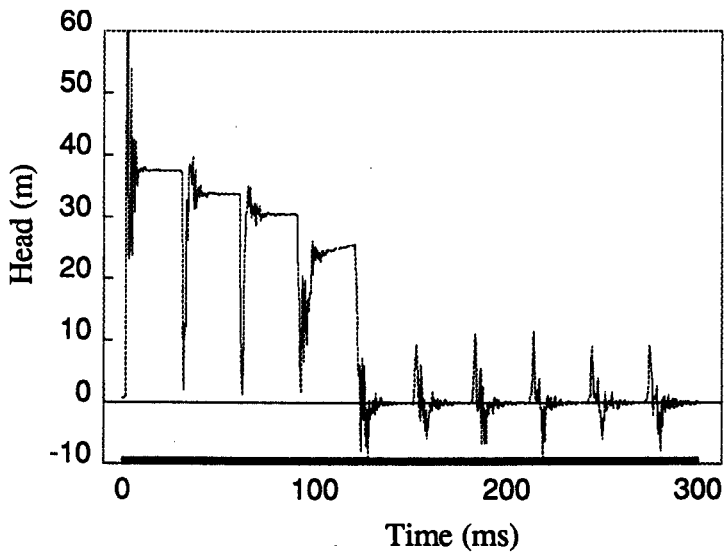

Fig 5. Simulated Pressure Transient.

IMPROVED DYNAMIC MODELLING OF THE IMPULSE VALVE.

Some recent work in the modelling of the Impulse Valve boundary condition has attempted to solve the inadequacy of the boundary condition described above,

allowing the modelling of the dynamic forces on the valve caused by the relative velocity between the valve plunger and the passing flow.
The amendments made to the boundary condition were undertaken following a realisation that the measured force characteristic remained constant once the valve plunger position exceeded a critical distance from the discharge orifice. The assumption was then made that the valve force in this position would be primarily related to the dynamic velocity between the fluid and the plunger, and that the effect of the relative motion of the valve body internal wall would be insignificant. To put it another way, it was assumed that the force on a plunger moving at 1m/s in a stationary fluid would be equivalent to that on a stationary plunger in a 1 m/s flow, provided the distance of the plunger from its seat was over a critical distance (see Fig 6.).
If this assumption is true as early results would suggest, a more accurate boundary condition of the impulse valve can be produced using this dynamic force

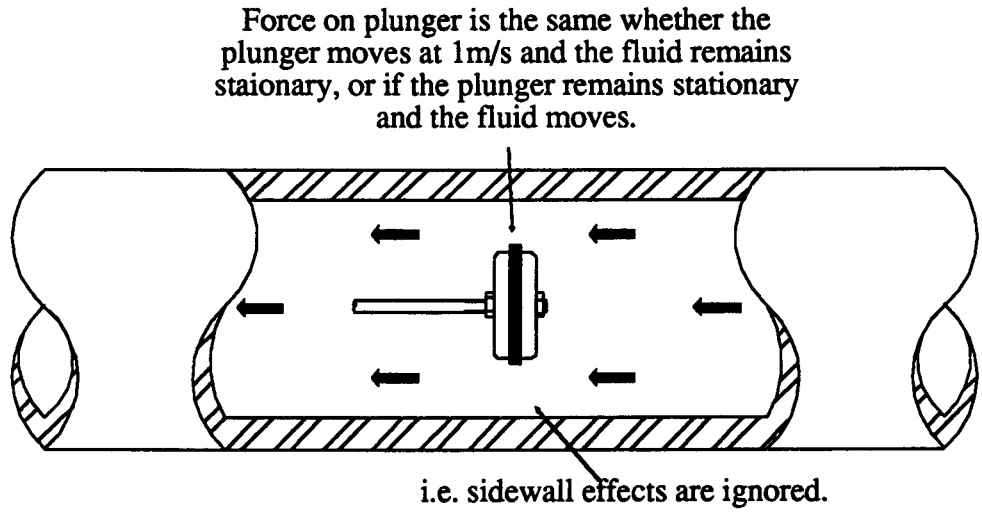

Fig 6. Valve Plunger in Free Pipe

coefficient. The dynamic component of the force coefficient is easily obtained from the calibration data, as it represents the linear element of equation (1). The dynamic boundary condition is then solved as before, except for every calculation of force on the valve, a dynamic component is summed with the statically calibrated component, as illustrated by equations 3 and 4.

NEW DYNAMIC VALVE CALIBRATION EQUATIONS

$$K_{fs} = 5.2827 \,.\, 10^{3} \,.\, e^{-1.862x} + 17.13 \,.\, e^{-0.4459} \qquad (3)$$

$$K_{fd} = 0.0414 \qquad (4)$$

where:-

K_{fs} = Static component of the force coefficient varying with displacement x
K_{fd} = Dynamic component of force coefficient.

IMMEDIATE APPLICATIONS OF THE SIMULATION

The simulation has been used to answer a number of specific questions regarding the operation of the hydraulic ram pump. These have included the substantiation or rejection of theoretical analyses, as well as questions relating to specific pump designs.

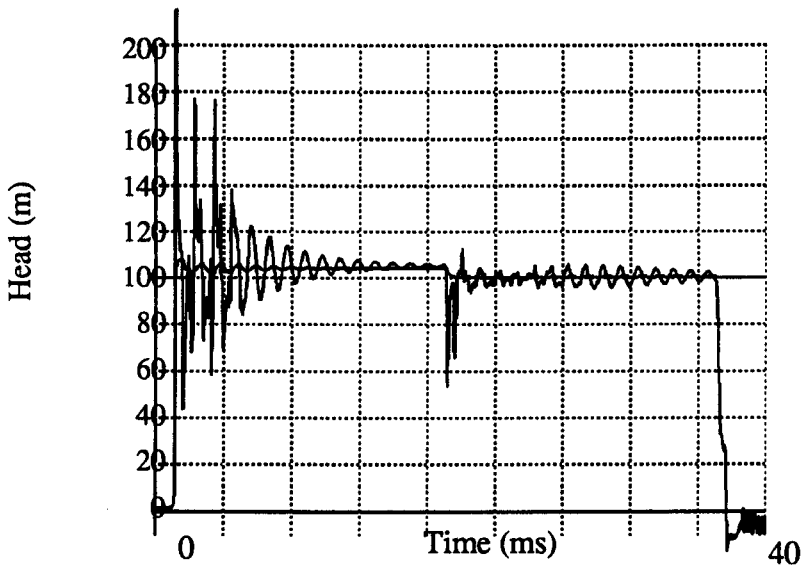

Fig 7. Simulated Pressure Transient - Valve Body = 50mm

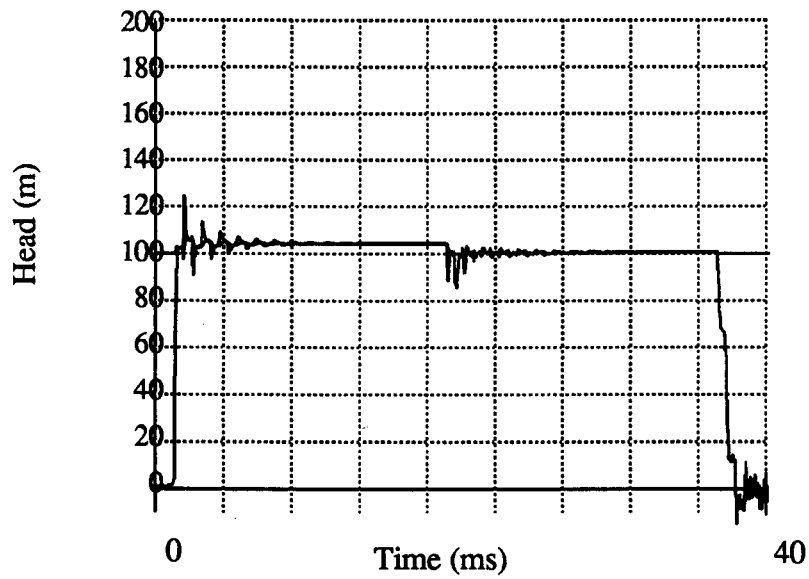

Fig 8. Simulated Pressure Transient - Valve Body = 100mm

Figs 7. and 8. illustrate the value of simulation techniques in the reduction of fatigue failures in pump design. The variation in pressure transient histories between Figs 7. and 8. was obtained by modifying the pipe diameter of a very small section of the pump body. This small modification to pump geometry can be seen to have a drastic effect on the magnitude of fatiguing transients experienced by the whole system.

A longer term application of the simulation is in the production of data beyond that readily achievable in the laboratory situation. Fig 9. demonstrates the value of the simulation for obtaining the large quantities of the type of data required to produce a complete pump characteristic. The graph shows the variation of power and efficiency with respect to a Joukowsky ratio, defined as the delivery pressure over the maximum attainable head at a given drive pipe cut off velocity (Joukowsky Head -see eqn 5). Laboratory measurement using high speed data sampling equipment has yielded a measured wave speed of 1350m/s for the 2" galvanised drive pipe.

$$\Delta H = \frac{c \,.V_0}{g} \qquad (5)$$

where :-

ΔH = Joukowsky Head [5]

c = Speed of sound in pipe

g = Acceleration due to gravity

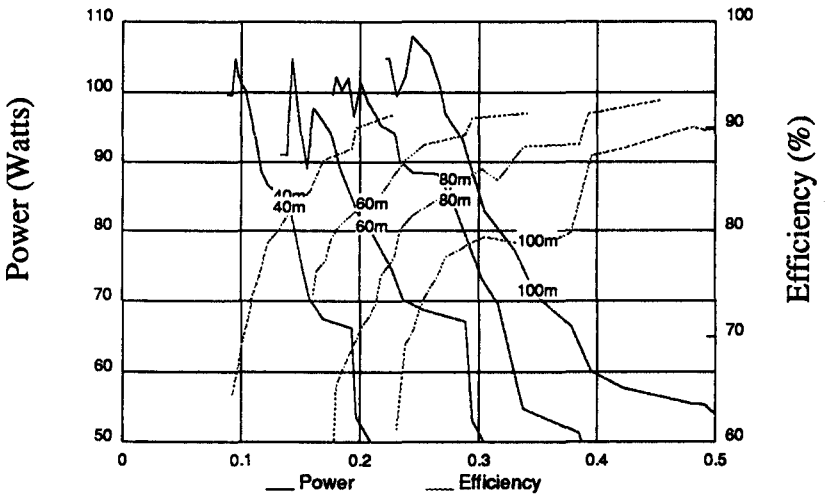

Fig 9. Simulated Power and Efficiency

The value of graphs of this type is primarily in the comparison of a variety of different valve bodies as minor changes in valve characteristic may have a more dramatic effect on power and efficiency than one would anticipate by merely viewing the head loss and force characteristic curves. Beyond this, a Joukowsky graph of this type represents the first step towards a global calibration of a hydraulic ram pump.

OTHER COMPUTATIONAL METHODS USED.

In addition to high speed A/D data sampling, and a method of characteristics simulation, a variety of computational methods have been employed in the development of hydraulic ram pump designs. The use of spreadsheet software has been intensive for a variety of applications involving the manipulation of large quantities of data. Fig 10. represents a range of acceleration efficiencies for a

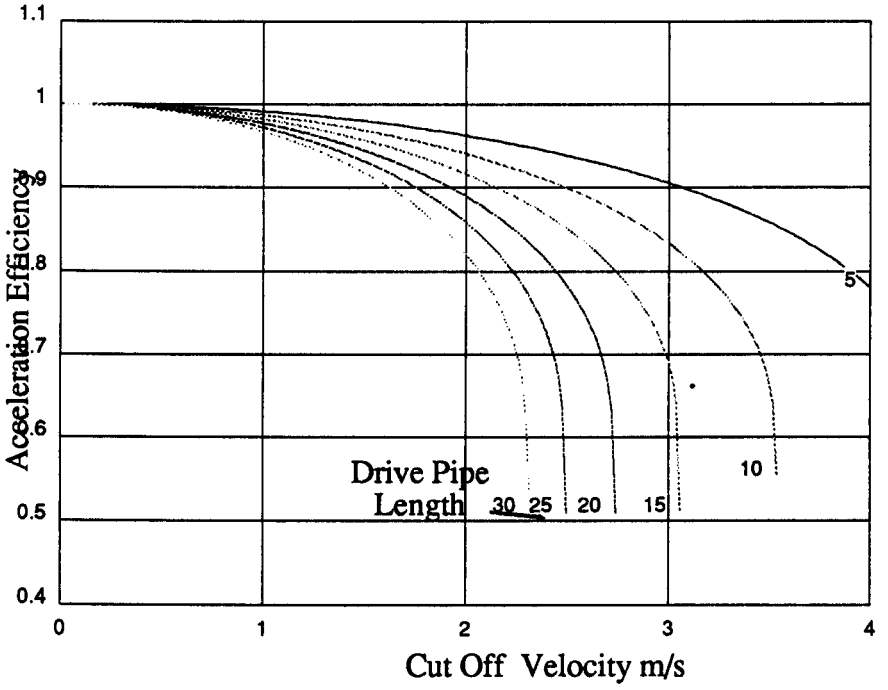

Fig 10. Acceleration Efficiency for Mk 6.4 with 50mm Drive

hydraulic ram pump operating with a range of drive pipe lengths at a fixed supply head of 5m. The curves were obtained using a spreadsheet to determine the changes in velocity and acceleration during the fluid acceleration cycle. Assuming the delivery period to be small in comparison with the acceleration period, it is possible to use this data to determine a mean drive pipe flow for a given cut off velocity. If this is related to a minimum flow(i.e. shortest acceleration- assuming no friction) it is possible to calculate an acceleration efficiency, based on the quantity of water unnecessarily flowing to waste.

Although the integrals represented here could have been achieved analytically, the adaptability of the spreadsheet provides a better environment to assess and modify calculations. The graph shown represents an important mile stone in the definition of the optimum operating point of the hydraulic ram if read in conjunction with Fig 9.

The use of curve fitting algorithms has also been of fundamental importance to the project. This is demonstrated by Fig 11. which was produced in a spreadsheet environment directly from the fitted force characteristic for D.T.U. Valve Mk 6.4.

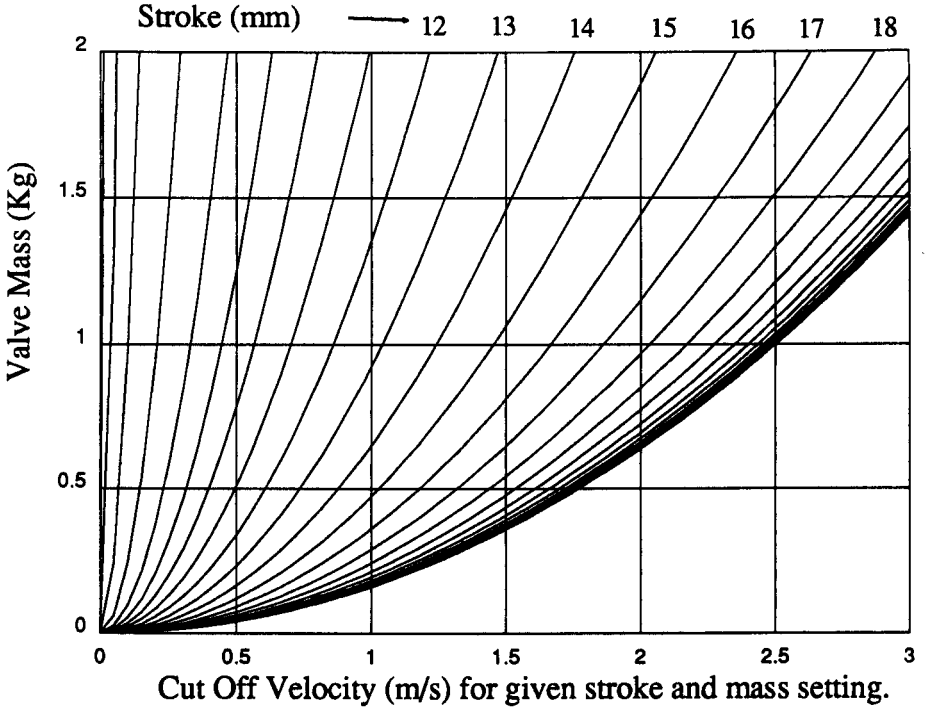

Fig 11. Force Curves for Valve Mk6.4 with 50mm Drive Pipe.

Diagrams of this type provide for the first time a means to determine quickly and accurately the cut off velocity in a hydraulic ram pump without the use of highly sophisticated experimental equipment. The accuracy of the graph has been ascertained by measuring the induced pressure transients for the various valve settings.

CONCLUSION

The Development Technology Unit has made a major step towards the global calibration of hydraulic ram pumps, and the production of designs suitable for manufacture in developing countries and maintainable at the village level. In this work the D.T.U. is maintaining close links with a water supply programme in Zaire which is supported by Tear Fund. This element of the project is taking the development work a step further by attempting to apply the technology at a participative level [6].

Computational methods have played a vital and increasing part of the described research undertaken at the University of Warwick. The usefulness of computer simulation in this development programme has been found to be closely related to the computational power available. The increasing availability of higher power computer systems will therefore clearly enhance the use of computer simulation in this type of development programme.

ACKNOWLEDGEMENTS

The Authors would wish to acknowledge the support obtained from the Overseas Development Administration, and the University of Warwick's Civil Engineering Research Fund for the research programme in the U.K. The Authors would also wish to acknowledge the support of TEAR Fund in their Zaire based water programme; the Mott MacDonald Charitable Trust for their support of the computational work involved in the project; and K.S.B. pumps for the generous supply of pumping equipment for use on test rigs.

REFERENCES

1. Kahangire P.O. Theory and design of the hydraulic ram pump. Proceedings of a workshop on Hydraulic Ram Pump (Hydram) Technology. IDRC. 1986

2. Mbwette T.S.A. and Protzen E.Th.P. Hydraulic Ram Pumps as potential pumping units for rural water supply in Tanzania. IDRC. 1986
Streeter

3. O'Brien M.P.O. and Gosline J.E. The Hydraulic Ram. University of California Publications in Engineering Vol. 3, No.1,pp1-58.

4. Wylie E.B. and Streeter V.L. Fluid Transients. FEB Press U.S.A. 1983.

5. Joukowsky J.N. Water Hammer. Proceedings of the American Waterworks Association Vol 24 1904 pp341-424.

6. Jeffery T.D. Fountain P.D. and Glover P.B.M. Development of the Hydraulic Ram Pump for Manufacture and Use in Developing Countries. Proceedings from the I.C.E symposium on Appropriate Technology 1990.

THE APPLICATION OF HYDRAULIC TRANSIENT ANALYSIS TO DESIGN OPTIMISATION ON THE HYDRAULIC RAM PUMP

L'APPLICATION D'UNE ANALYSE TRANSITOIRE HYDRAULIQUE À L'OPTIMISATION DU DESSIN SUR LE BÉLIER HYDRAULIQUE

P.B.M.GLOVER MSc BSc AMIMechE Research Associate	UNIVERSITY OF WARWICK Department of Engineering	United Kingdom
T.D.JEFFERY BSc Research Associate	UNIVERSITY OF WARWICK Department of Engineering	United Kingdom
Dr A. P. BOLDY PhD BSc C.Eng MICE Lecturer	UNIVERSITY OF WARWICK Department of Engineering	United Kingdom

Summary

This paper summarises some of the detailed analyses of the hydraulic ram pump which are being undertaken at the University of Warwick. The purpose of this work is primarily to develop designs suitable for manufacture in developing coutries, but also to aid the dissemination of the technology in rural areas. Detail is given of the use of calibration data in a computer simulation of the device, and the application of this is discussed. Clarification on the limitations of the methods used is also given.

Sommaire

Cet article résume certaines des analyses détaillées du beliér hydraulique que l'on s'engage à faire à l'Université de Warwick. Le but de ce travail est principalement de développer des dessins qui sont appropriés à la fabrication dans des pays en voie de développement, mais aussi d'aider dans la dissémination de la technologie dans des régions rurales. Par une simulation de l'appareil mis sur ordinator, on donne des détails qui concernent l'utilisation de l'information de calibration et on examine des applications résultantes. On donne aussi une clarification sur les limitations des méthodes employées.

Introduction

The hydraulic ram pump has been the subject of increasing interest in the area of small scale water supply and irrigation for developing countries. The device is a simple but effective water pump that operates by extracting energy from a fall of water. A typical system layout is shown in Figure 1. The attraction of the device for rural water projects lies in its simplicity, insignificant running costs, and its potential production as a VLOM device (Village Level Operation and Maintenance). The University of Warwick's Development Technology Unit (D.T.U) have been working to produce designs of the pump suitable for manufacture in developing countries.

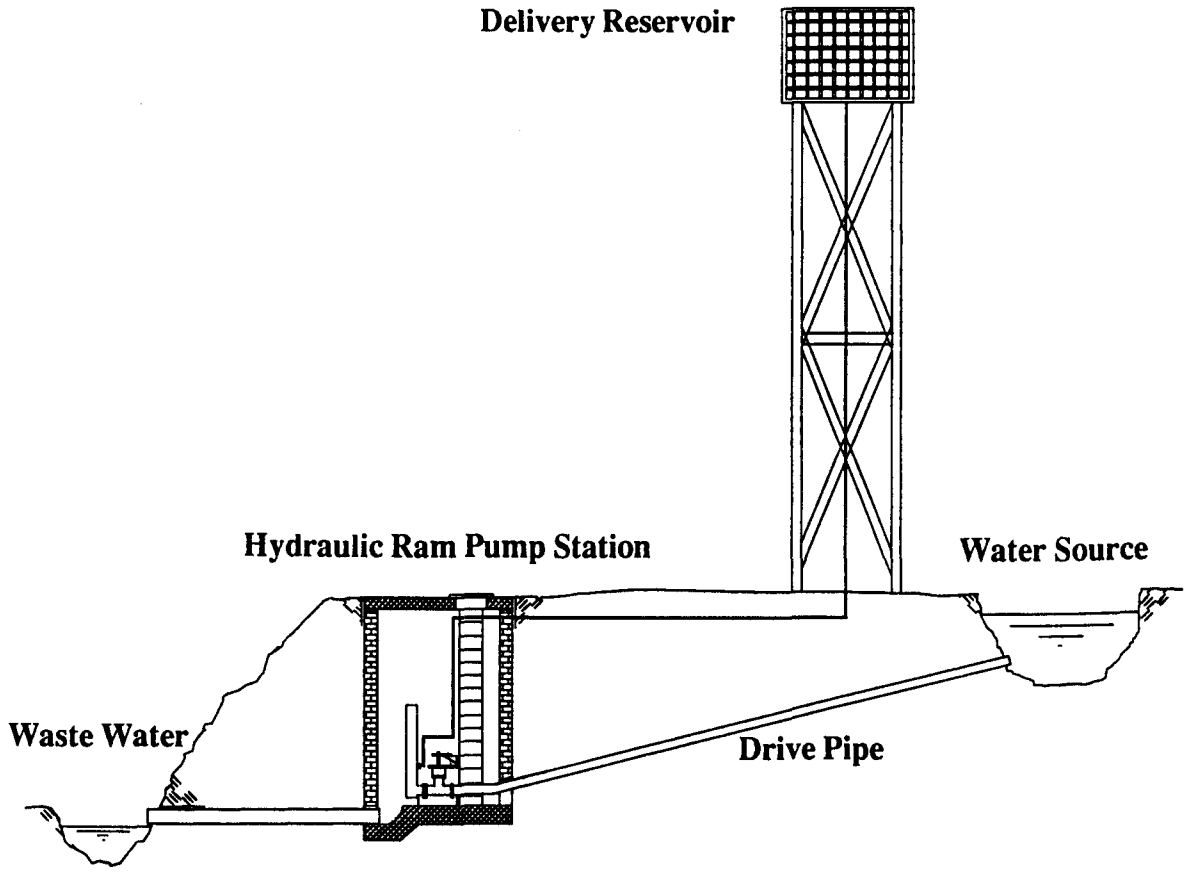

Figure 1. Typical Hydraulic Ram Installation.

Installation Typique du Bélier Hydraulique.

Although hydraulic ram pumps have been in production for in excess of two hundred years, many of the designs presently available require expensive casting techniques in their production, making them less than ideal for manufacture in developing countries, and unsuitable as a VLOM technology. It is these inadequacies that the University of Warwick's D.T.U. are attempting to address in the provision of new designs.

In addition to this deficiency, hydraulic ram design data presently available is often highly limited, causing water supply schemes to be either under or over designed, and often resulting in expensive failures. To quote two papers from a recent workshop on the hydraulic ram pump held in Tanzania:

> "Information on practical hydram sizes and installation limitations is often not available. Such information is necessary to prevent expensive failures in the field and arbitrary hydram designs and installations."-P.O.Kahangire[1].

> "From the point of view of water supply design, the engineers are only awaiting a hydraulic ram with established performance data so as to confidently incorporate it in their schemes."-T.S.A.Mbwette and E.Th.Protzen[2].

Recent work undertaken at the University of Warwick involving the use of computer simulation and analysis techniques has laid the foundations to providing comprehensive design literature for the designs produced by the Development Technology Unit, as well as identifying a methodology by which such data can be obtained for other hydraulic ram pump designs. This will hopefully lift the restriction on the wider dissemination of the technology.

How the Hydraulic Ram Works

The simplicity of the hydraulic ram pump represents one of its most attractive facets. The pump operates by extracting the energy from a large body of fluid as it falls through a small distance, and transferring this energy to a small quantity of the fluid which is delivered to a great height. Operation occurs around two simple valves; an impulse valve which closes automatically under dynamic drag forces; and a delivery valve which is a simple one way valve.

The pump undergoes a three stage cyclic operation; namely an acceleration phase, a delivery phase and a recoil phase. During the acceleration phase, water accelerates under gravity from the source to waste through a section of pipe known as the Drive Pipe, discharging through the Impulse Valve. (See Figure 2.) This process continues until such a time as the dynamic

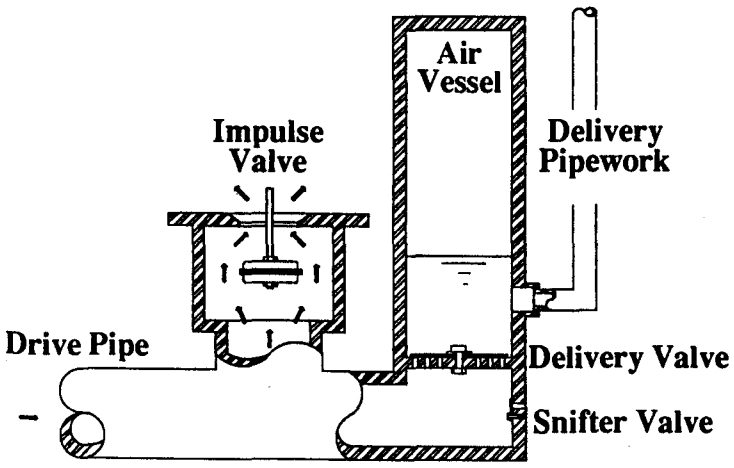

Water in the drive pipe accelerates under gravity, discharging to atmosphere through the impulse valve The valve plunger begins to move when the drag forces on it exceed its own weight.

Sous l'action de la gravitation, l'eau dans le tuyau d'alimentation s'accelère et s'évacue par la soupape d'arrêt. La soupape d'arrêt commence à se fermer quand la force du courant d'eau est plus grande que son poids.

Figure 2. The Acceleration Period.
L'Etape d'Accélération.

drag force on the impulse valve exceeds the force holding it open (typically its own weight), at which time the impulse valve begins to close. As the valve moves the valve orifice reduces and the drag forces increase accordingly. This results in a "snap shut" closure.

Once the impulse valve is closed, the water in the drive pipe is brought to rest. (Figure 3.) This inertial change causes a pressure rise in the drive pipe which allows the delivery phase to begin. When the transient pressure in the drive pipe exceeds that required for delivery it

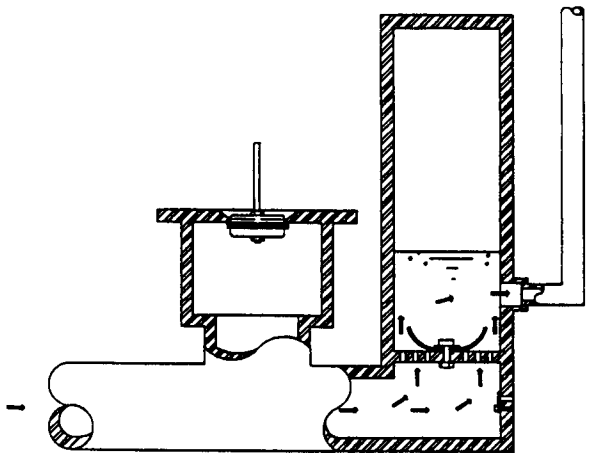

The impulse valve snaps shut under exponentially increasing drag forces. This induces a pressure rise that allows the delivery valve to open, and a small delivery to occur.

La soupape d'arrêt se ferme brusquement à cause de la force du courant d'eau qui s'augmente d'une manière exponentielle. Cette action provoque une augmentation de la pression qui ouvre la soupape de refoulement et permet un petit refoulement.

Figure 3. The Delivery Period.
L'Etape de Refoulement

causes the delivery valve to open and a small discharge to occur through the valve into a branching pipe. Pressure transients in this branch are cushioned by the presence of an air vessel. The delivery phase continues until the pressure in the drive pipe falls below the delivery pressure. When this happens the delivery valve closes, and any remaining velocity in the drive pipe causes a recoil to occur.(See Figure 4.)

The recoil phase represents a short period of reverse flow in the drive pipe. During this reverse flow, air enters into the drive pipe through a snifter valve (one way air valve) adjacent to the delivery valve. This entrained air passes through the delivery valve during the next delivery phase, and serves to replenish air lost into solution in the air vessel. During the recoil phase, the pressure below the impulse valve drops, allowing the valve to reopen under its own weight. This automatic reopening allows the whole process to start again with a new acceleration phase.

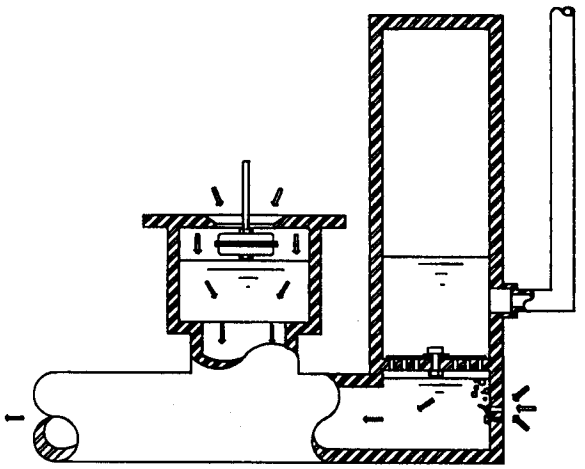

A negative pressure created by the fluid recoil allows the impulse valve to reopen, and also causes air to enter the body of the hydraulic ram.

La pression negative due au recul de l'eau permet l'ouverture de la soupape d'arrêt à nouveau. Celà aussi cause un ingrès d'air au corps de bélier.

Figure 4. The Recoil Period.
L'Etape de Recul.

In this way the pump operates continuously without any external energy input, delivering a small quantity of fluid on each full cycle. The rate of cycling varies depending on the particular pumping system characteristics, but 1 Hz is a typical cycle frequency.

Computer Simulation of the Hydraulic Ram

One highly significant aspect in the research associated with the development of cost effective and reliable hydraulic ram pumps and the provision of design literature has involved the use of computer based simulation and analysis techniques. A computer simulation of the Hydraulic Ram Pump was produced by the University's HYDROTransient SIMulation Unit.

The Unit's simulation uses a fixed grid method of characteristics solution for the pump, and has been developed alongside detailed measurement of actual pump performance. The simulation represents the hydraulic ram pump as a four pipe system including five boundary conditions. The majority of the boundary conditions are dealt with in a conventional manor[3], but the modelling of the impulse valve boundary condition required the use of some unusual methods. Accurate modelling of the impulse valve is important if the output from the simulation is to reliably reflect the operation of the pump.

To attain this accurate modelling, calibration data from particular impulse valve designs was used. The factors affecting the behaviour of a conventional impulse valve include: its maximum stroke, its mass, and its varying head loss and force characteristics. The varying head loss and force characteristics were determined by experimental measurement. This was done by fixing the impulse valve at a range of different strokes, and for each stroke position, varying the flow through the valve. For each steady flow rate set, readings were taken of head loss across the valve, and force on the valve. Graphs were then produced of the head loss and force characteristics for each of the valve positions. Curve fitting was then carried out on the data obtained, and as one would expect, both the head loss and the force data were found to follow a kQ^2 relationship; where k is a coefficient of force or head loss, and Q is the flow through the valve. Figure 5. shows the variation of the fitted head loss curves obtained for one of the D.T.U. valves as its position was varied from 40mm to 5mm from its seat.

Table 1 gives the head loss and force coefficients obtained using Nelder-Mead[5] curve fitting routines, for a range of different valve positions for one of the impulse valve's produced by the D.T.U. These curve fitting routines were then used again to obtain equations to describe the variation of these coefficients with valve position. These fitted curves are given in Figures

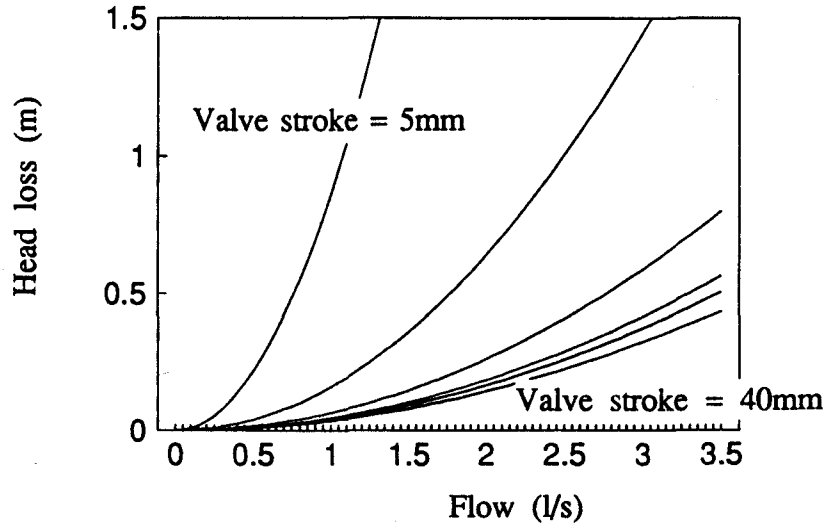

Figure 5. Impulse Valve Head Loss Characteristics.
Le Characteristiques de la Perte de Charge dans la Soupape d'Arrêt.

Table 1 gives the head loss and force coefficients obtained using Nelder-Mead curve fitting routines, for a range of different valve positions for one of the impulse valve's produced by the D.T.U. These curve fitting routines were then used again to obtain equations to describe the variation of these coefficients with valve position. These fitted curves are given in Figures 6. and 7. and the resulting equations are given as equations 1. and 2. These equations are specific to one particular valve, and can be used in conjunction with valve mass to fully describe the behaviour of a valve. Similar equations can relatively easily be obtained for the majority of valve types used in hydraulic ram pumps.

Table 1. Determined Head Loss and Force Coefficients.
Coéfficients de Perte de Charge et de Force Déterminées.

Valve Position(mm)	Kh	Kf
40	0.0381	-
35	0.0416	-
30	0.0414	-
25	0.0424	0.424
20	0.0462	0.43

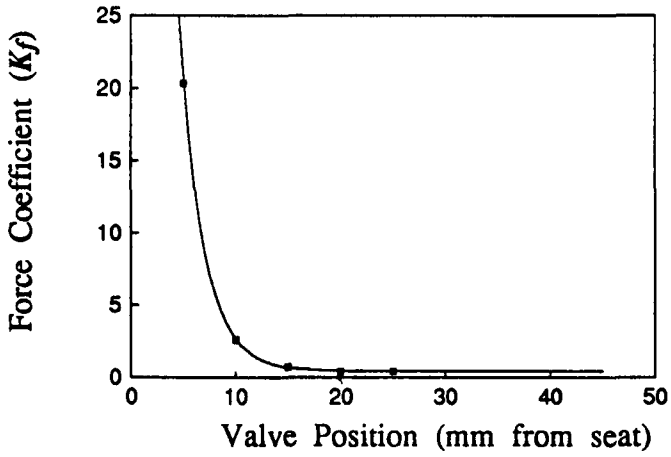

Figure 6.Variation of Force Coefficient with Displacement
Variation du Coéfficient de Force avec Déplacement

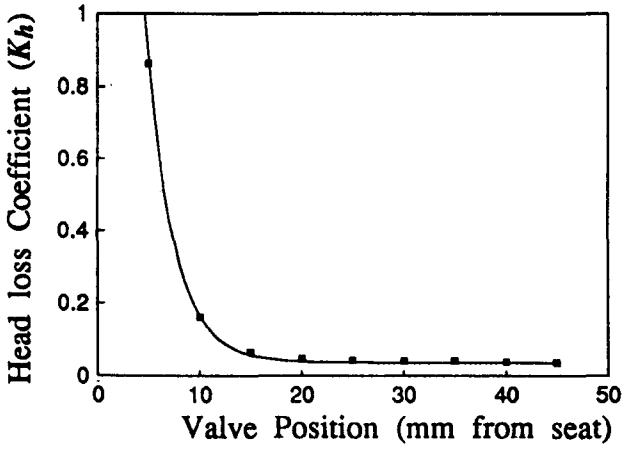

Figure 7.HeadLoss Coefficient Variation with Displacement
Variation du Coéfficient de Perte de Charge avec Déplacement

$$K_f = 180e^{-0.04407X} + 0.43 \quad (1)$$

$$K_h = 5.338e^{-3.726X} + 0.0355 \quad (2)$$

where : K_f = Impulse valve force coefficient

K_h = Impulse valve head loss coefficient

X = The displacement of the impulse valve from its seat(mm)

These equations provide the basis for the impulse valve boundary condition algorithm on the University of Warwick's simulation. The algorithm works by using a value of valve position calculated for a previous time step in conjunction with equation (1) to determine the force coefficient for the valve at the current position. From this, the force on the valve can be determined using the value of flow through the valve calculated for the previous time step in conjunction with equation (4). Once the force on the valve is known, the new valve position, velocity and acceleration can be determined using basic Newtonian equations of motion. Once the position of the valve is known the boundary condition can be simply solved using equation (3) where the value of K_h is obtained from equation (2).

$$H_f = K_h Q^2 \quad (3)$$

$$F = K_f Q^2 \quad (4)$$

where : H_f = Head loss across the impulse valve

Q = Flow through the valve

F = Force on the valve due to drag effects

This method for modelling the impulse valve is limited in so far as it is based on head loss and force coefficients obtained under steady flow conditions. However, if the time step used in the simulation is small enough, it is believed to represent a good approximation of valve behaviour. The time step used in a simulation of the hydraulic ram is typically 2.5 x 10^{-5}.

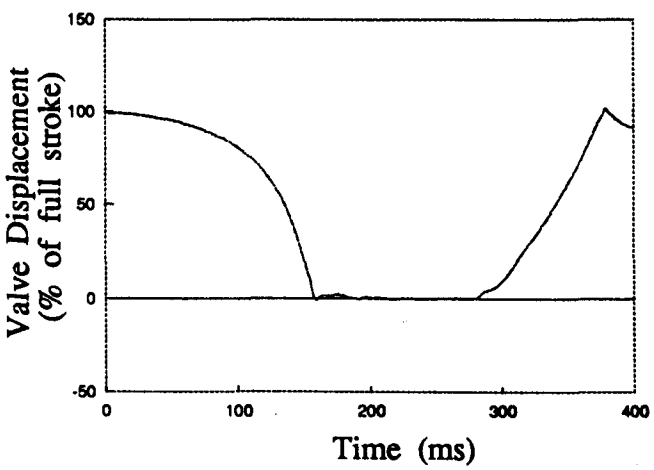

Figure 8. Measured Valve Displacement.
Soupape Déplacement Mesurée

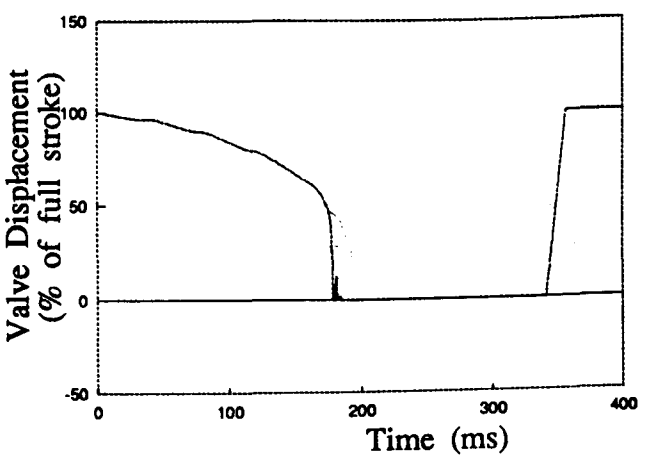

Figure 9. Simulated Valve Displacement.
Soupape Déplacement Simulée

Figures 8. and 9. illustrate valve position histories for measured and simulated data respectively. The measured trace was obtained using a linearly variable differential transformer sampled by a high speed analogue to digital converter.

The attraction of the method is that many valves can be quickly calibrated, provided calibration equipment is readily available. This allows more accurate modelling as it does not involve any of the approximations associated with dimensionless solutions to boundary conditions. The calibration of the impulse valve in this way is of wider significance in hydraulic ram pump and system design as the equations given can be used to determine the cut off velocity of a given valve and the head loss at various positions. These can be used to determine the maximum delivery head of a given pump, and indicate maximum efficiency settings.

It is hoped that the method of impulse valve calibration described here will be more widely adopted both for simulation purposes and normal calibration.

The Application of the Simulation.

The computer simulation has provided a very powerful tool for the purpose of pump design optimisation and the provision of performance data. The earliest application of the simulation was in the creation or confirmation of theories that describe the operation of the pump. To illustrate this figures 10. and 11. are respectively measured and simulated pressure time histories for a hydraulic ram pump. The similarity of the curves would confirm the accuracy of the simulation for the given operating conditions. Once this is assured, the simulation can offer significant insight into the pump's operation. Figure 12. represents the simulated variations in the drive pipe velocity for the same time period. Data of this type is very difficult and highly expensive to produce experimentally. This extra insight confirms some theoretical analyses(O'Brien

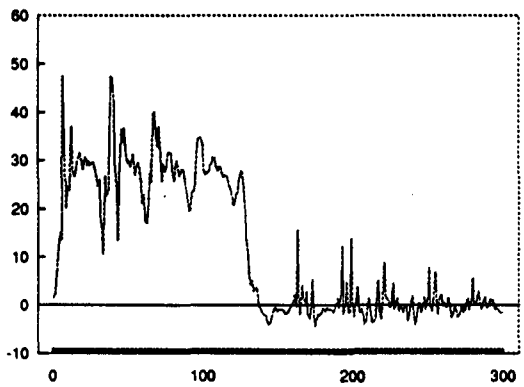

Figure 10. Measured Pressure Transient.
Pression Transitoire Mesurée

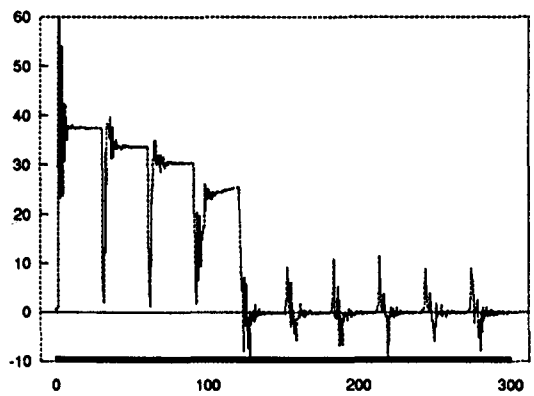

Figure 11. Simulated Pressure Transient.
Pression Transitoire Simulée

and Gosline) of the pump in a way that was previously impossible, and so enables a trustworthy analysis to be produced to determine important quantities such as volume delivered per cycle using explicit equations. It can be seen from Figure 12. that each pressure rise shown in Figures 10. and 11. is associated with a step down in velocity that is maintained for a time period 2L/a where L is the length of the drive pipe, and a is the wave speed. This is a direct confirmation of the theoretical analysis proposed by O'Brien and Gosline in 1933, but later ignored in many, more recent analyses of the pump.

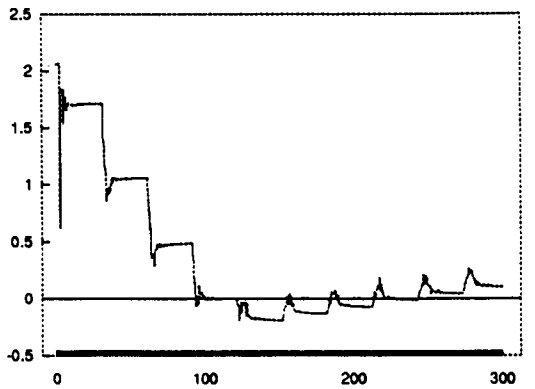

Figure 12. Simulated Transient Velocity.
Vitesse Transitoire Simulée

Although such information is a valuable insight into the operation of the hydraulic ram pump, the simulation is presently being used more directly on parametric studies to determine operational limits, and optimums for particular impulse valve designs. This procedure has been severely hampered by the length of the run times although recent attempts to reduce these have been successful, allowing more extensive studies to occur. Versions of the simulation have been set up to repeatedly simulate a pumping device under fixed operating conditions, but gradually varying an individual parameter. In this way the effect the parameter has on performance can be determined, and optimum and peripheral values can be identified.

One recent study involving such an iterative study of the significance of drive pipe length suggested a minimal fluctuation in output power for the D.T.U. impulse valve described above, for lengths ranging from 5m to 20m. A reduced performance was found beyond these values. Information of this type is specific to a particular device, and the tabulation of such data with each hydraulic ram pump produced would go some way towards meeting the need for better design data identified by Kahangire and also Mbwette and Protzen.

It is apparent that the University's simulation will be primarily involved in the production of tabular design data in this way. It is hoped that some further studies will yield information such as optimum impulse valve characteristics for a given pump as well as the more mundane yet needed data regarding optimum dimensions and settings.

Limitations of the Simulation.

One of the major difficulties associated with the simulation of the hydraulic ram are related to air entrainment. In its normal mode of operation, the air entrained through the snifter valve is delivered through the impulse valve during the delivery cycle and uniformly distributed by the turbulence present during delivery. The accuracy demonstrated in Figures 10. and 11. is attained by assuming a low, pressure independent wave speed in the section of pipe in the air vessel. This approximate modelling is adequate for the majority of operating conditions. However, if excessive air entrainment occurs through the impulse and snifter valves such that air travels up the drive pipe, significant inaccuracies can result.

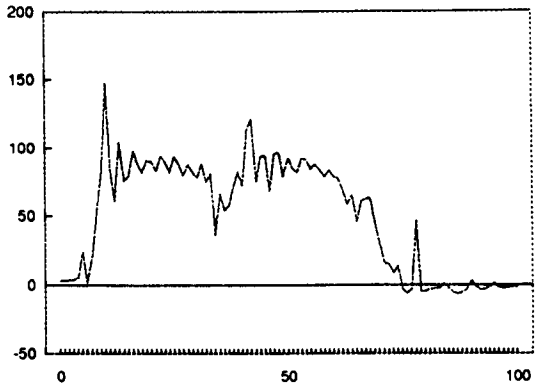

Figure 13.Measured Pressure Transient for an 84m Delivery.
Pression Transitoire Mesurée pour un Refoulement de 84m.

This is illustrated in Figure 13. which can be seen to deviate significantly from the simulated pressure time history in Figure 14. with respect to the period of the peaks. The reason for this can be determined from the simulated velocity history for the same operating conditions given in Figure 15. A large recoil velocity is found in the output. The effect of this on a conventional pump would be to induce large quantities of air into the drive pipe, which in turn would reduce the wave speed in the drive pipe. The simulation does not account for this as a drowned impulse valve is assumed.

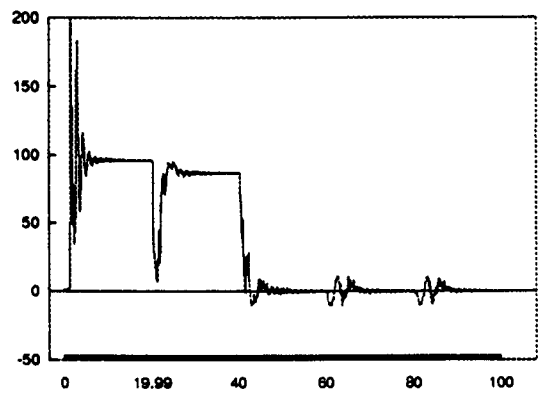

Figure 14. Simulated Pressure Transient.
Pression Transitoire Simulée.

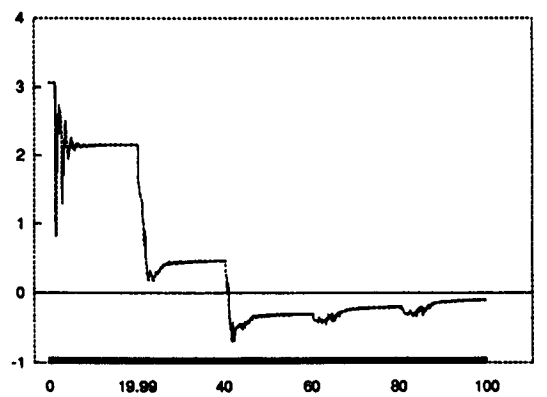

Figure 15. Simulated Velocity Transient.
Vitesse Transitoire Simulée.

It should be noted that this limitation in the analysis does not in any way invalidate the use of the simulation as a tool for optimisation, as hydraulic rams operating with air entrainment of this type are generally operating away from their performance optimum. It should also be noted that many impulse valves do operate in a semi flooded state as is modelled by the University's simulation. It is also interesting to note that air entrainment of the type illustrated has been the perceived cause of poor reliability in some high delivery head installations.

Conclusion

Some of the original aspects of the University of Warwick's computer simulation of the hydraulic ram pump have been discussed in detail. The analysis associated with the simulation is primarily being directed at the development of designs suitable for manufacture in developing countries. It is anticipated that the use of such sophisticated analytical tools will ensure the resulting designs are highly attractive in comparison with others commercially available, and the associated design literature will serve to enable wider dissemination of the technology. In areas in which the technology is appropriate, it offers an ideal solution to the human suffering associated with water porterage, and water washed diseases, without involving highly technical maintenance and external fuel supplies.

It is hoped that the methods described will be of benefit to others involved in similar analyses, as the ultimate provision of water supply systems is the main objective of the research being undertaken.

Acknowledgements.

The Authors would wish to acknowledge the sponsorship of the University of Warwick's Civil Engineering Research Fund and the generous support offered by K.S.B.(UK) Ltd. In addition to this, we would wish to acknowledge the Overseas Development Administration, and the Christian Charity Tear Fund for their commitment to the development of a pumping device suitable for manufacture and widespread use in the third world.

Bibliography.

1. P.O.Kahangire 1986.
Theory and design of the hydraulic ram pump.
Proceedings of a workshop on Hydraulic Ram Pump(Hydram) Technology. IDRC.

2. T.S.A.Mbwette and E.Th.P.Protzen 1986
Hydraulic ram pumps as potential pumping units for rural water supply in Tanzania.
IDRC.

3. V.L.Streeter and E.B.Wylie 1984.
Fluid Transients.
McGraw-Hill.

4. M.P.O'Brien and J.E.Gosline 1933.
The Hydraulic Ram
University of California Publications in Engineering Vol.3,No.1,pp1-58.

5.
Matlab
Mathworks Inc. Sherbourn MA U.S.A.

COMPUTER SIMULATION OF THE HYDRAULIC RAM PUMP

P.B.M. Glover BSc AMIMechE and

Dr A.P. Boldy BSc PhD C.Eng MICE,

HYDROtransient SIMulation Unit,

Department of Engineering,

The University of Warwick.

Summary

In this paper, the authors present the steps that are being taken to produce an accurate simulation of the hydraulic ram pump. The work is being carried out in conjunction with a product development project sponsored by the Overseas Development Administration, which in turn is associated with a rural water supply project for Zaire sponsored by Tear Fund. The project is of particular interest in the field of pressure surge analysis as it involves computer simulation of hydraulic transients for the purpose of harnessing as opposed to suppressing pressure surges.

1. Introduction

The hydraulic ram pump has experienced little development in recent years. In spite of the one and a half centuries that have lapsed since the first patents, it is now only deployed in relatively obscure sites. This can largely be explained in terms of the nature of water supply schemes in the majority of developed countries. These tend to treat large quantities of water and then provide a system of distribution that attempts to minimise wastage, so providing little scope for the use of hydraulic rams. In addition to this, high ram costs and poor system design literature have ensured that even duties ideally suited to the hydraulic ram are often performed by less suitable but better documented technologies.

Renewed interest in the hydraulic ram has stemmed from its minimal operational costs and high reliability which make it ideal for certain remote sites. A number of third world development organisations have shown keen interest in the use of the device for rural water supplies in circumstances where technical literacy is poor, and alternative power supplies are limited. Many attempts have been made to develop a reliable ram design that can be manufactured in developing countries, and also to adequately predict the performance of the pump to allow supply systems to be accurately designed. None of these have achieved any significant scale of success or adoption outside of the original project areas. With the sponsorship of the Overseas Development Administration, the University of Warwick's Development Technology Unit has set itself these objectives.

Previous attempts have often been hindered by poor understanding of the pump, and the complexity of the algorithms needed to describe its behaviour. It is believed that the production of a reliable computer simulation will help to clarify many misconceptions about the pumps operation, and provide a design tool for both pump and system development. To this end, the authors are working in collaboration with the Development Technology Unit on behalf of the University's HYDROtransient SIMulation Unit.

1.1 Mode of Operation

The hydraulic ram pump operates by inducing a pressure surge in a gravity fed conduit. This is produced by the rapid closure of a valve at the point of discharge. The increase in pressure allows a small flow through a non-return valve into a delivery pipe. The pressure surges are suppressed in the delivery pipe by the presence of an air vessel.

As back flow is limited by the non-return valve, the delivery pressure can greatly exceed the steady state pressure in the gravity fed conduit. Once the period of delivery is over, a quantity of water is once again wasted as the discharge valve is reopened and the water in the conduit is allowed to accelerate for the next pumping cycle. The pump is made to operate automatically by enabling the discharge valve to close under frictional drag, and then to reopen under the negative pressures experienced with the reflected pressure wave.

For the purpose of clarity, the main conduit will hitherto be referred to as "the drive pipe"; the discharge valve will be referred as "the impulse valve"; and the non-return valve as "the delivery valve", as illustrated in figure 2.

1.2 The present state of the research.

A one dimensional simulation of the pump's operation has been produced using the method of characteristics, and significant similarity with reality is already apparent. The process of modifying the simulation to as accurately as possible mimic the performance of the pump promises to be an arduous task involving the use of extensive experimental data alongside the development of improved theoretical algorithms. Possibilities for exploiting alternative methods of analysis are discussed in the paper.

2. Experimental Procedure.

In order to produce a simulation that can be used as a tool for pump design, it is necessary to provide a means by which extensive experimental data can be collected. In the first instance, this data is needed to pin-point necessary modifications to the program, but ultimately is required to quantify the value of any modifications identified by the simulation.

For this purpose, a hydraulic ram testing rig has been set up by the Development Technology Unit. The rig has capacity for testing two ram systems simultaneously, and offers a variable supply head of up to five metres. Water for the test rig is recirculated by a high quality submersible pump set, generously donated by KSB Pumps Ltd. A diagram of the complete test installation is given below.

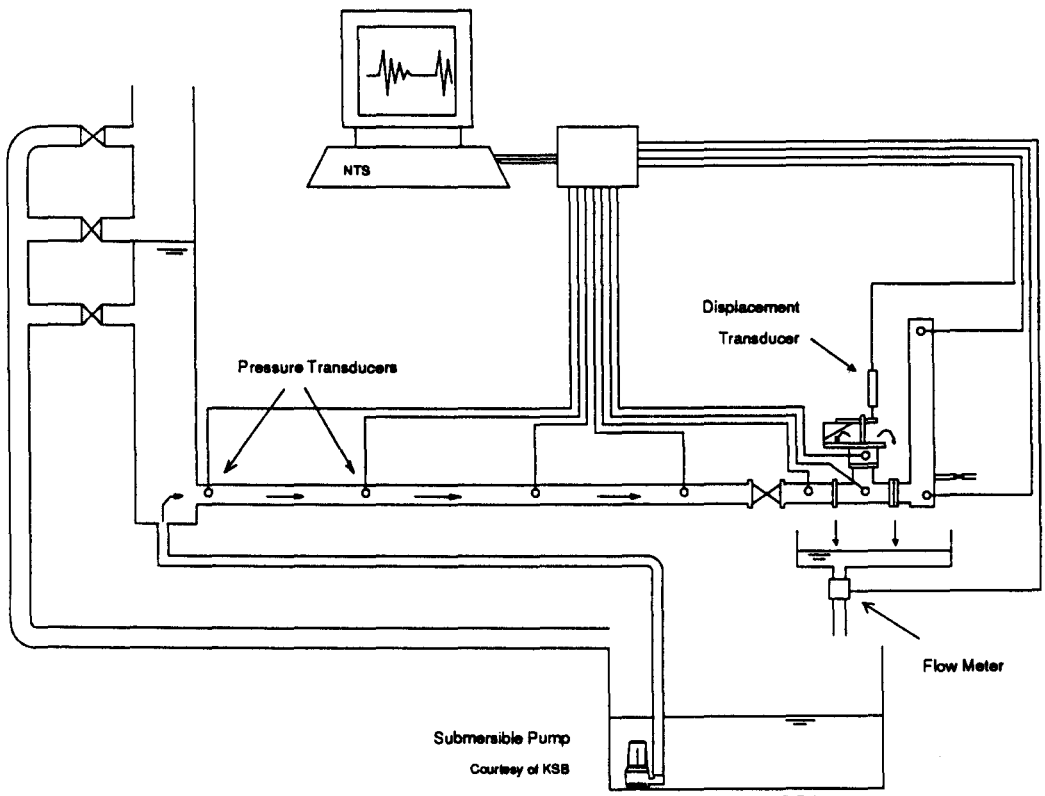

Figure1. The Experimental Test Rig (D.T.U.).

2.1 Instrumentation.

Pressure fluctuations in the body of the pump and the drive pipe are measured on the rig by a series of piezo-resistive pressure transducers. These are sampled by a 500kHz Analogue to Digital converter with fast response programmable gain amplifiers, from which samples are down loaded to a Northern Technology Systems Personal Computer.

A displacement transducer is used to monitor the position of the impulse valve, and with the help of the A/D converter, valve closure times can be accurately determined. A simple flow device giving a pulsed output for the data acquisition system, monitors drive pipe flows. This flowmeter is only useful for integrated flow monitoring and no facility is presently installed for monitoring transient velocities. Facility does however exist for more accurate, volumetric monitoring of flow rates.

It is hoped that, as the research continues, the instrumentation available will provide further insight into the pump's operation for the purposes of developing the simulation. Possible technologies for the measurement of transient velocities are presently under investigation, should they prove to be necessary additions to the rig.

The equipment described enables parameters such as wave speed, valve position delivery period and transient pressures to be measured accurately. A programme of testing is underway, using this equipment to build a database of pump characteristics, which in turn is being used to identify necessary improvements and modifications to the program.

3. The Development of a Simulation.

The first program developed was based on a simple one dimensional simulation of a gravity fed, single pipe system, using the method of characteristics. In an attempt to describe the operation of the hydraulic ram, a complex boundary condition was imposed on a node close to the discharge valve. This represented the operation of the delivery valve, the air vessel, and the delivery pipe. A simple valve closure boundary condition was included at the discharge point.

Although this simulation provided a useful insight into the pump's behaviour, and demanded relatively little computer time it was apparent that its simplicity would be restrictive. It is interesting to note that an attempt to keep the simulation as simple as possible created boundary conditions of such complexity as to limit the flexibility of the program, as well as only providing an approximate simulation of reality.

The present version of the simulation is based on a four pipe system with: reservoir, three way junction, impulse valve, and air vessel boundary conditions, as illustrated in figure 2. The basic structure of the program is significantly more complex than the previous version, but more flexible in that individual elements can be drastically changed without affecting the rest of the simulation. This is an important attribute in view of the planned programme of development.With the likelihood of air entrainment, it may also be necessary to account for a varying wave speed in one or more of the pipes.

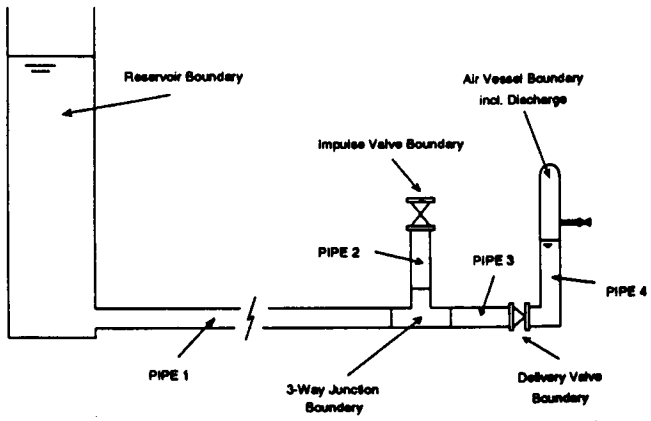

Figure 2. Elements Included in the Simulation.

The new structure is a much more accurate representation of the pump. Greater complexity may however, be necessary in future if a snifter valve(a small air inlet valve situated adjacent to the delivery valve on some ram pumps, for the purpose of replenishing the air supply in the air vessel), is to be simulated with any greater sophistication than simply imposing a slower wave speed in the relevant section of the pump.

3.1 The Impulse Valve Boundary Condition

The earlier version of the simulation incorporated a linearly varying dimensionless valve opening[3]. This is defined as:

$$\tau = \frac{Cd.A}{(Cd.A)o} \qquad -(1)$$

where τ = Dimensionless Valve Opening,

Cd = Discharge Coefficient,

A = Area of Valve Opening,

and o represents values at fully open position.

It was apparent from observation that this offers a poor representation of the impulse valve. A closer approximation was proposed using a two step closure. The second half of the valve's period involving a higher rate of closure. It is interesting to note that this is contradictory to recommended practice for the suppression of pressure surges. Figure 3 shows the nature of closure in the two simulations.

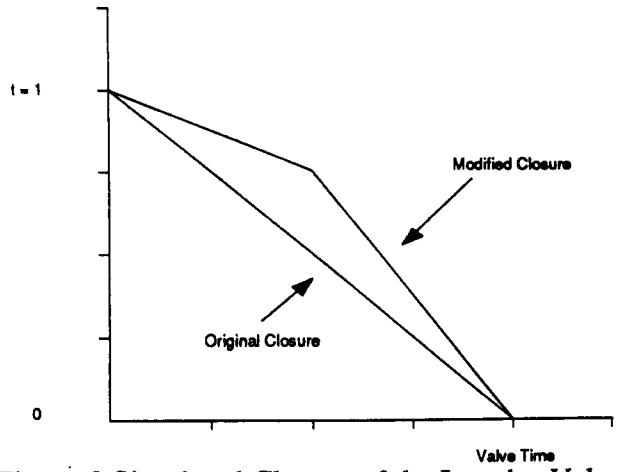

Figure 3.Simulated Closure of the Impulse Valve.

The displacement transducer offers a means for accurately measuring the time and form of the closure. An example trace produced by the displacement transducer is given in figure 4. (Note: A small degree of mechanical bounce is visible.)

In order to simulate the automatic operation, the valve closure is made to commence when a predefined reaction velocity is detected at the valve. Automatic reopening of the valve occurs when the pressure at the valve falls below atmospheric. At this stage the value of the dimensionless valve opening variable is returned to unity. This allows the water in the drive pipe to accelerate once more, in readiness for the next pumping cycle.

3.1.1. Limitations of theValve Boundary Condition.

The valve boundary condition described appears to provide an acceptable level of similarity with the actual impulse valve operation, but is quite restrictive as values such as valve closure time have to be input from experimental data.

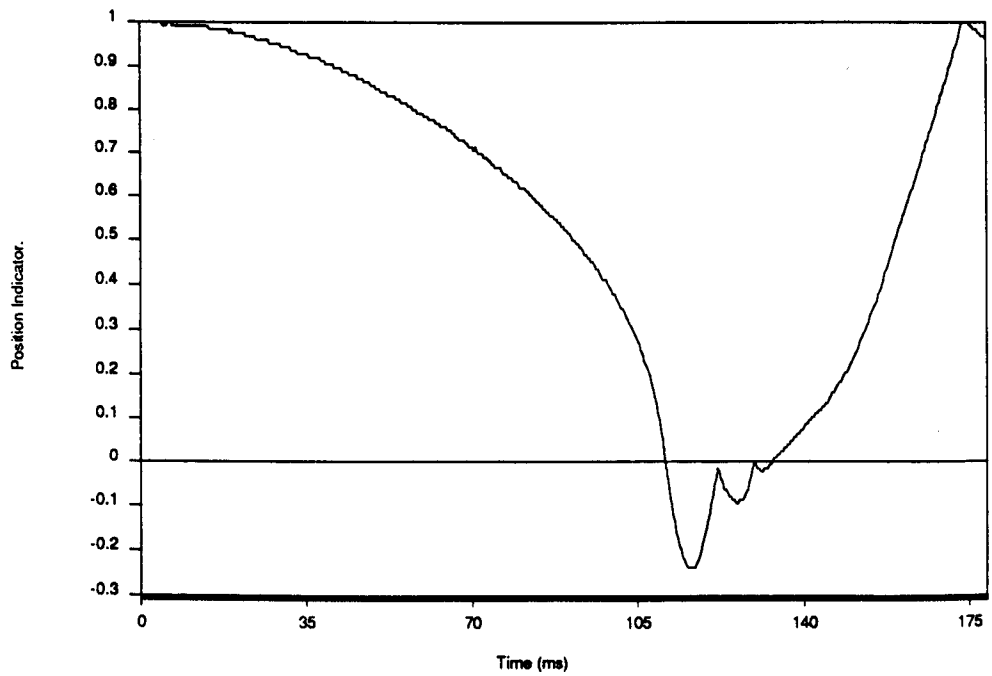

Figure 4. Trace of Impulse Valve Closure.

The displacement transducer offers a means by which steady state valve characteristics at various degrees of closure can be included in a complete valve characteristic algorithm that is based on the pressure differential across the valve. If successful, this will enable different system configurations to be simulated without modification to the boundary condition or the need for inputting a new closure time.

The present boundary condition also assumes instant reopening of the valve. This is probably acceptable as during the period of opening a small back flow is experienced, and a small quantity of air enters pipe2. It may however, prove necessary to include the reopening time and the effect of the air ingress, depending on the success of the simulation in its present form.

3.2. The Delivery Valve Boundary.

The delivery valve is simulated as a simple two way junction in which reverse flow is inhibited. It is likely that this will have to be modified to include the frictional loss across the valve, and the inertia of the valve, if a theoretical pump efficiency is to be accurately calculated. The present simulation is found to produce significantly better performance figures than those measured, indicating that this modification is necessary.

3.3. The Air Vessel Boundary Condition

The simulation adopts a conventional analysis of an air vessel in which the air is assumed to adhere to the relationship:

$$H.V^{\gamma} = \text{Constant} \qquad \text{- (2)}$$

where H = Absolute Head,

V = Air Volume present,

γ = The ratio of the Isobaric and Isochoric specific heat capacities for air.

The value of γ for a perfect gas varies between values of 1 and 1.4 depending on whether the process in question is isothermal or isentropic. A value of 1.2 is assumed for the purposes of the simulation, until such time as experimental data is found to disagree with this.

The calculation of discharge flow is included in the air vessel boundary condition. The characteristic of the receiving system is assumed to follow the relationship:

$$H_f = KQ^2 \qquad \text{- (3)}$$

where H_f = head loss due to friction

Q = the flow in the system

K = constant.

This relationship is compatible with a throttled head loss characteristic which is acceptable for comparison with experimental data where delivery occurs through a throttled valve.

The relationship is used to determine the discharge flow for a given pressure at each time interval. This flow is then subtracted from the calculated inflow to determine the change in volume in the air vessel. This is then used to calculate the associated pressure change using Equation (2).

For systems in which the air vessel is not adequately sized, it may be necessary to include transient calculations for the delivery system.

3.4 . Wave speed

The present simulation assumes a fixed wave speed and required the user to input a predetermined value. This enables a series of simulations to be run using different wave speeds to attempt to most accurately mimic recorded traces. This is an important facility at this stage of the development programme, as changes in wave speed have been found to significantly alter the form of the transient.

A wave speed of 1380m/s is calculated for the test rig using the well known formula:

$$c = \frac{1}{\sqrt{\rho\left(\frac{1}{K} + \frac{D}{T.E}\right)}}$$

where : c = Wave speed, K = Bulk Modulus of the Fluid,
ρ = Density of water, E = Elastic modulus of material,
T = Pipe wall thickness, D = Diameter.

Using the high speed A/D to measure wave speed, results of 1400m/s and below 700m/s were obtained for pipe 1 and 3 respectively. The result for pipe 3 was difficult to determine on account of the short distance involved.

It is anticipated that a variable wave speed may exist in pipe 3 on account of air entrainment through a snifter valve. If this greatly reduces the accuracy of the simulation using fixed wave speeds, it will be necessary to include a variable wave speed analysis for pipe 3 using interpolations. An accurate means for calculating the wave speed variations will then be required.

4. Results.

The problems involved in recording hydraulic transients and storing collected data in a form that is easily analysed, are well documented. Instrumentation and experimental accuracy for transient testing has become a well developed science, while difficulties of data manipulation and interpretation, continue to limit many development projects. Such problems become all the more severe when comparison is required between simulation and experiment.

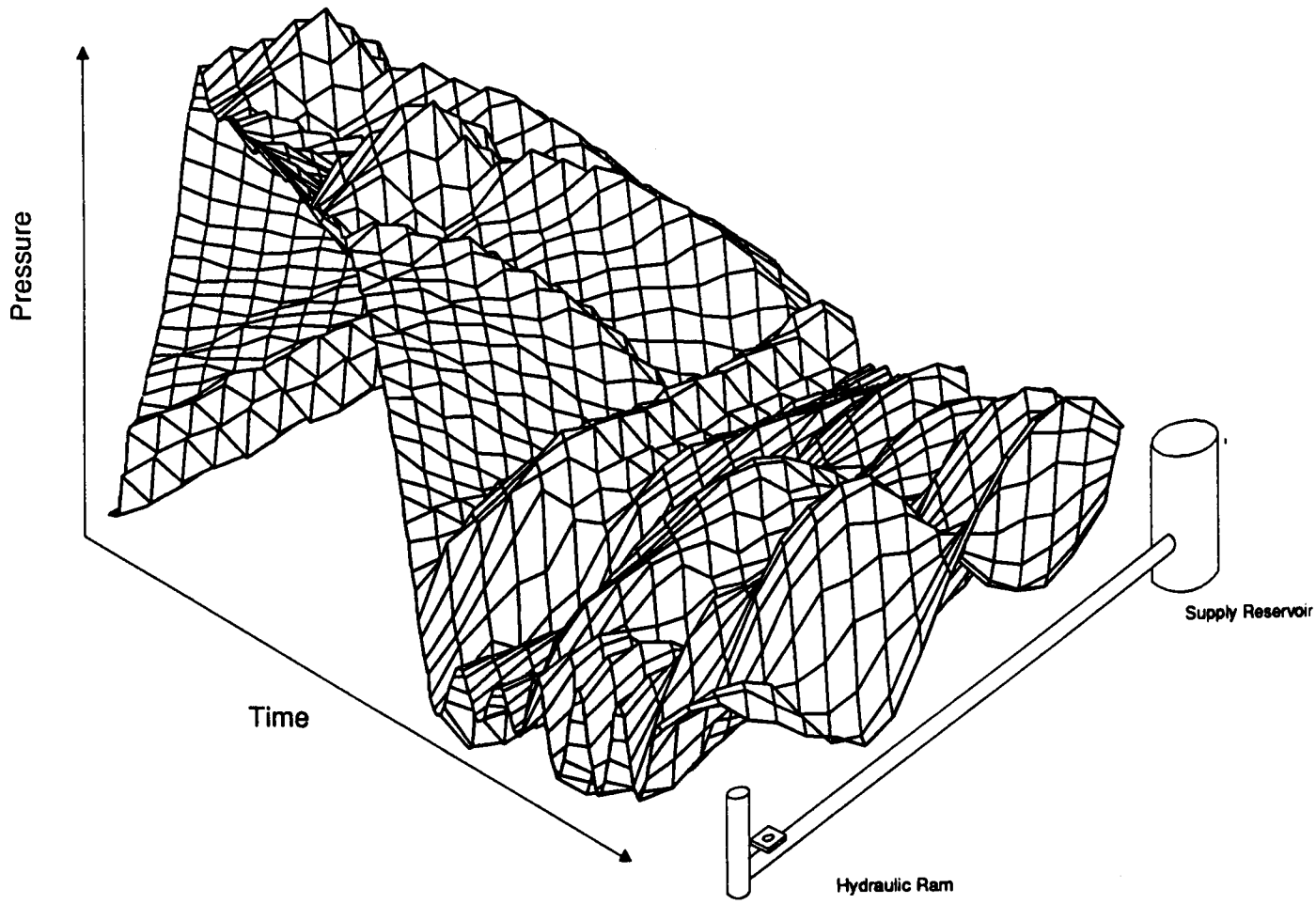

Figure 5. Simulated Pressure Transients in Drive Pipe.

A simple two dimensional representation of a transient at a single position on the main, is often the means by which comparisons are made. Although this is very useful for a measured comparison at the position in question, it does not provide enough information to visualise the interaction of various components. In an attempt to surmount this problem, three dimensional representations of pressure transients during the pumping cycle have been produced from both simulated and measured data. These are given as Figures 5. and 6. respectively.

The diagrams differ significantly in their resolution. This is largely explained by the experimental restrictions on the number of transducers available. However significant similarity is apparent between the two diagrams, and the resolution provided in Figure 5. is valuable for the interpretation of the measured transient in Figure 6.

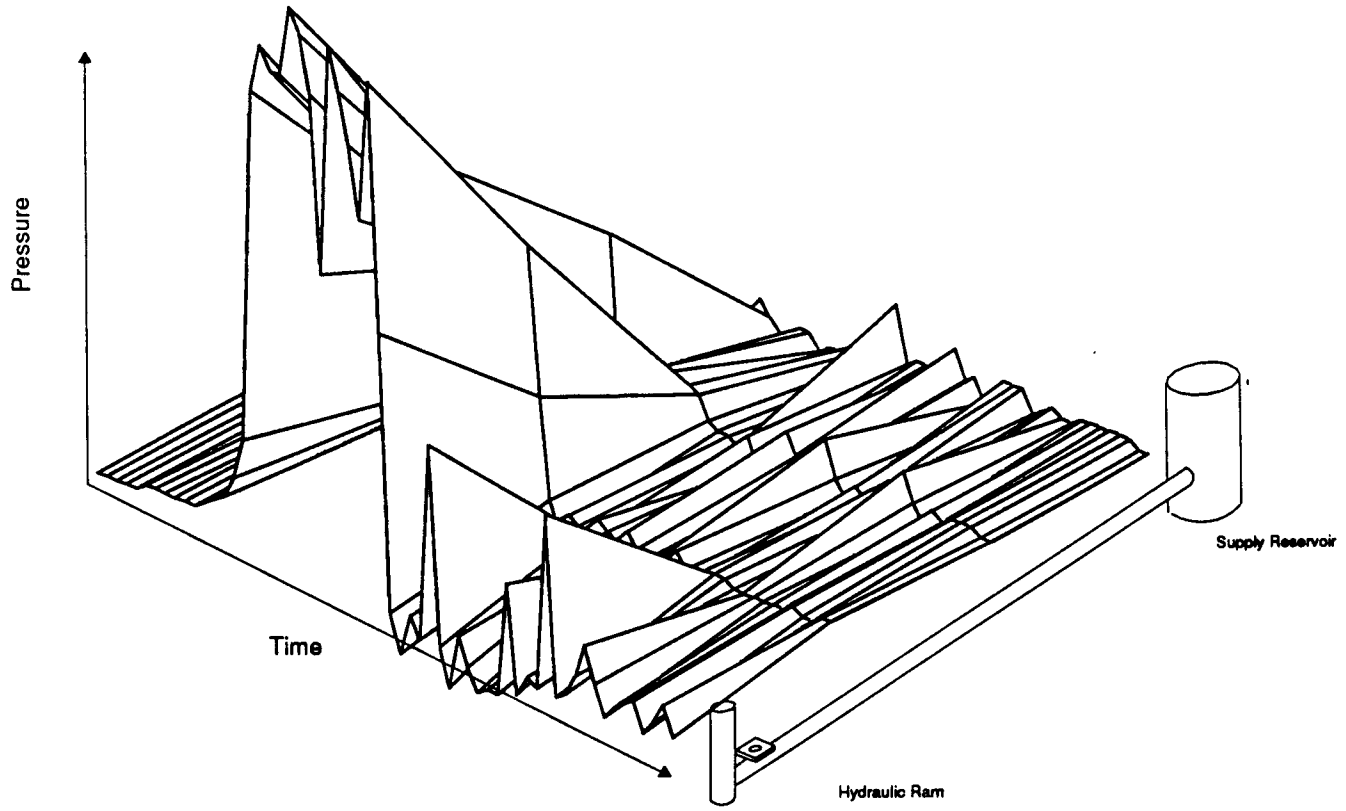

Figure 6.Measured Transient Pressures in Drive Pipe.

Attention is drawn to the period of high pressure delivery in both of the diagrams. It is noted that the shape of the transient in this section differs greatly between the measured and simulated diagrams. It has been found that the shape of the pressure fluctuation in this period is highly dependent on the wave speed in the various pipes. A process of tuning is therefore necessary to provide a more equal comparison. If this does not prove adequate, it may be necessary to incorporate a variable wave speed algorithm. This will drastically complicate the process of tuning.

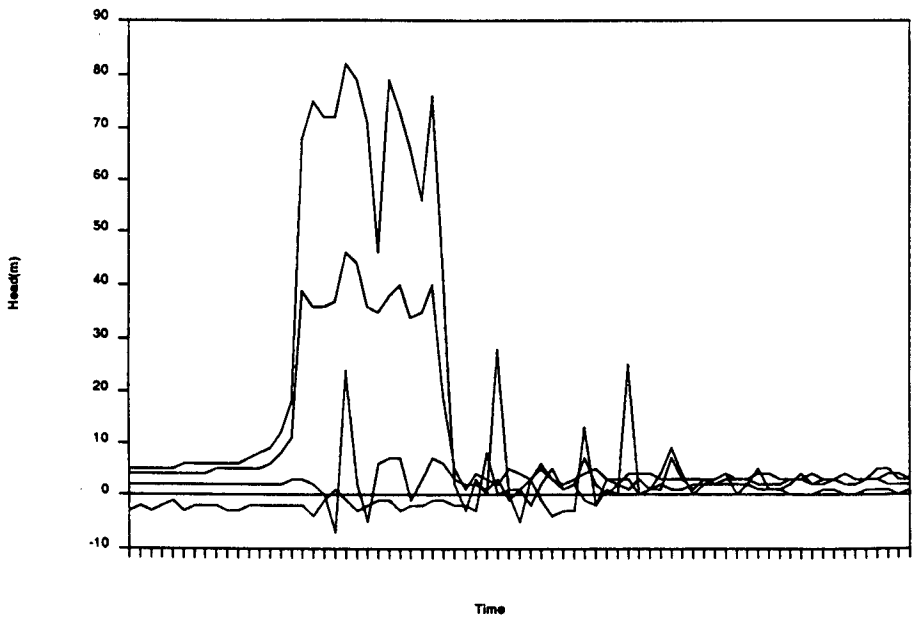

Figure 7.Transient Pressures Measured in the Drive Pipe.

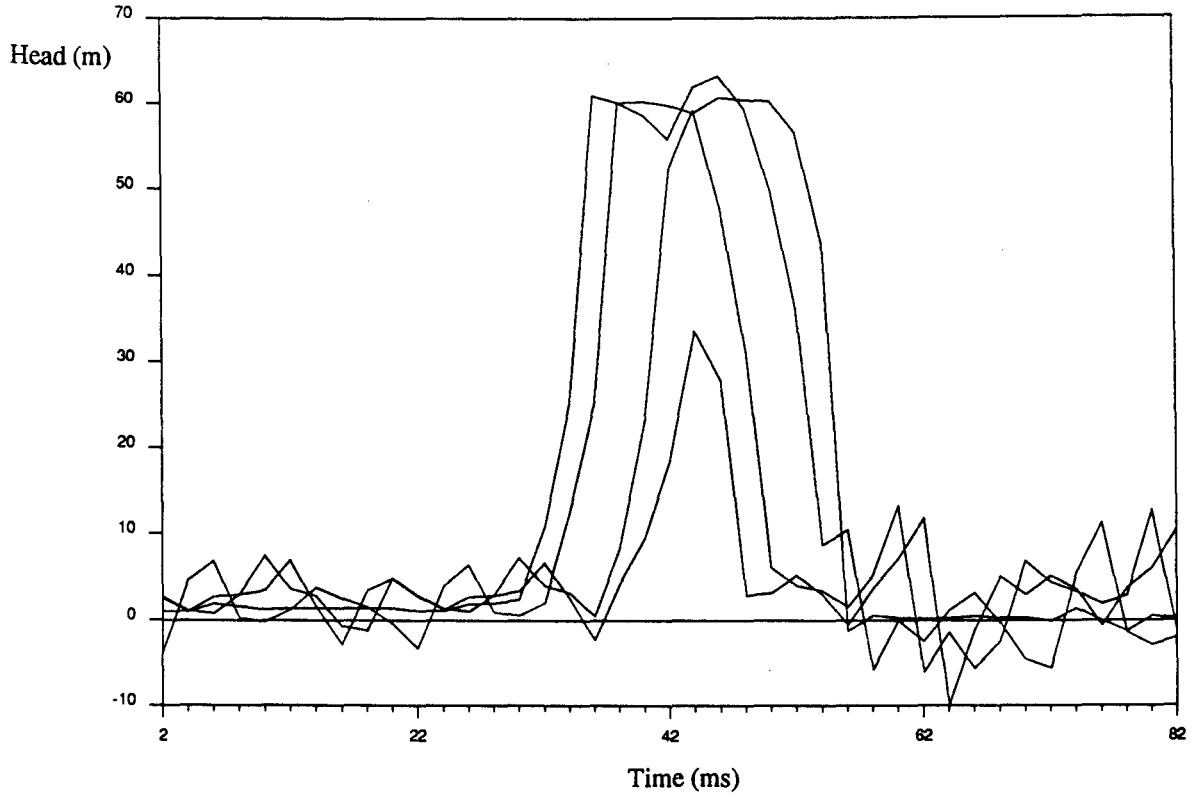

Figure 8.Transient Pressure Simulated for the Drive Pipe.

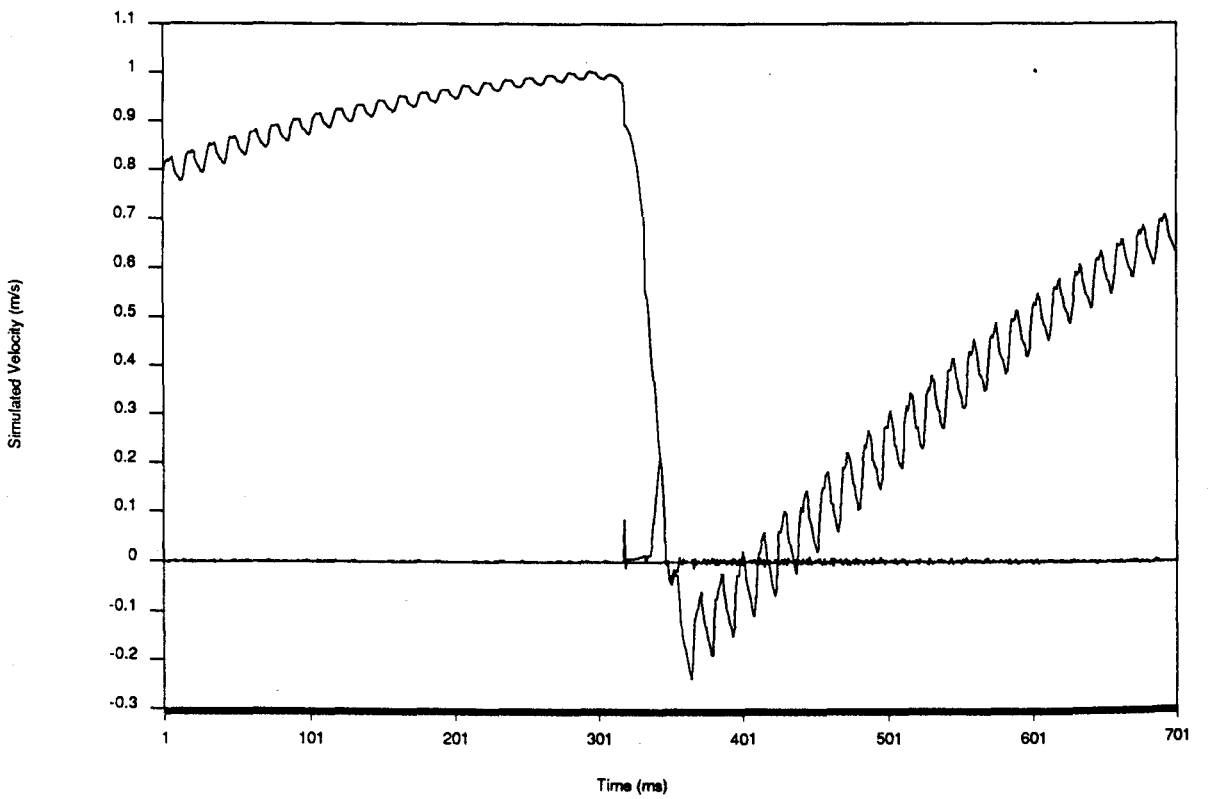

Figure 9.Simulated Velocities in Drive and Delivery Pipes.

Two dimensional plots of simulated and measured results are given in figures 7. and 8. for a series of positions on the drive pipe. Although the plots represent slightly different positions on the drive pipe, the similarity is apparent, while the need for some tuning of the program is also demonstrated.

Figure 9. is a two dimensional plot of the transient velocities simulated in the drive and delivery pipes. Once the program has been further modified and proven, information of this type will provide an accurate assessment of pump performance.

5. Conclusions.

It is apparent from the results given that the production of a reliable simulation for use as a design tool is highly feasible. The test installation produced by the Development Technology Unit, and the program development, represent major steps towards this goal. With further testing, and with the incorporation of the discussed modifications to the impulse valve and the delivery valve boundary conditions, the program should be capable of providing accurate performance predictions.

A new project will then commence using the program to identify necessary pump modifications and to produce design charts for engineers in the field. Once proved, the simulation will provide a means of assessing ram performance, modifying pump designs, and assessing alternative applications for the hydraulic ram phenomena.

6. Acknowledgements

The authors would wish to thank K.S.B. Pumps, Fluid Kinetics, Northern Technology Systems, and Severn Trent Water for their support in this research. They would also wish to acknowledge the University of Warwick's Civil Engineering Research Fund, the Development Technology Unit, the Overseas Development Administration and Tear Fund for their commitment to the development of a pumping device suitable for manufacture and widespread use in the third world.

7. References.

1. Rennie, L.C. and Bunt, E.A.:"The Automatic Hydraulic Ram". The South African Mechanical Engineer, Vol.31 October, 1981.

2. O'Brien, M.P. and Gosline, J.E.:"The Hydraulic Ram". University of California Publications in Engineering, Vol.3 January, 1933.

3. Krol, J.:"The Automatic Hydraulic Ram".Proc IMechE, Vol.165, 1951.

4. Schiller, E.J. and Kahangire, P.O.:"An Experimental Investigation and Design of Hydraulic Ram Pumps". International Journal for Development Technology, Vol.2, 173-183, 1984.

5. Wylie, E.B. and Streeter, V.L.:"Fluid Transients". N.Y., U.S.A., McGraw-Hill, 1978.

Appendix B. The Method of Characteristics

The method of characteristics solutions used in the researched simulation were primarily based on the work of Streeter and Wylie[30], although methods by J.A.Fox[33] and M.Hanif Chaudry[32] were used to provide parts of some of the boundary conditions.

The method of characteristics provides a means by which the partial differential equations of continuity and momentum may be represented by two total differential equations X1 and X3 which are only valid while two associated equations X2 and X4 are valid.

It is not necessary to cover the steps used to obtain these equations as they are well documented in a number of good texts[32][33][34], and an excellent coverage is given in Chapter 3 of Fluid Transients [30].

The four ordinary differential equations are given below:

$$\frac{g}{a}\cdot\frac{dH}{dt}+\frac{dV}{dt}+\frac{g}{a}.\sin\alpha+\frac{f.V.|V|}{2.D}=0 \qquad (B.1)$$

$$\frac{dx}{dt}=V+a \qquad (B.2)$$

$$\frac{-g}{a}\cdot\frac{dH}{dt}+\frac{dV}{dt}+\frac{g}{a}\sin\alpha+\frac{f.V.|V|}{2.D}=0 \qquad (B.3)$$

$$\frac{dx}{dt}=V-a \qquad (B.4)$$

where: a is the wave propagation velocity

The equations omit the convective acceleration term ie they assume that the characteristic lines pass through the mesh points therefore avoiding any interpolations.

The simulation produced uses a fixed time step, fixed wave speed solution, allowing a finite difference solution to be obtained for the above equations. This solution involves considering the pipe as a series of sections of length Δx where $\Delta x = c.\Delta t$ and c = speed of sound in the pipe. The finite difference solution for the equation is represented in the following equations which

are of the form that is easily implemented in computer code: (reproduced from "Fluid Transients"[30])

$$C+:\ H_{x_t} = C_p - \frac{a}{g.A}.Q_{x_t} \qquad (B.5)$$

$$C-:\ H_{x_t} = C_m + \frac{a}{g.A}.Q_{x_t} \qquad (B.6)$$

where Hx_t and Qx_t represent newly determined pressure and flow at the node being calculated and Cp and Cm are values determined from parameters for nodes a and b a distance Δx from the present calculation node at a simulation time Δt earlieras shown in Figure B.1. The values of Cp and Cm are obtained using the following equations:

$$C_p = h_{a_{t-\Delta t}} + \frac{a}{g.A}.Q_{a_{t-\Delta t}} - \frac{f.\Delta x}{2gDA^2}.Q_{a_{t-\Delta t}}|Q_{a_{t-\Delta t}}| \qquad (B.7)$$

$$C_m = h_{b_{t-\Delta t}} - \frac{a}{g.A}.Q_{b_{t-\Delta t}} + \frac{f.\Delta x}{2gDA^2}.Q_{b_{t-\Delta t}}|Q_{b_{t-\Delta t}}| \qquad (B.8)$$

Using these equations, the conditions at each of the nodes can be determined, providing the end conditions can be determined for each pipe at each time step. Figure B.1 demonstrates how the equations can be used to calculate the conditions along a full length of a pipe. The lines on the diagram represent the link between the known data used for each calculation at points a and b and the data calculated for the present node and time t.

In addition to providing a means for determining internal conditions in the simulated pipeline, the characteristic equations provide a means to define the behaviour of the pipeline with respect to boundaries. Using an independent equation in Q and H to describe the boundary, a complete boundary condition can be obtained by the simultaneous solution of the two equations. The C+ characteristic equations are used for downstream boundaries and C- for upstream. The individual boundary conditions used in the ram pump simulation are described in chapter 4.

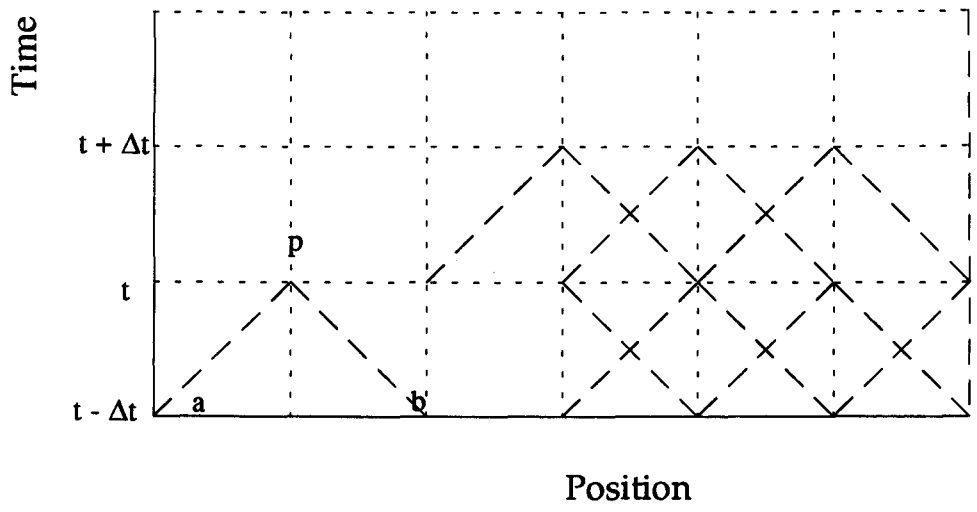

Figure B.1 Representation of the Method of Characteristics

Appendix C. Computer Methods Used

C.1 The Spreadsheet

C.1.1 What is a spreadsheet environment?

The spreadsheet is a type of application that has gained greater significance with the increased importance of the personal computer. The spreadsheet market was initially dominated by the Lotus 123 spreadsheet, but has since met increasing competition from other manufacturers. Currently the main packages are by Lotus, Microsoft, Borland, and Computer Associates. The original concept of a spreadsheet was to provide a computational tool for accountancy and financial analysis. However, it was found to be a very powerful tool for the engineer, and has been adopted widely. Some Engineering companies have attempted to substitute the majority of application production with spreadsheet analyses. The reason for this is clearly demonstrated by the flexibility of the spreadsheet based model described in chapter 5.

Although some modern spreadsheet packages differ from this description, classically spreadsheet packages are based around a two dimensional table of cells. Each cell as a reference column and row, and is identified using a cartesian like coordinate system. Each cell represents a computational pointer.

Each cell can be used to store a label, a number, or a function of the contents of other cells. It is this use of functions that make the spreadsheet so formidably adaptable. A classical application of a spreadsheet is demonstrated below. In this application data is inserted into a range of cells to represent the cost of product items. This data can then be analysed by inserting functions into cells. For example, the function sum(A5..A10) provides a summation of the cells in the range A5 to A10. Similarly, the function Max(A5..A10) will determine the maximum value in this range.

C.1.2 How is this useful to an engineer

Analysis of this type is of particular use to the engineer who is required to undertake a significant number of complex calculations repetitively, and often with subtle variations. Furthermore, the graphical and analytical facilities available in many modern spreadsheet packages provide a flexible means to visualise calculations and results.

Spreadsheets have been of such benefit to engineers that facilities have been developed to directly link spreadsheet analysis with computer aided design packages, while many simulation and analysis packages provide a facility to download data to a spreadsheet environment.

C.1.3 Relative and Absolute Cell Addresses

One of the particularly useful facets of the spreadsheet is related to cell addressing. It was mentioned above that it is possible to insert a function into a cell that refers to the contents of other cells. Typically these other cells are referenced by their coordinate position e.g. A8. However, most spreadsheets applications will consider this to be a relative reference. That is, relative to the position of the cell in which the function is inserted. For the simple case in which this cell is the only function, this is of no consequence.

It is possible to copy cells to other cells. So for example, if a function in a cell at an address B6, referenced a cell B7, but was then copied to an address G10, the function at G10 would actually reference G11. Illustrations of the power of this type of referencing are given in the following sections. However, this type of referencing can also lead to error. This is the case if it was actually required that the cell at G10 referenced B7. This situation is catered for by the use of an absolute reference. This is achieved by utilising the $ character before the co-ordinates of the referenced cell within the formula.

The following formula cold be inserted at cell F5: 2*F4+$H$4

If this cell is copied to cell T9, it will read: 2*T8+$H$4.

It can be seen from this example that the function at T9 refers to a relative address at T8, and an absolute address at $H$4. The value of this facility is well demonstrated in the model described in chapter 5.

It is of occasional benefit to utilise a partially absolute address. This is an address that references a cells coordinate with part of the coordinate an absolute reference, and the other an absolute. An example of this would be a function at G6: SQRT($H7). This function will clearly determine the square route of the value held at H7, and display this value at cell G6. If G6 is copied to J12, the partial referencing becomes apparent. J12 will the contain a function: SQRT($H13), the absolute referencing has ensured the newly addressed cell is in the same column, but the row has been referenced relatively.

C.1.4 Programming formulae

In modern spreadsheets a wide number of mathematical functions exist which can be deployed using referencing as described above. These include a full range of logic and loop functions. The loop functions are usually incorporated within a macro programming language that allows a given spreadsheet to be manipulated in an automatic fashion.

A particularly useful logic function is the classical programmers IF , THEN, ELSE. These are widely used within the model described in chapter 5. and allow the function in a given cell to depend on the results of a function. It is in this way that the full complexity of a hydraulic ram pump operation was modellable within a spreadsheet environment.

C.1.5 Trapezoidal Integration

A facet of the spreadsheet environment that was particularly beneficial to the modelling of a hydraulic ram pump was the facility to integrate a function that may not be mathematically specified, or solvable. If we consider the column of number A1 to A10 in the represented spreadsheet below to be for example delivery flows, it is possible to use a trapezoidal integration to determine the total delivered volume.

If each row represents the flow at a given time step, it is possible to calculate the flow that passes during a time step is column B. To do this, the formula at B2 should read =B1+DELTA T(A1+A2)/2. If this cell is then copied to the rest of the column, this column will representation a cumulative summation of the delivery flows. The final cell in this column will then represent the integration of the function described by the data in column A. In this way, it is possible to integrate a function when an analytical solution is not possible. The accuracy of this method relies on utilising a small time step increment between each row of data.

A similar approach can be adopted in the determination of a differential coefficient for a function described by a range of data.

C.1.6 Curve Fitting

Curve fitting techniques have been central to the solutions discussed in this thesis. A variety of methods have been adopted depending on the type of curve fit required. It was valuable to discover that the spreadsheet environment also provided a means by which curve fitting was possible.

Curve fitting can be achieved within a spreadsheet environment by the use of a linear regression facility available in many spreadsheet packages. These spreadsheets will allow a straight line to be fitted to a set of data to a quantified degree of correlation. At first impression this may appear to offer rather limited application, but the spreadsheet enables this facility to be adapted to a variety of problems.

For example, a classic experiment to determine the head loss in a pipe-work fitting will yield a range of data for flow and head loss. It is assumed that the relationship between the sets of experimental data will follow a relationship of the type $h_f = KQ^2$ in which h_f is the head loss in the fitting, Q is the flow through the fitting, and K is the unknown coefficient of proportionality. To obtain a curve fit of this type it is necessary to square the experimental flow data, and then utilise the linear regression facility to determine K.

This provides a very simple means of curve fitting. More functions can be fit to experimental data by utilising a multiple regression facility available in many spreadsheet environments.

C.1.7 Time based calculations

An inventive application of the spreadsheet environment was adopted in the development of the hydraulic ram pump model described in chapter 5. This utilised the spreadsheet to undertake time based calculations to determine the position of an impulse valve throughout its closure. This was achieved by utilising a single column of the spreadsheet as a incremental time record in which the first cell represents the time zero, and each row then represents an increment after the previous row. In this way it is possible to undertake calculations of time related variables such as acceleration, velocity and displacement using simple Newtonian mechanics for each of the time increments. As with the previous calculation, greatest accuracy in this method is obtained as the increment of time used approaches a minimum.

C.1.8 Optimisation - solver

A new facility increasingly available in the spreadsheet environment is the mathematical solver. This function allows the spreadsheet to determine a data value required in a given cell in order for a function elsewhere in the spreadsheet to reach a maximum, or a minimum, or a given value. In terms of the optimisation of design this is clearly a powerful tool. A function of this type could theoretically be applied to the model described in chapter 5 to obtain the maximum power setting or the maximum efficiency point.

The optimiser operates by using a search algorithm that modifies the input values with respect to the optimisation criteria. The sophistication of this facility was not found to be sophisticated enough to function with the complexity in the model of the hydraulic ram pump, but was used on smaller computational tasks.

C.2 Other software Used

For the purposes of analysis, the spreadsheet has provided the most flexible tool for the task. However, many of the more complex curve fitting tasks were achieved using the MATLAB package, which incorporates an implementation of the Nelder-Mead simplex algorithm. This proved particularly invaluable for obtaining accurate curve fitting on complex exponential functions.

For graphical production and the generation of engineering drawings the AutoCAD package was used. This also provided a means by which a 3 dimensional model of the hydraulic ram pump was generated, and provided a facility to manipulate and render (realistic colouring) the model.

Appendix D. Programme Listings

This section includes source code for the Pascal version of the simulation as well as the associated units and routines. The simulation has since been translated into the C language and had a variety of modifications and additions. The C listing is given in Appendix E.

THe majority of results given in this thesis are obtained using the C version of the simulation, but this version incorporates additional graphical routines which were not translated to C.

Ramsim Version T3G

List Of Constants Used

Angle1 = 0;{rads} - *Angle between pipe 1 and horizontal*

Angle2 = 0;{rads}- *Angle between pipe 2 and horizontal*

Angle3 = 1.571;{rads} - *Angle between pipe 3 and horizontal*

Angle4 = 1.571;{rads} - *Angle between pipe 4 and horizontal*

Area1=0.00196;{m^2} - *Area of Pipe 1*

Area2=0.00196;{m^2} - *Area of Pipe 2*

Area3=0.00196;{m^2} - *Area of Pipe 3*

Area4=0.00442;{m^2} - *Area of Pipe 4*

Delivery_Pressure=28;{m} - *Delivery pressure achieved by the pump*

Diameter1=0.05;{m}- *Diameter of Pipe 1*

Diameter2=0.05;{m} - *Diameter of Pipe 2*

Diameter3=0.05;{m} - *Diameter of Pipe 3*

Diameter4=0.075;{m}- *Diameter of Pipe 4*

Gravity = 9.80665;{m/s/s} - *Acceleration due to gravity*

InitFlow :real = 0.002;{cumecs} - *Estimate of initial flow in the drive pipe*

K = 0.0003;{m} - *Relative Roughness Coefficient*

Kdv = 200000; - *Coefficient of Friction for the Delivery Valve*

Length1 = 10;{m} - *Length of Pipe 1*

Length2 = 0.245;{m} - *Length of Pipe 2*

Length3 = 0.15;{m} - *Length of Pipe 3*

Length4 = 0.15;{m} - *Length of Pipe 4*

ResLevel = 3;{m} - *Reservoir Level*

Scale = 100;{m} - *Maximum pressure for graphed output*

TimeInt=0.000025;{secs} - *Time interval used in the simulation*

TimeLimit=0.2;{secs} - *Time limit of the simulation*

Valve_Area = 0.00181;{m^2} - *Area of impulse valve plunger face*

Valve_Coeff=1700; - *Coefficient of Friction for Discharge Valve*

Vessel_Height=0.5; - *Height of air vessel*

Valve_mass = 0.3;{Kg} - *Mass of Impulse Valve*

Valve_Stroke = 28; {mm} - *Maximum travel of impulse valve*

List of Global Variables Used of type Real

Valve_Displacement, - *Displacement of impulse valve plunger from its seat*

Old_Valve_Displacement, - *Displacement of impulse valve plunger after previous time step*

Valve_Velocity, - *Velocity of the impulse valve plunger*

Valve_Accn; - *Acceleration of the impulse valve plunger*

Ho, - *Head loss across impulse valve under initial conditions*

Kho, - *Impulse valve head loss coefficient for initial conditions*

Kh, - *Impulse valve head loss coefficient*

Kf, - *Impulse valve force coefficient*

Frifact - *Calculated friction factor of pipe in question*

WaveVel1, - *The velocity of sound in the Pipe 1*

WaveVel2, - *The velocity of sound in the Pipe 2*

WaveVel3, - *The velocity of sound in the Pipe 3*

WaveVel4; - *The velocity of sound in the Pipe 4*

Sin_Angle, - *Temporary variable to store sine of angle of pipe*

VP1, - *Velocity of fluid in the air vessel*

Level - *Level of fluid in the air vessel*

Discharge_Flow, - *Quantity of fluid discharged from the Hydraulic Ram Pump*

Junction_Pressure - *Pressure experienced at the three way junction*

Delivery_Flow - *Flow experienced through the delivery valve*

Sects1 - *Integer number of sections included in Pipe 1*

Sects2 - *Integer number of sections included in Pipe 2*

Sects3 - *Integer number of sections included in Pipe 3*

Sects4 - *Integer number of sections included in Pipe 4*

Count - *Integer number representing the number of time steps completed*

Dump_File - *Text file to which simulation output is sent*

LocalVel1 - *Array in which previous values of velocity are stored for each node of Pipe 1*

LocalPres1 -*Array in which previous values of pressure are stored for each node of Pipe 1*

NewVel1 - *Array in which latest values of velocity are stored for each node of Pipe 1*

NewPres1 - *Array in which latest values of pressure are stored for each node of Pipe 1*

LocalVel2,LocalPres2,NewVel2,NewPres2:
LocalVel3,LocalPres3,NewVel3,NewPres3:
LocalVel4,LocalPres4,NewVel4,NewPres4:

{ As above, but for Pipes 2, 3, and 4 respectively

Note:

It is apparent that the number of constants shown is high, and many of the constants defined would conventionally be included as variables. This was a concious attempt to reduce program complexity, and improve the efficiency of code during the development of the program. If at any stage, a user friendly interface is required for the simulation, these constants would either be converted to variables, or simply relabled as typed constants.
The proposed work, involving extensive sensitivity studies on various parameters effecting pump performance will require such modifications.

Routine to determine friction factor using Barr approximation

```
Function friction(Velocity,Diameter:real):real;     Parameters passed to the routine
 begin
  If Velocity <  0.8  then friction:= 0.02     This line ensures that a value of friction factor is
                                                defined for  low Reynolds numbers.
    begin
     frifact:= 2.34E-5 / exp(Ln(Abs(Velocity)*Diameter)*0.89);
     frifact:= ln(frifact + (k/(3.7*Diameter)))/2.30259;
     friction:= 0.25/(frifact*frifact);
    end;
 end;
```

Routine to determine stable initial conditions and set up initial grid

```
Procedure Initialise;
var Hf:real;
 begin
Discharge_Flow:=0;
{**************************************************
  CALCULATE STARTING FLOW FROM INITIAL ESTIMATE
              USING TEN ITERATIONS
**************************************************}
For I:= 1 to 10 do
 Begin
    Kho:= (5.338*EXP(-0.3726*Valve_Stroke) + 0.0355)*1E+6;
    F1:=Friction((InitFlow/Area1),Diameter1);
    F2:=Friction((InitFlow/Area2),Diameter2);
    InitFlow:=
       (1/(2*gravity*Sqr(Area1)))+Kho+(F1*Length1/(Sqr(Area1)*2*Diameter1*Gravity));
    InitFlow:=InitFlow+(F2*Length2/(Sqr(Area2)*2*Diameter2*Gravity));
    InitFlow:=Sqrt(ResLevel/InitFlow);
 end;

{**************************************************
    MINOR WAVE SPEED ADJUSTMENT TO ENSURE
     INTEGER NUMBER OF NODES ON EACH PIPE
**************************************************}
  Sects1:=trunc(Length1 /(TimeInt*WaveVel1) +0.5);
  Sects2:=trunc(Length2 /(TimeInt*WaveVel2) +0.5);
  Sects3:=trunc(Length3 /(TimeInt*WaveVel3) +0.5);
  Sects4:=trunc(Length4 /(TimeInt*WaveVel4) +0.5);
  WaveVel1:= Length1/(TimeInt*Sects1);
  WaveVel2:= Length2/(TimeInt*Sects2);
  WaveVel3:= Length3/(TimeInt*Sects3);
```

```
   WaveVel4:= Length4/(TimeInt*Sects4);
{*************************************************
 INITIALISE PIPE  PRESSURES AND VELOCITIES IN PIPE 1
 NOTE  : pipe positions are numbered from 3 wayjunction.
*************************************************}
   Velocity:=InitFlow /Area1;
   frifact:= friction(Velocity,Diameter1);
   Hf:= frifact*Length1*Velocity*Velocity/(2*Sects1*Gravity*Diameter1);
   LocalPres1[Sects1+1]:=ResLevel+Length1*sin(Angle1)-Velocity*Velocity*0.5/Gravity;
   LocalVel1[Sects1+1]:= Velocity;
   for Position:= 1 to Sects1 do
    begin
     LocalVel1[Position]:=Velocity;
     LocalPres1[Sects1+1-Position]:=
              LocalPres1[Sects1+1]-(Position*Hf)+Position*Length1*Sin(Angle1)/Sects1;
    end;
{*************************************************
        INITIALISE PIPE 2
*************************************************}
   Velocity:=InitFlow /Area2;
   frifact:= friction(Velocity,Diameter2);
   Hf:= frifact*Length2*Velocity*Velocity/(2*Sects2*Gravity*Diameter2);
   LocalPres2[1]:=LocalPres1[1];
   LocalVel2[1]:= Velocity;
   for Position:= 2 to Sects2 do
    begin
     LocalVel2[Position]:=Velocity;
LocalPres2[Position]:=LocalPres2[1]-(Position*Hf)-Position*Length2*Sin(Angle2)/Sects2;
    end;
{*************************************************
        INITIALISE PIPE 3
```

```
*****************************************************}
   for Position:= 0 to (Sects3-1) do
    begin
     LocalVel3[Position+1]:=0;
     LocalPres3[Position+1]:=LocalPres1[1]-Position*Length3*Sin(Angle3)/Sects3;
    end;
{*****************************************************
        INITIALISE PIPE 4
*****************************************************}
    for Position:= 0 to Sects4-1 do
    begin
     LocalVel4[Position+1]:=0;
LocalPres4[Sects4-Position]:=Delivery_Pressure+Position*Length4*Sin(Angle4)/Sects4;
    end;
{*****************************************************
      INITIALISE JUNCTION AND VALVES
*****************************************************}
  B9:=InitFlow*InitFlow/LocalPres2[Sects2];
  Valve_Displacement := Valve_Stroke;
  Valve_Accn:= 0;
  Valve_Velocity:=0;
  Kho := (5.338*EXP(-0.3726*Valve_Stroke) + 0.0355)*1E+6;
  Ho :=Kho*SQR(InitFlow);
  GrCount:=0;
 end;{******Initialise******}
```

Main Calculation Procedure

```
Procedure calculation;
 const
    Sample_Count:Integer=0; Typed constant - behaves as locally controlled global variable.
 var
  Time,c,B1,B2,B3,B4,B5,Q2,T9,xtmp,Tmp1,Tmp2,CP1,CM3:real;
   CM2,Tmp,a,b:Double;
  Has_P_Been_Pressed:char;
```

Procedure within main calculation to determine boundary conditions

```
Procedure Boundaries;
  Const
   Valve_Closing:Boolean = False;
```

Procedure to solve Air Vessel boundary condition

```
  Procedure Calc_AirVessel_Boundary;
     var
      Time,New_Level,Level_Change,Air_Pressure,New_Air_Pressure,Hp:real;
   Begin
      Level_Change:=TimeInt*LocalVel4[Sects4-1]-TimeInt*Discharge_Flow;
      New_Level:= Level+Level_Change;
      Tmp:=(Vessel_Height-Level)/(Vessel_Height-New_Level);
      Air_Pressure:=LocalPres4[Sects4]-level;
      New_Air_Pressure:=Power(tmp,1.2)*Air_Pressure;
      Hp:=New_Air_Pressure + New_Level;
      VP1:=LocalVel4[Sects4];
      VP1:= VP1 + Gravity*(LocalPres4[Sects4]-Hp)/WaveVel4;
VP1:=VP1-2*Frifact*LocalVel4[Sects4]*Abs(LocalVel4[Sects4])*TimeInt/Diameter4;
      NewPres4[Sects4]:=Hp;
      Localvel4[Sects4]:=VP1;
```

```
        Level:=New_Level;
        Discharge_Flow:=sqr(NewPres4[Sects4]/Valve_Coeff);
    end;
  Begin
{*****************************************************************
                RESERVOIR BOUNDARY
*****************************************************************}
    if LocalVel1[Sects1+1]=0 then NewPres1[Sects1+1]:=ResLevel
     else
      begin
       xtmp := LocalVel1[Sects1+1];
       c:= 0.25*(1-(xtmp/abs(xtmp)));
       NewPres1[Sects1+1]:= ResLevel-(c*xtmp*xtmp/Gravity);
      end;
    Velocity:= LocalVel1[Sects1];
    xtmp := abs(Velocity);
    frifact:= friction(xtmp,Diameter1);
    b:=0.5*frifact*Velocity*xtmp*TimeInt/Diameter1;
    c:=Gravity*(Velocity*Sin(Angle1)*TimeInt-LocalPres1[Sects1]);
    b:=Velocity+(c/WaveVel1)-b;
    NewVel1[Sects1+1]:=b + (Gravity*NewPres1[Sects1+1]/WaveVel1);
{*****************************************************************
                IMPULSE VALVE BOUNDARY
*****************************************************************}
    Old_Valve_Displacement:=Valve_Displacement;
    Velocity:=LocalVel2[Sects2-1];
    frifact:=friction(ABS(Velocity),Diameter2);
    a:=frifact*0.5*Velocity*abs(Velocity)*TimeInt/Diameter2;
a:=Velocity+Gravity*(LocalPres2[Sects2-1]-Velocity*sin(Angle2)*TimeInt)/WaveVel2-a;
    c:=Pi*Diameter2*Diameter2*0.25;
    b1:= c*a;
```

```
    B2:=-c*gravity/waveVel2;
    Valve_Displacement:=
      Valve_Displacement+Valve_Velocity*TimeInt*1000+Valve_Accn*TimeInt*1000/2;
    Valve_Velocity:= Valve_Velocity + Valve_Accn*TimeInt;
If Valve_Displacement  0.0000002 then
     Begin
      If Valve_Displacement  Valve_Stroke then
           Begin
            Valve_Displacement:= Valve_Stroke;
            Kf := (180*EXP(-0.4407*Valve_Displacement) + 0.43)*1E+6;
            Valve_Velocity := 0;
            Valve_Accn:= Gravity - Kf* SQR(c*Velocity)/Valve_Mass;
            If Valve_Accn  0 then Valve_Accn :=0;
           end
       else
           Begin
            Kf := (180*EXP(-0.4407*Valve_Displacement) + 0.43)*1E+6;
            Valve_Accn:= Gravity - Kf* SQR(c*Velocity)/Valve_Mass;
           end;
    end;
If Valve_Displacement 0.0000002 then
       Begin
        Valve_Accn:=Gravity*(1 - (LocalPres2[Sects2]*Valve_Area*1000/Valve_Mass));
         If Valve_Accn0 then
                    Begin
                     Valve_Accn:=0;
                     Valve_Velocity:=0;
                    end;
         If Valve_Displacement then Valve_displacement:=0;
        T9:=0;
       end
       else
```

```
        Begin
      Kh:= (5.338*EXP(-0.3726*Valve_Displacement) + 0.0355)*1E+6;
      T9:=SQRT(Kho/kh);
        end;
        (****** Boundary *******)
    B3:=B9*T9*T9;
    B4:=-B3/B2;
    B5:=B1*B3/B2;
    Q2:=0.5*(-B4+Sqrt(Abs(B4*B4-4*B5)));
    Newvel2[Sects2]:=Q2/c;
    Newpres2[Sects2]:=(Q2-B1)/B2;
{*********************************************************************
            THREE WAY JUNCTION
*********************************************************************}
Tmp:=
2*Friction(LocalVel1[2],Diameter1)*LocalVel1[2]*ABS(LocalVel1[2])/(Diameter1*Gravity);

Tmp1:=
2*Friction(LocalVel2[2],Diameter2)*LocalVel2[2]*ABS(LocalVel2[2])/(Diameter2*Gravity);

Tmp2:=
2*Friction(LocalVel3[2],Diameter3)*LocalVel3[2]*ABS(LocalVel3[2])/(Diameter3*Gravity);

CP1:=LocalPres1[2]+WaveVel1*((LocalVel1[2]/Gravity)-(tmp*TimeInt));
CM2:=LocalPres2[2]-WaveVel2*((LocalVel2[2]/Gravity)-(Tmp1*TimeInt));
CM3:=LocalPres3[2]-WaveVel3*((LocalVel3[2]/Gravity)-(Tmp2*TimeInt));
Junction_Pressure:=
(Gravity*(Area1/WaveVel1+Area2/WaveVel2+Area3/WaveVel3));
Junction_Pressure:=
((CP1*Area1*Gravity/WaveVel1)+
(CM2*Area2*Gravity/WaveVel2)+(CM3*Area3*Gravity/WaveVel3))/Junction_Pressure;
NewVel1[1]:=Gravity*(CP1-Junction_Pressure)/WaveVel1;
NewVel2[1]:=Gravity*(Junction_Pressure-CM2)/WaveVel2;
NewVel3[1]:=Gravity*(Junction_Pressure-CM3)/WaveVel3;
```

```
NewPres1[1]:=Junction_Pressure;
NewPres2[1]:=Junction_Pressure;
NewPres3[1]:=Junction_Pressure;
{**************************************************
        DELIVERY VALVE BOUNDARY CONDITION
**************************************************}
Velocity:= LocalVel3[Sects3-1];
Tmp:=2*Friction(Velocity,Diameter3)*Velocity*Abs(Velocity)/(Diameter3*Gravity);
CP1:=LocalPres3[Sects3-1]+WaveVel3*((LocalVel3[Sects3-1]/Gravity)-(Tmp*TimeInt));
Velocity:= LocalVel4[2];
Tmp:=2*Friction(Velocity,Diameter4)*Velocity*Abs(Velocity)/(Diameter4*Gravity);
CM2:=LocalPres4[2]-WaveVel4*((LocalVel4[2]/Gravity)-(Tmp*TimeInt));
Delivery_Flow:=Gravity*(CP1-CM2)/((WaveVel3/Area3)+(WaveVel4/Area4));

  If (CP1-CM2) 0 then
                Begin
                 Delivery_Flow:=0;
                 NewVel3[Sects3]:=0;
                 NewVel4[1]:=0;
                end
                Else
                Begin
      Delivery_Flow := -(WaveVel3/Area3+WaveVel4/Area4)/(2*Kdv*Gravity);
      Delivery_Flow := Delivery_Flow + SQRT(SQR(Delivery_Flow)+(CP1-CM2)/Kdv);
                 NewVel3[Sects3]:=Delivery_Flow/Area3;
                 NewVel4[1]:=Delivery_Flow/Area4;
                end;
  NewPres3[Sects3]:=CP1-Delivery_Flow*(WaveVel3/(Area3*Gravity));
  NewPres4[1]:=CM2+Delivery_Flow*WaveVel4/(Area4*Gravity);

 Calc_AirVessel_Boundary;
 End{******Boundaries*******};
```

```
  Begin {calculation}
   For count := 1 to round(timelimit/TimeInt)  Do
    Begin
{************************************************
    Characteristics Calculations for Pipe 1
************************************************}
     For Position := 2 to Sects1 Do
       Begin
(********** This is the C+ Characteristic ******************)
       tmp1 := 0.5 * TimeInt / Diameter1;
       Sin_Angle := Sin(Angle1);
       Velocity:=LocalVel1[Position + 1];
       Frifact:= friction(Abs(Velocity),Diameter1);
       a:=frifact * Velocity * Abs(Velocity)* tmp1;
       c:=Gravity *(LocalPres1[Position + 1] - Velocity* Sin_Angle);
       a:= Velocity + c/WaveVel1 - a;
(********** This is the C- Characteristic ******************)
       Velocity:= LocalVel1[Position - 1];
       frifact:=Friction(Abs(Velocity),Diameter1);
       b:= frifact  * Velocity * abs(Velocity) * tmp1;
       c:=Gravity*(Velocity *Sin_Angle*TimeInt-LocalPres1[Position-1]);
       b:=Velocity + c/WaveVel1 - b;
       Newvel1[Position] := 0.5*(a+b);
       Newpres1[Position] := 0.5*WaveVel1*(a-b)/Gravity;
       end;
{************************************************
    Characteristics Calculations for Pipe 2
************************************************}
     For Position := 2 to (Sects2-1) Do
       Begin
(********** This is the C+ Characteristic ******************)
```

```
        tmp1 := 0.5 * TimeInt / Diameter2;
        Sin_Angle := Sin(Angle2);
        Velocity:=LocalVel2[Position - 1];
        Frifact:= friction(Abs(Velocity),Diameter2);
        a:=frifact * Velocity * Abs(Velocity)* tmp1;
        c:=Gravity *(LocalPres2[Position - 1] - Velocity* Sin_Angle);
        a:= Velocity + c/WaveVel2 - a;
(********** This is the C- Characteristic ******************)
        Velocity:= LocalVel2[Position + 1];
        frifact:=Friction(Abs(Velocity),Diameter2);
        b:= frifact  * Velocity * abs(Velocity) * tmp1;
        c:=Gravity*(Velocity *Sin_Angle*TimeInt-LocalPres2[Position+1]);
        b:=Velocity + c/WaveVel2 - b;
        Newvel2[Position] := 0.5*(a+b);
        Newpres2[Position] := 0.5*WaveVel2*(a-b)/Gravity;
         end;
{*************************************************************
    Characteristics Calculations for Pipe 3
*************************************************************}
      For Position := 2 to (Sects3-1) Do
         Begin
(********** This is the C+ Characteristic ******************)
        tmp1 := 0.5 * TimeInt / Diameter3;
        Sin_Angle := Sin(Angle3);
        Velocity:=LocalVel3[Position - 1];
        Frifact:= friction(Abs(Velocity),Diameter3);
        a:=frifact * Velocity * Abs(Velocity)* tmp1;
        c:=Gravity *(LocalPres3[Position - 1] - Velocity* Sin_Angle);
        a:= Velocity + c/WaveVel3 - a;
(********** This is the C- Characteristic ******************)
        Velocity:= LocalVel3[Position + 1];
        frifact:=Friction(Abs(Velocity),Diameter3);
```

```
        b:= frifact  * Velocity * abs(Velocity) * tmp1;
        c:=Gravity*(Velocity *Sin_Angle*TimeInt-LocalPres3[Position+1]);
        b:=Velocity + c/WaveVel3 - b;
        Newvel3[Position] := 0.5*(a+b);
        Newpres3[Position] := 0.5*WaveVel3*(a-b)/Gravity;
         end;
{*************************************************************
    Characteristics Calculations for Pipe 4
*************************************************************}

     For Position := 2 to (Sects4-1) Do
        Begin
(********** This is the C+ Characteristic ******************)
        tmp1 := 0.5 * TimeInt / Diameter4;
        Sin_Angle := Sin(Angle4);
        Velocity:=LocalVel4[Position - 1];
        If Abs(Velocity) then a:= 0
         else Begin
        Frifact:= friction(Abs(Velocity),Diameter4);
        a:=frifact * Velocity * Abs(Velocity)* tmp1;
            end;
        c:=Gravity *(LocalPres4[Position - 1] - Velocity* Sin_Angle);
        a:= Velocity + c/WaveVel4 - a;
(********** This is the C- Characteristic ******************)
        Velocity:= LocalVel4[Position + 1];
        If Abs(Velocity) then b:= 0
         else Begin
        frifact:=Friction(Abs(Velocity),Diameter4);
        b:= frifact  * Velocity * abs(Velocity) * tmp1;
            end;
        c:=Gravity*(Velocity *Sin_Angle*TimeInt-LocalPres4[Position+1]);
        b:=Velocity + c/WaveVel4 - b;
```

```
        NewVel4[Position] := 0.5*(a+b);
        NewPres4[Position] := 0.5*WaveVel4*(a-b)/Gravity;
         end;
 Boundaries;

(*************************************************************
    FILE DUMP SECTION
                - Routine to dump each set of calculated  data to output file.
*************************************************************)

Sample_Count:=Sample_Count+1;
      If Sample_Count=Sample_Rate then
        Begin
      Time:=(count)*TimeInt;
 Dump_to_Disk(Time,valve_displacement,LocalVel1[22],localPres1[22],Dump_File);
       Sample_Count:=0;
        End;
(*************************************************************
    SCREEN OUTPUT FUNCTION
*************************************************************)
 SetViewPorts(0,0,0.5,0.25,-1,-1);
 TwoDV_Output (count,TimeInt,TimeLimit,NewVel1[1],LocalVel1[1]);
 SetViewPorts(0,0.25,0.5,0.5,-1,-1);
 TwoDV_Output
(count,TimeInt,TimeLimit,(Valve_Displacement/7),(Old_Valve_Displacement/7));

 SetViewPorts(0,0.5,1,1,-1,-1);
 setcolors(11);
 TwoD_Output(sects1,scale,count,TimeInt,TimeLimit,LocalPres1[22],NewPres1[22]);
 setcolors(12);
 TwoD_Output(sects4,scale,count,TimeInt,TimeLimit,LocalPres4[1],NewPres4[1]);
 setcolors(13);
```

```
{
TwoD_Output(sects2,scale,count,TimeInt,TimeLimit,LocalPres2[sects2],NewPres2[sects2]);
 setcolors(14);
TwoD_Output(sects3,scale,count,TimeInt,TimeLimit,LocalPres3[sects3],NewPres3[sects3]);
 }
{  SetViewPorts(0.5,0,1,0.5,-1,-1);

    ThreeD_Output(sects1,Scale,Count,TimeInt,TimeLimit,NewPres1,LocalPres1);
 }  {   ThreeD_Output(sects2,Scale,Count,TimeInt,TimeLimit,NewPres2,LocalPres2);
     ThreeD_Output(sects3,Scale,Count,TimeInt,TimeLimit,NewPres3,LocalPres3);
     ThreeD_Output(sects4,Scale,Count,TimeInt,TimeLimit,NewPres4,LocalPres4);
     readln;}
(*************************************************************
 UPDATE VALUES OF LOCALVEL AND LOCALPRES FOR NEXT CALCULATION
*************************************************************)
    for Position := 1 to Sects1+ 1 do
      begin
      If Nsewpres1[Position] -10 then Newpres1[Position]:=-10;
      LocalVel1[Position]:= NewVel1[Position];
      LocalPres1[Position]:= NewPres1[Position];
      end;
    for Position := 1 to Sects2 do
      begin
      If Newpres2[Position] -10 then Newpres2[Position]:=-10;
      LocalVel2[Position]:= NewVel2[Position];
      LocalPres2[Position]:= NewPres2[Position];
      end;
    for Position := 1 to Sects3 do
      begin
      If Newpres3[Position] -10 then Newpres3[Position]:=-10;
      LocalVel3[Position]:= NewVel3[Position];
      LocalPres3[Position]:= NewPres3[Position];
```

```
        end;
      for Position := 1 to Sects4 do
        begin
        If Newpres4[Position]  -10 then Newpres4[Position]:=-10;
        LocalVel4[Position]:= NewVel4[Position];
        LocalPres4[Position]:= NewPres4[Position];
        end;
    end;
  end;(****** Procedure Calculation*****************)
 begin {main program}
  Input;
  Initialise;
          Open_Dump_File('d:\RamSim.Out',Dump_File);
{          Dump_Info(Dump_File,Outputs1,Outputs2,Outputs3,Outputs4,
             Length1,Length2,Length3,Length4,
             Diameter1,Diameter2,Diameter3,Diameter4,
             WaveVel1,WaveVel2,WaveVel3,WaveVel4);
}          TdStart;
  SetViewPorts(0,0.5,1,1,3,2);
  TwoD_Set_Up(sects1,Length1,TimeLimit,Scale);
  SetViewPorts(0,0,0.5,0.25,14,0);
  TwoD_vSet_Up(TimeLimit);
  SetViewPorts(0,0.25,0.5,0.5,14,0);
 TwoD_VSet_Up(TimeLimit);
  SetViewPorts(0.5,0,1,0.5,10,11);
          ThreeD_Set_Up(sects1,Length1,TimeLimit,Scale);
          { ThreedSup(Sects1,Length1,timeLimit,Scale);}
           Calculation;
         Close(Dump_File);
         { TdFinish;}
end.
```

Use of View Ports allows various graphical output routines to be used simultaneously

The following code includes routines called from the main program, and allows the creation of a simple output file that includes all the necessary information about the simulation and provides a formatted output of data that allows for easy importing into other programs for analysis and plotting.

Unit FileOps;

Interface

```
Uses
Dos,Crt,HaloSurg;
Procedure Open_Dump_file(FileName:String; Var Dump_File:text);

Procedure Dump_Info(Var Dump_File:Text;
                    Outputs1,Outputs2,Outputs3,Outputs4:Integer;
                    Length1,Length2,Length3,Length4,
                    Diameter1,Diameter2,Diameter3,Diameter4,
                    WaveVel1,WaveVel2,WaveVel3,WaveVel4:real);
Procedure Dump_to_Disk(Time,Valve_Displacement,
                       Localvel,LocalPres:Real;var Dump_File:text);
```

Implementation

```
Procedure Open_Dump_file(FileName:String; Var Dump_File:text);
Begin
 {Initialise the disk dump file}
 Assign(Dump_File,FileName);
 Rewrite(Dump_File);
Writeln(Dump_File,'*************************************************************'
);
 Writeln(Dump_File,'*Method of Characteristics Simulation of the Hydrulic Ram*');
Writeln(Dump_File,'*************************************************************'
);

End;
Procedure Dump_Info(Var Dump_File:Text;
                    Outputs1,Outputs2,Outputs3,Outputs4:Integer;
                    Length1,Length2,Length3,Length4,
```

```
        Diameter1,Diameter2,Diameter3,Diameter4,
        WaveVel1,WaveVel2,WaveVel3,WaveVel4:real);
Var I:Integer;
Begin
 Writeln(Dump_File,'          Pipe    Pipe    Pipe    Pipe ');
 Writeln(Dump_File,'           1       2       3       4 ');
 Writeln(Dump_File,'          ____________________________________');
 Writeln(Dump_File,'Pipe Lengths (m)');
 Writeln(Dump_File,'          ',Real2Str(Length1),'  '
 ,Real2Str(Length2),'  ',Real2Str(Length3),'  ',Real2Str(Length4));
 Writeln(Dump_File,'Wave Velocities (m/s)');
 Writeln(Dump_File,'          ',Real2StrAB(WaveVel1,4,0),'
                                  ',Real2StrAB(WaveVel2,4,0),'      '
 ,Real2StrAB(WaveVel3,4,0),'      ',Real2StrAB(WaveVel4,4,0));
 Writeln(Dump_FIle,'Diameters (mm)');
 Writeln(Dump_File,'          ',Real2StrAB(1000*Diameter1,3,0),'
                                  ',Real2StrAB(1000*Diameter2,3,0),'      '
 ,Real2StrAB(1000*Diameter3,3,0),'      ',Real2StrAB(1000*Diameter4,3,0));
 Writeln(Dump_File,'Number of Outputs');
 Writeln(Dump_File,'
       ',IntoStr(Outputs1),InToStr(Outputs2),InToStr(Outputs3),InToStr(Outputs4));
 Writeln(Dump_File);
 Write(Dump_File,'Time ms  ');
 Write(Dump_File,'Pipe 1');
 For I:= 1 to Outputs1 do
  Begin
    Write(Dump_File,'      ');
  end;
 Write(Dump_File,'Pipe 2');
 For I:= 1 to Outputs2 do
  Begin
    Write(Dump_File,'      ');
```

```
 end;
Write(Dump_File,'Pipe 3');
For I:= 1 to Outputs3 do
 Begin
   Write(Dump_File,'       ');
 end;
Write(Dump_File,'Pipe 4');
Writeln(Dump_File);
Write(Dump_File,'         ');
For I := 1 to (Outputs1) do
 Begin
  Write(Dump_File,' Vel  Hd  ');
 end;
Write(Dump_File,'  ');
For I := 1 to (Outputs2) do
 Begin
  Write(Dump_File,' Vel  Hd  ');
 end;
Write(Dump_File,'  ');
For I := 1 to (Outputs3) do
 Begin
  Write(Dump_File,' Vel  Hd  ');
 end;
Write(Dump_File,'  ');
For I := 1 to (Outputs4) do
 Begin
  Write(Dump_File,' Vel  Hd  ');
 end;
Writeln(Dump_File);
Write(Dump_File,'__________');
For I := 1 to (Qutputs1) do
 Begin
```

```
    Write(Dump_File,'_____');
   end;
  Write(Dump_File,' ');
  For I := 1 to (Outputs2) do
   Begin
    Write(Dump_File,'_____');
   end;
  Write(Dump_File,' ');
  For I := 1 to (Outputs3) do
   Begin
    Write(Dump_File,'_____');
   end;
  Write(Dump_File,' ');
  For I := 1 to (Outputs4) do
   Begin
    Write(Dump_File,'_____');
   end;
    Writeln(Dump_File);
end;
Procedure Dump_to_Disk(Time,Valve_Displacement,Localvel,localpres:real;
                var Dump_File:text);
{Var Position:Integer;}
Begin
{******* Output for Pipe 1 ********}

  Writeln(Dump_File);
  Write(Dump_File,Real2StrAB((1000*Time),4,2),'    ');
{   For I:= 1 to Outputs1 do
  Begin
   Position:=OutPosit[1,I];
   Write(Dump_File,Real2StrAB(LocalVel1[Position],1,3),' ');
   Write(Dump_File,Real2Str(LocalPres1[Position]),' ');
```

```
    end;
     Write(Dump_File,' ');
    For I:= 1 to Outputs2 do
    Begin
     Write(Dump_File,Real2StrAB(LocalVel2[(OutPosit[2,I])],1,3),' ');
     Write(Dump_File,Real2Str(LocalPres2[(OutPosit[2,I])]),' ');
    end;
     Write(Dump_File,' ');
    For I:= 1 to Outputs3 do
    Begin
     Write(Dump_File,Real2StrAB(LocalVel3[(OutPosit[3,I])],1,3),' ');
     Write(Dump_File,Real2Str(LocalPres3[(OutPosit[3,I])]),' ');
    end;
     Write(Dump_File,' ');
    For I:= 1 to Outputs4 do
    Begin
     Write(Dump_File,Real2StrAB(LocalVel4[(OutPosit[3,I])],1,3),' ');
     Write(Dump_File,Real2Str(LocalPres4[(OutPosit[3,I])]),' ');
   end;
 }

    Write(Dump_File,Real2StrAB(Valve_Displacement,5,3));
    Write(Dump_File,' ');
    Write(Dump_File,Real2StrAB(LocalVel,5,3));
    Write(Dump_File,' ');
    Write(Dump_File,Real2StrAB(Localpres,5,3));

 end;

end.
```

The following code includes various routines which were produced to allow the simulation to utilise real time 2D and 3D graphical representations of the simulated transients:

```
Procedure tdFinish;
Procedure TwoD_Set_Up(sects,Length,TimeLimit:real;Scale:integer);
Procedure TwoD_Output
 (sects,scale:integer;
  count:longint;
  TimeInt,TimeLimit,LocalPres,NewPres:real);
Procedure TwoD_VSet_Up(TimeLimit:real);
Procedure TwoDV_Output
 (count:longint;
  TimeInt,TimeLimit,
  NewVel,LocalVel:real);
```

Implementation

```
Function Power(number,index:real) :real;
  begin
    Power := exp(Ln(Abs(number))*(index));
  end;
Function InToStr(i:longint):string;
   { Converts any integer type to a string }
 var s:string;
 Begin
   Str(i:4,s);
   IntoStr:=s;
 end;

Function Real2str(i:real):string;
   { Converts any real type to a string }
 var s:string;

 Begin
   Str(i:4:1,s);
   Real2Str:=s;
```

```
 end;
Function Real2strAB(i:real;A,B:Integer):string;
   { Converts any real type to a string }
 var s:string;

 Begin
  Str(i:A:B,s);
  Real2StrAB:=s;
 end;
Procedure Print_Picture;
var Has_P_Been_Pressed:char;
 Begin
     Has_P_Been_Pressed:=Readkey;
     If Has_P_Been_Pressed IN ['p','P'] then
        Begin
         SetPrns('D:\HALO\PRIN\Haloepjx.prn');
         GPrint;
        end;
 end;
Procedure TdStart;
 begin

SetDevs;
InitGraphicss(7);
SetDevs;
InitGraphicss(6);
SetWorlds(0,0,1000,1000);
LRecords(167,1);
LRecords(131,1);
LRecords(127,1);
LRecords(147,1);
 end;
```

```
Procedure ThreeD_Set_Up(sects,Length,TimeLimit:real;Scale:integer);
Begin
  {******** Set Up Axes for 3D Plot********}
{******* Draw Side Wall 1 *********}
MovAbss(156,757);
polyX[1]:= 156;   polyY[1]:=757;
polyX[2]:= 609; polyY[2]:= 980;
polyX[3]:= 609; polyY[3]:= 408;
polyX[4]:= 156;   polyY[4]:= 185;
polyX[5]:= 156;   polyY[5]:=757;
SetHatchStyles(1);
PolyFAbss(PolyX,PolyY,5,3);

MovAbss(609,980);
polyX[1]:= 609;   polyY[1]:=980;
polyX[2]:= 917; polyY[2]:= 886;
polyX[3]:= 917; polyY[3]:= 308;
polyX[4]:= 609;   polyY[4]:= 408;
polyX[5]:= 609;   polyY[5]:=980;
SetHatchStyles(1);
PolyFAbss(PolyX,PolyY,5,8);

{******* Draw Floor *******}
MovAbss(156,185);
polyX[1]:= 156; polyY[1]:=185;
polyX[2]:= 464; polyY[2]:= 86;
polyX[3]:= 917; polyY[3]:= 309;
polyX[4]:= 609; polyY[4]:= 409;
polyX[5]:= 156; polyY[5]:=185;
SetHatchStyles(1);
PolyFAbss(PolyX,PolyY,5,7);
```

```
{******* Draw Scale along length ********}
MovAbss(217,166);LnAbss(670,389);
MovAbss(280,146);LnAbss(733,368);
MovAbss(341,125);LnAbss(793,349);
MovAbss(403,106);LnAbss(856,329);


{******* Draw Scale across length ********}

MovAbss(202,209);LnAbss(509,109);
MovAbss(248,231);LnAbss(555,131);
MovAbss(292,251);LnAbss(600,151);
MovAbss(338,274);LnAbss(645,174);
MovAbss(383,297);LnAbss(691,197);
MovAbss(428,320);LnAbss(736,220);
MovAbss(473,343);LnAbss(781,243);
MovAbss(519,363);LnAbss(827,263);
MovAbss(564,386);LnAbss(872,286);

{******* Draw Base *********}

MovAbss(917,251);
polyX[1]:= 917; polyY[1]:=251;
polyX[2]:= 917; polyY[2]:=308;
polyX[3]:= 464; polyY[3]:=86;
polyX[4]:= 464; polyY[4]:=29;
polyX[5]:= 917; polyY[5]:=251;
SetHatchStyles(1);
PolyFAbss(PolyX,PolyY,5,13);
```

```
MovAbss(156,186);
polyX[1]:= 156; polyY[1]:=186;
polyX[2]:= 156; polyY[2]:=129;
polyX[3]:= 464; polyY[3]:=29;
polyX[4]:= 464; polyY[4]:=86;
polyX[5]:= 156; polyY[5]:=186;
SetHatchStyles(1);
PolyFAbss(PolyX,PolyY,5,5);

{******* Draw Scale ********}

MovAbss(217,166);LnAbss(217,109);
MovAbss(280,146);LnAbss(280,89);
MovAbss(341,126);LnAbss(341,69);
MovAbss(403,106);LnAbss(403,49);

{******* Draw base scale on length ********}

MovAbss(509,51);LnAbss(509,109);
MovAbss(555,74);LnAbss(555,131);
MovAbss(600,94);LnAbss(600,151);
MovAbss(645,117);LnAbss(645,174);
MovAbss(691,140);LnAbss(691,197);
MovAbss(736,163);LnAbss(736,220);
MovAbss(781,186);LnAbss(781,243);
MovAbss(827,206);LnAbss(827,263);
MovAbss(872,229);LnAbss(872,286);

{******** Labelling Base *******}
{******* Draw Base *********}
MovAbss(902,254);
polyX[1]:= 902; polyY[1]:=254;
```

```
polyX[2]:= 902; polyY[2]:=294;
polyX[3]:= 480; polyY[3]:=86;
polyX[4]:= 480; polyY[4]:=46;
polyX[5]:= 902; polyY[5]:=254;
SetHatchStyles(1);
PolyFAbss(PolyX,PolyY,5,0);

MovAbss(172,174);
polyX[1]:= 172; polyY[1]:=174;
polyX[2]:= 172; polyY[2]:=134;
polyX[3]:= 448; polyY[3]:=43;
polyX[4]:= 448; polyY[4]:=83;
polyX[5]:= 172; polyY[5]:=174;
SetHatchStyles(1);
PolyFAbss(PolyX,PolyY,5,0);

SetFonts('Halo104.fnt');
SetSTexts(20,1.5,0);
SetDegrees(1);
SetSTAngs(-12);
MovTCurAbss(178,134);
STexts('TIME (ms)');

MovAbss(336,100);LnAbss(417,74);
MovAbss(409,86);LnAbss(417,74);
MovAbss(409,71);LnAbss(417,74);
MovAbss(409,86);LnAbss(409,71);
SetSTAngs(18.75);
MovTCurAbss(70,80);
STexts('  0');
MovTCurAbss(131,60);
STexts(InToStr(Round(TimeLimit*1000/5)));
```

```
MovTCurAbss(193,40);
STexts(InToStr(Round(2*TimeLimit*1000/5)));
MovTCurAbss(254,20);
STexts(InToStr(Round(3*TimeLimit*1000/5)));
MovTCurAbss(318,0);
STexts(InToStr(Round(4*TimeLimit*1000/5)));

SetSTAngs(18.75);
MovTCurAbss(484,53);
STexts('DISTANCE from Ram (m)');



{*************** Pressure Scale ***************}

{******Zero Pressure Line*******}
  PolyX[1]:=(156+(453/(sects-1))-(453/(sects-1)));
  PolyY[1]:=(186+(528*(10)/Scale));
  PolyX[2]:=(156+(453*(sects)/(sects-1))-(453/(sects-1)));
  PolyY[2]:=(186+(222*(sects-1)/(sects-1))+(528*10/Scale));
  PolyX[3]:=(156+(453*(sects)/(sects-1))+(308)-(453/(sects-1)));
  PolyY[3]:=(186+(222*(sects-1)/(sects-1))-(100)+(528*10/Scale));
  PolyX[4]:=(156+(453/(sects-1))+(308)-(453/(sects-1)));
  PolyY[4]:=(186-(100)+(528*10/Scale));
  PolyX[5]:=(156+(453/(sects-1))-(453/(sects-1)));
  PolyY[5]:=(186+(528*(10)/Scale));
  MovAbss(PolyX[1],PolyY[1]);
  PolyLnAbss(PolyX,PolyY,5);
  MovTCurAbss(polyX[1]-25,PolyY[1]-30);
  STexts('0');
  MovTCurAbss(polyX[3]+31,PolyY[3]-30);
  STexts('0');
```

```
{***** The Next Pressure Lines and Labels ******}
For I:= 1 to 10 do
   begin
PolyX[1]:=1.5625*(100+(0.966*300/(sects-1))+(0.985 *0)-(0.966*300/(sects-1)));
PolyY[1]:=2.85714*(350-(285+(0.174 *0)-(185*(10+I*(scale-10)/10)/Scale)));
PolyX[2]:=1.5625*(100+(0.966*300*(sects)/(sects-1))+(0.985 *0)-(0.966*300/(sects-1)));
PolyY[2]:=2.85714*(350-(285-(0.258*300*(sects-1)/(sects-1))+(0.174
*0)-(185*(10+I*(scale-10)/10)/Scale)));
PolyX[3]:=1.5625*(100+(0.966*300*(sects)/(sects-1))+(0.985 *200)-(0.966*300/(sects-1)));
PolyY[3]:=2.85714*(350-(285-(0.258*300*(sects-1)/(sects-1))+(0.174
*200)-(185*(10+I*(scale-10)/10)/Scale)));

    SetColors(11);
    MovAbss(PolyX[1],PolyY[1]);
    LnAbss(PolyX[2],PolyY[2]);
    LnAbss(PolyX[3],PolyY[3]);

    SetColors(15);
    MovTCurAbss(PolyX[1]-72.5,PolyY[1]-50);
    SetSTAngs(18.75);
    STexts(InToStr(Round(I*Scale/10)));
    SetSTAngs(-12);
    MovTCurAbss(PolyX[3]-25,PolyY[3]-10);
    STexts(InToStr(Round(I*Scale/10)));
  end;

 polyX[1]:= 156;  polyY[1]:= 156;
 SetColors(15);
 polyX[3]:= 917;  polyY[3]:= 279;
```

```
   MovTCurAbss(polyX[3]+23,PolyY[3]);
   SetSTAngs(-12);
   STexts('-10');
   SetSTAngs(18.75);
   MovTCurAbss(polyX[1]-48,PolyY[1]);
   STexts('-10');
   PolyX[1]:=1.5625*(100+(0.966*300/(sects-1))+(0.985 *0)-(0.966*300/(sects-1)));
   PolyY[1]:=2.85714*(285+(0.174 *0)-(185*(10)/Scale));
   setColors(15);
   PolyX[3]:=1.5625*(100+(0.966*300*(sects)/(sects-1))+(0.985
*200)-(0.966*300/(sects-1)));
PolyY[3]:=2.85714*(285-(0.258*300*(sects-1)/(sects-1))+(0.174 *200)-(185*10/Scale));


{******* Label Chainage Scale *******}
SetSTAngs(-12);
MovTCurAbss(509,37);
STexts(Real2Str((length/10)));
MovTCurAbss(555,60);
STexts(Real2Str((2*length/10)));
MovTCurAbss(600,80);
STexts(Real2Str((3*length/10)));
MovTCurAbss(645,103);
STexts(Real2Str((4*length/10)));
MovTCurAbss(691,126);
STexts(Real2Str((5*length/10)));
MovTCurAbss(736,149);
STexts(Real2Str((6*length/10)));
MovTCurAbss(781,171);
STexts(Real2Str((7*length/10)));
MovTCurAbss(827,191);
STexts(Real2Str((8*length/10)));
```

```
MovTCurAbss(872,214);
STexts(Real2Str((9*length/10)));
MovTCurAbss(917,234);
STexts(Real2Str(Length));


MovTCurAbss(63,571);
SetSTAngs(90);
STexts('Head (metres)');

end;

Procedure ThreeDSUp(sects,Length,TimeLimit:real;Scale:integer);
Begin
  {******** Set Up Axes for 3D Plot********}
LOpens('Surgevp.plt',0,Offset);
SetViewPorts(0,0,0.75,0.6,3,2);
SetWindows(0,0,1000,1000);
SetLnStyles(1);
SetLnWidths(1);
MovAbss(609,408);
LnAbss(156,185);
MovAbss(609,408);
LnAbss(609,980);
Movabss(609,408);
LnAbss(917,308);
SetFonts('Halo104.fnt');
SetSTexts(20,1.5,0);
SetDegrees(1);
SetSTAngs(-12);
MovTCurAbss(917,308);
STexts('TIME (ms)');
```

```
SetSTAngs(18.75);
MovTCurAbss(156,185);
STexts('DISTANCE from Ram (m)');
LClose;
end;


Procedure ThreeD_Output
 (sects,scale:integer;
  count:longint;
  TimeInt,TimeLimit:real;
  NewPres,LocalPres:results);
const
GrCount:Integer=0;
tmpx :real = 0;
tmpx1:real = 0;
tmpy:real = 0;
tmpy1:real = 0;

var
   M,TimeSpacing,ChainageSpacing,PositionCount,Position:integer;
   temp1,temp3,temp4:real;

Begin
     Temp3 := 324*Count*TimeInt/TimeLimit;
     Temp4 := 324*(Count-1)*TimeInt/TimeLimit;
     GrCount:=GrCount+1;
     TimeSpacing:=Round(TimeLimit/(80*TimeInt));
     ChainageSpacing:=Round(sects/10);
     PositionCount := ChainageSpacing - 1;
     If GrCount = TimeSpacing then
```

```
    Begin
    For  position := 1 to sects do
      Begin
TmpX:=(156+(0.898*504*(Sects+1-position)/(sects-1))+(0.951
            *temp3)-(0.898*453/(sects-1)));
TmpY:=(186+(0.438*504*(Sects+1-position-1)/(sects-1))-(0.309*temp3)+(528*(NewPres[Pos
            ition]+10)/Scale));
TmpX1:=(156+(0.898*504*(Sects+1-position)/(sects-1))+(0.951
            *temp4)-(0.898*453/(sects-1)));
TmpY1:=(186+(0.438*504*(Sects+1-position-1)/(sects-1))-(0.309
            *temp4)+(528*(LocalPres[Position]+10)/Scale));

          If Position=1 then MovAbss(tmpX,tmpY);
          If Grcount=Timespacing then LnAbss(tmpX1,TmpY1);
        end;
    end;
    For  position := 1 to sects do
      Begin
       PositionCount:=PositionCount+1;
TmpX:=(156+(0.898*504*(Sects+1-position)/(sects-1))+(0.951
            *temp3)-(0.898*453/(sects-1)));
TmpY:=(186+(0.438*504*(Sects+1-position-1)/(sects-1))-(0.309*temp3)+(528*(NewPres[Pos
            ition]+10)/Scale));
TmpX1:=(156+(0.898*504*(Sects+1-position)/(sects-1))+(0.951
            *temp4)-(0.898*453/(sects-1)));
TmpY1:=(186+(0.438*504*(Sects+1-position-1)/(sects-1))-(0.309
            *temp4)+(528*(LocalPres[Position]+10)/Scale));
        If PositionCount = ChainageSpacing then
          Begin
            setcolors(12);
            MovAbss(TmpX1,TmpY1);
```

```
            LnAbss(TmpX,TmpY);
            PositionCount :=0
          end;
      end;
        If GrCount=TimeSpacing Then GrCount:=0;

end;    {***** 3D_Output *****}
Procedure TdFinish;
 begin
 LClose;
 end;
Procedure TwoD_Set_Up(sects,Length,TimeLimit:real;Scale:integer);
var
Y_Scale:integer;
Begin

SetFonts('d:\halo\plt\Halo106.fnt');

{******* Draw Y Axis *******}
Y_Scale:=Scale+10;
SetColors(15);
MovAbss(78,938);LnAbss(78,104);

{****LABELS****}
SetLnStyles(2);
SetSTexts(80,0.6,0);

For I := 1 to 10 do
   Begin
    MovTCurAbss(0,(100+((10+(Y_Scale-10)*I/10)*833/Y_Scale)));
    SetStAngs(0);
```

```
    STexts(InToStr(round(I*scale/10)));
    MovAbss(78,(104+((10+(Y_Scale-10)*I/10)*833/Y_Scale)));
    LnAbss(938,(104+((10+(Y_Scale-10)*I/10)*833/Y_Scale)));
   end;
  MovTCurAbss(0,(100+(10*833/Y_Scale)));
  STexts(InToStr(0));
  MovTCurAbss(0,100);
  STexts(InToStr(-10));


{******* Draw X Axis ********** Zero Position ******}
SetLnStyles(1);
SetcOLORS(15);
MovAbss(78,(104+(10*833/Y_Scale)));
LnAbss(938,(104+(10*833/Y_Scale)));
SetLnStyles(2);

For I := 1 to 10 do
   Begin
    MovTCurAbss((35+I*86),80);
    STexts(InToStr(round(I*TimeLimit*1000/10)));
    MovAbss((78+I*86),104);
    LnAbss((78+I*86),938);
   end;

SetLnStyles(1);

end;
Procedure TwoD_Output
 (sects,scale:integer;
  count:longint;
  TimeInt,TimeLimit,LocalPres,NewPres:real);
```

```
var
Old_X_Position,New_X_Position,Old_Y_Position,New_Y_Position:real;
Y_Scale:integer;

Begin

Y_Scale:=Scale+10;
Begin
Old_X_Position:=(78+(count-1)*TimeInt*859/TimeLImit);
New_X_Position:=(78+count*TimeInt*859/TimeLImit);
Old_Y_Position:=104+(10*833/Y_Scale)+(LocalPres*833/Y_Scale);
New_Y_Position:=104+(10*833/Y_Scale+NewPres*833/Y_Scale);
MovAbss(Old_X_Position,Old_Y_Position);
LnAbss(New_X_Position,New_Y_Position);
end;
end;

Procedure TwoD_VSet_Up(TimeLimit:real);
var
 Y_Scale:integer;
 Begin

  SetFonts('d:\halo\plt\Halo106.fnt');
  {******* Draw Y Axis *******}
  SetColors(15);
  MovAbss(78,938);LnAbss(78,104);

  {****LABELS****}
  SetLnStyles(2);
  SetSTexts(80,0.6,0);

For I := 1 to 10 do
```

```
    Begin
     MovTCurAbss(0,(100+(I*83)));
     SetStAngs(0);
     STexts(InToStr(I-5));
     MovAbss(78,(100+(I*83)));
     LnAbss(938,(100+(I*83)));
    end;

    {******* Draw X Axis ********** Zero Position ******}
    SetLnStyles(1);
    SetcOLORS(15);
    MovAbss(78,521);
    LnAbss(938,521);
    SetLnStyles(2);

For I := 1 to 10 do
    Begin
     MovTCurAbss((35+I*86),80);
     STexts(InToStr(round(I*TimeLimit*1000/10)));
     MovAbss((78+I*86),104);
     LnAbss((78+I*86),938);
    end;
SetLnStyles(1);
end;

Procedure TwoDV_Output
 (count:longint;
  TimeInt,TimeLimit,
  NewVel,LocalVel:real);
var
  Old_X_Position,New_X_Position,Old_Y_Position,New_Y_Position:real;
  Y_Scale:integer;
```

```
Begin
 Old_X_Position:=(78+(count-1)*TimeInt*859/TimeLImit);
 New_X_Position:=(78+count*TimeInt*859/TimeLImit);
 Old_Y_Position:=521+(LocalVel*83);
 New_Y_Position:=521+(NewVel*83);
 MovAbss(Old_X_Position,Old_Y_Position);
 LnAbss(New_X_Position,New_Y_Position);
end;
end.
```

Appendix E. Program Listing - C Code.

This appendix gives a listing of a version of the simulation that was coded in C. The C programming language was used in order to allow improved speed of execution for the simulation, and the deployment of the latest computing hardware.

```
/*

This Simulation of the hydraulic ram pump uses the method of
characteristics
calculate the progression of transients through the system.
The
simulation
varying pressures and velocities in four pipes:
Pipe 1 = Main drive pipe - linking supply reservoir to a 3 way
junction.(Position 1 is at Junction).
Pipe 2 = End section of drive pipe linking 3 way junction to
impulse valve.(Position 1 is at Junction).
Pipe 3 = Delivery pipe connecting 3 way junction to
delivery(reflux) valve.(Position 1 is at Junction).
Pipe 4 = Section of pipe making up the part of the air vessel
that is
permanently submerged.(Section 1 is at the Delivery Valve)
Note: Transients in the short fluctuating column of water that
is created
in the air vessel are not simulated in this program.
*****

*/
#include <stdio.h>
#include <stdlib.h>
#include <math.h>
#include <io.h>

#define  FALSE   0
#define  TRUE    1
/*#define  PI 3.1415927*/

#define  SQR(i)  i*i

#define  Gravity      9.80665
#define PI 3.142

float
K,Kdv,ResLevel,Valve Coeff,Diameter1,Diameter2,Diameter3,Diameter4;
float Area1,Area2,Area3,Area4,Angle1,Angle2,Angle3,Angle4;
float Length1,Length2,Length3,Length4;


float InitFlow;       /*cumecs*/
float Frequency[20];
float Valve_Velocity,Valve_Accn;
float
Ho,Khoinitapprox,Kho,Kh,Kf,Kfd,F1,F2,Frifact,WaveVel1,WaveVel2
;
float WaveVel3,WaveVel4;
float Tmp1,Sin Angle,Velocity,B9,B3;
float TermVel[20],TermAccn[20];
float TimeLimit,TimeInt;
int   Position,MassCount;
int   Sects1,Scale,outcount,outputcycle;
int Sects2,Sects3,Sects4;
float  Delivered Volume,Old Delivered Volume;
float  Wasted_Volume,Old_Wasted_Volume;
long   Count;
float  VP1,Level;
int    Delivery Pressure,DelPressCount;
double Junction Pressure;
double Discharge Flow;
int Delivery_Cycle_No,Waste_Cycle_No;


double Delivered_Volume_Data[15],Wasted_Volume_Data[15];
float
LocalVel1[1000],LocalPres1[1000],NewVel1[1000],NewPres1[1000];
float  LocalVel2[200], LocalPres2[200], NewVel2[200],
NewPres2[200];
float  LocalVel3[200], LocalPres3[200], NewVel3[200],
NewPres3[200];
float  LocalVel4[200], LocalPres4[200], NewVel4[200],
NewPres4[200];

/*DeliveryValve*/
int Delivery Valve Count,Delivery_Valve_Open;
double Delivery_Flow;
```

```
/*Valve Related*/
float
Valve_Displacement,Valve_Mass,Old_Valve_Displacement,Rel_Vel;
float
Valve Area,Valve Stroke,c,B1,B2,B4,B5,Q2,T9,xtmp,Tmp2,CP1,CM3;
double CM2,Tmp,a,b;
int Impulse_Valve_Closed,Impulse_Valve_Count;

/**Air Vessel**/
float
Vessel_Height,New_Level,Level_Change,Air_Pressure,New_Air_Pressure,Hp;

/*** Measure ***/
int Recoil,Delivery_Period,Recoil_Count;
float
Recoil Time,Recoil Data[15],Delivery_Time,Delivery_Time_Data[15];
float Impulse Close Time[10];
int Impulse_Closure_Count,Impulse_Valve_Closing;

FILE   *Dump_File;

/* Prototypes */
void Initialise(void);
void Calculation(void);
void input(void);
void Dump Data(void);
void Increment Length1(void);
void Dump Power(void);
void Pipe1 Characteristics(void);
void Pipe2 Characteristics(void);
void Pipe3 Characteristics(void);
void Pipe4 Characteristics(void);
void Reservoir Boundary(void);
void Impulse Valve Boundary(void);
void Three Way Junc Boundary(void);
void Delivery Valve Boundary(void);
void AirVessel Boundary(void);
void Update Arrays(void);
void Measure(void);

int main()
 {
 int I;
 input();
 Initialise();

Dump_File = fopen("output.txt","w");

for( I=1; I < 10; I++)
  {
Dump Data();
Calculation();
Dump Power();
Increment Length1();
Initialise();
   }
fclose(Dump File);
return 0;  }

float friction(float Velocity,float Diameter) {

 float frictval;

   if (Velocity < 1) frictval = 0.02;
   else {
     Frifact  = 2.34E-5 /
exp(log(fabs(Velocity)*Diameter)*0.89);
     Frifact  = log(Frifact + (K/(3.7*Diameter)))/2.30259;

     frictval = 0.25/(Frifact*Frifact);
   };
   return(frictval);
}
void input() {
    K=0.0002;
    Kdv=0.9;
    ResLevel=5;
    Valve Coeff=783000.00;
    Diameter1=0.05;
```

```
      Diameter2=0.1;
     Diameter3=0.05;
     Diameter4=0.1;
     Length1=6;
     Length2=0.3;/*0.245*/
     Length3=0.08;/*0.15*/
     Length4=0.08;/*0.158*/
     TimeInt=0.000025;
     outputcycle=10;
     TimeLimit=1.5;
     Valve Stroke=20;
     Valve Area=0.00342;/*0.00196 0.00181*/
     Vessel Height=0.5;
     WaveVel1 =1350;
     WaveVel2=1350;
     WaveVel3=1350;
     WaveVel4=80;
     Sects1 = 40;
     Sects2 = 3;
     Sects3 = 5;
     Sects4=5;
     Level=0;
     Scale=200;
     Delivery Pressure = 50;
     Valve_Mass = 0.5;
}
void Dump_Data()
  {

fprintf(Dump File,"~~~
```

```
    printf("%i \n",outputcycle);
    printf("Time     Complete    Valve Opening mm \n");

    }

void Dump_Power()
{
int I;
fprintf(Dump File,"                                                    \n");
   fprintf(Dump File,"Frequency |");
   for (I=0;I<Waste_Cycle_No;I++)
   {
   fprintf(Dump_File,"  %f    ",Frequency[I]);
   }
   fprintf(Dump File,"\n WasteVol  |");
   for (I=0;I<Waste_Cycle_No;I++)
   {
   fprintf(Dump_File,"  %f    ",Wasted_Volume_Data[I]);
   }
   fprintf(Dump File,"\n Delivered_Vol  |");
   for (I=0;I<Waste_Cycle_No;I++)
   {
   fprintf(Dump_File,"  %E    ",Delivered_Volume_Data[I]);
   }
   fprintf(Dump File,"\n DeliverTime  |");
   for (I=0;I<Waste_Cycle_No;I++)
   {
   fprintf(Dump_File,"  %f    ",Delivery_Time_Data[I]);
   }
   fprintf(Dump File,"\n RecoilTime  |");
   for (I=0;I<Waste_Cycle_No;I++)
   {
   fprintf(Dump_File,"  %f    ",Recoil_Data[I]);
   }
   fprintf(Dump File,"Power     |   %f\n",
   (1000*Delivered Volume Data[6]*9.81*Delivery_Pressure/Frequency[6]));
   fprintf(Dump File,"Eff       |   %f\n",
   (Delivered Volume Data[6]*Delivery Pressure/((Wasted_Volume_Data[6]+Delivered_Volume_Data[4])
   fprintf(Dump File,"Accn Pow  |   %f\n",
   (500*Areal*Length1*TermVel[6]*TermVel[6]/(Frequency[6]-Recoil_Data[6]-Delivery_Time_Data[6]))
   fprintf(Dump File,"Del  Pow  |   %f\n",
   (1000*Delivered Volume Data[6]*9.81*Delivery_Pressure/(Delivery_Time_Data[6]+Recoil_Data[6]))
   fprintf(Dump File,"Accn Eff  |   %f\n",
   (500*Areal*Length1*TermVel[6]*TermVel[6]/(1000*Wasted_Volume_Data[6]*9.81*ResLevel)));
   fprintf(Dump File,"Del  Eff  |   %f\n",
   (1000*Delivered Volume Data[6]*9.81*Delivery Pressure/(500*Areal*Length1*TermVel[6]*TermVel[6
   fprintf(Dump File,"CutoffVel    |    %f\n",TermVel[6]);
   fprintf(Dump File,"CutoffAccn    |    %f\n",TermAccn[6]);
   fprintf(Dump File,"Terminal  |    %f\n",(InitFlow/Areal));
fprintf(Dump_File,"\n ClosureTime  |");

   for (I=0;I<Waste_Cycle_No;I++)
   {
   fprintf(Dump_File,"  %f    ",Impulse_Close_Time[I]);
   }
   printf("\n Cutoff    |");
   for (I=0;I<Waste_Cycle_No;I++)
   {
   fprintf(Dump_File,"  %f    ",TermVel[I]);
   }

printf("                                                    \n");
   printf("WasteVol  |    %f      %f      %f  %f\n",
   Wasted Volume Data[1],Wasted Volume Data[2],Wasted_Volume_Data[3],Wasted_Volume_Data[4]);
   printf("DelivVol  |    %f      %f      %f  %f\n",
   Delivered Volume Data[1],Delivered Volume Data[2],Delivered_Volume_Data[3],Delivered_Volume_D
   printf("DelvTime  |    %f      %f      %f  %f\n",
   Delivery Time Data[1],Delivery Time Data[2],Delivery_Time_Data[3],Delivery_Time_Data[4]);
   printf("RecoTime  |    %f      %f      %f  %f\n",
   Recoil Data[1],Recoil Data[2],Recoil_Data[3],Recoil_Data[4]);
   printf("Power     |   %f\n",
   (1000*Delivered Volume Data[4]*9.81*Delivery_Pressure/Frequency[6]));
   printf("Eff       |   %f\n",
   (Delivered Volume Data[4]*Delivery_Pressure/((Wasted_Volume_Data[4]+Delivered_Volume_Data[4])
   printf("Accn Pow  |   %f\n",
   (500*Areal*Length1*TermVel[6]*TermVel[6]/(Frequency[6]-Recoil_Data[4]-Delivery_Time_Data[4]))
   printf("Del  Pow  |   %f\n",
   (1000*Delivered Volume Data[4]*9.81*Delivery_Pressure/(Delivery_Time_Data[4]+Recoil_Data[4]))
   printf("Accn Eff  |   %f\n",
```

```
    (500*Area1*Length1*TermVel[6]*TermVel[6]/(1000*Wasted_Volume_Data[4]*9.81*ResLevel)));
   printf("Del  Eff  |   %f\n",
   (1000*Delivered_Volume_Data[4]*9.81*Delivery_Pressure/(500*Area1*Length1*TermVel[6]*TermVel[6

   printf("Terminal  |    %f\n",(InitFlow/Area1));
   printf("ClosureTime    %f %f %f %f\n",Impulse_Close_Time[1],
Impulse_Close_Time[2],Impulse_Close_Time[3],Impulse_Close_Time[4]);

   }

void Increment_Length1()
  {
    Length1=Length1+1;
  }
void Initialise()
  {
   float Hf;
   int I;
   Discharge_Flow=0;
   Area1=PI*0.25*Diameter1*Diameter1;
   Area2=PI*0.25*Diameter2*Diameter2;
   Area3=PI*0.25*Diameter3*Diameter3;
   Area4=PI*0.25*Diameter4*Diameter4;

  /*************************************************
     CALCULATE STARTING FLOW FROM INITIAL ESTIMATE
  *************************************************/
    for( I=1; I < 11;I++)
      {
     Kho = (1.6569e+3*exp(-1.8748*Valve_Stroke) /* AAA */
        +5.1944*exp(-0.4360*Valve_Stroke)
/*   +2.887e-10*exp(0.3117*Valve_Stroke)**only needed for
strokes
over 40mm*/
        + 0.038)*1E+6;
     Khoinitapprox = (1.6569e+3*exp(-1.8748*Valve_Stroke) /*
AAA */    /*Khoinitapprox is used to start the pump with a lower initial velocity*/
        +5.1944*exp(-0.4360*Valve_Stroke)
/*   +2.887e-10*exp(0.3117*Valve_Stroke/2)**only needed for strokes over 40mm*/
        + 0.038)*1E+6;
     F1 = friction((InitFlow/Area1),Diameter1);
     F2 = friction((InitFlow/Area2),Diameter2);
     InitFlow = (1/(2*Gravity*Area1*Area1))
+Khoinitapprox+(F1*Length1/(Area1*Area1*2*Diameter1*Gravity));
     InitFlow =
InitFlow+(F2*Length2/(Area2*Area2)*2*Diameter2*Gravity);
     InitFlow = sqrt(ResLevel/InitFlow);
      };
   /*************************************************
        WAVE SPEED ADJUSTMENT
   *************************************************/
     Sects1 = floor(Length1/(TimeInt*WaveVel1)+0.5);
     Sects2 = floor(Length2/(TimeInt*WaveVel2)+0.5);
     Sects3 = floor(Length3/(TimeInt*WaveVel3)+0.5);
     Sects4 = floor(Length4/(TimeInt*WaveVel4)+0.5);
     WaveVel1 = Length1/(TimeInt*Sects1);
     WaveVel2 = Length2/(TimeInt*Sects2);
     WaveVel3 = Length3/(TimeInt*Sects3);
     WaveVel4 = Length4/(TimeInt*Sects4);
     /*************************************************
         Initialise Pipe 1
      Note: Pipe positions are numbered from junction.
     *************************************************/
     Velocity = InitFlow /Area1;
     Frifact = friction(Velocity,Diameter1);
Hf =
Frifact*Length1*Velocity*Velocity/(2*Sects1*Gravity*Diameter1);
LocalPres1[Sects1+1] =
ResLevel+Length1*sin(Angle1)-Velocity*Velocity*0.5/Gravity;
     LocalVel1[Sects1+1] = Velocity;
     for (Position=1;Position<=Sects1;Position++)
    {
LocalVel1[Position] = Velocity;
LocalPres1[Sects1+1-Position] =
LocalPres1[Sects1+1]-(Position*Hf)

+Position*Length1*sin(Angle1)/Sects1;
/*printf(" %f \n",LocalPres1[Sects1+1-Position]);*/
    };
```

```
      /*****************************************************
         Initialise Pipe 2
      *****************************************************/
      Velocity = InitFlow /Area2;
      Frifact = friction(Velocity,Diameter2);
      Hf =
Frifact*Length2*Velocity*Velocity/(2*Sects2*Gravity*Diameter2)
;
      LocalPres2[1] =LocalPres1[1];
      LocalVel2[1] = Velocity;
      for(Position=2;Position <= Sects2;Position++) {
       LocalVel2[Position] =Velocity;
       LocalPres2[Position]=LocalPres2[1]-(Position*Hf)-Position*Length2*sin(Angle2)/Sects2;
     };
      /*****************************************************
         Initialise Pipe 3
      *****************************************************/
      for(Position=0;Position <=(Sects3-1);Position++) {
     LocalVel3[Position+1] = 0;
     LocalPres3[Position+1] =
LocalPres1[1]-Position*Length3*sin(Angle3)/Sects3;
      };
      /*****************************************************
         Initialise Pipe 4
       *****************************************************/
      for(Position= 0;Position <=(Sects4-1);Position++) {
     LocalVel4[Position+1]=0;

LocalPres4[Sects4-Position]=Delivery_Pressure+Position*Length4
*sin(Angle4)/Sects4;
      };
      /*****************************************************
       Initialise Junction and Valves
      *****************************************************/
       B9 = InitFlow*InitFlow/LocalPres2[Sects2];
       Valve Displacement = Valve_Stroke;
       Valve Accn = 0;
       Valve Velocity = 0;
       Ho = Kho*InitFlow*InitFlow; /*AAA*/
       Old Delivered Volume = 0;
       Delivered Volume = 0;
       Wasted Volume = 0;
       Impulse Valve Closed = FALSE;
       Delivery Valve Open = FALSE;
       Delivery Period=FALSE;
       Delivery Cycle No = 0;
       Waste Cycle No = 0;
       Recoil Time=0;
       Recoil Count=0;
   } /******Initialise******/
void Pipe1_Characteristics()
    {
    /*****************************************************
        Characteristics Calculations for Pipe 1
    *****************************************************/
     Tmp1 = 0.5*TimeInt/Diameter1;
    for(Position=2;Position <= Sects1;Position++)
      {
     /*********** This is the C+ Characteristic
*****************/
     Sin Angle = sin(Angle1);
     Velocity = LocalVel1[Position+1];
    Frifact = friction(fabs(Velocity),Diameter1);
     a = Frifact*fabs(Velocity)*Velocity *  Tmp1;
     c = Gravity *(LocalPres1[Position+1] - Velocity*
Sin Angle);
     a = Velocity + c/WaveVel1 - a;
     /*********** This is the C- Characteristic
*****************/
    Velocity = LocalVel1[Position-1];
     b = Frifact*fabs(Velocity) * Velocity *  Tmp1;
     c =
Gravity*(Velocity*Sin Angle*TimeInt-LocalPres1[Position-1]);
     b = Velocity + c/WaveVel1 - b;
     NewVel1[Position] = 0.5*(a+b);
     NewPres1[Position] = 0.5*WaveVel1*(a-b)/Gravity;
      };
   }
void Pipe2_Characteristics()
```

```
    {
    /*****************************************************
          Characteristics Calculations for Pipe 2
     *****************************************************/
    for(Position = 2; Position <=(Sects2-1);Position++) {
    /*********** This is the C+ Characteristic
*****************/
    Tmp1 = 0.5 * TimeInt / Diameter2;
    Sin Angle = sin(Angle2);
    Velocity = LocalVel2[Position - 1];
    Frifact = friction(fabs(Velocity),Diameter2);
    a = Frifact * Velocity * fabs(Velocity)* Tmp1;
    c = Gravity *(LocalPres2[Position - 1] - Velocity*
Sin Angle);
    a = Velocity + c/WaveVel2 - a;
    /*********** This is the C- Characteristic
*****************/
    Velocity = LocalVel2[Position+1];
    Frifact = friction(fabs(Velocity),Diameter2);
    b = Frifact  * Velocity * fabs(Velocity) * Tmp1;
    c = Gravity*(Velocity
*Sin Angle*TimeInt-LocalPres2[Position+1]);
    b = Velocity + c/WaveVel2 - b;
    NewVel2[Position] = 0.5*(a+b);
    NewPres2[Position] = 0.5*WaveVel2*(a-b)/Gravity;
     };
}
void Pipe3_Characteristics()
    {
/*************************************************************
               Characteristics Calculations for Pipe 3

*************************************************************/
    for(Position=2;Position <=(Secs3-1);Position++)
     {
     /*********** This is the C+ Characteristic
*****************/
    Tmp1 = 0.5 * TimeInt / Diameter3;
    Sin Angle = sin(Angle3);
    Velocity =LocalVel3[Position - 1];
    Frifact = friction(fabs(Velocity),Diameter3);
    a = Frifact * Velocity * fabs(Velocity)* Tmp1;
    c = Gravity *(LocalPres3[Position - 1] - Velocity*
Sin Angle);
    a = Velocity + c/WaveVel3 - a;
     /*********** This is the C- Characteristic
*****************/
    Velocity= LocalVel3[Position+1];
    Frifact=friction(fabs(Velocity),Diameter3);
    b=Frifact  * Velocity * fabs(Velocity) * Tmp1;
    c=Gravity*(Velocity
*Sin Angle*TimeInt-LocalPres3[Position+1]);
    b=Velocity + c/WaveVel3 - b;
    NewVel3[Position] = 0.5*(a+b);
    NewPres3[Position] = 0.5*WaveVel3*(a-b)/Gravity;
    };
    }
void Pipe4_Characteristics()
    {
/*************************************************************
          Characteristics Calculations for Pipe 4

*************************************************************/
    for(Position=2;Position <=(Secs4-1);Position++)
     {
    /*********** This is the C+ Characteristic
*****************/
    Tmp1 = 0.5 * TimeInt / Diameter4;
    Sin Angle = sin(Angle4);
    Velocity=LocalVel4[Position - 1];
    if (fabs(Velocity)<0.001) a = 0;
    else {
      Frifact = friction(fabs(Velocity),Diameter4);
      a = Frifact * Velocity * fabs(Velocity)* Tmp1;
    };
    c =Gravity *(LocalPres4[Position - 1] - Velocity*
Sin Angle);
    a = Velocity + c/WaveVel4 - a;
    /*********** This is the C- Characteristic
```

```
*****************/
    Velocity = LocalVel4[Position + 1];
    if (fabs(Velocity)<0.001) b= 0;
    else {
      Frifact=friction(fabs(Velocity),Diameter4);
      b = Frifact  * Velocity * fabs(Velocity) * Tmp1;
    };
    c = Gravity*(Velocity
*Sin Angle*TimeInt-LocalPres4[Position+1]);
    b = Velocity + c/WaveVel4 - b;
    NewVel4[Position] = 0.5*(a+b);
    NewPres4[Position] = 0.5*WaveVel4*(a-b)/Gravity;
    };
  }
void Reservoir_Boundary()
      {

/*********************************************************
                Reservoir Boundary

*********************************************************/
     if (LocalVel1[Sects1+1]==0)
NewPres1[Sects1+1]=ResLevel;
     else
    {
      xtmp = LocalVel1[Sects1+1];
      c = 0.25*(1-(xtmp/fabs(xtmp)));
      NewPres1[Sects1+1] = ResLevel-(c*xtmp*xtmp/Gravity);
     };
     Velocity = LocalVel1[Sects1];
     xtmp  = fabs(Velocity);
     Frifact = friction(xtmp,Diameter1);
     b = 0.5*Frifact*Velocity*xtmp*TimeInt/Diameter1;
     c =
Gravity*(Velocity*sin(Angle1)*TimeInt-LocalPres1[Sects1]);
     b = Velocity+(c/WaveVel1)-b;
     NewVel1[Sects1+1] = b +
(Gravity*NewPres1[Sects1+1]/WaveVel1);
}
void Impulse_Valve_Boundary()
      {
/*********************************************************
               Impulse Valve Boundary
*********************************************************/
     Old Valve Displacement = Valve Displacement;
     Velocity = LocalVel2[Sects2-1];
     Frifact = friction(fabs(Velocity),Diameter2);
     a = Frifact*0.5*Velocity*fabs(Velocity)*TimeInt/Diameter2;
     a = Velocity+Gravity*(LocalPres2[Sects2-1]-Velocity*sin(Angle2)*TimeInt)/WaveVel2-a;
     c = PI*Diameter2*Diameter2*0.25;
     B1 = c*a;
     B2 = -c*Gravity/WaveVel2;
     Valve Displacement = Valve Displacement+Valve Velocity*TimeInt*1000+Valve_Accn*TimeInt*10(
     Valve Velocity = Valve Velocity + Valve_Accn*TimeInt;
     Rel Vel = Velocity+Valve Velocity;
  /***********************************
    Impulse Valve Open
  ***********************************/

  if (Valve_Displacement > 0.0000002)
   {
     Impulse Valve Closed=FALSE;
     Impulse Valve Count = 0;
     if (Valve_Displacement > Valve_Stroke)
      {
       Valve Displacement = Valve Stroke;
        Kf = (5.2827e+3*exp(-1.862*Valve Displacement)
           +17.1304*exp(-0.4459*Valve Displacement)
           +4.7e-6*exp(-0.1788*Valve_Displacement)
           +0.0414)*1E+6;
        Valve Velocity = 0;
        Valve Accn = Gravity - Kf*
SQR(c*Velocity)*Gravity/Valve Mass;
        if (Valve_Accn > 0)  Valve_Accn =0;
      }
     else
      {
       Kf  = (5.2827e+3*exp(-1.862*Valve Displacement)
           +17.1304*exp(-0.4459*Valve_Displacement)
```

```
            +4.7e-6*exp(-0.1788*Valve_Displacement)
          )*1E+6;

        Kfd = 0.0414e+6;
        Valve Accn =Gravity-(Kf* SQR(c*Velocity)+
       Kfd*c*c*Rel_Vel*fabs(Rel_Vel))*Gravity/Valve_Mass;
       };
     };
   /***********************************
     Impulse Valve Closed
   ************************************/

   if (Valve_Displacement<= 0.0000002)
     {
     Impulse_Valve_Count=Impulse_Valve_Count+1; /***to check
closure**/
     Valve Accn =
Gravity*(1-(LocalPres2[Sects2]*Valve_Area*1000/Valve_Mass));
     if (Valve_Accn<=0)
       {
      Valve Accn =0;
      Valve_Velocity =0;
       };
     if (Valve_Displacement<0) {Valve_Displacement=0;}
       T9 =0;
     }
     else
       {
       Kh = (1.6569e+3*exp(-1.8748*Valve Displacement)
       +5.1944*exp(-0.4360*Valve Displacement)
 /*+2.887e-10*exp(0.3117*Valve_Displacement)*only needed for
strokes over 40mm*/
          + 0.038)*1E+6;
     T9=sqrt(Kho/Kh);
       };
        /****** Boundary *******/
      B3=B9*T9*T9;
      B4=-B3/B2;
      B5=B1*B3/B2;
      Q2=0.5*(-B4+sqrt(fabs(B4*B4-4*B5)));
      NewVel2[Sects2]=Q2/c;
      NewPres2[Sects2]=(Q2-B1)/B2;

      /***********************************
      Detection of Terminal Velocity
      ***********************************/
     if(Impulse_Valve_Count==1)
     {
     TermVel[Waste Cycle No]=LocalVel1[1];
     TermAccn[Waste_Cycle_No]=(NewVel1[1]-LocalVel1[1])/TimeInt;
     }
      /*****************************************
            Detection of Permanent Valve Closure
            - for the purpose of integrating the
            wasted volume.
       *****************************************/
     if ((Impulse Valve Count * TimeInt>0.002) &
(Impulse_Valve_Count * TimeInt<0.00203))
       {
       Impulse Valve Closed=TRUE;
       Waste Cycle No=Waste Cycle No+1;
       Wasted Volume Data[Waste_Cycle_No]=Wasted_Volume;
       Wasted_Volume=0;
      };
      /*****************************************
            The integration of wasted volume
       *****************************************/
    Old_Wasted_Volume=Wasted_Volume;

Wasted Volume=Wasted Volume+TimeInt*Area2*(LocalVel2[Sects2]
          +(NewVel2[Sects2]-LocalVel2[Sects2])/2);

}
void Three_Way_Junc_Boundary()
    {
/*************************************************************
****
             Three Way Junction
```

```
**********************************************************
****/
Tmp=2*friction(LocalVel1[2],Diameter1)*LocalVel1[2]*fabs(LocalVel1[2])/(Diameter1*Gravity);
Tmp1=2*friction(LocalVel2[2],Diameter2)*LocalVel2[2]*fabs(LocalVel2[2])/(Diameter2*Gravity);
Tmp2=2*friction(LocalVel3[2],Diameter3)*LocalVel3[2]*fabs(LocalVel3[2])/(Diameter3*Gravity);
CP1=LocalPres1[2]+WaveVel1*((LocalVel1[2]/Gravity)-(Tmp*TimeInt));
CM2=LocalPres2[2]-WaveVel2*((LocalVel2[2]/Gravity)-(Tmp1*TimeInt));
CM3=LocalPres3[2]-WaveVel3*((LocalVel3[2]/Gravity)-(Tmp2*TimeInt));
Junction Pressure=(Gravity*(Area1/WaveVel1+Area2/WaveVel2+Area3/WaveVel3));
Junction Pressure=((CP1*Area1*Gravity/WaveVel1)+(CM2*Area2*Gravity/WaveVel2)
+(CM3*Area3*Gravity/WaveVel3))/Junction Pressure;
NewVel1[1] =Gravity*(CP1-Junction Pressure)/WaveVel1;
NewVel2[1] =Gravity*(Junction Pressure-CM2)/WaveVel2;
NewVel3[1] =Gravity*(Junction Pressure-CM3)/WaveVel3;
NewPres1[1] =Junction Pressure;
NewPres2[1] =Junction Pressure;
NewPres3[1] =Junction_Pressure;
}
void Delivery_Valve_Boundary()
    {
     /*************************************************
       Delivery Valv Boundary Condition
      *************************************************/
Velocity= LocalVel3[Secta3-1];
Tmp=2*friction(Velocity,Diameter3)*Velocity*fabs(Velocity)/(Diameter3*Gravity);
CP1=LocalPres3[Secta3-1]+WaveVel3*((LocalVel3[Secta3-1]/Gravity)-(Tmp*TimeInt));
Velocity= LocalVel4[2];
Tmp=2*friction(Velocity,Diameter4)*Velocity*fabs(Velocity)/(Diameter4*Gravity);
CM2=LocalPres4[2]-WaveVel4*((LocalVel4[2]/Gravity)-(Tmp*TimeInt));
Delivery Flow=Gravity*(CP1-CM2)/((WaveVel3/Area3)+(WaveVel4/Area4));
   if ((CP1-CM2) <= 0)
      {
      Delivery Flow=0;
      NewVel3[Secta3]=0;
      NewVel4[1]=0;
      }
   else
     {
      Delivery Period=TRUE;
      Delivery Valve Open=TRUE;
      Delivery Flow =
-(WaveVel3/Area3+WaveVel4/Area4)/(2*Kdv*Gravity);
      Delivery Flow = Delivery Flow +
sqrt((Delivery Flow*Delivery Flow)+(CP1-CM2)/Kdv);
      NewVel3[Secta3]=Delivery Flow/Area3;
      NewVel4[1]=Delivery_Flow/Area4;
   }

NewPres3[Secta3]=CP1-Delivery Flow*(WaveVel3/(Area3*Gravity));
   NewPres4[1]=CM2+Delivery Flow*WaveVel4/(Area4*Gravity);
    /*****************************************
       Checking for Delivery Valve Closure
     *****************************************/
if (Delivery_Valve_Open)
 {
   if (NewVel4[1]<=0)
Delivery Valve Count=Delivery Valve_Count+1;
   else Delivery Valve Count=0;
   if (((Delivery Valve Count*TimeInt) > 0.002) &
((Delivery_Valve_Count*TimeInt)<0.00203))
      {
     Delivery Period=FALSE;
     Delivery_Cycle_No=Delivery_Cycle_No+1;

     /******* Storing Integrated Volume and Frequency
Determination *******/

     if (Delivery Cycle No==1) Frequency[Delivery_Cycle_No]=Count*TimeInt;
     if (Delivery_Cycle_No>1)
    {
       Frequency[Delivery Cycle No-1]=Count*TimeInt
       -Frequency[Delivery Cycle No-1];
       Frequency[Delivery_Cycle_No]=Count*TimeInt;
    };


Delivered Volume Data[Delivery_Cycle_No]=Delivered_Volume;
        Delivered_Volume=0;
```

```
      };
      /*****************************************
       Integration of delivered volume
    *****************************************/
Old Delivered Volume=Delivered Volume;
Delivered Volume=Delivered Volume+TimeInt*Area3*(LocalVel3[Sects3]
       +(NewVel3[Sects3]-LocalVel3[Sects3])/2);
   if (!Delivery Valve Open) Delivered Volume=0;
 }; /********** Delivery Condition ***********/

}

void AirVessel_Boundary()
    {
Level Change=TimeInt*LocalVel4[Sects4-1]-(TimeInt*Discharge_Flow/Area4);
    New Level= Level+Level Change;
    Air_Pressure=LocalPres4[Sects4]-Level;

Tmp=pow((Vessel Height-Level),1.2)/pow((Vessel_Height-New_Level),1.2);
    New Air Pressure= Tmp*Air Pressure;
    Hp=New Air Pressure + New_Level;
    VP1=LocalVel4[Sects4];
    VP1= VP1 + Gravity*(LocalPres4[Sects4]-Hp)/WaveVel4;

    Frifact=friction(abs(LocalVel4[Sects4]),Diameter4);

VP1=VP1-2*Frifact*LocalVel4[Sects4]*fabs(LocalVel4[Sects4])*TimeInt/Diameter4;
    NewPres4[Sects4]=Hp;
    LocalVel4[Sects4]=VP1;
    Level=New Level;
    Tmp=(NewPres4[Sects4]-Delivery_Pressure)/Valve_Coeff;
    Discharge_Flow=sqrt(Tmp);

    }

void Update_Arrays()
    {
/*****************************************************************
       Update values of LocalVel and LocalPres for next
calculation

*****************************************************************/
      for (Position=1;Position <=Sects1+1;Position++)
     {
    if(NewPres1[Position] < -10) NewPres1[Position]=-10;
    LocalVel1[Position]= NewVel1[Position];
    LocalPres1[Position]= NewPres1[Position];
      };
      for (Position=1;Position <= Sects2;Position++)

     {
    if (NewPres2[Position] < -10) NewPres2[Position]=-10;
    LocalVel2[Position]= NewVel2[Position];
    LocalPres2[Position]= NewPres2[Position];
      };
      for (Position=1;Position<=Sects3;Position++)
     {
    if(NewPres3[Position] < -10) NewPres3[Position]=-10;
    LocalVel3[Position]= NewVel3[Position];
    LocalPres3[Position]= NewPres3[Position];
      };
      for(Position=1;Position<=Sects4;Position++)
     {
    if(NewPres4[Position] < -10) NewPres4[Position]=-10;
    LocalVel4[Position]= NewVel4[Position];
    LocalPres4[Position]= NewPres4[Position];
      };
 }
void Measure()
 {
/*****RecoilTime & DeliveryPeriod******/
if (Delivery Period) Recoil Time=0;
if ((LocalVel1[1]<-0.002) & (Recoil_Time==0))
   {
   Recoil=TRUE;
   }
if (Recoil) Recoil Time=Recoil Time+TimeInt;
if ((Recoil)&(LocalVel1[1]>-0.002)) ++Recoil_Count;
if (Recoil_Count*TimeInt>0.005)
```

```
    {
   Recoil=FALSE;
   Recoil Data[Delivery_Cycle_No]=Recoil_Time;
   Recoil Count=0;
Delivery Time Data[Delivery_Cycle_No]=Delivery_Time;
Delivery_Time=0;
   }
if (Delivery Period) Delivery Time=Delivery_Time+TimeInt;
/**** Impulse Valve Closure Time ****/
if (Valve_Displacement==Valve_Stroke)
    {
Impulse Closure Count=0;
Impulse_Valve_Closing=TRUE;
    }
if (Impulse Valve Closing) Impulse Closure Count++;
if (Impulse Valve Closed) Impulse Valve Closing=FALSE;
if (Impulse_Valve_Count==1)Impulse_Close_Time[Waste_Cycle_No]=Impulse_Closure_Count*TimeInt;
}


 /*calculation*/
void Calculation()
 {
   Count=1;
   outcount=outputcycle-1;
   while(Waste_Cycle_No<=8/*Count*TimeInt<=TimeLimit*/)
     {
   Count= Count+1;
    ++outcount;
    if (outcount==outputcycle)
          {
/* fprintf(Dump_File,"%6.5f   %6.2f   %6.3f   %6.2f   %6.3f
%5.2f   %6.3f
\n",(TimeInt*Count),LocalPres2[1],LocalVel2[1],LocalPres4[1],L
ocalVel4[1],Valve Displacement,LocalVel1[1]);
*/          outcount=0;

printf("%f      %3.1f      %f   %f   %f    %f \r",(TimeInt*Count),Impulse Close_Time[1],
Impulse Close_Time[2],Impulse_Close_Time[3],LocalVel1[1],Valve_Displacement);
          }
    Pipe1 Characteristics();
    Pipe2 Characteristics();
    Pipe3 Characteristics();
    Pipe4 Characteristics();
    Reservoir Boundary();
    Impulse Valve Boundary();
    Three Way Junc Boundary();
    Delivery Valve Boundary();
    AirVessel Boundary();
    Update Arrays();
    Measure();
     .
     };   /****** Procedure Calculation*****************/

}
```

Appendix F - Spreadsheet Formulae

This appendix is designed as a reference to understand the structure and content of the spreadsheet model described in chapter 5. The first part of the appendix up to page F8 is a snapshot preview of the spreadsheet as would be seen by an exploring user. The rest of the appendix gives the actual formulae contained in each of the spredsheet cell. It should be possible to use these to build a duplicate of the spreadsheet if an electronic copy is not available.

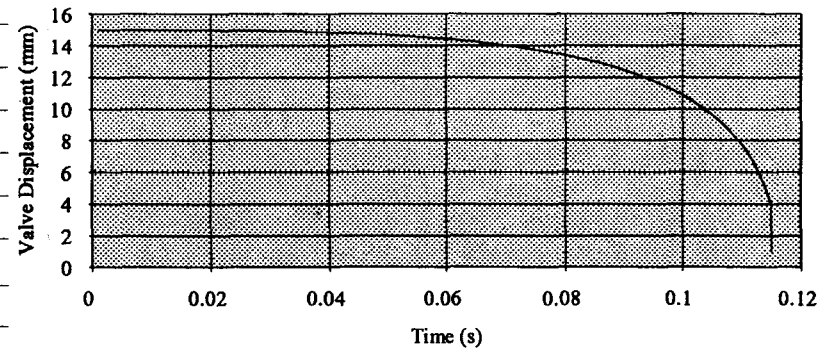

	J	K	L	M	N	O	P	Q	R	S	T
2											
3											
4											
5											
6											
7											
8											
9											
10								CL/2g	0.105122		
11								gxdH/c	0.653777	gKd/c	0.002383
12								Vel step	0.01	WavePerioc	0.014815
13											
14			DelFlow	DelFlow	Efficiency	DeliveryNos		Term Flow	VEL	Acc 1	Acc 2
15			0.034	0.039	67.62282	1		0	0	2.943	2.943
16								0.019638	0.01	2.943	2.943
17								0.039275	0.02	2.943	2.942902
18								0.058913	0.03	2.943	2.942646
19								0.07855	0.04	2.943	2.942255
20								0.098188	0.05	2.943	2.941735
21								0.117825	0.06	2.943	2.941092
22	e							0.137463	0.07	2.943	2.940328
23								0.1571	0.08	2.943	2.939445
24								0.176738	0.09	2.943	2.938444
25	Freque							0.196375	0.1	2.943	2.937328
26	Power Efficie							0.216013	0.11	2.943	2.936096
27								0.23565	0.12	2.943	2.934749
28								0.255288	0.13	2.943	2.933289

	U	V	W	X	Y	Z	AA	AB	AC	AD	AE
2											
3											
4											
5											
6											
7											
8											
9											
10											
11	Area10^-3	1.96375									
12											
13										Delivery Loss Model	
14	Time 1	Time 2	Q1	Q2	f						
15	0	0	0	0	0						
16	0.003398	0.003398	3.34E-05	3.34E-05	0.094525						
17	0.006796	0.006796	0.000133	0.000133	0.070607						
18	0.010194	0.010194	0.0003	0.0003	0.060852						
19	0.013592	0.013593	0.000534	0.000534	0.055244						
20	0.016989	0.016992	0.000834	0.000834	0.051498						
21	0.020387	0.020391	0.001201	0.001201	0.048775						
22	0.023785	0.023792	0.001635	0.001635	0.046683						
23	0.027183	0.027193	0.002135	0.002136	0.045012						
24	0.030581	0.030596	0.002702	0.002704	0.04364						
25	0.033979	0.034	0.003336	0.003339	0.042488						
26	0.037377	0.037405	0.004037	0.004042	0.041503						
27	0.040775	0.040812	0.004804	0.004811	0.040649						
28	0.044173	0.04422	0.005638	0.005647	0.039901						

	AF	AG	AH	AI	AJ	AK	AL	AM	AN	AO	AP
2											
3											
4											
5											
6											
7											
8											
9											
10											
11											
12										0.6322	
13											
14	Inst HL1	Inst HL2	Inst HL3	Inst HL4	Inst HL5	Inst HL6	Inst HL7		V0	V1	V2
15											
16	0	0	0	0	0	0	0	0	-0.6577	-1.95659	-3.32766
17	0	0	0	0	0	0	0	0.01	-0.64758	-1.94626	-3.31662
18	0	0	0	0	0	0	0	0.02	-0.63747	-1.93593	-3.30558
19	0	0	0	0	0	0	0	0.03	-0.62735	-1.92561	-3.29454
20	0	0	0	0	0	0	0	0.04	-0.61724	-1.91528	-3.28351
21	0	0	0	0	0	0	0	0.05	-0.60712	-1.90496	-3.27249
22	0	0	0	0	0	0	0	0.06	-0.59701	-1.89465	-3.26148
23	0	0	0	0	0	0	0	0.07	-0.5869	-1.88434	-3.25047
24	0	0	0	0	0	0	0	0.08	-0.57679	-1.87403	-3.23947
25	0	0	0	0	0	0	0	0.09	-0.56669	-1.86373	-3.22847
26	0	0	0	0	0	0	0	0.1	-0.55658	-1.85343	-3.21748
27	0	0	0	0	0	0	0	0.11	-0.54648	-1.84313	-3.2065
28	0	0	0	0	0	0	0	0.12	-0.53638	-1.83284	-3.19552

	AQ	AR	AS	AT	AU	AV	AW	AX	AY	AZ	BA
2											
3											
4											
5											
6											
7											
8											
9											
10											
11											
12											
13											
14	V3	v4	v5	v6	v7	No Dels	Delivered su	Volume	remainder	Recoil	DeliveryTim
15											
16	-4.88694	-6.70089	-8.90672	-11.7186	-15.5003	0	0	0	0	0	0
17	-4.87434	-6.68591	-8.8881	-11.6943	-15.4667	0	0	0	0.01	0.01	0
18	-4.86174	-6.67095	-8.86952	-11.67	-15.4331	0	0	0	0.02	0.02	0
19	-4.84916	-6.65601	-8.85096	-11.6458	-15.3997	0	0	0	0.03	0.03	0
20	-4.83659	-6.64109	-8.83244	-11.6217	-15.3663	0	0	0	0.04	0.04	0
21	-4.82403	-6.62618	-8.81394	-11.5975	-15.333	0	0	0	0.05	0.05	0
22	-4.81148	-6.61129	-8.79547	-11.5735	-15.2998	0	0	0	0.06	0.06	0
23	-4.79894	-6.59642	-8.77703	-11.5495	-15.2667	0	0	0	0.07	0.07	0
24	-4.78641	-6.58157	-8.75862	-11.5255	-15.2337	0	0	0	0.08	0.08	0
25	-4.7739	-6.56674	-8.74024	-11.5016	-15.2007	0	0	0	0.09	0.09	0
26	-4.7614	-6.55193	-8.72189	-11.4777	-15.1678	0	0	0	0.1	0.1	0
27	-4.7489	-6.53713	-8.70357	-11.4538	-15.135	0	0	0	0.11	0.11	0
28	-4.73642	-6.52235	-8.68527	-11.4301	-15.1023	0	0	0	0.12	0.12	0

	BB	BC	BD	BE	BF	BG	BH	BI	BJ	BK	BL
2											
3											
4											
5											
6											
7											
8											
9											f
10											**0.0284436**
11											Cutt Accn
12											**1.7982671**
13									Valve Closure Time Model		
14	RecoilTime					Recoil Pres:	Not OK		T	VFluid	AccnFluid
15										1.45	
16	0					3	20		0.001	1.451798	1.798267
17	0.003398					1.623853	20		0.002	1.453597	1.798267
18	0.006796					0.247706	20		0.003	1.455395	1.798267
19	0.010194					-1.12844	0		0.004	1.457193	1.798267
20	0.013592					-2.50459	0		0.005	1.458991	1.798267
21	0.016989					-3.88073	0		0.006	1.46079	1.798267
22	0.020387					-5.25688	0		0.007	1.462588	1.798267
23	0.023785					-6.63303	0		0.008	1.464386	1.798267
24	0.027183					-8.00917	0		0.009	1.466184	1.798267
25	0.030581					-9.38532	0		0.01	1.467983	1.798267
26	0.033979					-10.7615	0		0.011	1.469781	1.798267
27	0.037377					-12.1376	0		0.012	1.471579	1.798267
28	0.040775					-13.5138	0		0.013	1.473377	1.798267

	BM	BN	BO	BP	BQ	BR
2						
3						
4						
5						
6						
7						
8						
9						
10						
11						
12						
13						
14	WVolume	Kh	Kf	Av	Vv	S
15					0	15
16	0.002849	0.0455033	0.06273	0.028161	2.82E-05	14.99996
17	0.005702	0.0455033	0.0627304	0.040592	6.88E-05	14.99987
18	0.008558	0.0455034	0.0627312	0.053074	0.000122	14.99972
19	0.011418	0.0455037	0.0627326	0.065617	0.000187	14.9995
20	0.014281	0.0455042	0.0627347	0.078231	0.000266	14.9992
21	0.017148	0.0455049	0.0627376	0.090926	0.000357	14.99879
22	0.020019	0.0455059	0.0627414	0.103712	0.00046	14.99828
23	0.022893	0.0455072	0.0627463	0.116601	0.000577	14.99765
24	0.02577	0.0455089	0.0627524	0.129602	0.000707	14.99687
25	0.028651	0.045511	0.0627597	0.142727	0.000849	14.99595
26	0.031535	0.0455135	0.0627685	0.155986	0.001005	14.99487
27	0.034424	0.0455165	0.0627788	0.169392	0.001175	14.99361
28	0.037315	0.0455201	0.0627908	0.182955	0.001358	14.99216

	A	B	C	D	E	F	G	H	I	J	K	L	M	N
405						Stroke	Power	dflow	Frequency	Frequenc	Efficiency	Not OK	Q2(l/m)	Qratio
406						15	30.161	2.050380262	72.5936	83.475	67.62282	0	88.91	0.023061
407	iiii

	A	B	C	D	E
1					
2	**Hydraulic Ram Pump Perform**				
3	**INPUT**	Type data into yellow boxes - output is updated automatically			
4	SITE		DRIVE PIPE		VALVE
5	Drive Head (m)	3	Diameter (mm)	50	Stroke (mm)
6	Delivery Head(m)	30	Pipe Length(m)	10	Kf
7			relrough(k) (mm)	0.15	Ki
8			Wavespeed m/s	1320	Kd
9			CL Fittings	1.0625	Valve Mass kg
10	**OUTPUT**				Type cntrl I to recalculate charts
11	Power watts	=F15	Delivery l/m	=C15	Delivery' l/m
12	Freq b/m	=H15	Waste l/m	=A15	
13	Efficiency	=N15		=B15	
14	Waste	Waste nR	DFLOWL/M	dflow	Avpow
15	=60*(HLOOKUP("Q2",$A$14:$BH$400,$	=60*(HLOOKUP("Q2",$A$14:$BH$400,$I$7/$R$12+1)+$I$6)/(HLOOKUP("DeliveryTime",$A$14:$BH$400,$I$8/$R$12+1)+HLOOKUP("Time 2",$A$14:$BH$400,$I$7/$R$12+1)+$I$9)	=L15*60	=M15*60	=(F15+G15)/2
16					
17					
18					

	F	G
1		
2		
3		
4		Delivery Valve Swept Volume l
5	15	=IF($I$8<$I$7,"VALVE WILL NOT CLOSE with this setting","VALVE WILL CLOSE with this setting")
6	=5282.7*EXP(-1.862*F5)+17.1304*EXP(-0.4459*F5)+0.000047*EXP(-0.4459*F5)+0.0414	
7	=1656.9*EXP(-1.8748*F5)+5.1944*EXP(-0.436*F5)+0.038	
8	0.328	
9	0.507	
10		
11	=((+C15+D15)/2) -(O15*I4*B12)	Delivery' accounts for a partial realisation of recoil,
12		and delivery valve swept volume losses
13		
14	Power	
15	=IF(HLOOKUP("Acc 2",$A$14:$BH$400,$I$7/$R$12+1)<0,0,+L15*9.80665*$B$6)	=IF(HLOOKUP("Acc 2",$A$14:$BH$400,$I$7/$R$12+1)<0,0,+M15*9.80665*$B$6)
16		
17		
18		

F10

	H	I
1		
2		
3		
4		0.004
5		
6	Closure Waste Vol (l)	=$BM$310
7	Critical Velocity (m/s)	=ROUND((SQRT(F9/F6)/V11)+0.005,2)
8	Cutt off Velocity (m/s)	=$BK$310
9	closuretime (s)	=$BJ$310
10		
11		
12		
13	Power nR	
14	Frequency	FrequencynR
15	=60/((HLOOKUP("DeliveryTime",$A$14:$BH$400,$I$8/$R$12+1)+HLOOKUP("RecoilTime",$A$14:$BH$400,$I$8/$R$12+1)+HLOOKUP("Time 2",$A$14:$BH$400,$I$7/$R$12+1)+$I$9))	=60/(HLOOKUP("DeliveryTime",$A$14:$BH$400,$I$8/$R$12+1)+HLOOKUP("Time 2",$A$14:$BH$400,$I$7/$R$12+1)+$I$9)
16		
17		
18		

F11

	Q	R	S	T
10	CL/2g	=$D$9/(2*9.81)		
11	gxdH/c	=9.80665*B6/D8	gKd/c	=F8*9.80665/D8
12	Vel step	0.01	WavePeriod	=2*$D$6/D8
13				
14	Term Flow	VEL	Acc 1	Acc 2
15	=R15*$V$11	0	=9.81*($B$5)/$D$6	=(9.81/$D$6)*($B$5-(($R$10+$F$7*$V$11^2+Y15*$D$6/(2*0.001*$D$5*9.80665))*(R14)*(R14)))
16	=R16*$V$11	=(R12)	=9.81*($B$5)/$D$6	=(9.81/$D$6)*($B$5-(($R$10+$F$7*$V$11^2+Y16*$D$6/(2*0.001*$D$5*9.80665))*(R15)*(R15)))
17	=R17*$V$11	=(R16)+($R$12)	=9.81*($B$5)/$D$6	=(9.81/$D$6)*($B$5-(($R$10+$F$7*$V$11^2+Y17*$D$6/(2*0.001*$D$5*9.80665))*(R16)*(R16)))
18	=R18*$V$11	=(R17)+($R$12)	=9.81*($B$5)/$D$6	=(9.81/$D$6)*($B$5-(($R$10+$F$7*$V$11^2+Y18*$D$6/(2*0.001*$D$5*9.80665))*(R17)*(R17)))

	U	V	W	X	Y
10					
11	Area10^-3	=1000*3.142*(D5*10^(-3))^2/4			
12					
13					
14	Time 1	Time 2	Q1	Q2	f
15	0	0	0	0	0
16	=(R16-R15)/((S16+S15)/2)	=(R16-R15)/((T16+T15)/2)	=0.5*U16*R16*$V$11	=$V$11*(R15*(V16-V15)+(0.5*T16*(V16-V15)^2))+X15	=(1/(-2*(LOG(+$D$7/(3.7*$D$5)+(5.1286/(($D$5*R16/0.00114)^0.89)))))^2
17	=(R17-R16)/((S17+S16)/2)+U16	=(R17-R16)/((T17+T16)/2)+V16	=0.5*U17*R17*$V$11	=$V$11*(R16*(V17-V16)+(0.5*T17*(V17-V16)^2))+X16	=(1/(-2*(LOG(+$D$7/(3.7*$D$5)+(5.1286/(($D$5*R17/0.00114)^0.89)))))^2
18	=(R18-R17)/((S18+S17)/2)+U17	=(R18-R17)/((T18+T17)/2)+V17	=0.5*U18*R18*$V$11	=$V$11*(R17*(V18-V17)+(0.5*T18*(V18-V17)^2))+X17	=(1/(-2*(LOG(+$D$7/(3.7*$D$5)+(5.1286/(($D$5*R18/0.00114)^0.89)))))^2
19	=(R19-R18)/((S19+S18)/2)+U18	=(R19-R18)/((T19+T18)/2)+V18	=0.5*U19*R19*$V$11	=$V$11*(R18*(V19-V18)+(0.5*T19*(V19-V18)^2))+X18	=(1/(-2*(LOG(+$D$7/(3.7*$D$5)+(5.1286/(($D$5*R19/0.00114)^0.89)))))^2

	AF	AG	AH	AI
14	Inst HL1	Inst HL2	Inst HL3	Inst HL4
15				
16	=IF(AN16<0,0,+$Y16*$D$6*AN16^2/(2*0.001*$D$5*9.81))	=IF(AO16<0,0,+$Y16*$D$6*AO16^2/(2*0.001*$D$5*9.81))	=IF(AP16<0,0,+$Y16*$D$6*AP16^2/(2*0.001*$D$5*9.81))	=IF(AQ16<0,0,+$Y16*$D$6*AQ16^2/(2*0.001*$D$5*9.81))
17	=IF(AN17<0,0,+$Y17*$D$6*AN17^2/(2*0.001*$D$5*9.81))	=IF(AO17<0,0,+$Y17*$D$6*AO17^2/(2*0.001*$D$5*9.81))	=IF(AP17<0,0,+$Y17*$D$6*AP17^2/(2*0.001*$D$5*9.81))	=IF(AQ17<0,0,+$Y17*$D$6*AQ17^2/(2*0.001*$D$5*9.81))
18	=IF(AN18<0,0,+$Y18*$D$6*AN18^2/(2*0.001*$D$5*9.81))	=IF(AO18<0,0,+$Y18*$D$6*AO18^2/(2*0.001*$D$5*9.81))	=IF(AP18<0,0,+$Y18*$D$6*AP18^2/(2*0.001*$D$5*9.81))	=IF(AQ18<0,0,+$Y18*$D$6*AQ18^2/(2*0.001*$D$5*9.81))
19	=IF(AN19<0,0,+$Y19*$D$6*AN19^2/(2*0.001*$D$5*9.81))	=IF(AO19<0,0,+$Y19*$D$6*AO19^2/(2*0.001*$D$5*9.81))	=IF(AP19<0,0,+$Y19*$D$6*AP19^2/(2*0.001*$D$5*9.81))	=IF(AQ19<0,0,+$Y19*$D$6*AQ19^2/(2*0.001*$D$5*9.81))

F14

	AJ	AK	AL	AM
14	*Inst HL5*	*Inst HL6*	*Inst HL7*	
15				
16	=IF(AR16<0,0,+$Y16*$D$6*AR16^2/(2*0.001*$D$5*9.81))	=IF(AS16<0,0,+$Y16*$D$6*AS16^2/(2*0.001*$D$5*9.81))	=IF(AT16<0,0,+$Y16*$D$6*AT16^2/(2*0.001*$D$5*9.81))	=R15
17	=IF(AR17<0,0,+$Y17*$D$6*AR17^2/(2*0.001*$D$5*9.81))	=IF(AS17<0,0,+$Y17*$D$6*AS17^2/(2*0.001*$D$5*9.81))	=IF(AT17<0,0,+$Y17*$D$6*AT17^2/(2*0.001*$D$5*9.81))	=R16
18	=IF(AR18<0,0,+$Y18*$D$6*AR18^2/(2*0.001*$D$5*9.81))	=IF(AS18<0,0,+$Y18*$D$6*AS18^2/(2*0.001*$D$5*9.81))	=IF(AT18<0,0,+$Y18*$D$6*AT18^2/(2*0.001*$D$5*9.81))	=R17
19	=IF(AR19<0,0,+$Y19*$D$6*AR19^2/(2*0.001*$D$5*9.81))	=IF(AS19<0,0,+$Y19*$D$6*AS19^2/(2*0.001*$D$5*9.81))	=IF(AT19<0,0,+$Y19*$D$6*AT19^2/(2*0.001*$D$5*9.81))	=R18

AN16 - V1

=R15-$R$11-
9.80665*($F$8*$V$11^2*(R15$R$11)^2)/$D$8+9.80665*$F$7*R15^2*$V$11^2/$D$8

A016 - V2

=2*AN16-AM16-9.80665*($B$6-$B$5+AF16)/$D$8-9.80665*($F$8*(AN16-2*$R$11)^2)/$D$8

AP16 -V3

=AM16-2*AN16+2*AO16-9.80665*($B$6-$B$5+AG16)/$D$8-9.80665*($F$8*(AO16-
2*$R$11)^2*$V$11^2)/$D$8

AQ16 - V4

=-AM16+2*AN16-2*AO16+2*AP16-9.80665*($B$6-$B$5+AH16)/$D$8-9.80665*($F$8*(AP16-
2*$R$11)^2*$V$11^2)/$D$8

AR16 - V5

=+AM16-2*AN16+2*AO16-2*AP16+2*AQ16-9.80665*($B$6-$B$5+AI16)/$D$8-
9.80665*($F$8*(AQ16-2*$R$11)^2*$V$11^2)/$D$8

AS16 - V6

=-AM16+2*AN16-2*AO16+2*AP16-2*AQ16+2*AR16-9.80665*($B$6-$B$5+AJ16)/$D$8-
9.80665*($F$8*(AR16-2*$R$11)^2*$V$11^2)/$D$8

AT16 - V7

=+AM16-2*AN16+2*AO16-2*AP16+2*AQ16-2*AR16+2*AS16-9.80665*($B$6-
$B$5+AK16)/$D$8-9.80665*($F$8*(AS16-2*$R$11)^2*$V$11^2)/$D$8

AU16- V8

=-AM16+2*AN16-2*AO16+2*AP16-2*AQ16+2*AR16-2*AS16+2*AT16-9.80665*($B$6-
$B$5+AL16)/$D$8-9.80665*($F$8*(AT16-2*$R$11)^2*$V$11^2)/$D$8

AV16 - No. Dels

=IF(AN16<0,0,IF(AO16<0,1,IF(AP16<0,2,IF(AQ16<0,3,IF(AR16<0,4,IF(AS16<0,5,IF(AT16<0,6,IF
(AU16<0,7,10)))))))

AW16 - Delivered s

=R17*$V$11

AX16 - Volume

=AW16*$V$11

AY16 - Remainder

=IF(AV16=0,R15,VLOOKUP(AN16,AN16:AU400,AV16))

AZ16 - Recoil

=IF(AY16<$R$11,AY16,AY16-$R$11)

BA16 - Delivery Time

=IF(AY16<$R$11,+AV16*$T$12,$T$12*(AV16+1))

BB17 - Recoil Time

=AZ17/S16

BG16 - Recoil Pressure

=$B$5-$D$8*AZ16/9.81

BH16 - NOT OK

=IF(BG16>0,20,0)

	BJ
9	
10	
11	
12	
13	Valve Closure Time Model
14	T
15	
16	0.001
17	=IF(BR16<$F$5/4,BJ16,+BJ16+$BJ$16)
18	=IF(BR17<$F$5/4,BJ17,+BJ17+$BJ$16)
19	=IF(BR18<$F$5/4,BJ18,+BJ18+$BJ$16)
20	=IF(BR19<$F$5/4,BJ19,+BJ19+$BJ$16)
21	=IF(BR20<$F$5/4,BJ20,+BJ20+$BJ$16)
22	=IF(BR21<$F$5/4,BJ21,+BJ21+$BJ$16)
23	=IF(BR22<$F$5/4,BJ22,+BJ22+$BJ$16)
24	=IF(BR23<$F$5/4,BJ23,+BJ23+$BJ$16)
25	=IF(BR24<$F$5/4,BJ24,+BJ24+$BJ$16)
26	=IF(BR25<$F$5/4,BJ25,+BJ25+$BJ$16)
27	=IF(BR26<$F$5/4,BJ26,+BJ26+$BJ$16)
28	=IF(BR27<$F$5/4,BJ27,+BJ27+$BJ$16)
29	=IF(BR28<$F$5/4,BJ28,+BJ28+$BJ$16)
30	=IF(BR29<$F$5/4,BJ29,+BJ29+$BJ$16)
31	=IF(BR30<$F$5/4,BJ30,+BJ30+$BJ$16)

	BK
9	
10	
11	
12	
13	
14	VFluid
15	=$I$7
16	=IF(BR15<$F$5/4,BK15,IF(HLOOKUP("Acc 2",$A$14:$BH$400,$I$7/$R$12+1)<0,0,(BK15+HLOOKUP("Acc 2",$A$14:$BH$400,$I$7/$R
17	=IF(BR16<$F$5/4,BK16,IF(HLOOKUP("Acc 2",$A$14:$BH$400,$I$7/$R$12+1)<0,0,(BK16+HLOOKUP("Acc 2",$A$14:$BH$400,$I$7/$R
18	=IF(BR17<$F$5/4,BK17,IF(HLOOKUP("Acc 2",$A$14:$BH$400,$I$7/$R$12+1)<0,0,(BK17+HLOOKUP("Acc 2",$A$14:$BH$400,$I$7/$R
19	=IF(BR18<$F$5/4,BK18,IF(HLOOKUP("Acc 2",$A$14:$BH$400,$I$7/$R$12+1)<0,0,(BK18+HLOOKUP("Acc 2",$A$14:$BH$400,$I$7/$R
20	=IF(BR19<$F$5/4,BK19,IF(HLOOKUP("Acc 2",$A$14:$BH$400,$I$7/$R$12+1)<0,0,(BK19+HLOOKUP("Acc 2",$A$14:$BH$400,$I$7/$R
21	=IF(BR20<$F$5/4,BK20,IF(HLOOKUP("Acc 2",$A$14:$BH$400,$I$7/$R$12+1)<0,0,(BK20+HLOOKUP("Acc 2",$A$14:$BH$400,$I$7/$R
22	=IF(BR21<$F$5/4,BK21,IF(HLOOKUP("Acc 2",$A$14:$BH$400,$I$7/$R$12+1)<0,0,(BK21+HLOOKUP("Acc 2",$A$14:$BH$400,$I$7/$R
23	=IF(BR22<$F$5/4,BK22,IF(HLOOKUP("Acc 2",$A$14:$BH$400,$I$7/$R$12+1)<0,0,(BK22+HLOOKUP("Acc 2",$A$14:$BH$400,$I$7/$R
24	=IF(BR23<$F$5/4,BK23,IF(HLOOKUP("Acc 2",$A$14:$BH$400,$I$7/$R$12+1)<0,0,(BK23+HLOOKUP("Acc 2",$A$14:$BH$400,$I$7/$R
25	=IF(BR24<$F$5/4,BK24,IF(HLOOKUP("Acc 2",$A$14:$BH$400,$I$7/$R$12+1)<0,0,(BK24+HLOOKUP("Acc 2",$A$14:$BH$400,$I$7/$R
26	=IF(BR25<$F$5/4,BK25,IF(HLOOKUP("Acc 2",$A$14:$BH$400,$I$7/$R$12+1)<0,0,(BK25+HLOOKUP("Acc 2",$A$14:$BH$400,$I$7/$R
27	=IF(BR26<$F$5/4,BK26,IF(HLOOKUP("Acc 2",$A$14:$BH$400,$I$7/$R$12+1)<0,0,(BK26+HLOOKUP("Acc 2",$A$14:$BH$400,$I$7/$R
28	=IF(BR27<$F$5/4,BK27,IF(HLOOKUP("Acc 2",$A$14:$BH$400,$I$7/$R$12+1)<0,0,(BK27+HLOOKUP("Acc 2",$A$14:$BH$400,$I$7/$R
29	=IF(BR28<$F$5/4,BK28,IF(HLOOKUP("Acc 2",$A$14:$BH$400,$I$7/$R$12+1)<0,0,(BK28+HLOOKUP("Acc 2",$A$14:$BH$400,$I$7/$R
30	=IF(BR29<$F$5/4,BK29,IF(HLOOKUP("Acc 2",$A$14:$BH$400,$I$7/$R$12+1)<0,0,(BK29+HLOOKUP("Acc 2",$A$14:$BH$400,$I$7/$R
31	=IF(BR30<$F$5/4,BK30,IF(HLOOKUP("Acc 2",$A$14:$BH$400,$I$7/$R$12+1)<0,0,(BK30+HLOOKUP("Acc 2",$A$14:$BH$400,$I$7/$R

	BL
9	f
10	=HLOOKUP("f",$A$14:$BH$400,$I$7/$R$12+1)
11	Cutt Accn
12	=HLOOKUP("Acc 2",$A$14:$BH$400,$I$7/$R$12+1)
13	
14	AccnFluid
15	
16	=IF(BJ16<$T$12,$BL$12,9.81/$D$6*($B$5-BK16^2*($R$10+BN16*$V$11^2+$BL$10*$D$6/(2*0.001*$D$5*9.80665))))
17	=IF(BJ17<$T$12,$BL$12,9.81/$D$6*($B$5-BK17^2*($R$10+BN17*$V$11^2+$BL$10*$D$6/(2*0.001*$D$5*9.80665))))
18	=IF(BJ18<$T$12,$BL$12,9.81/$D$6*($B$5-BK18^2*($R$10+BN18*$V$11^2+$BL$10*$D$6/(2*0.001*$D$5*9.80665))))
19	=IF(BJ19<$T$12,$BL$12,9.81/$D$6*($B$5-BK19^2*($R$10+BN19*$V$11^2+$BL$10*$D$6/(2*0.001*$D$5*9.80665))))
20	=IF(BJ20<$T$12,$BL$12,9.81/$D$6*($B$5-BK20^2*($R$10+BN20*$V$11^2+$BL$10*$D$6/(2*0.001*$D$5*9.80665))))
21	=IF(BJ21<$T$12,$BL$12,9.81/$D$6*($B$5-BK21^2*($R$10+BN21*$V$11^2+$BL$10*$D$6/(2*0.001*$D$5*9.80665))))
22	=IF(BJ22<$T$12,$BL$12,9.81/$D$6*($B$5-BK22^2*($R$10+BN22*$V$11^2+$BL$10*$D$6/(2*0.001*$D$5*9.80665))))
23	=IF(BJ23<$T$12,$BL$12,9.81/$D$6*($B$5-BK23^2*($R$10+BN23*$V$11^2+$BL$10*$D$6/(2*0.001*$D$5*9.80665))))
24	=IF(BJ24<$T$12,$BL$12,9.81/$D$6*($B$5-BK24^2*($R$10+BN24*$V$11^2+$BL$10*$D$6/(2*0.001*$D$5*9.80665))))
25	=IF(BJ25<$T$12,$BL$12,9.81/$D$6*($B$5-BK25^2*($R$10+BN25*$V$11^2+$BL$10*$D$6/(2*0.001*$D$5*9.80665))))
26	=IF(BJ26<$T$12,$BL$12,9.81/$D$6*($B$5-BK26^2*($R$10+BN26*$V$11^2+$BL$10*$D$6/(2*0.001*$D$5*9.80665))))
27	=IF(BJ27<$T$12,$BL$12,9.81/$D$6*($B$5-BK27^2*($R$10+BN27*$V$11^2+$BL$10*$D$6/(2*0.001*$D$5*9.80665))))
28	=IF(BJ28<$T$12,$BL$12,9.81/$D$6*($B$5-BK28^2*($R$10+BN28*$V$11^2+$BL$10*$D$6/(2*0.001*$D$5*9.80665))))
29	=IF(BJ29<$T$12,$BL$12,9.81/$D$6*($B$5-BK29^2*($R$10+BN29*$V$11^2+$BL$10*$D$6/(2*0.001*$D$5*9.80665))))
30	=IF(BJ30<$T$12,$BL$12,9.81/$D$6*($B$5-BK30^2*($R$10+BN30*$V$11^2+$BL$10*$D$6/(2*0.001*$D$5*9.80665))))
31	=IF(BJ31<$T$12,$BL$12,9.81/$D$6*($B$5-BK31^2*($R$10+BN31*$V$11^2+$BL$10*$D$6/(2*0.001*$D$5*9.80665))))

	BM	BN
9		
10		
11		
12		
13		
14	WVolume	Kh
15		
16	=IF($F$5/4<BR16,+BM15+$V$11*$BJ$16*(BK15+BK16)/2,BM15)	=1656.9*EXP(-1.8748*F5)+5.1944*EXP(-0.436*F5)+0.038
17	=IF($F$5/4<BR17,+BM16+$V$11*$BJ$16*(BK16+BK17)/2,BM16)	=1656.9*EXP(-1.8748*BR15)+5.1944*EXP(-0.436*BR15)+0.03
18	=IF($F$5/4<BR18,+BM17+$V$11*$BJ$16*(BK17+BK18)/2,BM17)	=1656.9*EXP(-1.8748*BR16)+5.1944*EXP(-0.436*BR16)+0.03
19	=IF($F$5/4<BR19,+BM18+$V$11*$BJ$16*(BK18+BK19)/2,BM18)	=1656.9*EXP(-1.8748*BR17)+5.1944*EXP(-0.436*BR17)+0.03
20	=IF($F$5/4<BR20,+BM19+$V$11*$BJ$16*(BK19+BK20)/2,BM19)	=1656.9*EXP(-1.8748*BR18)+5.1944*EXP(-0.436*BR18)+0.03
21	=IF($F$5/4<BR21,+BM20+$V$11*$BJ$16*(BK20+BK21)/2,BM20)	=1656.9*EXP(-1.8748*BR19)+5.1944*EXP(-0.436*BR19)+0.03
22	=IF($F$5/4<BR22,+BM21+$V$11*$BJ$16*(BK21+BK22)/2,BM21)	=1656.9*EXP(-1.8748*BR20)+5.1944*EXP(-0.436*BR20)+0.03
23	=IF($F$5/4<BR23,+BM22+$V$11*$BJ$16*(BK22+BK23)/2,BM22)	=1656.9*EXP(-1.8748*BR21)+5.1944*EXP(-0.436*BR21)+0.03
24	=IF($F$5/4<BR24,+BM23+$V$11*$BJ$16*(BK23+BK24)/2,BM23)	=1656.9*EXP(-1.8748*BR22)+5.1944*EXP(-0.436*BR22)+0.03
25	=IF($F$5/4<BR25,+BM24+$V$11*$BJ$16*(BK24+BK25)/2,BM24)	=1656.9*EXP(-1.8748*BR23)+5.1944*EXP(-0.436*BR23)+0.03
26	=IF($F$5/4<BR26,+BM25+$V$11*$BJ$16*(BK25+BK26)/2,BM25)	=1656.9*EXP(-1.8748*BR24)+5.1944*EXP(-0.436*BR24)+0.03
27	=IF($F$5/4<BR27,+BM26+$V$11*$BJ$16*(BK26+BK27)/2,BM26)	=1656.9*EXP(-1.8748*BR25)+5.1944*EXP(-0.436*BR25)+0.03
28	=IF($F$5/4<BR28,+BM27+$V$11*$BJ$16*(BK27+BK28)/2,BM27)	=1656.9*EXP(-1.8748*BR26)+5.1944*EXP(-0.436*BR26)+0.03
29	=IF($F$5/4<BR29,+BM28+$V$11*$BJ$16*(BK28+BK29)/2,BM28)	=1656.9*EXP(-1.8748*BR27)+5.1944*EXP(-0.436*BR27)+0.03
30	=IF($F$5/4<BR30,+BM29+$V$11*$BJ$16*(BK29+BK30)/2,BM29)	=1656.9*EXP(-1.8748*BR28)+5.1944*EXP(-0.436*BR28)+0.03
31	=IF($F$5/4<BR31,+BM30+$V$11*$BJ$16*(BK30+BK31)/2,BM30)	=1656.9*EXP(-1.8748*BR29)+5.1944*EXP(-0.436*BR29)+0.03

	BO	BP
9		
10		
11		
12		
13		
14	Kf	Av
15		
16	=5282.7*EXP(-1.862*BR15)+17.1304*EXP(-0.4459*BR15)+0.000047*EXP(-0.4459*BR15)+0.04	=9.81*(+BO16*(BK16*$V$11)^2-$F$9)
17	=5282.7*EXP(-1.862*BR16)+17.1304*EXP(-0.4459*BR16)+0.000047*EXP(-0.4459*BR16)+0.04	=9.81*(+BO17*(BK17*$V$11)^2-$F$9)
18	=5282.7*EXP(-1.862*BR17)+17.1304*EXP(-0.4459*BR17)+0.000047*EXP(-0.4459*BR17)+0.04	=9.81*(+BO18*(BK18*$V$11)^2-$F$9)
19	=5282.7*EXP(-1.862*BR18)+17.1304*EXP(-0.4459*BR18)+0.000047*EXP(-0.4459*BR18)+0.04	=9.81*(+BO19*(BK19*$V$11)^2-$F$9)
20	=5282.7*EXP(-1.862*BR19)+17.1304*EXP(-0.4459*BR19)+0.000047*EXP(-0.4459*BR19)+0.04	=9.81*(+BO20*(BK20*$V$11)^2-$F$9)
21	=5282.7*EXP(-1.862*BR20)+17.1304*EXP(-0.4459*BR20)+0.000047*EXP(-0.4459*BR20)+0.04	=9.81*(+BO21*(BK21*$V$11)^2-$F$9)
22	=5282.7*EXP(-1.862*BR21)+17.1304*EXP(-0.4459*BR21)+0.000047*EXP(-0.4459*BR21)+0.04	=9.81*(+BO22*(BK22*$V$11)^2-$F$9)
23	=5282.7*EXP(-1.862*BR22)+17.1304*EXP(-0.4459*BR22)+0.000047*EXP(-0.4459*BR22)+0.04	=9.81*(+BO23*(BK23*$V$11)^2-$F$9)
24	=5282.7*EXP(-1.862*BR23)+17.1304*EXP(-0.4459*BR23)+0.000047*EXP(-0.4459*BR23)+0.04	=9.81*(+BO24*(BK24*$V$11)^2-$F$9)
25	=5282.7*EXP(-1.862*BR24)+17.1304*EXP(-0.4459*BR24)+0.000047*EXP(-0.4459*BR24)+0.04	=9.81*(+BO25*(BK25*$V$11)^2-$F$9)
26	=5282.7*EXP(-1.862*BR25)+17.1304*EXP(-0.4459*BR25)+0.000047*EXP(-0.4459*BR25)+0.04	=9.81*(+BO26*(BK26*$V$11)^2-$F$9)
27	=5282.7*EXP(-1.862*BR26)+17.1304*EXP(-0.4459*BR26)+0.000047*EXP(-0.4459*BR26)+0.04	=9.81*(+BO27*(BK27*$V$11)^2-$F$9)
28	=5282.7*EXP(-1.862*BR27)+17.1304*EXP(-0.4459*BR27)+0.000047*EXP(-0.4459*BR27)+0.04	=9.81*(+BO28*(BK28*$V$11)^2-$F$9)
29	=5282.7*EXP(-1.862*BR28)+17.1304*EXP(-0.4459*BR28)+0.000047*EXP(-0.4459*BR28)+0.04	=9.81*(+BO29*(BK29*$V$11)^2-$F$9)
30	=5282.7*EXP(-1.862*BR29)+17.1304*EXP(-0.4459*BR29)+0.000047*EXP(-0.4459*BR29)+0.04	=9.81*(+BO30*(BK30*$V$11)^2-$F$9)
31	=5282.7*EXP(-1.862*BR30)+17.1304*EXP(-0.4459*BR30)+0.000047*EXP(-0.4459*BR30)+0.04	=9.81*(+BO31*(BK31*$V$11)^2-$F$9)

	BQ	BR
9		
10		
11		
12		
13		
14	Vv	S
15	0	=$F$5
16	=BQ15+BP16*$BJ$16	=IF(BR15<$F$5/4,1,+BR15-1000*(BQ16*$BJ$16+0.5*BP16*$BJ$16^2))
17	=BQ16+BP17*$BJ$16	=IF(BR16<$F$5/4,1,+BR16-1000*(BQ17*$BJ$16+0.5*BP17*$BJ$16^2))
18	=BQ17+BP18*$BJ$16	=IF(BR17<$F$5/4,1,+BR17-1000*(BQ18*$BJ$16+0.5*BP18*$BJ$16^2))
19	=BQ18+BP19*$BJ$16	=IF(BR18<$F$5/4,1,+BR18-1000*(BQ19*$BJ$16+0.5*BP19*$BJ$16^2))
20	=BQ19+BP20*$BJ$16	=IF(BR19<$F$5/4,1,+BR19-1000*(BQ20*$BJ$16+0.5*BP20*$BJ$16^2))
21	=BQ20+BP21*$BJ$16	=IF(BR20<$F$5/4,1,+BR20-1000*(BQ21*$BJ$16+0.5*BP21*$BJ$16^2))
22	=BQ21+BP22*$BJ$16	=IF(BR21<$F$5/4,1,+BR21-1000*(BQ22*$BJ$16+0.5*BP22*$BJ$16^2))
23	=BQ22+BP23*$BJ$16	=IF(BR22<$F$5/4,1,+BR22-1000*(BQ23*$BJ$16+0.5*BP23*$BJ$16^2))
24	=BQ23+BP24*$BJ$16	=IF(BR23<$F$5/4,1,+BR23-1000*(BQ24*$BJ$16+0.5*BP24*$BJ$16^2))
25	=BQ24+BP25*$BJ$16	=IF(BR24<$F$5/4,1,+BR24-1000*(BQ25*$BJ$16+0.5*BP25*$BJ$16^2))
26	=BQ25+BP26*$BJ$16	=IF(BR25<$F$5/4,1,+BR25-1000*(BQ26*$BJ$16+0.5*BP26*$BJ$16^2))
27	=BQ26+BP27*$BJ$16	=IF(BR26<$F$5/4,1,+BR26-1000*(BQ27*$BJ$16+0.5*BP27*$BJ$16^2))
28	=BQ27+BP28*$BJ$16	=IF(BR27<$F$5/4,1,+BR27-1000*(BQ28*$BJ$16+0.5*BP28*$BJ$16^2))
29	=BQ28+BP29*$BJ$16	=IF(BR28<$F$5/4,1,+BR28-1000*(BQ29*$BJ$16+0.5*BP29*$BJ$16^2))
30	=BQ29+BP30*$BJ$16	=IF(BR29<$F$5/4,1,+BR29-1000*(BQ30*$BJ$16+0.5*BP30*$BJ$16^2))
31	=BQ30+BP31*$BJ$16	=IF(BR30<$F$5/4,1,+BR30-1000*(BQ31*$BJ$16+0.5*BP31*$BJ$16^2))

	F	G	H	I	J	K	L	M	N
405	Stroke	Power	dflow	Frequency	FrequencynR	Efficiency	Not OK	Q2(l/m)	Qratio
406	=$F$5	=F15	=C15	=IF(OR(H15<2*G406,H15<2*M406),H15,0)	=I15	=N15	=HLOOKUP("Not OK",$A$14:$BH$400,$I$8/$R$12+1)	=A15	=H406/M406
407									
408	5	0	0	0	765.30394131	0	0	11.4999	0
409	5.5	7.2208	0.883	0	568.66394694	42.621653	0	19.8472	0.044519132
410	6	11.988	1.466	0	509.21180901	64.796356	0	21.1730	0.069285825
411	6.5	15.334	1.876	0	460.48450673	76.548263	0	22.6363	0.082893626
412	7	17.350	2.123	0	423.55129062	80.725266	0	24.1775	0.087814082

Appendix G Impulse Valve Calibration Data

This appendix gives the valve calibration results obtained for the D.T.U. hydraulic ram pumps given in the drawings in Appendix H. The results were obtained by staff of the Development Technology Unit under the supervision of the author, using experimental methods designed by the author, and provide the raw data required to determine the calibration of a given valve as described in chapter 4. This data can therefore be used to provide design charts of the type illustrated in Appendix 9.

The results are obtained by the use of a load cell, and a manometer to calculate the force on a valve at a given flow, and the head loss across the valve respectively. For this reason, the results are given in milliVolts and mm of mercury, with conversions to kilogrammes, and metres of water given in an adjacent column. Head loss figures are given from tappings at two different positions on the pump body.

Calibration for Valve 6.4											
	Stroke =	70	Force Rating		Kf =	2.1756	Head Loss (mm Hg)				
					Kh =	1.0574		94			
	Flow (l/m)	(l/s)	(mV)	(kg)				3way		orifice	
	0	0.00	5.5	0			94	0	94	0	0
	30	0.50	4.81	0.522965			75	0.258307	94	0	0.258307
	40	0.67	4.28	0.924663			61	0.448638	94	0	0.448638
	50	0.83	3.54	1.485524			42	0.706945	94	0	0.706945
	60	1.00	2.62	2.18281			18	1.033228	94	0	1.033228
	70	1.17	1.6	2.955889			-9	1.400295	94	0	1.400295
	80	1.33	0.4	3.865393			-44	1.876124	94	0	1.876124
	90	1.50	-0.9	4.85069			-80	2.365547	94	0	2.365547
	100	1.67	-2.5	6.063362			-121	2.922947	94	0	2.922947
	110	1.83	-4.02	7.215401			-162	3.480346	93	0.013595	3.466751
	120	2.00	-6.01	8.723662			-218	4.241671	92	0.02719	4.214481
	130	2.17	-8.1	10.30772			-278	5.057377	91	0.040785	5.016592

	Stroke =	65	Force Rating		Kf =	0.5717	Head Loss (mm Hg)				
					Kh =	0.1017		94			
	Flow (l/m)	(l/s)	(mV)	(kg)				3way			
	0	0.00	5.45	0			94	0			
	30	0.50	5.28	0.128846			90	0.05438			
	40	0.67	5.13	0.242534			87	0.095166			
	50	0.83	4.94	0.386539			83	0.149546			
	60	1.00	4.66	0.598757			76	0.244712			
	70	1.17	4.41	0.788237			71	0.312687			
	80	1.33	4.1	1.023192			63	0.421448			
	90	1.50	3.73	1.303623			55	0.530209			
	100	1.67	3.29	1.637108			45	0.66616			
	110	1.83	2.81	2.00091			36	0.788516			
	120	2.00	2.41	2.304078			26	0.924467			
	130	2.17	1.84	2.736092			13	1.101203			
	140	2.33	1.27	3.168107			1	1.264344			
	150	2.50	0.69	3.6077			-12	1.441081			
	160	2.67	0.03	4.107928			-28	1.658602			
	170	2.83	-0.6	4.585418			-45	1.889719			
	180	3.00	-1.28	5.100803			-60	2.093645			
	190	3.17	-1.97	5.623768			-79	2.351952			

	Stroke =	60	Force Rating		Kf =	0.2275	Head Loss (mm Hg)				
					Kh =	0.1017		94			
	Flow (l/m)	(l/s)	(mV)	(kg)				3way		orifice	
	0	0.00	5.44	0			94	0	94	0	0
	30	0.50	5.37	0.053054			92	0.02719	94	0	0.02719
	40	0.67	5.31	0.09853			91	0.040785	93	0.013595	0.02719
	50	0.83	5.24	0.151584			89	0.067976	92	0.02719	0.040785
	60	1.00	5.14	0.227376			87	0.095166	90	0.05438	0.040785
	70	1.17	5.03	0.310747			83	0.149546	88	0.081571	0.067976
	80	1.33	4.91	0.401698			80	0.190331	86	0.108761	0.081571
	90	1.50	4.77	0.507807			76	0.244712	84	0.135951	0.108761
	100	1.67	4.6	0.636653			73	0.285497	82	0.163141	0.122356
	110	1.83	4.42	0.773079			69	0.339878	80	0.190331	0.149546
	120	2.00	4.24	0.909504			65	0.394258	77	0.231117	0.163141
	130	2.17	4.01	1.083826			59	0.475829	73	0.285497	0.190331
	140	2.33	3.78	1.258148			53	0.557399	69	0.339878	0.217522
	150	2.50	3.56	1.42489			48	0.625375	65	0.394258	0.231117
	160	2.67	3.3	1.621949			41	0.72054	61	0.448638	0.271902
	170	2.83	3.02	1.834167			33	0.829301	56	0.516614	0.312687
	180	3.00	2.74	2.046385			28	0.897277	51	0.584589	0.312687
	190	3.17	2.43	2.28134			19	1.019633	46	0.652565	0.367068
	200	3.33	2.14	2.501137			6	1.196369	40	0.734135	0.462233

	Stroke = 55		Force Rating		Kf =	0.1032	Head Loss (mm Hg)				
					Kh =	0.057		94			
	Flow (l/m)	(l/s)	(mV)	(kg)				3way			
	0	0.00	5.45	0			94	0			
	30	0.50	5.41	0.030317			93	0.013595			
	40	0.67	5.37	0.060634			92	0.02719			
	50	0.83	5.32	0.09853			90	0.05438			
	60	1.00	5.26	0.144005			88	0.081571			
	70	1.17	5.2	0.18948			86	0.108761			
	80	1.33	5.12	0.250114			84	0.135951			
	90	1.50	5.03	0.318327			81	0.176736			
	100	1.67	4.92	0.401698			78	0.217522			
	110	1.83	4.8	0.492648			76	0.244712			
	120	2.00	4.69	0.576019			73	0.285497			
	130	2.17	4.55	0.682128			69	0.339878			
	140	2.33	4.41	0.788237			66	0.380663			
	150	2.50	4.25	0.909504			61	0.448638			
	160	2.67	4.09	1.030772			57	0.503019			
	170	2.83	3.92	1.159618			51	0.584589			
	180	3.00	3.75	1.288464			47	0.63897			
	190	3.17	3.52	1.462786			41	0.72054			
	200	3.33	3.35	1.591633			36	0.788516			

	Stroke = 50		Force Rating		Kf =	0.1032	Head Loss (mm Hg)				
					Kh =	0.057		94			
	Flow (l/m)	(l/s)	(mV)	(kg)				3way		orifice	
	0	0.00	5.52	6.73E-16			94	0	94	0	0
	30	0.50	5.49	0.022738			93	0.013595	94	0	0.013595
	40	0.67	5.46	0.045475			92	0.02719	94	0	0.02719
	50	0.83	5.42	0.075792			90	0.05438	93	0.013595	0.040785
	60	1.00	5.37	0.113688			89	0.067976	91	0.040785	0.02719
	70	1.17	5.32	0.151584			88	0.081571	90	0.05438	0.02719
	80	1.33	5.26	0.197059			86	0.108761	90	0.05438	0.05438
	90	1.50	5.19	0.250114			85	0.122356	89	0.067976	0.05438
	100	1.67	5.11	0.310747			82	0.163141	87	0.095166	0.067976
	110	1.83	5.03	0.371381			81	0.176736	86	0.108761	0.067976
	120	2.00	4.95	0.432015			79	0.203927	85	0.122356	0.081571
	130	2.17	4.85	0.507807			75	0.258307	84	0.135951	0.122356
	140	2.33	4.77	0.56844			71	0.312687	82	0.163141	0.149546
	150	2.50	4.66	0.651811			68	0.353473	80	0.190331	0.163141
	160	2.67	4.55	0.735183			64	0.407853	78	0.217522	0.190331
	170	2.83	4.43	0.826133			61	0.448638	76	0.244712	0.203927
	180	3.00	4.32	0.909504			56	0.516614	74	0.271902	0.244712
	190	3.17	4.17	1.023192			51	0.584589	72	0.299092	0.285497
	200	3.33	4.03	1.129301			47	0.63897	70	0.326282	0.312687

	Stroke = 40		Force Rating		Kf = 0.0489		Head Loss (mm Hg)				
					Kh = 0.0273			94			
	Flow (l/m)	(l/s)	(mV)	(kg)				3way		orifice	
	0	0.00	5.44	0			94	0	94	0	0
	30	0.50	5.42	0.015158			93	0.013595	94	0	0.013595
	40	0.67	5.41	0.022738			92	0.02719	94	0	0.02719
	50	0.83	5.38	0.045475			92	0.02719	94	0	0.02719
	60	1.00	5.35	0.068213			91	0.040785	94	0	0.040785
	70	1.17	5.33	0.083371			90	0.05438	93	0.013595	0.040785
	80	1.33	5.29	0.113688			89	0.067976	92	0.02719	0.040785
	90	1.50	5.25	0.144005			88	0.081571	91	0.040785	0.040785
	100	1.67	5.2	0.181901			87	0.095166	90	0.05438	0.040785
	110	1.83	5.15	0.219797			84	0.135951	90	0.05438	0.081571
	120	2.00	5.1	0.257693			82	0.163141	88	0.081571	0.081571
	130	2.17	5.04	0.303168			80	0.190331	88	0.081571	0.108761
	140	2.33	4.97	0.356223			78	0.217522	86	0.108761	0.108761
	150	2.50	4.91	0.401698			75	0.258307	84	0.135951	0.122356
	160	2.67	4.83	0.462331			73	0.285497	82	0.163141	0.122356
	170	2.83	4.77	0.507807			70	0.326282	80	0.190331	0.135951
	180	3.00	4.69	0.56844			66	0.380663	78	0.217522	0.163141
	190	3.17	4.63	0.613915			63	0.421448	76	0.244712	0.176736
	200	3.33	4.55	0.674549			59	0.475829	73	0.285497	0.190331

	Stroke = 30		Force Rating		Kf = 0.0489		Head Loss (mm Hg)				
					Kh = 0.0273			94			
	Flow (l/m)	(l/s)	(mV)	(kg)				3way		orifice	
	0	0.00	8.1	0			94	0	95	0	0
	30	0.50	8.09	0.007579			93	0.013595	94	0.013595	0
	40	0.67	8.08	0.015158			93	0.013595	94	0.013595	0
	50	0.83	8.06	0.030317			92	0.02719	93	0.02719	0
30	60	1.00	8.04	0.045475			91	0.040785	92	0.040785	0
	70	1.17	8.02	0.060634			90	0.05438	91	0.05438	0
	80	1.33	7.99	0.083371			89	0.067976	90	0.067976	0
	90	1.50	7.96	0.106109			87	0.095166	89	0.081571	0.013595
	100	1.67	7.93	0.128846			85	0.122356	88	0.095166	0.02719
	110	1.83	7.89	0.159163			84	0.135951	87	0.108761	0.02719
	120	2.00	7.85	0.18948			83	0.149546	87	0.108761	0.040785
	130	2.17	7.81	0.219797			81	0.176736	86	0.122356	0.05438
	140	2.33	7.76	0.257693			79	0.203927	85	0.135951	0.067976
	150	2.50	7.72	0.28801			77	0.231117	83	0.163141	0.067976
	160	2.67	7.66	0.333485			75	0.258307	81	0.190331	0.067976
	170	2.83	7.6	0.37896			71	0.312687	79	0.217522	0.095166
	180	3.00	7.54	0.424435			68	0.353473	77	0.244712	0.108761
	190	3.17	7.46	0.485069			65	0.394258	75	0.271902	0.122356
	200	3.33	7.42	0.515386			63	0.421448	73	0.299092	0.122356

	Stroke = 25		Force Rating		Kf = 0.0414		Head Loss (mm Hg)					
					Kh = 0.0213			94				
	Flow (l/m)	(l/s)	(mV)	(kg)				3way				
	0	0.00	5.46	0			95	0	33	0	0
	30	0.50	5.45	0.007579			93	0.02719	32	0.013595	0.013595
	40	0.67	5.43	0.022738			93	0.02719	31	0.02719	0
	50	0.83	5.42	0.030317			92	0.040785	31	0.02719	0.013595
25	60	1.00	5.4	0.045475			91	0.05438	31	0.02719	0.02719
	70	1.17	5.38	0.060634			90	0.067976	30	0.040785	0.02719
	80	1.33	5.36	0.075792			89	0.081571	29	0.05438	0.02719
	90	1.50	5.33	0.09853			87	0.108761	29	0.05438	0.05438
	100	1.67	5.3	0.121267			86	0.122356	28	0.067976	0.05438
	110	1.83	5.27	0.144005			84	0.149546	27	0.081571	0.067976
	120	2.00	5.24	0.166742			84	0.149546	27	0.081571	0.067976
	130	2.17	5.2	0.197059			82	0.176736	26	0.095166	0.081571
	140	2.33	5.16	0.227376			80	0.203927	25	0.108761	0.095166
	150	2.50	5.12	0.257693			78	0.231117	23	0.135951	0.095166
	160	2.67	5.07	0.295589			76	0.258307	22	0.149546	0.108761
	170	2.83	5.03	0.325906			73	0.299092	21	0.163141	0.135951
	180	3.00	4.97	0.371381			71	0.326282	19	0.190331	0.135951
	190	3.17	4.91	0.416856			67	0.380663	17	0.217522	0.163141
	200	3.33	4.86	0.454752			65	0.407853	16	0.231117	0.176736

	Stroke = 20		Force Rating		Kf =	0.0432	Head Loss (mm Hg)				
				Kh = 0.0276				94			
	Flow (l/m)	(l/s)	(mV)	(kg)				3way			
	0	0.00	5.44	0			94	0	95	0	0
	30	0.50	5.42	0.015158			93	0.013595	94	0.013595	0
	40	0.67	5.41	0.022738			92	0.02719	94	0.013595	0.013595
	50	0.83	5.4	0.030317			92	0.02719	93	0.02719	0
20	60	1.00	5.38	0.045475			90	0.05438	92	0.040785	0.013595
	70	1.17	5.36	0.060634			90	0.05438	91	0.05438	0
	80	1.33	5.33	0.083371			88	0.081571	90	0.067976	0.013595
	90	1.50	5.31	0.09853			86	0.108761	89	0.081571	0.02719
	100	1.67	5.27	0.128846			85	0.122356	88	0.095166	0.02719
	110	1.83	5.24	0.151584			83	0.149546	87	0.108761	0.040785
	120	2.00	5.21	0.174322			83	0.149546	87	0.108761	0.040785
	130	2.17	5.16	0.212218			81	0.176736	86	0.122356	0.05438
	140	2.33	5.12	0.242534			78	0.217522	84	0.149546	0.067976
	150	2.50	5.08	0.272851			76	0.244712	83	0.163141	0.081571
	160	2.67	5.03	0.310747			73	0.285497	81	0.190331	0.095166
	170	2.83	4.98	0.348643			71	0.312687	78	0.231117	0.081571
	180	3.00	4.93	0.386539			69	0.339878	77	0.244712	0.095166
	190	3.17	4.88	0.424435			66	0.380663	75	0.271902	0.108761
	200	3.33	4.82	0.469911			62	0.435043	73	0.299092	0.135951

	Stroke = 15		Force Rating		Kf =	0.0743	Head Loss (mm Hg)				
				Kh = 0.0374				94			
	Flow (l/m)	(l/s)	(mV)	(kg)				3way			
	0	0.00	5.44	0					95	0	
	30	0.50	5.42	0.015158					94	0.013595	
	40	0.67	5.4	0.030317					94	0.013595	
	50	0.83	5.38	0.045475					93	0.02719	
	60	1.00	5.34	0.075792					92	0.040785	
	70	1.17	5.3	0.106109					91	0.05438	
	80	1.33	5.25	0.144005					90	0.067976	
	90	1.50	5.21	0.174322					89	0.081571	
	100	1.67	5.16	0.212218					88	0.095166	
	110	1.83	5.11	0.250114					86	0.122356	
	120	2.00	5.05	0.295589					85	0.135951	
	130	2.17	4.97	0.356223					83	0.163141	
	140	2.33	4.9	0.409277					81	0.190331	
	150	2.50	4.82	0.469911					78	0.231117	
	160	2.67	4.74	0.530544					76	0.258307	
	170	2.83	4.64	0.606336					73	0.299092	
	180	3.00	4.57	0.659391					70	0.339878	
	190	3.17	4.46	0.742762					66	0.394258	
	200	3.33	4.37	0.810975					64	0.421448	

	Stroke =	12	Force Rating		Kf =	0.1237	Head Loss (mm Hg)				
				Kh = 0.0534				94			
	Flow (l/m)	(l/s)	(mV)	(kg)				3way			
	0	0.00	5.44	0					94	0	
	30	0.50	5.41	0.022738					94	0	
	40	0.67	5.38	0.045475					93	0.013595	
	50	0.83	5.33	0.083371					92	0.02719	
	60	1.00	5.28	0.121267					90	0.05438	
	70	1.17	5.22	0.166742					89	0.067976	
	80	1.33	5.13	0.234955					87	0.095166	
	90	1.50	5.05	0.295589					85	0.122356	
	100	1.67	4.97	0.356223					83	0.149546	
	110	1.83	4.88	0.424435					81	0.176736	
	120	2.00	4.78	0.500227					79	0.203927	
	130	2.17	4.66	0.591178					76	0.244712	
	140	2.33	4.54	0.682128					73	0.285497	
	150	2.50	4.4	0.788237					70	0.326282	
	160	2.67	4.28	0.879188					66	0.380663	
	170	2.83	4.13	0.992876					63	0.421448	
	180	3.00	3.97	1.114143					58	0.489424	
	190	3.17	3.81	1.23541					54	0.543804	
	200	3.33	3.66	1.349098					50	0.598184	

	Stroke =	10	Force Rating		Kf =	0.2399	Head Loss (mm Hg)				
					Kh = 0.0932			94			
	Flow (l/m)	(l/s)	(mV)	(kg)				3way			
	0	0.00	5.43	0					94	0	
	30	0.50	5.37	0.045475					94	0	
	40	0.67	5.3	0.09853					92	0.02719	
	50	0.83	5.21	0.166742					91	0.040785	
	60	1.00	5.1	0.250114					89	0.067976	
	70	1.17	4.98	0.341064					86	0.108761	
	80	1.33	4.87	0.424435					84	0.135951	
	90	1.50	4.74	0.522965					80	0.190331	
	100	1.67	4.54	0.674549					76	0.244712	
	110	1.83	4.36	0.810975					72	0.299092	
	120	2.00	4.16	0.962559					68	0.353473	
	130	2.17	3.95	1.121722					63	0.421448	
	140	2.33	3.68	1.32636					56	0.516614	
	150	2.50	3.42	1.52342					52	0.570994	
	160	2.67	3.2	1.690162					46	0.652565	
	170	2.83	2.91	1.909959					39	0.747731	
	180	3.00	2.62	2.137335					32	0.842896	
	190	3.17	2.24	2.425345					24	0.951657	
	200	3.33	1.93	2.6603					16	1.060418	

	Stroke =	8	Force Rating		Kf =	0.5229	Head Loss (mm Hg)				
				Kh = 0.1852				94			
	Flow (l/m)	(l/s)	(mV)	(kg)				3way			
	0	0.00	8.08	0					94	0	
	30	0.50	7.95	0.09853					92	0.02719	
	40	0.67	7.79	0.219797					89	0.067976	
	50	0.83	7.61	0.356223					85	0.122356	
	60	1.00	7.37	0.538123					80	0.190331	
	70	1.17	7.18	0.682128					77	0.231117	
	80	1.33	6.9	0.894346					72	0.299092	
	90	1.50	6.57	1.14446					65	0.394258	
	100	1.67	6.15	1.462786					57	0.503019	
	110	1.83	5.76	1.758375					49	0.61178	
	120	2.00	5.34	2.076702					41	0.72054	
	130	2.17	4.82	2.47082					30	0.870086	
	140	2.33	4.36	2.819463					22	0.978847	
	150	2.50	3.8	3.243899					11	1.128393	
	160	2.67	3.14	3.744126					-4	1.33232	
	170	2.83	2.45	4.267091					-18	1.522651	
	180	3.00	1.92	4.668789					-28	1.658602	
	190	3.17	1.15	5.252387					-45	1.889719	

	Stroke =	6	Force Rating		Kf =	1.2975	Head Loss (mm Hg)				
					Kh = 0.4282			94			
	Flow (l/m)	(l/s)	(mV)	(kg)				3way			
	0	0.00	8.09	0					94	0	
	30	0.50	7.69	0.303168					86	0.108761	
	40	0.67	7.36	0.553282					80	0.190331	
	50	0.83	6.97	0.848871					74	0.271902	
	60	1.00	6.5	1.205093					66	0.380663	
	70	1.17	5.85	1.697741					55	0.530209	
	80	1.33	5.15	2.228286					41	0.72054	
	90	1.50	4.35	2.834622					26	0.924467	
	100	1.67	3.34	3.600121					8	1.169179	
	110	1.83	2.25	4.426254					-13	1.454676	
	120	2.00	1.18	5.237229					-33	1.726578	
	130	2.17	0	6.131575					-55	2.02567	
	140	2.33	-1.18	7.025921					-76	2.311167	
	150	2.50	-2.52	8.041534					-102	2.66464	
	160	2.67	-4.22	9.329998					-134	3.099683	

	Stroke =	5	Force Rating		Kf =	2.3616	Head Loss (mm Hg)				
					Kh = 0.7544			94			
	Flow (l/m)	(l/s)	(mV)	(kg)				3way			
	0	0.00	8.08	0					94	0	
	30	0.50	7.36	0.545703					81	0.176736	
	40	0.67	6.85	0.932242					72	0.299092	
	50	0.83	6.14	1.470365					60	0.462233	
	60	1.00	5.14	2.228286					42	0.706945	
	70	1.17	3.85	3.206003					21	0.992442	
	80	1.33	2.73	4.054873					0	1.277939	
	90	1.50	1.1	5.290283					-29	1.672197	
	100	1.67	-0.58	6.56359					-61	2.107241	
	110	1.83	-2.55	8.056692					-95	2.569474	
	120	2.00	-4.4	9.458845					-131	3.058898	

	Stroke =	4	Force Rating		Kf =	5.977	Head Loss (mm Hg)				
				Kh = 1.8519				94			
	Flow (l/m)	(l/s)	(mV)	(kg)				3way			
	0	0.00	8.08	0					94	0	
	30	0.50	6.34	1.318781					64	0.407853	
	40	0.67	4.74	2.531454					38	0.761326	
	50	0.83	2.99	3.857814					6	1.196369	
	60	1.00	0.05	6.0861					-44	1.876124	
	70	1.17	-2.7	8.17038					-94	2.555879	
	80	1.33	-5.8	10.51993					-147	3.276419	
	90	1.50	-9.8	13.55161					-214	4.187291	

CALIBRATION DATA FOR STREAMLINED M6.4s											
	STROKE	83									
	FLOW			FORCE				HEAD LOSS			
	l/m	l/s		mV	kg		3 WAY				ORIFICE
	0	0		5.45	0		91	0		92	0
	30	0.5		5.4	0.037896		90	0.013595		92	0
	40	0.666667		5.36	0.068213		89	0.02719		92	0
	50	0.833333		5.3	0.113688		88	0.040785		92	0
	60	1		5.23	0.166742		86	0.067976		91	0.013595
	70	1.166667		5.14	0.234955		85	0.081571		91	0.013595
	80	1.333333		5.05	0.303168		83	0.108761		91	0.013595
	90	1.5		4.93	0.394119		81	0.135951		91	0.013595
	100	1.666667		4.8	0.492648		78	0.176736		91	0.013595
	110	1.833333		4.66	0.598757		75	0.217522		91	0.013595
	120	2		4.52	0.704866		73	0.244712		92	0
	130	2.166667		4.36	0.826133		71	0.271902		93	-0.013595
	140	2.333333		4.2	0.9474		67	0.326282		93	-0.013595
	150	2.5		4.02	1.083826		63	0.380663		93	-0.013595
	160	2.666667		3.83	1.227831		60	0.421448		93	-0.013595
	170	2.833333		3.63	1.379415		56	0.475829		93	-0.013595
	180	3		3.42	1.538578		51	0.543804		93	-0.013595
	190	3.166667		3.22	1.690162		47	0.598184		93	-0.013595
	200	3.333333		3	1.856905		42	0.66616		93	-0.013595
										9	

	STROKE	80									
	FLOW			FORCE				HEAD LOSS			
	l/m	l/s		mV	kg		3 WAY				ORIFICE
	0	0		5.45	0		91	0		92	0
	30	0.5		5.43	0.015158		90	0.013595		92	0
	40	0.666667		5.41	0.030317		89	0.02719		92	0
	50	0.833333		5.38	0.053054		89	0.02719		91	0.013595
	60	1		5.34	0.083371		87	0.05438		91	0.013595
	70	1.166667		5.3	0.113688		87	0.05438		91	0.013595
	80	1.333333		5.25	0.151584		86	0.067976		91	0.013595
	90	1.5		5.2	0.18948		85	0.081571		90	0.02719
	100	1.666667		5.15	0.227376		83	0.108761		90	0.02719
	110	1.833333		5.08	0.28043		82	0.122356		90	0.02719
	120	2		5.01	0.333485		81	0.135951		90	0.02719
	130	2.166667		4.92	0.401698		79	0.163141		90	0.02719
	140	2.333333		4.85	0.454752		77	0.190331		90	0.02719
	150	2.5		4.78	0.507807		75	0.217522		90	0.02719
	160	2.666667		4.68	0.583599		72	0.258307		90	0.02719
	170	2.833333		4.58	0.659391		69	0.299092		89	0.040785
	180	3		4.48	0.735183		67	0.326282		89	0.040785
	190	3.166667		4.37	0.818554		64	0.367068		88	0.05438
	200	3.333333		4.28	0.886767		61	0.407853		88	0.05438

	STROKE	70									
	FLOW			FORCE				HEAD LOSS			
	l/m	l/s		mV	kg		3 WAY				ORIFICE
	0	0		5.45	0		91	0		92	0
	30	0.5		5.44	0.007579		90	0.013595		91	0.013595
	40	0.666667		5.42	0.022738		89	0.02719		91	0.013595
	50	0.833333		5.4	0.037896		89	0.02719		91	0.013595
	60	1		5.38	0.053054		88	0.040785		92	0
	70	1.166667		5.35	0.075792		87	0.05438		89	0.040785
	80	1.333333		5.32	0.09853		86	0.067976		89	0.040785
	90	1.5		5.3	0.113688		85	0.081571		89	0.040785
	100	1.666667		5.25	0.151584		84	0.095166		88	0.05438
	110	1.833333		5.2	0.18948		83	0.108761		87	0.067976
	120	2		5.16	0.219797		82	0.122356		87	0.067976
	130	2.166667		5.1	0.265272		81	0.135951		87	0.067976
	140	2.333333		5.05	0.303168		81	0.135951		87	0.067976
	150	2.5		5	0.341064		79	0.163141		87	0.067976
	160	2.666667		4.94	0.386539		77	0.190331		86	0.081571
	170	2.833333		4.85	0.454752		74	0.231117		85	0.095166
	180	3		4.8	0.492648		72	0.258307		85	0.095166
	190	3.166667		4.73	0.545703		70	0.285497		84	0.108761
	200	3.333333		4.65	0.606336		68	0.312687		83	0.122356

	STROKE	60									
	FLOW			FORCE				HEAD LOSS			
	l/m	l/s		mV	kg		3 WAY				ORIFICE
	0	0		5.45	0		91	0		93	0
	30	0.5		5.44	0.007579		90	0.013595		91	0.02719
	40	0.666667		5.42	0.022738		89	0.02719		91	0.02719
	50	0.833333		5.4	0.037896		89	0.02719		90	0.040785
	60	1		5.38	0.053054		89	0.02719		89	0.05438
	70	1.166667		5.36	0.068213		88	0.040785		89	0.05438
	80	1.333333		5.33	0.09095		87	0.05438		88	0.067976
	90	1.5		5.29	0.121267		86	0.067976		88	0.067976
	100	1.666667		5.25	0.151584		85	0.081571		87	0.081571
	110	1.833333		5.21	0.181901		83	0.108761		86	0.095166
	120	2		5.16	0.219797		82	0.122356		85	0.108761
	130	2.166667		5.12	0.250114		81	0.135951		84	0.122356
	140	2.333333		5.06	0.295589		80	0.149546		83	0.135951
	150	2.5		5.02	0.325906		79	0.163141		82	0.149546
	160	2.666667		4.94	0.386539		77	0.190331		80	0.176736
	170	2.833333		4.88	0.432015		75	0.217522		79	0.190331
	180	3		4.82	0.47749		73	0.244712		78	0.203927
	190	3.166667		4.74	0.538123		70	0.285497		76	0.231117
	200	3.333333		4.69	0.576019		68	0.312687		74	0.258307

	STROKE	50									
	FLOW			FORCE				HEAD LOSS			
	l/m	l/s		mV	kg		3 WAY				ORIFICE
	0	0		5.46	0		93	0		93	0
	30	0.5		5.44	0.015158		91	0.02719		92	0.013595
	40	0.666667		5.43	0.022738		91	0.02719		91	0.02719
	50	0.833333		5.42	0.030317		90	0.040785		91	0.02719
	60	1		5.39	0.053054		89	0.05438		90	0.040785
	70	1.166667		5.37	0.068213		89	0.05438		89	0.05438
	80	1.333333		5.35	0.083371		88	0.067976		89	0.05438
	90	1.5		5.32	0.106109		87	0.081571		88	0.067976
	100	1.666667		5.29	0.128846		85	0.108761		87	0.081571
	110	1.833333		5.25	0.159163		84	0.122356		86	0.095166
	120	2		5.21	0.18948		83	0.135951		85	0.108761
	130	2.166667		5.17	0.219797		83	0.135951		85	0.108761
	140	2.333333		5.13	0.250114		81	0.163141		84	0.122356
	150	2.5		5.08	0.28801		79	0.190331		83	0.135951
	160	2.666667		5.02	0.333485		78	0.203927		81	0.163141
	170	2.833333		4.96	0.37896		76	0.231117		79	0.190331
	180	3		4.9	0.424435		73	0.271902		77	0.217522
	190	3.166667		4.85	0.462331		71	0.299092		75	0.244712
	200	3.333333		4.79	0.507807		69	0.326282		73	0.271902

	STROKE	40									
	FLOW			FORCE				HEAD LOSS			
	l/m	l/s		mV	kg		3 WAY				ORIFICE
	0	0		5.47	0		91	0		93	0
	30	0.5		5.46	0.007579		90	0.013595		92	0.013595
	40	0.666667		5.45	0.015158		89	0.02719		91	0.02719
	50	0.833333		5.43	0.030317		89	0.02719		91	0.02719
	60	1		5.42	0.037896		88	0.040785		90	0.040785
	70	1.166667		5.4	0.053054		87	0.05438		89	0.05438
	80	1.333333		5.37	0.075792		86	0.067976		89	0.05438
	90	1.5		5.35	0.09095		85	0.081571		88	0.067976
	100	1.666667		5.32	0.113688		84	0.095166		87	0.081571
	110	1.833333		5.29	0.136426		83	0.108761		86	0.095166
	120	2		5.25	0.166742		82	0.122356		85	0.108761
	130	2.166667		5.21	0.197059		81	0.135951		84	0.122356
	140	2.333333		5.17	0.227376		80	0.149546		83	0.135951
	150	2.5		5.12	0.265272		79	0.163141		82	0.149546
	160	2.666667		5.07	0.303168		77	0.190331		81	0.163141
	170	2.833333		5.02	0.341064		75	0.217522		80	0.176736
	180	3		4.97	0.37896		74	0.231117		79	0.190331
	190	3.166667		4.91	0.424435		72	0.258307		78	0.203927
	200	3.333333		4.85	0.469911		70	0.285497		77	0.217522

	STROKE	30									
	FLOW			FORCE				HEAD LOSS			
	l/m	l/s		mV	kg		3 WAY				ORIFICE
	0	0		5.45	0		91	0		93	0
	30	0.5		5.44	0.007579		91	0		93	0
	40	0.666667		5.43	0.015158		90	0.013595		92	0.013595
	50	0.833333		5.42	0.022738		89	0.02719		91	0.02719
	60	1		5.41	0.030317		89	0.02719		91	0.02719
	70	1.166667		5.39	0.045475		88	0.040785		90	0.040785
	80	1.333333		5.37	0.060634		87	0.05438		89	0.05438
	90	1.5		5.35	0.075792		87	0.05438		89	0.05438
	100	1.666667		5.32	0.09853		86	0.067976		88	0.067976
	110	1.833333		5.29	0.121267		84	0.095166		87	0.081571
	120	2		5.26	0.144005		83	0.108761		86	0.095166
	130	2.166667		5.23	0.166742		82	0.122356		85	0.108761
	140	2.333333		5.2	0.18948		81	0.135951		85	0.108761
	150	2.5		5.15	0.227376		80	0.149546		85	0.108761
	160	2.666667		5.12	0.250114		79	0.163141		84	0.122356
	170	2.833333		5.08	0.28043		77	0.190331		83	0.135951
	180	3		5.04	0.310747		75	0.217522		81	0.163141
	190	3.166667		4.98	0.356223		72	0.258307		80	0.176736
	200	3.333333		4.94	0.386539		70	0.285497		78	0.203927

	STROKE	25									
	FLOW			FORCE				HEAD LOSS			
	l/m	l/s		mV	kg		3 WAY				ORIFICE
	0	0		5.45	0		91	0		94	0
	30	0.5		5.44	0.007579		91	0		94	0
	40	0.666667		5.43	0.015158		91	0		94	0
	50	0.833333		5.42	0.022738		90	0.013595		93	0.013595
	60	1		5.4	0.037896		89	0.02719		93	0.013595
	70	1.166667		5.38	0.053054		89	0.02719		92	0.02719
	80	1.333333		5.36	0.068213		88	0.040785		91	0.040785
	90	1.5		5.34	0.083371		87	0.05438		91	0.040785
	100	1.666667		5.31	0.106109		85	0.081571		90	0.05438
	110	1.833333		5.28	0.128846		84	0.095166		89	0.067976
	120	2		5.26	0.144005		83	0.108761		89	0.067976
	130	2.166667		5.22	0.174322		82	0.122356		88	0.081571
	140	2.333333		5.19	0.197059		81	0.135951		87	0.095166
	150	2.5		5.15	0.227376		79	0.163141		86	0.108761
	160	2.666667		5.11	0.257693		78	0.176736		85	0.122356
	170	2.833333		5.07	0.28801		77	0.190331		84	0.135951
	180	3		5.01	0.333485		74	0.231117		82	0.163141
	190	3.166667		4.96	0.371381		72	0.258307		81	0.176736
	200	3.333333		4.92	0.401698		70	0.285497		79	0.203927

	STROKE	20									
	FLOW			FORCE				HEAD LOSS			
	l/m	l/s		mV	kg		3 WAY				ORIFICE
	0	0		5.54	0		91	0		93	0
	30	0.5		5.52	0.015158		90	0.013595		91	0.02719
	40	0.666667		5.51	0.022738		89	0.02719		91	0.02719
	50	0.833333		5.49	0.037896		89	0.02719		90	0.040785
	60	1		5.47	0.053054		88	0.040785		89	0.05438
	70	1.166667		5.44	0.075792		87	0.05438		89	0.05438
	80	1.333333		5.41	0.09853		87	0.05438		88	0.067976
	90	1.5		5.38	0.121267		86	0.067976		87	0.081571
	100	1.666667		5.34	0.151584		85	0.081571		86	0.095166
	110	1.833333		5.3	0.181901		84	0.095166		85	0.108761
	120	2		5.25	0.219797		83	0.108761		85	0.108761
	130	2.166667		5.21	0.250114		81	0.135951		84	0.122356
	140	2.333333		5.16	0.28801		79	0.163141		83	0.135951
	150	2.5		5.1	0.333485		77	0.190331		82	0.149546
	160	2.666667		5.04	0.37896		75	0.217522		81	0.163141
	170	2.833333		4.97	0.432015		73	0.244712		79	0.190331
	180	3		4.91	0.47749		71	0.271902		78	0.203927
	190	3.166667		4.85	0.522965		69	0.299092		76	0.231117
	200	3.333333		4.78	0.576019		66	0.339878		74	0.258307

	STROKE	15									
	FLOW			FORCE				HEAD LOSS			
	l/m	l/s		mV	kg		3 WAY				ORIFICE
	0	0		5.45	0		93	0		94	0
	30	0.5		5.42	0.022738		91	0.02719		93	0.013595
	40	0.666667		5.39	0.045475		89	0.05438		93	0.013595
	50	0.833333		5.35	0.075792		89	0.05438		91	0.040785
	60	1		5.31	0.106109		88	0.067976		91	0.040785
	70	1.166667		5.25	0.151584		86	0.095166		89	0.067976
	80	1.333333		5.18	0.204638		84	0.122356		88	0.081571
	90	1.5		5.1	0.265272		83	0.135951		87	0.095166
	100	1.666667		5.02	0.325906		81	0.163141		85	0.122356
	110	1.833333		4.95	0.37896		79	0.190331		84	0.135951
	120	2		4.84	0.462331		77	0.217522		82	0.163141
	130	2.166667		4.73	0.545703		75	0.244712		81	0.176736
	140	2.333333		4.62	0.629074		73	0.271902		79	0.203927
	150	2.5		4.5	0.720024		69	0.326282		75	0.258307
	160	2.666667		4.38	0.810975		67	0.353473		73	0.285497
	170	2.833333		4.24	0.917084		63	0.407853		71	0.312687
	180	3		4.11	1.015613		60	0.448638		68	0.353473
	190	3.166667		3.95	1.13688		56	0.503019		65	0.394258
	200	3.333333		3.77	1.273306		51	0.570994		61	0.448638

	STROKE	12									
	FLOW			FORCE				HEAD LOSS			
	l/m	l/s		mV	kg		3 WAY				ORIFICE
	0	0		5.51	0		114	0		114	0
	30	0.5		5.46	0.037896		113	0.013595		113	0.013595
	40	0.666667		5.41	0.075792		112	0.02719		113	0.013595
	50	0.833333		5.33	0.136426		110	0.05438		111	0.040785
	60	1		5.25	0.197059		108	0.081571		109	0.067976
	70	1.166667		5.14	0.28043		106	0.108761		107	0.095166
	80	1.333333		5.03	0.363802		104	0.135951		105	0.122356
	90	1.5		4.9	0.462331		102	0.163141		103	0.149546
	100	1.666667		4.77	0.560861		100	0.190331		102	0.163141
	110	1.833333		4.61	0.682128		97	0.231117		99	0.203927
	120	2		4.44	0.810975		94	0.271902		96	0.244712
	130	2.166667		4.24	0.962559		90	0.326282		93	0.285497
	140	2.333333		4.04	1.114143		87	0.367068		89	0.339878
	150	2.5		3.83	1.273306		84	0.407853		85	0.394258
	160	2.666667		3.6	1.447628		77	0.503019		80	0.462233
	170	2.833333		3.33	1.652266		71	0.584589		76	0.516614
	180	3		3.1	1.826588		66	0.652565		72	0.570994
	190	3.166667		2.81	2.046385		61	0.72054		66	0.652565
	200	3.333333		2.51	2.273761		55	0.802111		62	0.706945

	STROKE	10									
	FLOW			FORCE				HEAD LOSS			
	l/m	l/s		mV	kg		3 WAY				ORIFICE
	0	0		5.48	0		115	0		114	0
	30	0.5		5.37	0.083371		113	0.02719		113	0.013595
	40	0.666667		5.29	0.144005		111	0.05438		113	0.013595
	50	0.833333		5.16	0.242534		108	0.095166		111	0.040785
	60	1		4.99	0.371381		105	0.135951		109	0.067976
	70	1.166667		4.81	0.507807		102	0.176736		107	0.095166
	80	1.333333		4.62	0.651811		99	0.217522		105	0.122356
	90	1.5		4.4	0.818554		97	0.244712		103	0.149546
	100	1.666667		4.12	1.030772		92	0.312687		102	0.163141
	110	1.833333		3.8	1.273306		85	0.407853		99	0.203927
	120	2		3.51	1.493103		79	0.489424		96	0.244712
	130	2.166667		3.14	1.773533		73	0.570994		93	0.285497
	140	2.333333		2.75	2.069122		67	0.652565		89	0.339878
	150	2.5		2.31	2.402607		59	0.761326		85	0.394258
	160	2.666667		1.89	2.720934		51	0.870086		80	0.462233
	170	2.833333		1.36	3.122631		42	0.992442		76	0.516614
	180	3		0.89	3.478854		33	1.114798		72	0.570994
	190	3.166667		0.3	3.903289		25	1.223559		66	0.652565
	200	3.333333		-0.15	4.244353		15	1.35951		62	0.706945

	STROKE	8									
	FLOW			FORCE				HEAD LOSS			
	l/m	l/s		mV	kg		3 WAY				ORIFICE
	0	0		5.5	0		116	0		114	0
	30	0.5		5.12	0.28801		109	0.095166		113	0.013595
	40	0.666667		4.85	0.492648		104	0.163141		113	0.013595
	50	0.833333		4.46	0.788237		98	0.244712		111	0.040785
	60	1		3.99	1.14446		92	0.326282		109	0.067976
	70	1.166667		3.39	1.599212		86	0.407853		107	0.095166
	80	1.333333		2.66	2.152494		74	0.570994		105	0.122356
	90	1.5		1.79	2.811884		61	0.747731		103	0.149546
	100	1.666667		1.01	3.403062		48	0.924467		102	0.163141
	110	1.833333		0.01	4.160982		34	1.114798		99	0.203927
	120	2		-0.97	4.903744		18	1.33232		96	0.244712
	130	2.166667		-2.28	5.89662		-1	1.590627		93	0.285497
	140	2.333333		-3.66	6.94255		-22	1.876124		89	0.339878
	150	2.5		-5.05	7.996059		-42	2.148026		85	0.394258
	160	2.666667		-6.52	9.110202		-66	2.474308		80	0.462233
	170	2.833333		-8.3	10.4593		-94	2.854971		76	0.516614
	180	3		-10.04	11.77808		-119	3.194849		72	0.570994

	STROKE	6									
	FLOW			FORCE				HEAD LOSS			
	l/m	l/s		mV	kg		3 WAY				ORIFICE
	0	0		5.46	0		116	0		114	0
	30	0.5		4.48	0.742762		100	0.217522		100	0.190331
	40	0.666667		3.53	1.462786		86	0.407853		86	0.380663
	50	0.833333		2.26	2.425345		69	0.63897		70	0.598184
	60	1		0.38	3.850235		43	0.992442		43	0.965252
	70	1.166667		-1.63	5.373655		13	1.400295		15	1.345915
	80	1.333333		-2.97	6.389268		-20	1.848934		-20	1.821743
	90	1.5		-7.17	9.572533		-67	2.487903		-63	2.406333
	100	1.666667		-10.97	12.45263		-121	3.222039		-118	3.154063
	110	1.833333		-15.8	16.11338		-192	4.187291		-190	4.13291

Valve M6.4s

	STROKE	5									
	FLOW			FORCE				HEAD LOSS			
	l/m	l/s		mV	kg		3 WAY				ORIFICE
	0	0		5.46	0		116	0		114	0
	30	0.5		1.83	2.751251		65	0.69335		64	0.679755
	40	0.666667		-1.65	5.388813		15	1.373105		15	1.345915
	50	0.833333		-7.48	9.807488		-66	2.474308		-65	2.433523
	60	1		-17.97	17.75807		-218	4.540763		-212	4.432003

CALIBRATION OF I.V. M6.5 - 5" BODY										
STROKE	90									
	Flow		Force					HEAD LOSS		
l/min	l/sec		mV	Kg			3 Way		Orifice	
0	0		5.52	6.73E-16		114	0		114	0
30	0.5		5.31	0.159163		110	0.05438		113	0.013595
40	0.666667		5.04	0.363802		103	0.149546		113	0.013595
50	0.833333		4.73	0.598757		97	0.231117		113	0.013595
60	1		4.35	0.886767		89	0.339878		113	0.013595
70	1.166667		3.9	1.227831		80	0.462233		113	0.013595
80	1.333333		3.43	1.584053		70	0.598184		113	0.013595
90	1.5		2.84	2.031226		59	0.747731		113	0.013595
100	1.666667		2.21	2.508716		45	0.938062		114	0
110	1.833333		1.52	3.031681		30	1.141988		114	0
120	2		0.83	3.554646		15	1.345915		114	0
130	2.166667		0.04	4.153403		-2	1.577032		115	-0.013595
140	2.333333		-0.77	4.767318		-19	1.808148		116	-0.02719
150	2.5		-1.6	5.396392		-37	2.05286		116	-0.02719
160	2.666667		-2.54	6.108837		-56	2.311167		116	-0.02719
170	2.833333		-3.63	6.93497		-82	2.66464		116	-0.02719
180	3		-4.6	7.670153		-104	2.963732		116	-0.02719

G33

STROKE	80									
	Flow		Force					HEAD LOSS		
l/min	l/sec		mV	Kg			3 Way		Orifice	
0	0		5.53	0		114	0		114	0
30	0.5		5.48	0.037896		113	0.013595		113	0.013595
40	0.666667		5.42	0.083371		112	0.02719		113	0.013595
50	0.833333		5.35	0.136426		111	0.040785		112	0.02719
60	1		5.27	0.197059		109	0.067976		111	0.040785
70	1.166667		5.17	0.272851		108	0.081571		110	0.05438
80	1.333333		5.06	0.356223		106	0.108761		109	0.067976
90	1.5		4.94	0.447173		103	0.149546		107	0.095166
100	1.666667		4.77	0.576019		100	0.190331		106	0.108761
110	1.833333		4.62	0.689707		98	0.217522		104	0.135951
120	2		4.45	0.818554		95	0.258307		102	0.163141
130	2.166667		4.24	0.977717		92	0.299092		100	0.190331
140	2.333333		4.06	1.114143		89	0.339878		98	0.217522
150	2.5		3.84	1.280885		85	0.394258		96	0.244712
160	2.666667		3.63	1.440049		82	0.435043		94	0.271902
170	2.833333		3.36	1.644687		79	0.475829		91	0.312687
180	3		3.12	1.826588		75	0.530209		89	0.339878
190	3.166667		2.85	2.031226		71	0.584589		87	0.367068
200	3.333333		2.57	2.243444		65	0.66616		83	0.421448

STROKE	70									
	Flow		Force					HEAD LOSS		
l/min	l/sec		mV	Kg			3 Way		Orifice	
0	0		5.53	0		114	0		114	0
30	0.5		5.49	0.030317		113	0.013595		114	0
40	0.666667		5.45	0.060634		112	0.02719		113	0.013595
50	0.833333		5.42	0.083371		112	0.02719		113	0.013595
60	1		5.37	0.121267		111	0.040785		112	0.02719
70	1.166667		5.31	0.166742		110	0.05438		111	0.040785
80	1.333333		5.24	0.219797		109	0.067976		110	0.05438
90	1.5		5.16	0.28043		107	0.095166		110	0.05438
100	1.666667		5.04	0.371381		105	0.122356		109	0.067976
110	1.833333		4.93	0.454752		103	0.149546		108	0.081571
120	2		4.82	0.538123		101	0.176736		106	0.108761
130	2.166667		4.7	0.629074		99	0.203927		105	0.122356
140	2.333333		4.57	0.727603		97	0.231117		104	0.135951
150	2.5		4.45	0.818554		95	0.258307		103	0.149546
160	2.666667		4.29	0.939821		93	0.285497		102	0.163141
170	2.833333		4.13	1.061088		90	0.326282		101	0.176736
180	3		3.97	1.182356		88	0.353473		100	0.190331
190	3.166667		3.78	1.32636		85	0.394258		98	0.217522
200	3.333333		3.59	1.470365		82	0.435043		96	0.244712

STROKE	60									
	Flow		Force					HEAD LOSS		
l/min	l/sec		mV	Kg			3 Way		Orifice	
0	0		5.53	0		114	0		114	0
30	0.5		5.5	0.022738		113	0.013595		114	0
40	0.666667		5.47	0.045475		113	0.013595		113	0.013595
50	0.833333		5.43	0.075792		112	0.02719		113	0.013595
60	1		5.39	0.106109		111	0.040785		112	0.02719
70	1.166667		5.34	0.144005		110	0.05438		112	0.02719
80	1.333333		5.28	0.18948		109	0.067976		112	0.02719
90	1.5		5.21	0.242534		108	0.081571		111	0.040785
100	1.666667		5.14	0.295589		106	0.108761		110	0.05438
110	1.833333		5.06	0.356223		104	0.135951		109	0.067976
120	2		4.97	0.424435		103	0.149546		108	0.081571
130	2.166667		4.87	0.500227		102	0.163141		107	0.095166
140	2.333333		4.76	0.583599		101	0.176736		107	0.095166
150	2.5		4.65	0.66697		99	0.203927		106	0.108761
160	2.666667		4.54	0.750341		97	0.231117		106	0.108761
170	2.833333		4.41	0.848871		96	0.244712		106	0.108761
180	3		4.28	0.9474		93	0.285497		105	0.122356
190	3.166667		4.13	1.061088		90	0.326282		104	0.135951
200	3.333333		3.98	1.174776		88	0.353473		103	0.149546

STROKE	50									
	Flow		Force					HEAD LOSS		
l/min	l/sec		mV	Kg			3 Way		Orifice	
0	0		5.53	0		116	0		114	0
30	0.5		5.51	0.015158		114	0.02719		114	0
40	0.666667		5.48	0.037896		113	0.040785		113	0.013595
50	0.833333		5.44	0.068213		112	0.05438		113	0.013595
60	1		5.4	0.09853		111	0.067976		113	0.013595
70	1.166667		5.36	0.128846		110	0.081571		112	0.02719
80	1.333333		5.31	0.166742		110	0.081571		111	0.040785
90	1.5		5.25	0.212218		108	0.108761		110	0.05438
100	1.666667		5.17	0.272851		107	0.122356		110	0.05438
110	1.833333		5.11	0.318327		106	0.135951		109	0.067976
120	2		5.02	0.386539		104	0.163141		108	0.081571
130	2.166667		4.93	0.454752		102	0.190331		108	0.081571
140	2.333333		4.83	0.530544		100	0.217522		107	0.095166
150	2.5		4.74	0.598757		99	0.231117		106	0.108761
160	2.666667		4.62	0.689707		98	0.244712		106	0.108761
170	2.833333		4.5	0.780658		97	0.258307		106	0.108761
180	3		4.39	0.864029		94	0.299092		106	0.108761
190	3.166667		4.27	0.95498		92	0.326282		105	0.122356
200	3.333333		4.13	1.061088		89	0.367068		104	0.135951

G37

STROKE	40									
	Flow		Force					HEAD LOSS		
l/min	l/sec		mV	Kg			3 Way		Orifice	
0	0		5.53	0		114	0		114	0
30	0.5		5.5	0.022738		113	0.013595		114	0
40	0.666667		5.48	0.037896		112	0.02719		113	0.013595
50	0.833333		5.44	0.068213		112	0.02719		113	0.013595
60	1		5.41	0.09095		111	0.040785		112	0.02719
70	1.166667		5.37	0.121267		110	0.05438		112	0.02719
80	1.333333		5.31	0.166742		109	0.067976		111	0.040785
90	1.5		5.25	0.212218		108	0.081571		110	0.05438
100	1.666667		5.19	0.257693		107	0.095166		109	0.067976
110	1.833333		5.12	0.310747		105	0.122356		108	0.081571
120	2		5.04	0.371381		104	0.135951		108	0.081571
130	2.166667		4.95	0.439594		103	0.149546		107	0.095166
140	2.333333		4.86	0.507807		100	0.190331		106	0.108761
150	2.5		4.77	0.576019		99	0.203927		106	0.108761
160	2.666667		4.65	0.66697		98	0.217522		105	0.122356
170	2.833333		4.53	0.75792		97	0.231117		105	0.122356
180	3		4.44	0.826133		95	0.258307		104	0.135951
190	3.166667		4.32	0.917084		93	0.285497		103	0.149546
200	3.333333		4.19	1.015613		91	0.312687		102	0.163141

G38

STROKE	30									
	Flow		Force					HEAD LOSS		
l/min	l/sec		mV	Kg			3 Way		Orifice	
0	0		5.53	0		114	0		114	0
30	0.5		5.51	0.015158		113	0.013595		114	0
40	0.666667		5.48	0.037896		112	0.02719		113	0.013595
50	0.833333		5.46	0.053054		112	0.02719		113	0.013595
60	1		5.43	0.075792		112	0.02719		112	0.02719
70	1.166667		5.39	0.106109		111	0.040785		112	0.02719
80	1.333333		5.36	0.128846		110	0.05438		111	0.040785
90	1.5		5.31	0.166742		109	0.067976		110	0.05438
100	1.666667		5.25	0.212218		107	0.095166		110	0.05438
110	1.833333		5.19	0.257693		106	0.108761		109	0.067976
120	2		5.13	0.303168		105	0.122356		108	0.081571
130	2.166667		5.06	0.356223		104	0.135951		108	0.081571
140	2.333333		4.98	0.416856		102	0.163141		107	0.095166
150	2.5		4.91	0.469911		101	0.176736		106	0.108761
160	2.666667		4.83	0.530544		99	0.203927		106	0.108761
170	2.833333		4.73	0.606336		98	0.217522		106	0.108761
180	3		4.63	0.682128		97	0.231117		105	0.122356
190	3.166667		4.52	0.765499		95	0.258307		104	0.135951
200	3.333333		4.42	0.841291		93	0.285497		103	0.149546

STROKE	20									
	Flow		Force					HEAD LOSS		
l/min	l/sec		mV	Kg			3 Way		Orifice	
0	0		5.53	0		114	0		114	0
30	0.5		5.51	0.015158		113	0.013595		114	0
40	0.666667		5.5	0.022738		112	0.02719		114	0
50	0.833333		5.48	0.037896		112	0.02719		113	0.013595
60	1		5.45	0.060634		111	0.040785		113	0.013595
70	1.166667		5.42	0.083371		110	0.05438		112	0.02719
80	1.333333		5.39	0.106109		109	0.067976		112	0.02719
90	1.5		5.35	0.136426		108	0.081571		111	0.040785
100	1.666667		5.3	0.174322		107	0.095166		110	0.05438
110	1.833333		5.26	0.204638		106	0.108761		110	0.05438
120	2		5.21	0.242534		104	0.135951		109	0.067976
130	2.166667		5.15	0.28801		103	0.149546		108	0.081571
140	2.333333		5.09	0.333485		102	0.163141		108	0.081571
150	2.5		5.02	0.386539		101	0.176736		107	0.095166
160	2.666667		4.97	0.424435		100	0.190331		107	0.095166
170	2.833333		4.9	0.47749		99	0.203927		107	0.095166
180	3		4.83	0.530544		98	0.217522		107	0.095166
190	3.166667		4.75	0.591178		96	0.244712		106	0.108761
200	3.333333		4.66	0.659391		94	0.271902		105	0.122356

STROKE	15									
	Flow		Force					HEAD LOSS		
l/min	l/sec		mV	Kg			3 Way		Orifice	
0	0		5.53	0		115	0		114	0
30	0.5		5.51	0.015158		114	0.013595		114	0
40	0.666667		5.49	0.030317		113	0.02719		113	0.013595
50	0.833333		5.46	0.053054		112	0.040785		113	0.013595
60	1		5.42	0.083371		111	0.05438		112	0.02719
70	1.166667		5.37	0.121267		110	0.067976		112	0.02719
80	1.333333		5.31	0.166742		109	0.081571		111	0.040785
90	1.5		5.24	0.219797		108	0.095166		110	0.05438
100	1.666667		5.16	0.28043		106	0.122356		108	0.081571
110	1.833333		5.09	0.333485		105	0.135951		108	0.081571
120	2		5.01	0.394119		103	0.163141		107	0.095166
130	2.166667		4.92	0.462331		102	0.176736		106	0.108761
140	2.333333		4.82	0.538123		100	0.203927		106	0.108761
150	2.5		4.71	0.621495		99	0.217522		105	0.122356
160	2.666667		4.63	0.682128		97	0.244712		104	0.135951
170	2.833333		4.52	0.765499		95	0.271902		104	0.135951
180	3		4.41	0.848871		93	0.299092		103	0.149546
190	3.166667		4.27	0.95498		91	0.312687		101	0.176736
200	3.333333		4.14	1.053509		89	0.339878		99	0.203927

STROKE	12									
	Flow		Force					HEAD LOSS		
l/min	l/sec		mV	Kg			3 Way		Orifice	
0	0		5.53	0		115	0		114	0
30	0.5		5.5	0.022738		114	0.013595		114	0
40	0.666667		5.46	0.053054		113	0.02719		113	0.013595
50	0.833333		5.41	0.09095		112	0.040785		112	0.02719
60	1		5.34	0.144005		111	0.05438		111	0.040785
70	1.166667		5.26	0.204638		110	0.067976		110	0.05438
80	1.333333		5.16	0.28043		108	0.095166		109	0.067976
90	1.5		5.05	0.363802		106	0.122356		108	0.081571
100	1.666667		4.92	0.462331		104	0.149546		106	0.108761
110	1.833333		4.8	0.553282		102	0.176736		105	0.122356
120	2		4.66	0.659391		100	0.203927		104	0.135951
130	2.166667		4.51	0.773079		98	0.231117		102	0.163141
140	2.333333		4.42	0.841291		97	0.244712		102	0.163141
150	2.5		4.25	0.970138		95	0.271902		101	0.176736
160	2.666667		4.08	1.098984		93	0.299092		100	0.190331
170	2.833333		3.88	1.250568		90	0.339878		98	0.217522
180	3		3.67	1.409732		87	0.380663		96	0.244712
190	3.166667		3.46	1.568895		83	0.435043		93	0.285497
200	3.333333		3.24	1.735637		79	0.489424		90	0.326282

STROKE	10									
	Flow		Force					HEAD LOSS		
l/min	l/sec		mV	Kg			3 Way		Orifice	
0	0		5.61	0		114	0		114	0
30	0.5		5.56	0.037896		113	0.013595		113	0.013595
40	0.666667		5.48	0.09853		112	0.02719		113	0.013595
50	0.833333		5.39	0.166742		110	0.05438		111	0.040785
60	1		5.27	0.257693		109	0.067976		110	0.05438
70	1.166667		5.12	0.371381		107	0.095166		108	0.081571
80	1.333333		4.96	0.492648		105	0.122356		106	0.108761
90	1.5		4.79	0.621495		102	0.163141		104	0.135951
100	1.666667		4.58	0.780658		100	0.190331		102	0.163141
110	1.833333		4.39	0.924663		97	0.231117		100	0.190331
120	2		4.25	1.030772		96	0.244712		100	0.190331
130	2.166667		4.01	1.212672		93	0.285497		98	0.217522
140	2.333333		3.75	1.409732		90	0.326282		96	0.244712
150	2.5		3.47	1.621949		86	0.380663		94	0.271902
160	2.666667		3.19	1.834167		82	0.435043		90	0.326282
170	2.833333		2.85	2.09186		78	0.489424		86	0.380663
180	3		2.53	2.334394		73	0.557399		82	0.435043
190	3.166667		2.18	2.599667		68	0.625375		78	0.489424
200	3.333333		1.8	2.887676		63	0.69335		73	0.557399

STROKE	8									
	Flow		Force					HEAD LOSS		
l/min	l/sec		mV	Kg			3 Way		Orifice	
0	0		5.56	6.73E-16		114	0		114	0
30	0.5		5.46	0.075792		112	0.02719		113	0.013595
40	0.666667		5.32	0.181901		110	0.05438		111	0.040785
50	0.833333		5.17	0.295589		109	0.067976		109	0.067976
60	1		4.97	0.447173		107	0.095166		108	0.081571
70	1.166667		4.71	0.644232		104	0.135951		105	0.122356
80	1.333333		4.48	0.818554		100	0.190331		102	0.163141
90	1.5		4.16	1.061088		97	0.231117		99	0.203927
100	1.666667		3.8	1.33394		94	0.271902		96	0.244712
110	1.833333		3.64	1.455207		92	0.299092		94	0.271902
120	2		3.28	1.728058		87	0.367068		91	0.312687
130	2.166667		2.85	2.053964		82	0.435043		87	0.367068
140	2.333333		2.42	2.37987		77	0.503019		82	0.435043
150	2.5		1.97	2.720934		72	0.570994		78	0.489424
160	2.666667		1.42	3.13779		65	0.66616		72	0.570994
170	2.833333		0.9	3.531908		59	0.747731		66	0.652565
180	3		0.37	3.933606		53	0.829301		61	0.72054
190	3.166667		-0.18	4.350462		44	0.951657		54	0.815706
200	3.333333		-0.79	4.812794		37	1.046823		48	0.897277

STROKE	6									
	Flow		Force					HEAD LOSS		
l/min	l/sec		mV	Kg			3 Way		Orifice	
0	0		5.53	0		114	0		114	0
30	0.5		5.3	0.174322		111	0.040785		111	0.040785
40	0.666667		4.99	0.409277		108	0.081571		107	0.095166
50	0.833333		4.65	0.66697		104	0.135951		104	0.135951
60	1		4.23	0.985296		100	0.190331		100	0.190331
70	1.166667		3.73	1.364256		95	0.258307		96	0.244712
80	1.333333		3.25	1.728058		90	0.326282		92	0.299092
90	1.5		2.72	2.129756		84	0.407853		86	0.380663
100	1.666667		2	2.675459		77	0.503019		80	0.462233
110	1.833333		1.18	3.296953		69	0.61178		70	0.598184
120	2		0.43	3.865393		60	0.734135		64	0.679755
130	2.166667		-0.42	4.509626		50	0.870086		54	0.815706
140	2.333333		-1.4	5.252387		40	1.006037		44	0.951657
150	2.5		-2.45	6.048204		29	1.155584		34	1.087608
160	2.666667		-3.6	6.919812		15	1.345915		22	1.250749
170	2.833333		-4.8	7.829316		2	1.522651		10	1.41389
180	3		-6.03	8.761558		-11	1.699388		-1	1.563437
190	3.166667		-7.41	9.807488		-26	1.903314		-16	1.767363

STROKE	5									
	Flow		Force					HEAD LOSS		
l/min	l/sec		mV	Kg			3 Way		Orifice	
0	0		5.53	0		114	0		114	0
30	0.5		5.01	0.394119		108	0.081571		108	0.081571
40	0.666667		4.35	0.894346		102	0.163141		102	0.163141
50	0.833333		3.63	1.440049		94	0.271902		95	0.258307
60	1		2.76	2.099439		86	0.380663		86	0.380663
70	1.166667		1.87	2.773988		78	0.489424		78	0.489424
80	1.333333		0.82	3.569804		69	0.61178		70	0.598184
90	1.5		-0.5	4.570259		54	0.815706		56	0.788516
100	1.666667		-2.1	5.782932		38	1.033228		40	1.006037
110	1.833333		-3.82	7.086554		22	1.250749		24	1.223559
120	2		-5.54	8.390177		2				

Stroke =	60						
Flow			Force			Head Loss	
l/min	l/sec		mV	kg		mmHg	mH2O
0	0		2.52	0		127	0
30	0.5		2.51	0.007579		126	0.013595
40	0.666667		2.5	0.015158		126	0.013595
50	0.833333		2.49	0.022738		126	0.013595
60	1		2.47	0.037896		125	0.02719
70	1.166667		2.45	0.053054		124	0.040785
80	1.333333		2.43	0.068213		124	0.040785
90	1.5		2.41	0.083371		123	0.05438
100	1.666667		2.39	0.09853		122	0.067976
110	1.833333		2.37	0.113688		122	0.067976
120	2		2.34	0.136426		121	0.081571
130	2.166667		2.31	0.159163		120	0.095166
140	2.333333		2.28	0.181901		119	0.108761
150	2.5		2.25	0.204638		118	0.122356
160	2.666667		2.21	0.234955		116	0.149546
170	2.833333		2.16	0.272851		115	0.163141
180	3		2.11	0.310747		114	0.176736
190	3.166667		2.06	0.348643		112	0.203927
200	3.333333		2.02	0.37896		110	0.231117

Stroke =	50						
Flow			Force			Head Loss	
l/min	l/sec		mV	kg		mmHg	mH2O
0	0		2.53	3.37E-16		128	0
30	0.5		2.52	0.007579		126	0.02719
40	0.666667		2.51	0.015158		126	0.02719
50	0.833333		2.5	0.022738		125	0.040785
60	1		2.49	0.030317		124	0.05438
70	1.166667		2.48	0.037896		124	0.05438
80	1.333333		2.46	0.053054		124	0.05438
90	1.5		2.44	0.068213		123	0.067976
100	1.666667		2.42	0.083371		122	0.081571
110	1.833333		2.4	0.09853		121	0.095166
120	2		2.38	0.113688		121	0.095166
130	2.166667		2.36	0.128846		120	0.108761
140	2.333333		2.34	0.144005		118	0.135951
150	2.5		2.32	0.159163		117	0.149546
160	2.666667		2.3	0.174322		116	0.163141
170	2.833333		2.27	0.197059		115	0.176736
180	3		2.21	0.242534		114	0.190331
190	3.166667		2.17	0.272851		112	0.217522
200	3.333333		2.13	0.303168		111	0.231117

Stroke =	40						
Flow			Force			Head Loss	
l/min	l/sec		mV	kg		mmHg	mH2O
0	0		2.59	0		128	0
30	0.5		2.58	0.007579		127	0.013595
40	0.666667		2.57	0.015158		126	0.02719
50	0.833333		2.57	0.015158		125	0.040785
60	1		2.56	0.022738		124	0.05438
70	1.166667		2.55	0.030317		124	0.05438
80	1.333333		2.54	0.037896		123	0.067976
90	1.5		2.53	0.045475		122	0.081571
100	1.666667		2.51	0.060634		122	0.081571
110	1.833333		2.5	0.068213		121	0.095166
120	2		2.48	0.083371		120	0.108761
130	2.166667		2.46	0.09853		120	0.108761
140	2.333333		2.44	0.113688		119	0.122356
150	2.5		2.42	0.128846		118	0.135951
160	2.666667		2.4	0.144005		117	0.149546
170	2.833333		2.39	0.151584		116	0.163141
180	3		2.37	0.166742		114	0.190331
190	3.166667		2.34	0.18948		112	0.217522
200	3.333333		2.31	0.212218		110	0.244712

Stroke =	30						
Flow			Force			Head Loss	
l/min	l/sec		mV	kg		mmHg	mH2O
0	0		2.52	0		129	0
30	0.5		2.51	0.007579		127	0.02719
40	0.666667		2.51	0.007579		125	0.05438
50	0.833333		2.5	0.015158		125	0.05438
60	1		2.5	0.015158		125	0.05438
70	1.166667		2.49	0.022738		125	0.05438
80	1.333333		2.48	0.030317		123	0.081571
90	1.5		2.47	0.037896		122	0.095166
100	1.666667		2.46	0.045475		122	0.095166
110	1.833333		2.45	0.053054		121	0.108761
120	2		2.43	0.068213		120	0.122356
130	2.166667		2.42	0.075792		118	0.149546
140	2.333333		2.4	0.09095		117	0.163141
150	2.5		2.38	0.106109		116	0.176736
160	2.666667		2.36	0.121267		114	0.203927
170	2.833333		2.33	0.144005		114	0.203927
180	3		2.32	0.151584		112	0.231117
190	3.166667		2.31	0.159163		110	0.258307
200	3.333333		2.28	0.181901		109	0.271902

Stroke =	20						
Flow			Force			Head Loss	
l/min	l/sec		mV	kg		mmHg	mH2O
0	0		2.53	3.37E-16		126	0
30	0.5		2.52	0.007579		126	0
40	0.666667		2.51	0.015158		125	0.013595
50	0.833333		2.5	0.022738		124	0.02719
60	1		2.49	0.030317		124	0.02719
70	1.166667		2.47	0.045475		123	0.040785
80	1.333333		2.45	0.060634		122	0.05438
90	1.5		2.43	0.075792		121	0.067976
100	1.666667		2.41	0.09095		120	0.081571
110	1.833333		2.39	0.106109		119	0.095166
120	2		2.37	0.121267		118	0.108761
130	2.166667		2.34	0.144005		116	0.135951
140	2.333333		2.31	0.166742		115	0.149546
150	2.5		2.27	0.197059		113	0.176736
160	2.666667		2.24	0.219797		111	0.203927
170	2.833333		2.2	0.250114		109	0.231117
180	3		2.16	0.28043		107	0.258307
190	3.166667		2.12	0.310747		105	0.285497
200	3.333333		2.08	0.341064		103	0.312687

Stroke =	15						
Flow			Force			Head Loss	
l/min	l/sec		mV	kg		mmHg	mH2O
0	0		2.51	3.37E-16		126	0
30	0.5		2.5	0.007579		126	0
40	0.666667		2.47	0.030317		125	0.013595
50	0.833333		2.45	0.045475		124	0.02719
60	1		2.42	0.068213		122	0.05438
70	1.166667		2.39	0.09095		121	0.067976
80	1.333333		2.35	0.121267		120	0.081571
90	1.5		2.3	0.159163		118	0.108761
100	1.666667		2.27	0.181901		117	0.122356
110	1.833333		2.21	0.227376		116	0.135951
120	2		2.16	0.265272		114	0.163141
130	2.166667		2.09	0.318327		112	0.190331
140	2.333333		2.03	0.363802		109	0.231117
150	2.5		1.96	0.416856		106	0.271902
160	2.666667		1.89	0.469911		104	0.299092
170	2.833333		1.8	0.538123		102	0.326282
180	3		1.71	0.606336		98	0.380663
190	3.166667		1.62	0.674549		94	0.435043
200	3.333333		1.52	0.750341		90	0.489424

Stroke =	10						
Flow			Force			Head Loss	
l/min	l/sec		mV	kg		mmHg	mH2O
0	0		2.49	0		126	0.095166
30	0.5		2.42	0.053054		124	0.122356
40	0.666667		2.35	0.106109		123	0.135951
50	0.833333		2.26	0.174322		121	0.163141
60	1		2.16	0.250114		118	0.203927
70	1.166667		2.04	0.341064		116	0.231117
80	1.333333		1.91	0.439594		113	0.271902
90	1.5		1.78	0.538123		110	0.312687
100	1.666667		1.61	0.66697		106	0.367068
110	1.833333		1.42	0.810975		102	0.421448
120	2		1.22	0.962559		97	0.489424
130	2.166667		0.99	1.13688		92	0.557399
140	2.333333		0.72	1.341519		86	0.63897
150	2.5		0.48	1.52342		79	0.734135
160	2.666667		0.2	1.735637		73	0.815706
170	2.833333		-0.02	1.90238		64	0.938062
180	3		-0.33	2.137335		56	1.046823
190	3.166667		-0.66	2.387449		50	1.128393
200	3.333333		-0.98	2.629983		42	1.237154

Appendix H

This appendix gives engineering drawings for the hydraulic ram pumps of the University of Warwick's Development Technology Unit. These designs were developed over a number of years by a team of engineers including the author. The drawings here were produced byTim Jeffery of the D.T.U., and the designs are currently being manufactured in a number of African countries. The design charts and computer tools developed relate specifically to these designs although are applicable to others. (see chapter 7)

DTU M8 2"
STEEL RAM PUMP

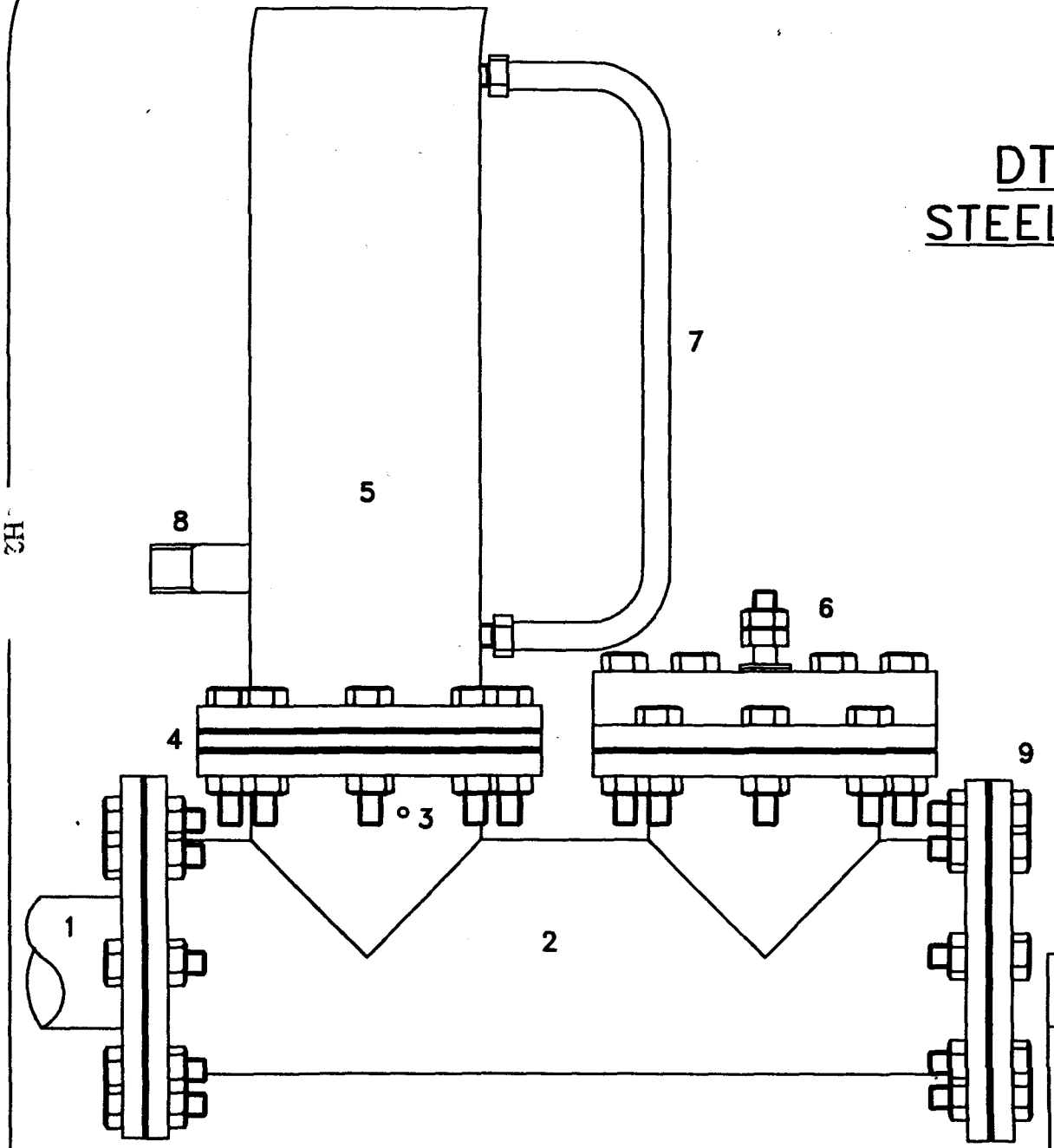

PARTS LIST

1 DRIVE PIPE
2 PUMP BODY
3 SNIFTER VALVE
4 DELIVERY VALVE
5 AIR VESSEL
6 IMPULSE VALVE ASSEMBLY
7 AIR SIGHT TUBE
8 DELIVERY PIPE
9 END PLATE

DEVELOPMENT TECHNOLOGY UNIT
UNIVERSITY OF WARWICK, COVENTRY, UK

M8

ASSEMBLY DRAWING

DTU M6 2"
STEEL RAM PUMP

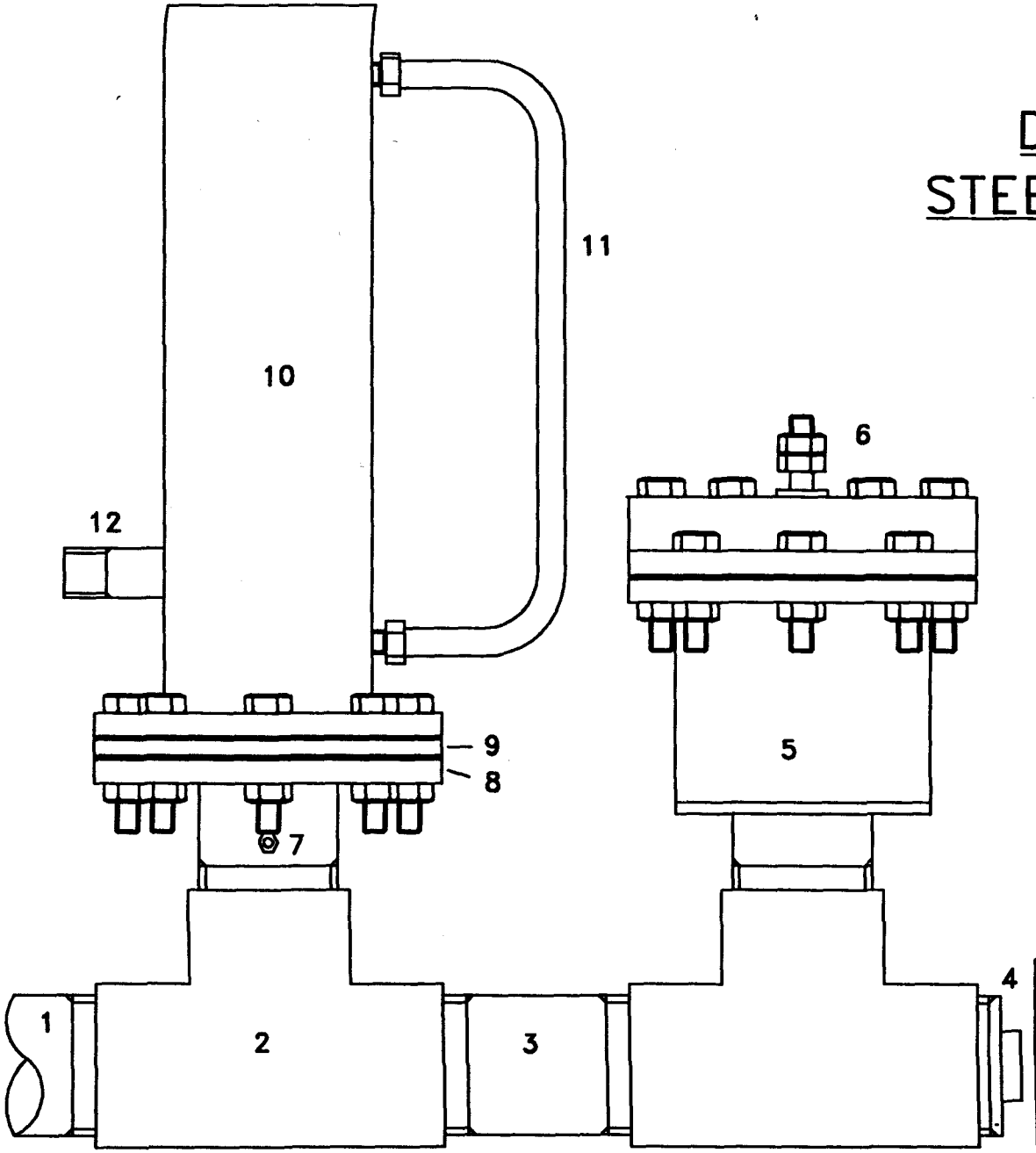

PARTS LIST

1 DRIVE PIPE
2 2" GALV. TEE
3 2" GALV NIPPLE
4 2" GALV PLUG
5 IMPULSE VALVE BODY
6 IMPULSE VALVE ASSEMBLY
7 SNIFTER VALVE
8 SNIFTER HOUSING
9 DELIVERY VALVE
10 AIR VESSEL
11 AIR SIGHT TUBE
12 DELIVERY PIPE

DEVELOPMENT TECHNOLOGY UNIT
UNIVERSITY OF WARWICK, COVENTRY, UK

M6

ASSEMBLY DRAWING

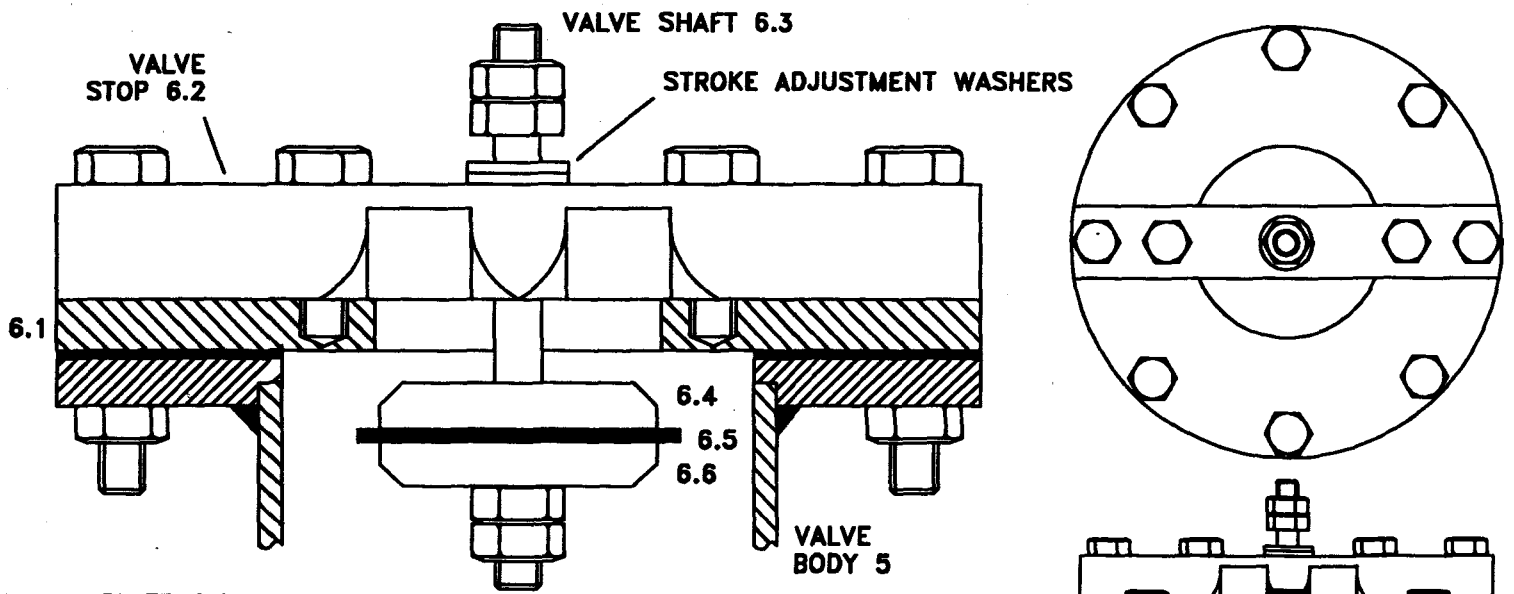

VALVE PLATE 6.1
VALVE PLUG 6.4
VALVE RUBBER 6.5
ADDITIONAL WEIGHT 6.6

BOLTS: 2off M10x60
2off M10x30
6off M10x35/40

NOTES

1 VALVE RUBBER (6.5) TO BE MIN 6mm THICK AND ⌀76mm
2 VALVE WEIGHTS (6.6) CAN BE ADDED TO ALTER PERFORMANCE USE STEEL DISCS OF IDENTIACL DIA TO VALVE PLUG (6.4)
3 ALL PARTS PAINTED OR GALVANISED AND THREADS PROTECTED WITH A HEAVY WATERPROOF GREASE
4 GALVANISED OR STAINLESS STEEL NUTS AND BOLTS SHOULD BE USED IF AVAILABLE

DEVELOPMENT TECHNOLOGY UNIT
UNIVERSITY OF WARWICK, COVENTRY, UK

M6 & M8 IMPULSE VALVE ASSEMBLY DRAWING

IV64ASS

H4

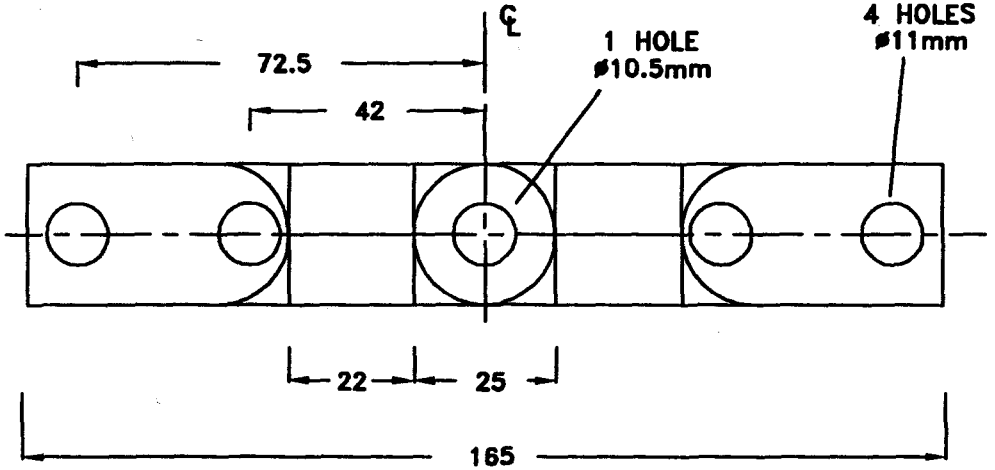

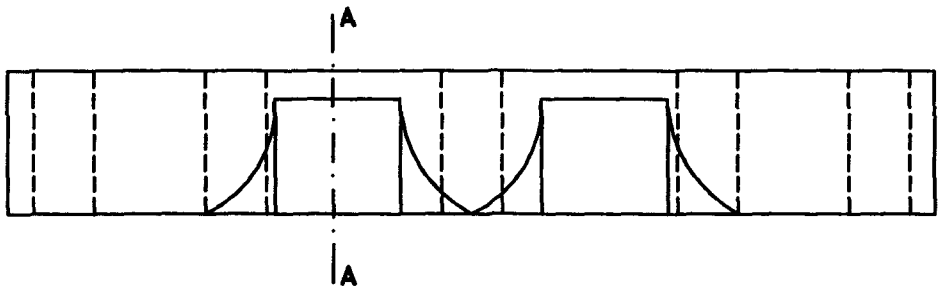

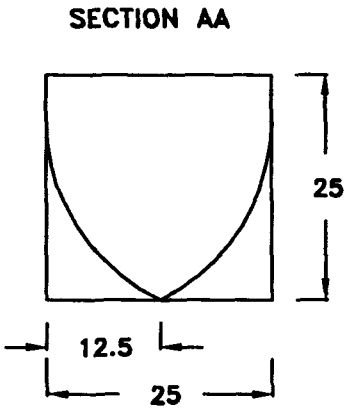

NOTE: 1. STREAMLINING SECTIONS TO BE MANUFACTURED BY FILING
2. MATERIAL: MILD STEEL (OR STAINLESS IF AVAILABLE)

NOT TO SCALE

DEVELOPMENT TECHNOLOGY UNIT
UNIVERSITY OF WARWICK, COVENTRY, UK

M6 & M8

IMPULSE VALVE STOP

IV64P1

H5

VALVE PLUG

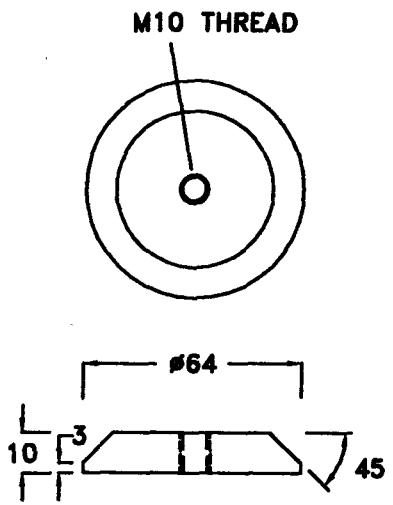

VALVE PLATE

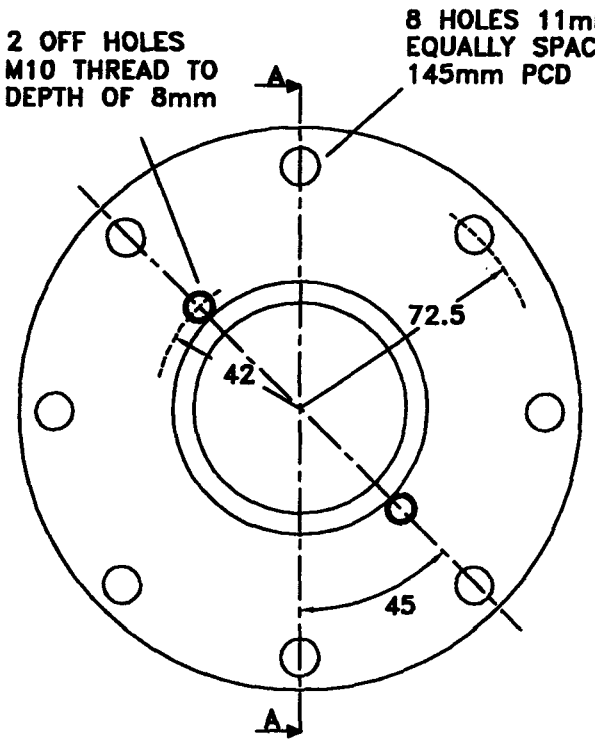

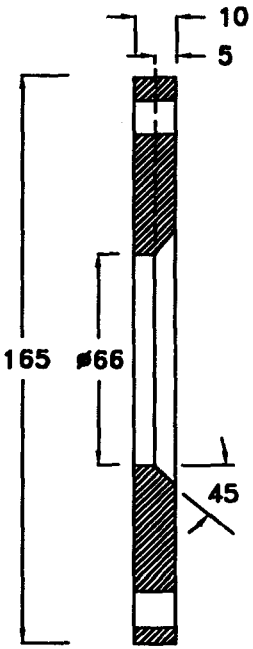

SECTION AA

VALVE STEM

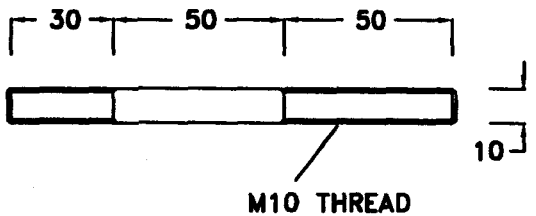

NOT TO SCALE

DEVELOPMENT TECHNOLOGY UNIT
UNIVERSITY OF WARWICK, COVENTRY, UK

M6 & M8

IMPULSE VALVE PARTS

IV64P

9H

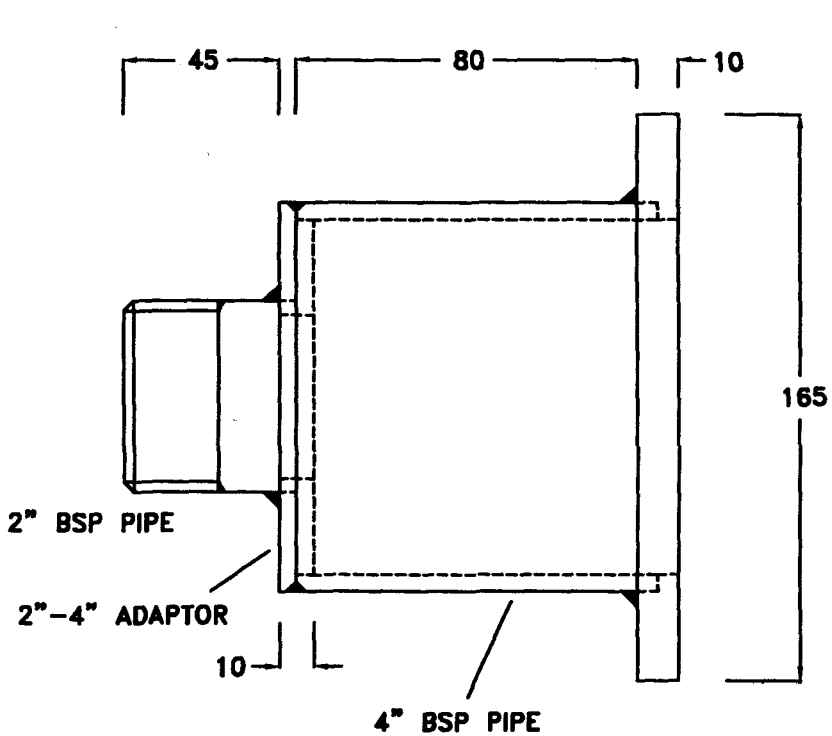

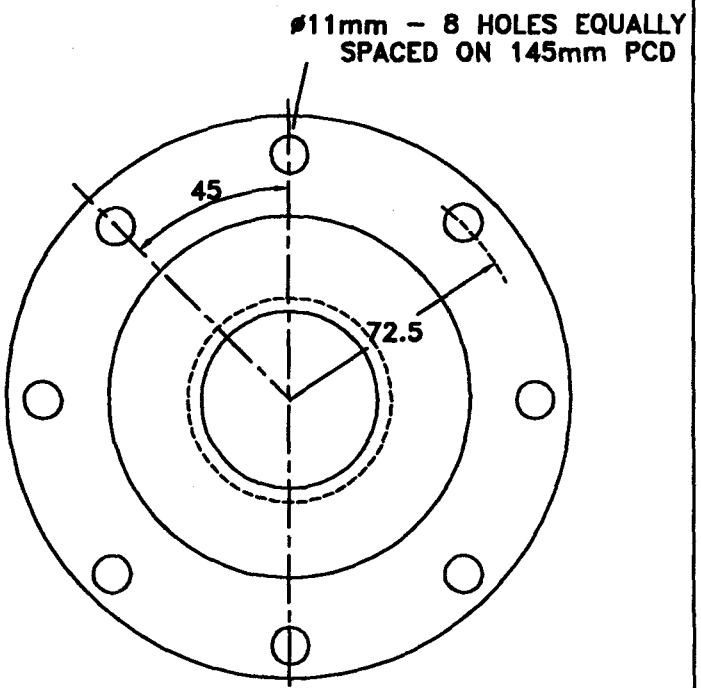

NOT TO SCALE

NOTE: 1. ALL PARTS MILD STEEL
2. ALL JOINTS WELDED
3. ADAPTOR AND FLANGE CONNECTED TO PIPE USING TOP HAT SECTION
4. ALL TO BE PAINTED – 2 COATS MIN. OR GALVANIZED

DEVELOPMENT TECHNOLOGY UNIT
UNIVERSITY OF WARWICK, COVENTRY, UK

M6 IMPULSE VALVE BODY

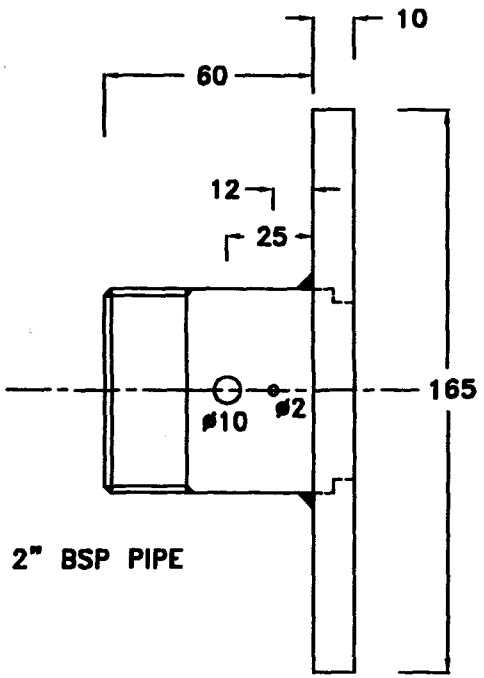

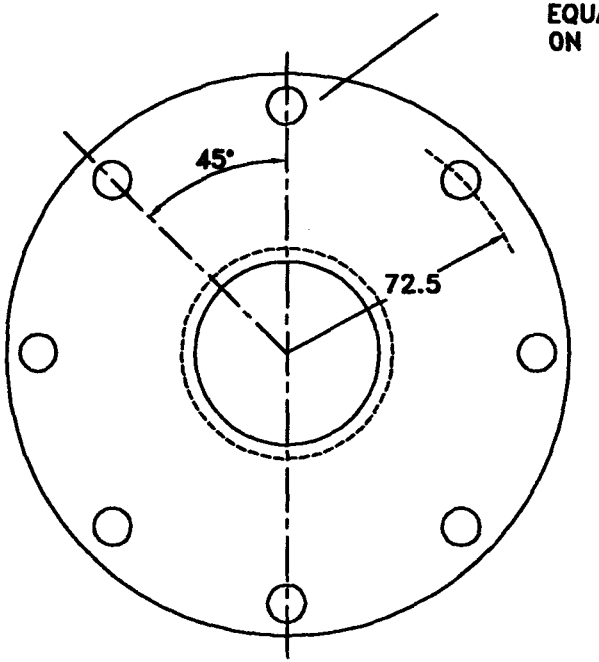

NOTE: 1. ALL PARTS MILD STEEL
2. ALL JOINTS WELDED

DEVELOPMENT TECHNOLOGY UNIT
UNIVERSITY OF WARWICK, COVENTRY, UK

M6

DELIVERY VALVE ADAPTOR

DVB64

H8

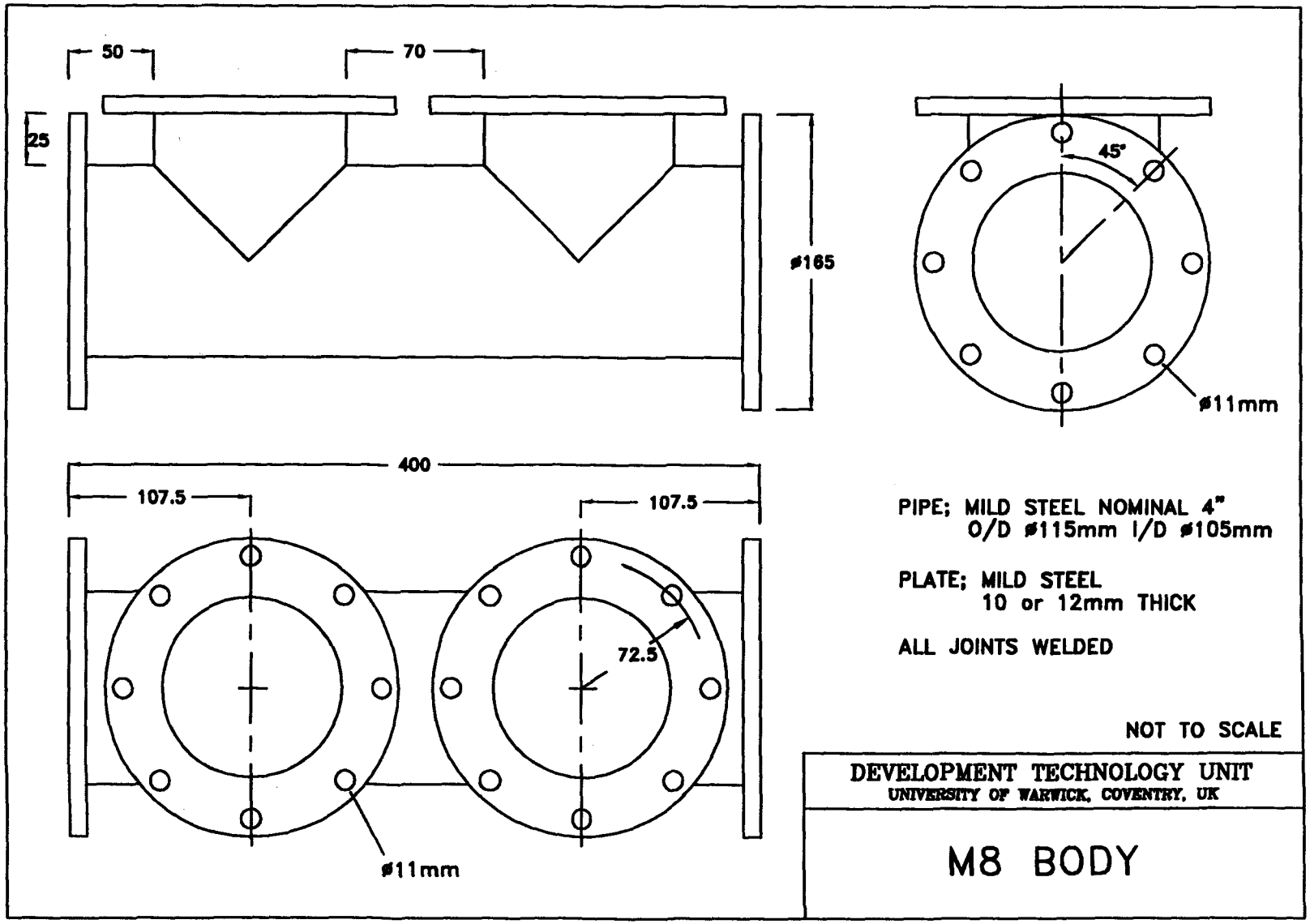
50
70
25
ø165
45°
ø11mm
400
107.5
107.5
72.5
ø11mm
PIPE; MILD STEEL NOMINAL 4"
O/D ø115mm I/D ø105mm
PLATE; MILD STEEL
10 or 12mm THICK
ALL JOINTS WELDED
NOT TO SCALE
DEVELOPMENT TECHNOLOGY UNIT
UNIVERSITY OF WARWICK, COVENTRY, UK
M8 BODY

M84BODY

6H

FLAP TYPE

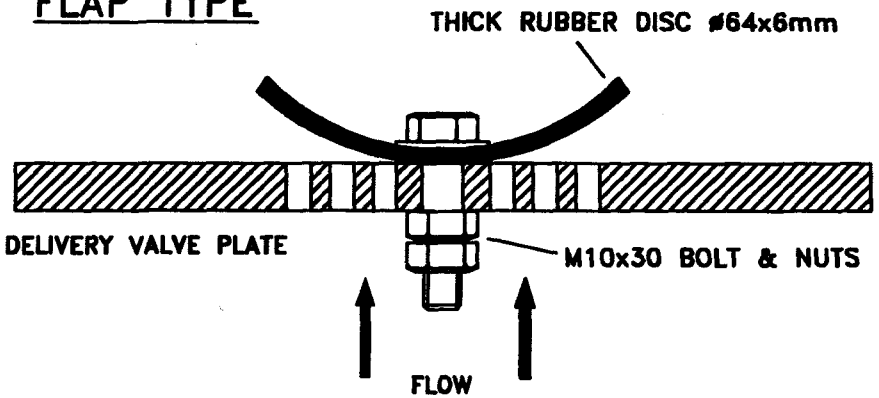

FLAP TYPE SNIFTER

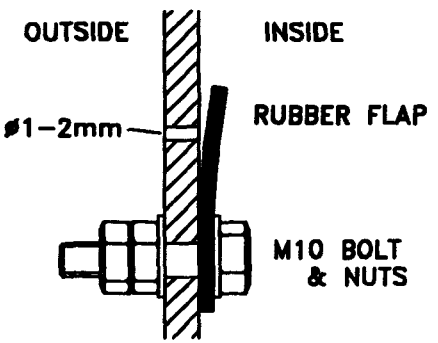

POPPET TYPE

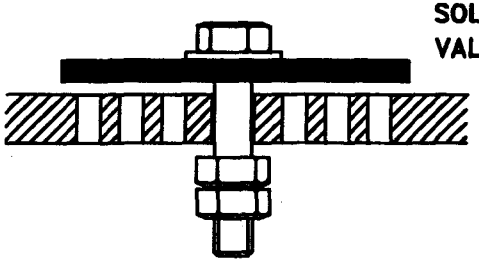

SOLID RUBBER DISC ø64mm
VALVE STROKE = 3mm

DEVELOPMENT TECHNOLOGY UNIT
UNIVERSITY OF WARWICK, COVENTRY, UK

M6 & M8

DELIVERY & SNIFTER VALVE ASSEMBLIES

DV64ASS

H10

8 HOLES ⌀11mm
EQUISPACED ON 145mm PCD

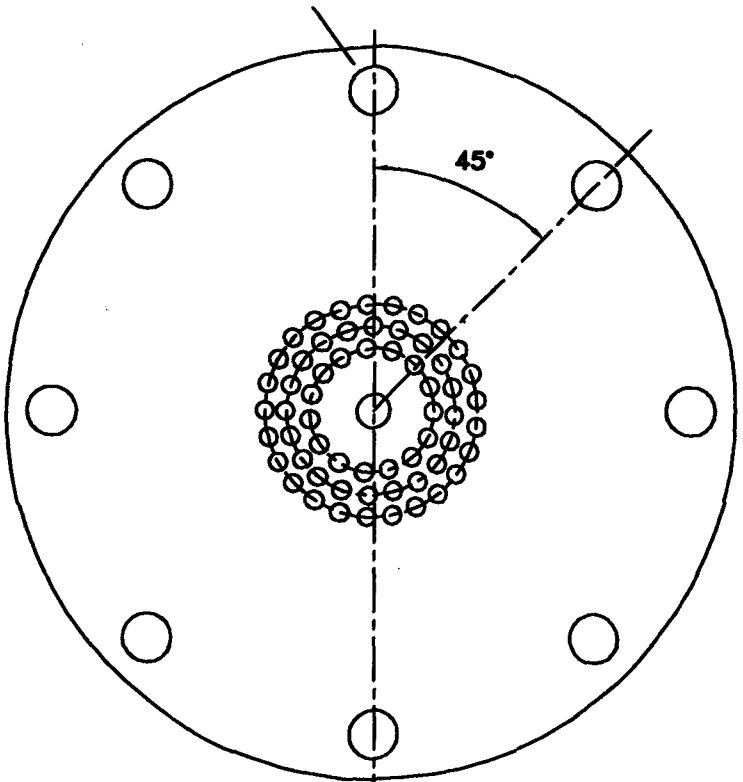

CENTRE HOLE ⌀10mm
OTHER HOLES ⌀4mm EQUISPACED ON
PCR's OF 14, 19 & 24mm
ALL HOLES DEBURRED AND CHAMPHERED
ON ONE SIDE ONLY UNTIL HOLES CONNECT
MIN DISTANCE BETWEEN HOLES 1.5mm

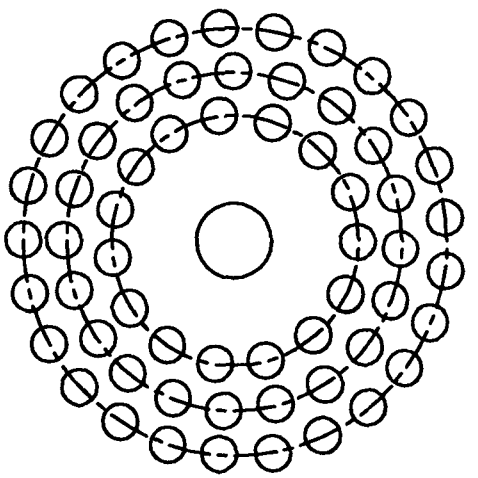

NOT TO SCALE

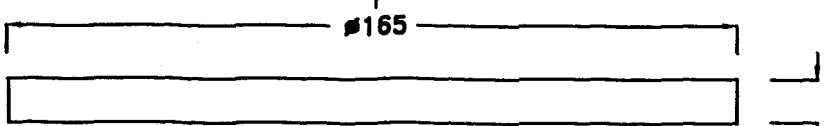

THROUGH HOLES NOT SHOWN

DEVELOPMENT TECHNOLOGY UNIT
UNIVERSITY OF WARWICK, COVENTRY, UK

M6 & M8

DELIVERY VALVE PLATE

H11

DV64

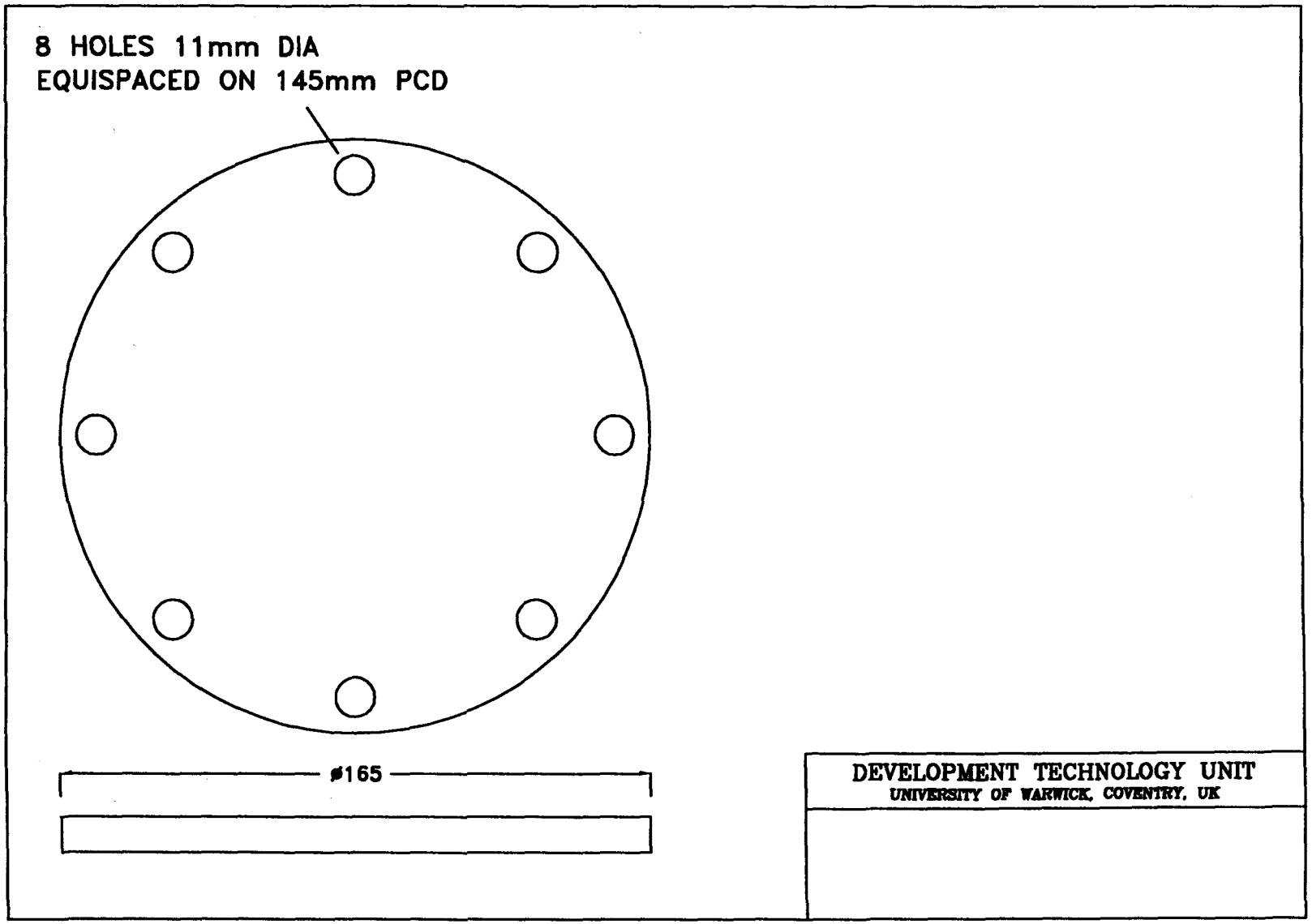
8 HOLES 11mm DIA
EQUISPACED ON 145mm PCD
ø165
DEVELOPMENT TECHNOLOGY UNIT
UNIVERSITY OF WARWICK, COVENTRY, UK

H12

DV64

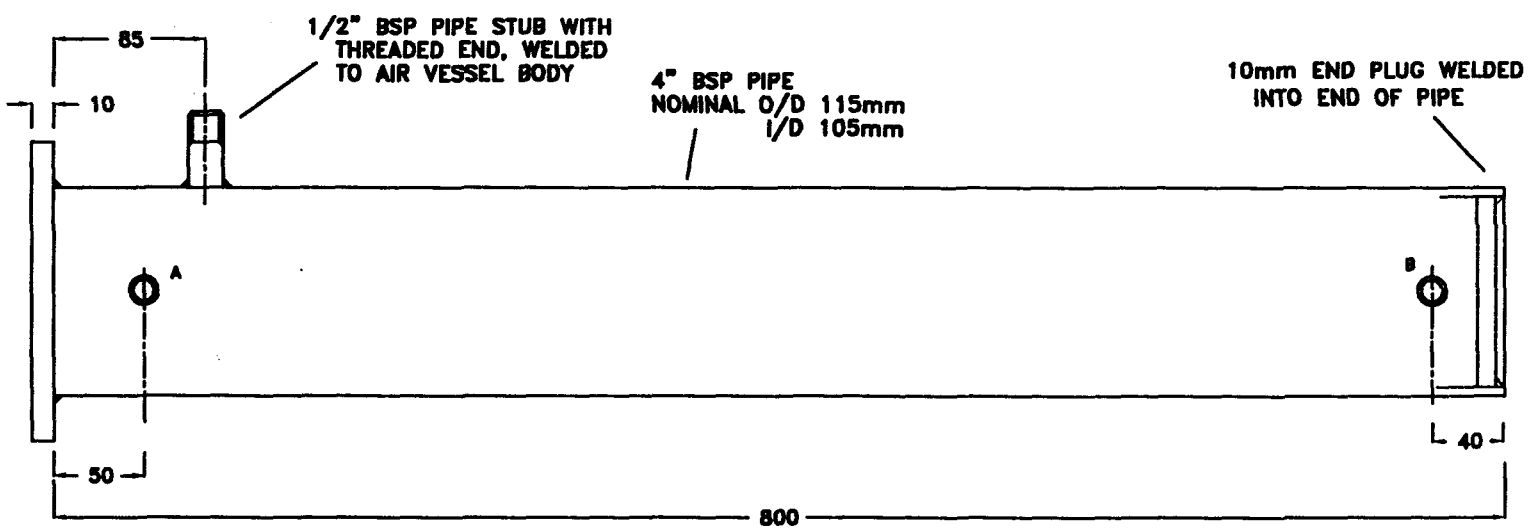

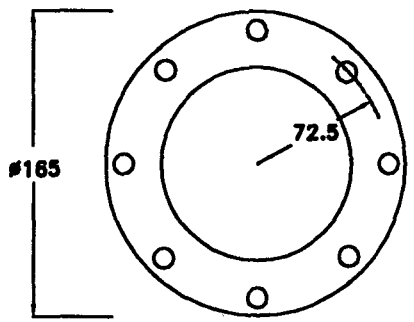

FLANGE DETAIL: WELDED TO AIR VESSEL AS SHOWN
8 OFF 11mm DIA HOLES EQUALLY SPACED ON 145mm PCD

NOTE; ALL PARTS TO BE PAINTED WITH UNDERCOAT AND TOPCOAT INSIDE AND OUT AFTER WELDING

ITEMS MARKED A & B ARE POSITIONS OF CONNECTIONS FOR SIGHT TUBE. IF INCLUDED THESE SHOULD BE MADE TO SUIT TUBE AND FITTINGS AVAILABLE

NOT TO SCALE

DEVELOPMENT TECHNOLOGY UNIT
UNIVERSITY OF WARWICK, COVENTRY, UK

M6 & M8

AIR VESSEL

AV64

Appendix I. Design Charts.

The production of design charts for the hydraulic ram pump is seen as one of the most significant products of the research described in this thesis. The wider deployment of hydraulic ram pumps has been greatly restricted by the lack of useful design data. As is described in the main thesis, the operation of the hydraulic ram pump is often highly variable, for this reason, for accurate prediction of pump performance it is necessary to use a computer model as described in chapter 5. However, the design charts given overleaf give a guideline for a typical range of hydraulic ram installations. These are similar in this respect to the centrifugal pump tombstone charts provided by many manufacturers.

The first range of charts give an indication of the likely performance of a given pump type over a range of possible duties. These charts can be used to select the optimum drive head, or number of units for a given required duty. As hydraulic ram pump installations are potentially quite expensive, charts of this type will avoid poor system selection.

The charts folowing this are charts obtained directly from the computer model output. These give the full characteristic of the D.T.U. hydraulic ram pumps for a range of likely configurations. The charts can be used to directly determine tuning of the devices, and predict conditions under which operation may be unreliable. The charts give in tabular form the perfomance of the units with maximum stroke, and then graphically represent their performance over the full range of adjustment. The charts assume a standard weighted valve, and a typical drive pipe length of three times the drive head. Using the computer model, it is possible to produce charts of this type for peculiar configurations, and varying drive pipe diameters, and hydraulic ram pump types.

Flow Chart for D.T.U. Mk6.4 Hydraulic Ram with 3m Drive Head and 10m Drive Pipe

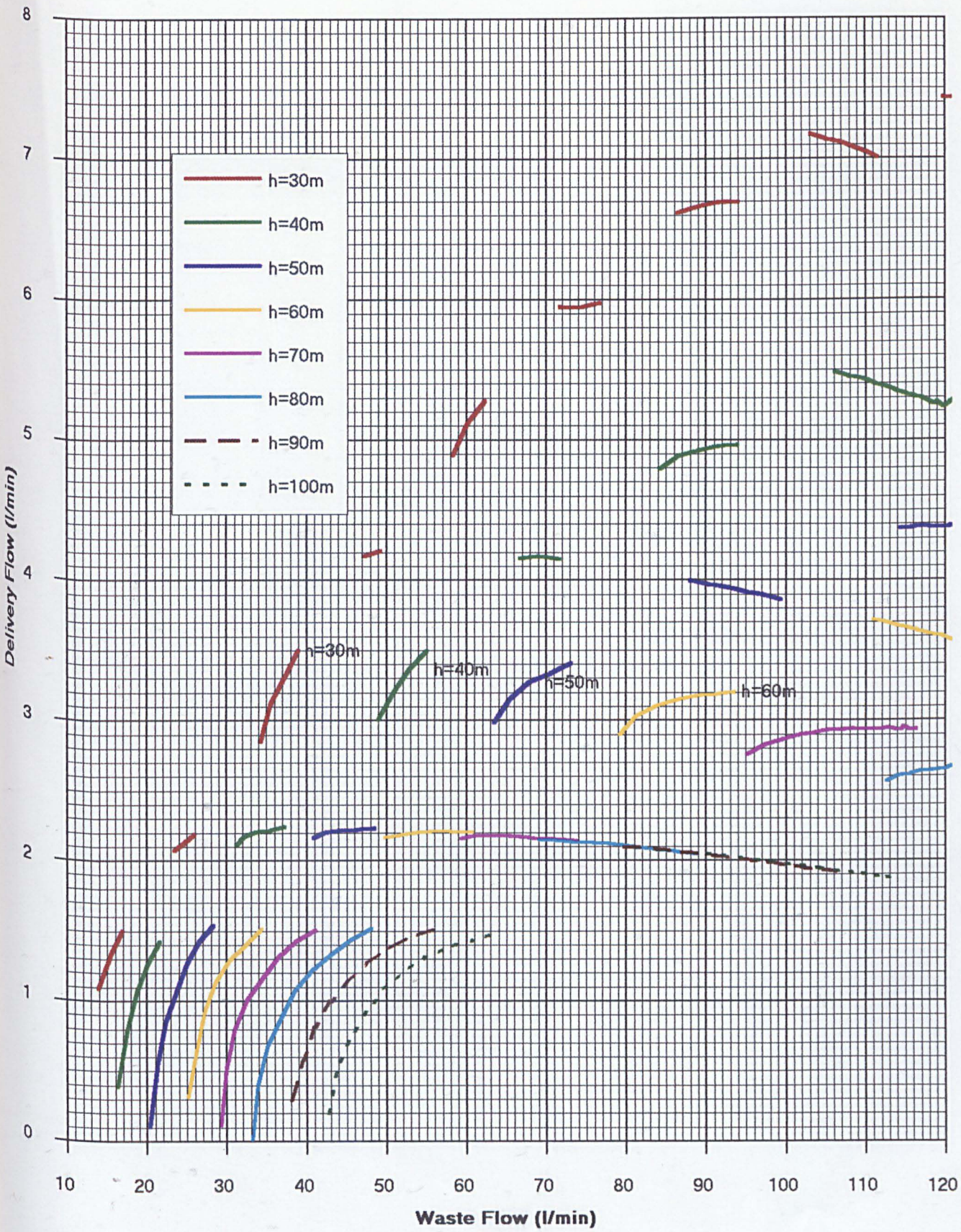

Flow Chart for D.T.U.Mk 6.4 Hydraulic Ram with 5m Drive Head and 15m Drive Pipe

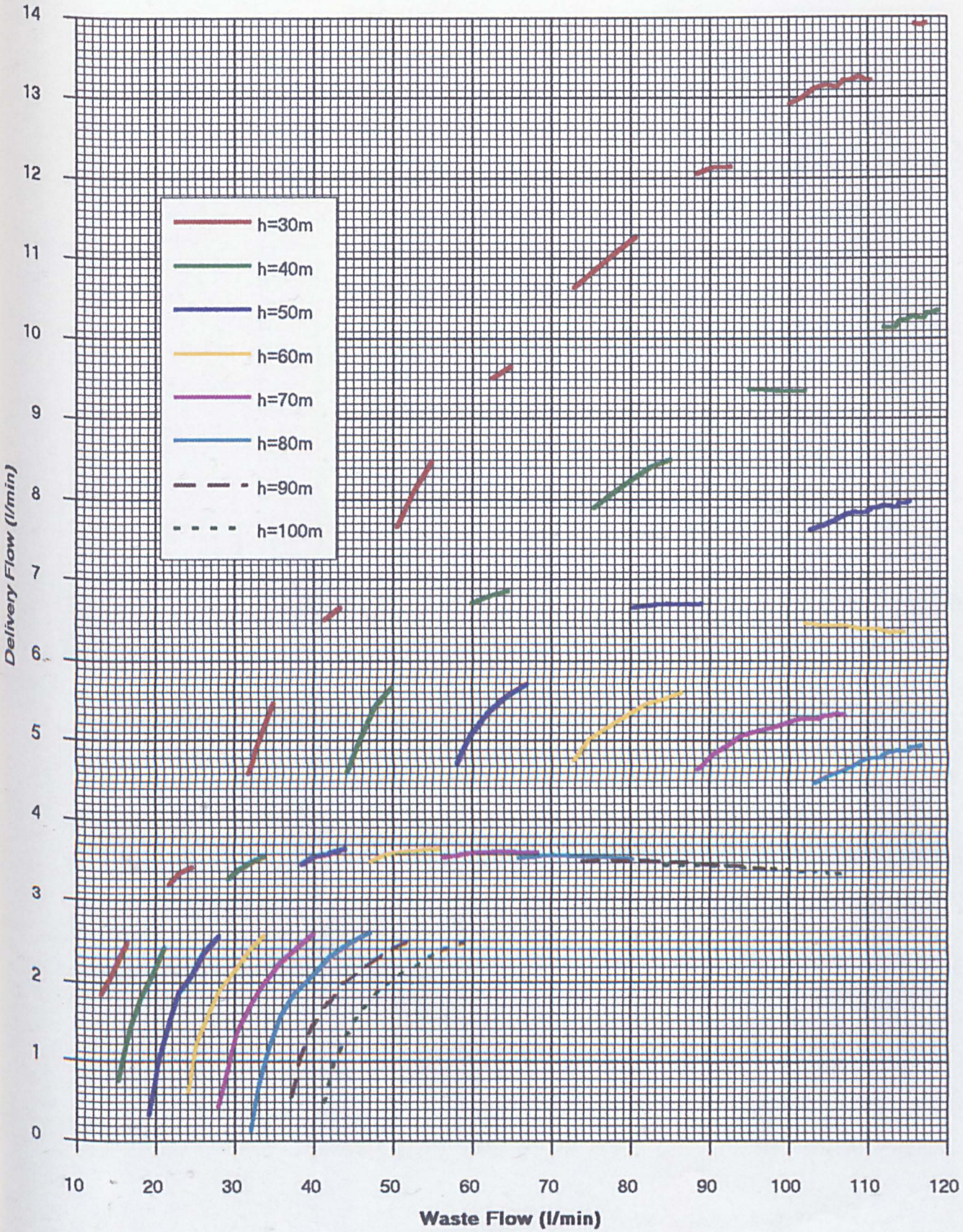

Flow Chart for D.T.U. Mk6.4 Hydraulic Ram with 8m Drive Head and 24m Drive Pipe

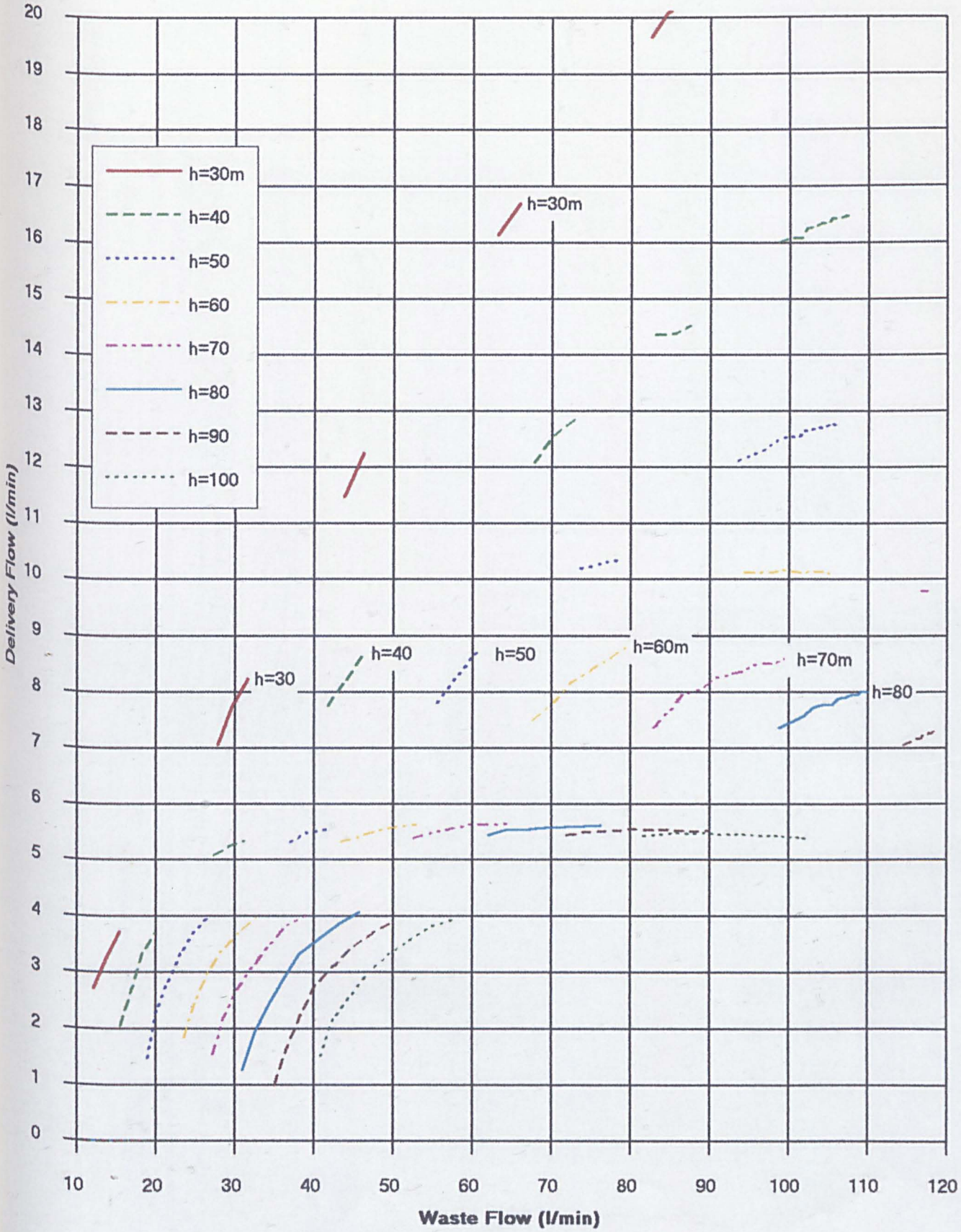

Hydraulic Ram Pump Performance Model

INPUT

SITE		DRIVE PIPE		VALVE	
Drive Head (m)	3	Diameter (mm)	50	Stroke (mm)	23.5
Delivery Head(m)	50	Pipe Length(m)	10	Kf	0.041881891
		relrogh(k) (mm)	0.15	Ki	0.038184397
		Wavespeed m/s	1350	Kd	0.328
		CL Fittings	2.0625	Valve Mass kg	0.507

Delivery Valve Swept Volume l	0.008
VALVE WILL CLOSE with this setting	
Closure Waste Vol (l)	0.746
Critical Velocity (m/s)	1.78
Cutt off Velocity (m/s)	2.04
closuretime (s)	0.200

OUTPUT

Power watts	35.84	Delivery l/m	4.39	Delivery' l/m	3.223206199
Freq b/m	54.83	Waste l/m	124.79		
Efficiency	56.58		133.52		

Delivery' accounts for a partial realisation of recoil, and delivery valve swept volume losses

Pump Performance Range

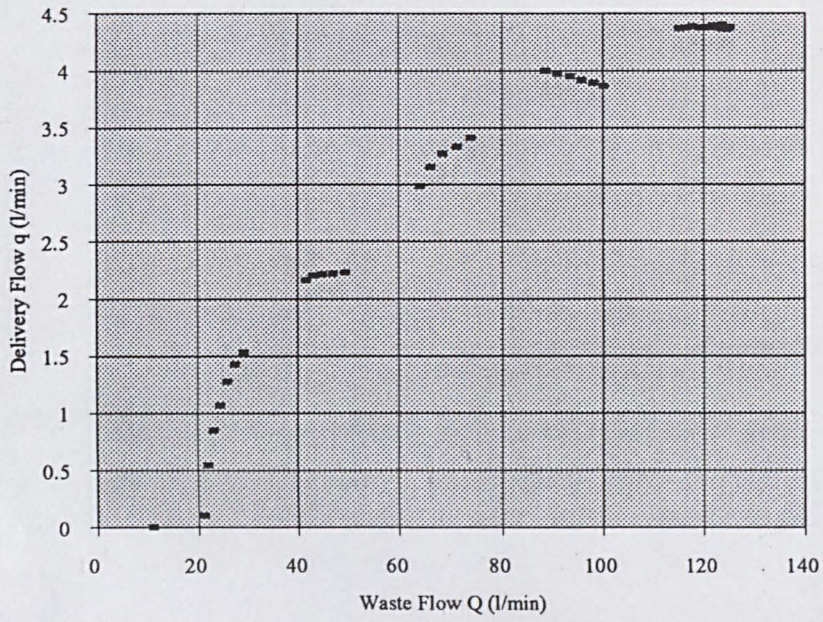

Performance Chart for Hydraulic Ram Pump

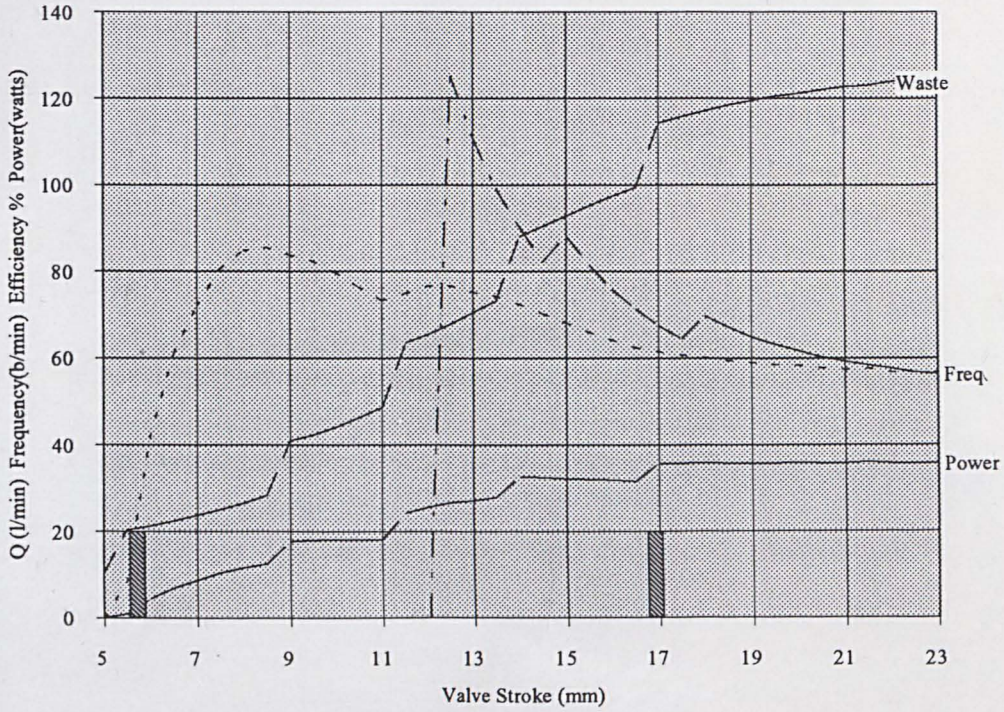

The shaded bars indicate strokes at which the impulse valve may not reopen.

Hydraulic Ram Pump Performance Model

INPUT

SITE		DRIVE PIPE		VALVE		Delivery Valve Swept Volume l	0.008
Drive Head (m)	3	Diameter (mm)	50	Stroke (mm)	23.5	VALVE WILL CLOSE with this setting	
Delivery Head(m)	60	Pipe Length(m)	10	Kf	0.041881891	Closure Waste Vol (l)	0.746
		relrogh(k) (mm)	0.15	Ki	0.038184397	Critical Velocity (m/s)	1.78
		Wavespeed m/s	1350	Kd	0.328	Cutt off Velocity (m/s)	2.04
		CL Fittings	2.0625	Valve Mass kg	0.507	closuretime (s)	0.200

OUTPUT

Power watts	34.81	Delivery l/m	3.55	Delivery' l/m	2.834753976
Freq b/m	54.08	Waste l/m	123.10		
Efficiency	56.06		133.52		

Delivery' accounts for a partial realisation of recoil, and delivery valve swept volume losses

Pump Performance Range

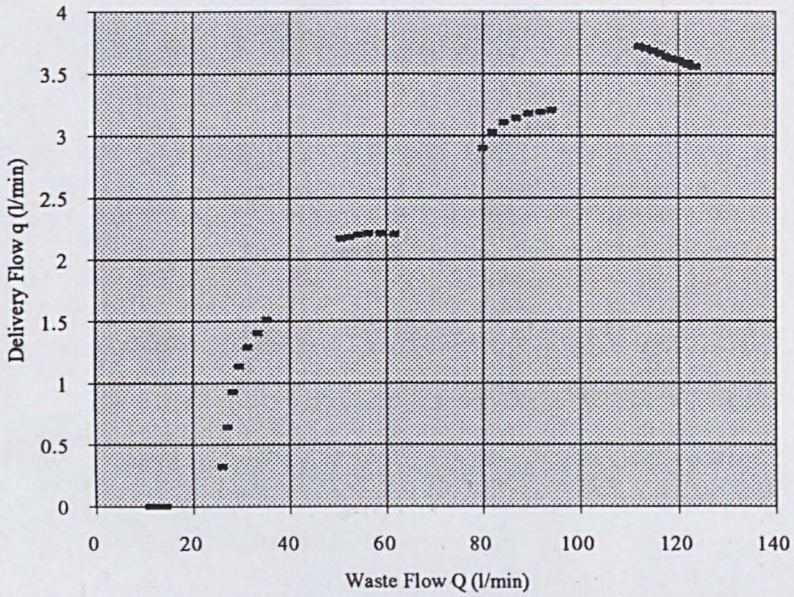

Performance Chart for Hydraulic Ram Pump

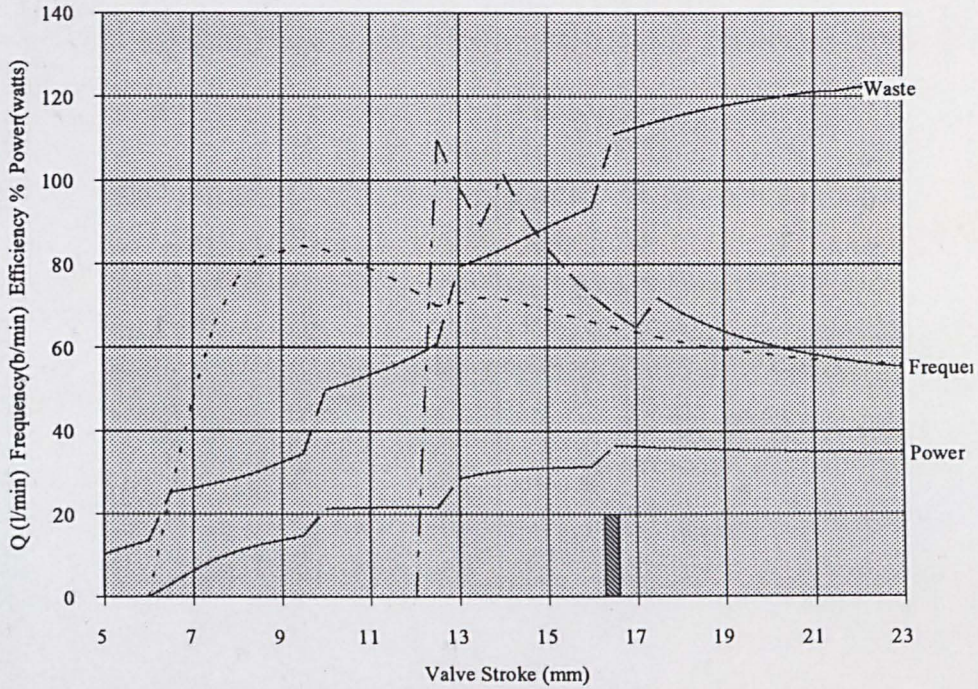

The shaded bars indicate strokes at which the impulse valve may not reopen.

Hydraulic Ram Pump Performance Model

INPUT

SITE		DRIVE PIPE		VALVE		Delivery Valve Swept Volume l	0.008
Drive Head (m)	3	Diameter (mm)	50	Stroke (mm)	23.5	VALVE WILL CLOSE with this setting	
Delivery Head(m)	70	Pipe Length(m)	10	Kf	0.041881891	Closure Waste Vol (l)	0.746
		relrogh(k) (mm)	0.15	Ki	0.038184397	Critical Velocity (m/s)	1.78
		Wavespeed m/s	1350	Kd	0.328	Cutt off Velocity (m/s)	2.04
		CL Fittings	2.0625	Valve Mass kg	0.507	closuretime (s)	0.200

OUTPUT

Power watts	33.66	Delivery l/m	2.94	Delivery' l/m	2.359051672
Freq b/m	51.27	Waste l/m	116.69		
Efficiency	57.39		135.49		

Delivery' accounts for a partial realisation of recoil, and delivery valve swept volume losses

Pump Performance Range

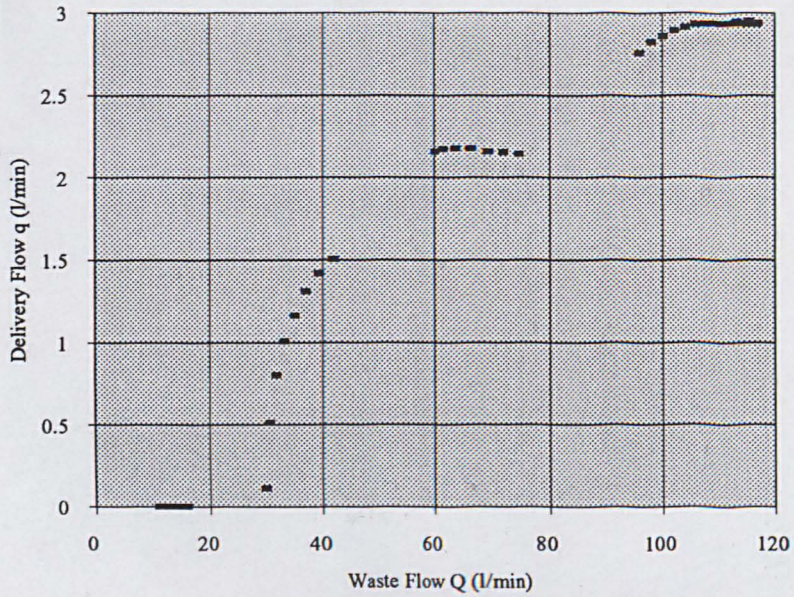

Performance Chart for Hydraulic Ram Pump

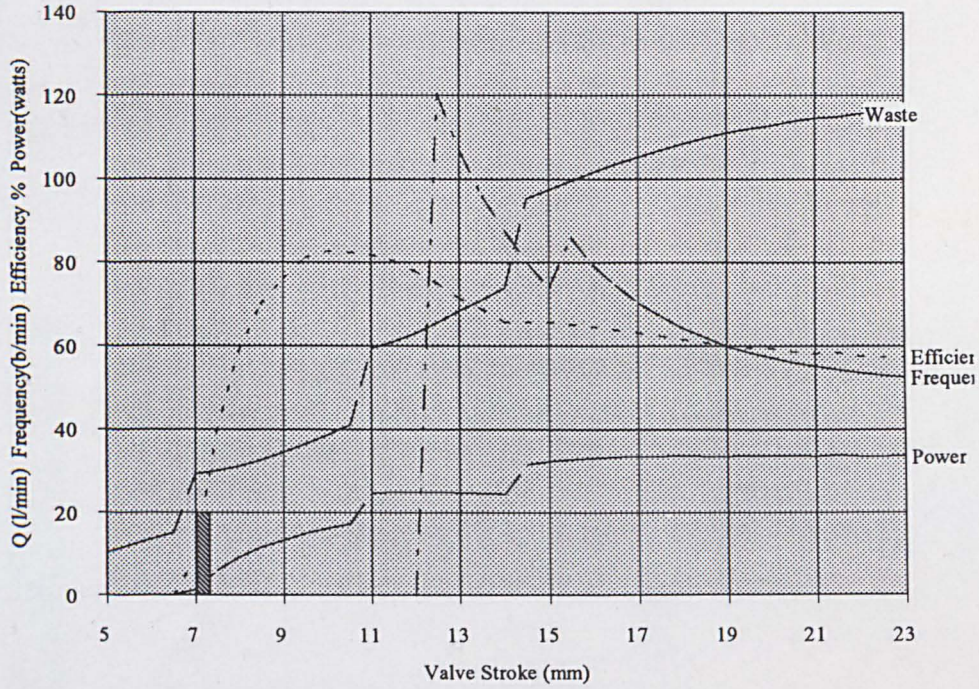

The shaded bars indicate strokes at which the impulse valve may not reopen.

Hydraulic Ram Pump Performance Model

INPUT

SITE		DRIVE PIPE		VALVE		Delivery Valve Swept Volume l	0.008
Drive Head (m)	3	Diameter (mm)	50	Stroke (mm)	23.5	VALVE WILL CLOSE with this setting	
Delivery Head(m)	80	Pipe Length(m)	10	Kf	0.041881891	Closure Waste Vol (l)	0.746
		relrogh(k) (mm)	0.15	Ki	0.038184397	Critical Velocity (m/s)	1.78
		Wavespeed m/s	1350	Kd	0.328	Cutt off Velocity (m/s)	2.04
		CL Fittings	2.0625	Valve Mass kg	0.507	closuretime (s)	0.200

OUTPUT

Power watts	35.11	Delivery l/m	2.69	Delivery' l/m	1.930576639
Freq b/m	54.65	Waste l/m	124.39		
Efficiency	56.35		135.49		

Delivery' accounts for a partial realisation of recoil, and delivery valve swept volume losses

Pump Performance Range

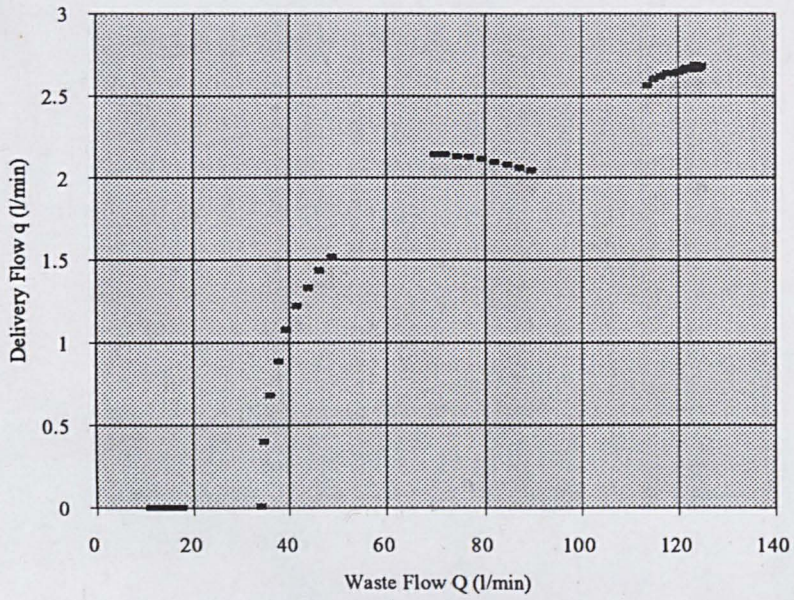

Performance Chart for Hydraulic Ram Pump

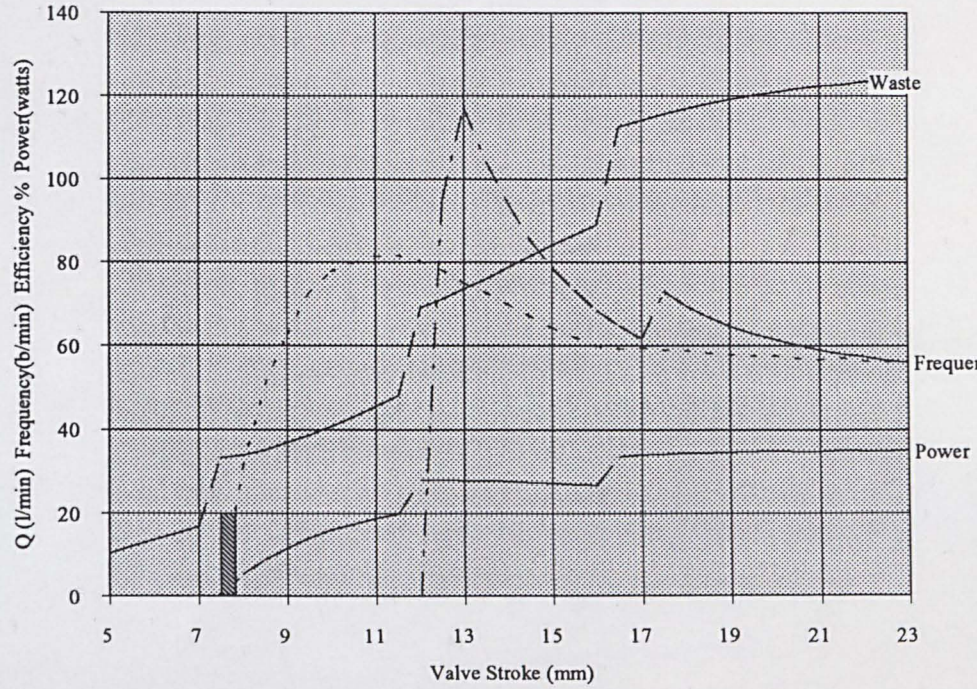

The shaded bars indicate strokes at which the impulse valve may not reopen.

Hydraulic Ram Pump Performance Model

INPUT

SITE		DRIVE PIPE		VALVE		Delivery Valve Swept Volume l	0.008
Drive Head (m)	3	Diameter (mm)	50	Stroke (mm)	23.5	VALVE WILL CLOSE with this setting	
Delivery Head(m)	90	Pipe Length(m)	10	Kf	0.041881891	Closure Waste Vol (l)	0.746
		relrogh(k) (mm)	0.15	Ki	0.038184397	Critical Velocity (m/s)	1.78
		Wavespeed m/s	1350	Kd	0.328	Cutt off Velocity (m/s)	2.04
		CL Fittings	2.0625	Valve Mass kg	0.507	closuretime (s)	0.200

OUTPUT

Power watts	35.17	Delivery l/m	2.39	Delivery' l/m	1.475413811
Freq b/m	58.52	Waste l/m	133.19		
Efficiency	52.91		135.49		

Delivery' accounts for a partial realisation of recoil, and delivery valve swept volume losses

Pump Performance Range

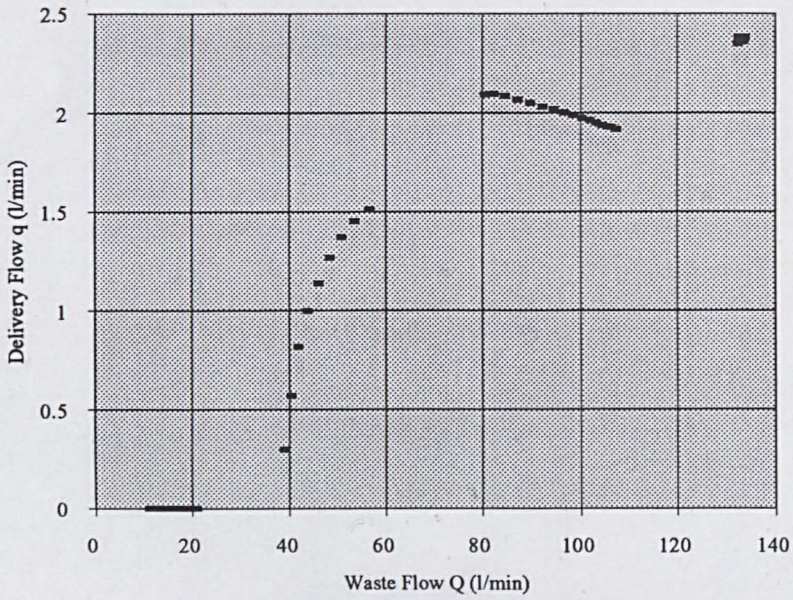

Performance Chart for Hydraulic Ram Pump

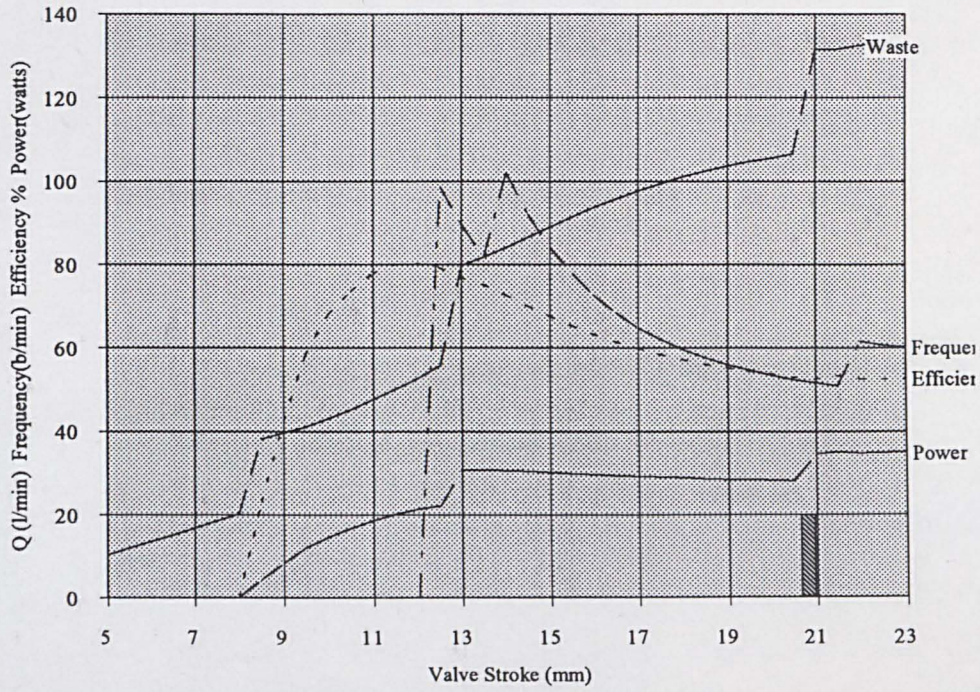

The shaded bars indicate strokes at which the impulse valve may not reopen.

Hydraulic Ram Pump Performance Model

INPUT

SITE		DRIVE PIPE		VALVE		Delivery Valve Swept Volume l	0.008
Drive Head (m)	5	Diameter (mm)	50	Stroke (mm)	23.5	VALVE WILL CLOSE with this setting	
Delivery Head(m)	40	Pipe Length(m)	15	Kf	0.041881891	Closure Waste Vol (l)	0.685
		relrogh(k) (mm)	0.15	Ki	0.038184397	Critical Velocity (m/s)	1.78
		Wavespeed m/s	1350	Kd	0.328	Cutt off Velocity (m/s)	2.12
		CL Fittings	2.0625	Valve Mass kg	0.507	closuretime (s)	0.180

OUTPUT

Power watts	67.28	Delivery l/m	10.29	Delivery' l/m	8.537819524	Delivery' accounts for a partial realisation of recoil, and delivery valve swept volume losses
Freq b/m	62.52	Waste l/m	119.40			
Efficiency	63.48		125.15			

Pump Performance Range

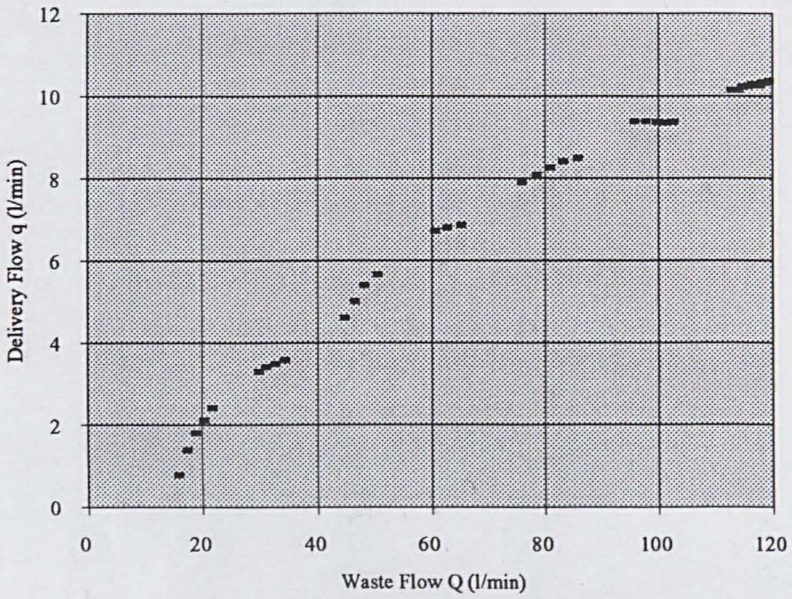

Performance Chart for Hydraulic Ram Pump

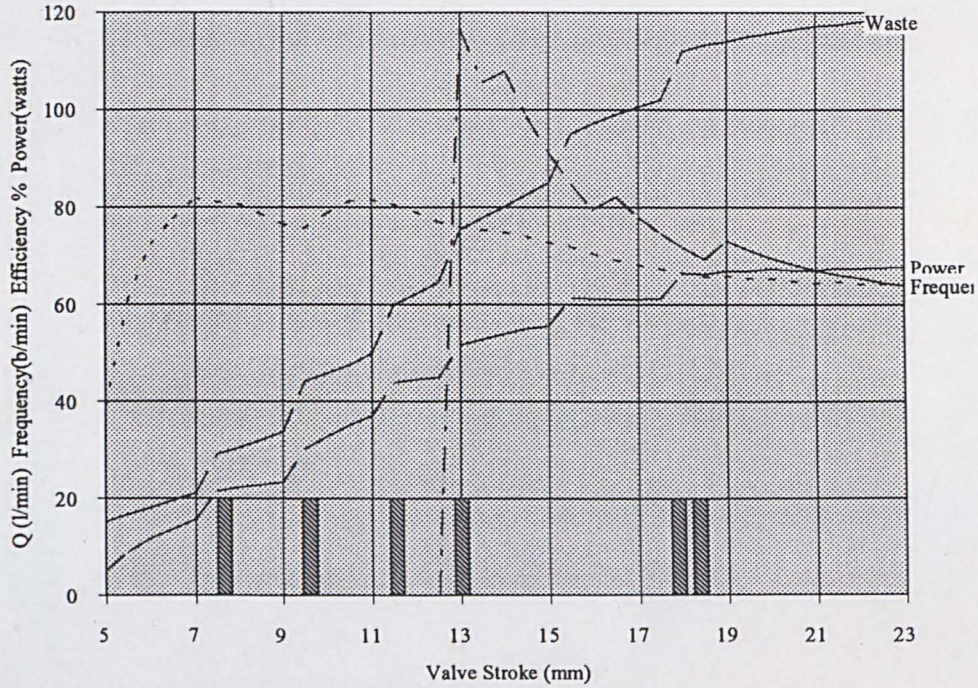

The shaded bars indicate strokes at which the impulse valve may not reopen.

Hydraulic Ram Pump Performance Model

INPUT

SITE		*DRIVE PIPE*		*VALVE*	
Drive Head (m)	5	Diameter (mm)	50	Stroke (mm)	23.5
Delivery Head(m)	50	Pipe Length(m)	15	Kf	0.041881891
		relrogh(k) (mm)	0.15	Ki	0.038184397
		Wavespeed m/s	1350	Kd	0.328
		CL Fittings	2.0625	Valve Mass kg	0.507

Delivery Valve Swept Volume l 0.008

VALVE WILL CLOSE with this setting

Closure Waste Vol (l)	0.685
Critical Velocity (m/s)	1.78
Cutt off Velocity (m/s)	2.12
closuretime (s)	0.180

OUTPUT

Power watts	64.83	Delivery l/m	7.93	Delivery' l/m	6.899789081
Freq b/m	60.69	Waste l/m	115.91		
Efficiency	64.06		128.26		

Delivery' accounts for a partial realisation of recoil, and delivery valve swept volume losses

Pump Performance Range

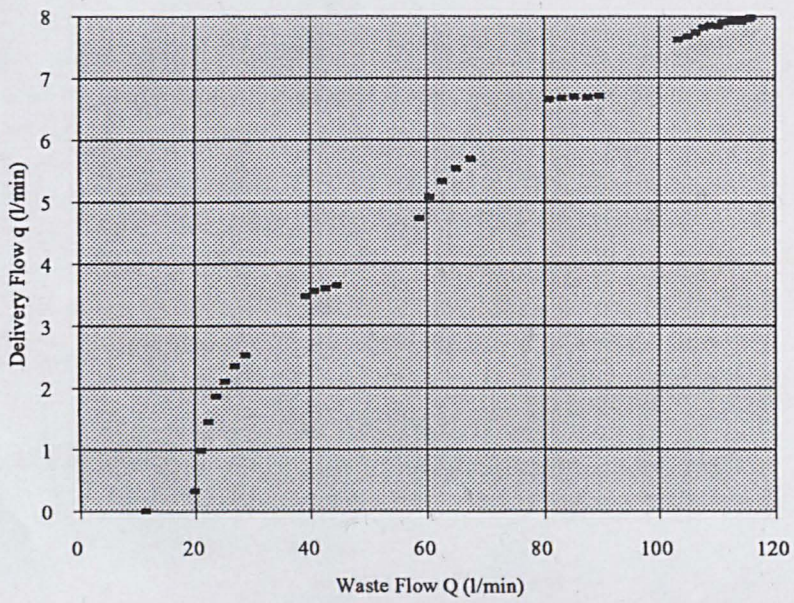

Performance Chart for Hydraulic Ram Pump

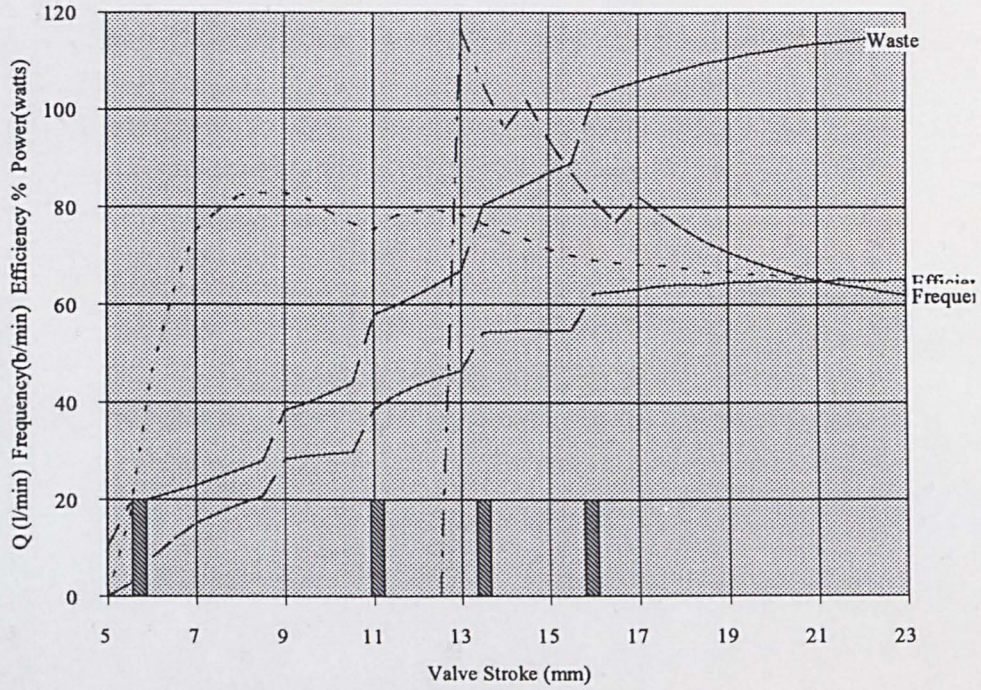

The shaded bars indicate strokes at which the impulse valve may not reopen.

Hydraulic Ram Pump Performance Model

INPUT

SITE		DRIVE PIPE		VALVE	
Drive Head (m)	5	Diameter (mm)	50	Stroke (mm)	23.5
Delivery Head(m)	60	Pipe Length(m)	15	Kf	0.041881891
		relrogh(k) (mm)	0.15	Ki	0.038184397
		Wavespeed m/s	1350	Kd	0.328
		CL Fittings	2.0625	Valve Mass kg	0.507

Delivery Valve Swept Volume l	0.008
VALVE WILL CLOSE with this setting	
Closure Waste Vol (l)	0.685
Critical Velocity (m/s)	1.78
Cutt off Velocity (m/s)	2.12
closuretime (s)	0.180

OUTPUT

Power watts	61.98	Delivery l/m	6.32	Delivery' l/m	5.715203742
Freq b/m	60.30	Waste l/m	115.16		
Efficiency	62.43		128.26		

Delivery' accounts for a partial realisation of recoil, and delivery valve swept volume losses

Pump Performance Range

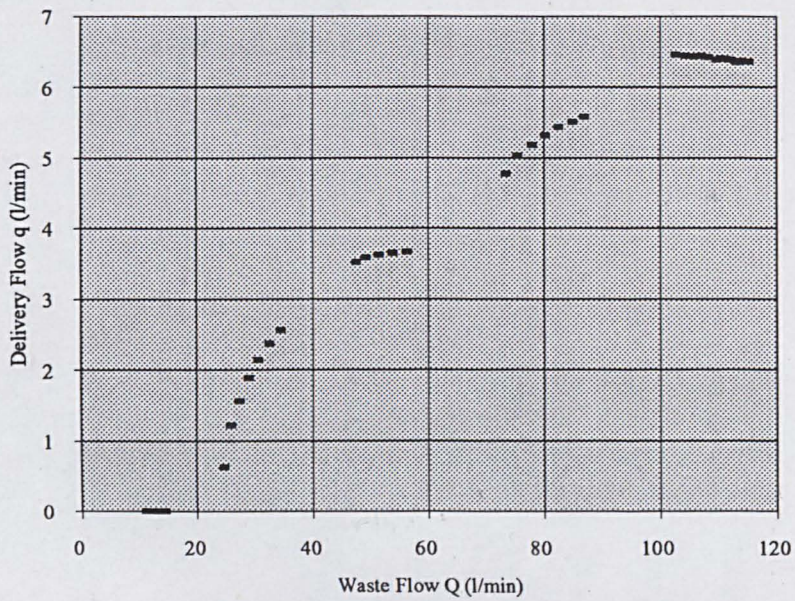

Performance Chart for Hydraulic Ram Pump

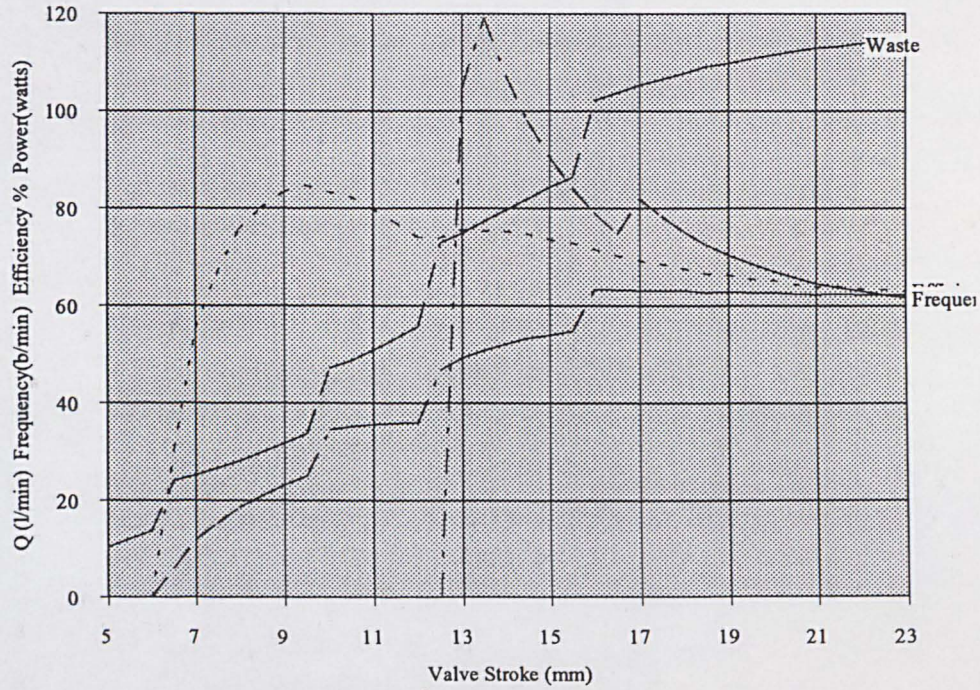

The shaded bars indicate strokes at which the impulse valve may not reopen.

Hydraulic Ram Pump Performance Model

INPUT

SITE		*DRIVE PIPE*		*VALVE*	
Drive Head (m)	5	Diameter (mm)	50	Stroke (mm)	23.5
Delivery Head(m)	70	Pipe Length(m)	15	Kf	0.041881891
		relrogh(k) (mm)	0.15	Ki	0.038184397
		Wavespeed m/s	1350	Kd	0.328
		CL Fittings	2.0625	Valve Mass kg	0.507

Delivery Valve Swept Volume l 0.008

VALVE WILL CLOSE with this setting

Closure Waste Vol (l)	0.685
Critical Velocity (m/s)	1.78
Cutt off Velocity (m/s)	2.12
closuretime (s)	0.180

OUTPUT

Power watts	69.92	Delivery l/m	6.11	Delivery' l/m	5.103887684
Freq b/m	66.09	Waste l/m	126.21		
Efficiency	64.66		128.26		

Delivery' accounts for a partial realisation of recoil, and delivery valve swept volume losses

Pump Performance Range

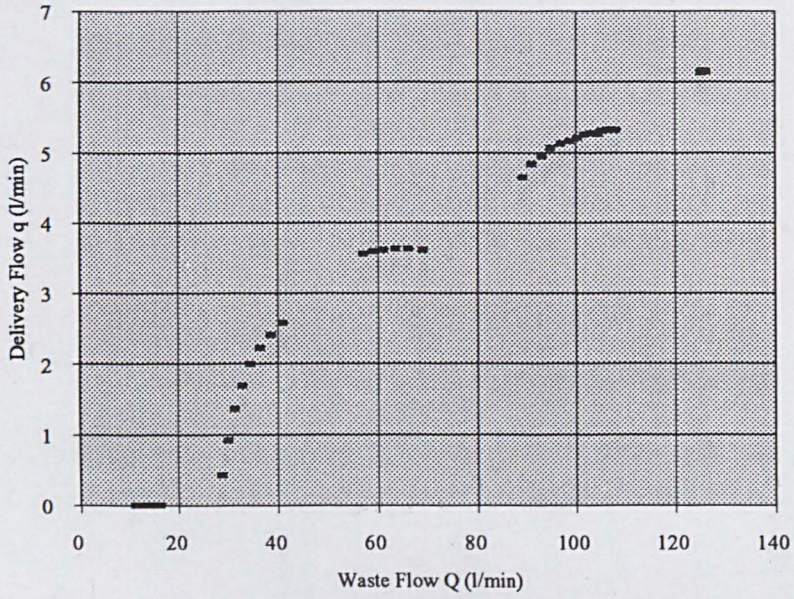

Performance Chart for Hydraulic Ram Pump

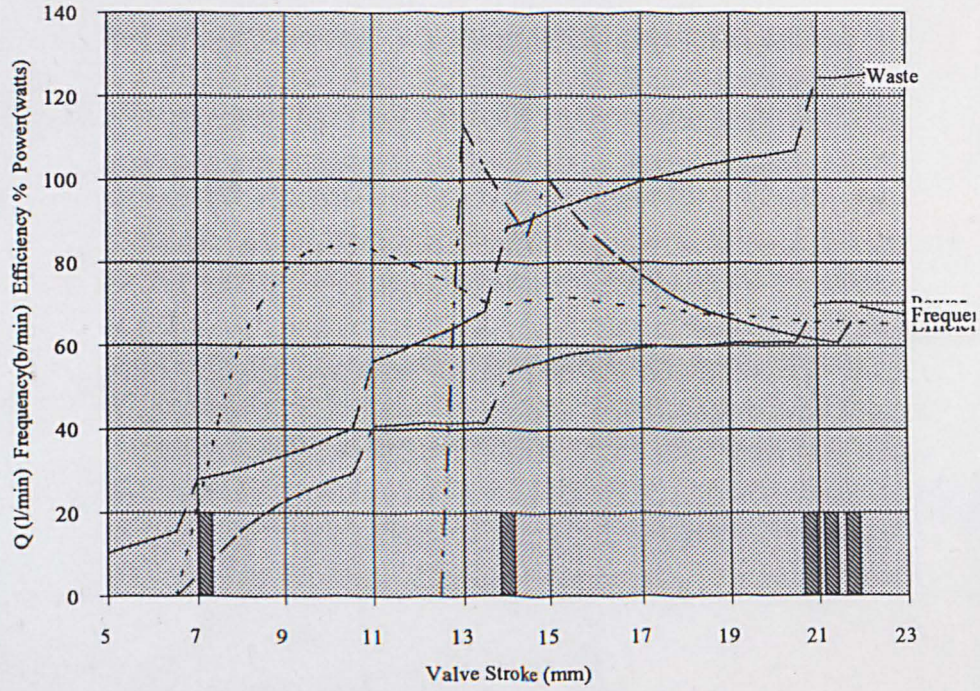

The shaded bars indicate strokes at which the impulse valve may not reopen.

Hydraulic Ram Pump Performance Model

INPUT

SITE		DRIVE PIPE		VALVE	
Drive Head (m)	5	Diameter (mm)	50	Stroke (mm)	23.5
Delivery Head(m)	80	Pipe Length(m)	15	Kf	0.041881891
		relrogh(k) (mm)	0.15	Ki	0.038184397
		Wavespeed m/s	1350	Kd	0.328
		CL Fittings	2.0625	Valve Mass kg	0.507

Delivery Valve Swept Volume l	0.008
VALVE WILL CLOSE with this setting	
Closure Waste Vol (l)	0.685
Critical Velocity (m/s)	1.78
Cutt off Velocity (m/s)	2.12
closuretime (s)	0.180

OUTPUT

Power watts	64.39	Delivery l/m	4.92	Delivery' l/m	4.237802671
Freq b/m	61.47	Waste l/m	117.39		
Efficiency	64.42		131.53		

Delivery' accounts for a partial realisation of recoil, and delivery valve swept volume losses

Pump Performance Range

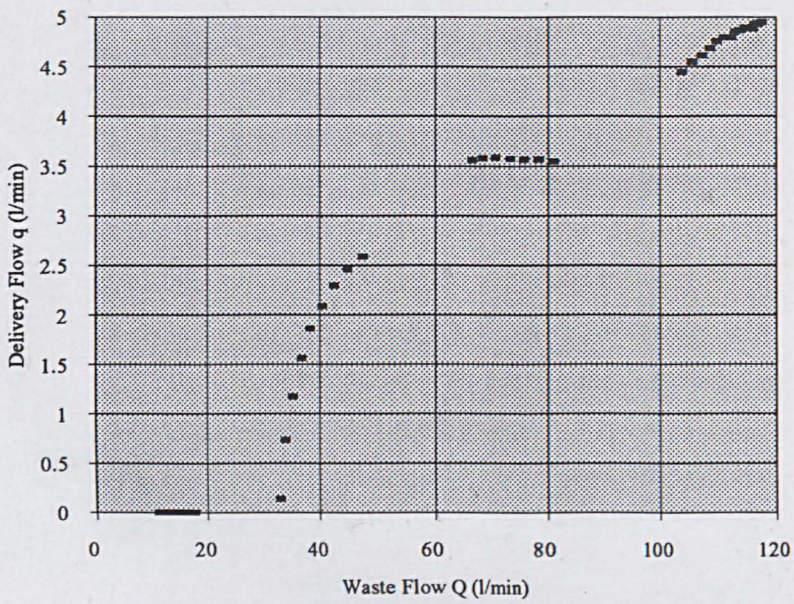

Performance Chart for Hydraulic Ram Pump

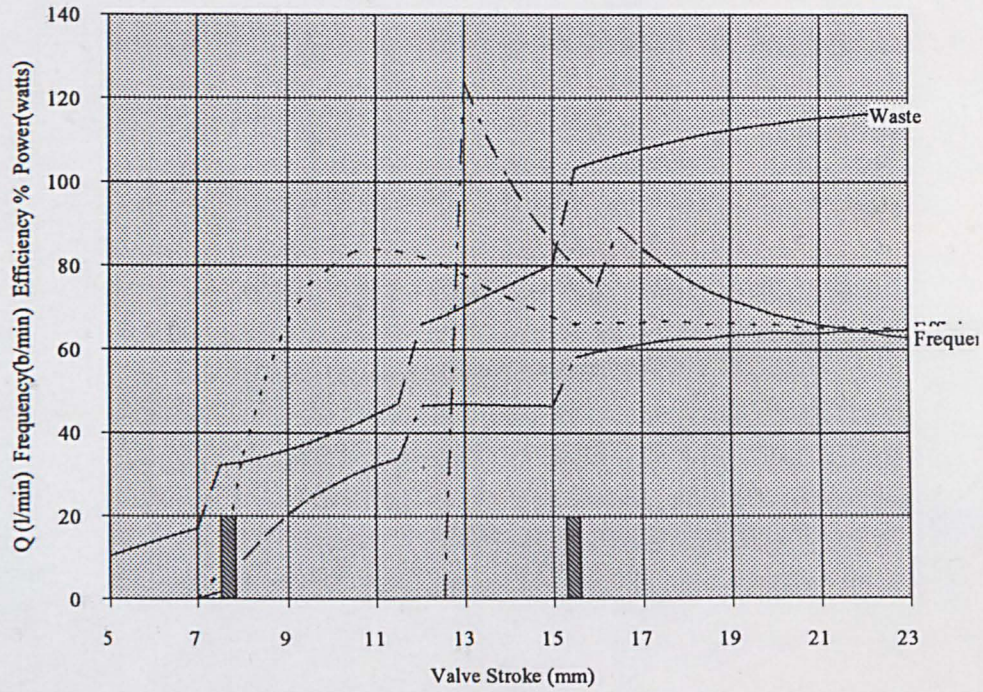

The shaded bars indicate strokes at which the impulse valve may not reopen.

Hydraulic Ram Pump Performance Model

INPUT

SITE		DRIVE PIPE		VALVE	
Drive Head (m)	5	Diameter (mm)	50	Stroke (mm)	23.5
Delivery Head(m)	90	Pipe Length(m)	15	Kf	0.041881891
		relrogh(k) (mm)	0.15	Ki	0.038184397
		Wavespeed m/s	1350	Kd	0.328
		CL Fittings	2.0625	Valve Mass kg	0.507

Delivery Valve Swept Volume l	0.008
VALVE WILL CLOSE with this setting	
Closure Waste Vol (l)	0.685
Critical Velocity (m/s)	1.78
Cutt off Velocity (m/s)	2.12
closuretime (s)	0.180

OUTPUT

Power watts	65.62	Delivery l/m	4.46	Delivery' l/m	3.509234792
Freq b/m	65.87	Waste l/m	125.79		
Efficiency	61.65		131.53		

Delivery' accounts for a partial realisation of recoil, and delivery valve swept volume losses

Pump Performance Range

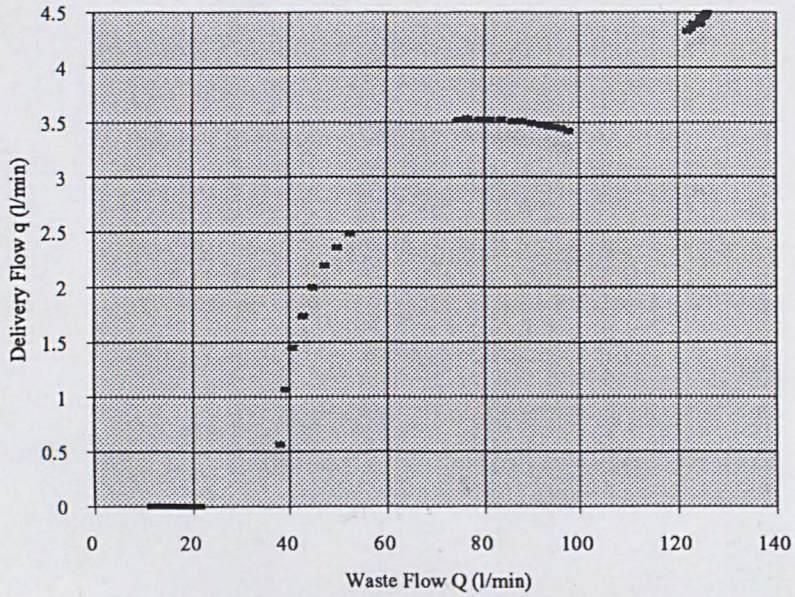

Performance Chart for Hydraulic Ram Pump

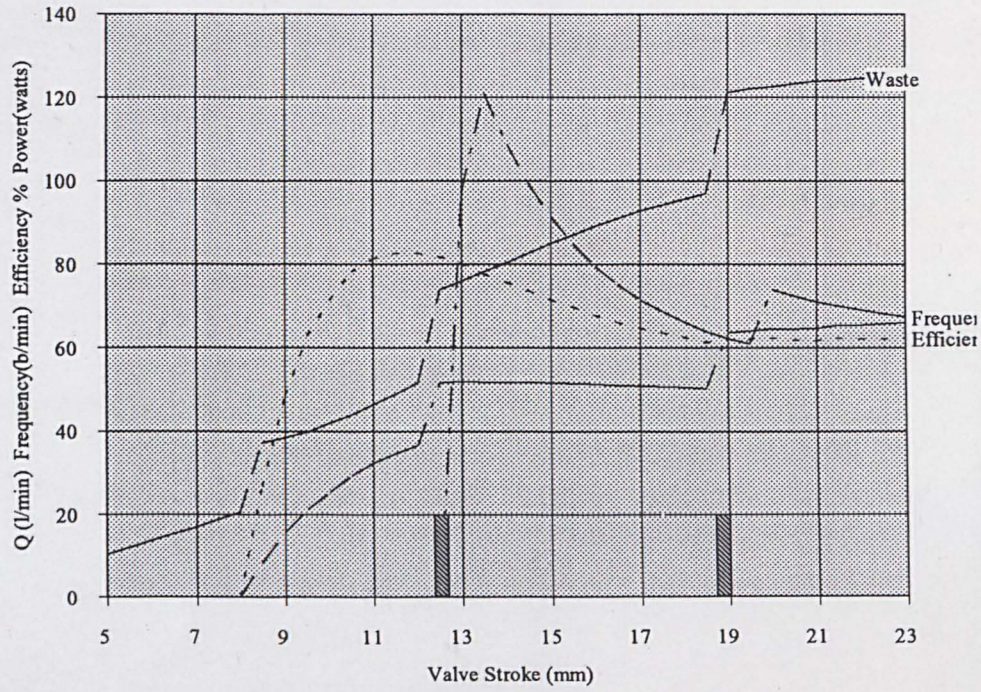

The shaded bars indicate strokes at which the impulse valve may not reopen.

Hydraulic Ram Pump Performance Model

INPUT

SITE		DRIVE PIPE		VALVE		Delivery Valve Swept Volume l	0.008
Drive Head (m)	5	Diameter (mm)	50	Stroke (mm)	23.5	VALVE WILL CLOSE with this setting	
Delivery Head(m)	100	Pipe Length(m)	15	Kf	0.041881891	Closure Waste Vol (l)	0.685
		relrogh(k) (mm)	0.15	Ki	0.038184397	Critical Velocity (m/s)	1.78
		Wavespeed m/s	1350	Kd	0.328	Cutt off Velocity (m/s)	2.12
		CL Fittings	2.0625	Valve Mass kg	0.507	closuretime (s)	0.180

OUTPUT

Power watts	54.44	Delivery l/m	3.33	Delivery' l/m	3.243979203	Delivery' accounts for a partial realisation of recoil, and delivery valve swept volume losses
Freq b/m	56.49	Waste l/m	107.88			
Efficiency	59.90		131.53			

Pump Performance Range

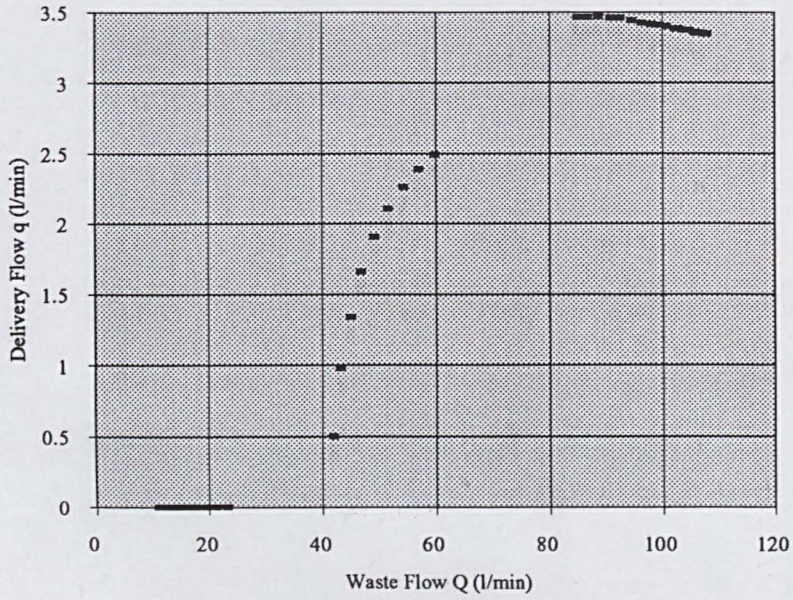

Performance Chart for Hydraulic Ram Pump

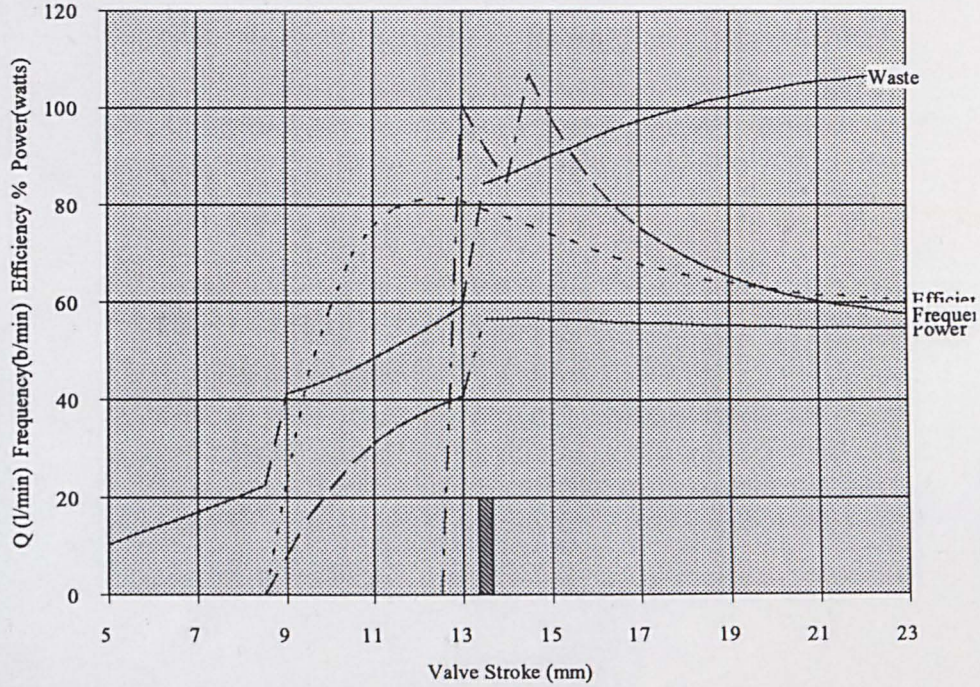

The shaded bars indicate strokes at which the impulse valve may not reopen.

Hydraulic Ram Pump Performance Model

INPUT

SITE		DRIVE PIPE		VALVE	
Drive Head (m)	8	Diameter (mm)	50	Stroke (mm)	23.5
Delivery Head(m)	50	Pipe Length(m)	24	Kf	0.041881891
		relrogh(k) (mm)	0.15	Ki	0.038184397
		Wavespeed m/s	1350	Kd	0.328
		CL Fittings	2.0625	Valve Mass kg	0.507

Delivery Valve Swept Volume l	0.008
VALVE WILL CLOSE with this setting	
Closure Waste Vol (l)	0.670
Critical Velocity (m/s)	1.78
Cutt off Velocity (m/s)	2.14
closuretime (s)	0.175

OUTPUT

Power watts	113.07	Delivery l/m	13.84	Delivery' l/m	12.3862263
Freq b/m	62.94	Waste l/m	115.93		
Efficiency	66.64		116.96		

Delivery' accounts for a partial realisation of recoil, and delivery valve swept volume losses

Pump Performance Range

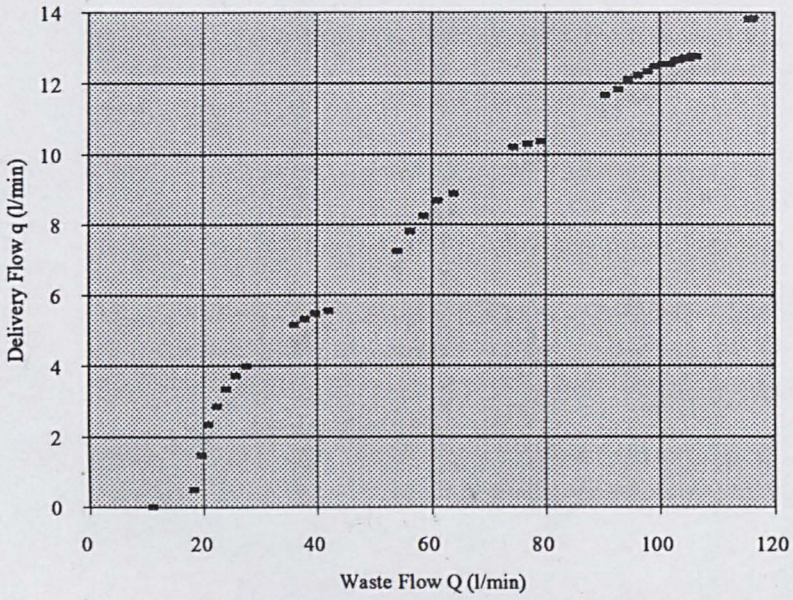

Performance Chart for Hydraulic Ram Pump

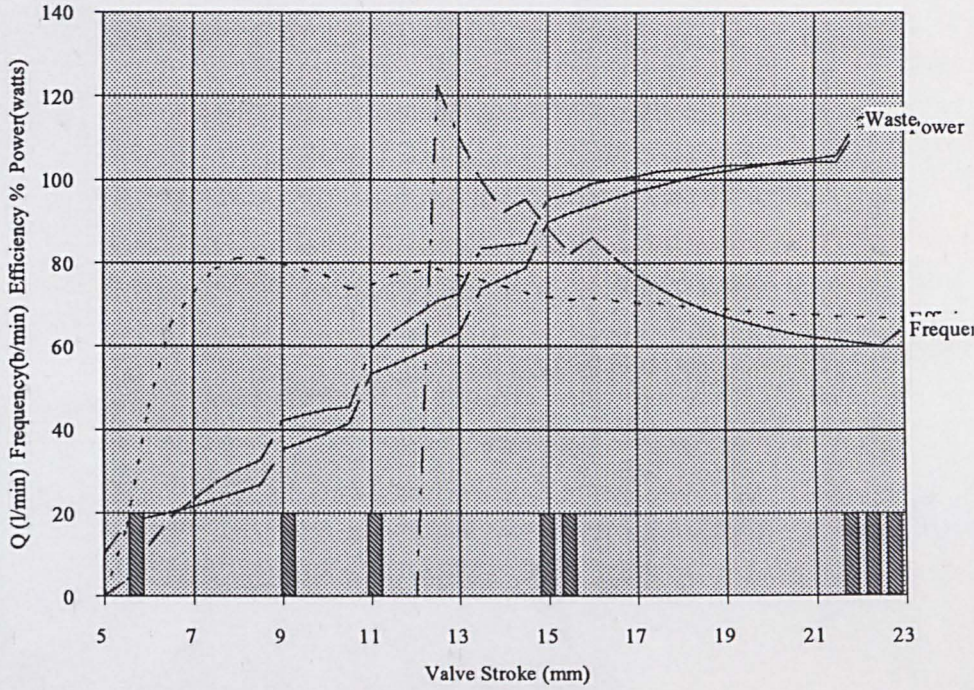

The shaded bars indicate strokes at which the impulse valve may not reopen.

Hydraulic Ram Pump Performance Model

INPUT

SITE		DRIVE PIPE		VALVE	
Drive Head (m)	8	Diameter (mm)	50	Stroke (mm)	23.5
Delivery Head(m)	60	Pipe Length(m)	24	Kf	0.041881891
		relrogh(k) (mm)	0.15	Ki	0.038184397
		Wavespeed m/s	1350	Kd	0.328
		CL Fittings	2.0625	Valve Mass kg	0.507

Delivery Valve Swept Volume l	0.008
VALVE WILL CLOSE with this setting	
Closure Waste Vol (l)	0.670
Critical Velocity (m/s)	1.78
Cutt off Velocity (m/s)	2.14
closuretime (s)	0.175

OUTPUT

Power watts	112.15	Delivery l/m	11.44	Delivery' l/m	9.94829569
Freq b/m	65.13	Waste l/m	119.96		
Efficiency	65.28		121.53		

Delivery' accounts for a partial realisation of recoil, and delivery valve swept volume losses

Pump Performance Range

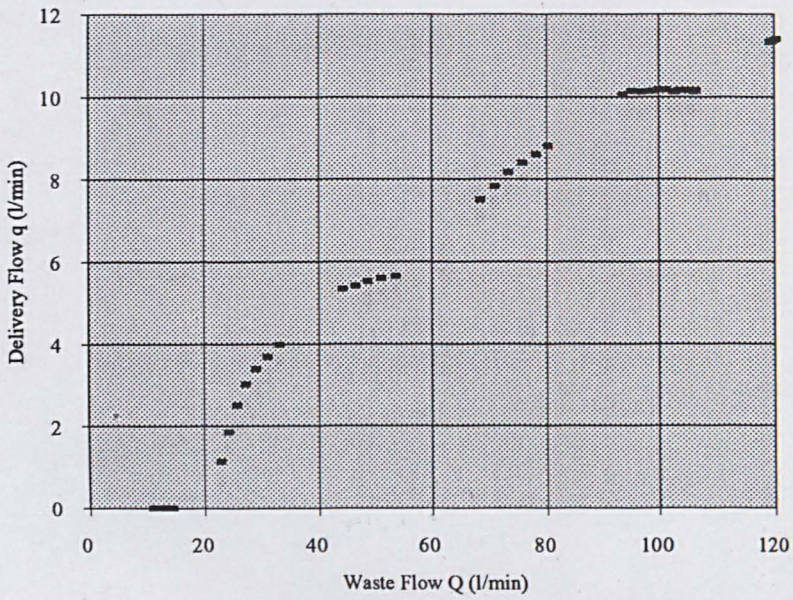

Performance Chart for Hydraulic Ram Pump

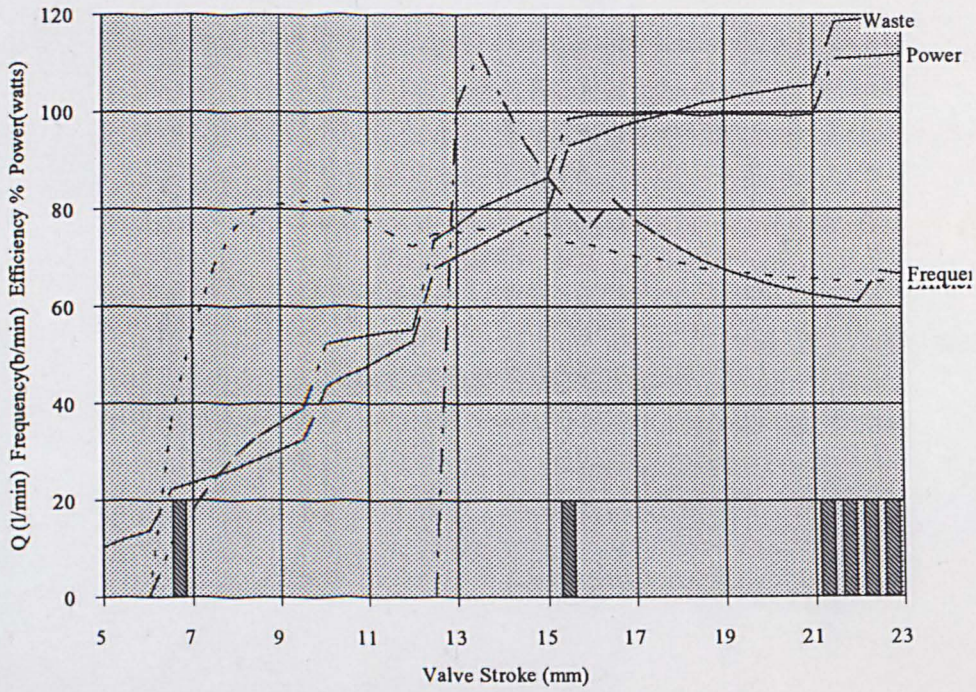

The shaded bars indicate strokes at which the impulse valve may not reopen.

Hydraulic Ram Pump Performance Model

INPUT

SITE		DRIVE PIPE		VALVE		Delivery Valve Swept Volume l	0.008
Drive Head (m)	8	Diameter (mm)	50	Stroke (mm)	23.5	VALVE WILL CLOSE with this setting	
Delivery Head(m)	70	Pipe Length(m)	24	Kf	0.041881891	Closure Waste Vol (l)	0.670
		relrogh(k) (mm)	0.15	Ki	0.038184397	Critical Velocity (m/s)	1.78
		Wavespeed m/s	1350	Kd	0.328	Cutt off Velocity (m/s)	2.14
		CL Fittings	2.0625	Valve Mass kg	0.507	closuretime (s)	0.175

OUTPUT

Power watts	112.14	Delivery l/m	9.80	Delivery' l/m	8.930349803
Freq b/m	63.99	Waste l/m	117.85		
Efficiency	67.18		121.53		

Delivery' accounts for a partial realisation of recoil, and delivery valve swept volume losses

Pump Performance Range

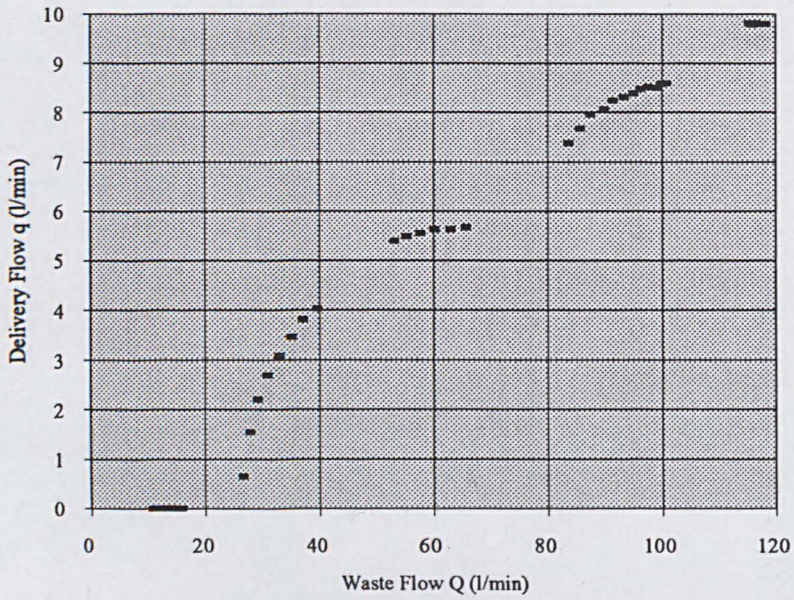

Performance Chart for Hydraulic Ram Pump

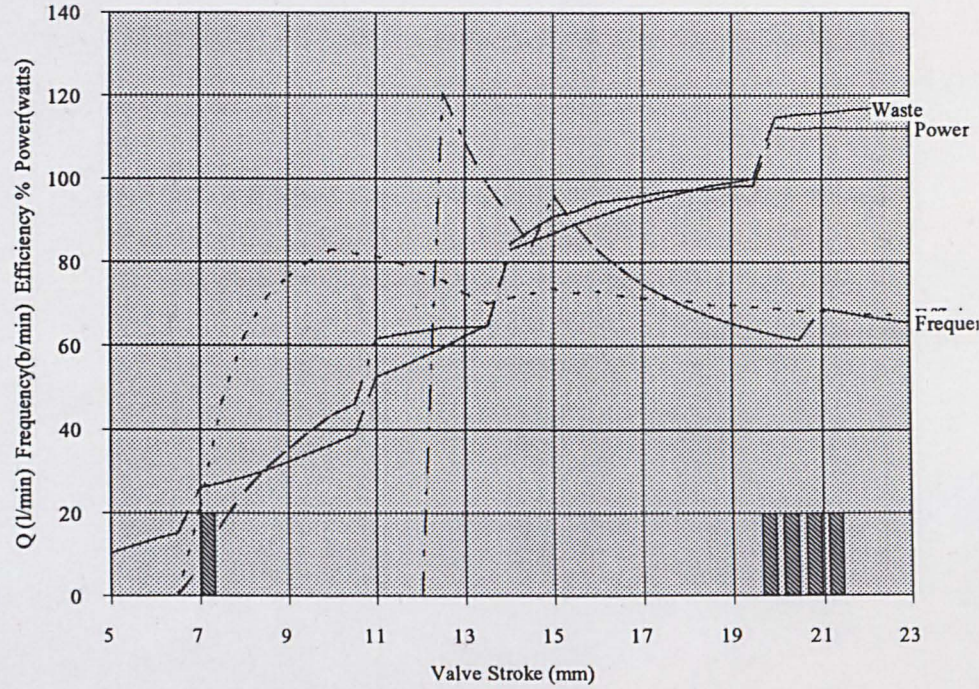

The shaded bars indicate strokes at which the impulse valve may not reopen.

Hydraulic Ram Pump Performance Model

INPUT

SITE		DRIVE PIPE		VALVE	
Drive Head (m)	8	Diameter (mm)	50	Stroke (mm)	23.5
Delivery Head(m)	80	Pipe Length(m)	24	Kf	0.041881891
		relrogh(k) (mm)	0.15	Ki	0.038184397
		Wavespeed m/s	1350	Kd	0.328
		CL Fittings	2.0625	Valve Mass kg	0.507

Delivery Valve Swept Volume l	0.008

VALVE WILL CLOSE with this setting

Closure Waste Vol (l)	0.670
Critical Velocity (m/s)	1.78
Cutt off Velocity (m/s)	2.14
closuretime (s)	0.175

OUTPUT

Power watts	105.45	Delivery l/m	8.06	Delivery' l/m	7.646688679
Freq b/m	60.44	Waste l/m	111.32		
Efficiency	67.55		126.47		

Delivery' accounts for a partial realisation of recoil, and delivery valve swept volume losses

Pump Performance Range

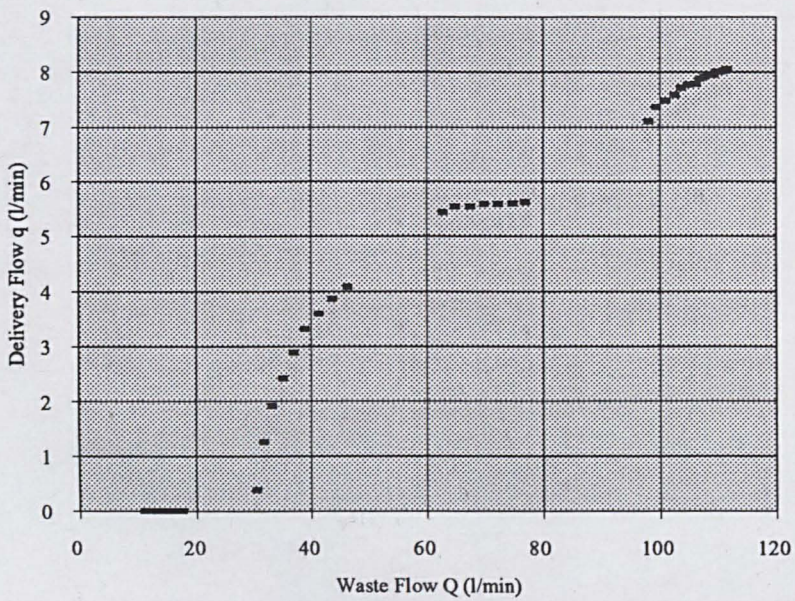

Performance Chart for Hydraulic Ram Pump

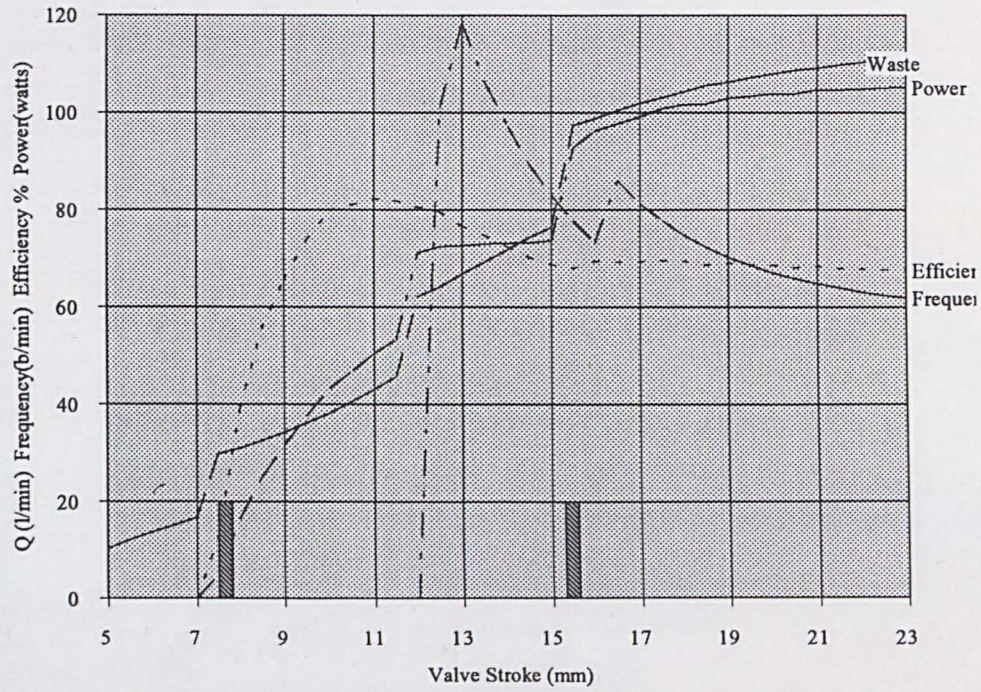

The shaded bars indicate strokes at which the impulse valve may not reopen.

Hydraulic Ram Pump Performance Model

INPUT

SITE		DRIVE PIPE		VALVE		Delivery Valve Swept Volume l	0.008
Drive Head (m)	8	Diameter (mm)	50	Stroke (mm)	23.5	VALVE WILL CLOSE with this setting	
Delivery Head(m)	90	Pipe Length(m)	24	Kf	0.041881891	Closure Waste Vol (l)	0.670
		relrogh(k) (mm)	0.15	Ki	0.038184397	Critical Velocity (m/s)	1.78
		Wavespeed m/s	1350	Kd	0.328	Cutt off Velocity (m/s)	2.14
		CL Fittings	2.0625	Valve Mass kg	0.507	closuretime (s)	0.175

OUTPUT

Power watts	108.13	Delivery l/m	7.35	Delivery' l/m	6.542864406	Delivery' accounts for a partial realisation of recoil, and delivery valve swept volume losses
Freq b/m	64.68	Waste l/m	119.12			
Efficiency	65.39		126.47			

Pump Performance Range

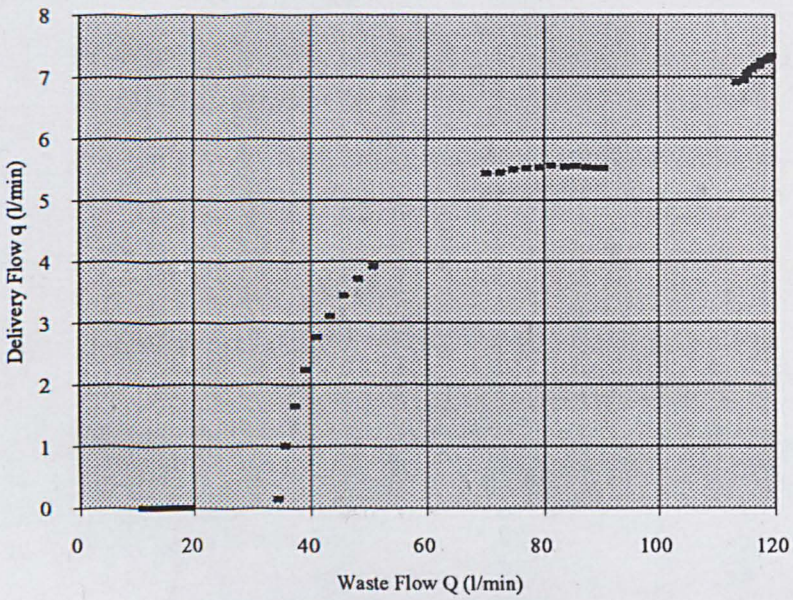

Performance Chart for Hydraulic Ram Pump

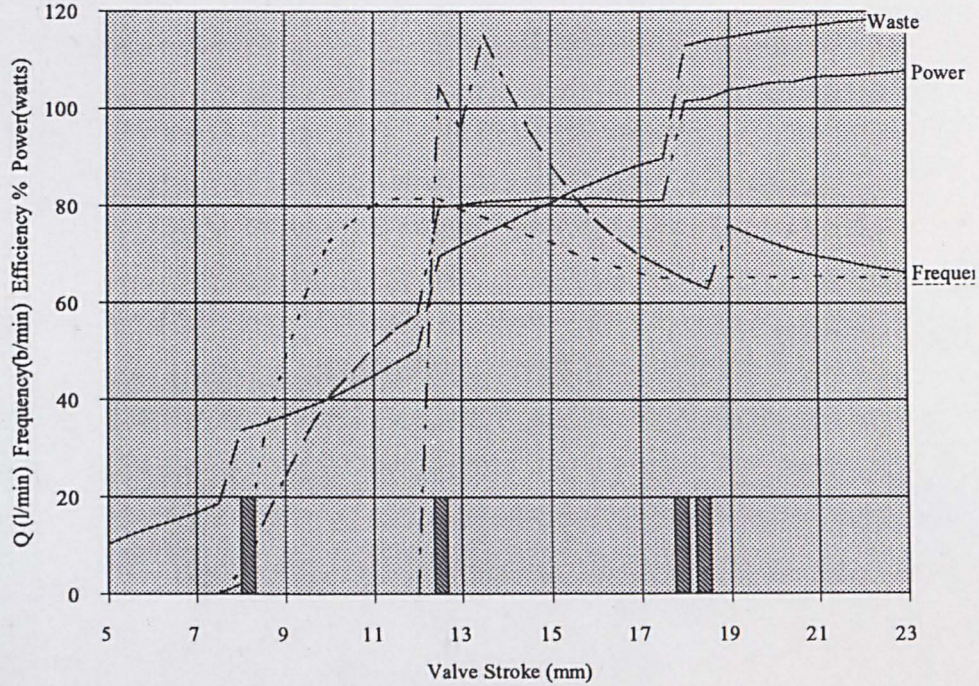

The shaded bars indicate strokes at which the impulse valve may not reopen.

Hydraulic Ram Pump Performance Model

INPUT

SITE		DRIVE PIPE		VALVE	
Drive Head (m)	8	Diameter (mm)	50	Stroke (mm)	23.5
Delivery Head(m)	100	Pipe Length(m)	24	Kf	0.041881891
		relrogh(k) (mm)	0.15	Ki	0.038184397
		Wavespeed m/s	1350	Kd	0.328
		CL Fittings	2.0625	Valve Mass kg	0.507

Delivery Valve Swept Volume l	0.008
VALVE WILL CLOSE with this setting	
Closure Waste Vol (l)	0.670
Critical Velocity (m/s)	1.78
Cutt off Velocity (m/s)	2.14
closuretime (s)	0.175

OUTPUT

Power watts	88.04	Delivery l/m	5.39	Delivery' l/m	5.555914324
Freq b/m	55.88	Waste l/m	102.91		
Efficiency	62.17		126.47		

Delivery' accounts for a partial realisation of recoil, and delivery valve swept volume losses

Pump Performance Range

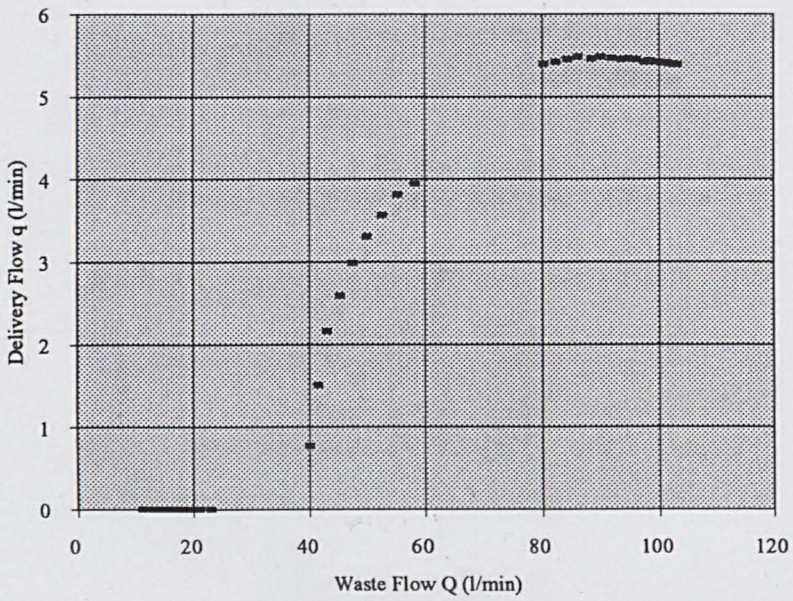

Performance Chart for Hydraulic Ram Pump

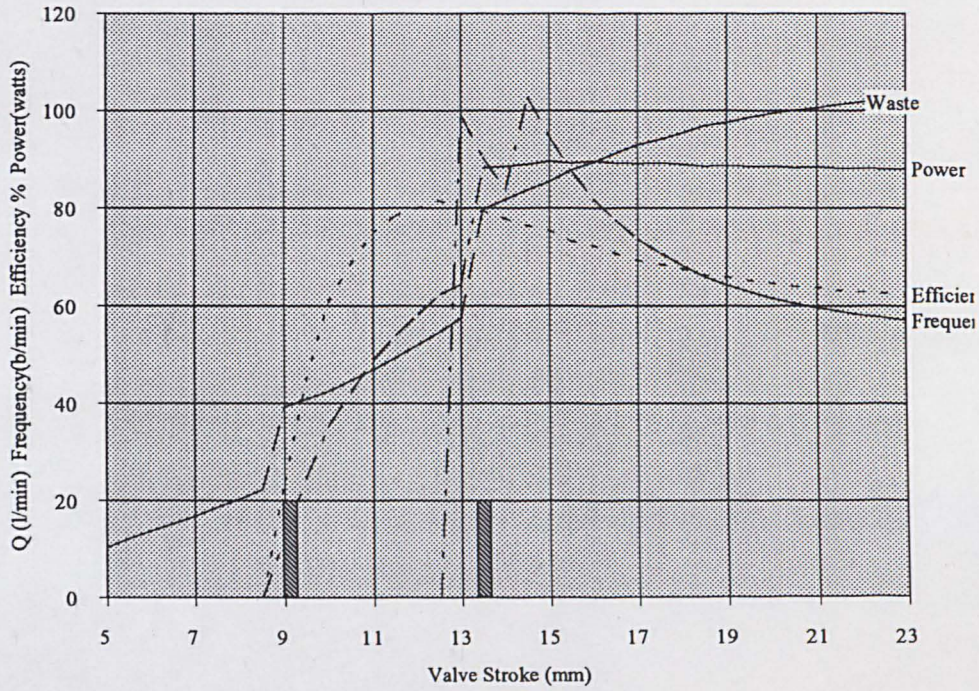

The shaded bars indicate strokes at which the impulse valve may not reopen.

Hydraulic Ram Pump Performance Model

INPUT

SITE		DRIVE PIPE		VALVE		Delivery Valve Swept Volume l	0.008
Drive Head (m)	10	Diameter (mm)	50	Stroke (mm)	23.5	VALVE WILL CLOSE with this setting	
Delivery Head(m)	50	Pipe Length(m)	30	Kf	0.041881891	Closure Waste Vol (l)	0.664
		relrogh(k) (mm)	0.15	Ki	0.038184397	Critical Velocity (m/s)	1.78
		Wavespeed m/s	1350	Kd	0.328	Cutt off Velocity (m/s)	2.15
		CL Fittings	2.0625	Valve Mass kg	0.507	closuretime (s)	0.173

OUTPUT

Power watts	138.66	Delivery l/m	16.97	Delivery' l/m	15.70842054	Delivery' accounts for a partial realisation of recoil, and delivery valve swept volume losses
Freq b/m	60.35	Waste l/m	109.77			
Efficiency	66.94		112.22			

Pump Performance Range

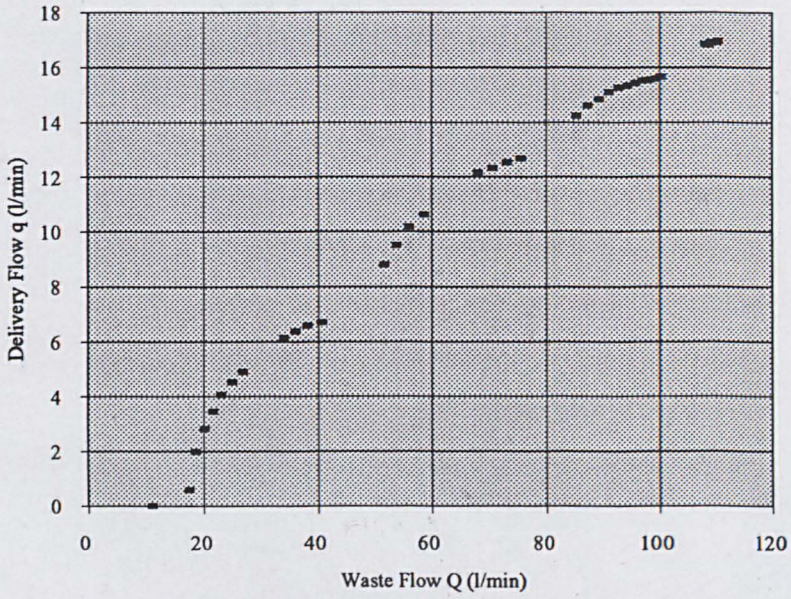

Performance Chart for Hydraulic Ram Pump

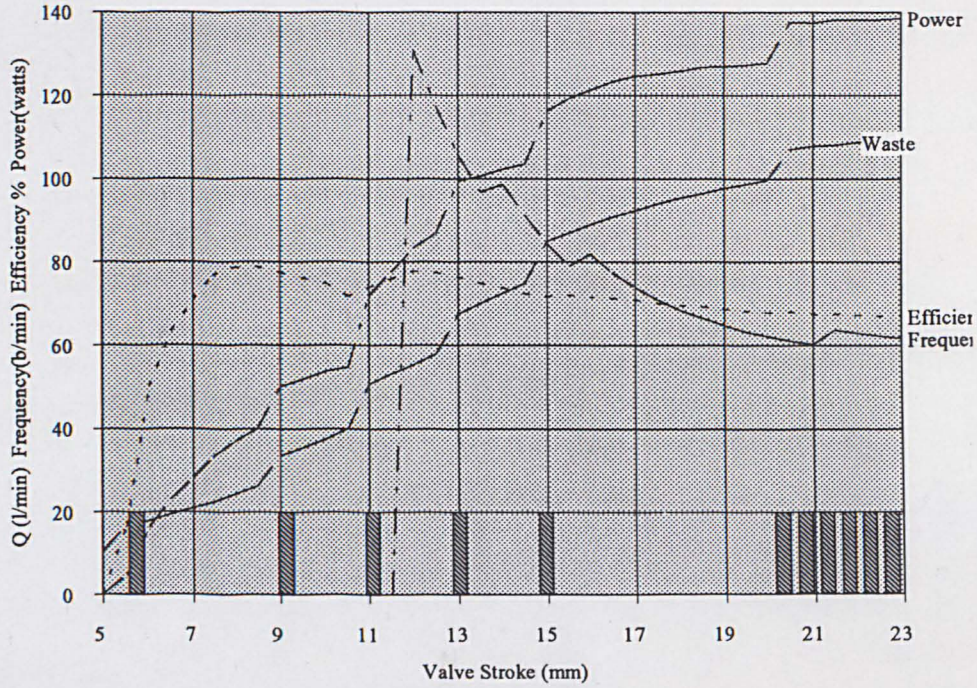

The shaded bars indicate strokes at which the impulse valve may not reopen.

Hydraulic Ram Pump Performance Model

INPUT

SITE		DRIVE PIPE		VALVE		Delivery Valve Swept Volume l	0.008
Drive Head (m)	10	Diameter (mm)	50	Stroke (mm)	23.5	VALVE WILL CLOSE with this setting	
Delivery Head(m)	60	Pipe Length(m)	30	Kf	0.041881891	Closure Waste Vol (l)	0.664
		relrogh(k) (mm)	0.15	Ki	0.038184397	Critical Velocity (m/s)	1.78
		Wavespeed m/s	1350	Kd	0.328	Cutt off Velocity (m/s)	2.15
		CL Fittings	2.0625	Valve Mass kg	0.507	closuretime (s)	0.173

OUTPUT

Power watts	139.45	Delivery l/m	14.22	Delivery' l/m	12.90649428
Freq b/m	62.92	Waste l/m	114.44		
Efficiency	66.32		117.60		

Delivery' accounts for a partial realisation of recoil, and delivery valve swept volume losses

Pump Performance Range

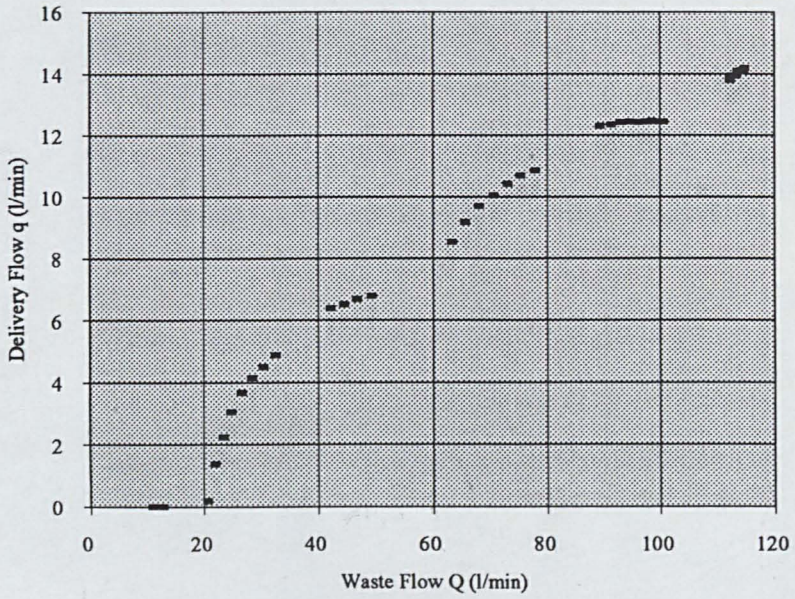

Performance Chart for Hydraulic Ram Pump

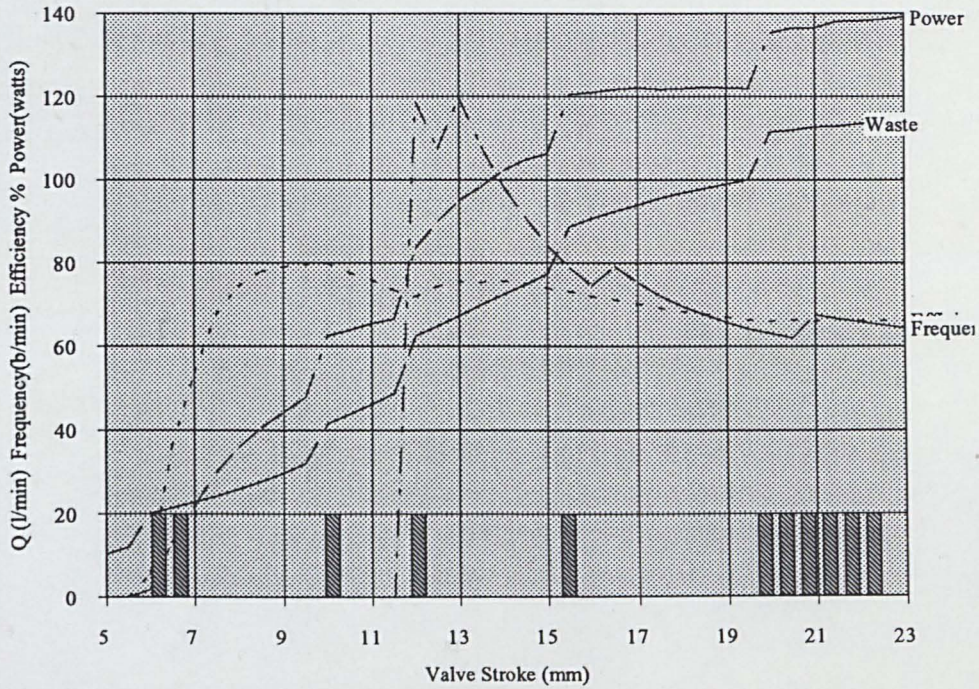

The shaded bars indicate strokes at which the impulse valve may not reopen.

Hydraulic Ram Pump Performance Model

INPUT

SITE		DRIVE PIPE		VALVE		Delivery Valve Swept Volume l	0.008
Drive Head (m)	10	Diameter (mm)	50	Stroke (mm)	23.5	VALVE WILL CLOSE with this setting	
Delivery Head(m)	70	Pipe Length(m)	30	Kf	0.041881891	Closure Waste Vol (l)	0.664
		relrogh(k) (mm)	0.15	Ki	0.038184397	Critical Velocity (m/s)	1.78
		Wavespeed m/s	1350	Kd	0.328	Cutt off Velocity (m/s)	2.15
		CL Fittings	2.0625	Valve Mass kg	0.507	closuretime (s)	0.173

OUTPUT

Power watts	138.42	Delivery l/m	12.10	Delivery' l/m	11.32696221	Delivery' accounts for a partial realisation of recoil, and delivery valve swept volume losses
Freq b/m	62.33	Waste l/m	113.36			
Efficiency	67.50		117.60			

Pump Performance Range

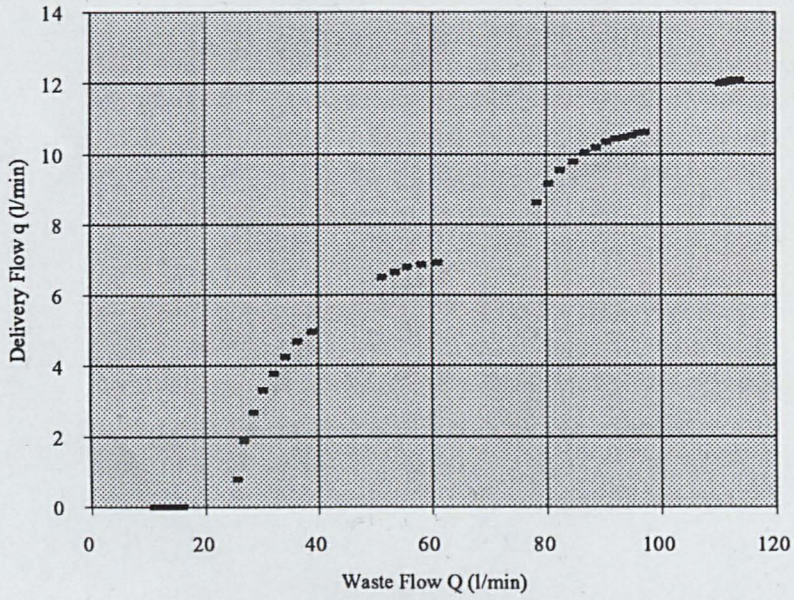

Performance Chart for Hydraulic Ram Pump

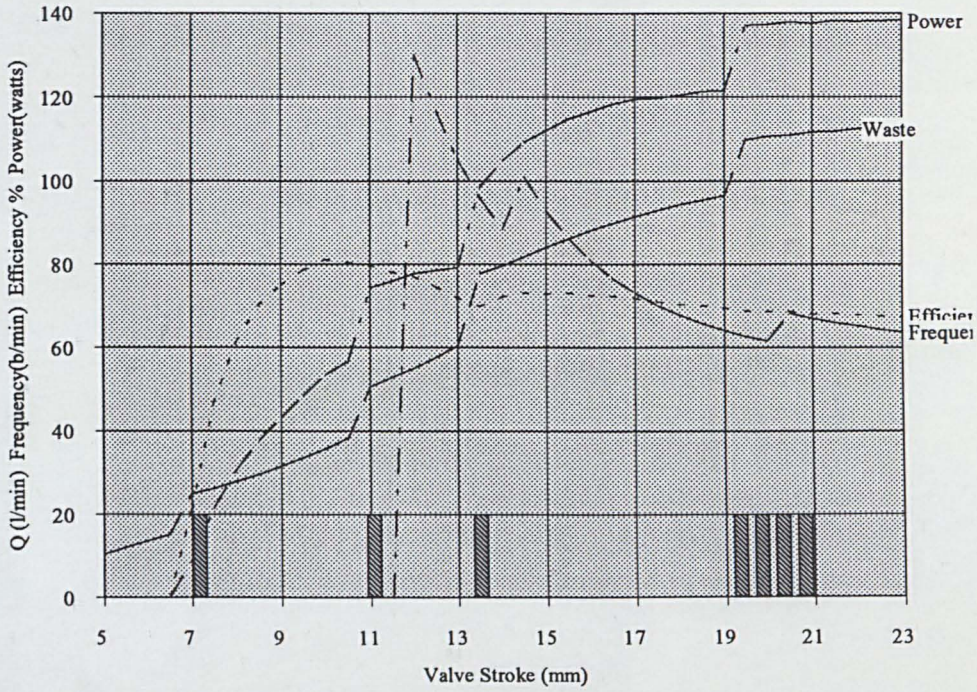

The shaded bars indicate strokes at which the impulse valve may not reopen.

Hydraulic Ram Pump Performance Model

INPUT

SITE		DRIVE PIPE		VALVE		Delivery Valve Swept Volume l	0.008
Drive Head (m)	10	Diameter (mm)	50	Stroke (mm)	23.5	VALVE WILL CLOSE with this setting	
Delivery Head(m)	80	Pipe Length(m)	30	Kf	0.041881891	Closure Waste Vol (l)	0.664
		relrogh(k) (mm)	0.15	Ki	0.038184397	Critical Velocity (m/s)	1.78
		Wavespeed m/s	1350	Kd	0.328	Cutt off Velocity (m/s)	2.15
		CL Fittings	2.0625	Valve Mass kg	0.507	closuretime (s)	0.173

OUTPUT

Power watts	131.77	Delivery l/m	10.08	Delivery' l/m	9.841410696	Delivery' accounts for a partial realisation of recoil, and delivery valve swept volume losses
Freq b/m	59.47	Waste l/m	108.16			
Efficiency	68.19		123.51			

Pump Performance Range

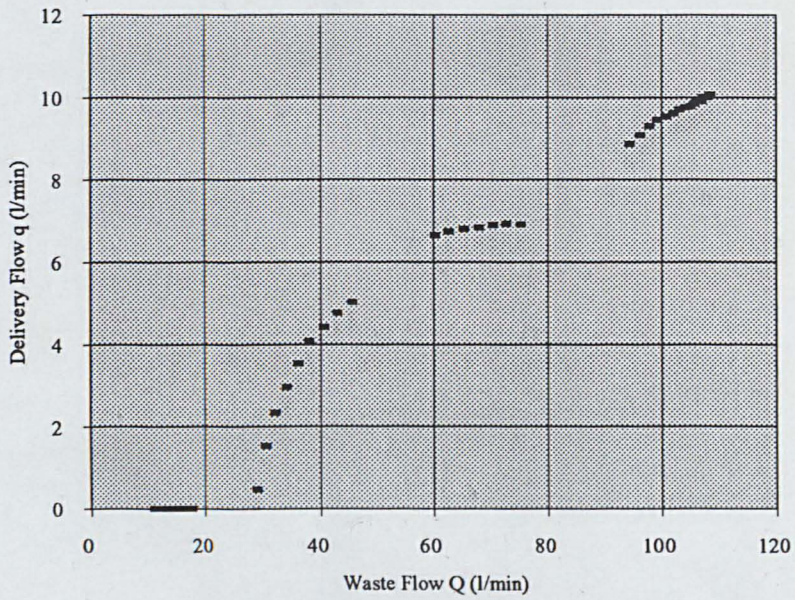

Performance Chart for Hydraulic Ram Pump

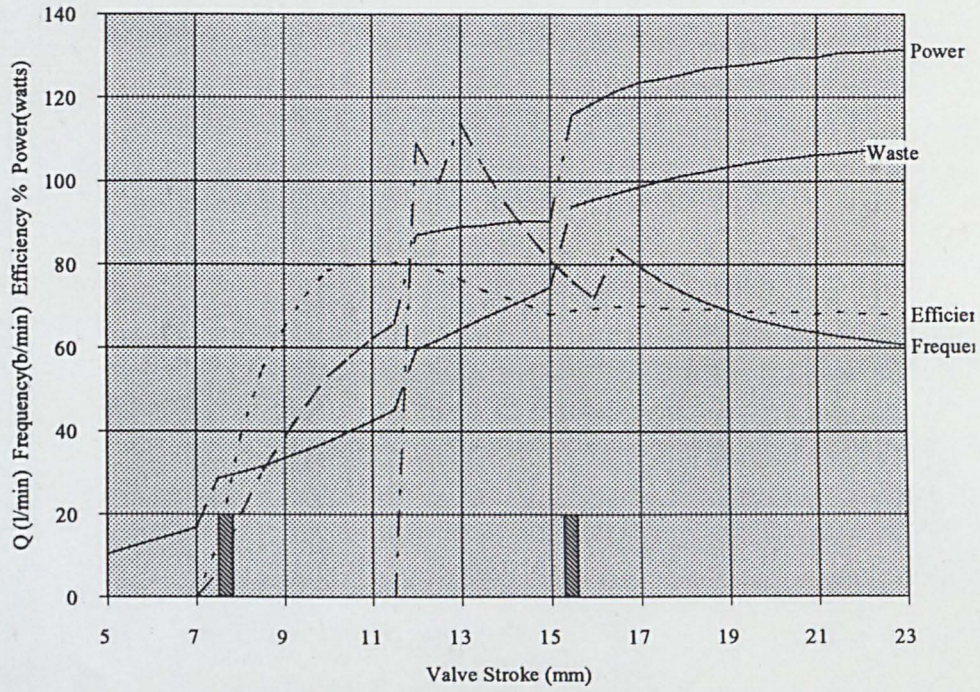

The shaded bars indicate strokes at which the impulse valve may not reopen.

Hydraulic Ram Pump Performance Model

INPUT

SITE		DRIVE PIPE		VALVE	
Drive Head (m)	12	Diameter (mm)	50	Stroke (mm)	23.5
Delivery Head(m)	100	Pipe Length(m)	36	Kf	0.041881891
		relrogh(k) (mm)	0.15	Ki	0.038184397
		Wavespeed m/s	1350	Kd	0.328
		CL Fittings	2.0625	Valve Mass kg	0.507

Delivery Valve Swept Volume l	0.008
VALVE WILL CLOSE with this setting	
Closure Waste Vol (l)	0.661
Critical Velocity (m/s)	1.78
Cutt off Velocity (m/s)	2.16
closuretime (s)	0.172

OUTPUT

Power watts	129.87	Delivery l/m	7.95	Delivery' l/m	8.409025653
Freq b/m	54.57	Waste l/m	98.51		
Efficiency	62.20		120.82		

Delivery' accounts for a partial realisation of recoil, and delivery valve swept volume losses

Pump Performance Range

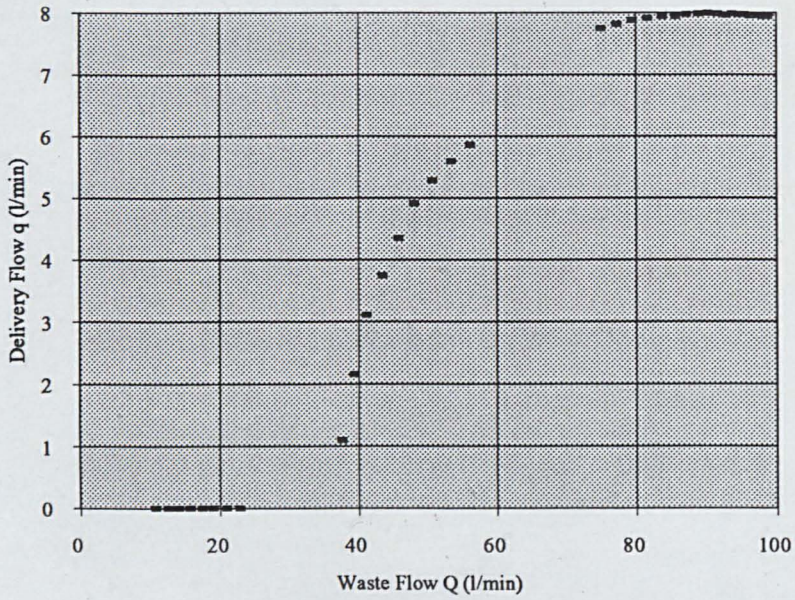

Performance Chart for Hydraulic Ram Pump

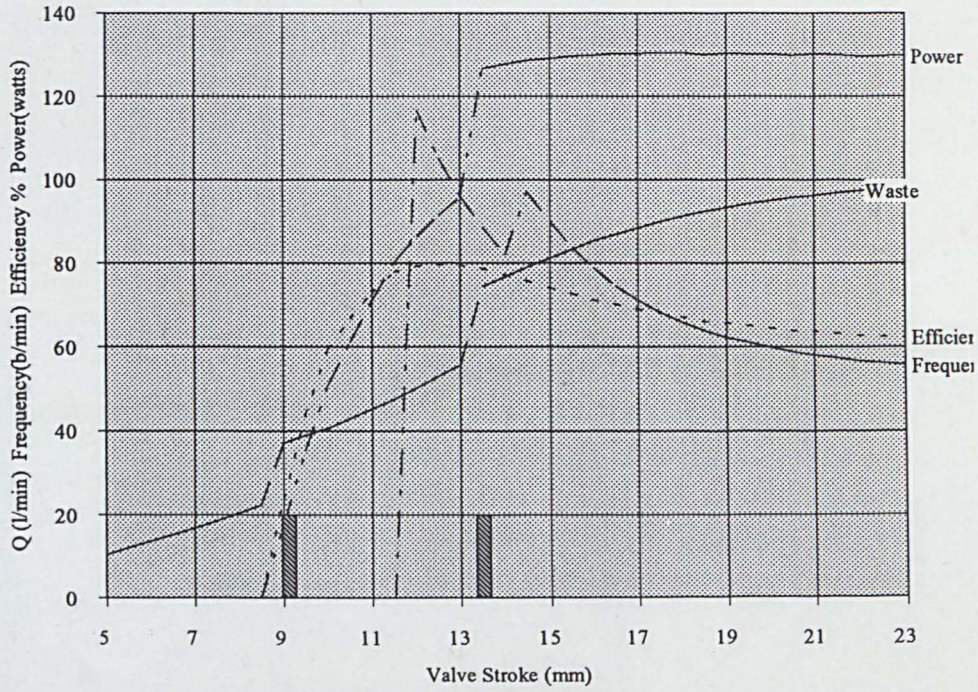

The shaded bars indicate strokes at which the impulse valve may not reopen.

Hydraulic Ram Pump Performance Model

INPUT

SITE		DRIVE PIPE		VALVE		Delivery Valve Swept Volume l	0.008
Drive Head (m)	12	Diameter (mm)	50	Stroke (mm)	23.5	VALVE WILL CLOSE with this setting	
Delivery Head(m)	90	Pipe Length(m)	36	Kf	0.041881891	Closure Waste Vol (l)	0.661
		relrogh(k) (mm)	0.15	Ki	0.038184397	Critical Velocity (m/s)	1.78
		Wavespeed m/s	1350	Kd	0.328	Cutt off Velocity (m/s)	2.16
		CL Fittings	2.0625	Valve Mass kg	0.507	closuretime (s)	0.172

OUTPUT

Power watts	160.76	Delivery l/m	10.93	Delivery' l/m	10.32022495	Delivery' accounts for a partial realisation of recoil, and delivery valve swept volume losses
Freq b/m	62.46	Waste l/m	112.76			
Efficiency	66.27		120.82			

Pump Performance Range

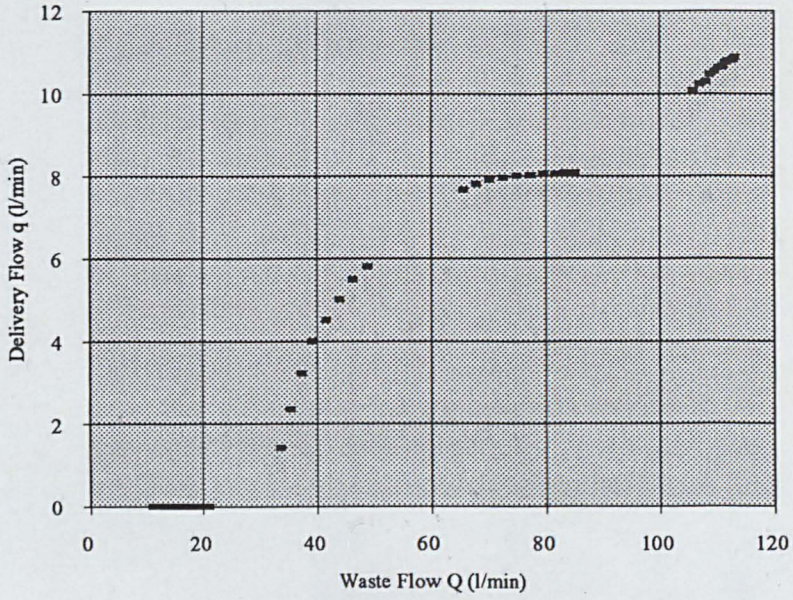

Performance Chart for Hydraulic Ram Pump

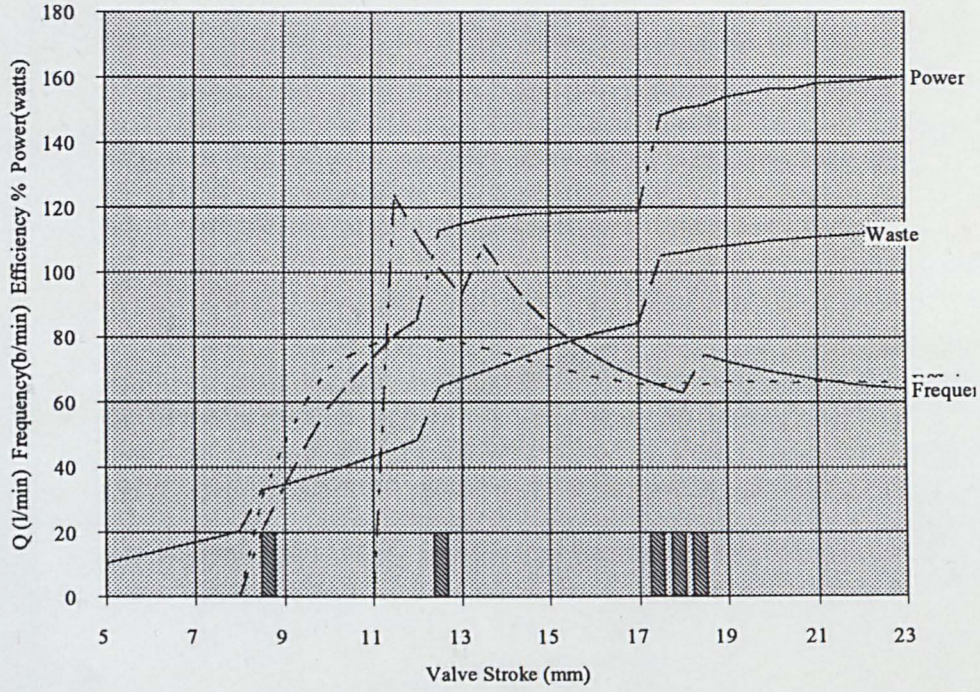

The shaded bars indicate strokes at which the impulse valve may not reopen.

Hydraulic Ram Pump Performance Model

INPUT

SITE		DRIVE PIPE		VALVE		Delivery Valve Swept Volume l	0.008
Drive Head (m)	12	Diameter (mm)	50	Stroke (mm)	23.5	VALVE WILL CLOSE with this setting	
Delivery Head(m)	80	Pipe Length(m)	36	Kf	0.041881891	Closure Waste Vol (l)	0.661
		relrogh(k) (mm)	0.15	Ki	0.038184397	Critical Velocity (m/s)	1.78
		Wavespeed m/s	1350	Kd	0.328	Cutt off Velocity (m/s)	2.16
		CL Fittings	2.0625	Valve Mass kg	0.507	closuretime (s)	0.172

OUTPUT

Power watts	156.51	Delivery l/m	11.97	Delivery' l/m	11.89464921	Delivery' accounts for a partial realisation of recoil, and delivery valve swept volume losses
Freq b/m	58.51	Waste l/m	105.63			
Efficiency	67.86		120.82			

Pump Performance Range

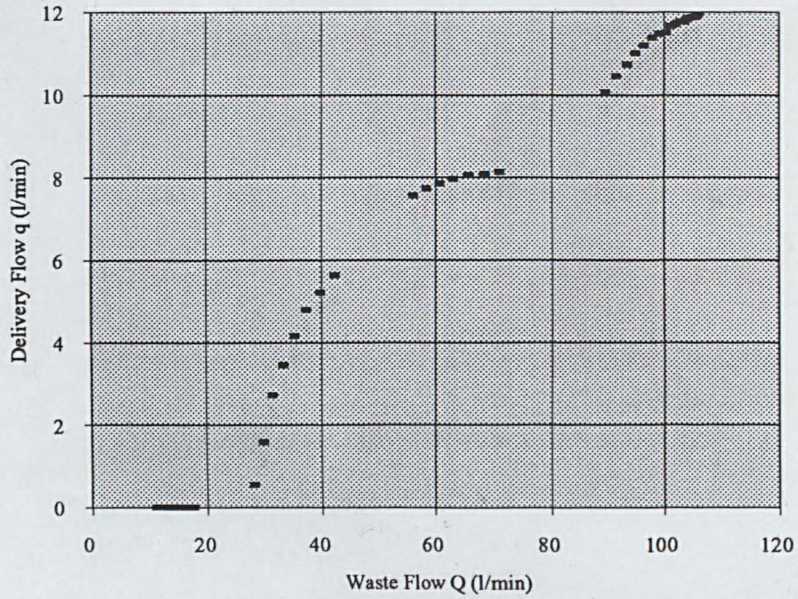

Performance Chart for Hydraulic Ram Pump

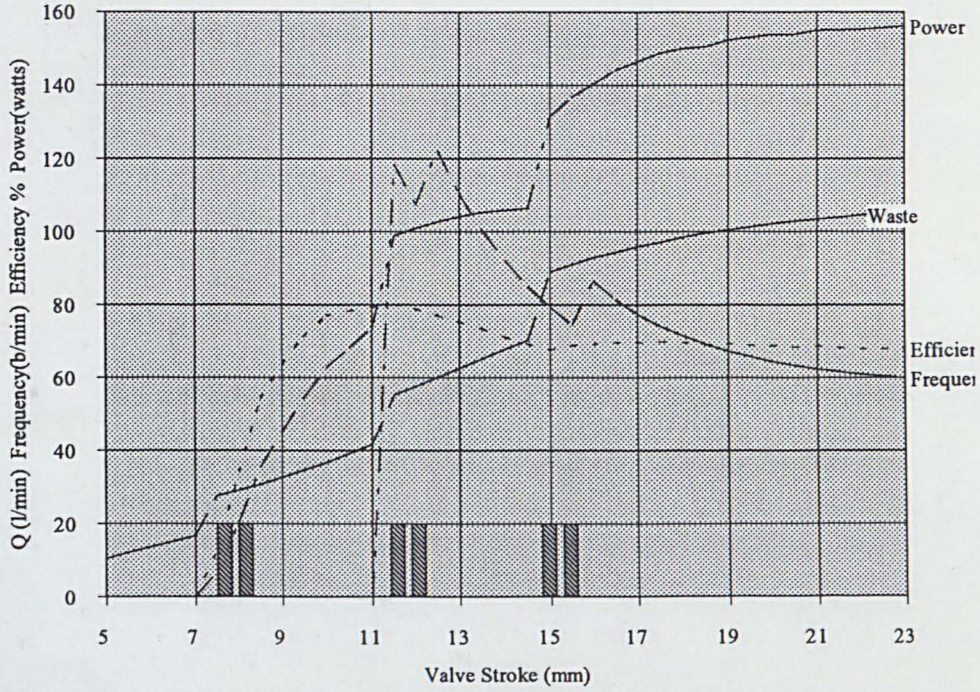

The shaded bars indicate strokes at which the impulse valve may not reopen.

Hydraulic Ram Pump Performance Model

INPUT

SITE		DRIVE PIPE		VALVE		Delivery Valve Swept Volume l	0.008
Drive Head (m)	12	Diameter (mm)	50	Stroke (mm)	23.5	VALVE WILL CLOSE with this setting	
Delivery Head(m)	70	Pipe Length(m)	36	Kf	0.041881891	Closure Waste Vol (l)	0.661
		relrogh(k) (mm)	0.15	Ki	0.038184397	Critical Velocity (m/s)	1.78
		Wavespeed m/s	1350	Kd	0.328	Cutt off Velocity (m/s)	2.16
		CL Fittings	2.0625	Valve Mass kg	0.507	closuretime (s)	0.172

OUTPUT

Power watts	162.67	Delivery l/m	14.22	Delivery' l/m	13.53195374
Freq b/m	60.73	Waste l/m	109.64		
Efficiency	66.97		114.04		

Delivery' accounts for a partial realisation of recoil, and delivery valve swept volume losses

Pump Performance Range

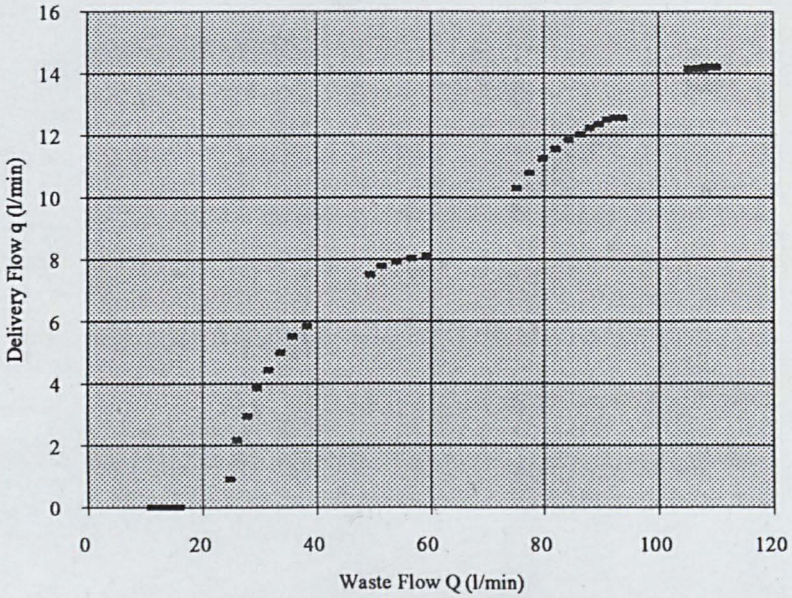

Performance Chart for Hydraulic Ram Pump

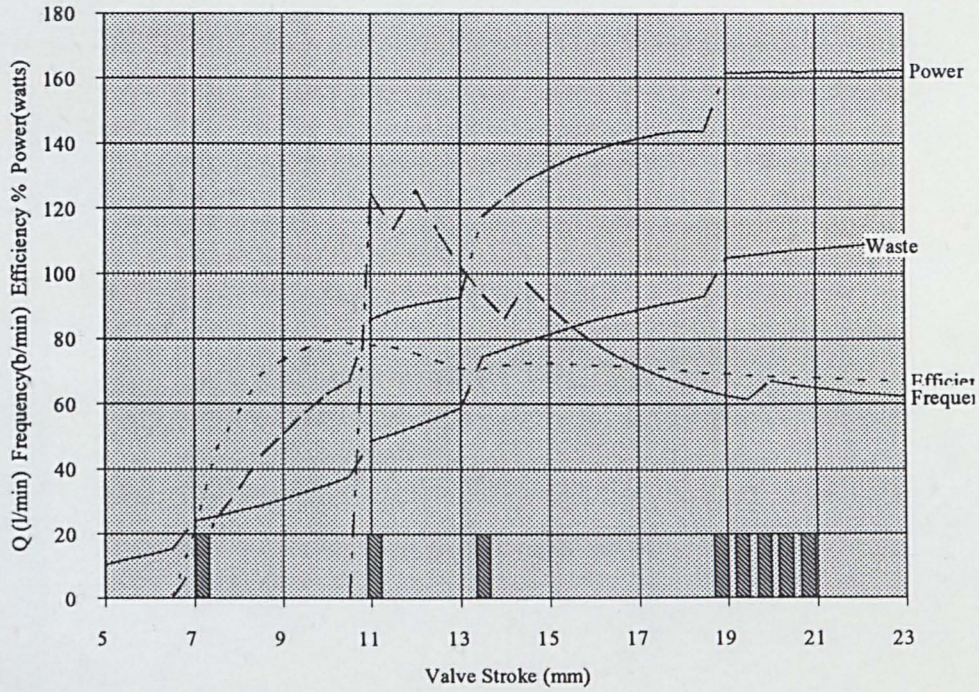

The shaded bars indicate strokes at which the impulse valve may not reopen.

Hydraulic Ram Pump Performance Model

INPUT

SITE		DRIVE PIPE		VALVE	
Drive Head (m)	12	Diameter (mm)	50	Stroke (mm)	23.5
Delivery Head(m)	60	Pipe Length(m)	36	Kf	0.041881891
		relrogh(k) (mm)	0.15	Ki	0.038184397
		Wavespeed m/s	1350	Kd	0.328
		CL Fittings	2.0625	Valve Mass kg	0.507

Delivery Valve Swept Volume l	0.008
VALVE WILL CLOSE with this setting	
Closure Waste Vol (l)	0.661
Critical Velocity (m/s)	1.78
Cutt off Velocity (m/s)	2.16
closuretime (s)	0.172

OUTPUT

Power watts	164.71	Delivery l/m	16.80	Delivery' l/m	15.65868396
Freq b/m	60.83	Waste l/m	109.82		
Efficiency	66.33		114.04		

Delivery' accounts for a partial realisation of recoil, and delivery valve swept volume losses

Pump Performance Range

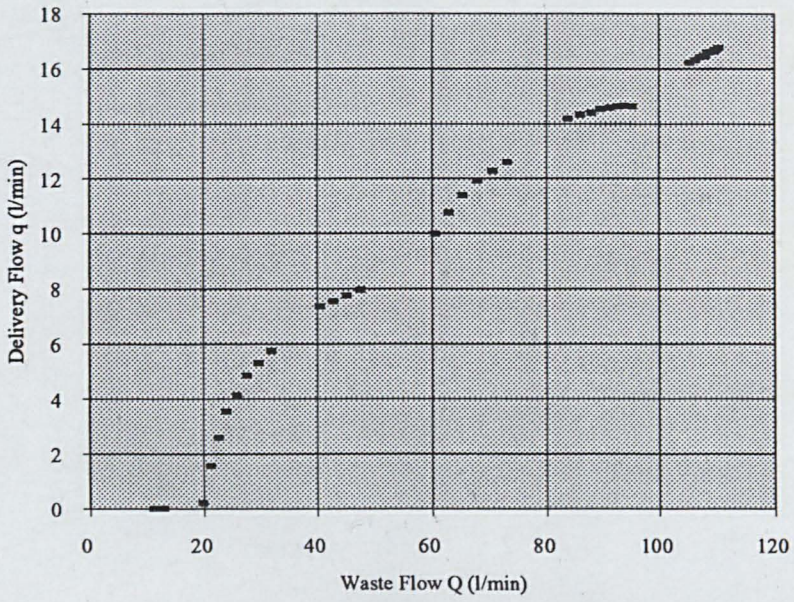

Performance Chart for Hydraulic Ram Pump

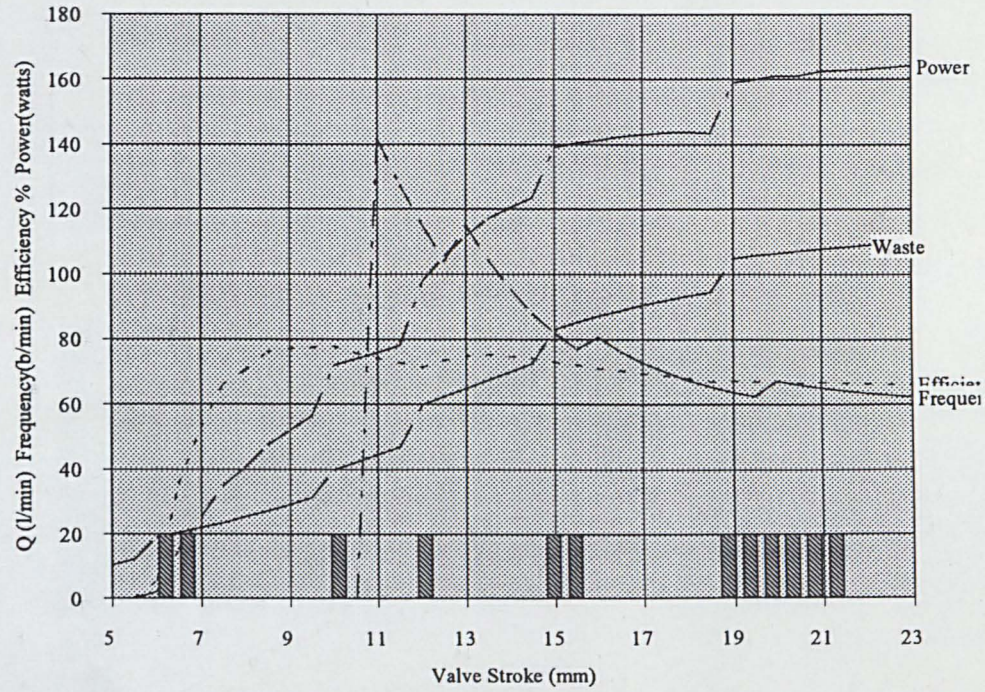

The shaded bars indicate strokes at which the impulse valve may not reopen.

Hydraulic Ram Pump Performance Model

INPUT

SITE		DRIVE PIPE		VALVE		Delivery Valve Swept Volume l	0.008
Drive Head (m)	12	Diameter (mm)	50	Stroke (mm)	23.5	VALVE WILL CLOSE with this setting	
Delivery Head(m)	50	Pipe Length(m)	36	Kf	0.041881891	Closure Waste Vol (l)	0.661
		relrogh(k) (mm)	0.15	Ki	0.038184397	Critical Velocity (m/s)	1.78
		Wavespeed m/s	1350	Kd	0.328	Cutt off Velocity (m/s)	2.16
		CL Fittings	2.0625	Valve Mass kg	0.507	closuretime (s)	0.172

OUTPUT

Power watts	162.01	Delivery l/m	19.82	Delivery' l/m	18.75212444
Freq b/m	57.95	Waste l/m	104.61		
Efficiency	66.38		107.98		

Delivery' accounts for a partial realisation of recoil, and delivery valve swept volume losses

Pump Performance Range

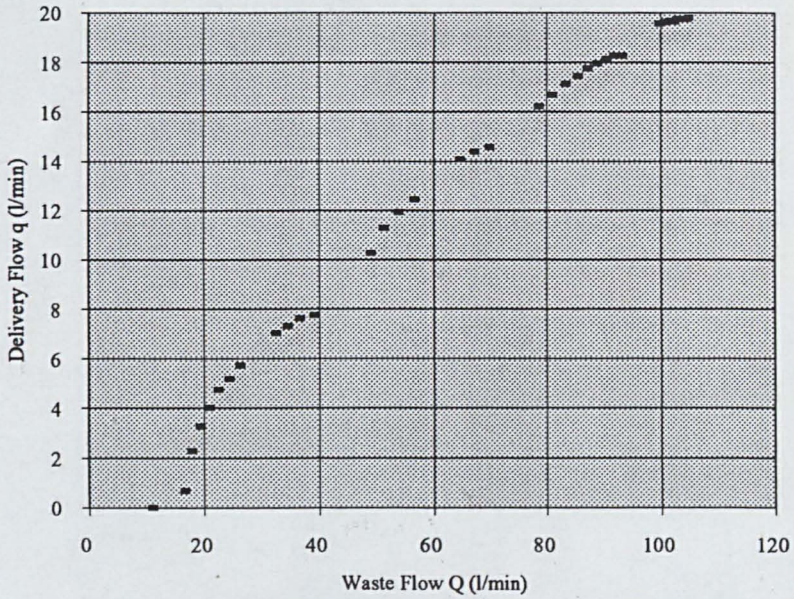

Performance Chart for Hydraulic Ram Pump

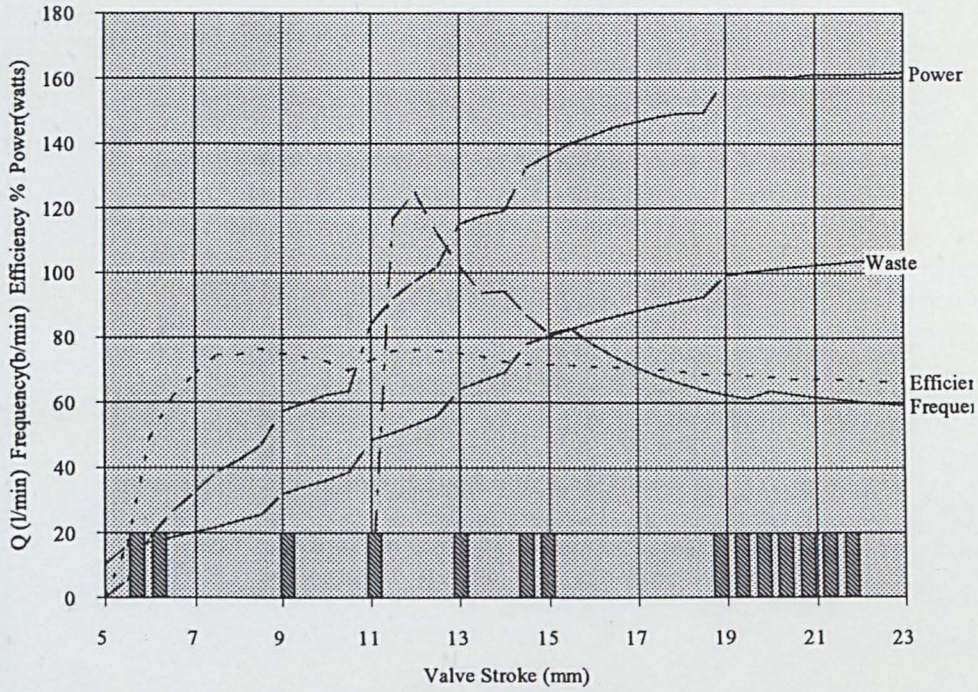

The shaded bars indicate strokes at which the impulse valve may not reopen.

Hydraulic Ram Pump Performance Model

INPUT

SITE		DRIVE PIPE		VALVE	
Drive Head (m)	10	Diameter (mm)	50	Stroke (mm)	23.5
Delivery Head(m)	100	Pipe Length(m)	30	Kf	0.041881891
		relrogh(k) (mm)	0.15	Ki	0.038184397
		Wavespeed m/s	1350	Kd	0.328
		CL Fittings	2.0625	Valve Mass kg	0.507

Delivery Valve Swept Volume l	0.008

VALVE WILL CLOSE with this setting

Closure Waste Vol (l)	0.664
Critical Velocity (m/s)	1.78
Cutt off Velocity (m/s)	2.15
closuretime (s)	0.173

OUTPUT

Power watts	109.51	Delivery l/m	6.70	Delivery' l/m	7.028519777
Freq b/m	55.22	Waste l/m	100.43		
Efficiency	62.54		123.51		

Delivery' accounts for a partial realisation of recoil, and delivery valve swept volume losses

Pump Performance Range

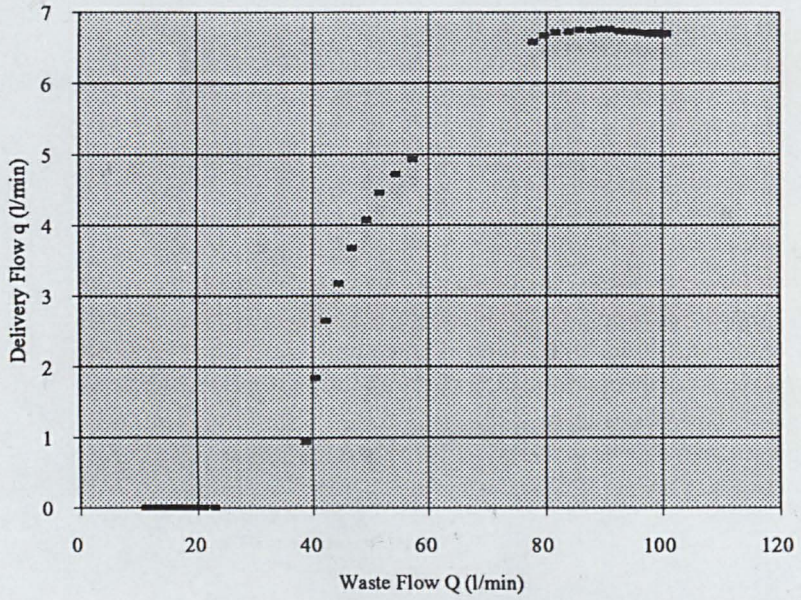

Performance Chart for Hydraulic Ram Pump

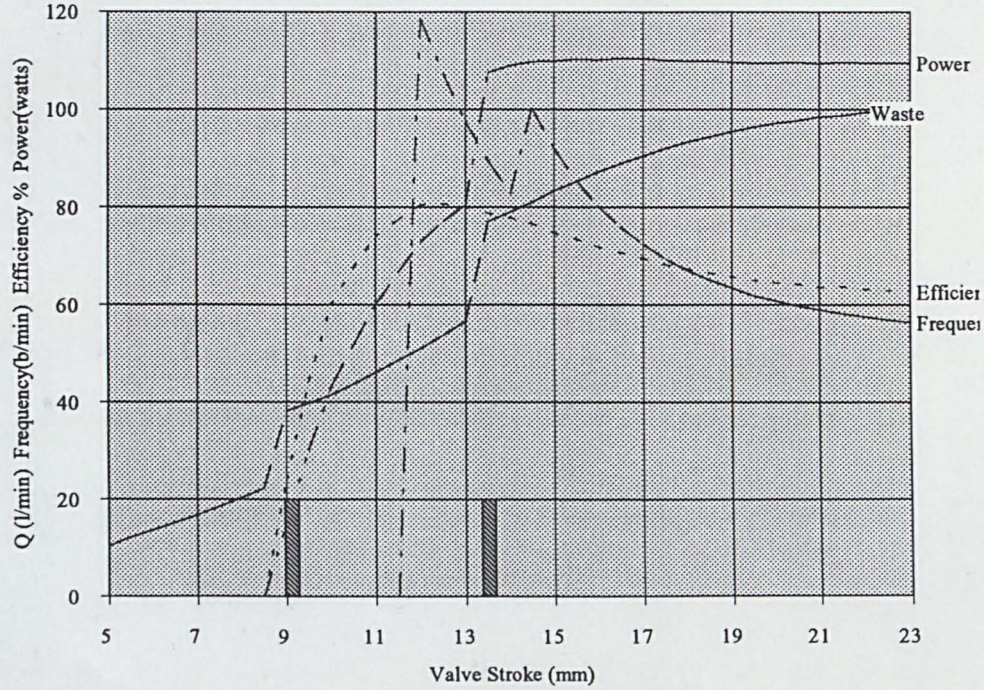

The shaded bars indicate strokes at which the impulse valve may not reopen.

Hydraulic Ram Pump Performance Model

INPUT

SITE		DRIVE PIPE		VALVE		Delivery Valve Swept Volume l	0.008
Drive Head (m)	10	Diameter (mm)	50	Stroke (mm)	23.5	VALVE WILL CLOSE with this setting	
Delivery Head(m)	90	Pipe Length(m)	30	Kf	0.041881891	Closure Waste Vol (l)	0.664
		relrogh(k) (mm)	0.15	Ki	0.038184397	Critical Velocity (m/s)	1.78
		Wavespeed m/s	1350	Kd	0.328	Cutt off Velocity (m/s)	2.15
		CL Fittings	2.0625	Valve Mass kg	0.507	closuretime (s)	0.173

OUTPUT

Power watts	135.35	Delivery l/m	9.20	Delivery' l/m	8.499355579
Freq b/m	63.56	Waste l/m	115.60		
Efficiency	66.36		123.51		

Delivery' accounts for a partial realisation of recoil, and delivery valve swept volume losses

Pump Performance Range

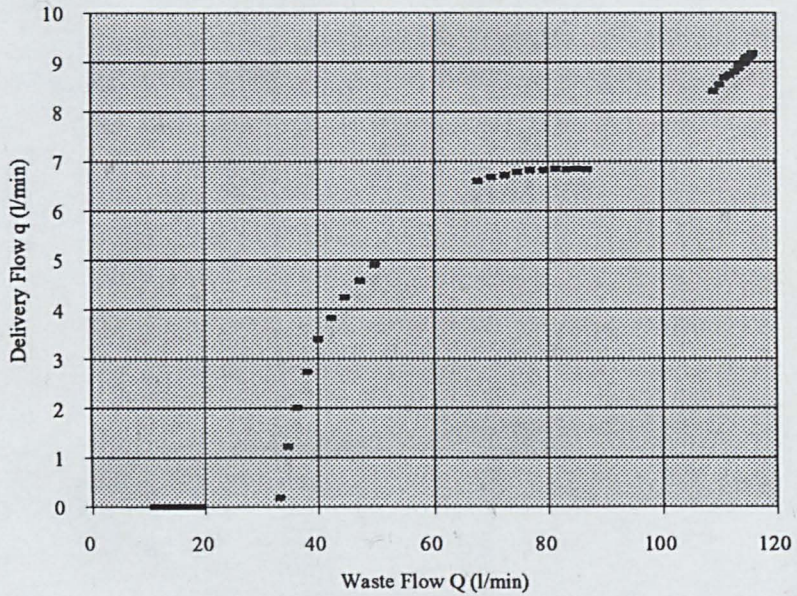

Performance Chart for Hydraulic Ram Pump

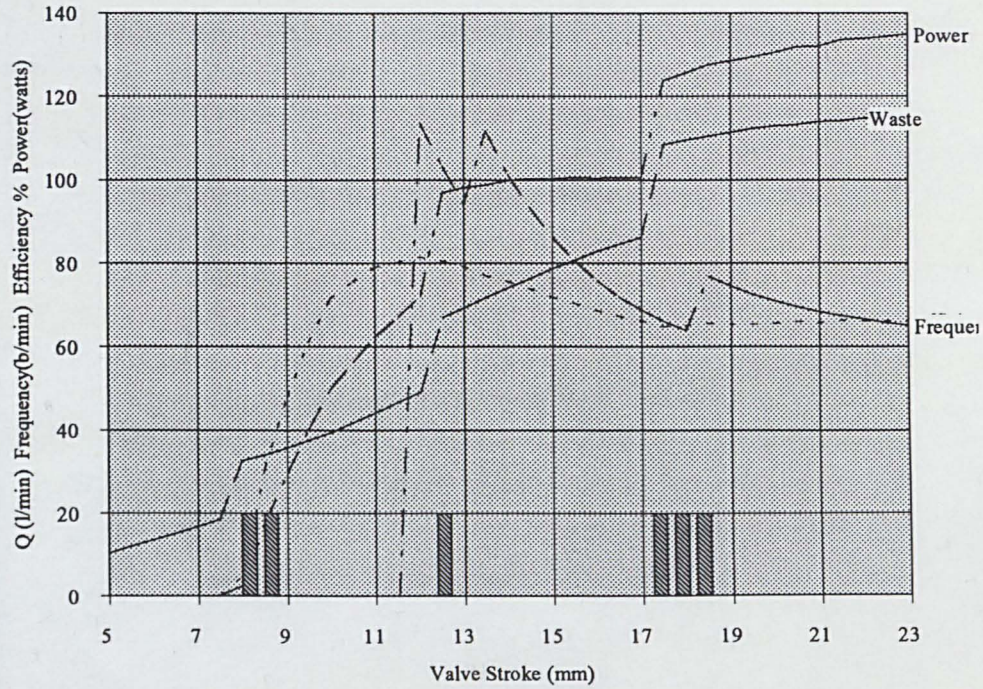

The shaded bars indicate strokes at which the impulse valve may not reopen.

INPUT

SITE		DRIVE PIPE		VALVE	
Drive Head (m)	15	Diameter (mm)	50	Stroke (mm)	23.5
Delivery Head(m)	100	Pipe Length(m)	45	Kf	0.041881891
		relrogh(k) (mm)	0.15	Ki	0.038184397
		Wavespeed m/s	1350	Kd	0.328
		CL Fittings	2.0625	Valve Mass kg	0.507

Delivery Valve Swept Volume l	0.008

VALVE WILL CLOSE with this setting

Closure Waste Vol (l)	0.657
Critical Velocity (m/s)	1.78
Cutt off Velocity (m/s)	2.16
closuretime (s)	0.171

OUTPUT

Power watts	197.54	Delivery l/m	12.09	Delivery' l/m	11.09881728
Freq b/m	64.80	Waste l/m	116.12		
Efficiency	62.85		117.07		

Delivery' accounts for a partial realisation of recoil, and delivery valve swept volume losses

Pump Performance Range

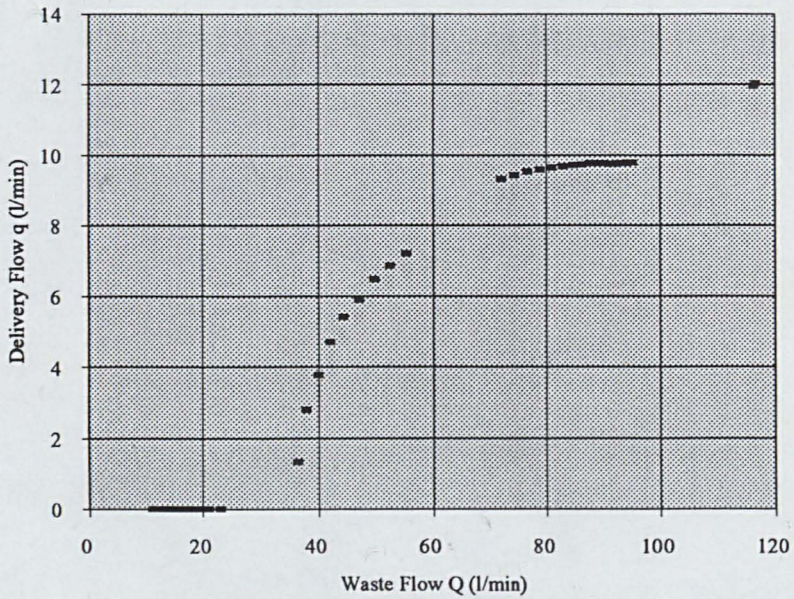

Performance Chart for Hydraulic Ram Pump

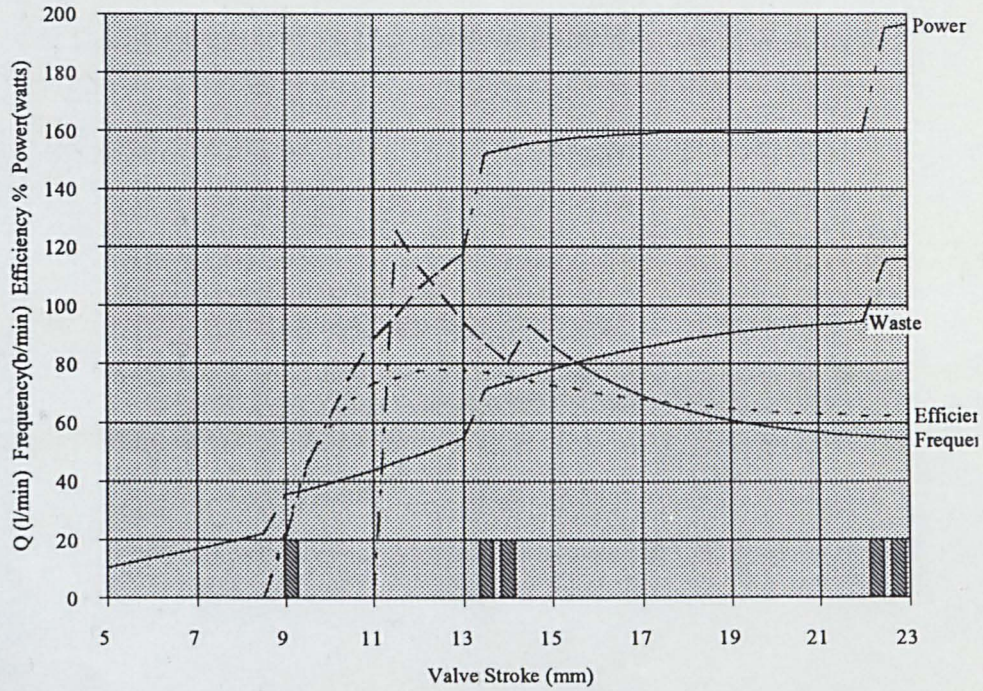

The shaded bars indicate strokes at which the impulse valve may not reopen.

INPUT

SITE		DRIVE PIPE		VALVE	
Drive Head (m)	15	Diameter (mm)	50	Stroke (mm)	23.5
Delivery Head(m)	90	Pipe Length(m)	45	Kf	0.041881891
		relrogh(k) (mm)	0.15	Ki	0.038184397
		Wavespeed m/s	1350	Kd	0.328
		CL Fittings	2.0625	Valve Mass kg	0.507

Delivery Valve Swept Volume l	0.008

VALVE WILL CLOSE with this setting

Closure Waste Vol (l)	0.657
Critical Velocity (m/s)	1.78
Cutt off Velocity (m/s)	2.16
closuretime (s)	0.171

OUTPUT

Power watts	199.13	Delivery l/m	13.54	Delivery' l/m	13.10155647
Freq b/m	60.55	Waste l/m	108.52		
Efficiency	66.55		117.07		

Delivery' accounts for a partial realisation of recoil, and delivery valve swept volume losses

Pump Performance Range

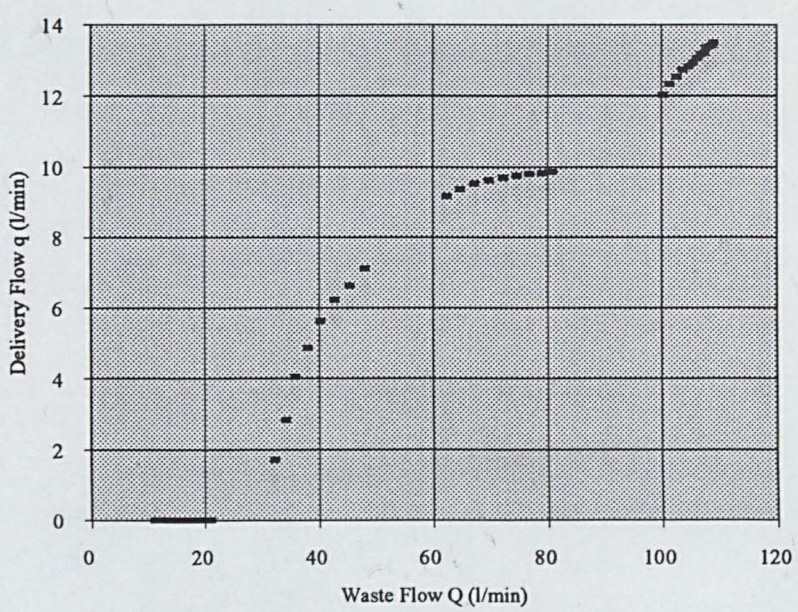

Performance Chart for Hydraulic Ram Pump

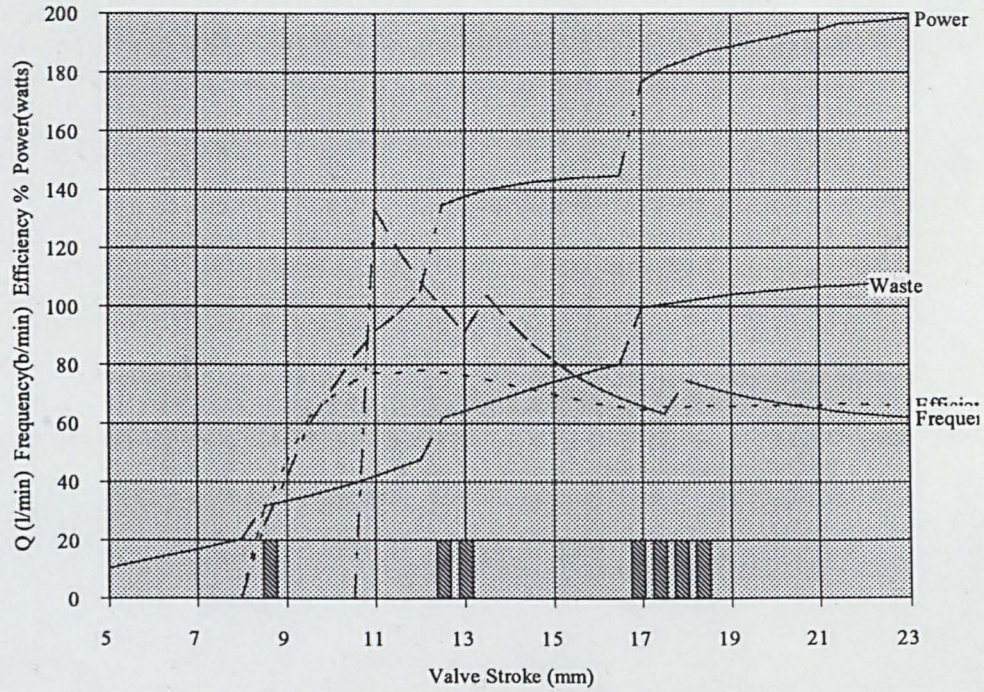

The shaded bars indicate strokes at which the impulse valve may not reopen.

Hydraulic Ram Pump Performance Model

INPUT

SITE		DRIVE PIPE		VALVE	
Drive Head (m)	15	Diameter (mm)	50	Stroke (mm)	23.5
Delivery Head(m)	80	Pipe Length(m)	45	Kf	0.041881891
		relrogh(k) (mm)	0.15	Ki	0.038184397
		Wavespeed m/s	1350	Kd	0.328
		CL Fittings	2.0625	Valve Mass kg	0.507

Delivery Valve Swept Volume l: 0.008

VALVE WILL CLOSE with this setting

Closure Waste Vol (l)	0.657
Critical Velocity (m/s)	1.78
Cutt off Velocity (m/s)	2.16
closuretime (s)	0.171

OUTPUT

Power watts	193.61	Delivery l/m	14.81	Delivery' l/m	15.00293661
Freq b/m	56.84	Waste l/m	101.86		
Efficiency	67.69		117.07		

Delivery' accounts for a partial realisation of recoil, and delivery valve swept volume losses

Pump Performance Range

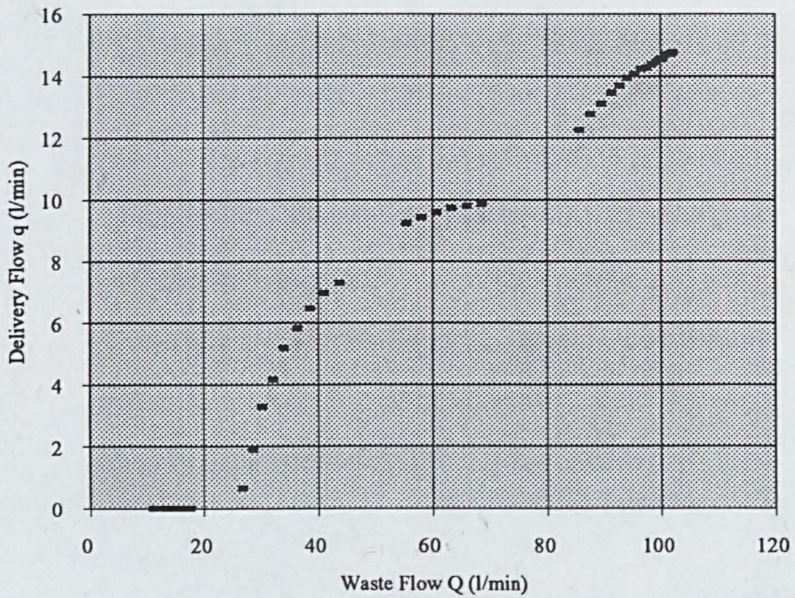

Performance Chart for Hydraulic Ram Pump

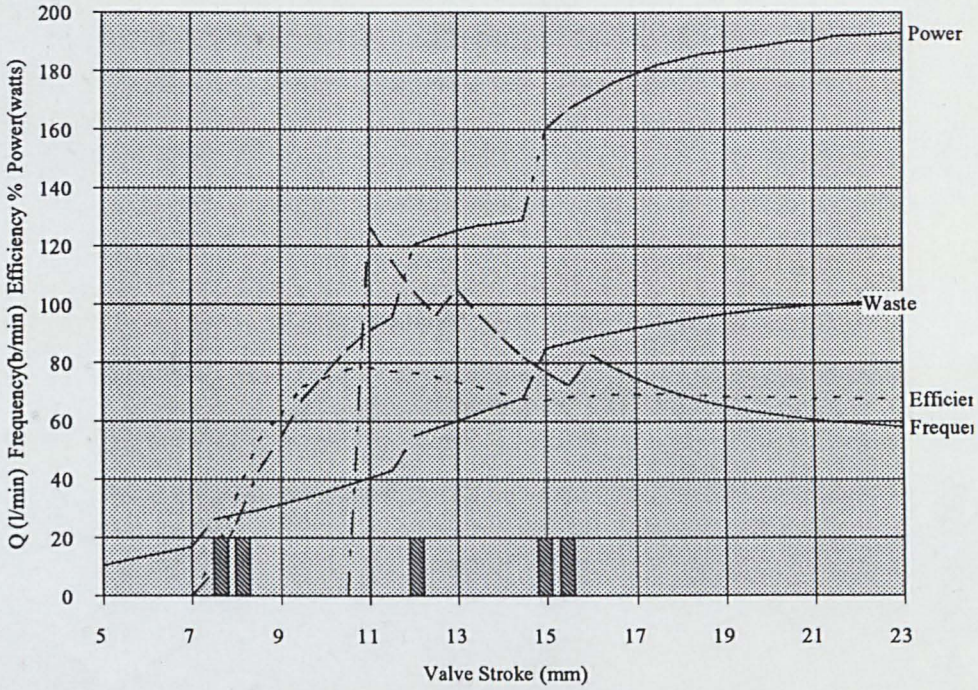

The shaded bars indicate strokes at which the impulse valve may not reopen.

Hydraulic Ram Pump Performance Model

INPUT

SITE		DRIVE PIPE		VALVE		Delivery Valve Swept Volume l	0.008
Drive Head (m)	15	Diameter (mm)	50	Stroke (mm)	23.5	VALVE WILL CLOSE with this setting	
Delivery Head(m)	70	Pipe Length(m)	45	Kf	0.041881891	Closure Waste Vol (l)	0.657
		relrogh(k) (mm)	0.15	Ki	0.038184397	Critical Velocity (m/s)	1.78
		Wavespeed m/s	1350	Kd	0.328	Cutt off Velocity (m/s)	2.16
		CL Fittings	2.0625	Valve Mass kg	0.507	closuretime (s)	0.171

OUTPUT

Power watts	197.94	Delivery l/m	17.30	Delivery' l/m	16.77527447
Freq b/m	58.18	Waste l/m	104.26		
Efficiency	66.42		109.15		

Delivery' accounts for a partial realisation of recoil, and delivery valve swept volume losses

Pump Performance Range

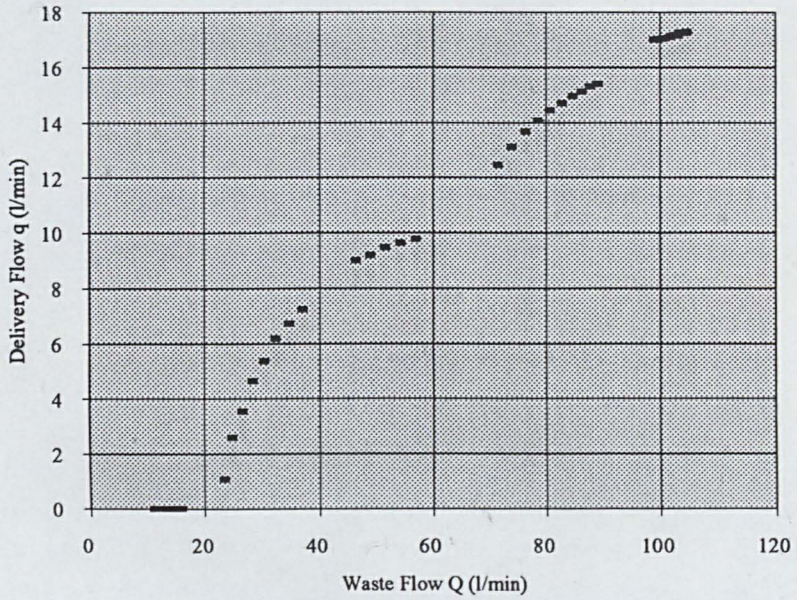

Performance Chart for Hydraulic Ram Pump

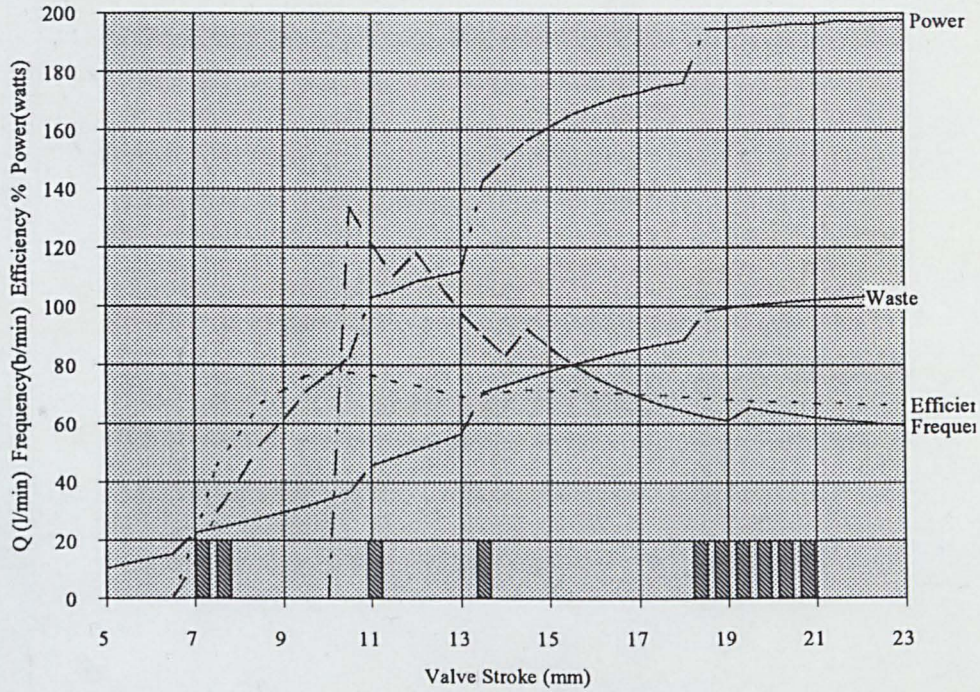

The shaded bars indicate strokes at which the impulse valve may not reopen.

Hydraulic Ram Pump Performance Model

INPUT

SITE		DRIVE PIPE		VALVE	
Drive Head (m)	15	Diameter (mm)	50	Stroke (mm)	23.5
Delivery Head(m)	60	Pipe Length(m)	45	Kf	0.041881891
		relrogh(k) (mm)	0.15	Ki	0.038184397
		Wavespeed m/s	1350	Kd	0.328
		CL Fittings	2.0625	Valve Mass kg	0.507

Delivery Valve Swept Volume l	0.008

VALVE WILL CLOSE with this setting

Closure Waste Vol (l)	0.657
Critical Velocity (m/s)	1.78
Cutt off Velocity (m/s)	2.16
closuretime (s)	0.171

OUTPUT

Power watts	202.38	Delivery l/m	20.64	Delivery' l/m	19.83427903
Freq b/m	57.66	Waste l/m	103.33		
Efficiency	66.59		109.15		

Delivery' accounts for a partial realisation of recoil, and delivery valve swept volume losses

Pump Performance Range

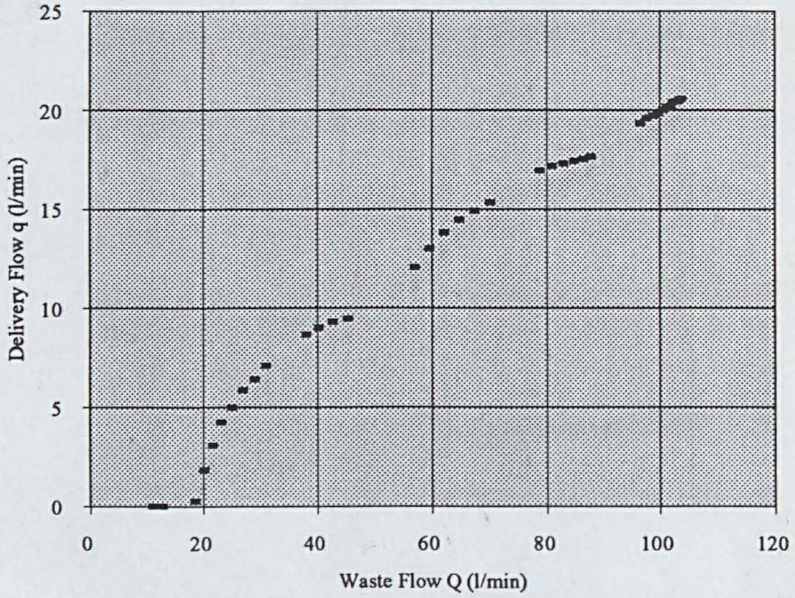

Performance Chart for Hydraulic Ram Pump

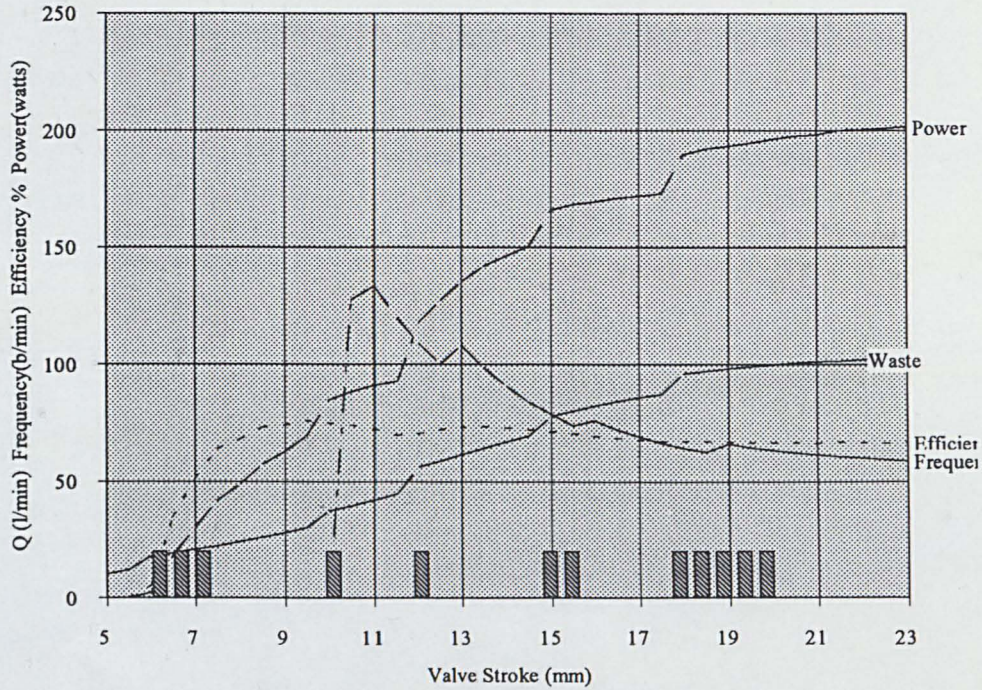

The shaded bars indicate strokes at which the impulse valve may not reopen.

Hydraulic Ram Pump Performance Model

INPUT

SITE		DRIVE PIPE		VALVE		Delivery Valve Swept Volume l	0.008
Drive Head (m)	15	Diameter (mm)	50	Stroke (mm)	23.5	VALVE WILL CLOSE with this setting	
Delivery Head(m)	50	Pipe Length(m)	45	Kf	0.041881891	Closure Waste Vol (l)	0.657
		relrogh(k) (mm)	0.15	Ki	0.038184397	Critical Velocity (m/s)	1.78
		Wavespeed m/s	1350	Kd	0.328	Cutt off Velocity (m/s)	2.16
		CL Fittings	2.0625	Valve Mass kg	0.507	closuretime (s)	0.171

OUTPUT

Power watts	205.17	Delivery l/m	25.11	Delivery' l/m	23.30304692
Freq b/m	56.96	Waste l/m	102.07		
Efficiency	65.80		102.23		

Delivery' accounts for a partial realisation of recoil, and delivery valve swept volume losses

Pump Performance Range

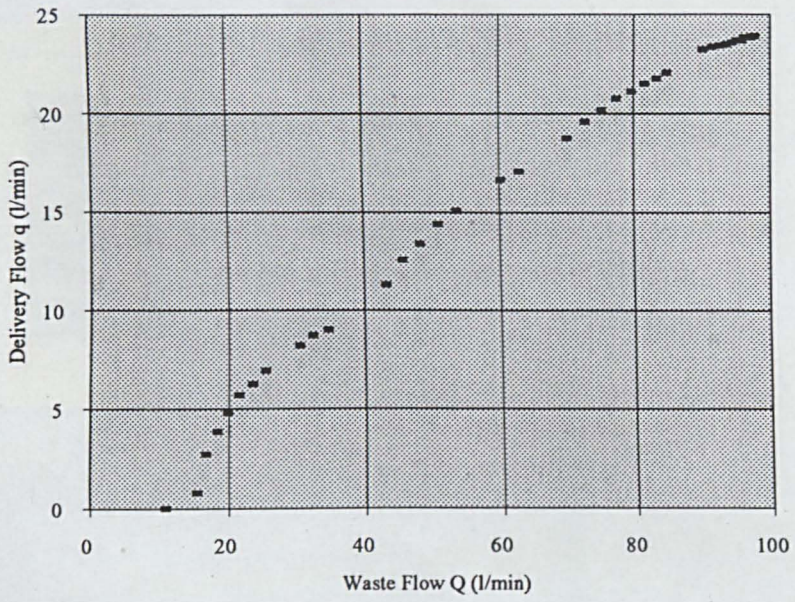

Performance Chart for Hydraulic Ram Pump

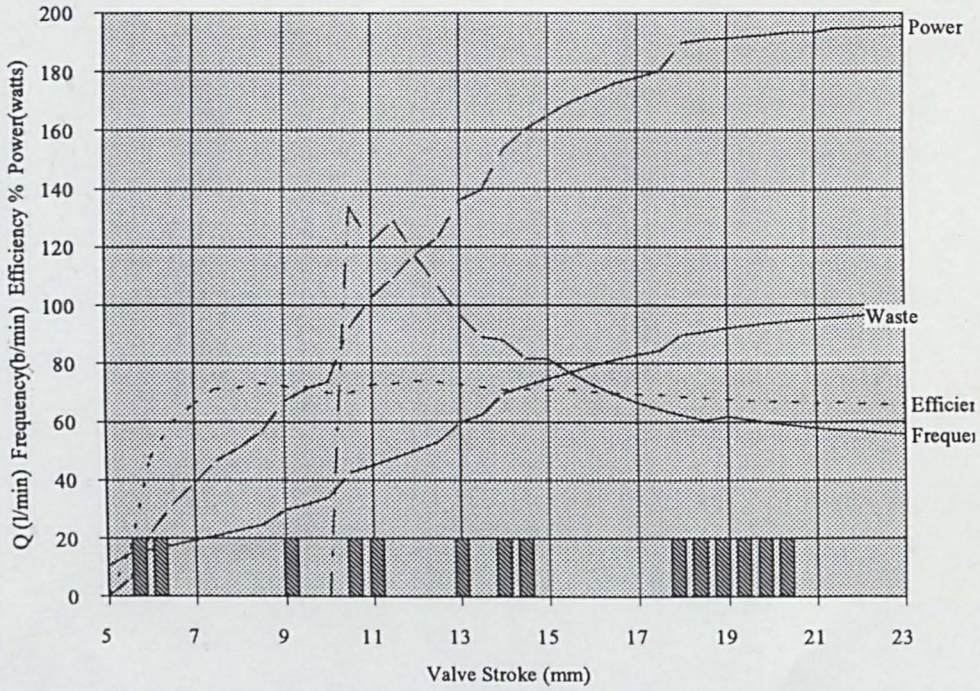

The shaded bars indicate strokes at which the impulse valve may not reopen.